FOUNDATION-SOIL INTERACTION ANALYSIS OF BRIDGES – VOLUMES I AND II

WA-RD 324.1

Research Report
April 1993

Washington State Department of Transportation

Washington State Transportation Commission
Planning and Capital Program Management
in cooperation with:
U.S. DOT - Federal Highway Administration

Manual of Practice
Foundation-Soil Interaction Analysis of Bridges
Volume I

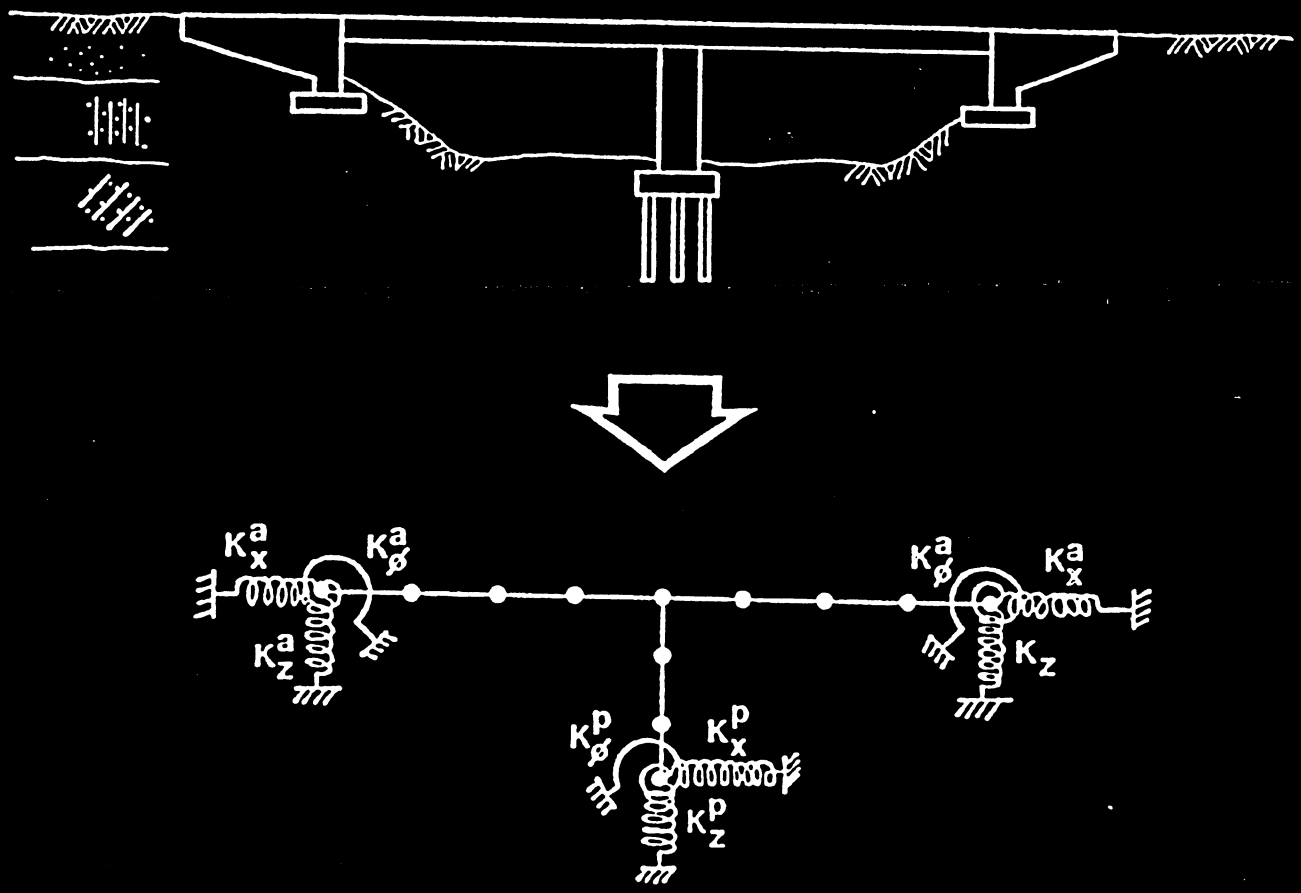

Prepared for:
Washington Department of Transportation

Prepared by:
Dames & Moore
Seattle, WA
and
Inca Engineers
Bellevue, WA

April 1993

FOREWORD

Dames & Moore and their subcontractor, Inca Engineers, have prepared this Manual of Practice for conducting bridge foundation-soil interaction analyses. The manual is intended to assist engineers in the Bridge Design office at the Washington State Department of Transportation (WSDOT) who perform dynamic analysis of bridge-foundation systems. The primary purpose of the manual is to present practical and accurate methods for estimating the foundation stiffness matrices for abutment or pier foundations supported on footings or piles. These matrices are needed for soil-structure interaction analysis to more accurately determine the seismic loads acting on the bridge superstructure and on the abutment and pier foundations.

This Manual of Practice consists of two volumes. Volume I presents five bridge example problems:

1. Coldwater Creek
2. Deadwater Slough
3. Ebey Slough
4. Northrup Way
5. FHWA

The first four examples are actual WSDOT bridges and the fifth example is a fictitious bridge that appeared in a 1991 FHWA course notebook on seismic design of highway bridges.

Volume II presents the input and output files of the SEISAB computer program for the dynamic soil-structure interaction analysis of bridges. The SEISAB computer program is currently used by WSDOT in the seismic design of Washington state bridges.

Dames & Moore recommends the FHWA and Novak methods to estimate bridge foundation stiffness matrices. These methodologies are presented in detail in the Coldwater Creek example problem in Volume I. In this example, the basic theory and relevant equations or inputs for implementing these methodologies are provided first and are immediately followed by their application to the Coldwater Creek bridge. The appropriate equations or inputs from the FHWA and Novak methodologies presented in the Coldwater Creek example problem are identified and applied in the other four bridge example problems.

Volume I also contains three appendices. The basis for the recommendation of the FHWA and Novak methods is provided in Appendix A, which is a reproduction of the 1992 Dames & Moore report to WSDOT on the evaluation of methods to estimate foundation stiffnesses. Appendix B consists of selected pages from the BMCOL 76 computer program user guide; this computer program, which computes the load-deflection and moment-rotation curves for single piles, is part of the FHWA methodology. Appendix C presents the method for transforming the foundation stiffness matrices from one coordinate system to another. This transformation process is important because the coordinate systems assumed in the FHWA and Novak methods are generally different and therefore are not necessarily the same as the SEISAB coordinate system. Coordinate transformations are also discussed in the Coldwater Creek example problem.

EXAMPLE NO. 1

COLDWATER CREEK BRIDGE

TABLE OF CONTENTS

Section		Page
1.0	**DESCRIPTION OF BRIDGE AND FOUNDATION SOILS**	1
2.0	**SEISMIC DESIGN PARAMETERS**	2
3.0	**SOIL PROPERTIES**	2
4.0	**PIER 1 STIFFNESS CALCULATION - FHWA METHOD**	3
4.1	PILE-STIFFNESS CALCULATION	4
4.1.1	Estimation of H-pile Parameters	5
4.1.2	Computation of t-z Curves	6
4.1.2.1	General Procedure	6
4.1.2.2	Application to Coldwater Creek Bridge Abutment Piles	8
4.1.3	Computation of Q-z Curve	10
4.1.3.1	General Procedure	10
4.1.3.2	Application to Coldwater Creek Bridge Abutment Piles	11
4.1.4	Computation of p-y Curves	11
4.1.4.1	General Procedure	11
4.1.4.2	Application to Coldwater Creek Bridge Abutment Piles	14
4.1.5	Preparation of BMCOL-76 Input	17
4.1.6	BMCOL-76 Output	17
4.1.7	Calculation of Pile-Head Stiffnesses	18
4.1.8	Calculation of Pile-Group Stiffness Matrix	19
4.1.8.1	Assumptions	19
4.1.8.2	Preparation of GPILE Input	19
4.1.8.3	GPILE Output	21
4.2	ABUTMENT FOOTING STIFFNESSES	21
4.2.1	Model and Assumptions	22
4.2.2	Calculation of Footing Stiffnesses	23
4.2.2.1	General Procedure.	23
4.2.2.2	Application to Coldwater Creek Abutment Footing.	25
4.3	ABUTMENT WALL STIFFNESS	28
4.3.1	Model and Assumptions	28
4.3.2	Calculation of Wall Stiffnesses	29
4.3.2.1	General Procedure.	29
4.3.2.2	Application to Coldwater Creek Abutment Wall.	30
4.4	TOTAL ABUTMENT STIFFNESS MATRIX	31
4.4.2	Application to Coldwater Creek Abutment.	32

5.0 PIER 1 STIFFNESS CALCULATION - NOVAK METHOD 34
5.1 PILE AND FOOTING SIDE STIFFNESS 35
5.1.1 Soil Model 35
5.1.2 Preparation of DYNA3 Input 36
5.1.3 DYNA3 Output 37
5.2 ABUTMENT WALL STIFFNESS 38
5.3 TOTAL PIER 1 STIFFNESS MATRIX 38

6.0 PIER 2 (FOOTING) STIFFNESS CALCULATION - FHWA METHOD 39
6.1 MODEL AND ASSUMPTIONS 39
6.2 CALCULATION OF FOOTING STIFFNESS 41

7.0 PIER 2 (FOOTING) STIFFNESS CALCULATION - NOVAK METHOD ... 43
7.1 SOIL MODEL 43
7.2 PREPARATION OF DYNA3 INPUT 44
7.3 DYNA3 OUTPUT 44

8.0 PIER 3 AND PIER 4 FOUNDATION STIFFNESSES 45
8.1 PIER 3 FOUNDATION STIFFNESSES 45
8.1.1 FHWA Method 45
8.1.2 Novak Method 46
8.2 PIER 4 FOUNDATION STIFFNESSES 46
8.2.1 FHWA Method 46
8.2.2 Novak Method 48

9.0 APPLICATION TO SEISAB-I BRIDGE ANALYSIS 49
9.1 BENT 2 MODEL 49
9.2 BENT 3 MODEL 50
9.3 BENT 4 MODEL 53
9.4 BENT 5 MODEL 54
9.5 LOAD MODEL 54
9.6 DISCUSSION OF THE INPUT FILE 55
9.7 DISCUSSION OF THE OUTPUT FILE 55

SEC. 2, T. 9 N., R. 4 E., W.M.

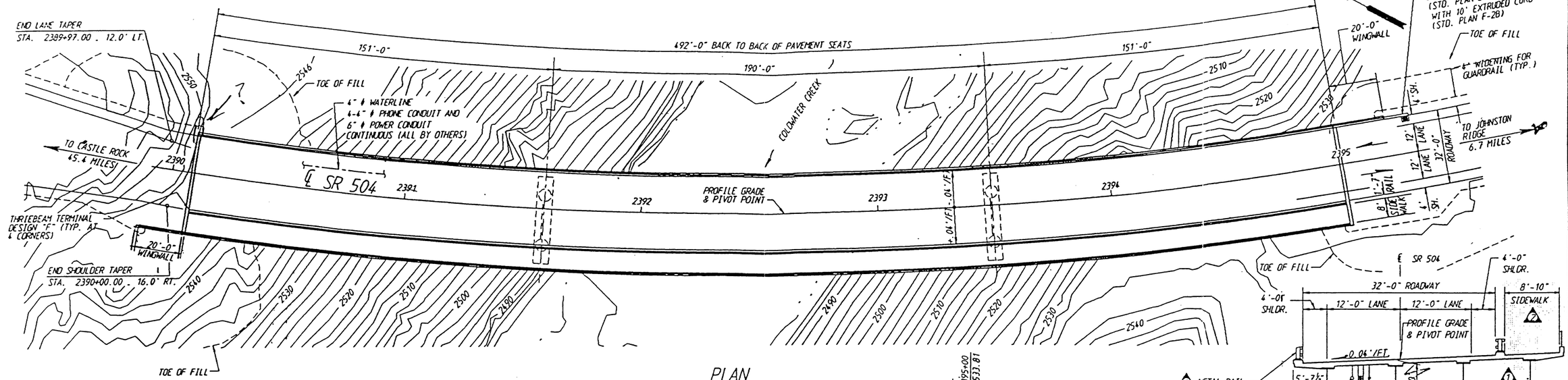

PLAN

BEARING OF ALL PIERS ARE NORMAL TO ℄ SR 504

SCALE 1" = 20'

CURVE DATA					
P.I. STATION	Δ	RADIUS	TANGENT	LENGTH	BK. TANGENT
2393+22.76	28° 18' 18" LT.	1500'	378.24'	741.02'	S17° 25' 06"E

P.I.V.C. STA. 2395+00
ELEV. 2533.81

-6.1876 % +0.4952 %

1000 V.C.

SR 504 PROFILE

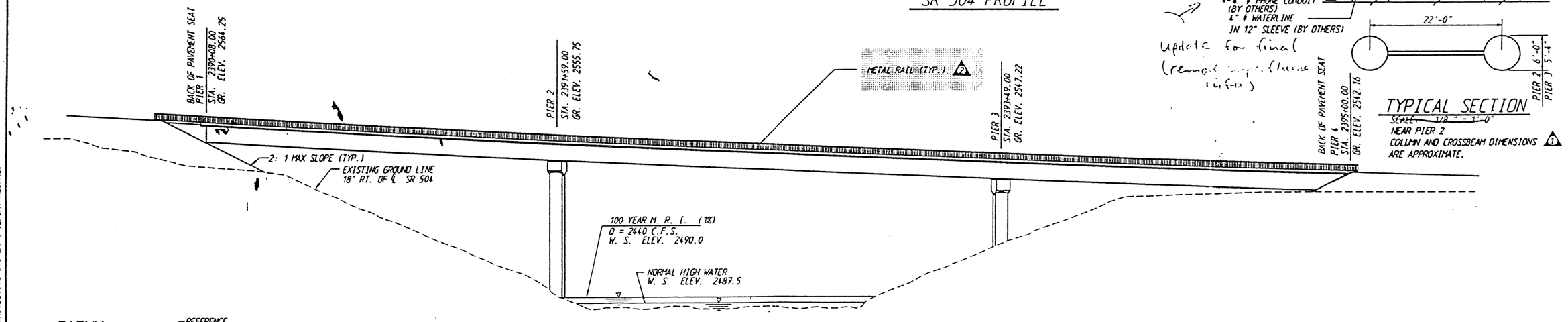

DATUM

NATL. GEOD. VERT.
DATUM OF 1929,
ADJUSTED 1947

ELEVATION

GRADE ELEVATIONS SHOWN ARE FINISH GRADES ON ℄ SR 504
AT TOP OF ROADWAY SLAB AND ARE EQUAL TO PROFILE GRADE.
FOR EMBANKMENT DETAILS AT BRIDGE ENDS. SEE STANDARD PLAN H-9.

NOTE: VENT SEALS AT ELEV. 2488.5

TYPICAL SECTION

SCALE 1/8" = 1'-0"

NEAR PIER 2
COLUMN AND CROSSBEAM DIMENSIONS 1
ARE APPROXIMATE.

Update for final
(remove superfluous
info)

COMPOSITE
STEEL PLATE GIRDER
LOADING: HS-25
OR
TWO 24K AXLES @ 4' CTRS.

Coast Guard Permit Requ. NO
Permit Target Date ——

BRIDGE WITH APPROACH FILLS
8'-0" STEEL PLATE GIRDER
DECK PROTECTIVE SYSTEM 1 (EPOXY REBARS)

SR 504 JOB NO. 7002 SHEET 1

LAYOUT APPROVED BY:

Allan H. Walley 1/21/92
BRIDGE & STRUCTURES ENGINEER

Gerald E. Smith 3-4-92
DISTRICT ADMINISTRATOR

Bridge Design Engr. Myn Lui 1/92					
Supervisor					
Designed By	6-92	2 ADDED BALLASTER SIDEWALK RAIL			
Checked By M. H. B. 1-92		AND 8"-10" SIDEWALK			
Detailed By J. M. A. / S. D. F. 1-92					
Bridge Projects Engr. Karl Koh 1-92	3-92	1 ADDED METAL RAIL, 8'-0" SIDEWALK,	SDF	MHL	
Prelim. Plan By S. D. FAIRCHILD 1-92		ROUND COLUMNS AND FOURTH GIRDER			
Architect/Specialist R. Mays 1/92	DATE	REVISION	BY	APP'D	

REGION NO.	STATE	FED. AID PROJ. NO.	SHEET NO.	TOTAL SHEETS
10	WASH.			
JOB NUMBER				

BRIDGE AND STRUCTURES

ALLAN H. WALLEY — STATE OF WASHINGTON — REGISTERED PROFESSIONAL ENGINEER (EXPIRES 12/15/93)

Washington State Department of Transportation

Figure 1.1

PRELIMINARY PLAN

BRIDGE SHEET NO. 7
SHEETS OF SHEETS

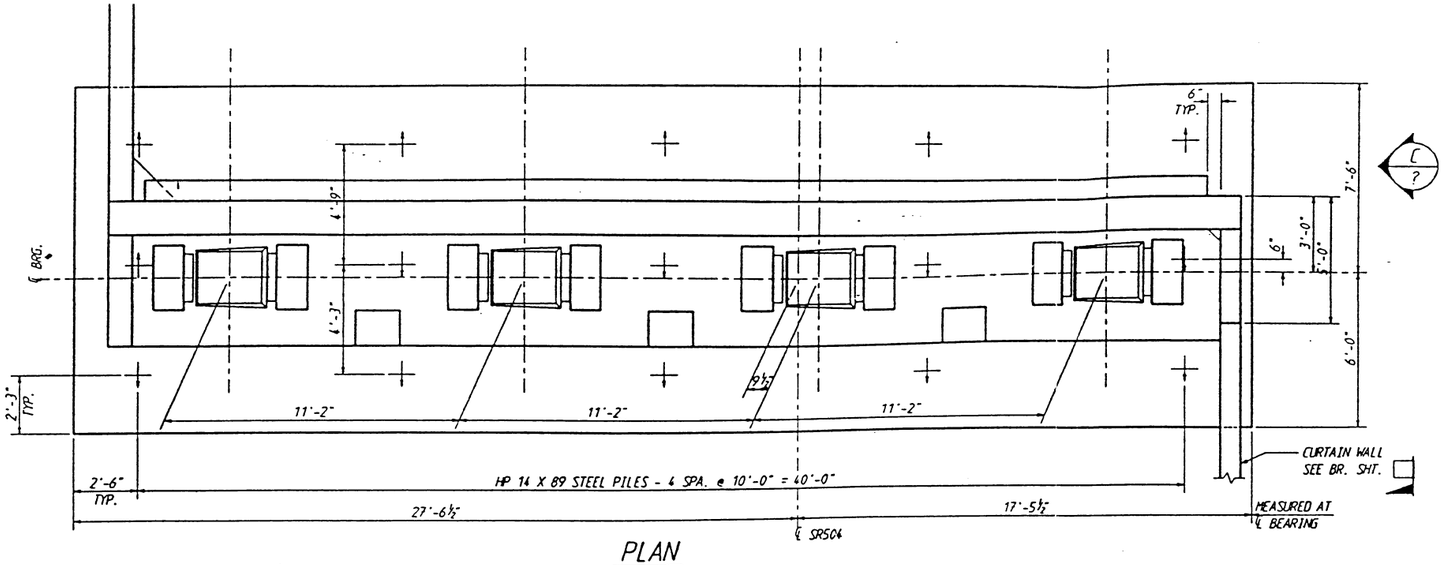

PLAN

+ DENOTES PILE AND DIRECION OF 4½ 12 BATTER.

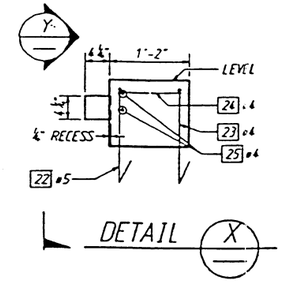

DETAIL X

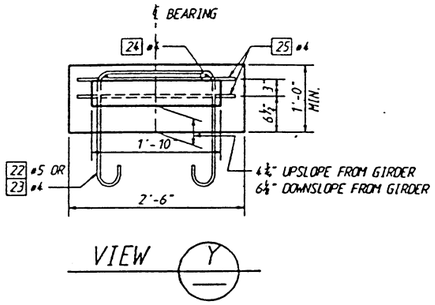

VIEW Y

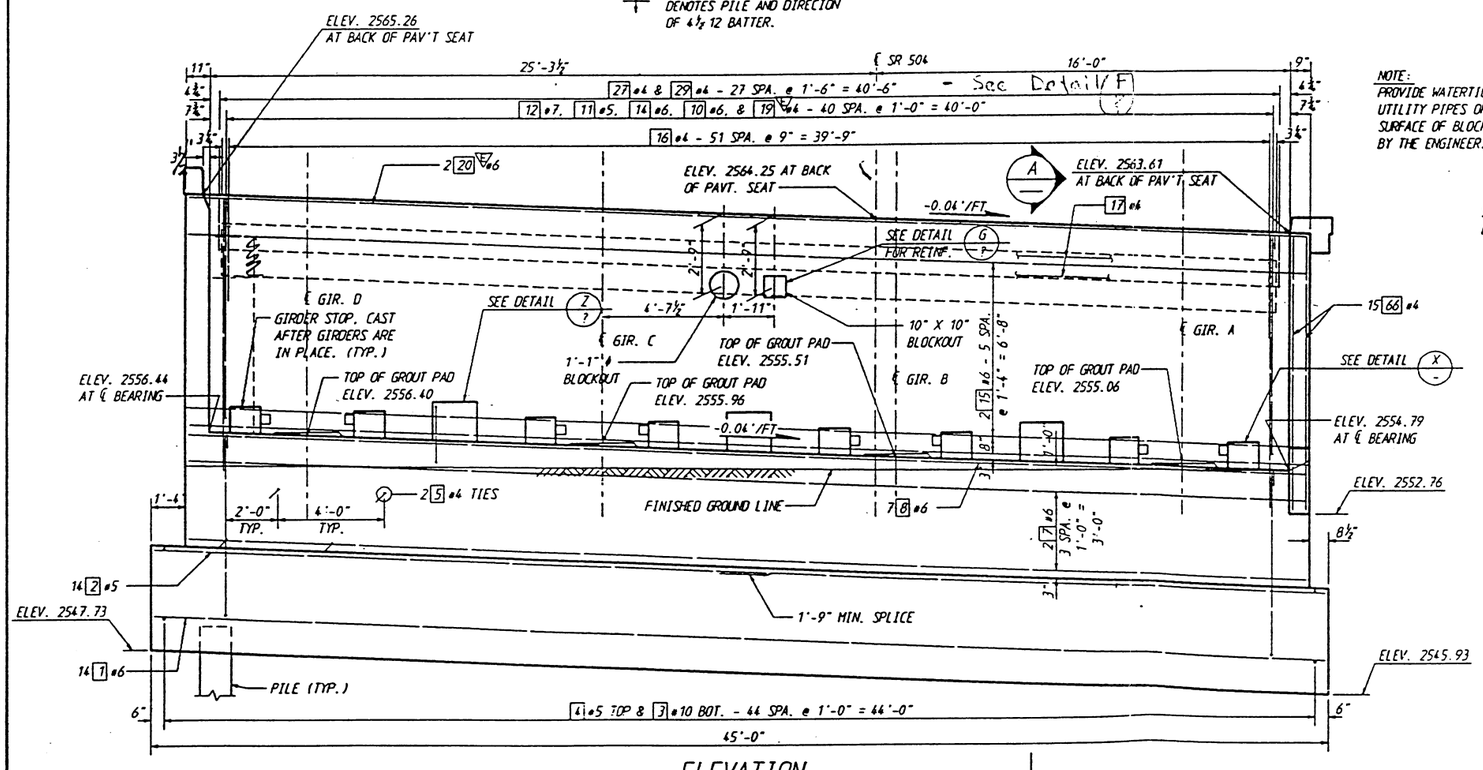

ELEVATION

SHOWN LOOKING BACK ON STATIONING

NOTE:
PROVIDE WATERTIGHT SEAL BETWEEN UTILITY PIPES OR DUCTS AND CONCRETE SURFACE OF BLOCKOUT. TO BE APPROVED BY THE ENGINEER. TYPICAL FOR PIERS 1&4.

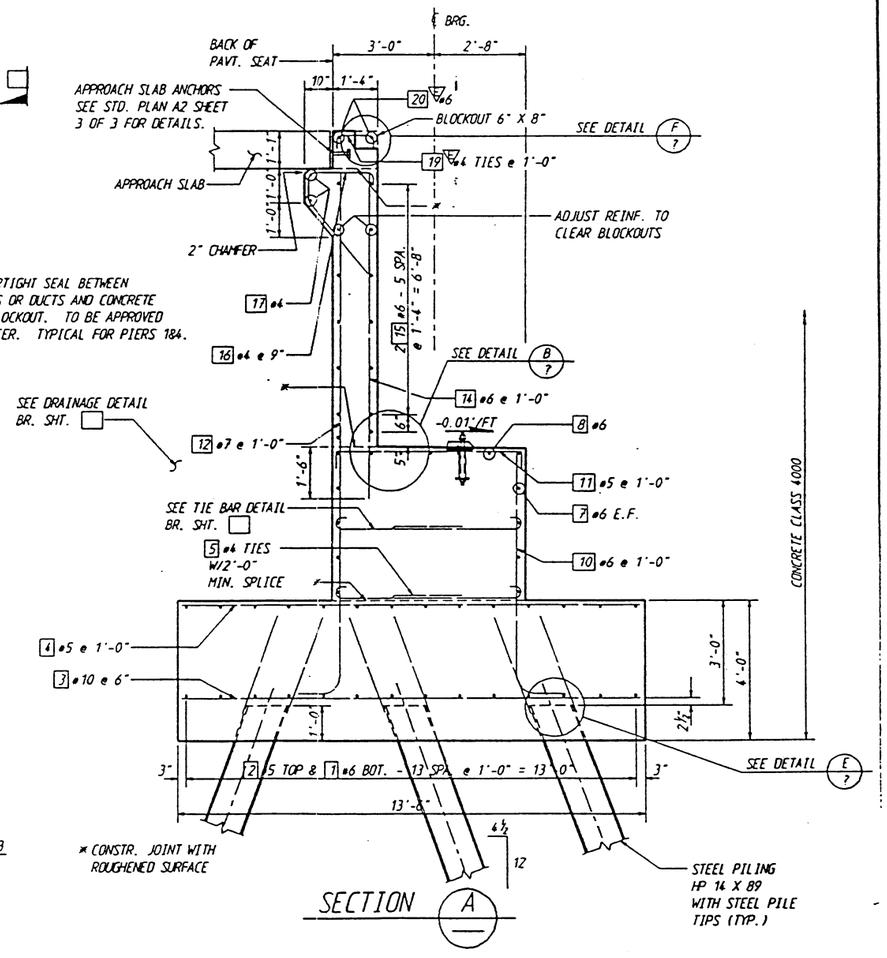

SECTION A

BR ^() JOB NO. ^() SHEET ^()

Bridge Design Engr.					REGION NO.	STATE	FED. AID PROJ. NO.	SHEET NO.	TOTAL SHEETS
Supervisor					10	WASH.			
Designed By ^()					JOB NUMBER				
Checked By ^()									
Detailed By ^()									
Bridge Projects Engr.									
Prelim. Plan By									
Architect/Specialist	DATE	REVISION	BY	APP'D					

BRIDGE AND STRUCTURES

ALLAN H. WALLEY — STATE OF WASHINGTON — REGISTERED PROFESSIONAL ENGINEER — EXPIRES 12/15/93

COLD_LKROOT:\000000.FGB\PIER1.FGB:1 09-JUN-92

Washington State Department of Transportation

Figure 1.2a

PIER 1

BRIDGE SHEET NO. ^()

SHEET

OF SHEETS

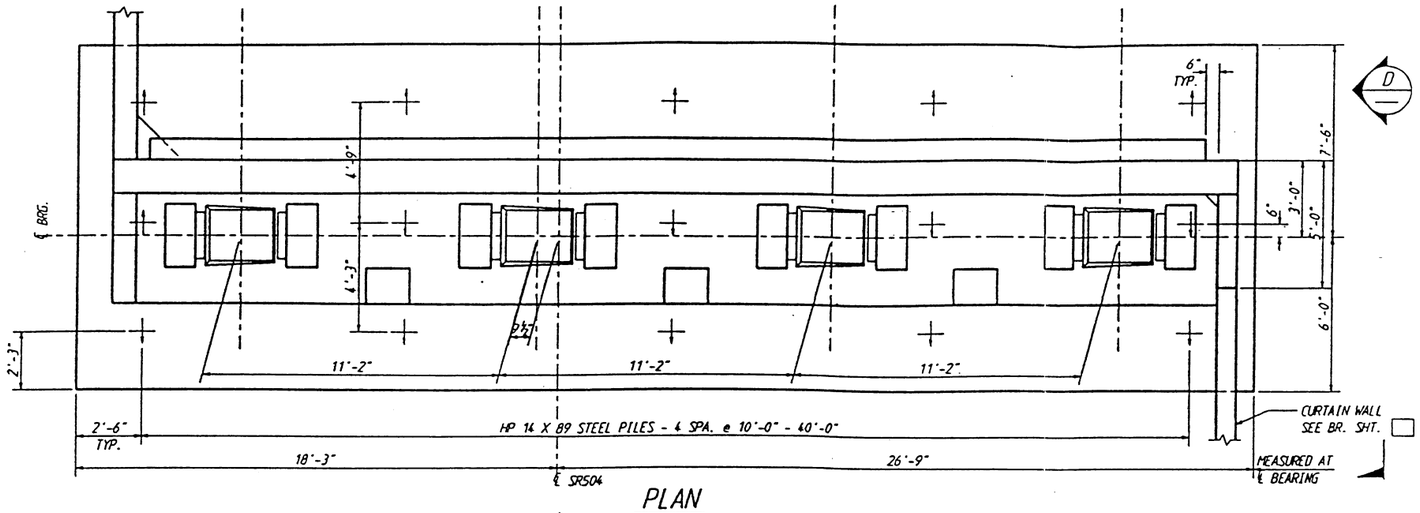

PLAN

DENOTES PILE AND DIRECTION OF 4½ 12 BATTER.

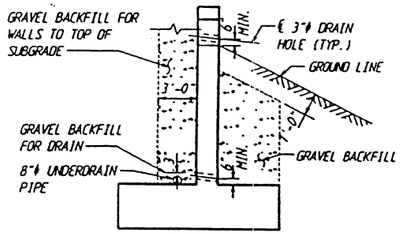

DRAINAGE DETAIL

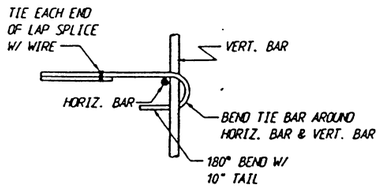

TIE BAR DETAIL

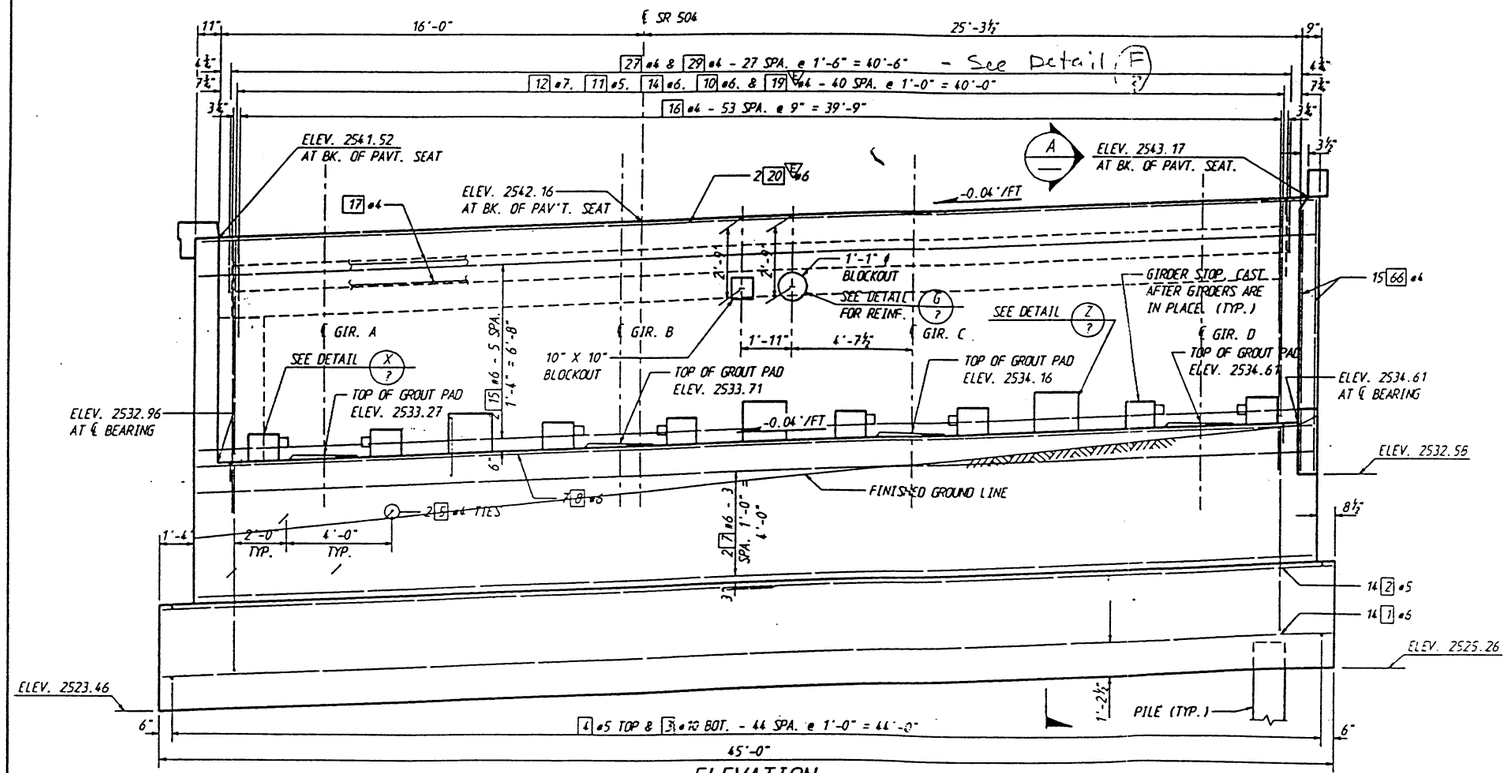

ELEVATION

SHOWN LOOKING AHEAD ON STATIONING

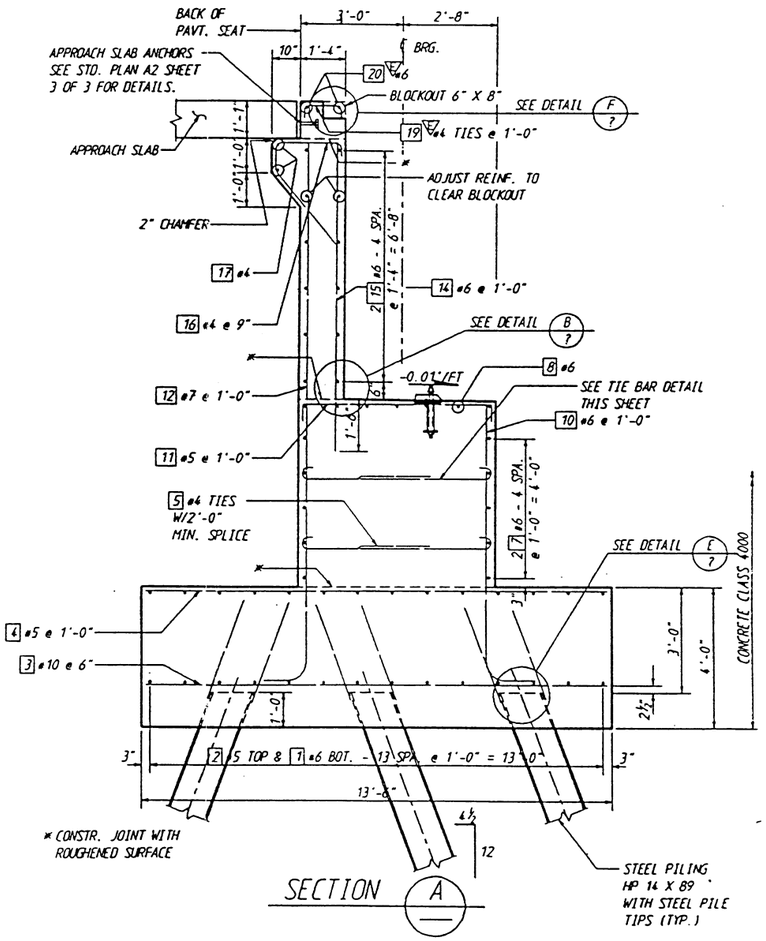

SECTION A

Bridge Design Engr.					DESIGN OC	STATE	FED. AID PROJ. NO	SHEET NO.	TOTAL SHEETS
Supervisor					10	WASH.			
Designed By ^()					JOB NUMBER				
Checked By ^()									
Detailed By ^()									
Bridge Projects Engr.									
Prelim. Plan By									
Architect/Specialist	DATE	REVISION	BY	APP'D					

BRIDGE AND STRUCTURES

ALLAN H. WALLEY — STATE OF WASHINGTON — REGISTERED PROFESSIONAL ENGINEER — EXPIRES 12/15/93

COLD_LKFOOT:\000000.FGB\PIER4.FGB:1 09-JUN-92

Washington State Department of Transportation

Figure 1.2b

PIER 4

SHEET NO. ^() OF SHEETS

SR ^() JOB NO. ^() SHEET ^()

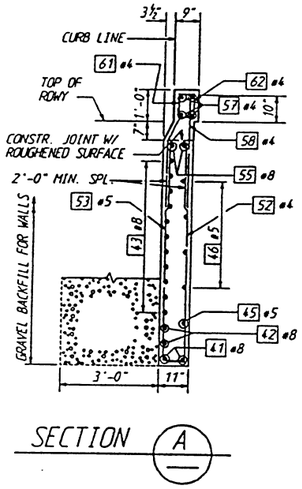

SECTION A

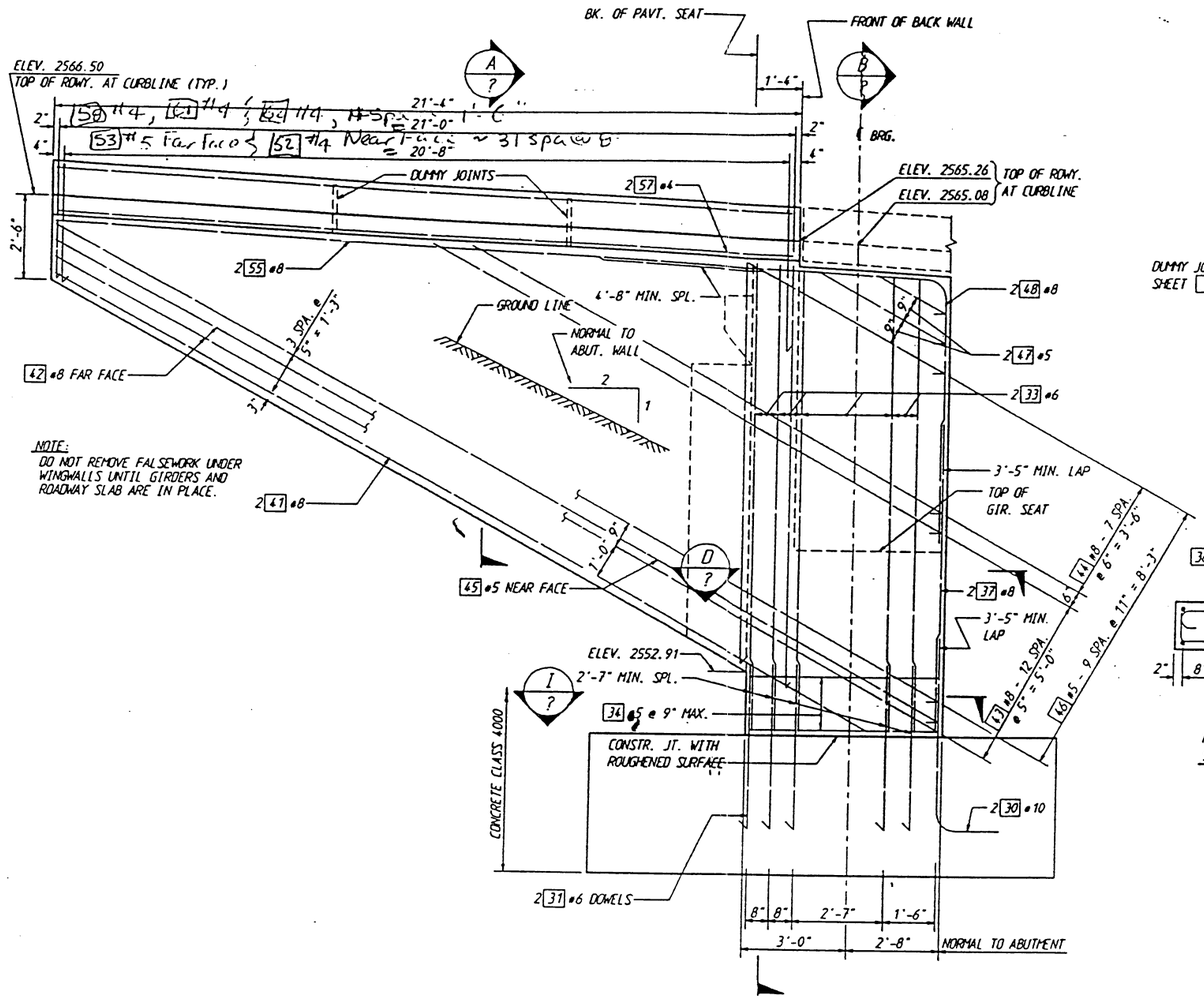

WINGWALL OUTSIDE ELEVATION
PIER 1

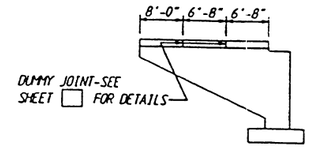

ELEVATION

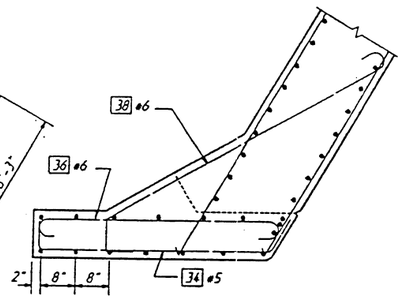

SECTION I
FOR REINF. NOT SHOWN SEE DETAIL D

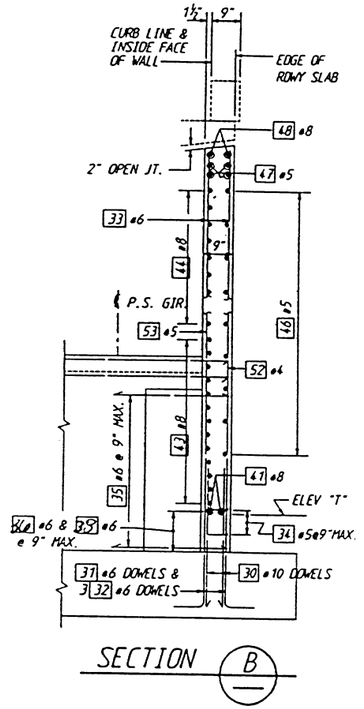

SECTION B

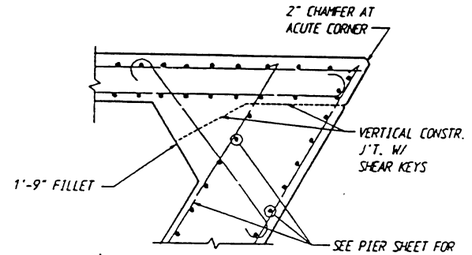

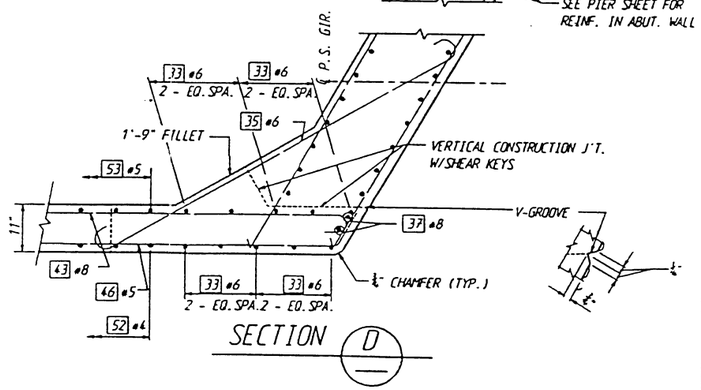

SECTION D

BR ^() JOB NO. ^() SHEET ^()

Bridge Design Engr.					REGION NO.	STATE	FED. AID PROJ. NO.	SHEET NO.	TOTAL SHEETS
Supervisor					10	WASH.			
Designed By ^()					JOB NUMBER				
Checked By ^()									
Detailed By ^()									
Bridge Projects Engr.									
Prelim. Plan By									
Architect/Specialist	DATE	REVISION	BY	APP'D					

BRIDGE AND STRUCTURES

ALLAN H. WALLEY — STATE OF WASHINGTON — REGISTERED PROFESSIONAL ENGINEER — EXPIRES 12/15/93

COLO_LKROOT:(000000.FGB)WMP1.FGB:1 08-JUN-92

Washington State Department of Transportation

Figure 1.3a

PIER 1 WINGWALL

BRIDGE SHEET ^()

SHEET OF SHEETS

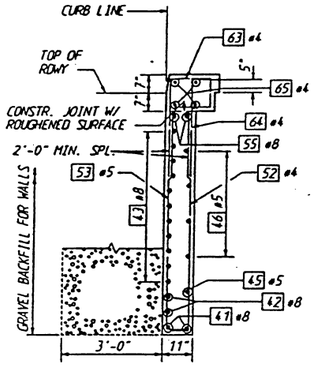

SECTION A

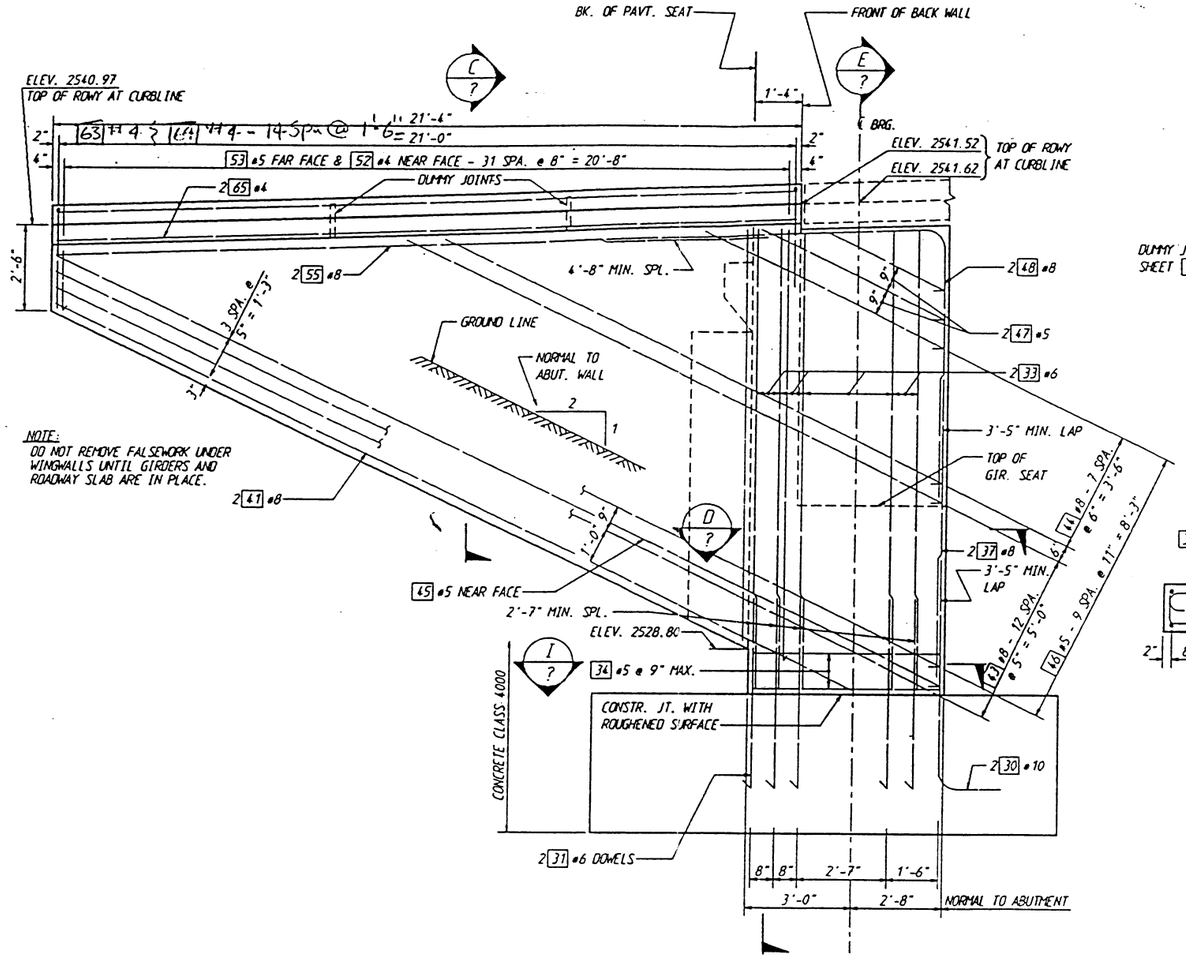

WINGWALL OUTSIDE ELEVATION
PIER 4

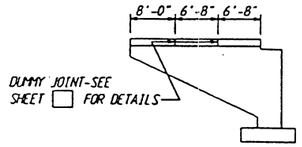

ELEVATION

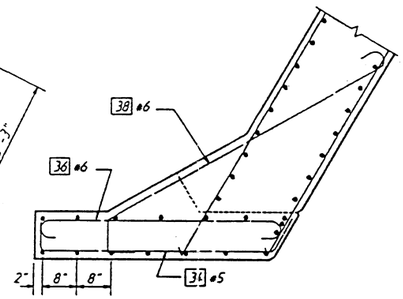

SECTION I
FOR REINF. NOT SHOWN SEE DETAIL D

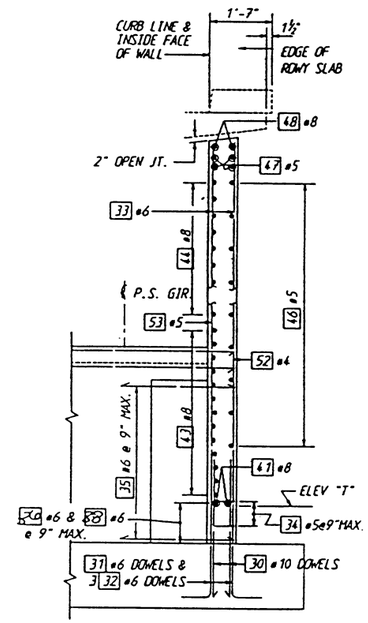

SECTION B

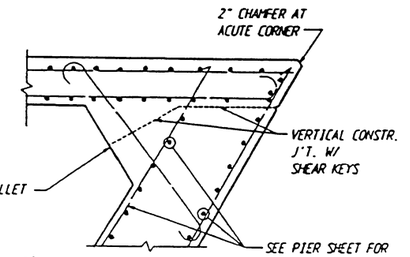

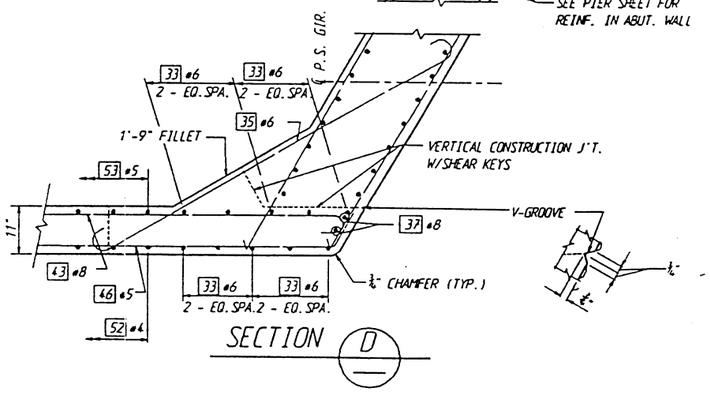

SECTION D

SR ^() JOB NO. ^() SHEET ^()

					REGION NO	STATE	FED. AID PROJ. NO	SHEET NO	TOTAL SHEETS
Bridge Design Engr.					10	WASH.			
Supervisor					JOB NUMBER				
Designed By ^()									
Checked By ^()									
Detailed By ^()									
Bridge Projects Engr.									
Prelim. Plan By									
Architect/Specialist	DATE	REVISION	BY	APP'D					

BRIDGE AND STRUCTURES

ALLAN H. WALLEY STATE OF WASHINGTON 16540 REGISTERED PROFESSIONAL ENGINEER EXPIRES 12/15/93

COLO_1:KROOT:\G00000.FGB\WMP4.FGB:1 08-JUN-92

Washington State Department of Transportation

Figure 1.3b

PIER 4 WINGWALL

BRIDGE SHEET NO ^()

SHEET ∝

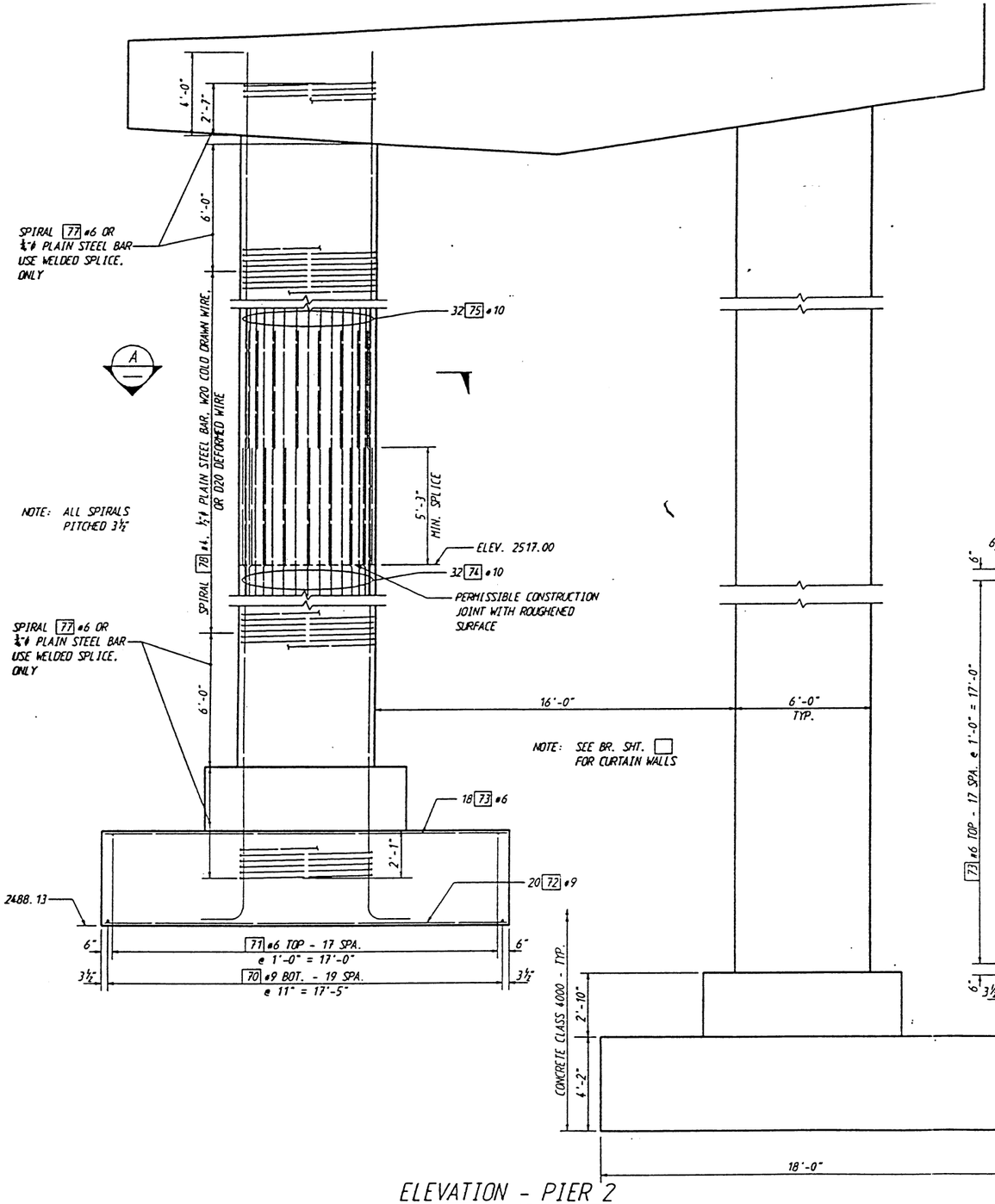

ELEVATION - PIER 2

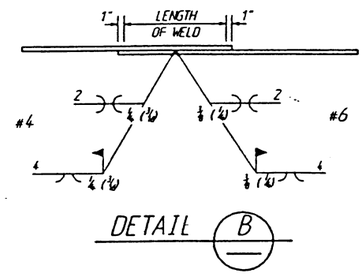

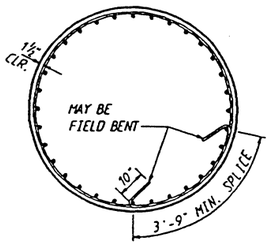

HOOKS SHALL BE PLACED TO AVOID VERTICAL REINFORCEMENT.
NOTE: FOR WELDED SPLICE ALTERNATE SEE DETAIL B

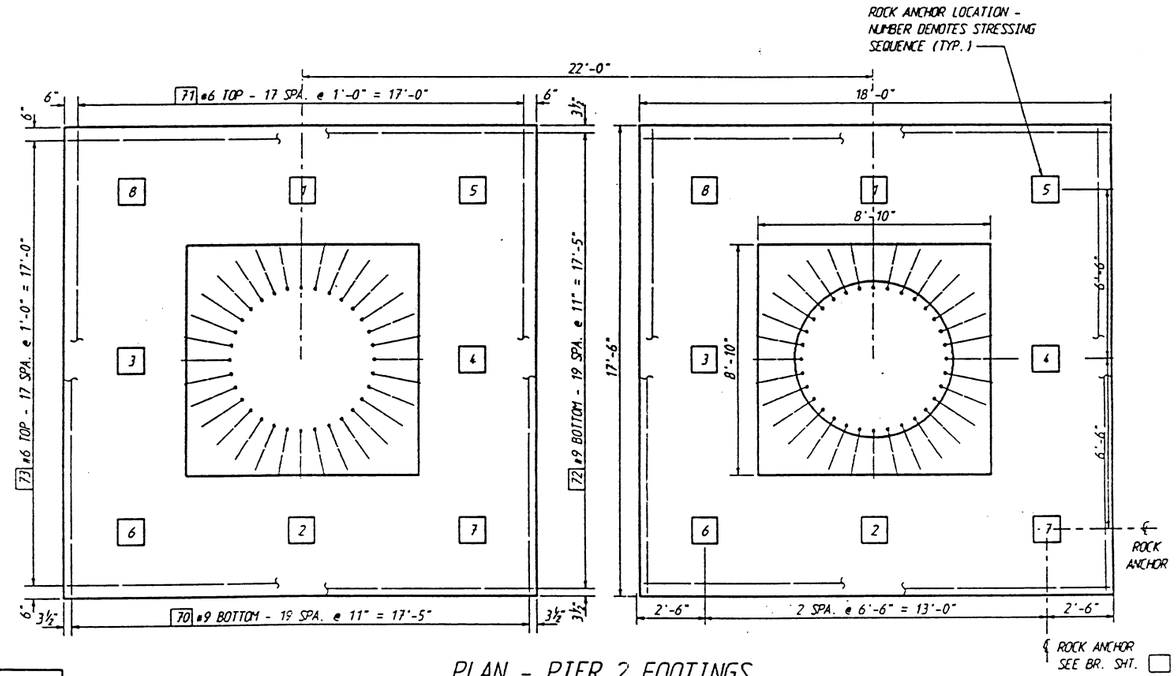

PLAN - PIER 2 FOOTINGS

SR ^() JOB NO. ^() SHEET ^()

Bridge Design Engr.					REGION NO.	STATE	FED. AID PROJ. NO.	SHEET NO.	TOTAL SHEETS	BRIDGE AND STRUCTURES
Supervisor					10	WASH.				
Designed By ^()					JOB NUMBER					
Checked By ^()										
Detailed By ^()										
Bridge Projects Engr.										
Prelim. Plan By										
Architect/Specialist	DATE	REVISION		SY	APP'D					

ALLAN H. MALLEY — STATE OF WASHINGTON — REGISTERED PROFESSIONAL ENGINEER — EXPIRES 12/15/93

COLO_LKROOT:(FGB)PIER2_COLUMN.FGB;1 05-JUN-92

Washington State Department of Transportation

Figure 1.4a

PIER 2

BRIDGE SHEET NO. ^() OF SHEETS

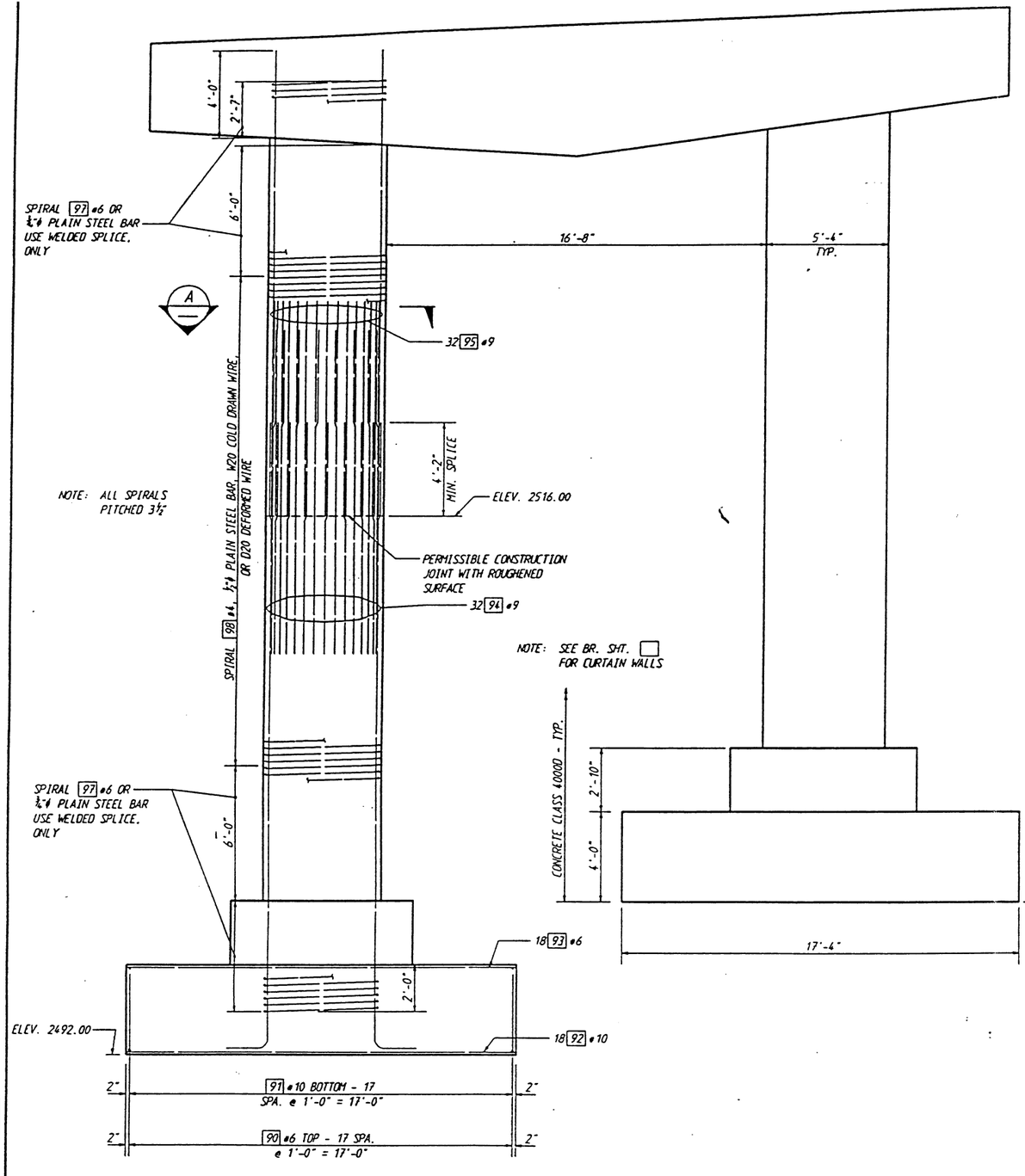

ELEVATION - PIER 3

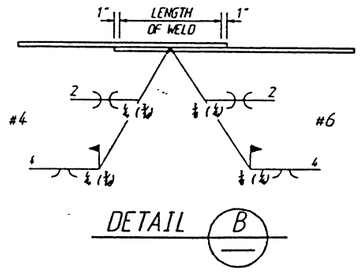

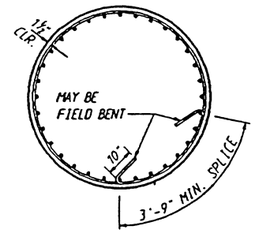

HOOKS SHALL BE PLACED TO AVOID VERTICAL REINFORCEMENT.
NOTE: FOR WELDED SPLICE ALTERNATE SEE DETAIL B

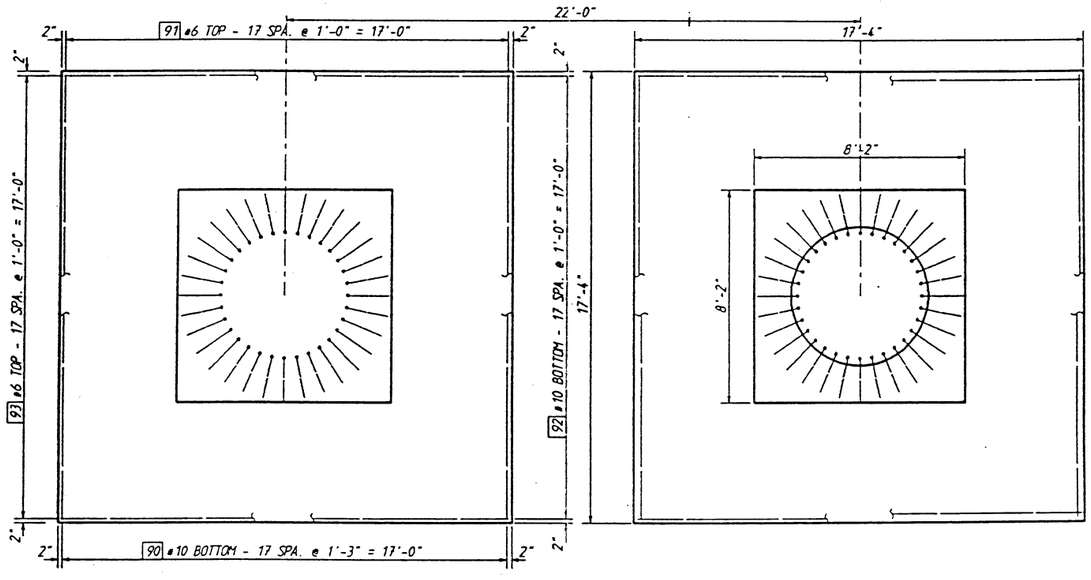

PLAN - PIER 3 FOOTINGS

SR ^() JOB NO. ^() SHEET ^()

					REGION NO.	STATE	FED. AID PROJ. NO.	SHEET NO.	TOTAL SHEETS
Bridge Design Engr.					10	WASH.			
Supervisor									
Designed By ^()					JOB NUMBER				
Checked By ^()									
Detailed By ^()									
Bridge Projects Engr.									
Prelim. Plan By									
Architect/Specialist	DATE	REVISION	BY	APP'D					

BRIDGE AND STRUCTURES

ALLAN H. MALLEY — STATE OF WASHINGTON — REGISTERED PROFESSIONAL ENGINEER — EXPIRES 12/15/93

COLD_1:\KROOT:\FGB\PIER3_COLUMN.FGB:1 08-JUN-92

Washington State Department of Transportation

Figure 1.4b

PIER 3

BRIDGE SHEET NO. ^()
SHEET OF SHEETS

1.0 DESCRIPTION OF BRIDGE AND FOUNDATION SOILS

The Coldwater Creek Bridge is a 3-span, slightly-curved, composite-steel, plate-girder bridge approximately 500 feet long (Figure 1.1). The seat-type (or L) abutments (Piers 1 and 4) at the ends of the bridge (Figures 1.2a and 1.2b) are supported by three rows of battered H piles (HP 14 x 89 - 5 per row) which penetrate through a medium dense sandy gravel and terminate in Andesite bedrock. The piles are about 30 feet long and are embedded one foot in a concrete pile cap, 45' long x 13'6" wide x 4' thick, which supports the seat-type abutment. A construction joint with a roughened surface separates the cap from the abutment seat. The concrete abutment walls are 1'5" thick and are approximately 10 feet high. A construction joint with a roughened surface separates the wall from the seat. Continuous reinforcing steel bars pass through this construction joint and the joint between the seat and the cap.

Triangular-shaped concrete wingwalls, approximately 20 feet long, are attached to each side of the abutments (Figures 1.3a and 1.3b). The soil behind the abutment-wingwall system is predominantly stiff fill.

Each of the two intermediate bents (Piers 2 and 3) consists of a reinforced concrete cross beam supporting the girders (Figures 1.4a and 1.4b). This cross beam in turn is supported by two cylindrical reinforced concrete columns, six feet in diameter. Each column is supported by a square concrete footing that bears on the Andesite bedrock. The dimensions of the Pier 2 and Pier 3 footings are 18'x18'x4'-2" thick and 17'-4" x 17'-4" x 4' thick, respectively.

2.0 SEISMIC DESIGN PARAMETERS

The ground acceleration coefficient for the seismic design of the Coldwater Creek Bridge was 0.55. The appropriate soil category was Soil Type I, which is bedrock or shallow stiff soil over bedrock. The ATC-6, 5% damped response spectrum (Figure 2.1) for this soil type was normalized to 0.55 g and was used in the dynamic response analysis of the bridge by WSDOT. This same spectrum will be used in the example problem presented herein for the bridge. The spectrum will be modified where appropriate to account for the 7½ % damping recommended for those modes of vibration where soil-structure interaction is significant.

3.0 SOIL PROPERTIES

The soil parameters provided by WSDOT for the fill and sandy gravel soil layers are:

γ = total density in pcf
c = cohesion in psf
ϕ = friction angle in degrees
k = modulus of subgrade reaction in pci
G = low-strain shear modulus in psf or ksf
ν = Poisson's Ratio

Values of G, ν, and γ were also provided to characterize the Andesite bedrock.

Because the behavior of soil is nonlinear during strong shaking, simple procedures were implemented to approximately account for the effect of this nonlinearity on the computation of the abutment and pier foundation stiffnesses. These procedures are described below, and they are illustrated in the subsequent sections dealing with the foundation stiffness computations.

Normalized 5%
Damped Response Spectrum

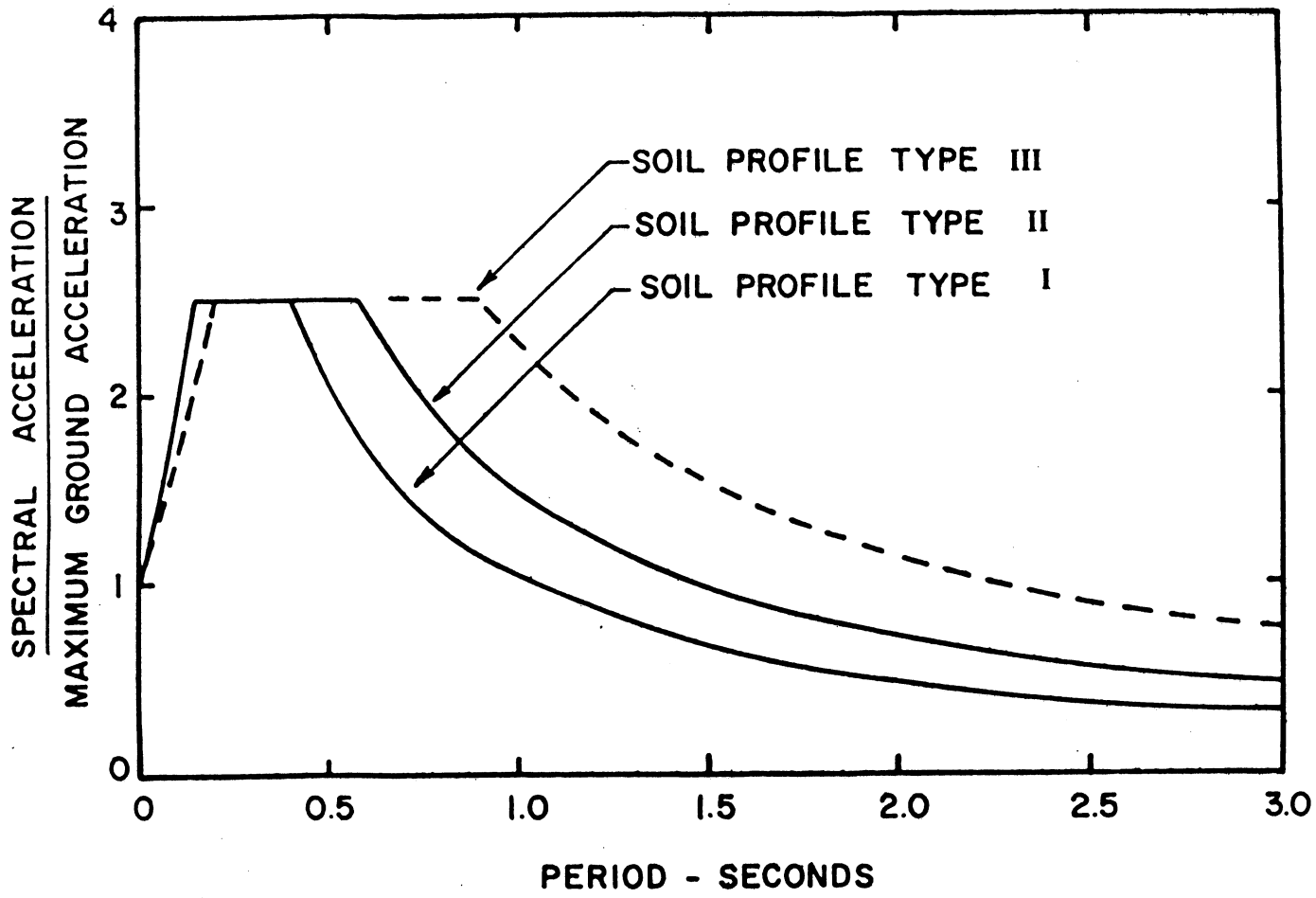

Reference: ATC-6 (1978)

Figure 2.1

At locations where the ground acceleration coefficient Z is less than 0.2, then modifications to the low-strain elastic soil properties or the load-deflection curves for the piles (i.e. t-z, Q-z, and p-y curves) are not recommended.

However, at locations of high ground acceleration where $Z \geq 0.2$, then the following modifications are recommended in the FHWA and Novak methods. For footings and abutment walls, reduce the low-strain G value by 50%. Implement the same reduction in G for the pile-head stiffness calculation using the Novak method. For the calculation of the pile-head stiffness following the FHWA approach, compute the t-z, Q-z, and p-y curves using the low strain G or k values and reduce the resulting t, z, and p amplitudes by 50%

The above recommendations are suitable for locations where soil liquefaction is not anticipated. If soil liquefaction is expected for a given Z value, then site-specific studies are recommended to determine the extent of the liquefaction before estimating soils properties.

4.0 PIER 1 STIFFNESS CALCULATION - FHWA METHOD

In this section the calculation of foundation stiffnesses using the FHWA (1986) method is presented in detail for Piers 1 and 2 of the Coldwater Creek Bridge. (The use of the Novak method is illustrated in Section 5.0). Because Piers 3 and 4 are similar to Piers 2 and 1, respectively, only the final results of the stiffness calculations will be presented for Piers 3 and 4.

A side-elevation view of the abutment and the soil-property profile at Pier 1 (NW Abutment) is shown in Figure 4.1. The basic approach to compute the foundation stiffness matrix at this pier is to first compute the pile-group stiffness, abutment-footing (pile cap) stiffness, and abutment-wall stiffness, and then combine these stiffnesses to

obtain the abutment stiffness matrix at a specified point on the abutment foundation. This point (Point O in Figure 4.1) is located on top of the 4-foot thick footing at its geometric center.

4.1 PILE-STIFFNESS CALCULATION

Individual pile-head stiffnesses are first computed at the point where the piles enter the abutment footing. Several steps are involved in this calculation. First, the appropriate length parameters of the HP 14 x 89 piles are estimated (Section 4.1.1) and used in the calculation of the so-called t-z (vertical load - vertical deflection), Q-z (tip load - tip deflection), and p-y (lateral load - lateral deflection) curves.

The t-z and p-y curves specify the resistances provided by the soil bearing against the pile subjected to vertical and axial loads, and can be visualized as the force-deformation relationships of springs attached to small incremental pile segments comprising the pile. The Q-z curve is simply the force-deflection relationship of the pile tip and end-bearing soils. The calculation of the t-z and Q-z curves is illustrated in Sections 4.1.2 and 4.1.3, respectively; the p-y curve calculation is illustrated in Section 4.1.4. These curves are input to the computer program BMCOL-76 (Matlock et al, 1981) , which computes the load-deflection curves of the pile head under either the pinned-head or fixed-head condition for pile-head fixity. For this example problem, a pinned connection was assumed. The input to the BMCOL-76 program is described in Section 4.1.5 and the output is presented in Section 4.1.6. It should be noted that this program is similar to the COM624 program that has been used by WSDOT.

Because t-z, Q-z, and p-y curves are nonlinear, the pile-head load-deflection curves are also nonlinear. The procedure to compute the pile-head stiffnesses from the pile-head load-deflection curves is described in Section 4.1.7. This procedure approximately considers the nonlinear soil behavior due to strong ground shaking.

Pier 1 Abutment Profile

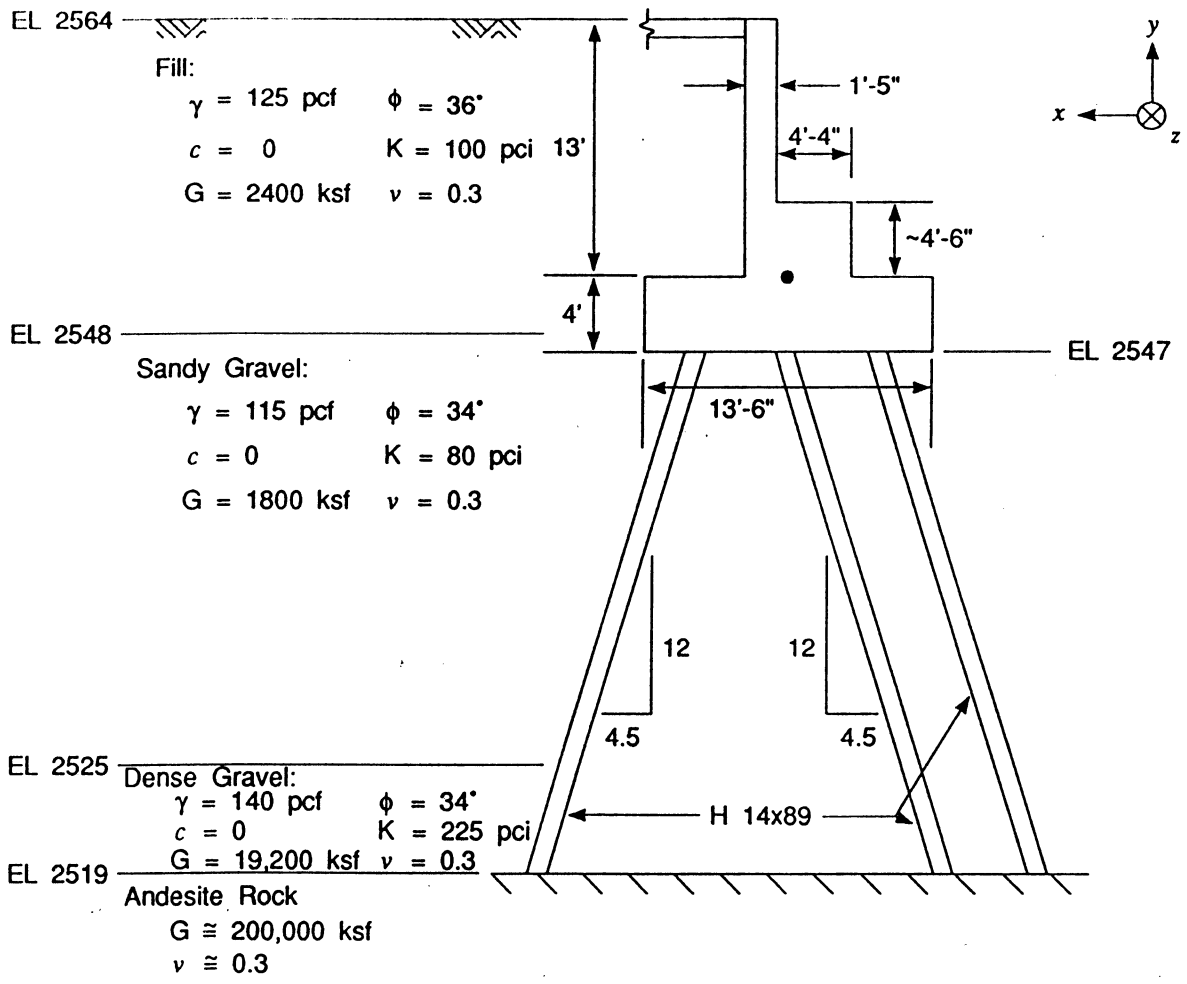

Water Table at EL 2495

Figure 4.1

The final step is to compute the pile-group stiffness matrix by using the GPILE program. Per the recommendation in the Task 1 report (Appendix A), group effects are neglected. The preparation of the input file and listing of the output from the GPILE program is presented in Section 4.1.8. The resulting pile-group stiffness matrix is listed in Section 4.1.9.

4.1.1 Estimation of H-pile Parameters

The cross-sectional dimensions and properties of the HP 14 x 89 pile are provided in Table 4.1, taken from the AISC Manual. In the figure of the H section shown in this table, the symbols d and b_f demote the depth of the section and the width of the flange, respectively. For the calculation of the t-z and Q-z curves in the next section, the pile perimeter, s, is the relevant parameter, and it is defined as the perimeter of a circumscribed rectangle of length, d, and width, b_f. Thus, for the HP 14 x 89 pile (Table 4.1),

$$s = 2(d + b_f) = 2(13.83 \text{ in} + 14.695 \text{ in})$$

or $s = 57.05$ in.

For the calculation of the p-y curves, the dimension of the side of the circumscribed rectangle normal to the applied load is the proper length parameter. Thus, for loads normal to the web (i.e. loads parallel to x-x axis in the Table 4.1 figure), d = 13.83" is used as the length. For loads normal to the flange, b_f = 14.695" is used.

The cross-sectional area of the H pile from Table 4.1 is A = 26.1 in^2. The moments of inertia from Table 4.1 are I_{xx} = 904 in^4 and I_{yy} = 326 in^4. The Young's modulus of the steel H-pile is the standard value, E = 29 x 10^6 psi.

Thus, the axial (EA) and flexual (EI) rigidities are:

$EA = 7.569\ E\ 08\ lb$

$EI_{xx} = 2.622\ E\ 10\ lb\text{-}in^2$

$EI_{yy} = 9.454\ E\ 09\ lb\text{-}in^2$

The above information was used in the calculation of the t-z, Q-z, and p-y curves, and the load-deflection curves of the pile-head.

4.1.2 Computation of t-z Curves

4.1.2.1 General Procedure. The procedure for computing the t-z curve was adapted from information in Vijayvergiya (1977), Scott (1981), API-RP2A (1991), and NAVFAC (1986). The general formula relating the axial resistance (force) provided by the soil per unit pile length, t, and vertical pile deflection, z, is (Vijayvergiya, 1977).

$$t = t_{max} \tanh(z / z_{ref}) \tag{4.1}$$

where t_{max} is the maximum resistance and z_{ref} is a reference deflection. The form of this hyperbolic t-z curve is plotted in Figure 4.2. The parameters, t_{max} and z_{ref}, are computed from the following formulas:

$$t_{max} = f \cdot s \tag{4.2}$$

$$z_{ref} = f / \bar{k} \tag{4.3}$$

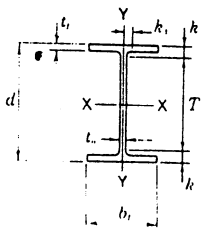

HP SHAPES
Dimensions

Designation	Area A	Depth d		Web Thickness t_w		$\frac{t_w}{2}$	Flange Width b_f		Flange Thickness t_f		Distance T	Distance k	Distance k_1
	In.^{2}	In.		In.		In.	In.		In.		In.	In.	In.
HP 14x117	34.4	14.21	14 1/4	0.805	13/16	7/16	14.885	14 7/8	0.805	13/16	11 1/4	1 1/2	1 1/16
x102	30.0	14.01	14	0.705	11/16	3/8	14.785	14 3/4	0.705	11/16	11 1/4	1 3/8	1
x 89	26.1	13.83	13 7/8	0.615	5/8	5/16	14.695	14 3/4	0.615	5/8	11 1/4	1 5/16	15/16
x 73	21.4	13.61	13 5/8	0.505	1/2	1/4	14.585	14 5/8	0.505	1/2	11 1/4	1 3/16	7/8
HP 13x100	29.4	13.15	13 1/8	0.765	3/4	3/8	13.205	13 1/4	0.765	3/4	10 1/4	1 7/16	1
x 87	25.5	12.95	13	0.665	11/16	3/8	13.105	13 1/8	0.665	11/16	10 1/4	1 3/8	15/16
x 73	21.6	12.75	12 3/4	0.565	9/16	5/16	13.005	13	0.565	9/16	10 1/4	1 1/4	15/16
x 60	17.5	12.54	12 1/2	0.460	7/16	1/4	12.900	12 7/8	0.460	7/16	10 1/4	1 1/8	7/8
HP 12x 84	24.6	12.28	12 1/4	0.685	11/16	3/8	12.295	12 1/4	0.685	11/16	9 1/2	1 3/8	1
x 74	21.8	12.13	12 1/8	0.605	5/8	5/16	12.215	12 1/4	0.610	5/8	9 1/2	1 5/16	15/16
x 63	18.4	11.94	12	0.515	1/2	1/4	12.125	12 1/8	0.515	1/2	9 1/2	1 1/4	7/8
x 53	15.5	11.78	11 3/4	0.435	7/16	1/4	12.045	12	0.435	7/16	9 1/2	1 1/8	7/8
HP 10x 57	16.8	9.99	10	0.565	9/16	5/16	10.225	10 1/4	0.565	9/16	7 5/8	1 3/16	13/16
x 42	12.4	9.70	9 3/4	0.415	7/16	1/4	10.075	10 1/8	0.420	7/16	7 5/8	1 1/16	3/4
HP 8x 36	10.6	8.02	8	0.445	7/16	1/4	8.155	8 1/8	0.445	7/16	6 1/8	15/16	5/8

HP SHAPES
Properties

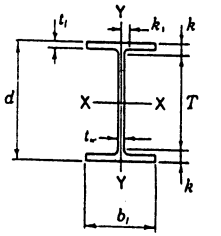

Nominal Wt. per Ft.	Compact Section Criteria $\frac{b_f}{2t_f}$	Compact Section Criteria F_y'	Compact Section Criteria $\frac{d}{t_w}$	Compact Section Criteria F_y'''	r_T	$\frac{d}{A_f}$	Elastic Properties Axis X-X I	Axis X-X S	Axis X-X r	Axis Y-Y I	Axis Y-Y S	Axis Y-Y r	Torsional constant J	Plastic Modulus Z_x	Plastic Modulus Z_y
Lb.		Ksi		Ksi	In.		In.^{4}	In.^{3}	In.	In.^{4}	In.^{3}	In.	In.^{4}	In.^{3}	In.^{3}
117	9.2	49.4	17.7	—	4.00	1.19	1220	172	5.96	443	59.5	3.59	8.02	194	91.4
102	10.5	38.4	19.9	—	3.97	1.34	1050	150	5.92	380	51.4	3.56	5.40	169	78.8
89	11.9	29.6	22.5	—	3.94	1.53	904	131	5.88	326	44.3	3.53	3.60	146	67.7
73	14.4	20.3	27.0	—	3.90	1.85	729	107	5.84	261	35.8	3.49	2.01	118	54.6
100	8.6	56.7	17.2	—	3.54	1.30	886	135	5.49	294	44.5	3.16	6.25	153	68.6
87	9.9	43.5	19.5	—	3.51	1.49	755	117	5.45	250	38.1	3.13	4.12	131	58.5
73	11.5	31.9	22.6	—	3.47	1.74	630	98.8	5.40	207	31.9	3.10	2.54	110	48.8
60	14.0	21.5	27.3	—	3.43	2.11	503	80.3	5.36	165	25.5	3.07	1.39	89.0	39.0
84	9.0	52.5	17.9	—	3.29	1.46	650	106	5.14	213	34.6	2.94	4.24	120	53.2
74	10.0	42.1	20.0	—	3.26	1.63	569	93.8	5.11	186	30.4	2.92	2.98	105	46.6
63	11.8	30.5	23.2	—	3.23	1.91	472	79.1	5.06	153	25.3	2.88	1.83	88.3	38.7
53	13.8	22.0	27.1	—	3.20	2.25	393	66.8	5.03	127	21.1	2.86	1.12	74.0	32.2
57	9.0	51.6	17.7	—	2.74	1.73	294	58.8	4.18	101	19.7	2.45	1.97	66.5	30.3
42	12.0	29.4	23.4	—	2.69	2.29	210	43.4	4.13	71.7	14.2	2.41	0.81	48.3	21.8
36	9.2	50.3	18.0	—	2.18	2.21	119	29.8	3.36	40.3	9.88	1.95	0.77	33.6	15.2

Thus, the axial (EA) and flexual (EI) rigidities are:

$EA = 7.569\ E\ 08\ lb$

$EI_{xx} = 2.622\ E\ 10\ lb\text{-}in^2$

$EI_{yy} = 9.454\ E\ 09\ lb\text{-}in^2$

The above information was used in the calculation of the t-z, Q-z, and p-y curves, and the load-deflection curves of the pile-head.

4.1.2 Computation of t-z Curves

4.1.2.1 General Procedure. The procedure for computing the t-z curves was adapated from information in Vijayvergiya (1977), Scott (1981), API-RP2A (1991), and NAVFAC (1986). The general formula relating the axial resistance (force) provided by the soil per unit pile length, t, and vertical pile deflection, z, is (Vijayvergiya, 1977):

$$t = t_{max}\tanh(z/z_{ref}) \tag{4.1}$$

where t_{max} is the maximum resistance and z_{ref} is a reference deflection. The form of this hyperbolic t-z curve is plotted in Figure 4.2 The parameters, t_{max} and z_{ref}, are computed from the following formulas:

$$t_{max} = f \cdot s \tag{4.2}$$

$$z_{ref} = f / \bar{k} \tag{4.3}$$

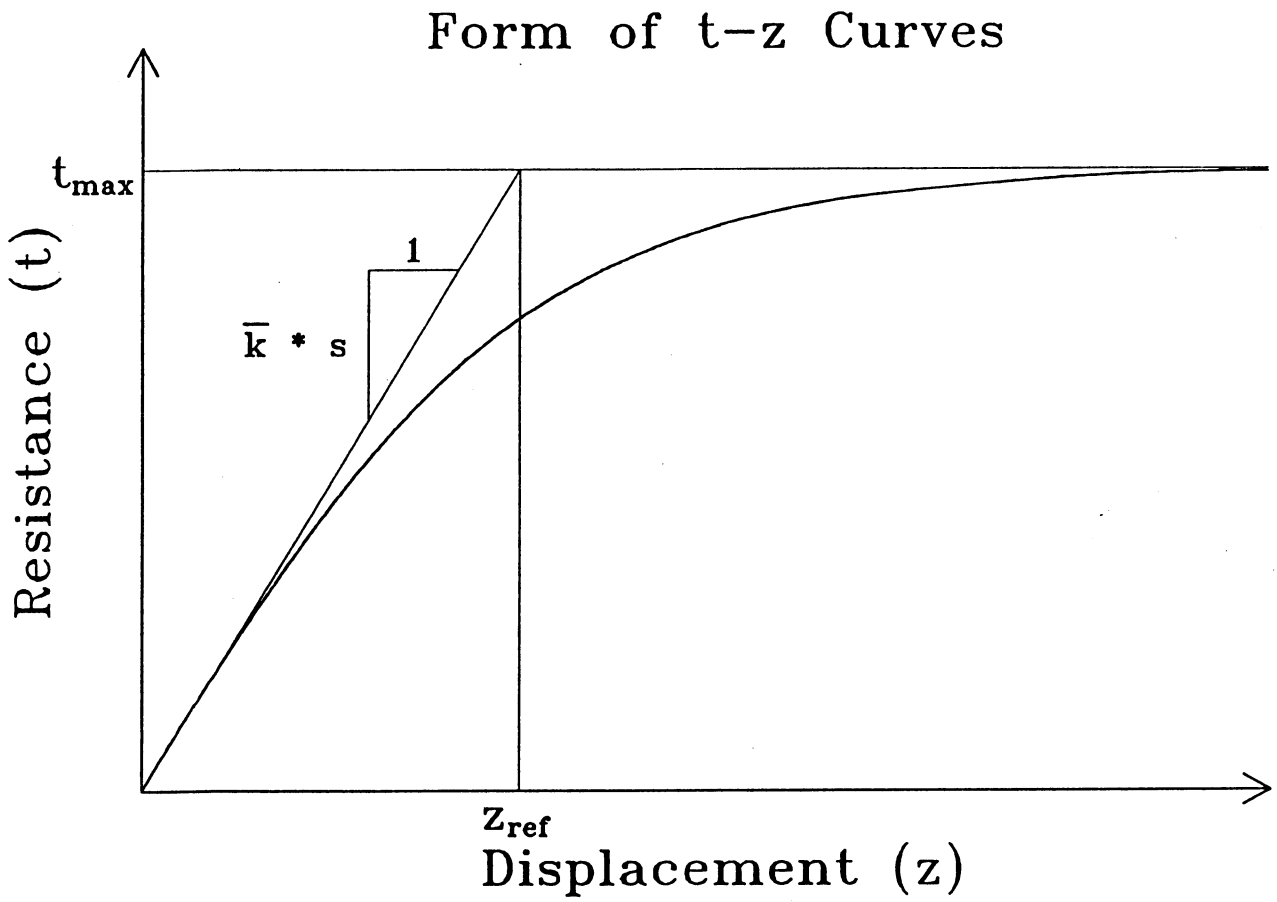
Form of t–z Curves
t_{max}
1
$\bar{k}$ * s
Resistance (t)
z_{ref}
Displacement (z)

Figure 4.2

where f is the pile-shaft friction in units of stress, s is the equivalent pile perimeter (see Section 4.1.1), and $\bar{k}$ is a stiffness parameter given by (Scott, 1981),

$$\bar{k} = G\pi/2s \tag{4.4}$$

In Equation (4.4), G is the soil shear modulus. As shown in Figure 4.2, the initial slope of the t-z curve is $\bar{k} \cdot s$.

The pile-shaft friction is computed from the following formula in API RP2A (1991):

$$f = \begin{cases} c & (\textit{cohesive soils}) \\ Kp_o \tan\delta & (\textit{cohesionless soils}) \end{cases} \tag{4.5}$$

where c = undrained shear strength or cohesion of soil,
K = coefficient of lateral earth pressure (ratio of horizontal to vertical normal effective stress),
p_o = effective overburden pressure at point in question, and
δ = friction angle between soil and pile wall.

According to API RP2A (1991),

$$K = \begin{cases} 0.8 & (\textit{open-ended piles}) \\ 1.0 & (\textit{closed-ended or plugged piles}) \end{cases} \tag{4.6}$$

Although values of δ are suggested in API RP2A, the following values are preferred (NAVFAC, 1986)

$$\delta = \begin{cases} 20° \text{ (steel piles)} \\ 0.75\phi \text{ (concrete and timber piles)} \end{cases} \quad (4.7)$$

where ϕ is the friction angle (in degrees) of the cohesionless soil.

4.1.2.2 Application to Coldwater Creek Bridge Abutment Piles. The calculation of the t-z curves for input to the BMCOL-76 program is described below for piles supporting the NW abutment (Pier 1). The pile batter is not considered in these calculations; the piles are assumed to be vertical. However, pile batter is considered in the calculation of the pile-group stiffnesses (Section 4.1.8).

Because the soil surrounding the piles is cohesionless, the relevant soil parameters are p_o, ϕ, and G. The values of these parameters are shown in Figure 4.3, as taken from Figure 4.1. The input to BMCOL-76 only requires that the t-z curves be computed at the top and bottom of each soil layer (i.e. at Elevations A, B, C, and D in Figure 4.3). The calculation of the t-z curve is illustrated at Elevation A = 2547 ft (at base of the pile cap). The following equations and figures are used:

Eqn. (4.5): $f = Kp_o \tan \delta$ (cohesionless soil - sandy gravel)
Eqn. (4.6): K = 0.8 (H pile is open-ended)
Figures 4.1 & 4.3: p_o = 2.12 ksf (= 125 pcf x 16 ft + 115 pcf x 1 ft), 1k = 1,000 lb
Eqn. (4.7): δ = 20° (H pile is steel)
Therefore, f = 0.8(2.12 ksf) tan (20°)
= 0.62 ksf

From Section 4.1.1, s = 57.06 in = 4.76 ft; use this value to compute t_{max}.

Parameters for Computation of T-Z Curves at Elevations A, B, C, and D

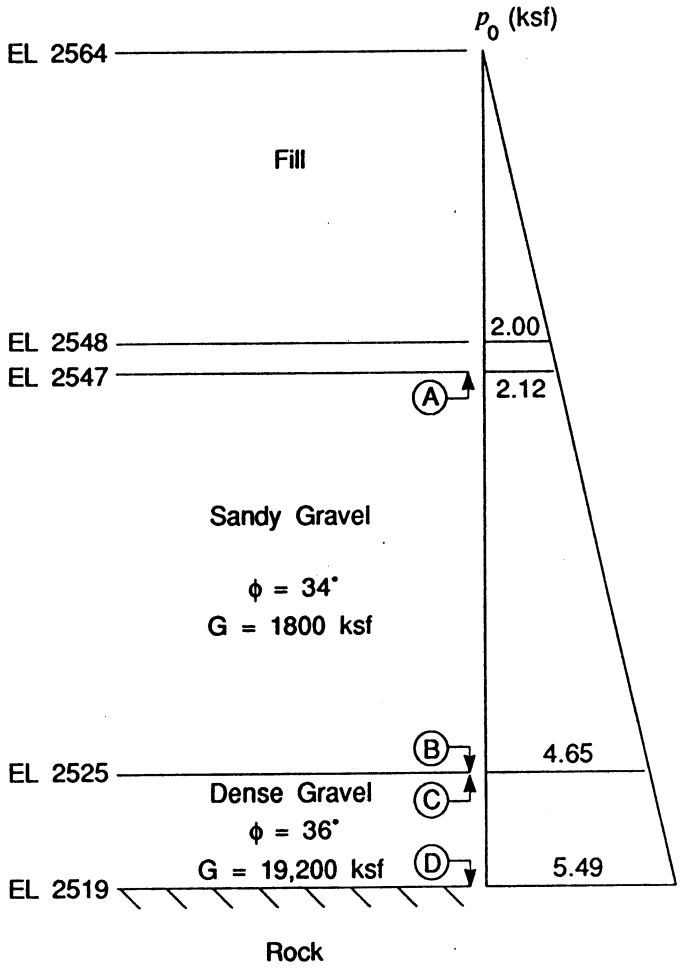

Notes

p_0 Effective Overburden Pressure

ϕ Friction Angle

G Low Strain Shear Modulus

Figure 4.3

Eqn. (4.2): $t_{max} = f \cdot s$

$= (0.62 \text{ ksf})(4.76 \text{ ft})$

$= 2.95 \text{ kpf}$

Compute the length parameter, z_{ref}:

Eqn. (4.3): $z_{ref} = f/\bar{k}$

Eqn. (4.4): $\bar{k} = G\pi/2s$

Figures 4.1&4.3: $G = 1800 \; ksf$

Therefore, $z_{ref} = \dfrac{(0.62 \; ksf)(2)(4.76 \; ft)}{(1800 \; ksf)(3.14)} = 0.00104 \; ft = 0.0125 \; in$

The above calculation pertains to ground acceleration coefficients, Z < 0.2. For this example, Z = 0.55. Therefore, reduce t_{max} in Equation (4.1) by 50% per the recommendation in Section 3.0, and construct the t-z curve. Thus,

$$t = t_{max} \tanh(z/z_{ref}) = \left(\frac{2.95 \; kpf}{2}\right)\tanh\left(\frac{z}{0.0125 \; in}\right)$$

A plot of this t-z curve is shown in Figure 4.4, where the units of t_{max} are lb/in (rather than kpf as in the above equation).

A spread sheet containing the values of 10 points on the t-z curves at seven depths within the soil profile is provided in Table 4.2. The t-z curves for the last four depths in this table were input to the BMCOL-76 program; these depths correspond to Points A, B, C, and D in Figure 4.3.

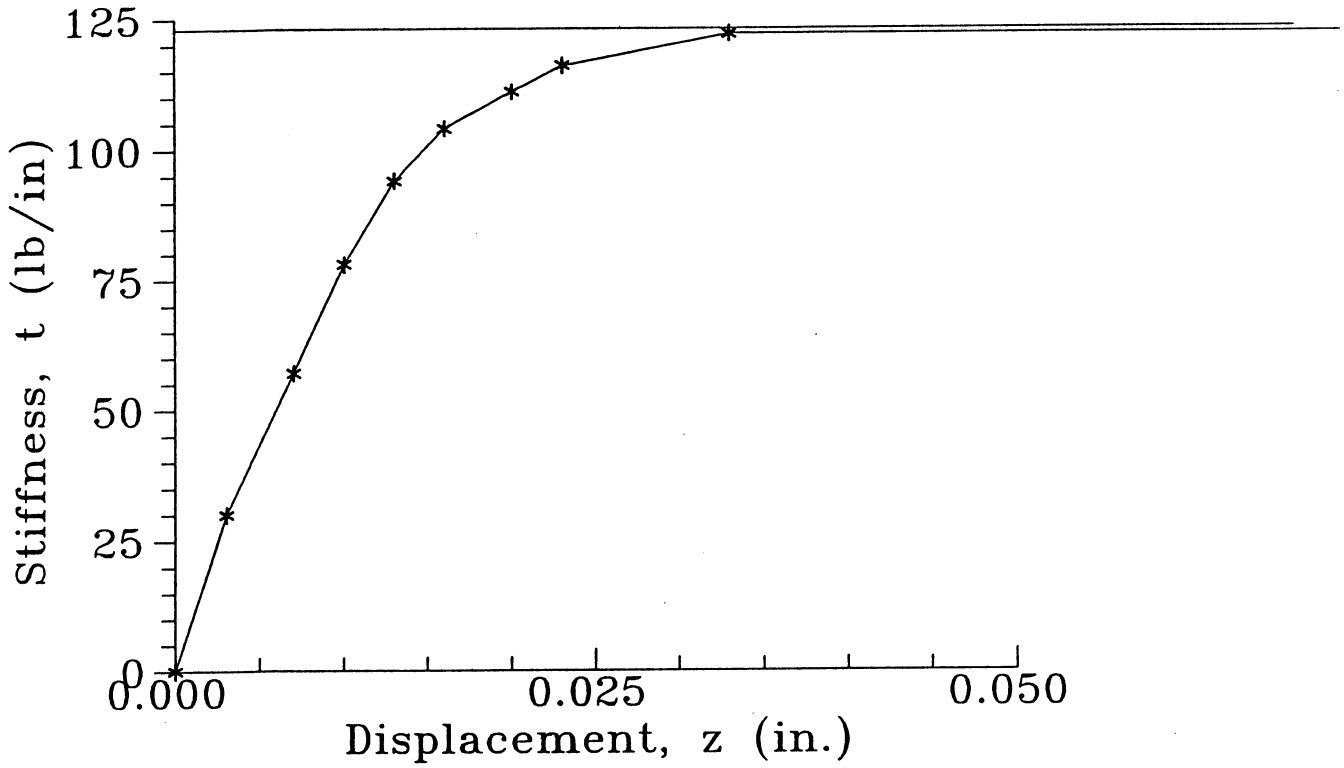
125
100
75
50
25
0
Stiffness, t (lb/in)
0.000
0.025
0.050
Displacement, z (in.)

Figure 4.4

T-Z CURVES

Bridge: Coldwater Creek Overcrossing Pier 1 : high strain case

Ground Surface Elevation:	2564			
Depth to water table:	69	ft	Elev: 2495	ft
Average Pile Perimeter:	57.06	in		
Pile Tip Area:	203.3	in²		
Pile Type:	S	T=Timber,C=Concrete,S=Steel		
	O	O= Open Ended, D=Displacement		

SOIL	DEPTH	ELEV.	GAMMA	PHI	c	G	k	Po	Delta	f	f	Ks	Tmax	Zref
	ft	ft	γ	ϕ	ksf	psf	API RP2A	ksf	δ	ksf	psi	pci	lb/in	in
SAND	0	2564	125	36	-	2.40E+06	0.8	0.00	20	0.00	0.00	459	0	0.000
SAND	16	2548	125	36	-	2.40E+06	0.8	2.00	20	0.58	4.04	459	115	0.009
SAND	16	2548	115	34	-	1.80E+06	0.8	2.00	20	0.58	4.04	344	115	0.012
SAND	17	2547	115	34	-	1.80E+06	0.8	2.12	20	0.62	4.28	344	122	0.012
SAND	39	2525	115	34	-	1.80E+06	0.8	4.65	20	1.35	9.39	344	268	0.027
SAND	39	2525	140	34	-	1.92E+07	0.8	4.65	20	1.35	9.39	3671	268	0.003
SAND	45	2519	140	34	-	1.92E+07	0.8	5.49	20	1.60	11.09	3671	316	0.003

	DEPTH	ELEV.	Tmax	Zref										
	ft	ft	lb/in	in										
SAND	0	2564	0	0.0000	T (lb/in)	0	0	0	0	0	0	0	0	0	0
					Z (in.)	0.0000	0.0000	0.0000	0.0000	0.0000	0.0000	0.0000	0.0000	0.0000	2.0000
SAND	16	2548	115	0.0088	T (lb/in)	0	28	53	73	88	98	104	109	114	115
					Z (in.)	0.0000	0.0022	0.0044	0.0066	0.0088	0.0110	0.0132	0.0154	0.0220	2.0000
SAND	16	2548	115	0.0118	T (lb/in)	0	28	53	73	88	98	104	109	114	115
					Z (in.)	0.0000	0.0029	0.0059	0.0088	0.0118	0.0147	0.0176	0.0206	0.0294	2.0000
SAND	17	2547	122	0.0124	T (lb/in)	0	30	56	77	93	104	110	115	120	122
					Z (in.)	0.0000	0.0031	0.0062	0.0093	0.0124	0.0155	0.0186	0.0217	0.0311	2.0000
SAND	39	2525	268	0.0273	T (lb/in)	0	66	124	170	204	227	243	252	264	268
					Z (in.)	0.0000	0.0068	0.0136	0.0205	0.0273	0.0341	0.0409	0.0478	0.0682	2.0000
SAND	39	2525	268	0.0026	T (lb/in)	0	66	124	170	204	227	243	252	264	268
					Z (in.)	0.0000	0.0006	0.0013	0.0019	0.0026	0.0032	0.0038	0.0045	0.0064	2.0000
SAND	45	2519	316	0.0030	T (lb/in)	0	77	146	201	241	268	286	298	312	316
					Z (in.)	0.0000	0.0008	0.0015	0.0023	0.0030	0.0038	0.0045	0.0053	0.0076	2.0000
					T (lb/in)										
					Z (in.)										
					T (lb/in)										
					Z (in.)										
					T (lb/in)										
					Z (in.)										

Note: Q-Z curve omitted. Bedrock tip condition treated as fixed.

Table 4.2

4.1.3 Computation of Q-z Curve

4.1.3.1 General Procedure. The procedure for computing the Q-z curve for each pile tip was adapted from information in Vijayvergiya (1977), Scott (1981), API-RP2A (1991), and NAVFAC (1986). This formulation is similar to that for the t-z curves. The general formula relating the resistance (vertical force) provided by soil bearing against the pile tip, Q, and the vertical tip deflection, z, is (Vijayvergiya, 1977)

$$Q = Q_{max} \tanh(z / z_{ref}) \tag{4.8}$$

where Q_{max} is the maximum resistance and z_{ref} is a reference deflection. These parameters are computed from the following formulas:

$$Q_{max} = Aq \tag{4.9}$$

$$z_{ref} = q / \bar{k}_t \tag{4.10}$$

where A is the cross-sectional area of the pile, q is the unit end bearing in units of stress, and $\bar{k}_t$ is a stiffness parameter given by Scott (1981),

$$\bar{k}_t = G\pi / 4s \tag{4.11}$$

The initial slope of the Q-z curve is $\bar{k}_t \cdot A$, as shown in Figure 4.5.

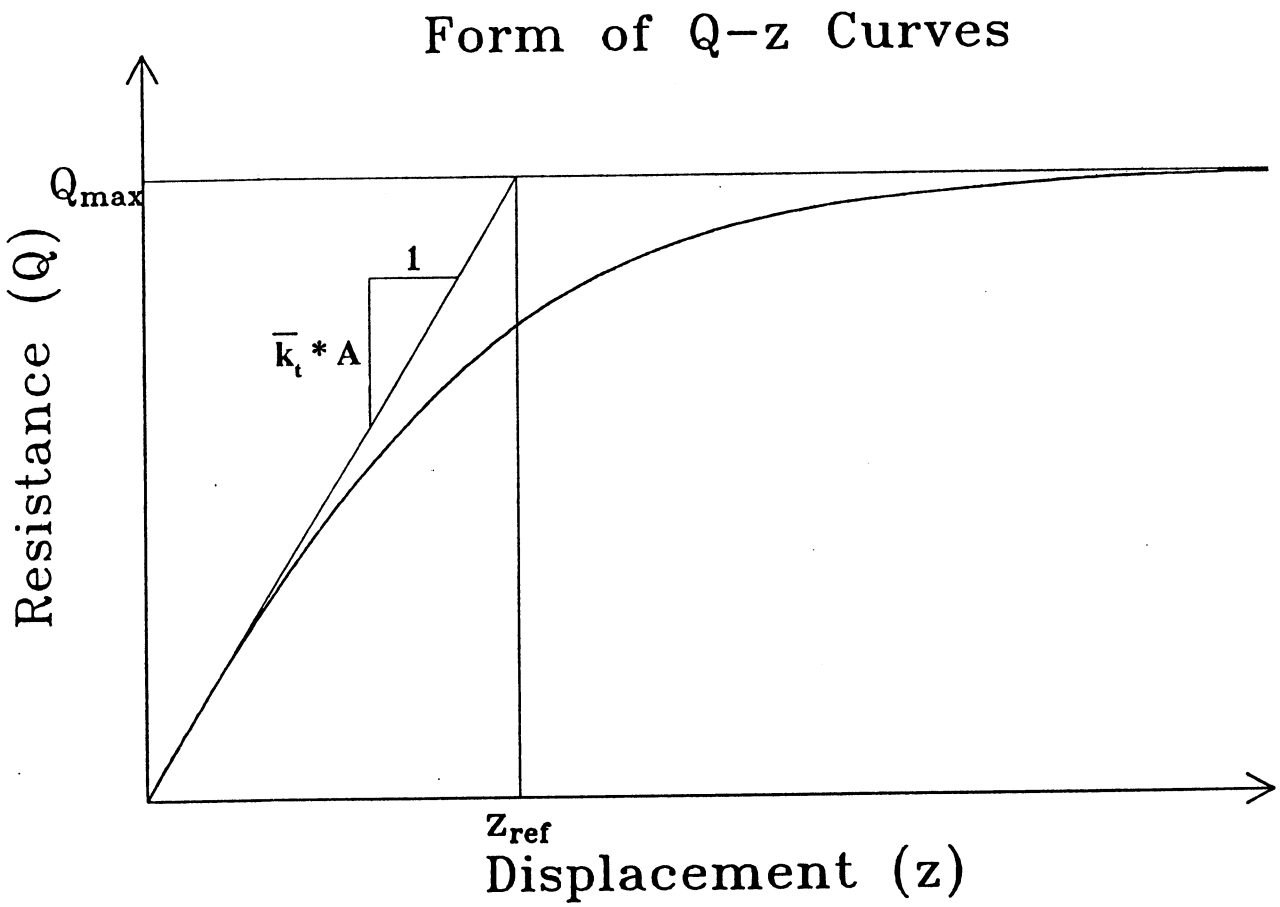
Form of Q–z Curves
Qmax
1
$\bar{k}_t * A$
Resistance (Q)
z_{ref}
Displacement (z)

Figure 4.5

The unit end bearing, q, is given by (API RP2A, 1991),

$$q = \begin{cases} 9c & (cohesive\ soils) \\ p_o N_q & (cohesionless\ soils) \end{cases} \qquad (4.12)$$

where c = undrained shear strength,

p_o = effective overburden pressure at the pile tip, and

N_q = dimensionless bearing capacity factor.

Values of N_q as a function of friction angle, ϕ, are provided in Table 4.3, taken from NAVFAC (1986).

For situations where the piles bear on bedrock, the development of Q-z curves is not recommended. In this case, the axial displacement of the pile tip is set equal to zero in the BMCOL-76 program input file.

4.1.3.2 Application to Coldwater Creek Bridge Abutment Piles. The calculation of the Q-z curves for input to the BMCOL-76 program is not required for piles supporting the NW abutment (Pier 1) because the pile tips bear on the Andesite bedrock as shown in Figure 4.1. Rather, the axial displacement of each pile tip was set equal to zero in the BMCOL-76 input file per the recommendation above.

4.1.4 Computation of p-y Curves

4.1.4.1 General Procedure. The procedure for computing the p-y curves was taken from API RP2A (1991). In this reference, formulas are provided that relate the lateral resistance (load) provided by the soil per unit length of pile, p, and the lateral pile deflection, y. The same functional form used for the t-z and Q-z curves (i.e. Eqns. 4.1

Capacity parameters of single pile in granular soils.

BEARING CAPACITY FACTORS - N_q

ϕ* (DEGREES)	26	28	30	31	32	33	34	35	36	37	38	39	40
N_q (DRIVEN PILE DISPLACE-MENT)	10	15	21	24	29	35	42	50	62	77	86	120	145
N_q** (DRILLED PIERS)	5	8	10	12	14	17	21	25	30	38	43	60	72

* LIMIT ϕ TO 28° IF JETTING IS USED

** (A) IN CASE A BAILER OR GRAB BUCKET IS USED BELOW GROUNDWATER TABLE, CALCULATE END BEARING BASED ON ϕ NOT EXCEEDING 28°.

(B) FOR PIERS GREATER THAN 24-INCH DIAMETER, SETTLEMENT RATHER THAN BEARING CAPACITY USUALLY CONTROLS THE DESIGN. FOR ESTIMATING SETTLEMENT, TAKE 50% OF THE SETTLEMENT FOR AN EQUIVALENT FOOTING RESTING ON THE SURFACE OF COMPARABLE GRANULAR SOILS. (CHAPTER 5, DM-7.1).

Ref.: NAVFAC (1986)

Table 4.3

and 4.8), is also used for the p-y curves for sands. A different functional form is used for clays.

p-y Curves for Sands. The general formula for the p-y curve is

$$p = \bar{A} p_u \tanh(y / y_c) \tag{4.13}$$

where: $\bar{A}$ is a factor to account for cyclic or static loading conditions; p_u is the ultimate bearing capacity at depth H and is in units of force/length; and, y_c is a reference length. The parameters $\bar{A}$, p_u, and y_c are computed from the following formulas:

$$\bar{A} = 0.9 \text{ (cyclic or earthquake loads)} \tag{4.14}$$

$$p_u = \min \begin{Bmatrix} (C_1 H + C_2 D) p_o \\ C_3 D p_o \end{Bmatrix} \tag{4.15}$$

$$y_c = \frac{\bar{A} p_u}{kH} \tag{4.16}$$

where: C_1, C_2, and C_3 are functions of friction angle, ϕ, and are plotted in Figure 4.6; D is the average (or equivalent) pile diameter; p_o is the effective overburden pressure at depth H; and, k is the modulus of subgrade reaction in units of force/length^3 and is given in Figure 4.6 as a function of ϕ. For cylindrical piles of constant cross section, D is the outside pile diameter; for tapered cylindrical piles that are fully embedded in the

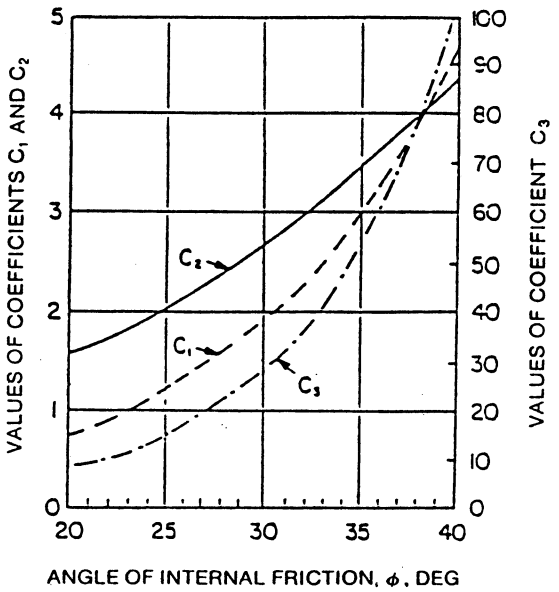

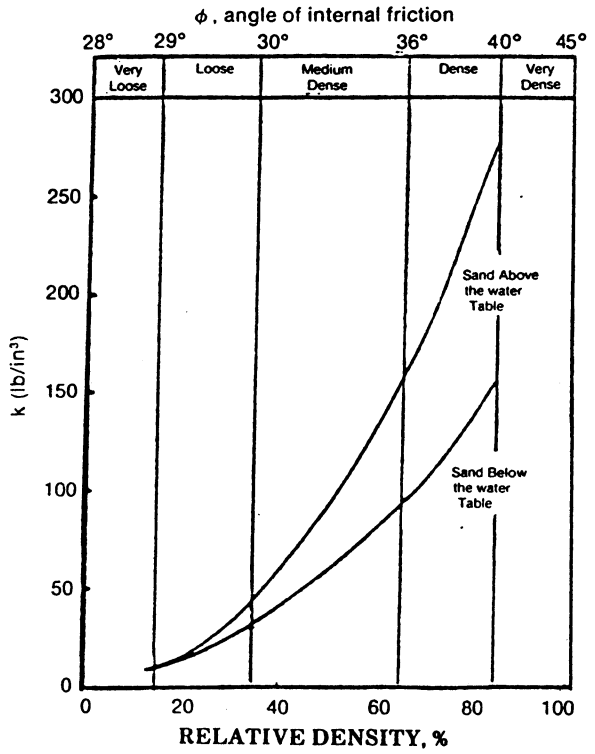

Graphs used to develop P-Y curves for sands.

Ref.: API RPZA (1991)

Figure 4.6

soil, D is the average pile diameter from the pile top to depth, H. For floating tapered piles, D is the average pile diameter from the ground surface to depth, H.

For rectangular pile cross-sections, D is the length of the side normal to the loading direction. In the case of H piles, D is either the flange length, b_f, or the depth of the section, d (see Table 4.1), whichever is normal to the loading direction. For octagonal piles, D is the diameter of a circle that circumscribes the octagonal section.

The notation, min { }, in Equation (4.15) for p_u means that the value of p_u to be used is the smaller of the two values obtained from the top and bottom expressions with the { }.

p-y Curves for Clay. The general formula for the p-y curve is

$$p = \begin{cases} 1/2 p_u' (y/y_c)^{1/3}, & y \le 8y_c \\ p_u', & y > 8y_c \end{cases} \tag{4.17}$$

where p_u' is the ultimate resistance in units of force/length of pile, and y_c is a reference length.

The parameters p_u' and y_c are computed from the following formulas:

$$p_u' = \min \begin{Bmatrix} 3cD + p_o D + JcH \\ 9cD \end{Bmatrix} \tag{4.18}$$

$$y_c = 2.5 \epsilon_c D \tag{4.19}$$

where, as before: c is the undrained shear strength; p_o is the effective overburden pressure, H is the depth, and D is the average or equivalent pile diameter. The parameter, J, is a dimensionless empirical constant ranging from 0.25 (soft clays) to 0.5 (medium and stiff clays), and the parameter, ϵ_c is the strain which occurs at one-half the maximum undrained compressive strength. The parameter, ϵ_c, usually ranges between 0.005 and 0.020. In the absence of field or laboratory test data, the values recommended for J and ϵ_c are summarized in Table 4.4.

TABLE 4.4
RECOMMENDED VALUES OF J AND ϵ_c FOR CLAY

CLAY CONSISTENCY	J	ϵ_c
Soft	0.25	0.020
Medium	0.50	0.010
Stiff	0.50	0.005

4.1.4.2 Application to Coldwater Creek Bridge Abutment Piles. The calculation of the p-y curves for input to the BMCOL-76 program is described below for piles supporting the NW abutment. The pile batter is not considered in these calculations.

As previously noted in the calculation of the t-z curves, the soil surrounding the piles is cohesionless. The relevant soil parameters are provided in Figure 4.3, taken from Figure 4.1. As with the t-z curves, the input to BMCOL-76 only requires that the p-y curves be computed at the top and bottom of each soil layer (i.e. at elevations A, B, C, and D in Figure 4.3). The calculation of the p-y curve is illustrated for loading in the y direction (transverse direction) at Elevation A = 2547 ft (at base of pile cap). The H piles are oriented such that the direction normal to the web of each pile is parallel to the y direction (see Figures 1.1 and 4.1). The following parameters are first computed:

Eqn. (4.14): $\bar{A} = 0.9$

Eqn. (4.15): $p_u = \min \left\{ \begin{matrix} (C_1 H + C_2 D) p_o \\ C_3 D p_o \end{matrix} \right\}$

Eqn. (4.15): $y_c = \dfrac{\bar{A} p_u}{kH}$

For calculation of p_u , obtain the following parameter values:

Figure 4.3: H = 2564 ft - 2547 ft = 17 ft

Figure 4.1: $\phi = 34°$

Section 4.1.1: D = 13.83 in = 1.15 ft (= d, depth of H section)

Figures 4.1 & 4.3: p_o = 2.12 ksf (= 125 pcf x 16 ft + 115 pcf x 1 ft)

Figure 4.6: For $\phi = 34°$, $C_1 = 2.8$, $C_2 = 3.3$, $C_3 = 47$

Therefore,

$$p_u = \min \left\{ \begin{matrix} (2.8\ x\ 17\ ft + 3.3\ x\ 1.15\ ft)2.12\ ksf \\ (47\ x\ 1.15\ ft)2.12\ ksf \end{matrix} \right\} = \min \left\{ \begin{matrix} 109\ kpf \\ 115\ kpf \end{matrix} \right\} = 109\ kpf$$

For the calculation of y_c, obtain k = 80 pci = 0.080 kci from Figure 4.1.

Therefore,

$$y_c = \frac{0.9(109\ kpf)}{(0.080\ kci)(17\ ft)}\ x\ (\frac{1\ ft^3}{1728\ in^3}) = 0.042\ ft = 0.501\ in$$

The above calculation pertains to ground acceleration coefficients, Z < 0.2. For this example, Z = 0.55. Therefore, reduce $\bar{A}p_u$ in Equation (4.13) by 50% per the recommendation in Section 3.0 and construct the p-y curve. Thus,

$$p = \bar{A}p_u \tanh(y/y_c) = \left(\frac{(0.9)(109\ kpf)}{2}\right)\tanh(y/0.501\ in)$$

Implementing the above calculation procedure for the x (longitudinal) direction yields the same p-y curve at Elevation A = 2547 ft. However, at greater depths, different values of p_u are computed for the two directions, and thus the longitudinal and transverse p-y curves at these depths are different.

Spread sheets containing the values of 10 points on the p-y curves at seven depths within the abutment soil profile are provided in Table 4.5 (transverse direction) and

Table 4.6 (longitudinal direction). The p-y curves for the last four depths in this table were input to the BMCOL-76 program; these depths correspond to Points A, B, C, and D in Figure 4.3.

4.1.5 Preparation of BMCOL-76 Input

The user guide titled, GUIDE FOR DATA INPUT FOR BMCOL-76, is provided in Appendix B. The text accompanying the guide is reproduced from the BMCOL-76 manual (Matlock et al, 1981), and is also provided in this Appendix. Users should read this text before attempting to prepare the input to the BMCOL-76 program. Upon reading the input guide and accompanying text, users will note some notational differences between this material and the material in Section 4.1. For example, the guide sheets use the symbols Q and U to represent either t and z, Q and z, or p and y.

The input files for the axial load and transverse lateral load cases of the Pier 1 piles of the Coldwater Creek bridge are presented as Tables 4.7 and 4.8, respectively. A similar input file was prepared for the longitudinal lateral load case.

4.1.6 BMCOL-76 Output

A detailed output file for the axial load case is shown in Table 4.9 for a 500-lb axial load applied to the top of the H pile. A summary of the axial pile-head loads versus axial deflections at five locations along the pile is provided in Table 4.10. The data in Table 4.10 were extracted from output files similar to Table 4.9. Station No. 0 in Table 4.10 represents the pile head. The deflections listed for this station were used to construct the axial load-deflection curve for the pile head (Figure 4.7), which was in turn

P-Y CURVE

Worksheet to link with: e:\wash_dot\examples\coldwatr\axial\tz_one.xls
(including path and extension)

Bridge:	Coldwater Creek Overcrossing Pier 1 : high strain case (transverse)			
Ground Surface Elevation:	2564			
Depth to water table:	69	ft	Elev: 2495	ft
Average Pile Diameter:	13.83	in		
Pile Type:	S	T=Timber,C=Concrete,S=Steel		
	O	O= Open Ended, D=Displacement		

SOIL	DEPTH	ELEV.	GAMMA	PHI (deg)	c	PHI (rad)	Po	Ko	α	β	C1	C2	C3	k	Pu	Yc
	ft	ft	γ	ϕ	ksf	ϕ	ksf		rad	rad				lb / in^3	lb/in	in
SAND	0	2564	125	36	-	0.63	0.00	0.41	0.31	1.1	3.3	3.6	61	100	0	0.00
SAND	16	2548	125	36	-	0.63	2.00	0.41	0.31	1.1	3.3	3.6	61	100	9404	0.44
SAND	16	2548	115	34	-	0.59	2.00	0.44	0.30	1.1	2.8	3.3	47	80	8066	0.47
SAND	17	2547	115	34	-	0.59	2.12	0.44	0.30	1.1	2.8	3.3	47	80	9022	0.50
SAND	39	2525	115	34	-	0.59	4.65	0.44	0.30	1.1	2.8	3.3	47	80	21122	0.51
SAND	39	2525	140	34	-	0.59	4.65	0.44	0.30	1.1	2.8	3.3	47	225	21122	0.18
SAND	45	2519	140	34	-	0.59	5.49	0.44	0.30	1.1	2.8	3.3	47	225	24942	0.18
0		0	0	0	0.00	0.00										
0		0	0	0	0.00	0.00										
0		0	0	0	0.00	0.00										

Note : Ko = 1 - sin ϕ; α = ϕ/2; β =45+ϕ/2. These parameters can alternatively be used to compute C1, C2, and C3 using formulas in 1980 Bogard and Matlock paper, "Simplified Calculation of p-y Curves for Laterally Loaded Piles in Sand."

SOIL	DEPTH	ELEV.	Pu	Yc											
	ft	ft	lb/in	in											
SAND	0	2564	0	0.000	P (lb/in)	0	0	0	0	0	0	0	0	0	0
					Y (in.)	0.000	0.000	0.000	0.000	0.000	0.000	0.000	0.000	0.000	2.000
SAND	16	2548	9404	0.441	P (lb/in)	0	1036	1956	2688	3223	3590	3830	4080	4175	4231
					Y (in.)	0.000	0.110	0.220	0.331	0.441	0.551	0.661	0.882	1.102	2.000
SAND	16	2548	8066	0.473	P (lb/in)	0	889	1677	2305	2764	3079	3286	3499	3581	3628
					Y (in.)	0.000	0.118	0.236	0.354	0.473	0.591	0.709	0.945	1.182	2.000
SAND	17	2547	9022	0.498	P (lb/in)	0	994	1876	2579	3092	3444	3675	3914	4005	4057
					Y (in.)	0.000	0.124	0.249	0.373	0.498	0.622	0.746	0.995	1.244	2.000
SAND	39	2525	21122	0.508	P (lb/in)	0	2328	4392	6037	7239	8063	8603	9163	9378	9498
					Y (in.)	0.000	0.127	0.254	0.381	0.508	0.635	0.762	1.015	1.269	2.000
SAND	39	2525	21122	0.181	P (lb/in)	0	2328	4392	6037	7239	8063	8603	9163	9378	9505
					Y (in.)	0.000	0.045	0.090	0.135	0.181	0.226	0.271	0.361	0.451	2.000
SAND	45	2519	24942	0.185	P (lb/in)	0	2749	5187	7129	8548	9521	10159	10820	11074	11224
					Y (in.)	0.000	0.046	0.092	0.139	0.185	0.231	0.277	0.370	0.462	2.000
					P (lb/in)										
					Y (in.)										
					P (lb/in)										
					Y (in.)										
					P (lb/in)										
					Y (in.)										

Table 4.5

P-Y CURVES

Worksheet to link with: e:\wash_dot\examples\coldwatr\axial\tz_one.xls
(including path and extension)

Bridge: Coldwater Creek Overcrossing Pier 1 : high strain case (longitudinal)
Ground Surface Elevation: 2564
Depth to water table: 69 ft Elev: 2495 ft
Average Pile Diameter: 14.7 in
Pile Type: S T=Timber,C=Concrete,S=Steel
O O= Open Ended, D=Displacement

SOIL	DEPTH ft	ELEV. ft	GAMMA γ	PHI (deg) ϕ	c ksf	PHI (rad) ϕ	Po ksf	Ko	α rad	β rad	C1	C2	C3	k lb / in^3	Pu lb/in	Yc in
SAND	0	2564	125	36	-	0.63	0.00	0.41	0.31	1.1	3.3	4	61	100	0	0.00
SAND	16	2548	125	36	-	0.63	2.00	0.41	0.31	1.1	3.3	4	61	100	9448	0.44
SAND	16	2548	115	34	-	0.59	2.00	0.44	0.30	1.1	2.8	3	47	80	8106	0.47
SAND	17	2547	115	34	-	0.59	2.12	0.44	0.30	1.1	2.8	3	47	80	9063	0.50
SAND	39	2525	115	34	-	0.59	4.65	0.44	0.30	1.1	2.8	3	47	80	22451	0.54
SAND	39	2525	140	34	-	0.59	4.65	0.44	0.30	1.1	2.8	3	47	225	22451	0.19
SAND	45	2519	140	34	-	0.59	5.49	0.44	0.30	1.1	2.8	3	47	225	26511	0.20
0		0	0	0	0.00	0.00										
0		0	0	0	0.00	0.00										
0		0	0	0	0.00	0.00										

SOIL	DEPTH ft	ELEV. ft	Pu lb/in	Yc in											
SAND	0	2564	0	0.000	P (lb/in)	0	0	0	0	0	0	0	0	0	0
					Y (in.)	0.000	0.000	0.000	0.000	0.000	0.000	0.000	0.000	0.000	2.000
SAND	16	2548	9448	0.443	P (lb/in)	0	1041	1965	2700	3238	3606	3848	4098	4194	4250
					Y (in.)	0.000	0.111	0.221	0.332	0.443	0.554	0.664	0.886	1.107	2.000
SAND	16	2548	8106	0.475	P (lb/in)	0	893	1686	2317	2778	3094	3302	3516	3599	3646
					Y (in.)	0.000	0.119	0.237	0.356	0.475	0.594	0.712	0.950	1.187	2.000
SAND	17	2547	9063	0.500	P (lb/in)	0	999	1885	2590	3106	3460	3692	3932	4024	4076
					Y (in.)	0.000	0.125	0.250	0.375	0.500	0.625	0.750	1.000	1.250	2.000
SAND	39	2525	22451	0.540	P (lb/in)	0	2474	4669	6417	7694	8570	9145	9739	9968	10091
					Y (in.)	0.000	0.135	0.270	0.405	0.540	0.675	0.810	1.079	1.349	2.000
SAND	39	2525	22451	0.192	P (lb/in)	0	2474	4669	6417	7694	8570	9145	9739	9968	10103
					Y (in.)	0.000	0.048	0.096	0.144	0.192	0.240	0.288	0.384	0.480	2.000
SAND	45	2519	26511	0.196	P (lb/in)	0	2922	5513	7577	9086	10120	10798	11501	11770	11930
					Y (in.)	0.000	0.049	0.098	0.147	0.196	0.245	0.295	0.393	0.491	2.000
					P (lb/in)										
					Y (in.)										
					P (lb/in)										
					Y (in.)										
					P (lb/in)										

Table 4.6

```
   COLDWATER CREEK OVERCROSSING-----                                    IDENTIFICATION OF RUN (2 LINES)
---AXIAL PILE CAPACITY-PIER 1----
1000      AXIAL LOAD 500 LB APPLIED LOAD                                IDENTIFICATION OF PROBLEM
        1        0       28       12.                                  TABLE 1: PROGRAM CONTROL DATA
       30        0    0    0    0        1    2   12        1    1     TABLE 2: AXIAL CONTROL DATA (2 CARDS)
              100.  1.00E-08         0    3    5   10   28                      ITERATION CONTROL DATA
       28                0.                                            TABLE 3: SPECIFIED DEFLECTIONS
        0   28      7.569E+08                                          TABLE 4: FIXED VALUES OF AXIAL STIFFNESS AND LOAD
            0                    500.
        0        1  -1.2E+01  1.00E-03   10    1                       TABLE 5: AXIAL SUPPORT CURVES
                                0   30   56   77   93  104  110  115  120  122
                                0    3    6    9   12   16   19   22   31 2000
           22    0  -1.2E+01  1.00E-03   10    1
                                0   66  124  170  204  227  243  252  264  268
                                0    7   14   21   27   34   41   48   68 2000
       22        1  -1.2E+01  1.00E-04   10    1
                                0   66  124  170  204  227  243  252  264  268
                                0    6   13   19   26   32   38   45   64 2000
           28    0  -1.2E+01  1.00E-04   10    1
                                0   77  146  201  241  268  286  298  312  316
                                0    8   15   23   30   38   45   53   76 2000
1001      AXIAL LOAD PIER 1000 APPLIED LOAD                             NEXT PROBLEM
        1        0       28       12.                                  TABLE 1: PROGRAM CONTROL DATA
       30        0    1    0    1        0    2    0        1    1     TABLE 2: AXIAL CONTROL DATA (2 CARDS)
              100.  1.00E-10         0    3    5   10   28                      ITERATION CONTROL DATA
        0   28      7.569E+08                                          TABLE 4: FIXED VALUES OF AXIAL STIFFNESS AND LOAD
        0    0                   1000.                                NOTE : TABLES 3 AND 5 ARE EQUAL TO PREVIOUS PROBLEM
1004      AXIAL LOAD PIER 2500 APPLIED LOAD                             NEXT PROBLEM
        1        0       28       12.                                  TABLE 1: PROGRAM CONTROL DATA
       30        0    1    0    1        0    2    0        1    1     TABLE 2: AXIAL CONTROL DATA (2 CARDS)
              100.  1.00E-10         0    3    5   10   28                      ITERATION CONTROL DATA
        0   28      7.569E+08                                          TABLE 4: FIXED VALUES OF AXIAL STIFFNESS AND LOAD (UPD
        0    0                   2500.                                NOTE : TABLES 3 AND 5 ARE EQUAL TO PREVIOUS PROBLEM
1005      AXIAL LOAD PIER 5000 APPLIED LOAD                             NEXT PROBLEM  . . .
        1        0       28       12.
       30        0    1    0    1        0    2    0        1    1
              100.  1.00E-10         0    3    5   10   28
        0   28      7.569E+08
        0    0                   5000.
1006      AXIAL LOAD PIER 7500 APPLIED LOAD
        1        0       28       12.
       30        0    1    0    1        0    2    0        1    1
              100.  1.00E-10         0    3    5   10   28
        0   28      7.569E+08
        0    0                   7500.
1007      AXIAL LOAD PIER 10000 APPLIED LOAD
        1        0       28       12.
       30        0    1    0    1        0    2    0        1    1
              100.  1.00E-10         0    3    5   10   28
        0   28      7.569E+08
        0    0                  10000.
1009      AXIAL LOAD PIER 15000 APPLIED LOAD
        1        0       28       12.
       30        0    1    0    1        0    2    0        1    1
              100.  1.00E-10         0    3    5   10   28
```

```
        0   28      7.569E+08
        0    0                  15000.
1011     AXIAL LOAD PIER 20000 APPLIED LOAD
        1        0        28       12.
       30        0    1   0    1        0    2    0        1    1
              100.  1.00E-10         0    3    5   10   28
        0   28      7.569E+08
        0    0                  20000.
1114     AXIAL LOAD PIER 25000 APPLIED LOAD
        1        0        28       12.
       30        0    1   0    1        0    2    0        1    1
              100.  1.00E-10         0    3    5   10   28
        0   28      7.569E+08
        0    0                  25000.
1115     AXIAL LOAD PIER 30000 APPLIED LOAD
        1        0        28       12.
       30        0    1   0    1        0    2    0        1    1
              100.  1.00E-10         0    3    5   10   28
        0   28      7.569E+08
        0    0                  30000.
1117     AXIAL LOAD PIER 40000 APPLIED LOAD
        1        0        28       12.
       30        0    1   0    1        0    2    0        1    1
              100.  1.00E-10         0    3    5   10   28
        0   28      7.569E+08
        0    0                  40000.
1118     AXIAL LOAD PIER 50000 APPLIED LOAD
        1        0        28       12.
       30        0    1   0    1        0    2    0        1    1
              100.  1.00E-10         0    3    5   10   28
        0   28      7.569E+08
        0    0                  50000.
1119     AXIAL LOAD PIER 60000 APPLIED LOAD
        1        0        28       12.
       30        0    1   0    1        0    2    0        1    1
              100.  1.00E-10         0    3    5   10   28
        0   28      7.569E+08
        0    0                  60000.
1120     AXIAL LOAD PIER 70000 APPLIED LOAD
        1        0        28       12.
       30        0    1   0    1        0    2    0        1    1
              100.  1.00E-10         0    3    5   10   28
        0   28      7.569E+08
        0    0                  70000.
1121     AXIAL LOAD PIER 100000 APPLIED LOAD
        1        0        28       12.
       30        0    1   0    1        0    2    0        1    1
              100.  1.00E-10         0    3    5   10   28
        0   28      7.569E+08
        0    0                 100000.
1122     AXIAL LOAD PIER 200000 APPLIED LOAD
        1        0        28       12.
       30        0    1   0    1        0    2    0        1    1
              100.  1.00E-10         0    3    5   10   28
        0   28      7.569E+08
```

Table 4.7 (cont.)

```
        0    0                    200000.
1123     AXIAL LOAD PIER 300000 APPLIED LOAD
        1         0         28        12.
       30         0    1    0    1         0    2    0         1    1
                100.  1.00E-10         0    3    5   10   28
        0   28       7.569E+08
        0    0                    300000.
1124     AXIAL LOAD PIER 400000 APPLIED LOAD
        1         0         28        12.
       30         0    1    0    1         0    2    0         1    1
                100.  1.00E-10         0    3    5   10   28
        0   28       7.569E+08
        0    0                    400000.
1125     AXIAL LOAD PIER 500000 APPLIED LOAD
        1         0         28        12.
       30         0    1    0    1         0    2    0         1    1
                100.  1.00E-10         0    3    5   10   28
        0   28       7.569E+08
        0    0                    500000.
1126     AXIAL LOAD PIER 600000 APPLIED LOAD
        1         0         28        12.
       30         0    1    0    1         0    2    0         1    1
                100.  1.00E-10         0    3    5   10   28
        0   28       7.569E+08
        0    0                    600000.
1127     AXIAL LOAD PIER 700000 APPLIED LOAD
        1         0         28        12.
       30         0    1    0    1         0    2    0         1    1
                100.  1.00E-10         0    3    5   10   28
        0   28       7.569E+08
        0    0                    700000.
1127     AXIAL LOAD PIER 1000000 APPLIED LOAD
        1         0         28        12.
       30         0    1    0    1         0    2    0         1    1
                100.  1.00E-10         0    3    5   10   28
        0   28       7.569E+08
        0    0                   1000000.
STOP
```

Table 4.7 (cont.)

```
  COLDWATER CREEK OVERCROSSING-----                                  IDENTIFICATION OF RUN (2 LINES)
---AXIAL PILE CAPACITY-PIER 1----
1000      AXIAL LOAD 500 LB APPLIED LOAD                             IDENTIFICATION OF PROBLEM
    AXIAL    MIRROR                    NUMBER OF INCREMENT
  PROBLEM    INPUT                    INCREMENTS LENGTH
      1        0        28       12.                                TABLE 1: PROGRAM CONTROL DATA

     MAX    ENTER 1 TO HOLD PRIOR    LENGTH OF TABLES    LINEAR OUTPUT
   ITERS   DISPL U TBL7 TBL8 TBL9      TBL3 TBL4 TBL5      SOLN FORCE COMPONENTS
     30        0    0    0    0         1    2   12         1    1      TABLE 2: AXIAL CONTROL DATA (2 CARDS)
             MAX       DEFL       LIST OF MONITOR STATIONS
            DEFL        TOL
             100.  1.00E-08        0    3    5   10   28                    ITERATION CONTROL DATA

     STN      DEFL
              TYPE     DEFL      SLOPE
      28                 0.                                          TABLE 3: SPECIFIED DEFLECTIONS

    STN1 STN2          AXIAL    AXIAL
                     STIFFNESS    LOAD
       0   28       7.569E+08                                        TABLE 4: FIXED VALUES OF AXIAL STIFFNESS AND LOAD
           0                      500.

    STN1  STN2 CONT. Q MULT    U MULT  NPTS SYMM
       0         1  -1.2E+01  1.00E-03   10    1                    TABLE 5: AXIAL SUPPORT CURVES
                              0   30   56   77   93  104  110  115  120  122
                              0    3    6    9   12   16   19   22   31 2000
            22    0  -1.2E+01  1.00E-03   10    1
                              0   66  124  170  204  227  243  252  264  268
                              0    7   14   21   27   34   41   48   68 2000
      22          1  -1.2E+01  1.00E-04   10    1
                              0   66  124  170  204  227  243  252  264  268
                              0    6   13   19   26   32   38   45   64 2000
            28    0  -1.2E+01  1.00E-04   10    1
                              0   77  146  201  241  268  286  298  312  316
                              0    8   15   23   30   38   45   53   76 2000

================================================================================

1001      AXIAL LOAD PIER 1000 APPLIED LOAD                          NEXT PROBLEM
    AXIAL    MIRROR                    NUMBER OF INCREMENT
  PROBLEM    INPUT                    INCREMENTS LENGTH
      1        0        28       12.                                TABLE 1: PROGRAM CONTROL DATA

     MAX    ENTER 1 TO HOLD PRIOR    LENGTH OF TABLES    LINEAR OUTPUT
   ITERS   DISPL U TBL3 TBL4 TBL5      TBL3 TBL4 TBL5      SOLN FORCE COMPONENTS
     30        0    1    0    1         0    2    0         1    1      TABLE 2: AXIAL CONTROL DATA (2 CARDS)
             MAX       DEFL       LIST OF MONITOR STATIONS
            DEFL        TOL
             100.  1.00E-10        0    3    5   10   28                    ITERATION CONTROL DATA

    STN1 STN2          AXIAL    AXIAL
                     STIFFNESS    LOAD
       0   28       7.569E+08                                        TABLE 4: FIXED VALUES OF AXIAL STIFFNESS AND LOAD
       0    0                     1000.                             NOTE : TABLES 3 AND 5 ARE EQUAL TO PREVIOUS PROBLE
>>>>>>>>>>>>>>>>>>>>>>>>>>>>>>>>>>>>>>>>>>>>>>>>>>>>>>>>>>>>>>>>>>>>>>>>>>>>>>>
<<<<<<<<<<<<<<<<<<<<<<<<<<<<<<<<<<<<<<<<<<<<<<<<<<<<<<<<<<<<<<<<<<<<<<<<<<<<<<<

STOP
```

Table 4.7 (cont.)

```
---COLDWATER CREEK OVERCROSSING PIER 1 : TRANSVERSE -----                    IDENTIFICATION OF RUN (2 LINES)
-------FIXED HEAD & PINNED HEAD
1014      LATERAL LOAD ABUT 100 lb APPLIED LOAD FIXED HEAD                  IDENTIFICATION OF PROBLEM
        2         0                                28     12.              TABLE 1: PROGRAM CONTROL DATA
       30         0    0    0    0         1    2   12          0    1     TABLE 6: LATERAL CONTROL DATA (2 CARDS)
              100.  1.00E-10          0    3    6   10   28                        ITERATION CONTROL DATA
        0         2            .00000001                                    TABLE 7: SPECIFIED DEFLECTIONS AND SLOPES
        0   28      9.454E+09                                              TABLE 8: FIXED VALUES OF LATERAL STIFFNESS AND LOAD
        0    0                      100.
        0         1  -1.2E+03  1.00E-02   10    1                          TABLE 9: LATERAL SUPPORT CURVES
                                 0   10   19   26   31   34   37   39   40   41
                                 0   12   25   37   50   62   75  100  124  200
            22    0  -1.2E+03  1.00E-02   10    1
                                 0   23   44   60   72   81   86   92   94   95
                                 0   13   25   38   51   64   76  102  127  200
       22         1  -1.2E+03  1.00E-02   10    1
                                 0   23   44   60   72   81   86   92   94   95
                                 0    5    9   14   18   23   27   36   45  200
            28    0  -1.2E+03  1.00E-02   10    1
                                 0   27   52   71   85   95  102  108  111  112
                                 0    5    9   14   19   23   28   37   46  200
1017      LATERAL LOAD ABUT 1000 LB APPLIED LOAD FIXED HEAD                 NEXT PROBLEM
        2         0                                28      12.              TABLE 1: PROGRAM CONTROL DATA
       30         0    1    0    1         0    2    0          0    1     TABLE 6: LATERAL CONTROL DATA (2 CARDS)
              100.  1.00E-10          0    3    6   10   28                        ITERATION CONTROL DATA
        0   28      9.454E+09                                              TABLE 8: FIXED VALUES OF LATERAL STIFFNESS AND LOAD
        0    0                     1000.                                   NOTE : TABLES 7 AND 9 ARE EQUAL TO PREVIOUS PROBLEM
1018      LATERAL LOAD ABUT 3000 LB APPLIED LOAD FIXED HEAD                 NEXT PROBLEM
        2         0                                28      12.              TABLE 1: PROGRAM CONTROL DATA
       30         0    1    0    1         0    2    0          0    1     TABLE 6: LATERAL CONTROL DATA (2 CARDS)
              100.  1.00E-10          0    3    6   10   28                        ITERATION CONTROL DATA
        0   28      9.454E+09                                              TABLE 8: FIXED VALUES OF LATERAL STIFFNESS AND LOAD (U
        0    0                     3000.                                   NOTE : TABLES 7 AND 9 ARE EQUAL TO PREVIOUS PROBLEM
1019      LATERAL LOAD ABUT 5000 LB APPLIED LOAD FIXED HEAD                 NEXT PROBLEM  . . .
        2         0                                28      12.
       30         0    1    0    1         0    2    0          0    1
              100.  1.00E-10          0    3    6   10   28
        0   28      9.454E+09
        0    0                     5000.
1020      LATERAL LOAD ABUT 7000 LB APPLIED LOAD FIXED HEAD
        2         0                                28      12.
       30         0    1    0    1         0    2    0          0    1
              100.  1.00E-10          0    3    6   10   28
        0   28      9.454E+09
        0    0                     7000.
1021      LATERAL LOAD ABUT 10000 LB APPLIED LOAD FIXED HEAD
        2         0                                28      12.
       30         0    1    0    1         0    2    0          0    1
              100.  1.00E-10          0    3    6   10   28
        0   28      9.454E+09
        0    0                    10000.
1023      LATERAL LOAD ABUT 15000 LB APPLIED LOAD FIXED HEAD
        2         0                                28      12.
       30         0    1    0    1         0    2    0          0    1
              100.  1.00E-10          0    3    6   10   28
```

```
        0   28      9.454E+09
        0    0                  15000.
1024     LATERAL LOAD ABUT 20000 LB APPLIED LOAD FIXED HEAD
        2         0                          28       12.
       30         0    1    0    1         0    2    0         0    1
             100.  1.00E-10         0    3    6   10   28
        0   28      9.454E+09
        0    0                  20000.
1025     LATERAL LOAD ABUT 40000 LB APPLIED LOAD FIXED HEAD
        2         0                          28       12.
       30         0    1    0    1         0    2    0         0    1
             100.  1.00E-10         0    3    6   10   28
        0   28      9.454E+09
        0    0                  40000.
1126     LATERAL LOAD ABUT 60000 LB APPLIED LOAD FIXED HEAD
        2         0                          28       12.
       30         0    1    0    1         0    2    0         0    1
             100.  1.00E-10         0    3    6   10   28
        0   28      9.454E+09
        0    0                  60000.
1127     LATERAL LOAD ABUT 100000 LB APPLIED LOAD FIXED HEAD
        2         0                          28       12.
       30         0    1    0    1         0    2    0         0    1
             100.  1.00E-10         0    3    6   10   28
        0   28      9.454E+09
        0    0                 100000.
1128     LATERAL LOAD ABUT 200000 LB APPLIED LOAD FIXED HEAD
        2         0                          28       12.
       30         0    1    0    1         0    2    0         0    1
             100.  1.00E-10         0    3    6   10   28
        0   28      9.454E+09
        0    0                 200000.
1130     LATERAL LOAD ABUT 300000 LB APPLIED LOAD FIXED HEAD
        2         0                          28       12.
       30         0    1    0    1         0    2    0         0    1
             100.  1.00E-10         0    3    6   10   28
        0   28      9.454E+09
        0    0                 300000.
1014     LATERAL LOAD ABUT 100 lb APPLIED LOAD-PINNED HEAD
        2         0                          28      12.
       30         0    0    0    1         0    2    0         0    1
             100.  1.00E-10         0    3    6   10   28
        0   28      9.454E+09
        0    0                   100.

1017     LATERAL LOAD ABUT 500 LB APPLIED LOAD-PINNED HEAD
        2         0                          28       12.
       30         0    0    0    1         0    2    0         0    1
             100.  1.00E-10         0    3    6   10   28
        0   28      9.454E+09
        0    0                   500.
1019     LATERAL LOAD ABUT 1000 LB APPLIED LOAD-PINNED HEAD
        2         0                          28       12.
       30         0    0    0    1         0    2    0         0    1
             100.  1.00E-10         0    3    6   10   28
```

```
NEXT PROBLEM
TABLE 1: PROGRAM CONTROL DATA
TABLE 6: LATERAL CONTROL DATA (2 CARDS)
          ITERATION CONTROL DATA
TABLE 8: FIXED VALUES OF LATERAL STIFFNESS AND LOA
NOTE : TABLE 9 IS EQUAL TO PREVIOUS PROBLEM
       TABLE 7 OMITTED FOR PINNED HEAD PROBLEM
NEXT PROBLEM . . .
```

Table 4.8 (cont.)

```
        0   28      9.454E+09
        0    0                    1000.
1021     LATERAL LOAD ABUT 3000 LB APPLIED LOAD-PINNED HEAD
        2         0                              28       12.
       30         0    0    0    1         0    2    0         0    1
              100.  1.00E-10         0    3    6   10   28
        0   28      9.454E+09
        0    0                    3000.
1023     LATERAL LOAD ABUT 5000 LB APPLIED LOAD-PINNED HEAD
        2         0                              28       12.
       30         0    0    0    1         0    2    0         0    1
              100.  1.00E-10         0    3    6   10   28
        0   28      9.454E+09
        0    0                    5000.
1022     LATERAL LOAD ABUT 7000 LB APPLIED LOAD-PINNED HEAD
        2         0                              28       12.
       30         0    0    0    1         0    2    0         0    1
              100.  1.00E-10         0    3    6   10   28
        0   28      9.454E+09
        0    0                    7000.
1024     LATERAL LOAD ABUT 10000 LB APPLIED LOAD-PINNED HEAD
        2         0                              28       12.
       30         0    0    0    1         0    2    0         0    1
              100.  1.00E-10         0    3    6   10   28
        0   28      9.454E+09
        0    0                   10000.
1125     LATERAL LOAD ABUT 15000 LB APPLIED LOAD-PINNED HEAD
        2         0                              28       12.
       30         0    0    0    1         0    2    0         0    1
              100.  1.00E-10         0    3    6   10   28
        0   28      9.454E+09
        0    0                   15000.
1126     LATERAL LOAD ABUT 20000 LB APPLIED LOAD-PINNED HEAD
        2         0                              28       12.
       30         0    0    0    1         0    2    0         0    1
              100.  1.00E-10         0    3    6   10   28
        0   28      9.454E+09
        0    0                   20000.
1127     LATERAL LOAD ABUT 40000 LB APPLIED LOAD-PINNED HEAD
        2         0                              28       12.
       30         0    0    0    1         0    2    0         0    1
              100.  1.00E-10         0    3    6   10   28
        0   28      9.454E+09
        0    0                   40000.
1128     LATERAL LOAD ABUT 60000 LB APPLIED LOAD-PINNED HEAD
        2         0                              28       12.
       30         0    0    0    1         0    2    0         0    1
              100.  1.00E-10         0    3    6   10   28
        0   28      9.454E+09
        0    0                   60000.
1129     LATERAL LOAD ABUT 100000 LB APPLIED LOAD-PINNED HEAD
        2         0                              28       12.
       30         0    0    0    1         0    2    0         0    1
              100.  1.00E-10         0    3    6   10   28
        0   28      9.454E+09
```

Table 4.8 (cont.)

```
        0    0                  100000.
1130     LATERAL LOAD ABUT 200000 LB APPLIED LOAD-PINNED HEAD
        2         0                          28       12.
       30         0    0    0    1         0    2    0         0    1
              100.  1.00E-10         0    3    6   10   28
        0   28      9.454E+09
        0    0                  200000.
1131     LATERAL LOAD ABUT 400000 LB APPLIED LOAD-PINNED HEAD
        2         0                          28       12.
       30         0    0    0    1         0    2    0         0    1
              100.  1.00E-10         0    3    6   10   28
        0   28      9.454E+09
        0    0                  400000.
1132     LATERAL LOAD ABUT 600000 LB APPLIED LOAD-PINNED HEAD
        2         0                          28       12.
       30         0    0    0    1         0    2    0         0    1
              100.  1.00E-10         0    3    6   10   28
        0   28      9.454E+09
        0    0                  600000.
1133     LATERAL LOAD ABUT 800000 LB APPLIED LOAD-PINNED HEAD
        2         0                          28       12.
       30         0    0    0    1         0    2    0         0    1
              100.  1.00E-10         0    3    6   10   28
        0   28      9.454E+09
        0    0                  800000.
STOP
```

Table 4.8 (cont.)

```
1                                                                    I-----TRIM
     PROGRAM BMCOL76 - IBM PC DECK - MATLOCK, BOGARD
     DATE OF LATEST REVISION  10 FEB 1987


       COLDWATER CREEK OVERCROSSING-----
     ---AXIAL PILE CAPACITY-PIER 1----
     1000      AXIAL LOAD 500 LB APPLIED LOAD
             1         0        28 1.200D+01         0 0.000D-01
            30         0    0    0    0         1    2   12         1    1
               1.000D+02 1.000D-08         0    1    5   10   28
            28           0.000D-01
             0   28    0 7.569D+08 0.000D-01 0.000D-01
             0    0    0 0.000D-01 5.000D+02 0.000D-01
             0    0    1-1.200D+01 1.000D-03   10    1 0.000D-01
                                0   30   56   77   93  104  110  115  120  122
                                0    3    6    9   12   16   19   22   31 2000
             0   22    0-1.200D+01 1.000D-03   10    1 0.000D-01
                                0   66  124  170  204  227  243  252  264  268
                                0    7   14   21   27   34   41   48   68 2000
            22    0    1-1.200D+01 1.000D-04   10    1 0.000D-01
                                0   66  124  170  204  227  243  252  264  268
                                0    6   13   19   26   32   38   45   64 2000
             0   28    0-1.200D+01 1.000D-04   10    1 0.000D-01
                                0   77  146  201  241  268  286  298  312  316
                                0    8   15   23   30   38   45   53   76 2000
                                                                     I-----TRIM
1                                                                    I-----TRIM
     PROGRAM BMCOL76 - IBM PC DECK - MATLOCK, BOGARD
     DATE OF LATEST REVISION  10 FEB 1987


       COLDWATER CREEK OVERCROSSING-----
     ---AXIAL PILE CAPACITY-PIER 1----



     PROB
     1000      AXIAL LOAD 500 LB APPLIED LOAD


     TABLE 1 - PROGRAM CONTROL DATA

         PROBLEM TYPE (1=AX,2=LAT,3=COMB)                          1

         NUM AXIAL INCREMENTS                                     28
         AXIAL INCREMENT LENGTH                            1.200D+01

         DATA CARD LISTING (1=NO)                                  0



     TABLE 2 - AXIAL CONTROL DATA
```

	DISPLS U(I)	TABLE NUMBER 3	4	5
PRIOR-DATA OPTIONS (1 = HOLD)	0	0	0	0
NUM CARDS INPUT THIS PROBLEM		1	2	12
OUTPUT OPTION (0 = TABLE 12 ONLY, 1 = TABLES 12 AND 13)				1
PLOT OPTION (1=PRINTER, 2=CALCOMP, 3=BOTH)				1

AXIAL ITERATION CONTROL DATA

MAX NUM OF ITERATIONS					30
DISPL CLOSURE TOLERANCE					1.000D-08
MAX ALLOWABLE DISPLACEMENT					1.000D+02
LIST OF MONITOR STATIONS	0	1	5	10	28

TABLE 3 - SPECIFIED DISPLACEMENTS

STA	DISPLACEMENT
28	0.000D-01

TABLE 4 - AXIAL STIFFNESS AND LOAD DATA

FROM	TO	CONTD	AE	Q	S
0	28	0	7.569D+08	0.000D-01	0.000D-01
0	0	0	0.000D-01	5.000D+02	0.000D-01

TABLE 5 - AXIAL LOAD AND SUPPORT CURVES

FROM	TO	CONTD	Q-MULTIPLIER	U-MULTIPLIER	POINTS	SYM OPT	U-OFFSET
0		1	-1.200D+01	1.000D-03	10	1	0.000D-01
Q-VALUE			0.	30.	56.	77.	93.	104.	110.	115.	120.	122.
U-VALUE			0.	3.	6.	9.	12.	16.	19.	22.	31.	2000.

FROM	TO	CONTD	Q-MULTIPLIER	U-MULTIPLIER	POINTS	SYM OPT	U-OFFSET
22	0		-1.200D+01	1.000D-03	10	1	0.000D-01
Q-VALUE			0.	66.	124.	170.	204.	227.	243.	252.	264.	268.

Table 4.9 (cont.)

U-VALUE 0. 7. 14. 21. 27. 34. 41. 48. 68. 2000.

FROM	TO	CONTD	Q-MULTIPLIER	U-MULTIPLIER	POINTS	SYM	OPT	U-OFFSET
22	1		-1.200D+01	1.000D-04	10	1		0.000D-01

Q-VALUE 0. 66. 124. 170. 204. 227. 243. 252. 264. 268.

U-VALUE 0. 6. 13. 19. 26. 32. 38. 45. 64. 2000.

FROM	TO	CONTD	Q-MULTIPLIER	U-MULTIPLIER	POINTS	SYM	OPT	U-OFFSET
28	0		-1.200D+01	1.000D-04	10	1		0.000D-01

Q-VALUE 0. 77. 146. 201. 241. 268. 286. 298. 312. 316.

U-VALUE 0. 8. 15. 23. 30. 38. 45. 53. 76. 2000.

I-----TRIM
1 I-----TRIM

COLDWATER CREEK OVERCROSSING-----
---AXIAL PILE CAPACITY-PIER 1----

PROB (CONTD)
1000 AXIAL LOAD 500 LB APPLIED LOAD

TABLE 11 - AXIAL ITERATION MONITOR DATA

ITER NUM	OFF CURVES	NUM STAS NOT CLOSED	DISPLS AT STAS NUM 0	1	5	10	28
1	NO	28	1.507D-04	1.429D-04	1.143D-04	8.336D-05	0.000D-01
2	NO	0	1.507D-04	1.429D-04	1.143D-04	8.336D-05	0.000D-01

I-----TRIM
1 I-----TRIM

PROGRAM BMCOL76 - IBM PC DECK - MATLOCK, BOGARD
DATE OF LATEST REVISION 10 FEB 1987

COLDWATER CREEK OVERCROSSING-----
---AXIAL PILE CAPACITY-PIER 1----

PROB (CONTD)
1000 AXIAL LOAD 500 LB APPLIED LOAD

TABLE 12 - RESULTS OF ITERATION NUM 2

Table 4.9 (cont.)

ASTERISKS * INDICATE VALUES AFFECTED BY SPECIFIED DISPLACEMENTS

STA I	DIST ALONG BMCOL	DISPL	AXIAL THRUST	LIN+NONL REACTION
0	0.000D-01	1.507D-04		-9.040D+00
			-4.910D+02	
1	1.200D+01	1.429D-04		-1.710D+01
			-4.739D+02	
2	2.400D+01	1.354D-04		-1.616D+01
			-4.577D+02	
3	3.600D+01	1.281D-04		-1.525D+01
			-4.424D+02	
4	4.800D+01	1.211D-04		-1.438D+01
			-4.281D+02	
5	6.000D+01	1.143D-04		-1.354D+01
			-4.145D+02	
6	7.200D+01	1.077D-04		-1.273D+01
			-4.018D+02	
7	8.400D+01	1.014D-04		-1.194D+01
			-3.898D+02	
8	9.600D+01	9.520D-05		-1.119D+01
			-3.787D+02	
9	1.080D+02	8.919D-05		-1.045D+01
			-3.682D+02	
10	1.200D+02	8.336D-05		-9.743D+00
			-3.585D+02	
11	1.320D+02	7.767D-05		-9.054D+00
			-3.494D+02	
12	1.440D+02	7.213D-05		-8.386D+00
			-3.410D+02	
13	1.560D+02	6.673D-05		-7.737D+00
			-3.333D+02	
14	1.680D+02	6.144D-05		-7.105D+00
			-3.262D+02	
15	1.800D+02	5.627D-05		-6.489D+00
			-3.197D+02	
16	1.920D+02	5.120D-05		-5.889D+00
			-3.138D+02	
17	2.040D+02	4.623D-05		-5.302D+00
			-3.085D+02	
18	2.160D+02	4.134D-05		-4.728D+00
			-3.038D+02	
19	2.280D+02	3.652D-05		-4.166D+00
			-2.996D+02	
20	2.400D+02	3.177D-05		-3.614D+00
			-2.960D+02	
21	2.520D+02	2.708D-05		-3.072D+00
			-2.929D+02	
22	2.640D+02	2.243D-05		-1.608D+01
			-2.768D+02	
23	2.760D+02	1.804D-05		-2.332D+01
			-2.535D+02	

Table 4.9 (cont.)

24	2.880D+02	1.403D-05		-1.774D+01
			-2.358D+02	
25	3.000D+02	1.029D-05		-1.273D+01
			-2.231D+02	
26	3.120D+02	6.751D-06		-8.169D+00
			-2.149D+02	
27	3.240D+02	3.344D-06		-3.954D+00
			-2.109D+02	
28	3.360D+02	0.000D-01		0.000D-01

STA I	DIST ALONG BMCOL	DISPL	AXIAL THRUST	LIN+NONL REACTION

THE MAXIMUM ARITHMETIC ROUND-OFF ERROR CHECK WAS -1.504D-12 FORCE UNITS

I-----TRIM

1 I-----TRIM

PROGRAM BMCOL76 - IBM PC DECK - MATLOCK, BOGARD
DATE OF LATEST REVISION 10 FEB 1987

COLDWATER CREEK OVERCROSSING-----
---AXIAL PILE CAPACITY-PIER 1----

PROB (CONTD)
1000 AXIAL LOAD 500 LB APPLIED LOAD

TABLE 13 - INDIVIDUAL AXIAL REACTIONS AND FORCES

STA	QAE	QQ	QS	QSTAR
0	-4.910D+02	5.000D+02	-9.040D+00	-6.477D-13
1	1.710D+01	0.000D-01	-1.710D+01	5.265D-13
2	1.616D+01	0.000D-01	-1.616D+01	1.273D-12
3	1.525D+01	0.000D-01	-1.525D+01	3.191D-14
4	1.438D+01	0.000D-01	-1.438D+01	-1.504D-12
5	1.354D+01	0.000D-01	-1.354D+01	-4.394D-13
6	1.273D+01	0.000D-01	-1.273D+01	-3.425D-13
7	1.194D+01	0.000D-01	-1.194D+01	-1.227D-13
8	1.119D+01	0.000D-01	-1.119D+01	-7.716D-13
9	1.045D+01	0.000D-01	-1.045D+01	1.273D-14
10	9.743D+00	0.000D-01	-9.743D+00	-1.201D-12
11	9.054D+00	0.000D-01	-9.054D+00	2.788D-13
12	8.386D+00	0.000D-01	-8.386D+00	4.393D-13
13	7.737D+00	0.000D-01	-7.737D+00	-3.768D-13
14	7.105D+00	0.000D-01	-7.105D+00	-1.206D-13
15	6.489D+00	0.000D-01	-6.489D+00	-1.571D-13
16	5.889D+00	0.000D-01	-5.889D+00	1.327D-13

Table 4.9 (cont.)

17	5.302D+00	0.000D-01	-5.302D+00	1.734D-13
18	4.728D+00	0.000D-01	-4.728D+00	-3.658D-13
19	4.166D+00	0.000D-01	-4.166D+00	2.468D-13
20	3.614D+00	0.000D-01	-3.614D+00	-1.129D-13
21	3.072D+00	0.000D-01	-3.072D+00	3.066D-13
22	1.608D+01	0.000D-01	-1.608D+01	7.195D-14
23	2.332D+01	0.000D-01	-2.332D+01	4.320D-14
24	1.774D+01	0.000D-01	-1.774D+01	1.742D-13
25	1.273D+01	0.000D-01	-1.273D+01	-3.786D-14
26	8.169D+00	0.000D-01	-8.169D+00	3.199D-14
27	3.954D+00	0.000D-01	-3.954D+00	1.672D-14
28	2.109D+02	0.000D-01	0.000D-01	-2.109D+02

STA	QAE	QQ	QS	QSTAR

1 AXIAL DISPLACEMENT ALONG BMCOL

STA NUM	AXIAL DISPLACEMENT
0	1.507D-04
1	1.429D-04
2	1.354D-04
3	1.281D-04
4	1.211D-04
5	1.143D-04
6	1.077D-04
7	1.014D-04
8	9.520D-05
9	8.919D-05
10	8.336D-05
11	7.767D-05
12	7.213D-05
13	6.673D-05
14	6.144D-05
15	5.627D-05

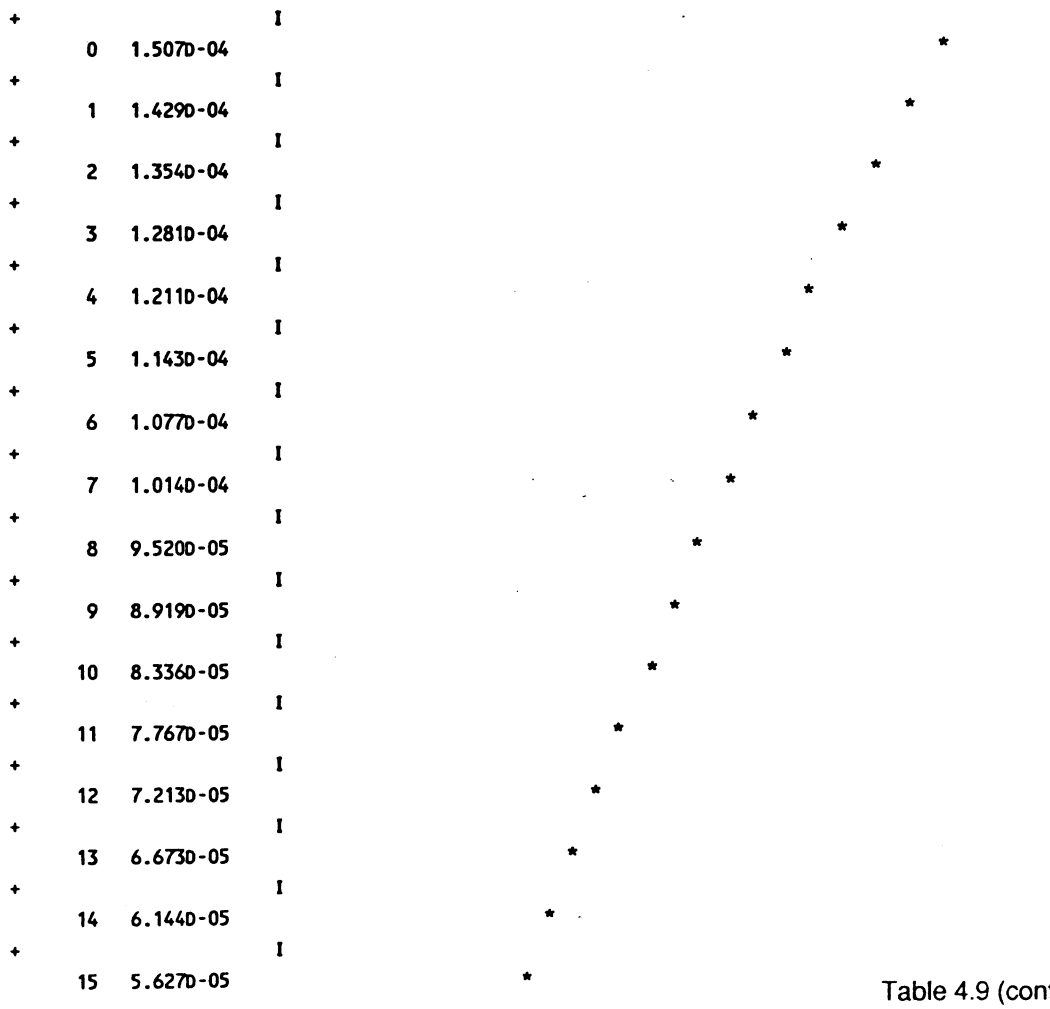

Table 4.9 (cont.)

```
+                    I
     16  5.120D-05                  *
+                    I
     17  4.623D-05                 *
+                    I
     18  4.134D-05                *
+                    I
     19  3.652D-05               *
+                    I
     20  3.177D-05              *
+                    I
     21  2.708D-05             *
+                    I
     22  2.243D-05           *
+                    I
     23  1.804D-05         *
+                    I
     24  1.403D-05       *
+                    I
     25  1.029D-05      *
+                    I
     26  6.751D-06    *
+                    I
     27  3.344D-06   *
+                    I
     28  0.000D-01   *
                                                                I-----TRIM
1                          AXIAL THRUST ALONG BMCOL

    BAR   AXIAL
    NUM   THRUST

                                                                I-----TRIM
+
      1  -4.910D+02   *
+
      2  -4.739D+02      *
+
      3  -4.577D+02         *
+
      4  -4.424D+02            *
+
      5  -4.281D+02               *
+
      6  -4.145D+02                  *
+
      7  -4.018D+02                     *
+
      8  -3.898D+02                       *
+
      9  -3.787D+02                          *
+
     10  -3.682D+02                            *
+
     11  -3.585D+02                              *
```

Table 4.9 (cont.)

```
+
      12  -3.494D+02                                  *
+
      13  -3.410D+02                                 *
+
      14  -3.333D+02                                *
+
      15  -3.262D+02                               *
+
      16  -3.197D+02                              *
+
      17  -3.138D+02                             *
+
      18  -3.085D+02                            *
+
      19  -3.038D+02                           *
+
      20  -2.996D+02                          *
+
      21  -2.960D+02                         *
+
      22  -2.929D+02                        *
+
      23  -2.768D+02                      *
+
      24  -2.535D+02                   *
+
      25  -2.358D+02                 *
+
      26  -2.231D+02               *
+
      27  -2.149D+02             *
+
      28  -2.109D+02           *
                                                    I-----TR
1                    AXIAL LIN+NONL REACTIONS ALONG BMCOL

     STA   LIN+NONL
     NUM   REACTION

                                                    I-----TR
+                                                   I
       0  -9.040D+00                          *
+                                                   I
       1  -1.710D+01                    *
+                                                   I
       2  -1.616D+01                   *
+                                                   I
       3  -1.525D+01                  *
+                                                   I
       4  -1.438D+01                 *
+                                                   I
       5  -1.354D+01                *
+                                                   I
       6  -1.273D+01               *
```

Table 4.9 (cont.)

```
+                                                        I
   7  -1.194D+01                      *
+                                                        I
   8  -1.119D+01                       *
+                                                        I
   9  -1.045D+01                        *
+                                                        I
  10  -9.743D+00                         *
+                                                        I
  11  -9.054D+00                          *
+                                                        I
  12  -8.386D+00                           *
+                                                        I
  13  -7.737D+00                            *
+                                                        I
  14  -7.105D+00                             *
+                                                        I
  15  -6.489D+00                              *
+                                                        I
  16  -5.889D+00                               *
+                                                        I
  17  -5.302D+00                                *
+                                                        I
  18  -4.728D+00                                 *
+                                                        I
  19  -4.166D+00                                  *
+                                                        I
  20  -3.614D+00                                   *
+                                                        I
  21  -3.072D+00                                    *
+                                                        I
  22  -1.608D+01                *
+                                                        I
  23  -2.332D+01   *
+                                                        I
  24  -1.774D+01              *
+                                                        I
  25  -1.273D+01                    *
+                                                        I
  26  -8.169D+00                          *
+                                                        I
  27  -3.954D+00                                *
+                                                        I
  28   0.000D-01                                         *
                                                          I-----TRIM
```

Table 4.9 (cont.)

1000 AXIAL LOAD 500 LB APPLIED LOAD

ITER NUM	OFF CURVES	NUM STAS NOT CLOSED	DISPLS AT STAS NUM 0	1	5	10	28
2	NO	0	1.507D-04	1.429D-04	1.143D-04	8.336D-05	0.000D

1001 AXIAL LOAD PIER 1000 APPLIED LOAD

ITER NUM	OFF CURVES	NUM STAS NOT CLOSED	DISPLS AT STAS NUM 0	1	5	10	28
2	NO	0	3.013D-04	2.858D-04	2.286D-04	1.667D-04	0.000D

1004 AXIAL LOAD PIER 2500 APPLIED LOAD

ITER NUM	OFF CURVES	NUM STAS NOT CLOSED	DISPLS AT STAS NUM 0	1	5	10	28
2	NO	0	7.534D-04	7.144D-04	5.716D-04	4.168D-04	0.000D

1005 AXIAL LOAD PIER 5000 APPLIED LOAD

ITER NUM	OFF CURVES	NUM STAS NOT CLOSED	DISPLS AT STAS NUM 0	1	5	10	28
2	NO	0	1.507D-03	1.429D-03	1.143D-03	8.336D-04	0.000D

1006 AXIAL LOAD PIER 7500 APPLIED LOAD

ITER NUM	OFF CURVES	NUM STAS NOT CLOSED	DISPLS AT STAS NUM 0	1	5	10	28
2	NO	0	2.260D-03	2.143D-03	1.715D-03	1.250D-03	0.000D

1007 AXIAL LOAD PIER 10000 APPLIED LOAD

ITER NUM	OFF CURVES	NUM STAS NOT CLOSED	DISPLS AT STAS NUM 0	1	5	10	28
3	NO	0	3.013D-03	2.858D-03	2.286D-03	1.667D-03	0.000D

1009 AXIAL LOAD PIER 15000 APPLIED LOAD

ITER NUM	OFF CURVES	NUM STAS NOT CLOSED	DISPLS AT STAS NUM 0	1	5	10	28
3	NO	0	4.542D-03	4.308D-03	3.448D-03	2.514D-03	0.000D

1011 AXIAL LOAD PIER 20000 APPLIED LOAD

ITER NUM	OFF CURVES	NUM STAS NOT CLOSED	DISPLS AT STAS NUM 0	1	5	10	28
3	NO	0	6.088D-03	5.776D-03	4.627D-03	3.376D-03	0.000D

1114 AXIAL LOAD PIER 25000 APPLIED LOAD

ITER NUM	OFF CURVES	NUM STAS NOT CLOSED	DISPLS AT STAS NUM 0	1	5	10	28
3	NO	0	7.658D-03	7.268D-03	5.827D-03	4.256D-03	0.000D

1115 AXIAL LOAD PIER 30000 APPLIED LOAD

ITER NUM	OFF CURVES	NUM STAS NOT CLOSED	DISPLS AT STAS NUM 0	1	5	10	28
4	NO	0	9.252D-03	8.784D-03	7.050D-03	5.151D-03	0.000D

1117 AXIAL LOAD PIER 40000 APPLIED LOAD

ITER NUM	OFF CURVES	NUM STAS NOT CLOSED	DISPLS AT STAS NUM 0	1	5	10	28
4	NO	0	1.253D-02	1.190D-02	9.573D-03	7.006D-03	0.000D

Table 4.10

1118 AXIAL LOAD PIER 50000 APPLIED LOAD

ITER NUM	OFF CURVES	NUM STAS NOT CLOSED	DISPLS AT STAS NUM 0	1	5	10	28
4	NO	0	1.596D-02	1.518D-02	1.224D-02	8.977D-03	0.000D+00

1119 AXIAL LOAD PIER 60000 APPLIED LOAD

ITER NUM	OFF CURVES	NUM STAS NOT CLOSED	DISPLS AT STAS NUM 0	1	5	10	28
4	NO	0	1.953D-02	1.859D-02	1.503D-02	1.105D-02	0.000D+00

1120 AXIAL LOAD PIER 70000 APPLIED LOAD

ITER NUM	OFF CURVES	NUM STAS NOT CLOSED	DISPLS AT STAS NUM 0	1	5	10	28
5	NO	0	2.319D-02	2.209D-02	1.792D-02	1.321D-02	0.000D+00

1121 AXIAL LOAD PIER 100000 APPLIED LOAD

ITER NUM	OFF CURVES	NUM STAS NOT CLOSED	DISPLS AT STAS NUM 0	1	5	10	28
4	NO	0	3.475D-02	3.317D-02	2.712D-02	2.014D-02	0.000D+00

1122 AXIAL LOAD PIER 200000 APPLIED LOAD

ITER NUM	OFF CURVES	NUM STAS NOT CLOSED	DISPLS AT STAS NUM 0	1	5	10	28
5	NO	0	7.646D-02	7.330D-02	6.091D-02	4.609D-02	0.000D+00

1123 AXIAL LOAD PIER 300000 APPLIED LOAD

ITER NUM	OFF CURVES	NUM STAS NOT CLOSED	DISPLS AT STAS NUM 0	1	5	10	28
5	NO	0	1.200D-01	1.153D-01	9.656D-02	7.382D-02	0.000D+00

1124 AXIAL LOAD PIER 400000 APPLIED LOAD

ITER NUM	OFF CURVES	NUM STAS NOT CLOSED	DISPLS AT STAS NUM 0	1	5	10	28
4	NO	0	1.642D-01	1.578D-01	1.328D-01	1.021D-01	0.000D+00

1125 AXIAL LOAD PIER 500000 APPLIED LOAD

ITER NUM	OFF CURVES	NUM STAS NOT CLOSED	DISPLS AT STAS NUM 0	1	5	10	28
4	NO	0	2.085D-01	2.006D-01	1.692D-01	1.306D-01	0.000D+00

1126 AXIAL LOAD PIER 600000 APPLIED LOAD

ITER NUM	OFF CURVES	NUM STAS NOT CLOSED	DISPLS AT STAS NUM 0	1	5	10	28
4	NO	0	2.528D-01	2.433D-01	2.056D-01	1.591D-01	0.000D+00

1127 AXIAL LOAD PIER 700000 APPLIED LOAD

ITER NUM	OFF CURVES	NUM STAS NOT CLOSED	DISPLS AT STAS NUM 0	1	5	10	28
4	NO	0	2.972D-01	2.861D-01	2.420D-01	1.876D-01	0.000D+00

1127 AXIAL LOAD PIER 1000000 APPLIED LOAD

ITER NUM	OFF CURVES	NUM STAS NOT CLOSED	DISPLS AT STAS NUM 0	1	5	10	28
4	NO	0	4.304D-01	4.145D-01	3.514D-01	2.732D-01	0.000D+00

Table 4.10 (cont.)

used to estimate the axial stiffness. The output files for the lateral load-deflection cases are not presented because they are similar in content to the output files for the axial load case. Rather, the resulting lateral load-deflection curves for the pile head are presented in Figure 4.8 (transverse direction) and Figure 4.9 (longitudinal direction). These curves were used to estimate the lateral stiffnesses of the pile.

4.1.7 Calculation of Pile-Head Stiffnesses

The pile-head stiffnesses are computed from the load-deflection curves in Figures 4.7, 4.8, and 4.9 as follows. For the axial load case, the axial pile-head stiffness is the slope of the load-deflection curve (Figure 4.7) at the origin (i.e. the initial tangent slope). For the two lateral load cases, the lateral pile-head stiffness is the slope of straight line from the origin to the point on the load-deflection curve corresponding to 0.50 in deflection. These rules for estimating pile-head stiffnesses were based on the results of the Task 1 study and discussions with I.P. Lam and L. Cheang of Earth Mechanics, Inc., subcontractor on this project.

Under the assumption that the H piles at Pier 1 are pinned to the abutment footing, the pile-head stiffnesses resulting from the implementation of the above procedure (see Figures 4.7, 4.8, and 4.9) are as follows:

$K_z = 3.1 \times 10^6$ lb/in (Axial)

$K_y = 1.7 \times 10^5$ lb/in (Transverse)

$K_x = 2.2 \times 10^5$ lb/in (Longitudinal)

Pile Head Load-Deflection Curve

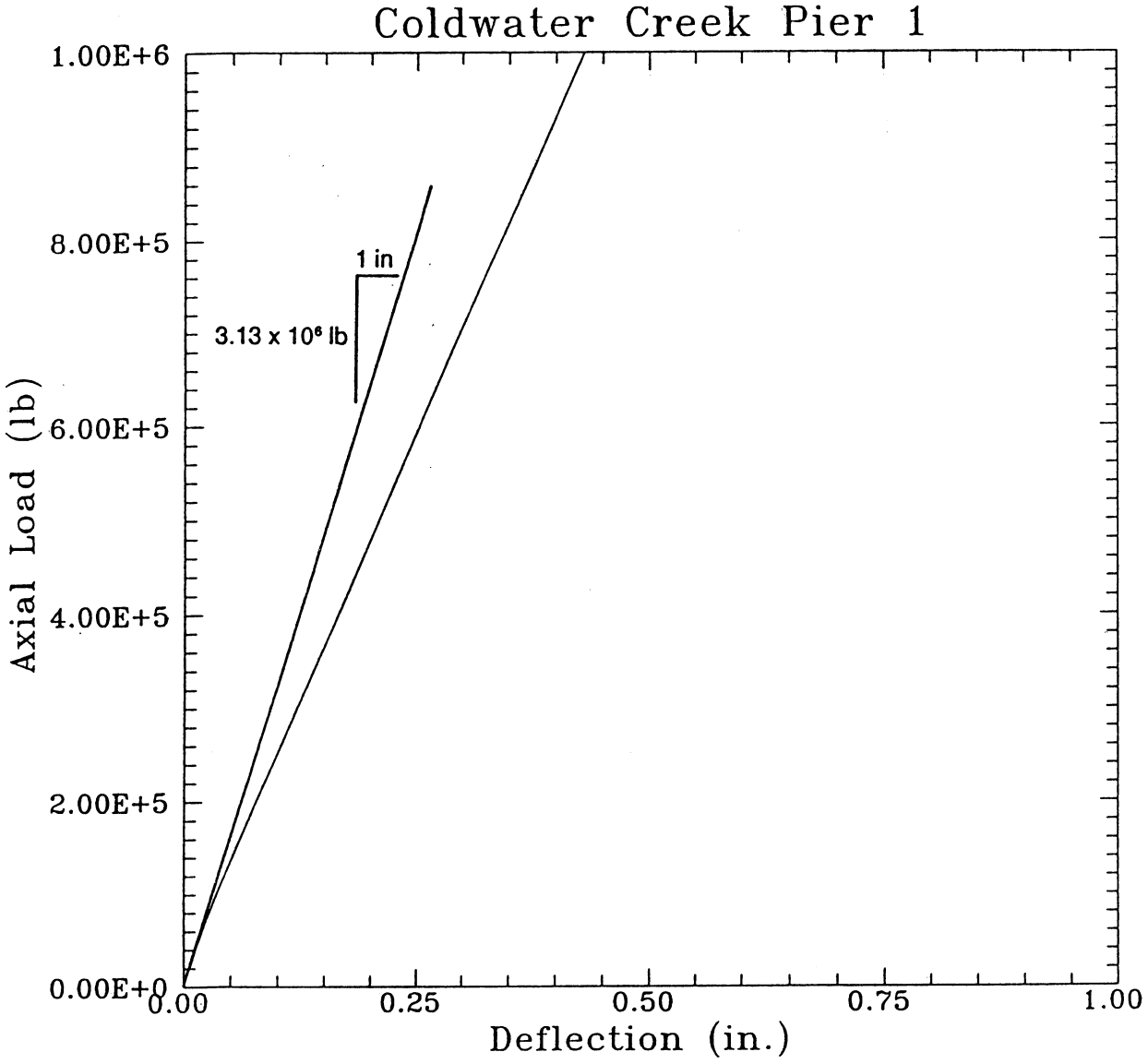

Figure 4.7

Pile Head Load-Deflection Curves

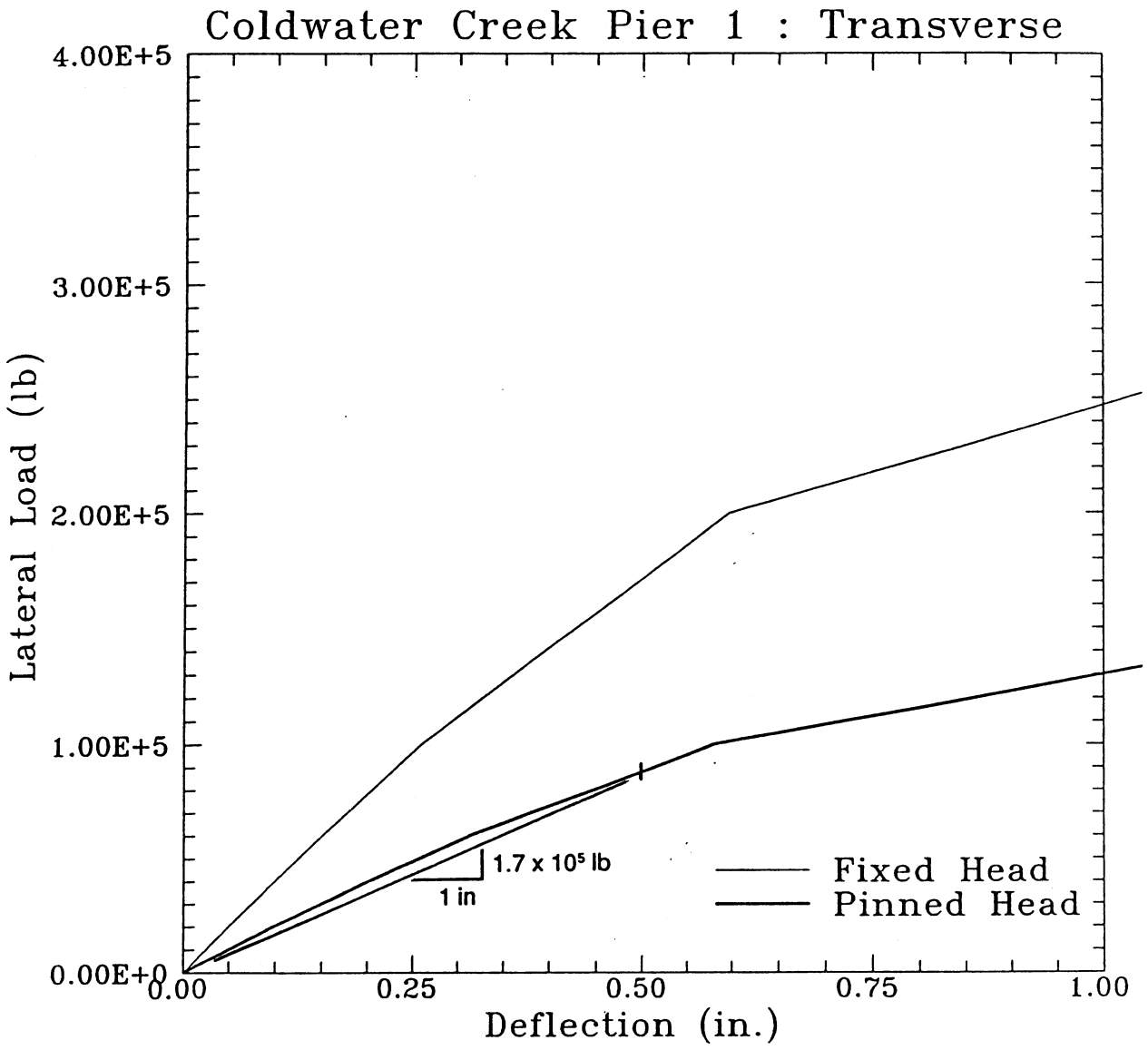

Figure 4.8

Pile Head Load-Deflection Curves

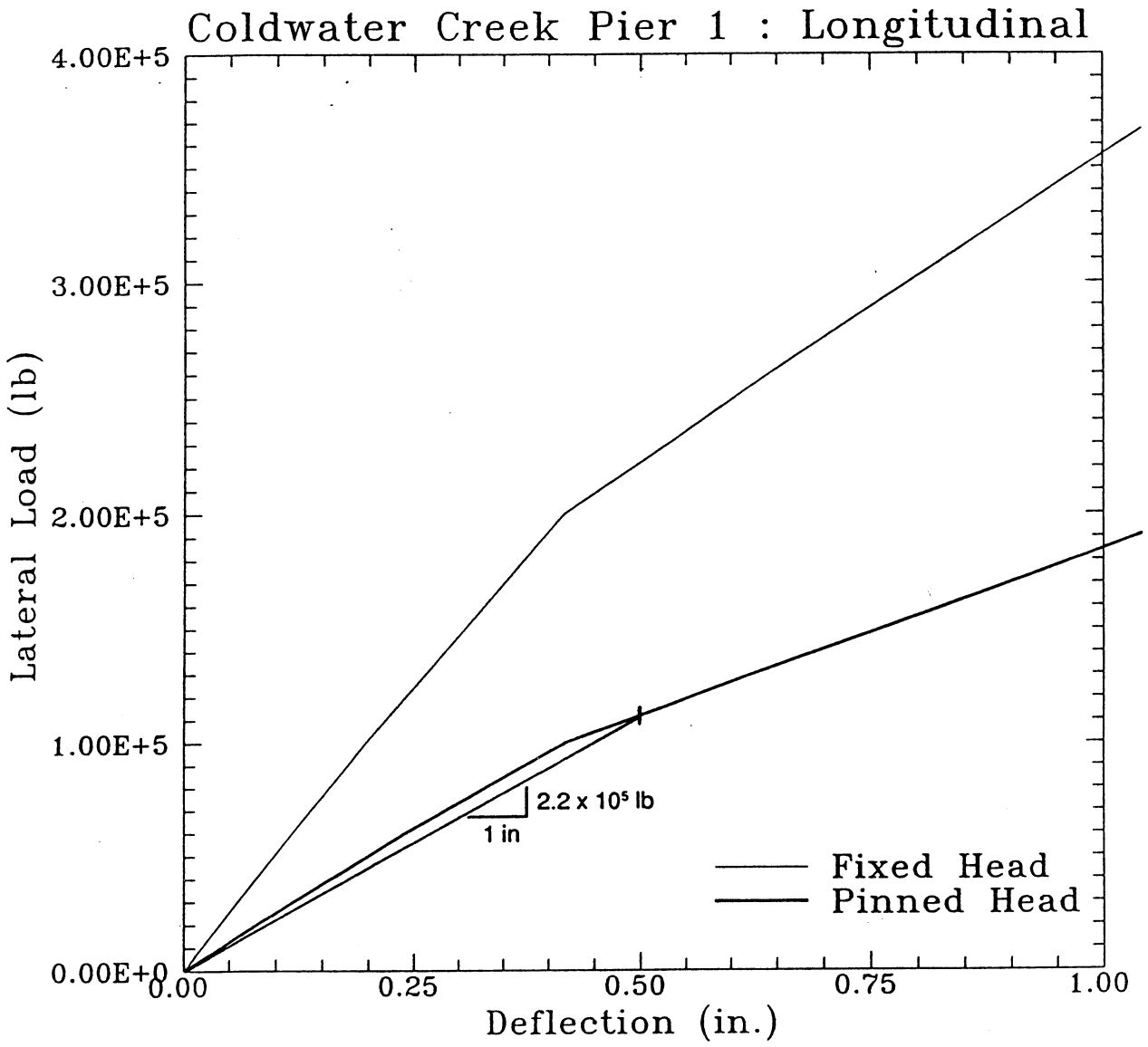

Figure 4.9

These stiffness values apply to each H-pile at Elevation 2547 in Figure 4.1 (pile head location or bottom of pile cap).

4.1.8 Calculation of Pile-Group Stiffness Matrix

4.1.8.1 Assumptions. Two key assumptions are made in order to compute the 6 x 6 pile-group stiffness matrix: (1) pile-group effects (i.e. pile-soil-pile interaction) is neglected, and (2) the individual pile-head stiffnesses computed in Section 4.1.7 apply to a local coordinate system coincidental with the principal axes of each pile (i.e. the axial stiffness, K_z, is associated with the local z axis, which is parallel to the direction along the length of the pile; the transverse stiffness, K_y, is associated with the local y axis, which is coincident with the x-x axis of the H-pile section (Table 4.1); and, the longitudinal stiffness, K_x, is associated with the local x axis is coincident with the y-y axis of the H-pile section).

The first assumption is based on the recommendation in the Task 1 report. The second assumption is required to account for the effect of the pile batter, which is considered in the GPILE program.

4.1.8.2 Preparation of GPILE Input. The GPILE program is currently used by WSDOT to compute the pile-group stiffness matrix given the individual pile-head stiffnesses and the location and batter of the piles. At Pier 1, the location of the geometric center of each of the 15 piles at the bottom of the pile cap is shown in Figure 4.10. Also shown is the orientation of the pile-cap global coordinate system in GPILE. All piles lie in a vertical (xy) plane, and the batter is 20.56° with respect to the vertical axis.

Pier 1 Pile Cap and Battered Pile System and G Pile Coordinate System and Batter Convention

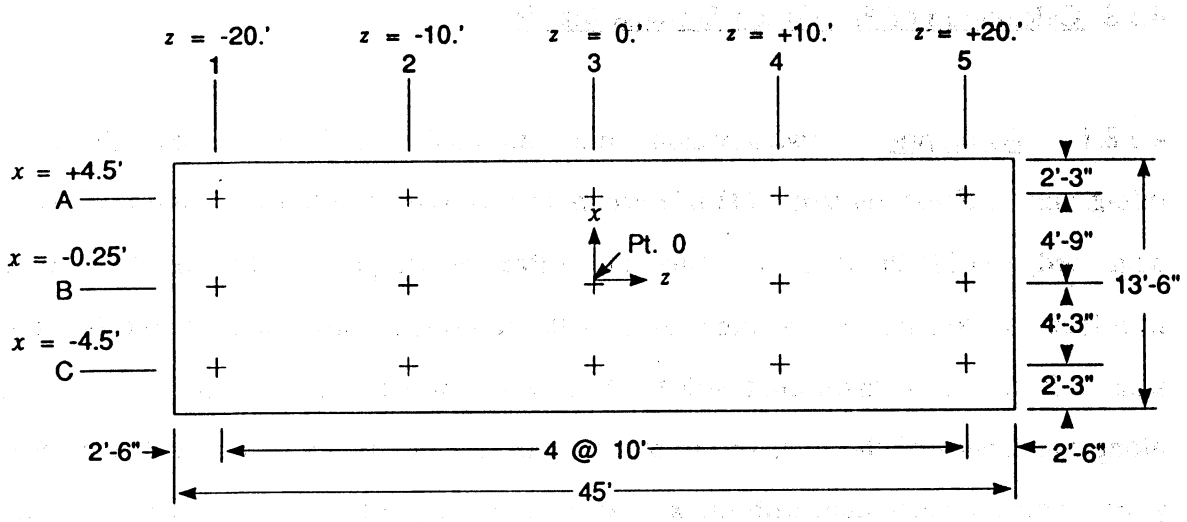

PLAN

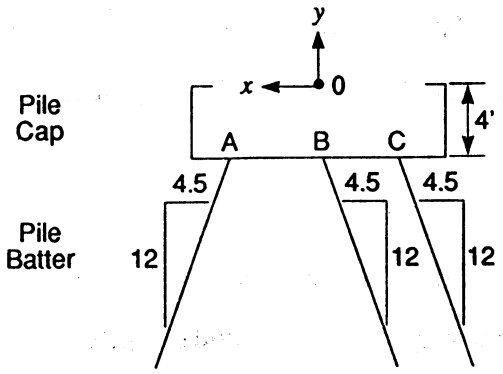

Pile Batter Planes

Row A - β = 0°
Row B - β = 180°
Row C - β = 180°

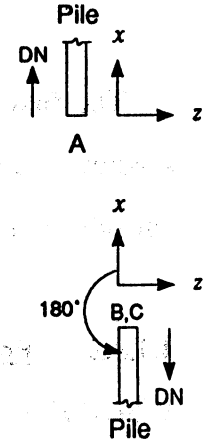

ELEVATION

Batter, B = 4.5

Batter $< = \tan^{-1}\left(\frac{4.5}{12}\right) = 20.56°$

Figure 4.10

The GPILE input file for the Pier 1 piles is listed in Table 4.11. The origin of global xyz coordinate system is fixed at Point O in Figures 4.1 and 4.10. This point is located on the top face of the Pier 1 pile cap at the geometric center of this face. The orientations of the global x, y, and z axes are parallel with the principal axes of the pile cap.[1] The pile cap 6 x 6 stiffness matrix [K] is defined with respect to the global coordinate system as follows:

$$\underline{F} = [K]\underline{u} \tag{4.20}$$

where $\underline{F}$ and $\underline{u}$ are the force and displacement vectors given by

$$\underline{F} = (F_x, F_y, F_z, M_x, M_y, M_z)^T \tag{4.21}$$

$$\underline{u} = (\delta_x, \delta_x, \delta_y, \delta_z, \theta_x, \theta_y, \theta_z)^T \tag{4.22}$$

where: F_i is the force acting along the global i axis; M_i is the moment acting about the global i axis; δ_i is the displacement along the global i axis; and θ_i is the rotation about the global i axis (i = x, y, z). Positive forces, F_i, and positive deflections, δ_i, act in the positive i directions; moments, M_i, and rotations, θ_i, are positive according to the right-hand rule convention.

---

[1]For this document, the orientation of the global coordinate system at any pier foundation is defined as follows. The x axis is in the longitudinal direction, which is exactly or approximately parallel to the direction of traffic on the bridge. This axis corresponds to one of the principal horizontal axes of the rectangular foundation. The z axis is in the transverse direction, and the y axis is in the vertical direction. The positive y direction is up. This convention is used in SEISAB also.

```
COLDWATER CREEK OVERCROSSING PILE STIFFNESS - PIER 1          JOB TITLE
   15    1    1                                               # PILE, # PILE TYPES, # LOADS
   4.5  -4. -20.    0.   4.5   1                              PILE X, Y, Z, BATTER ANGLE, BATER, PILE TYPE
  -0.25 -4. -20.  180.   4.5   1
  -4.5  -4. -20.  180.   4.5   1
   4.5  -4. -10.    0.   4.5   1
  -0.25 -4. -10.  180.   4.5   1
  -4.5  -4. -10.  180.   4.5   1
   4.5  -4.   0.    0.   4.5   1
  -0.25 -4.   0.  180.   4.5   1
  -4.5  -4.   0.  180.   4.5   1
   4.5  -4.  10.    0.   4.5   1
  -0.25 -4.  10.  180.   4.5   1
  -4.5  -4.  10.  180.   4.5   1
   4.5  -4.  20.    0.   4.5   1
  -0.25 -4.  20.  180.   4.5   1
  -4.5  -4.  20.  180.   4.5   1
1 37200000.  2040000.  2640000. 0. 0. 0. 0. 0. 0. 0.   PILE STIFFNESS VALUES
1 0. 0. 0. 0. 0. 0.                                     LOAD CONDITIONS
```

Table 4.11

The geometry and batter of the individual piles is defined with respect to the global coordinate system. This information is contained in lines 3 through 17 of the GPILE input file (Table 4.11). Each line represents a pile. For example, line 3 represents Pile No. 1 in Figure 4.10. The first three entries (4.5, -4., -20.) in this line are the x, y, z coordinates in units of feet. The fourth entry (0.) is the batter angle, which is the angle between the batter plane and the xy plane as shown in Figure 4.10. The fifth entry (4.50) is the batter, B, which is the horizontal deviation from a vertical pile over a 12-unit vertical distance, i.e. B = 12 tan (20.56°). The sixth entry is the pile type.

The second, third, and fourth entries of Line 18 are the axial, transverse, and longitudinal pile-head stiffnesses in units of lb/ft and were taken from Section 4.1.7.

4.1.8.3 GPILE Output The GPILE output file for Pier 1 is shown in Table 4.12. The global group stiffness matrix, [K], and the local group stiffness matrix are listed. The global group stiffness matrix is used in the abutment stiffness calculation Section 4.4. The local group stiffness matrix is not used because this matrix is for a different orientation of the global coordinate system.

4.2 ABUTMENT FOOTING STIFFNESSES

As recommended in the Task 1 report, the foundation stiffnesses of the pile caps are also computed assuming the caps are footings fully embedded in the surrounding soil. These footing stiffnesses (along with the stiffness contributions from the abutment wall) are added to the pile-group stiffnesses to obtain the total abutment stiffness matrix.

WASHINGTON STATE DEPARTMENT OF TRANSPORTATION 10/13/92 TIME 12:13:23 PAGE 5
*** GROUP PILE ANALYSIS *** REV 4/12/88

COLDWATER CREEK OVERCROSSING PILE STIFFNESS - PIER 1

GLOBAL GROUP STIFFNESS MATRIX:

	FX	FY	FZ	MX	MY	MZ
δX	0.104E+09	0.568E+08	0.838E+01	0.725E+01	0.350E+02	-0.111E+09
δY	0.568E+08	0.494E+09	0.196E+02	0.828E+02	0.232E+02	0.186E+09
δZ	0.838E+01	0.196E+02	0.306E+08	-0.122E+09	0.255E+07	-0.130E+02
θX	0.245E+02	0.937E+02	-0.122E+09	0.993E+11	-0.114E+11	-0.390E+02
θY	0.706E+02	0.582E+02	0.255E+07	-0.114E+11	0.211E+11	-0.180E+03
θZ	-0.111E+09	0.186E+09	-0.130E+02	-0.418E+02	-0.224E+02	0.413E+10

LOCAL GROUP STIFFNESS MATRIX:

	FX	FY	FZ	MX	MY	MZ
δX	0.494E+09	-0.568E+08	0.196E+02	0.232E+02	-0.828E+02	0.186E+09
δY	-0.568E+08	0.104E+09	-0.838E+01	-0.350E+02	0.725E+01	0.111E+09
δZ	0.196E+02	-0.838E+01	0.306E+08	0.255E+07	0.122E+09	-0.130E+02
θX	0.582E+02	-0.706E+02	0.255E+07	0.211E+11	0.114E+11	-0.180E+03
θY	-0.937E+02	0.245E+02	0.122E+09	0.114E+11	0.993E+11	0.390E+02
θZ	0.186E+09	0.111E+09	-0.130E+02	-0.224E+02	0.418E+02	0.413E+10

Table 4.12

4.2.1 Model and Assumptions

The theoretical model for estimating the stiffnesses of an embedded footing is taken from pages 40-51 of Volume II of the FHWA (1986) report. The model consists of a rigid massless footing in a linear elastic half space. The elastic properties characterizing the half space are Poisson's Ratio, ν, and shear modulus, G.

The origin of the global coordinate system for the footing is also located on the top face of the footing at its geometric center, but the orientation is different from the orientation of the global coordinate system used for the GPILE pile-group stiffness calculations. However, the sign conventions for the force and displacement vectors in both systems are the same. Consequently, Equations (4.20), (4.21), and (4.22) for the pile-group stiffnesses also apply for the footing stiffnesses.[2]

The footing stiffness matrix, [K], is assumed to be diagonal (i.e., off diagonal terms are zero), which is considered a reasonable assumption for footings supporting abutments and intermediate pier foundations. To be consistent with Equations (4.20),

---

[2]The foundation stiffnesses for another coordinate system that has the same origin as the original coordinate system, but which has the axes labeled differently (e.g. the +x axis in the new system is the -z axis in the original system, etc.), can be obtained by a coordinate transformation or can be computed by the following simple procedure. For example, the FHWA coordinate system for a rectangular footing or pile cap is shown in Figure 4.11. The GPILE coordinate system is shown in Figure 4.10. Comparing the two systems, it is apparent that $x_{FHWA} = x_{GPILE}$, $y_{FHWA} = z_{GPILE}$, $z_{FHWA} = -y_{GPILE}$. Therefore, to convert the stiffnesses derived from the FHWA coordinate system to the GPILE coordinate system, do the following: (1) replace the y subscript with the z subscript in the F_y and M_y elements of the FHWA force vector and do a similar subscript replacement with the δ_y and θ_y FHWA displacement vector, (2) in a similar manner, replace the z subscript with the y subscript and change the sign of the affected force and displacement vector elements from plus (+) to minus (-), and (3) write out the resulting six equations and rearrange their order such that resulting force and displacement vectors have the same x, y, z order as in Eqns. (4.21) and (4.22), and that the signs of the elements of these vectors are all positive. The resulting stiffness matrix is the [K] in Eqn. (4.20) in the GPILE coordinate system.

(4.21), and (4.22), the subscript notation adopted for the diagonal elements, $K_{ii} = K_i$, is as follows: $K_i = K_x$, $K_2 = K_y$, $K_3 = K_z$, $K_4 = K_{\theta x}$, $K_5 = K_{\theta y}$, $K_6 = K_{\theta z}$.

4.2.2 Calculation of Footing Stiffnesses

4.2.2.1 General Procedure. The diagonal stiffnesses of the embedded footing are approximated by (FHWA, 1986)

$$K_i = \alpha_i \cdot \beta_i \cdot K_i^o \tag{4.23}$$

where: K_i° is the i^{th} diagonal value of the 6 x 6 stiffness matrix of an equivalent circular surface footing; α_i is a scalar factor that accounts for the footing being rectangular; and β_i is a scalar factor that accounts for the footing embedment.

The values of K_i° are calculated using the following formulas:

$$\textit{Vertical translation: } K_z^o = \frac{4GR}{1 - \nu} \tag{4.24}$$

$$\textit{Horizontal translation: } K_x^o = K_y^o = \frac{8GR}{2 - \nu} \tag{4.25}$$

$$\textit{Rotation about vertical axis: } K_{\theta z}^o = \frac{16GR_z^3}{3} \tag{4.26}$$

$$\textit{Rotation about x horizontal axis:}\quad K^{o}_{\theta x} = \frac{8GR_x^3}{3(1 - \nu)} \tag{4.27}$$

$$\textit{Rotation about y horizontal axis:}\quad K^{o}_{\theta y} = \frac{8GR_y^3}{3(1 - \nu)} \tag{4.28}$$

where R, R_x, R_y, and R_z are the equivalent radii for translation and rotation. The formulas for R are given in Figure 4.11, taken from the aforementioned FHWA (1986) report.

The shape factors, α_i, for the various stiffnesses are plotted as a function of the footing length to width ratio, L/B, in Figure 4.12 (FHWA, 1986). The embedment factors, $ß_i$, are plotted in Figure 4.13 as a function of the footing thickness to equivalent radius ratio (FHWA, 1986). for translational stiffnesses, R is used to compute this ratio; for rotational stiffnesses, $K_{\theta x}$, $K_{\theta y}$, and $K_{\theta z}$, the appropriate values of equivalent radius are R_x, R_y and R_z, respectively (Figure 4.11).

In order to compute [K], values of G and υ for an equivalent half space must be estimated from a soil profile that usually consists of more than one soil layer, each one having different elastic properties. The recommended procedure (Gazetas, 1983) is to use the values of G and ν at a depth, h, beneath the bottom of the footing equal to the radius of the equivalent circular foundation, i.e.

RECTANGULAR FOOTING

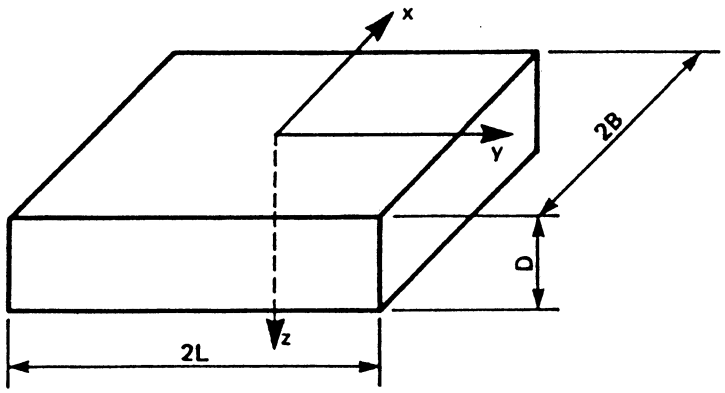

EQUIVALENT CIRCULAR FOOTING

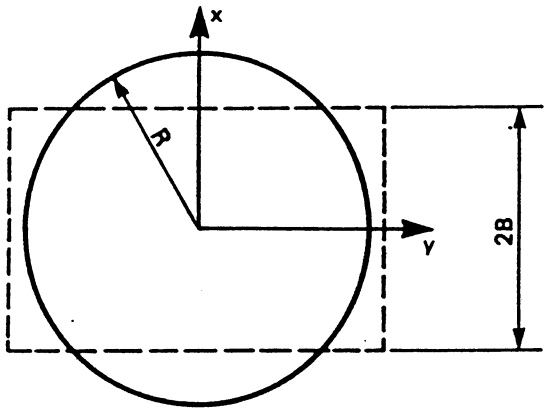

EQUIVALENT RADIUS:

TRANSLATIONAL: $R = \sqrt{\frac{4BL}{\pi}}$

ROTATIONAL: $R = \left[\frac{(2B)(2L)^3}{3\pi}\right]^{1/4}$ .....(x–AXIS ROCKING)

$R = \left[\frac{(2B)^3(2L)}{3\pi}\right]^{1/4}$ .....(y–AXIS ROCKING)

$R = \left[\frac{4BL(4B^2 + 4L^2)}{6\pi}\right]^{1/4}$ .....(z–AXIS TORSION)

Procedure for calculating equivalent radius of a rectangular footing.

ef.: FHWA (1986)

Figure 4.11

$$h = R = \left(\frac{4BL}{\pi}\right)^{1/2} \qquad (4.29)$$

where 4BL is the area of the rectangular footing of width 2B and length 2L (see Figure 4.11).

To account for the reduction in G during strong shaking, the low-strain G value should be modified following the recommendations in Section 3.0, i.e., if the acceleration coefficient, $Z < 0.2$, then use the low-strain G; if $Z \geq 0.2$, then reduce G by 50%.

4.2.2.2 Application to Coldwater Creek Abutment Footing. The calculation of the footing (pile cap) stiffness matrix for the Pier 1 abutment is described below.

The footing dimensions from Figures 4.1 and 4.10 are:

Length:	2L = 45 ft	
Width:	2B = 13.5 ft	
Thickness:	D = 4 ft	(footing assumed to be fully embedded; see Section 6.1 for example dealing with partially embedded footing.)

Compute the effective soil depth:

Eqn. (4.29): $h = \left(\frac{4BL}{\pi}\right)^{1/2} = \left(\frac{(45\ ft)(13.5\ ft)}{\pi}\right)^{1/2} = 13.9\ ft$

Select the G and ν values at h = 13.9 ft beneath the bottom of footing:

Figure 4.1: G = 1800 ksf, ν = 0.3

This modulus is the low-strain G. Because Z ≥ 0.2, reduce G by 50%. Thus, for subsequent calculations, use G = 900 ksf. Compute equivalent radii, R, R_x, R_y, and R_z, of the rectangular foundation using formula in Figure 4.11:

Translation: $R = h = 13.9\ ft$

Rotation: (about x axis) $$R_x = \left[\frac{(2B)(2L)^3}{3\pi}\right]^{1/4} = \left[\frac{(13.5)(45)^3}{3\pi}\right]^{1/4} = 19.0\ ft$$

Rotation: (about y axis) $$R_y = \left[\frac{(2L)(2B)^3}{3\pi}\right]^{1/4} = \left[\frac{(45)(13.5)^3}{3\pi}\right]^{1/4} = 10.4\ ft$$

Rotation: (about z axis) $$R_z = \left[\frac{4BL(4B^2 + 4L^2)}{6\pi}\right]^{1/4} = \left[\frac{(13.5)(45)(13.5^2 + 45^2)}{6\pi}\right]^{1/4} = 16.3\ ft$$

Compute the stiffnesses of equivalent circular footing, K_i^c:

Eqn. (4.24): $$K_z^o = \frac{4GR}{1 - \nu} = \frac{4(900\ ksf)(13.9\ ft)}{1 - 0.3} \times \left(\frac{1{,}000\ lb}{1k}\right) = 7.15 \times 10^7\ lb/ft$$

Eqn. (4.25): $$K_x^o = K_y^o = \frac{8GR}{2 - \nu} = \frac{8(900\ ksf)(13.9\ ft)}{2 - 0.3} \times \left(\frac{1{,}000\ lb}{1k}\right) = 5.89 \times 10^7\ lb/ft$$

Eqn. (4.26): $$K^{o}_{\theta z} = \frac{16GR_z^3}{3} = \frac{16(900\ ksf)(16.3\ ft)^3}{3} \times \left(\frac{1{,}000\ lb}{1k}\right) = 2.08 \times 10^{10}\ lb\text{-}ft$$

Eqn. (4.27): $$K^{o}_{\theta x} = \frac{8GR_x^3}{3(1 - \nu)} = \frac{8(900\ ksf)(19.0\ ft)^3}{3(1 - 0.3)} \times \left(\frac{1{,}000\ lb}{1k}\right) = 2.35 \times 10^{10}\ lb\text{-}ft$$

Eqn. (4.28): $$K^{o}_{\theta y} = \frac{8GR_y^3}{3(1 - \nu)} = \frac{8(900\ ksf)(10.4\ ft)^3}{3(1 - 0.3)} \times \left(\frac{1{,}000\ lb}{1k}\right) = 3.86 \times 10^{9}\ lb\text{-}ft$$

Compute values of α_i and $ß_i$ by first calculating L/B and D/R ratios:

L/B = 3.33

D/R = 4/13.9 = 0.288 (translation)

D/R_x = 0.211, D/R_y = 0.385, D/R_z = 0.245 (rotation)

The corresponding values of α_i and $ß_i$ were read from Figures 4.12 and 4.13, respectively, and are summarized in Table 4.13 below, along with the stiffnesses K_i° and the final stiffnesses $K_i = \alpha_i \cdot ß_1 \cdot K_i^{\circ}$ (Eqn. 4.22).

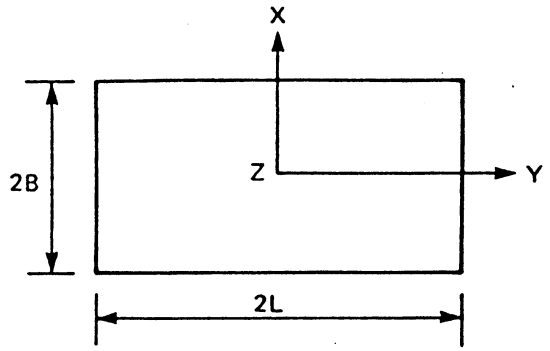

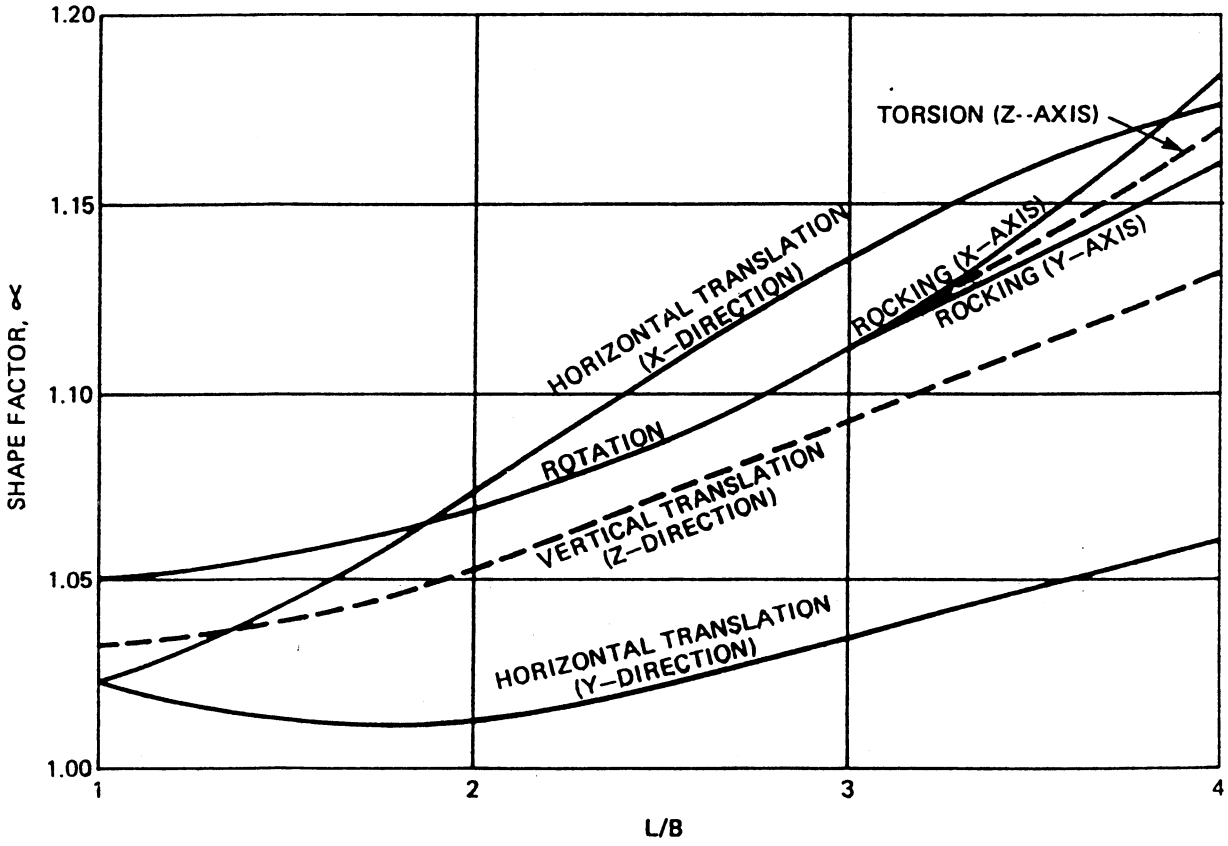

Shape factor for rectangular footings.

f.: FHWA (1986)

Figure 4.12

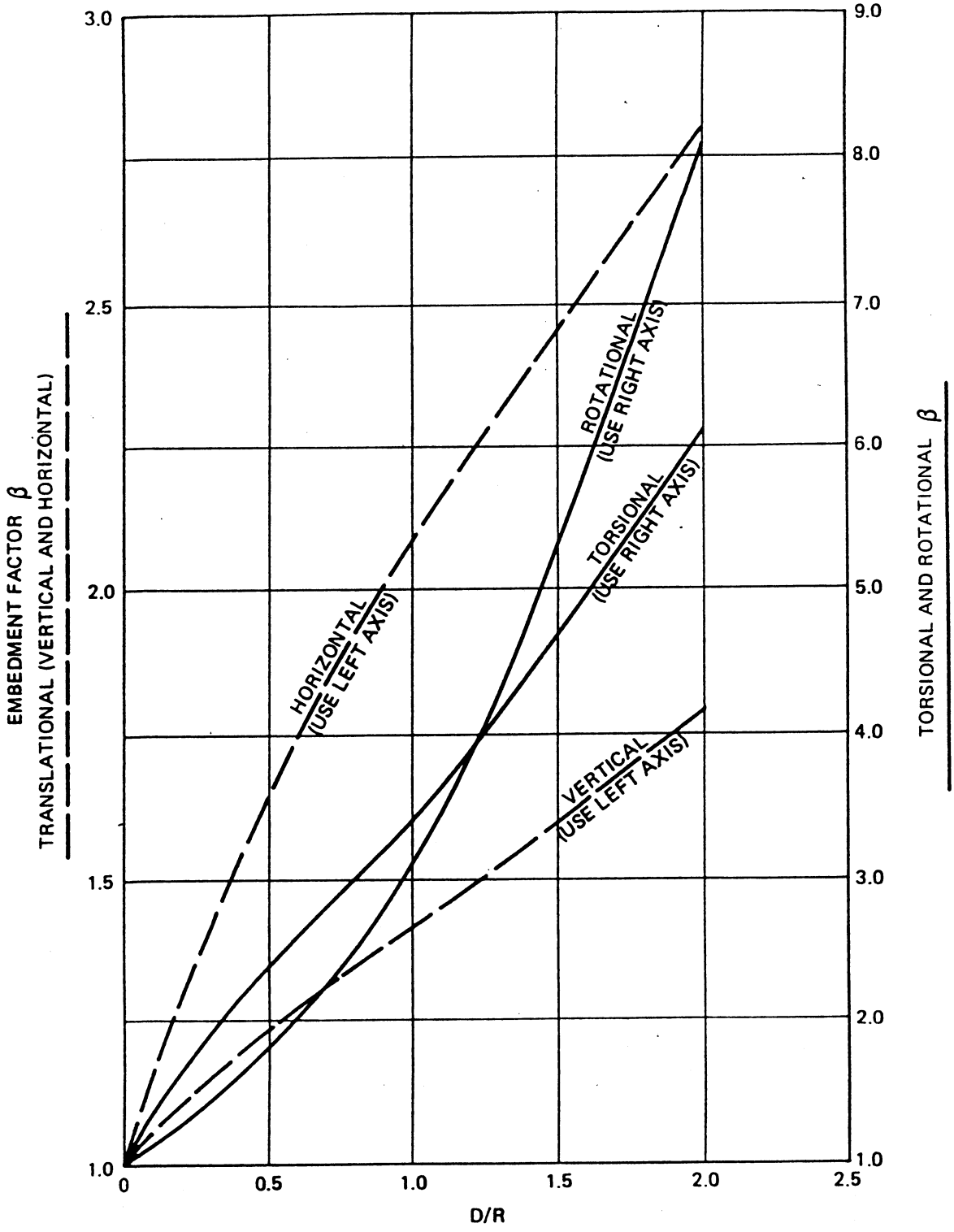

Embedment factor of footings.

Ref.: FHWA (1986)

Figure 4.13

TABLE 4.13
CALCULATION OF PIER 1 FOOTING STIFFNESSES

	K_i^o	α_i	$ß_i$	K_i
K_x (lb/ft)	5.89×10^7	1.15	1.41	9.55×10^7
K_y (lb/ft)	5.89×10^7	1.04	1.41	8.64×10^7
K_z(lb/ft)	7.15×10^7	1.11	1.15	9.13×10^7
$K_{\theta x}$ (lb-ft)	2.35×10^{10}	1.13	1.29	3.43×10^{10}
$K_{\theta y}$ (lb-ft)	3.86×10^9	1.13	1.60	6.98×10^9
$K_{\theta z}$ (lb-ft)	2.08×10^{10}	1.13	1.76	4.14×10^{10}

Thus, the diagonal elements of the diagonal footing stiffness matrix, [K], are the values in the last column in Table 4.13. This stiffness matrix applies to the FHWA coordinate system. Elements of this matrix will be rearranged in Section 4.4 to be compatible with the global coordinate system in Figure 4.1.

4.3 ABUTMENT WALL STIFFNESS

As recommended in the Task 1 report, the stiffness due to the passive resistance of abutment backfill soil is also computed and added to the pile-group and footing stiffnesses.

4.3.1 Model and Assumptions

The model for estimating the translational and rotational stiffnesses of the abutment wall-backfill system is shown in Figure 4.14, taken from the FHWA (1986) report. These stiffnesses are due to the normal pressure exerted on the wall by the backfill as the wall translates into it. Other stiffnesses, such as those arising from shearing forces acting on

the wall during transverse translation of the wall or the torsional stiffness of the wall about a vertical axis, are assumed to be negligible.

4.3.2 Calculation of Wall Stiffnesses

4.3.2.1 General Procedure. The formulas for the translational stiffness, K_x , and the rotational stiffness, $K_{\theta y}$, are (FHWA, 1986)

$$K_x = 0.425 E_s B_w \tag{4.30}$$

$$K_{\theta z} = 0.072 E_s B_w H_w^2 \tag{4.31}$$

where: E_s is the elastic (Youngs) modulus of the backfill soil;[3] B_w is the length of the abutment wall (i.e. the dimension of the wall normal to 2-D section view in Figure 4.14); and H_w is the height of the wall. The stiffnesses given by Equations (4.30) and (4.31) apply to a point on the wall at a height, $h_1 = 0.37H_w$, above the base of the wall. For most applications, the stiffnesses are defined at the base of the wall. The stiffnesses at this point are obtained by a simple transformation as shown in Figure 4.14. The formulas for these stiffnesses are (FHWA, 1986)

$$K_x = 0.425 E_s B_w \tag{4.32}$$

$$K_{\theta z} = 0.425 E_s B_w h_1^2 + 0.072 E_s B_w H_w^2 \tag{4.33}$$

[3]See Section 8.2.1 for the evaluation of E_s when the backfill soil consists of two or more layers.

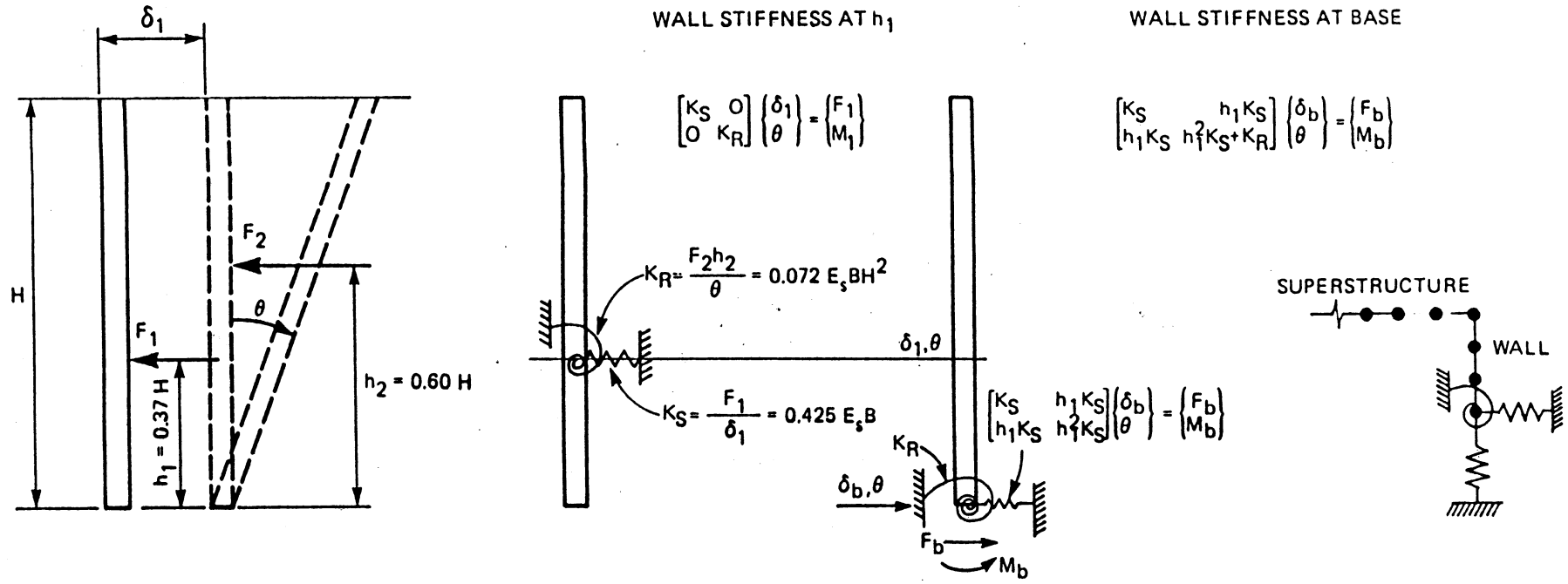

(A) SOLUTION FROM FORCED WALL PRESSURE

(B) SIMPLIFIED MODEL

(C) TRANSFORMATION OF SPRING POSITION

(D) ABUTMENT MODEL

NOTE:

F_1 = FORCE AT HEIGHT h_1 ABOVE BASE OF WALL
F_2 = FORCE AT HEIGHT h_2 ABOVE BASE OF WALL
F_b = FORCE AT BASE OF WALL
M_1 = MOMENT AT HEIGHT h_1 ABOVE BASE OF WALL
M_b = MOMENT AT BASE OF WALL
B = WIDTH OF ABUTMENT WALL

Figure 4.14

Procedure to incorporate wall stiffness in abutment stiffness model.

Ref.: FHWA (1986)

$$K_{x\theta z} = 0.425 E_s B_w h_1 \qquad (4.34)$$

where $K_{x\theta z}$ is the cross coupling (off-diagonal) stiffness which results from the transformation (see Figure 4.14).

The elastic modulus, E_s, is obtained from the shear modulus, G, and Poisson's ratio, ν, by using the formula

$$E_s = 2G(1 + \nu) \qquad (4.35)$$

4.3.2.2 Application to Coldwater Creek Abutment Wall. The abutment-wall stiffness computation is illustrated for the Pier 1 abutment. The abutment wall height is assumed to be the distance from the top of the pile cap (i.e. Point 0 in Figure 4.14) to the top of the abutment. The stiffnesses are computed at Point 0.

Obtain the appropriate length dimensions from Figures 1.2 and 4.1:

B_w = 4.5' - (8.5") - (1' - 4") = 43 ft

H_w = 13 ft

Thus, $h_1 = 0.37H_w$ = 4.8 ft

Compute E_s using the high strain G, which is 50% less than the low-strain G of 2400 ksf as explained in the abutment footing calculation:

Eqn. (4.35): $E_s = 2G(1 + \nu) = 2(1200\ ksf)(1 + 0.3) = 3{,}120\ ksf$

Using the global coordinate system in Figure 4.1, the wall stiffnesses at Point 0 are:

Eqn. (4.32): $K_x = 0.425E_sB_w = 0.425(3{,}120\ ksf)(43\ ft)\ x \left(\frac{1{,}000\ lb}{1k}\right) = 5.70\ x\ 10^7\ lb/ft$

Eqn.(4.33): $K_{\theta z} = (0.425E_sB_w)h_1^2 + 0.072E_sB_wH_w^2$
$= (5.70\ x\ 10^7\ lb/ft)(4.8\ ft)^2 + 0.072(3.12\ x\ 10^6\ psf)(43\ ft)(13\ ft)^2$
$= 2.95\ x\ 10^9\ lb\text{-}ft$

Eqn. (4.34): $K_{x\theta z} = -(0.425E_sB_w)h_1 = -(5.70\ x\ 10^7\ lb/ft)(4.8\ ft) = -2.74\ x\ 10^8\ lb$

The minus sign in Eqn. (4.34) results from the fact that the sign convention for forces (moments) and displacements (rotations) in the FHWA (1986) report is slightly different from the convention adopted herein.

4.4 TOTAL ABUTMENT STIFFNESS MATRIX

4.4.1 General Procedure.

The total abutment stiffness matrix, $[K_t]$, at a given point is approximated as the sum of the stiffness matrices for the piles, $[K_p]$, footing or pile cap, $[K_f]$, and abutment wall, $[K_w]$, i.e.

$$[K_t] = [K_p] + [K_f] + [K_w] \qquad (4.36)$$

Although this formula is simple, it is important to note that $[K_p]$, $[K_f]$, and $[K_w]$ must be computed at the same point in the same coordinate system used for the piles, footings, and wall.

4.4.2 Application to Coldwater Creek Abutment. The stiffness matrices $[K_p]$, $[K_f]$, and $[K_w]$ for the abutment system at Pier 1 were constructed from the stiffness calculations presented in Sections 4.1, 4.2, and 4.3, respectively. The xyz coordinate system is oriented as shown in Figure 4.1 with the origin at Point 0.

The 6 x 6 stiffness matrices are:

From Table 4.12,

$$[K_p] = \begin{bmatrix} 1.04E8 & 5.68E7 & 8.38E0 & 7.25E0 & 3.50E1 & -1.11E8 \\ 5.68E7 & 4.94E8 & 1.96E1 & 8.28E1 & 2.32E1 & 1.86E8 \\ 8.38E0 & 1.96E1 & 3.06E7 & -1.22E8 & 2.55E6 & -1.30E1 \\ 2.45E1 & 9.37E1 & -1.22E8 & 9.93E10 & -1.14E10 & -3.90E1 \\ 7.06E1 & 5.82E1 & 2.55E6 & -1.14E10 & 2.11E10 & -1.80E2 \\ -1.11E8 & 1.86E8 & -1.30E1 & -4.18E1 & -2.24E1 & 4.13E9 \end{bmatrix}$$

From Table 4.13 (after converting from the FHWA to GPILE coordinate system),

$$\text{diag } [K_f] = \begin{bmatrix} 9.55E7 & & & & & \\ & 9.13E7 & & & & \\ & & 8.64E7 & & & \\ & & & 3.43E10 & & \\ & & & & 4.14E10 & \\ & & & & & 6.98E9 \end{bmatrix}$$

From Section (4.3.2.2),

$$[K_w] = \begin{bmatrix} 5.70E7 & 0 & 0 & 0 & 0 & -2.74E8 \\ 0 & 0 & 0 & 0 & 0 & 0 \\ 0 & 0 & 0 & 0 & 0 & 0 \\ 0 & 0 & 0 & 0 & 0 & 0 \\ 0 & 0 & 0 & 0 & 0 & 0 \\ -2.74E8 & 0 & 0 & 0 & 0 & 2.95E9 \end{bmatrix}$$

The values for $[K_p]$ were taken from the output of GPILE. Note that in some cases, $K_{ij} \neq K_{ji}$, which is not correct because, theoretically, $[K_p]$ is symmetric. Furthermore, some of the off-diagonal terms are quite small relative to other off-diagonal and diagonal terms. Theoretically, these small off-diagonal terms should be zero and are not zero because of a numerical precision deficiency in the GPILE program. The values of the other elements in $[K_p]$ are correct. For simplicity, the small elements in $[K_p]$ that should be zero will be set equal to zero. The revised $[K_p]$ is

$$[K_p] = \begin{bmatrix} 1.04E8 & 5.68E7 & 0 & 0 & 0 & -1.11E8 \\ 5.68E7 & 4.94E8 & 0 & 0 & 0 & 1.86E8 \\ 0 & 0 & 3.06E7 & -1.22E8 & 2.55E6 & 0 \\ 0 & 0 & -1.22E8 & 9.93E10 & -1.14E10 & 0 \\ 0 & 0 & 2.55E6 & -1.14E10 & 2.11E10 & 0 \\ -1.11E8 & 1.86E8 & 0 & 0 & 0 & 4.13E9 \end{bmatrix}$$

Using this revised $[K_p]$,

$$[K_t] = \begin{bmatrix} 2.57E8 & 5.68E7 & 0 & 0 & 0 & -3.85E8 \\ 5.68E7 & 5.85E8 & 0 & 0 & 0 & 1.86E8 \\ 0 & 0 & 1.17E8 & -1.22E8 & 2.55E6 & 0 \\ 0 & 0 & -1.22E8 & 1.34E11 & -1.14E10 & 0 \\ 0 & 0 & 2.55E6 & -1.14E10 & 6.25E10 & 0 \\ -3.85E8 & 1.86E8 & 0 & 0 & 0 & 1.41E10 \end{bmatrix}$$

The units are lb and ft.

5.0 PIER 1 STIFFNESS CALCULATION - NOVAK METHOD

The calculation of foundation stiffnesses using the Novak method is much simpler than the FHWA method primarily because a single computer program (DYNA3) is available to do all the required calculations. Furthermore, the theory upon which the program is based assumes linear elastic response of the soil-foundation system; consequently, fewer soil properties are required to characterize the soil medium, and

nonlinear load-deflection relationships between the pile and soil (t-z, Q-z, p-y curves) are not required.

5.1 PILE AND FOOTING SIDE STIFFNESS

The Task 1 report recommended the use of the Pile & Footing Side option within the Novak computer program. With this option, the total pile-cap stiffness is the sum of the stiffnesses from the pile group and the passive resistance of the soil against the sides of the pile cap.

5.1.1 Soil Model

The soil model is shown in Figure 5.1, which was adapted from information in Figure 4.1. Note that shear-wave velocity, V_s, is given as an elastic property, rather than the shear modulus, G. In computing $V_s = \sqrt{G/\gamma_m}$ (where γ_m = mass density), the low-strain shear modulus values in Figure 4.1 were reduced by 50% to account for high soil strain.

Besides V_s, the other new soil parameter not shown in Figure 4.1 is the soil damping ratio for shear deformation, ζ. Values of $\zeta \leq 0.05$ are typically assumed and within this range, the effect of this parameter on the stiffness calculation is negligible. For this and all other example problems, $\zeta = 0.03$ was arbitrarily assumed.

Soil Model for Novak Stiffness Calculation for Pile and Footing Side Case at Pier 1

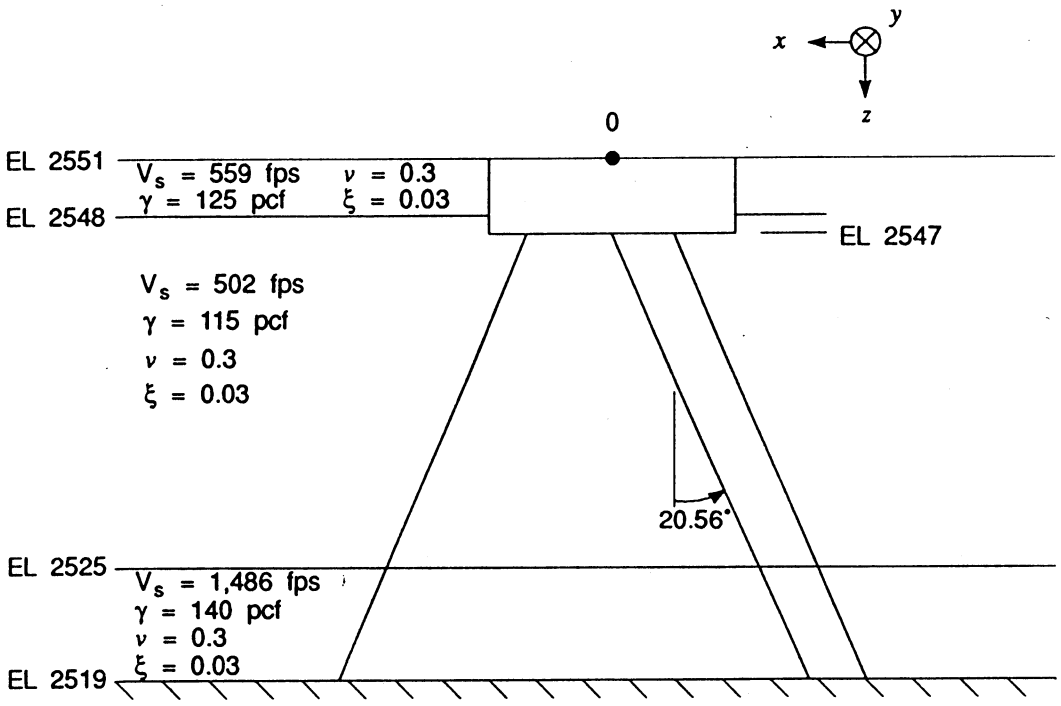

NOTES

V_s Shear-wave velocity $=\sqrt{G/\gamma_m}$, where G is the high-strain value of shear modulus = 50% of the low-strain G value in Figure 4.1. The parameter γ_m is mass density.

ξ Soil damping ratio (assumed).

xyz Coordinate system in this figure is oriented differently from the one in Figure 4.1. In Novak's model, the *z* coordinate axis is positive downward.

Figure 5.1

5.1.2 Preparation of DYNA3 Input

The input file for Novak's DYNA3 computer program to estimate the foundation stiffnesses at Point 0 in Figure 5.1 is provided in Table 5.1. Most of the inputs are easily understood after reading the comment statements to the right of each line of input data. However, several lines require additional clarification. The line reading "CONSTANTS = 0., 0., 4.0," is explained in the comment as "x, y, z of Cg." For dynamic analysis, Novak's program computes the stiffness matrix at the center-of-gravity (Cg) of the foundation or pile cap. For the calculation of the stiffness matrix only, the location of the center-of-gravity of the pile cap is not important, and therefore this line in the program is used to specify the location where the stiffness is to be computed. The z value is the height above the bottom of the pile cap to the desired point (in this case, Point 0). The value is 4.0 and the sign is positive.

Further into the same "CONSTANTS = " data, there appears the number, 0.05, which is explained in the comment as "RADIATION DAMPING IN THE PILE." Values of 0.05 are typically assumed, but the effect of this parameter on the computed stiffness is small.

The number following the 0.05 RADIATION DAMPING IN PILE number is the value 3.00, which is the EFFECTIVE SHEAR AREA COEFFICIENT. In the DYNA3 user guide, Novak provides values of this parameter for circular and rectangular pile cross sections. For flexible pile foundations (which are the ones mostly encountered in practice, including the example problems in this manual), the stiffness calculation is not sensitive to this parameter. In this example, the coefficient was estimated as A/A_w, where A is the cross-sectional area of the H pile (26.1 in^2), and $A_w = t_w d$ is the area of

```
TITLE=COLDWATER CREEK PIER 1 [ PILES + EMBEDMENT ] [k, ft, s]
MATRIX                    | SPECIFY MATRIX OUTPUT OF STIFFNESS AND DAMPING
GRAVITY=32.2              | g
FOUNDATION=PILE           | FOUNDATION TYPE
RECTANGULAR=13.5,45.0     | PILE CAP DIMENSIONS
MASS=0,0,0,0,0,0,0        | MASS PROPERTIES OF FOUNDATION, NO EFFECT ON STIFFN
LAYERS=2                  | # OF SOIL LAYERS IN WHICH PILES ARE EMBEDDED
PINNED=15                 | PILE HEAD CONDITION AND # OF PILES
 1 -4.50  -20.            | PILE #, X AND Y COORDINATE OF PILE HEAD
 2 -0.25  -20.
 3  4.50  -20.
 4 -4.50  -10.
 5 -0.25  -10.
 6  4.50  -10.
 7 -4.50    0.
 8 -0.25    0.
 9  4.50    0.
10 -4.50   10.
11 -0.25   10.
12  4.50   10.
13 -4.50   20.
14 -0.25   20.
15  4.50   20.
CONSTANTS=0.,0.,4.0,      | X, Y, Z OF Cg
          28.,.089,0.,    | PILE LENGTH, PILE WEIGHT/UNIT LENGTH, STATIC LOAD
          0.3,0.05,       |  POISSON'S RATIO, RADIATION DAMPING IN PILE
          3.00, 4.2E06    | EFFECTIVE SHEAR AREA COEFFICIENT, Epile
ELEMENT
1  22.0  0.58  0.61  0.18  0.016 0.044 0.060
                          | LAYER THICKNESS, X RADIUS, Y RADIUS, AREA, Ix, Iy,
2   6.0  0.58  0.61  0.18  0.016 0.044 0.060
END-BEARING               | END-BEARING/FLOATING SWITCH
NO-INTERACTION            | NEGLECT INTERACTION
BATTERED                  | BATTER DESCRIPTION
 1  XZ  -20.56            | PILE #, DIRECTION OF BATTER, ANGLE OF BATTER
 2  XZ  -20.56
 3  XZ   20.56
 4  XZ  -20.56
 5  XZ  -20.56
 6  XZ   20.56
 7  XZ  -20.56
 8  XZ  -20.56
 9  XZ   20.56
10  XZ  -20.56
11  XZ  -20.56
12  XZ   20.56
13  XZ  -20.56
14  XZ  -20.56
15  XZ   20.56
SOIL
CONSTANTS
1  502. .115 0.3 0.03     | SOIL PARAMETERS : Vs, GAMMA, NU, DAMPING
2 1486. .140 0.3 0.03
BELOW
4632. .150 .3 0.03        | SOIL PROPERTIES BELOW PILE TIP
```

Table 5.1

```
EMBEDDED=2                | # OF LAYERS OVERLYING CAP
1  1. 502. .115 0.3 0.03  | LOWEST LAYER : THICKNESS, Vs, GAMMA, NU, DAMPING
2  3. 559. .125 0.3 0.03  | NEXT LAYER : THICKNESS, Vs, GAMMA, NU, DAMPING
LOAD=HARMONIC             | LOAD IDENTIFIER : SINE WAVE
CONSTANTS        | DEFINES MINIMAL LOAD, DOES NOT AFFECT STIFFNESS PROPERTIES
NONQUADRATIC
0.001  0.001  0.001  0.0  10.  0.0  0.  0.  0.
RUN                       | BEGIN EXECUTION
```

Table 5.1 (cont.)

the web (8.5 in^2) where most of the shear stress is located when the applied loading is normal to the face of the flange. Thus, the coefficient is 26.1/8.5 = 3. For loading in the other direction, the coefficient was estimated as 1.4. However, because the coefficient is not important for flexible piles, a value of 3.0 was selected for both directions.

In the next two lines, the value of 0.58 for X RADIUS is one-half of the H-pile flange width in ft; the value of 0.61 for Y RADIUS is one-half of the depth of the H-pile section in ft. In the same two lines, J is the polar moment of inertia in ft^4.

The first three numbers (0.001) of the last data line in the input file refer to the beginning frequency, ending frequency, and frequency increment in rad/sec. Recall that the Task 1 report recommended the computation of static stiffnesses instead of dynamic stiffnesses. Because the DYNA3 program does not compute static stiffnesses, dynamic stiffnesses computed by the program at an extremely low frequency (0.001 rad/sec) are equivalent to static stiffnesses.

5.1.3 DYNA3 Output

The output file from the DYNA3 program is listed in Table 5.2. The stiffnesses are in units of kips and ft. The values of CROSS-STIFFNESS (YZ PLANE) and CROSS-STIFFNESS (XZ PLANE) refer to $K_{y\theta x}$ and $K_{x\theta y}$, respectively.

```
**************************************************
*                                                *
*        D Y N A 3   S I M U L A T I O N         *
*                                                *
*              RUN DATE -  1992/10/16            *
*              TIME     -  15:54:11              *
*              REVISION -  1991/07/30            *
*                                                *
**************************************************

COLDWATER CREEK PIER 1 [ PILES + EMBEDMENT ] [k ft s]

                                   RESULTS
                                   *******


FREQUENCY  -      .0010
*********


STIFFNESS CONSTANTS (K)
***********************

HORIZONTAL TRANSLATION  (X) ...  1.51128E+05
HORIZONTAL TRANSLATION  (Y) ...  1.04428E+05
VERTICAL TRANSLATION  (Z) .....  5.33056E+05
ROTATION ABOUT  (X) ...........  1.11843E+08
ROTATION ABOUT  (Y) ...........  1.08986E+07
TORSION ABOUT  (Z) ............  4.37764E+07
CROSS-STIFFNESS (YZ PLANE) ....  3.84868E+05
CROSS-STIFFNESS (XZ PLANE) .... -5.71670E+05

DAMPING CONSTANTS (C)
*********************
HORIZONTAL TRANSLATION  (X) ...  5.71625E+06
HORIZONTAL TRANSLATION  (Y) ...  3.35145E+06
VERTICAL TRANSLATION  (Z) .....  2.30259E+07
ROTATION ABOUT  (X) ...........  4.76598E+09
ROTATION ABOUT  (Y) ...........  4.40973E+08
TORSION ABOUT  (Z) ............  1.55510E+09
CROSS-DAMPING  (YZ PLANE) .....  1.24179E+07
CROSS-DAMPING  (XZ PLANE) ..... -2.18771E+07
```

Table 5.2

5.2 ABUTMENT WALL STIFFNESS

The Task 1 report noted that the abutment-wall stiffness could be computed using Novak's method for a footing on an elastic half space whose properties are those of the backfill soil. However, the FHWA approach for retaining walls (Section 4.3) is slightly preferred over the Novak method. The stiffness matrix obtained using the FHWA method was presented in Section 4.4.

5.3 TOTAL PIER 1 STIFFNESS MATRIX

The total abutment stiffness matrix is $[K_t] = [K_{pfs}] + [K_w]$, where $[K_{pfs}]$ is the "pile + footing side" stiffness matrix, and K_w is the abutment wall stiffness matrix. From Table 5.2 of Section 5.1.3,

$$[K_{pfs}] = \begin{bmatrix} 1.51E8 & 0 & 0 & 0 & -5.72E8 & 0 \\ 0 & 1.04E8 & 0 & 3.85E8 & 0 & 0 \\ 0 & 0 & 5.33E8 & 0 & 0 & 0 \\ 0 & 3.85E8 & 0 & 1.12E11 & 0 & 0 \\ -5.72E8 & 0 & 0 & 0 & 1.09E10 & 0 \\ 0 & 0 & 0 & 0 & 0 & 4.38E10 \end{bmatrix}$$

The units are lb and ft.

Because the coordinate system in Figure 4.1 is different from the Novak coordinate system (Figure 5.1), elements of $[K_w]$ from Section 4.4 were rearranged to be consistent with the coordinate system in Figure 5.1. Thus,

$$[K_w] = \begin{bmatrix} 5.70E7 & 0 & 0 & 0 & -2.74E8 & 0 \\ 0 & 0 & 0 & 0 & 0 & 0 \\ 0 & 0 & 0 & 0 & 0 & 0 \\ 0 & 0 & 0 & 0 & 0 & 0 \\ -2.74E8 & 0 & 0 & 0 & 2.95E9 & 0 \\ 0 & 0 & 0 & 0 & 0 & 0 \end{bmatrix}$$

Therefore,

$$[K_t] = \begin{bmatrix} 2.08E8 & 0 & 0 & 0 & -8.46E8 & 0 \\ 0 & 1.04E8 & 0 & 3.85E8 & 0 & 0 \\ 0 & 0 & 5.33E8 & 0 & 0 & 0 \\ 0 & 3.85E8 & 0 & 1.12E11 & 0 & 0 \\ -8.46E8 & 0 & 0 & 0 & 1.39E10 & 0 \\ 0 & 0 & 0 & 0 & 0 & 4.38E10 \end{bmatrix}$$

Note that $[K_t]$ is the stiffness matrix at Point 0 for the global coordinate system defined in Figure 5.1.

6.0 PIER 2 (FOOTING) STIFFNESS CALCULATION - FHWA METHOD

6.1 MODEL AND ASSUMPTIONS

Pier 2 of the Coldwater Creek bridge consists of two columns, each supported by a square concrete footing, 18 ft x 18 ft x 4 ft-2 in thick, embedded in the Andesite bedrock. The NE footing is embedded 3 ft in the bedrock, while the SW footing is

completely buried, as shown in Figure 6.1. Also shown in the figure are the elastic properties of the bedrock (G = 200,000 ksf, ν = 0.3). Usually, foundations on bedrock are considered fixed against translations and rotations. However, for this example, the foundation stiffnesses will be computed using the method presented in Section 4.2 with one small modification.

The modification is made to the definition of D in the FHWA method to account for surface or partially embedded footings (rather than fully embedded footings, which the FHWA method assumes in all cases). Herein, D is defined as the embedment depth, which must be $\leq$ footing thickness for all applications. The footing dimensions are:

length = 2L = width = 2B = 18 ft

The embedment of the NE footing is:

D_{NE} = 3 ft

The embedment of the SW footing is:

D_{SW} = 4 ft - 2 in = 4.17 ft

Because the bedrock extends to great depths with presumably no change in elastic properties, the effective depth, h, need not be computed in this case.

Because Z $\geq$ 0.2, G is reduced by 50% to 100,000 ksf.

Eqn. (4.27 and 4.28):

$$K^o_{\theta x} = K^o_{\theta y} = \frac{8GR_x^3}{3(1 - \nu)} \qquad since\ R_x = R_y$$

$$= \frac{8(100{,}000\ ksf)(10.3\ ft)^3}{3(1 - 0.3)} \times \left(\frac{1{,}000\ lb}{1k}\right)$$

$$= 4.16 \times 10^{11}\ lb\text{-}ft$$

Values of α_i and β_i for L/B = 1 and D/R = 3/10.2 = 0.29 (NE footing) and D/R = 4.17/10.2 = 0.41 (SW footing) were read from Figures 4.12 and 4.13, and are summarized in Table 6.1 below[4]. Also listed in the table are the values of K_i^o and the final stiffnesses (K_i) computed for both footings. The stiffnesses, K_i, pertain to the top of the footing (Point 0) for the coordinate system shown in Figure 6.1.

[4]For square footings, $D/R \simeq D/R_x = D/R_y = D/R_z$; therefore, use D/R value to computer β_i.

Soil Model for FHWA Stiffness Calculation of Footings at Pier 2

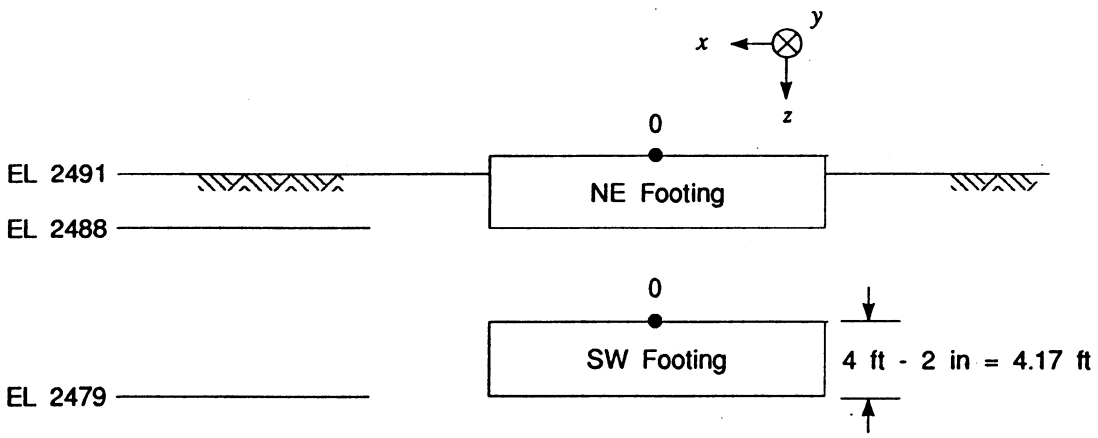

Adesite Bedrock: G = 200,000 ksf
ν = 0.3
γ = 150 pcf

NOTE

G is low strain shear modulus.

Figure 6.1

TABLE 6.1
CALCULATION OF PIER 2 FOOTING STIFFNESSES

	K_i^o	α_i	β_i		K_i	
			NE Footing	SW Footing	NE Footing	SW Footing
K_x(x 10^9 lb/ft)	4.80	1.02	1.42	1.55	6.95	7.59
K_y(x 10^9 lb/ft)	4.80	1.02	1.42	1.55	6.95	7.59
K_z(x 10^9 lb/ft)	5.83	1.03	1.15	1.20	6.91	7.21
$K_{\theta x}$(x 10^{11} lb-ft)	4.16	1.05	1.44	1.63	6.29	7.12
$K_{\theta y}$(x 10^{11} lb-ft)	4.16	1.05	1.44	1.63	6.29	7.12
$K_{\theta z}$(x 10^{11} lb-ft)	5.83	1.05	1.92	2.19	11.8	13.4

The table shows that the stiffnesses associated with the fully embedded footing (SW footing) are about 5-15% greater than those for the partially embedded footing (NE footing). Because each footing is square, the horizontal translational stiffnesses of a particular footing, K_x and K_y , are equal, and the rotational stiffnesses, $K_{\theta x}$ and $K_{\theta y}$, are also equal.

7.0 PIER 2 (FOOTING) STIFFNESS CALCULATION - NOVAK METHOD

7.1 SOIL MODEL

The description of the Pier 2 footings was given in Section 6.0; the footing-soil (bedrock) system was shown in Figure 6.1. The soil (bedrock) parameters and footing model for the Novak stiffness calculation are shown in Figure 7.1. The value of V_s was

Soil Model for Novak Stiffness Calculation of Footings at Pier 2

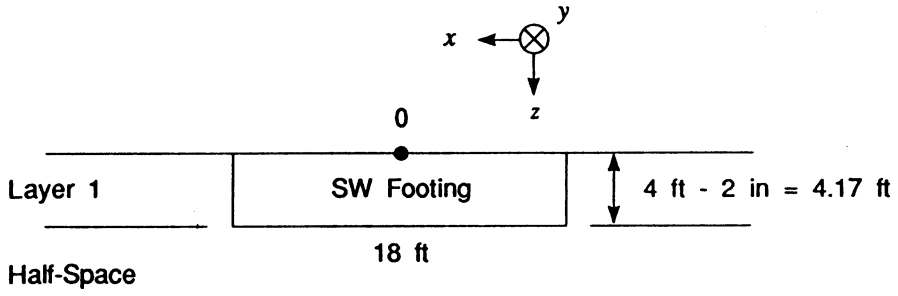

Soil Properties for Layer 1 and Half-Space are the same.

V_s = 4,633 fps ν = 0.3

γ = 150 pcf ξ = 0.03

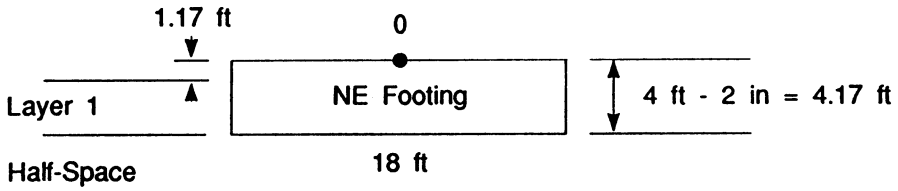

V_s = 4,633 fps ν = 0.3

γ = 150 pcf ξ = 0.03

NOTE

$V_s = \sqrt{G/\gamma_m}$ where: G = 10^8psf = 50% of value in Figure 6.1, and γ_m = mass density.

Figure 7.1

computed from the high strain shear modulus, G = 100,000 ksf. The damping ratio for the soil was assumed to be ζ = 0.03.

7.2 PREPARATION OF DYNA3 INPUT

The DYNA3 input files for the SW and NE footings at Pier 2 are listed in Tables 7.1 and 7.2, respectively. The inputs are self explanatory after reading the discussion of inputs for the Pier 1 stiffness calculation (Section 5.1.2). Note that the line, "CONSTANTS = 0., 0., 4.17," in both tables defines the location of the point (Point 0 in Figure 7.1) where the stiffnesses are computed[5].

7.3 DYNA3 OUTPUT

The DYNA3 output files for the SW and NE footings are listed in Tables 7.3 and 7.4, respectively. As with the Pier 1 example (Section 5.1.3), the values of CROSS-STIFFNESS (YZ PLANE) and CROSS-STIFFNESS (XZ PLANE) refer to $K_{y\theta x}$ and $K_{x\theta y}$, respectively.

[5]Novak's program can include the overburden soil directly above the top of a buried footing. However, consistent with the FHWA approach, this overburden is ignored, and the embedment is defined as the thickness of the footing.

```
TITLE=COLDWATER CREEK OVERCROSSING PIER 2 SW FOOTING [k ft s]
MATRIX                    | SPECIFY MATRIX OUTPUT OF STIFFNESS AND DAMPING
GRAVITY=32.2              | g
FOUNDATION=HALF-SPACE     | FOUNDATION TYPE
RECTANGULAR=18.,18.       | FOOTING DIMENSIONS
MASS=0,0,0,0,0,0,0        | MASS PROPERTIES OF FOUNDATION, NO EFFECT ON STIFFNI
CONSTANTS=0.,0.,4.17      | X, Y, Z OF Cg
SOIL
CONSTANTS=1               | # OF SOIL LAYERS
1 4.17 4632. .150 0.3 0.03 | SOIL PARAMETERS FOR LAYER 1: LAYER THICKNESS, Vs
                                                          GAMMA, NU, DAMPING
BELOW
4632. .150 0.3 0.03       | SOIL PROPERTIES BELOW FOOTING
LOAD=HARMONIC
CONSTANTS         | DEFINES MINIMAL LOAD, DOES NOT AFFECT STIFFNESS PROPERTIES
NONQUADRATIC
0.001  0.001  0.001  0.  0.  0.  0.  0.  0.
RUN
```

Table 7.1

```
TITLE=COLDWATER CREEK OVERCROSSING PIER 2 NE FOOTING [k ft s]
MATRIX                    | SPECIFY MATRIX OUTPUT OF STIFFNESS AND DAMPING
GRAVITY=32.2              | g
FOUNDATION=HALF-SPACE     | FOUNDATION TYPE
RECTANGULAR=18.,18.       | FOOTING DIMENSIONS
MASS=0,0,0,0,0,0,0        | MASS PROPERTIES OF FOUNDATION, NO EFFECT ON STIFFNESS
CONSTANTS=0.,0.,4.17      | X, Y, Z OF Cg
SOIL
CONSTANTS=1               | # OF SOIL LAYERS
1 3. 4632. .150 0.3 0.03  | SOIL PARAMETERS FOR LAYER 1: LAYER THICKNESS, Vs,
                                                         GAMMA, NU, DAMPING
BELOW
4632. .150 0.3 0.03       | SOIL PROPERTIES BELOW FOOTING
LOAD=HARMONIC
CONSTANTS         | DEFINES MINIMAL LOAD, DOES NOT AFFECT STIFFNESS PROPERTIES
NONQUADRATIC
0.001  0.001  0.001  0.  0.  0.  0.  0.  0.
RUN
```

Table 7.2

```
*************************************************
*                                               *
*        D Y N A 3   S I M U L A T I O N        *
*                                               *
*             RUN DATE -  1992/10/16            *
*             TIME     -  15:41:22              *
*             REVISION -  1991/07/30            *
*                                               *
*************************************************

COLDWATER CREEK OVERCROSSING PIER 2 SW FOOTING [k ft

                                    RESULTS
                                    *******


FREQUENCY  -     .0010
*********

STIFFNESS CONSTANTS (K)
***********************

HORIZONTAL TRANSLATION  (X) ...  6.21016E+06
HORIZONTAL TRANSLATION  (Y) ...  6.21016E+06
VERTICAL TRANSLATION  (Z) .....  6.46740E+06
ROTATION ABOUT  (X) ...........  6.42372E+08
ROTATION ABOUT  (Y) ...........  6.42372E+08
TORSION ABOUT  (Z) ............  1.13069E+09
CROSS-STIFFNESS (YZ PLANE) ....  2.29072E+07
CROSS-STIFFNESS (XZ PLANE) .... -2.29072E+07

DAMPING CONSTANTS (C)
*********************
HORIZONTAL TRANSLATION  (X) ...  1.86322E+08
HORIZONTAL TRANSLATION  (Y) ...  1.86322E+08
VERTICAL TRANSLATION  (Z) .....  1.94042E+08
ROTATION ABOUT  (X) ...........  1.92713E+10
ROTATION ABOUT  (Y) ...........  1.92713E+10
TORSION ABOUT  (Z) ............  3.39208E+10
CROSS-DAMPING  (YZ PLANE) .....  6.87267E+08
CROSS-DAMPING  (XZ PLANE) ..... -6.87267E+08
```

Table 7.3

```
**************************************************
*                                                *
*        D Y N A 3   S I M U L A T I O N         *
*                                                *
*             RUN DATE -  1992/10/16             *
*             TIME     -  15:41:14               *
*             REVISION -  1991/07/30             *
*                                                *
**************************************************

COLDWATER CREEK OVERCROSSING PIER 2 NE FOOTING [k ft s]

                                    RESULTS
                                    *******


FREQUENCY  -      .0010
*********


STIFFNESS CONSTANTS (K)
***********************

HORIZONTAL TRANSLATION  (X) ...  5.80791E+06
HORIZONTAL TRANSLATION  (Y) ...  5.80791E+06
VERTICAL TRANSLATION  (Z) .....  6.28016E+06
ROTATION ABOUT  (X) ...........  6.03417E+08
ROTATION ABOUT  (Y) ...........  6.03417E+08
TORSION ABOUT  (Z) ............  9.75605E+08
CROSS-STIFFNESS (YZ PLANE) ....  2.26719E+07
CROSS-STIFFNESS (XZ PLANE) .... -2.26719E+07

DAMPING CONSTANTS (C)
*********************
HORIZONTAL TRANSLATION  (X) ...  1.74252E+08
HORIZONTAL TRANSLATION  (Y) ...  1.74252E+08
VERTICAL TRANSLATION  (Z) .....  1.88422E+08
ROTATION ABOUT  (X) ...........  1.81027E+10
ROTATION ABOUT  (Y) ...........  1.81027E+10
TORSION ABOUT  (Z) ............  2.92681E+10
CROSS-DAMPING  (YZ PLANE) .....  6.80206E+08
CROSS-DAMPING  (XZ PLANE) ..... -6.80206E+08
```

Table 7.4

8.0 PIER 3 AND PIER 4 FOUNDATION STIFFNESSES

The FHWA and Novak methods were applied to Pier 3 and Pier 4. Because these pier foundations are similar to the Pier 1 and Pier 2 foundations, only the final results of the stiffness calculations are presented in Section 8.1 (Pier 3) and Section 8.2 (Pier 4). The stiffnesses are computed at the same point on the Pier 4 abutment (i.e., top of pile cap) and intermediate Pier 3 footing (i.e., top of footing) as in the Piers 1 and 2 stiffness calculations.

8.1 PIER 3 FOUNDATION STIFFNESSES

8.1.1 FHWA Method

The final Pier 3 foundation stiffnesses are summarized in Table 8.1 below. The coordinate system is defined as shown in Figure 6.1 for Pier 2. Both Pier 3 footings are 17.33 ft x 17.33 ft x 4.0 ft, and thus are slightly smaller than the Pier 2 footings. The Pier 3 footings are completely embedded in Andesite bedrock, the same material supporting the Pier 2 footings. Because the embedments ratio is identical for both Pier 3 footings, the stiffnesses are the same for both footings as shown in Table 8.1.

TABLE 8.1
PIER 3 FOOTING STIFFNESSES - FHWA METHOD

	NE Footing	SW Footing
K_x (x 10^9 lb/ft)	7.28	7.28
K_y (x 10^9 lb/ft)	7.28	7.28
K_z (x 10^9 lb/ft)	6.91	6.91
$K_{\theta x}$ (x 10^{11} lb-ft)	6.83	6.83
$K_{\theta y}$ (x 10^{11} lb-ft)	6.83	6.83
$K_{\theta z}$ (x 10^{11} lb-ft)	12.8	12.8

8.1.2 Novak Method

The DYNA3 output files for the SW and NE footings are listed in Tables 8.2 and 8.3, respectively. The coordinate system is defined as shown in Figure 7.1.

8.2 PIER 4 FOUNDATION STIFFNESSES

8.2.1 FHWA Method

The final Pier 4 foundation stiffness matrix is:

$$[K_t] = \begin{bmatrix} 2.56E8 & -5.84E7 & 0 & 0 & 0 & -3.90E98 \\ -5.84E7 & 6.00E8 & 0 & 0 & 0 & -1.91E8 \\ 0 & 0 & 1.21E8 & -1.37E8 & -2.85E6 & 0 \\ 0 & 0 & -1.37E8 & 1.36E11 & 1.17E10 & 0 \\ 0 & 0 & -2.85E6 & 1.17E10 & 6.38E10 & 0 \\ -3.90E8 & -1.91E8 & 0 & 0 & 0 & 1.47E10 \end{bmatrix}$$

```
**************************************************
*                                                *
*        D Y N A 3   S I M U L A T I O N         *
*                                                *
*              RUN DATE -  1992/10/16            *
*              TIME     -  15:41:48              *
*              REVISION -  1991/07/30            *
*                                                *
**************************************************

COLDWATER CREEK OVERCROSSING PIER 3 SW FOOTING [k ft

                                    RESULTS
                                    *******


FREQUENCY  -      .0010
*********


STIFFNESS CONSTANTS (K)
***********************

HORIZONTAL TRANSLATION  (X) ...   5.97392E+06
HORIZONTAL TRANSLATION  (Y) ...   5.97392E+06
VERTICAL TRANSLATION  (Z) .....   6.22430E+06
ROTATION ABOUT  (X) ...........   5.72197E+08
ROTATION ABOUT  (Y) ...........   5.72197E+08
TORSION ABOUT  (Z) ............   1.00726E+09
CROSS-STIFFNESS (YZ PLANE) ....   2.11453E+07
CROSS-STIFFNESS (XZ PLANE) .... -2.11453E+07

DAMPING CONSTANTS (C)
*********************
HORIZONTAL TRANSLATION  (X) ...   1.79234E+08
HORIZONTAL TRANSLATION  (Y) ...   1.79234E+08
VERTICAL TRANSLATION  (Z) .....   1.86748E+08
ROTATION ABOUT  (X) ...........   1.71661E+10
ROTATION ABOUT  (Y) ...........   1.71661E+10
TORSION ABOUT  (Z) ............   3.02177E+10
CROSS-DAMPING  (YZ PLANE) .....   6.34403E+08
CROSS-DAMPING  (XZ PLANE) ..... -6.34403E+08
```

Table 8.2

```
**************************************************
*                                                *
*        D Y N A 3   S I M U L A T I O N         *
*                                                *
*              RUN DATE -  1992/10/16            *
*              TIME     -  15:41:39              *
*              REVISION -  1991/07/30            *
*                                                *
**************************************************

COLDWATER CREEK OVERCROSSING PIER 3 NE FOOTING [k ft s]

                                    RESULTS
                                    *******


FREQUENCY  -     .0010
*********


STIFFNESS CONSTANTS (K)
***********************

HORIZONTAL TRANSLATION  (X) ...  5.97392E+06
HORIZONTAL TRANSLATION  (Y) ...  5.97392E+06
VERTICAL TRANSLATION  (Z) .....  6.22430E+06
ROTATION ABOUT  (X) ...........  5.72197E+08
ROTATION ABOUT  (Y) ...........  5.72197E+08
TORSION ABOUT  (Z) ............  1.00726E+09
CROSS-STIFFNESS (YZ PLANE) ....  2.11453E+07
CROSS-STIFFNESS (XZ PLANE) .... -2.11453E+07

DAMPING CONSTANTS (C)
*********************
HORIZONTAL TRANSLATION  (X) ...  1.79234E+08
HORIZONTAL TRANSLATION  (Y) ...  1.79234E+08
VERTICAL TRANSLATION  (Z) .....  1.86748E+08
ROTATION ABOUT  (X) ...........  1.71661E+10
ROTATION ABOUT  (Y) ...........  1.71661E+10
TORSION ABOUT  (Z) ............  3.02177E+10
CROSS-DAMPING  (YZ PLANE) .....  6.34403E+08
CROSS-DAMPING  (XZ PLANE) ..... -6.34403E+08
```

Table 8.3

The units are lb and ft. The coordinate system is defined as shown in Figure 8.1 with the origin at Point 0. Note that this global system is the same as the one for Pier 1 in Figure 4.1, although Pier 4 in Figure 8.1 is approximately a mirror image of Pier 1 in Figure 4.1.[6]

The computation of $[K_t] = [K_p] + [K_f] + [K_w]$ was straightforward; however, the computation of $[K_w]$ requires some explanation because the backfill behind the abutment wall consists of 2 soil layers (Figure 8.1). Because the FHWA method for computing $[K_w]$ assumes a single layer, homogeneous backfill, the 2-layered system in Figure 8.1 was converted to an equivalent single layer by calculating an average Youngs modulus $\overline{E_s}$ over the height of the wall using the general formula:

$$\overline{E_s} = \left(\sum_{i=1}^{n} h_i \, E_{si} \right) \Big/ \left(\sum_{i=1}^{n} h_i \right) \qquad (8.1)$$

where: H_i is the thickness of layer i bearing against the wall; E_{si} is the Youngs modulus for layer, i; and $\sum_{i=1}^{n} h_i = H_w$, the height of the wall.

[6]Piers 1 and 4 would be exact mirror images of each other in Figures 4.1 and 8.1 if the abutment wall heights and the soil profiles were identical at both piers.

Backfill Soil Properties at Pier 4 Abutment

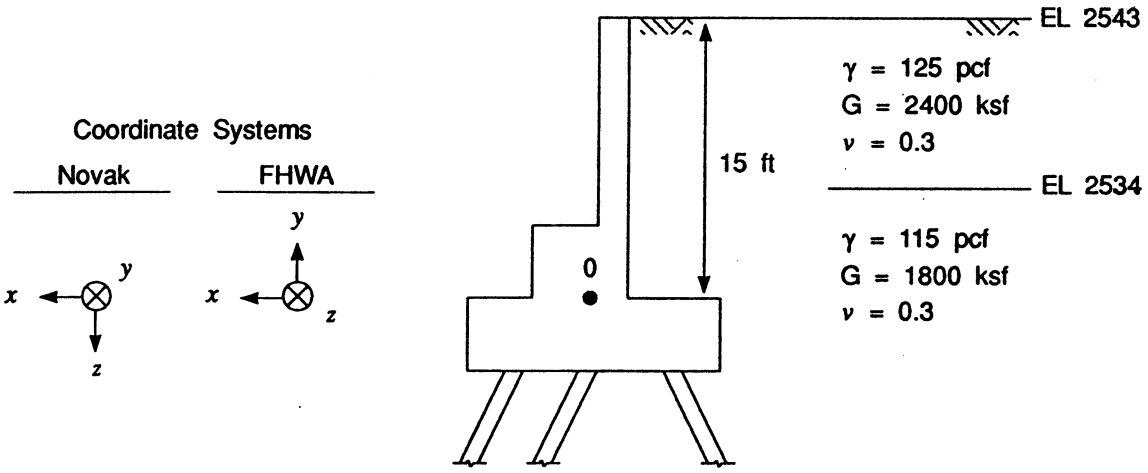

NOTES

G Low strain shear modulus

E Youngs Modulus = 2G(1+ν)

Figure 8.1

Referring to Figure 8.1,

h_1 = 9 ft

h_2 = 6 ft

E_{s1} = 6,240 ksf (low strain)

E_{s2} = 4,680 ksf (low strain)

Substituting these values into Eqn. (8.1) yielded $\overline{E_s}$ = 5,616 ksf. This value was reduced by 50% to obtain the high strain value. This high strain value (2,808 ksf) was used to compute $[K_w]$.

8.2.2 Novak Method

The final Pier 4 foundation stiffness matrix is:

$$[K_i] = \begin{bmatrix} 1.95E8 & 0 & 0 & 0 & -8.57E8 & 0 \\ 0 & 1.01E8 & 0 & 3.85E8 & 0 & 0 \\ 0 & 0 & 5.06E8 & 0 & 0 & 0 \\ 0 & 3.85E8 & 0 & 1.06E11 & 0 & 0 \\ -8.57E8 & 0 & 0 & 0 & 1.37E10 & 0 \\ 0 & 0 & 0 & 0 & 0 & 3.99E10 \end{bmatrix}$$

The units are lb and ft. The coordinate system is shown in Figure 8.1 with the origin at Point 0. Relative to the entire bridge, this coordinate system is oriented the same as the coordinate system in Figure 5.1 for Pier 1.

9.0 APPLICATION TO SEISAB-I BRIDGE ANALYSIS

This example illustrates the use of SEISAB-I in conducting a response spectrum dynamic analysis of the Coldwater Creek Bridge, to illustrate the application of methods presented in this report. The designer is assumed to have a working knowledge of SEISAB-I. The SEISABPC version of SEISAB-I with program updates through 1.3.3 was used for all analysis in this report.

The bridge is described in Section 1.0. In the example, Pier 1 abutment, Pier 2, Pier 3 and Pier 4 abutment are modeled in SEISAB-I analysis as Bent 2, 3, 4 and 5, respectively. The structure model is illustrated in Figure 9.1.

9.1 BENT 2 MODEL

In order to apply support stiffness [K] at the footing level and to model a free superstructure connection, it is necessary to model each abutment as a single column bent. The column section properties are calculated to model the abutment seat at each location. Since abutment items are required by SEISAB they are included but assigned zero stiffness.

The 5.25 inch gap and elastomeric bumper resisting longitudinal load at each abutment is idealized as an elastic bearing element located at the top of the bent column. The bearing longitudinal shear stiffness KFIF1 is determined by trial to output the longitudinal shear force required to provide longitudinal displacement of the bearing compatible with the actual inelastic condition. The bearing displacement is determined as the product of the longitudinal shear force (Column Top Longitudinal Shear, LC 3) and the input stiffness KFIF1.

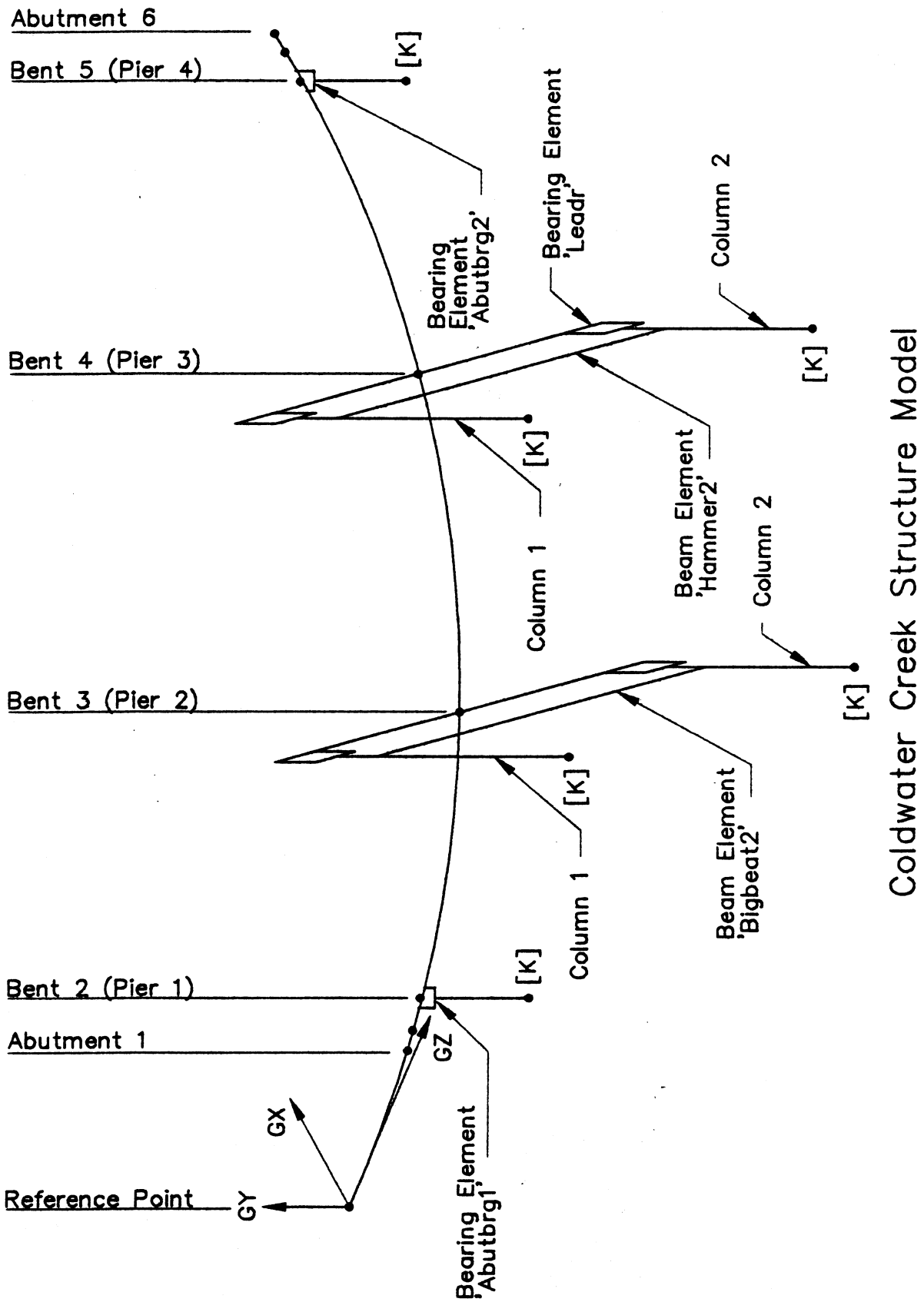
Abutment 6
Bent 5 (Pier 4)
Bent 4 (Pier 3)
Bent 3 (Pier 2)
Bent 2 (Pier 1)
Abutment 1
Reference Point
GX
GY
GZ
[K]
Bearing Element 'Abutbrg2'
Bearing Element 'Leadr'
Column 2
Column 1
Beam Element 'Hammer2'
Beam Element 'Bigbeat2'
Bearing Element 'Abutbrg1'
Coldwater Creek Structure Model

Figure 9.1

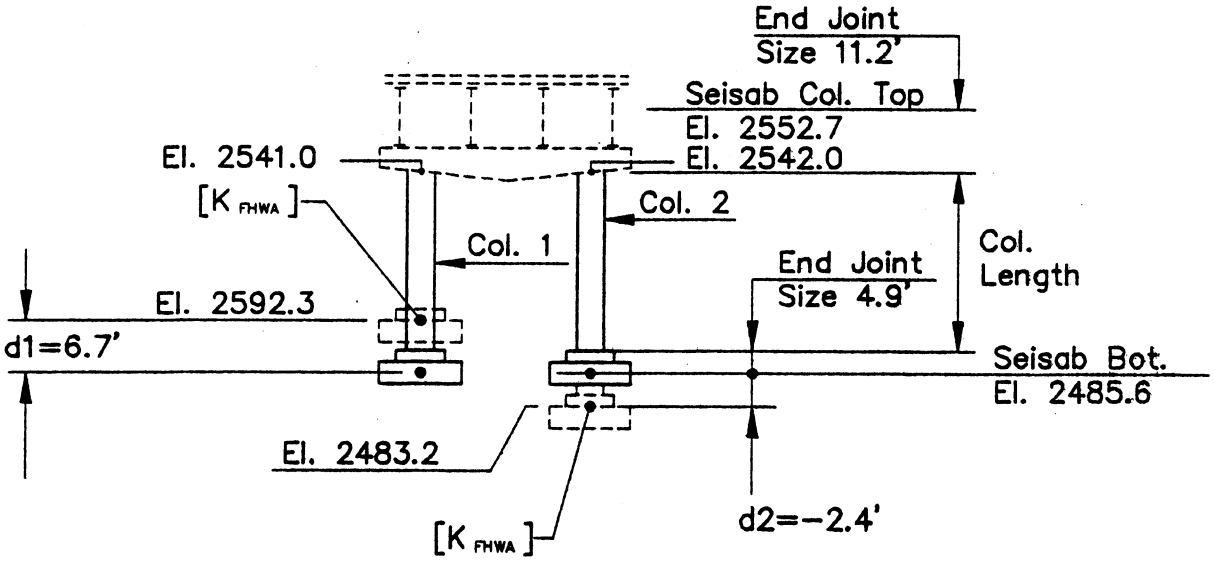

Bent 3 (Pier 2)

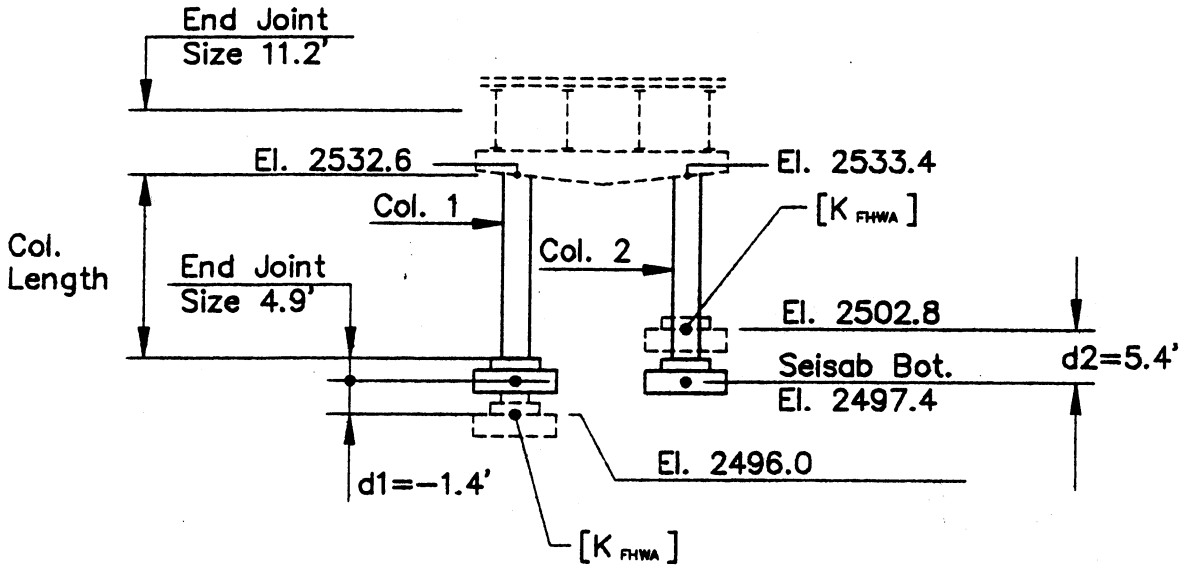

Bent 4 (Pier 3)

Figure 9.2

The foundation stiffness matrix $[K_t]$ given in Section 4.4.2 is in the GPILE coordinate system. The units are lb and ft.

$$[K_t] = \begin{bmatrix} 2.57E8 & 5.68E7 & 0 & 0 & 0 & -3.85E8 \\ & 5.85E8 & 0 & 0 & 0 & 1.86E8 \\ & & 1.17E8 & -1.22E8 & 2.55E6 & 0 \\ \text{symmetrical} & & & 1.34E11 & -1.14E10 & 0 \\ & & & & 6.25E10 & 0 \\ & & & & & 1.41E10 \end{bmatrix}$$

Converting to the SEISAB-I coordinate system by reversing signs on X and Z values and changing from lb to kip units, the SEISAB-I input stiffness matrix for model Bent 2 is:

$$[K_{SEISAB}] = \begin{bmatrix} 2.27E5 & -5.68E7 & 0 & 0 & 0 & -3.85E5 \\ -5.68E7 & 5.85E5 & 0 & 0 & 0 & -1.86E5 \\ & & 1.17E5 & -1.22E5 & -2.55E3 & 0 \\ \text{symmetrical} & & & 1.34E8 & 1.14E7 & 0 \\ & & & & 6.25E7 & 0 \\ & & & & & 1.14E7 \end{bmatrix}$$

9.2 BENT 3 MODEL

Base isolation bearings supporting each girder at the bridge piers are combined and modeled as bearing elements positioned at the top of each bent column. SEISAB-I allows only column top bearing locations. The bent cap, positioned above the bearing in the model, is represented as a "Special Cap" and, therefore, displaces with the superstructure. Beam elements are added between columns near the top of each bent to model the actual column restraint provided by the pier cap.

In order to model equal column lengths at a given bent, a SEISAB-I requirement, section properties for each column are modified to yield actual column stiffnesses while maintaining one average length. Each foundation stiffness matrix [K_f] must be converted to the SEISAB-I coordinate system and transformed in position vertically to the center of the model footing. Figure 9.2 shows relative locations of column footings.

The foundation stiffness matrix [K_f] for Bent 3 Col 1 (Pier 2 NE Footing) is given in Table 6.1 and designated below as [K_{FHWA}]. The stiffness matrix is first converted from FHWA coordinate system to SEISAB-I coordinate system using method given in Appendix C-1.

$$[K_{FHWA}] = \begin{bmatrix} 6.95E9 & 0 & 0 & 0 & 0 & 0 \\ & 6.95E9 & 0 & 0 & 0 & 0 \\ & & 6.91E9 & 0 & 0 & 0 \\ \text{symmetrical} & & & 6.29E11 & 0 & 0 \\ & & & & 6.29E11 & 0 \\ & & & & & 11.8E11 \end{bmatrix}$$

$$[K_{SEISAB}] = \begin{bmatrix} 6.95E9 & 0 & 0 & 0 & 0 & 0 \\ & 6.91E9 & 0 & 0 & 0 & 0 \\ & & 6.95E9 & 0 & 0 & 0 \\ \text{symmetrical} & & & 6.29E11 & 0 & 0 \\ & & & & 11.8E11 & 0 \\ & & & & & 6.29E11 \end{bmatrix}$$

The stiffnesses are calculated at the top of each actual footing and, therefore, must be transformed in position vertically to the center of the modeled column footings. The rigid body transformation derivation is included in Appendix C-3. The resulting transformed stiffness matrix is now developed for h = 6.7 ft.

$$[K_{SEISAB}] = \begin{bmatrix} 6.95E9 & 0 & 0 & 0 & -6.7(6.95E9) & 0 \\ & 6.91E9 & 0 & 6.7(6.91E9) & 0 & 0 \\ & & 6.95E9 & 0 & 0 & 0 \\ & & & (6.7)^2 6.91E9 + 6.29E11 & 0 & 0 \\ & & & & (6.7)^2 6.95E9 + 11.8E11 & 0 \\ & & & & & 6.29E11 \end{bmatrix}$$

After converting from lb to kip units, the SEISAB-I input stiffness matrix for Model Bent 3 Column 1 is:

$$[K_{SEISAB}] = \begin{bmatrix} 6.95E6 & 0 & 0 & 0 & -4.66E7 & 0 \\ & 6.91E6 & 0 & 4.63E7 & 0 & 0 \\ & & 6.95E6 & 0 & 0 & 0 \\ & & & 9.39E8 & 0 & 0 \\ & & & & 1.49E9 & 0 \\ & & & & & 6.29E8 \end{bmatrix}$$

Similarly, the model transformed stiffness matrix for Bent 3 Column 2 is developed.

$$[K_{FHWA}] = \begin{bmatrix} 7.59E9 & 0 & 0 & 0 & 0 & 0 \\ & 7.59E9 & 0 & 0 & 0 & 0 \\ & & 7.21E9 & 0 & 0 & 0 \\ \text{symmetrical} & & & 7.12E11 & 0 & 0 \\ & & & & 7.12E11 & 0 \\ & & & & & 13.4E11 \end{bmatrix}$$

$$[K_{SEISAB}] = \begin{bmatrix} 7.59E9 & 0 & 0 & 0 & 0 & 0 \\ & 7.21E9 & 0 & 0 & 0 & 0 \\ & & 7.59E9 & 0 & 0 & 0 \\ \text{symmetrical} & & & 7.12E11 & 0 & 0 \\ & & & & 13.4E11 & 0 \\ & & & & & 7.12E11 \end{bmatrix}$$

Transform restraint to mid-depth of Ftg h = h_2 = - 2.4 ft.

$[K_{SEISAB}]$ = MID-DEPTH FOOTING

7.59E9	0	0	0	2.4(7.59)E9	0
	7.21E9	0	-2.4(7.21)E9	0	0
		7.59E9	0	0	0
symmetrical			$(2.4)^2$7.21E9 +7.12E11	0	0
				$(2.4)^2$7.59E9 +13.4E11	0
					7.12E11

After converting from lb to kip units, the SEISAB-I input stiffness matrix for Model Bent 3 Column 2 is:

$[K_{SEISAB}]$ = MID-DEPTH FOOTING

7.59E6	0	0	0	1.82E7	0
	7.21E6	0	-1.73E7	0	0
		7.59E6	0	0	0
symmetrical			7.54E8	0	0
				1.38E9	0
					7.12E8

9.3 BENT 4 MODEL

Following are the SEISAB-I input stiffness matrices for Model Bent 4 foundations.

Bent 4 Column 1

$[K_{SEISAB}]$ = MID-DEPTH FOOTING

7.28E6	0	0	0	1.02E7	0
	6.91E6	0	-9.67E6	0	0
		7.28E6	0	0	0
symmetrical			1.35E7	0	0
				1.29E9	0
					6.83E8

Bent 4 Column 2

$$[K_{SEISAB}] = \text{MID-DEPTH FOOTING}$$

$$\begin{bmatrix} 7.28E6 & 0 & 0 & 0 & -3.93E7 & 0 \\ & 6.91E6 & 0 & 3.73E7 & 0 & 0 \\ & & 7.28E6 & 0 & 0 & 0 \\ \text{symmetrical} & & & 8.85E8 & 0 & 0 \\ & & & & 1.49E9 & 0 \\ & & & & & 6.29E8 \end{bmatrix}$$

9.4 BENT 5 MODEL

The SEISAB-I input stiffness matrix for Model Bent 5 foundation is developed using methods described for Model Bent 2.

$$[K_{SEISAB}] =$$

$$\begin{bmatrix} 2.58E5 & -5.84E4 & 0 & 0 & 0 & -3.90E5 \\ & 6.01E5 & 0 & 0 & 0 & -1.91E5 \\ & & 1.22E5 & -1.37E5 & -2.85E3 & 0 \\ \text{symmetrical} & & & 1.39E8 & 1.17E7 & 0 \\ & & & & 6.00E7 & 0 \\ & & & & & 1.48E7 \end{bmatrix}$$

9.5 LOAD MODEL

The RESPONSE SPECTRUM must be input using the SEISAB ARBITRARY CURVE option in order to include the effect of damping of base isolation bearings. The isolation modes are the first 2 primary modes. The response spectrum used in this example was supplied by WSDOT. Spectrum modification discussed in Task 1 Report, Section 6.2 is not required because the total length of the bridge is greater than 250 ft.

9.6 DISCUSSION OF THE INPUT FILE

The default units used in this example are kips, feet, seconds and radians.

The abutment-to-superstructure connections are specified as FIXED. To release the abutments and transfer all abutment forces to the dummy replacement bent, all abutment foundation spring values are set to zero in the FOUNDATION block.

The bent-to-superstructure connections are specified as FIXED by default.

All column tops are specified as FREE in order to activate BEARING ELEMENTS located at the top of each column.

COLUMN TOP JOINT SIZE is specified to provide a rigid element from the top of each model column (superstructure centroid) to the top of each actual column so that true column stiffness is represented.

9.7 DISCUSSION OF THE OUTPUT FILE

Several iterative runs with varying BEARING KFIF1 stiffnesses were required to match the model displacement of bearing elements at Bent 2 and Bent 5 to the nonlinear displacement of the actual gap and bumper. Results of each run were checked to:

1. Ascertain that the specified number of modes was found.
2. Confirm that output displacement matches that used to estimate KFIF1.
3. Ascertain that the period of the first longitudinal and transverse modes fall within the isolated region of the response spectrum.

EXAMPLE NO. 2

DEADWATER SLOUGH BRIDGE

TABLE OF CONTENTS

Section — Page

1.0 DESCRIPTION OF BRIDGE AND FOUNDATION SOILS 1

2.0 SEISMIC DESIGN PARAMETERS 1

3.0 SOIL PROPERTIES 2

4.0 PIER 1 STIFFNESS CALCULATION - FHWA METHOD 2
- 4.1 PILE-STIFFNESS CALCULATION 3
  - 4.1.1 Estimation of Pile Parameters 4
  - 4.1.2 Computation of t-z Curves 5
    - 4.1.2.1 General Procedure 5
    - 4.1.2.2 Application to Deadwater Slough Bridge Abutment Piles. 5
  - 4.1.3 Computation of Q-z Curve 7
    - 4.1.3.1 General Procedure 7
    - 4.1.3.2 Application to Deadwater Slough Bridge Abutment Piles 7
  - 4.1.4 Computation of p-y Curves 9
    - 4.1.4.1 General Procedure 9
    - 4.1.4.2 Application to Deadwater Slough Bridge Abutment Piles 9
  - 4.1.5 Preparation of BMCOL-76 Input 11
  - 4.1.6 BMCOL-76 Output 11
  - 4.1.7 Calculation of Pile-Head Stiffnesses 11
  - 4.1.8 Calculation of Pile-Group Stiffness Matrix 12
    - 4.1.8.1 Assumptions 12
    - 4.1.8.2 Preparation of GPILE Input 12
    - 4.1.8.3 GPILE Output 12
- 4.2 ABUTMENT FOOTING STIFFNESSES 13
  - 4.2.1 Model and Assumptions 13
  - 4.2.2 Calculation of Footing Stiffnesses 13
    - 4.2.2.1 General Procedure. 13
    - 4.2.2.2 Application to Deadwater Slough Abutment Footing. 13
- 4.3 ABUTMENT WALL STIFFNESS 16
  - 4.3.1 Model and Assumptions 16
  - 4.3.2 Calculation of Wall Stiffnesses 17
    - 4.3.2.1 General Procedure. 17
    - 4.3.2.2 Application to Deadwater Slough Abutment Wall. 17
- 4.4 TOTAL ABUTMENT STIFFNESS MATRIX 18
  - 4.4.2 Application to Deadwater Slough Abutment. 19

TABLE OF CONTENTS (Continued)

Section	Page
5.0 PIER 1 STIFFNESS CALCULATION - NOVAK METHOD	20
5.1 PILE AND FOOTING SIDE STIFFNESS	21
5.1.1 Soil Model	21
5.1.2 Preparation of DYNA3 Input	21
5.1.3 DYNA3 Output	23
5.2 ABUTMENT WALL STIFFNESS	23
5.3 TOTAL PIER 1 STIFFNESS MATRIX	23
6.0 PIER 2 STIFFNESS CALCULATION - FHWA METHOD	25
6.1 PILE STIFFNESS CALCULATION	26
6.1.1 Preparation of BMCOL-76 Input	28
6.1.2 BMCOL-76 Output	28
6.1.3 Calculation of Pile Head Stiffnesses	29
7.0 PIER 2 STIFFNESS CALCULATION - NOVAK METHOD	30
7.1 SOIL MODEL	30
7.2 PREPARATION OF DYNA3 INPUT	30
7.3 DYNA3 OUTPUT	30
8.0 PIER 3 AND PIER 4 FOUNDATION STIFFNESSES	31
8.1 PIER 3 FOUNDATION STIFFNESSES	31
8.1.1 FHWA Method	31
8.1.2 Novak Method	32
8.2 PIER 4 FOUNDATION STIFFNESSES	33
8.2.1 FHWA Method	33
8.2.2 Novak Method	33

9.0 APPLICATION TO SEISAB-I BRIDGE ANALYSIS 37
9.1 ABUTMENT 1 MODEL 37
9.1.1 FHWA Method 37
9.1.2 Novak Method 38
9.2 BENT 2 MODEL 38
9.2.1 FHWA Method 38
9.2.2 Novak Method 39
9.3 BENT 3 AND ABUTMENT 4 MODELS 40
9.3.1 FHWA Method 40
9.3.2 Novak Method 40
9.4 LOAD MODEL 40

1.0 DESCRIPTION OF BRIDGE AND FOUNDATION SOILS

The Deadwater Slough Bridge is a 3-span, slightly-curved, prestressed concrete-girder bridge approximately 220 feet long (Figure 1.1). The monolithic abutments (Piers 1 and 4) at the ends of the bridge (Figure 1.2) are each supported by one row of seven vertical, 2' diameter, cylindrical concrete piles with a tubular steel casing. The piles (Figure 1.3) penetrate through a soft to medium stiff clay overlying medium dense to dense silty fine sand. The piles, which are about 45 feet long at Pier 1 and about 60 feet long at Pier 4, are embedded in a concrete pile cap, 4' wide x 3' thick, which supports a small abutment approximately 5' high and 4' thick. The concrete girders are placed in the abutment as shown in Figure 1.2.

Each of the two intermediate bents (Piers 2 and 3) consists of a reinforced concrete cross beam supporting the girders (Figure 1.4). This cross beam in turn is supported by seven vertical, 2' diameter reinforced concrete columns. The columns extend into soils similar to those at the abutments. The subsurface portions of the columns (piles) are encased with tubular steel, 3/8" thick. The piles extend to depths of approximately 33 ft (Pier 2) and 50 ft (Pier 3).

2.0 SEISMIC DESIGN PARAMETERS

The ground acceleration coefficient for the seismic design of the Deadwater Slough Bridge was 0.25. The appropriate soil category was Soil Type II, which is deep stiff soil over bedrock. The ATC-6, 5% damped response spectrum (Figure 2.1) for this soil type was normalized to 0.25 g and was used in the dynamic response analysis of the bridge by WSDOT. This same spectrum will be used in the example problem presented herein for the bridge. The spectrum will be modified where appropriate to account for the 7½ % damping recommended for those modes of vibration where soil-structure interaction is significant.

CURVE DATA						
PI STATION	Δ	RADIUS	TANGENT	LENGTH	BK. TANGENT	S
HA 42+63.74	82°56'05"LT.	550.00'	486.04'	796.12'	N83°58'43"E	0.08'/FT.

T. 29 N., R. 5 E., W.M.

SR 2

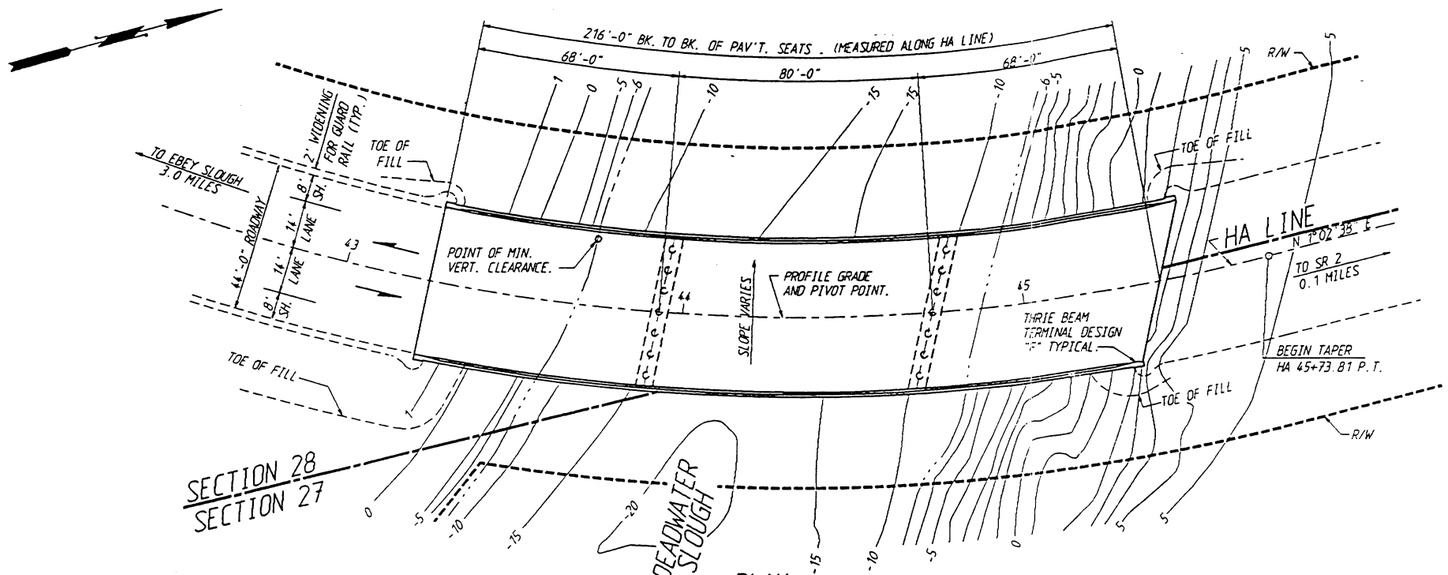

PLAN

BEARINGS OF ALL PIERS IS N 63°02'08" W FOR EMBANKMENT DETAILS AT BRIDGE ENDS. SEE ST'D. PLAN H-9.

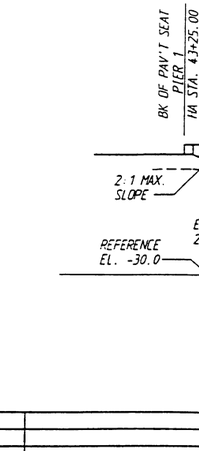

HA LINE PROFILE

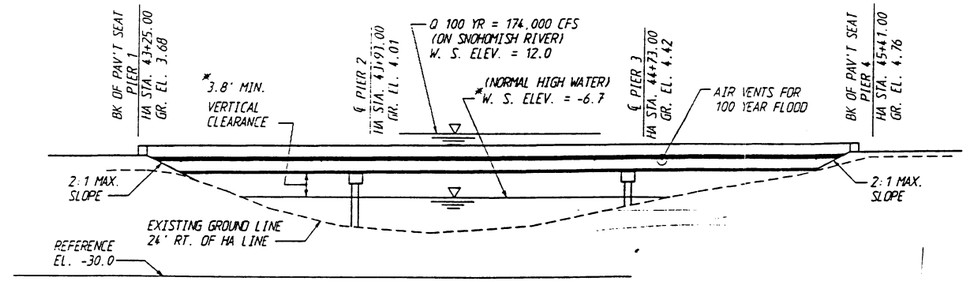

ELEVATION

GRADE ELEVATIONS SHOWN ARE FINISH GRADES AT TOP OF ROADWAY SLAB ON HA LINE AND ARE EQUAL TO PROFILE GRADE.
Q 500 YR = 243,900 CFS (ON SNOHOMISH RIVER) W.S. ELEV. 14.0
* WATER SURFACE ELEVATION IS DEPENDENT ON DIKE DISTRICT PUMPING.

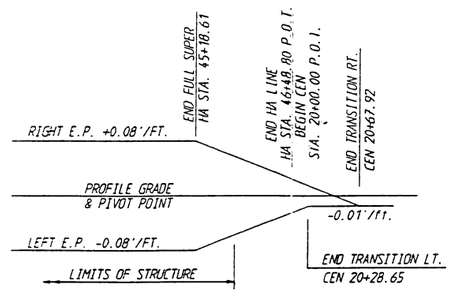

SUPERELEVATION DIAGRAM

DATUM

NATL. GEOD. VERT. DATUM OF 1929

GENERAL NOTES

1. ALL MATERIAL AND WORKMANSHIP SHALL BE IN ACCORDANCE WITH THE REQUIREMENTS OF THE STATE OF WASHINGTON DEPARTMENT OF TRANSPORTATION STANDARD SPECIFICATIONS FOR ROAD
2. THIS STRUCTURE HAS BEEN DESIGNED IN ACCORDANCE WITH THE REQUIREMENTS OF THE 1989 AASHTO STANDARD SPECIFICATIONS AND INTERIMS THROUGH 1991 FOR HIGHWAY BRIDGES. ALL PRESTRESSED CONCRETE ELEMENTS HAVE BEEN DESIGNED FOR SERVICE LOAD STRESSES AND CHECKED FOR THE REQUIREMENTS OF LOAD FACTOR DESIGN. ALL OTHER STRUCTURAL ELEMENTS ARE DESIGNED IN ACCORDANCE WITH THE REQUIREMENTS FOR LOAD FACTOR DESIGN.
3. SEISMIC DESIGN OF THIS STRUCTURE CONFORMS WITH THE PROVISIONS OF THE AASHTO GUIDE SPECIFICATIONS FOR SEISMIC DESIGN OF HIGHWAY BRIDGES, DATED 1983 AND INTERIMS THROUGH 1991. AN ACCELERATION COEFFICIENT OF 0.25 HAS BEEN USED.
4. FOOTING ELEVATIONS AND SUBSTRUCTURE DETAILS ARE SUBJECT TO CHANGE, DEPENDING UPON FOUNDATION MATERIAL ENCOUNTERED. REINFORCING STEEL FOR FOOTINGS, ABUTMENT WALLS AND COLUMNS SHALL NOT BE CUT UNTIL FINAL ELEVATIONS HAVE BEEN DETERMINED AND SUBSTRUCTURE DETAILS HAVE BEEN MODIFIED.
5. THE CONCRETE IN THE SEALS AND SHAFTS SHALL BE CLASS 4000W. THE CONCRETE IN THE SUPERSTRUCTURE INCLUDING ROADWAY DECK AND CROSSBEAMS SHALL BE CLASS 5000. ALL OTHER CONCRETE SHALL BE CLASS 4000.
6. ALL STEEL CASINGS FOR CONCRETE PILING SHALL BE DRIVEN TO A MINIMUM PILE TIP ELEVATION AS REQUIRED TO MEET THE PILE CAPACITY TABULATED ON BRIDGE SHEET 14, THE MAXIMUM DESIGN AXIAL LOADS ARE AT THE TOP OF THE PILES.
7. FALSEWORK SHALL BE CAREFULLY RELEASED TO PREVENT IMPACT OR UNDUE STRESS IN THE STRUCTURE.
8. ALL STEEL SHALL BE AASHTO M 183 AND GALVANIZED AFTER FABRICATION ACCORDING TO AASHTO M 111, UNLESS NOTED OTHERWISE.
9. ALL BOLTS EXCEPT AS NOTED SHALL BE AASHTO M 164 AND SHALL HAVE STANDARD NUTS AND WASHERS AND GALVANIZED ACCORDING TO AASHTO M 232. ALL SCREWS AND MISCELLANEOUS FASTENERS SHALL BE ASTM A 307 AND GALVANIZED ACCORDING TO AASHTO M 232.
10. ALL BOLT HOLE SIZES SHALL BE 1/16" DIAMETER LARGER THAN BOLT DIAMETER. BOLT LENGTHS NOT SHOWN SHALL BE AS REQUIRED TO FIT.
11. UNLESS OTHERWISE SHOWN ON THE PLANS, CONCRETE COVER MEASURED FROM THE FACE OF THE CONCRETE TO THE FACE OF ANY REINFORCEMENT BAR SHALL BE 2 1/2" AT THE TOP OF THE ROADWAY SLAB, 1" AT THE BOTTOM OF THE ROADWAY SLAB, 2 1/2" AT THE BOTTOM OF FOOTING AND 1 1/2" AT ALL OTHER LOCATIONS.

P.C. GIRDERS (W50G)
CONTINUOUS FOR LIVE LOAD
LOADING HS-25
OR
TWO 24K AXLES 4' CTRS

Bridge Design Engr.					REGION NO.	STATE	FED. AID PROJ. NO.	SHEET NO.	TOTAL SHEETS
Supervisor					10	WASH.			
Designed By R.L. LIPTAK 4/92					JOB NUMBER				
Checked By J. KAPUR 4/92									
Detailed By JCE (AGA INC), REL 4/92									
Bridge Projects Engr. K.N. KIRKER 12-91									
Prelim. Plan By G.E.C.MINNS 11-92									
Architect/Specialist R. MAYS 12-91	DATE	REVISION	BY	APP'D					

BRIDGE AND STRUCTURES

ALLAN H. WALLEY — STATE OF WASHINGTON — 12347 — REGISTERED PROFESSIONAL ENGINEER — EXPIRES 12/15/93

DEADWATERROOT:\FGB\LAYOUT.FGB:1 09-JUN-92

Washington State Department of Transportation

LAYOUT

BRIDGE SHEET NO. 1

SHEET OF SHEETS

C.S.3106.PROJ. NO. L0666B.DIST. NO. 1.SNOHOMISH RIVER TO EBEY SLOUGH EAST BOUND BRIDGE REPL. STAGE 2.DEADWATER SLOUGH (HA LINE)

Figure 1.1

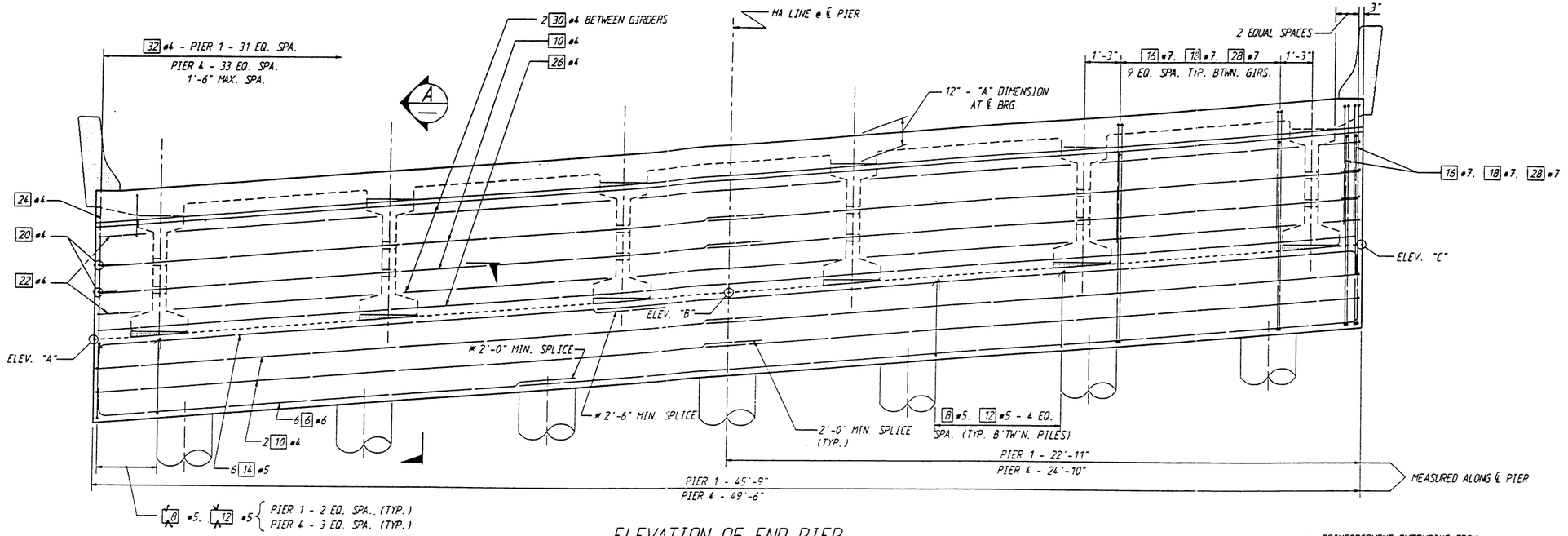

ELEVATION OF END PIER

PIER 1 SHOWN - PIER 4 SIMILAR AS NOTED LOOKING BACK ON STA.
* ALTERNATE LOCATION OF SPLICE

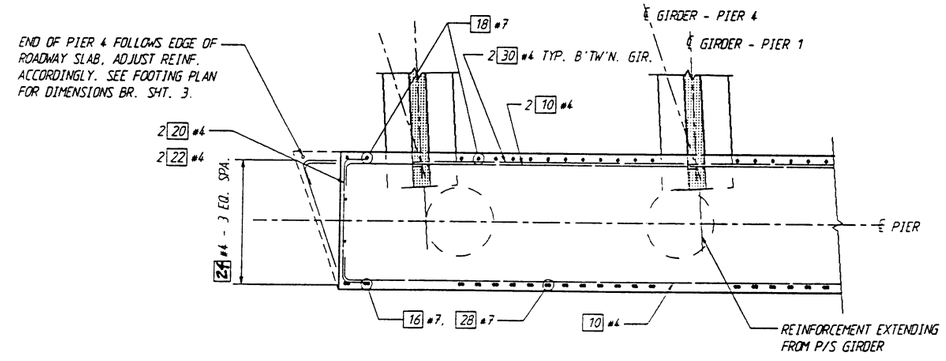

SECTION (B)

ELEVATIONS ALONG ℄ PIER

PIER #	"A"	"B"	"C"
1	-3.44	-1.61	0.22
4	-2.01	-0.54	1.11

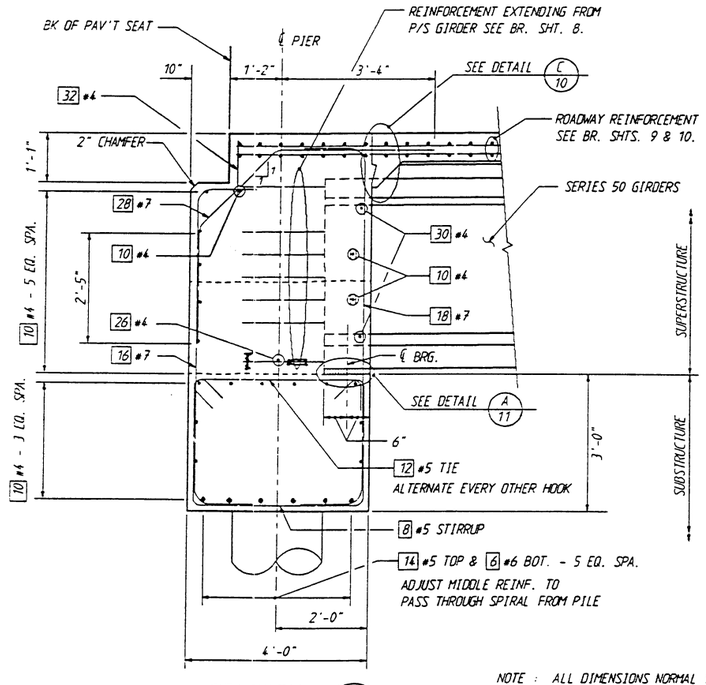

SECTION (A) PIERS 1 & 4

NOTE : ALL DIMENSIONS NORMAL TO ℄ PIER.

Design Engr.					REGION NO.	STATE	FED. AID PROJ. NO.	SHEET NO.	TOTAL SHEETS	BRIDGE AND STRUCTURES
Supervisor					10	WASH.				
Designed By R.E. LIPTAK 4/92					JOB NUMBER					
Checked By J. KAPUR 4/92										
Detailed By B.H. CREWS 4/92										
Bridge Projects Engr.										
Quantities Plan By										
Architect/Specialist	DATE	REVISION	BY	APP'D						

ALLAN H. WALLEY — STATE OF WASHINGTON — 1934 — REGISTERED PROFESSIONAL ENGINEER — EXPIRES 12/13/93

DEADWATERROOT:\FGB\PIER_1-4.FGB;1 11-JUN-92

Washington State Department of Transportation

PIERS 1 & 4

BRIDGE SHEET NO. 5 — SHEET OF SHEETS

Figure 1.2

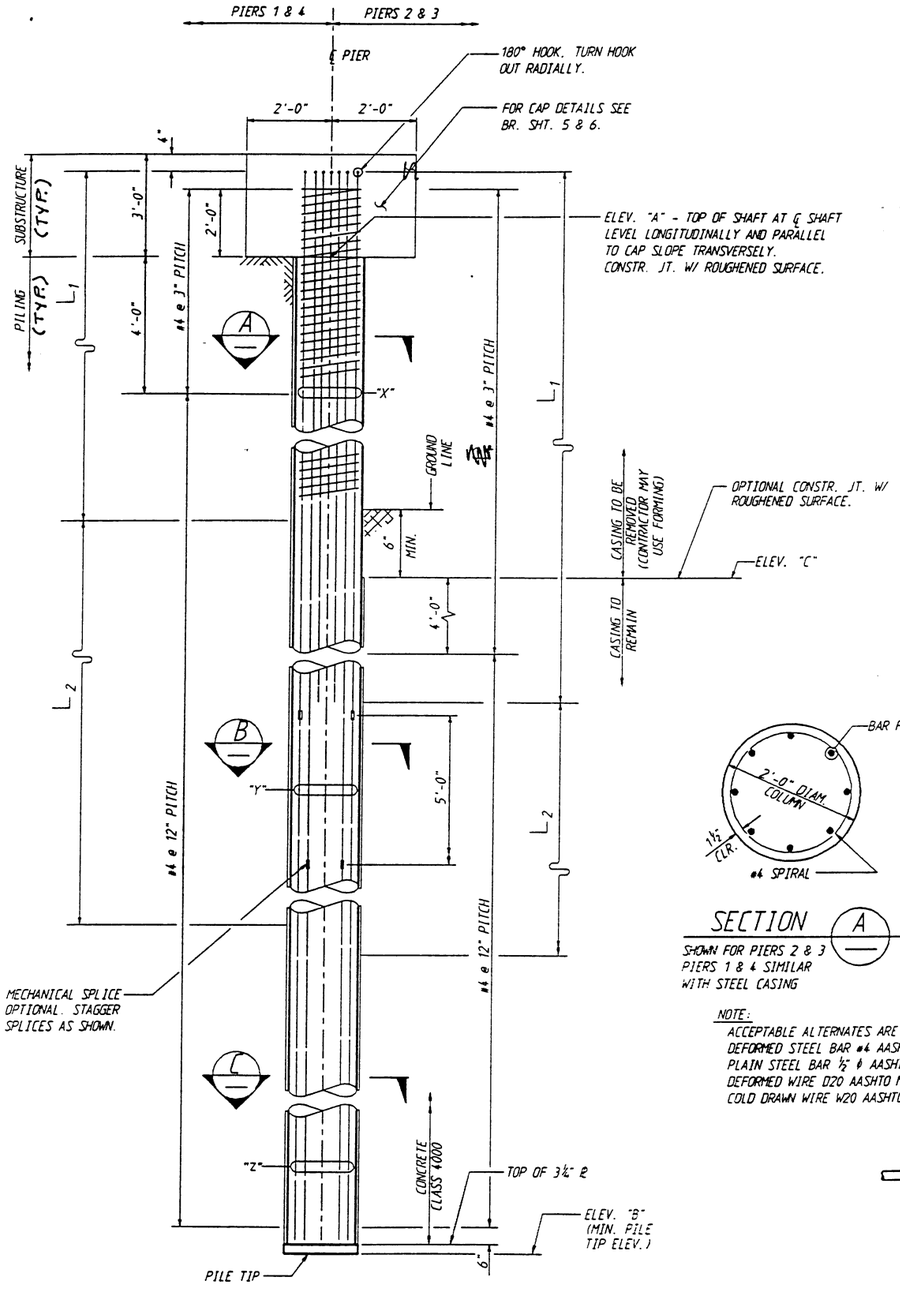

TYPICAL ELEVATION

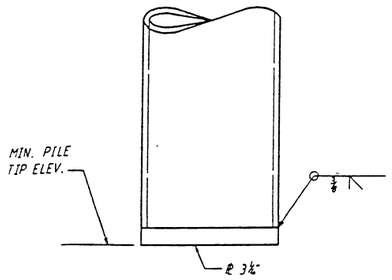

STANDARD PILE TIP DETAIL

* PIER		BAR F SIZE	BAR F NO. OF BARS X	Y	Z	L_1	L_2	ELEVATIONS A	B	C	REQUIRED PILE CAPACITY (TONS)
1	A	8	8	6	4			-6.17		-	
	B							-5.65		-	
	C							-5.13		-	
	D							-4.61		-	
	E							-4.09		-	
	F							-3.57		-	
	G							-3.05		-	
2 **	A							-5.81		-15.5	
	B							-5.30			
	C							-4.79			
	D							-4.28			
	E							-3.77			
	F							-3.25			
	G							-2.74			
3 **	A							-5.35		-10.5	
	B							-4.90			
	C							-4.37			
	D							-3.88			
	E							-3.38			
	F							-2.89			
	G							-2.40			
4	A							-4.72		-	
	B							-4.34			
	C							-3.95			
	D							-3.54			
	E							-3.14			
	F							-2.71		-	
	G							-2.27			

* PILE ORIENTATION IS LOOKING AHEAD ON STATION, LEFT TO RIGHT.
** CONTRACTOR TO VERIFY THAT ELEV. "C" IS A MINIMUM OF 6" BELOW NATURAL GROUND.

SECTION A

SHOWN FOR PIERS 2 & 3
PIERS 1 & 4 SIMILAR
WITH STEEL CASING

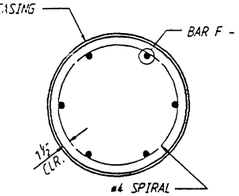

SECTION B

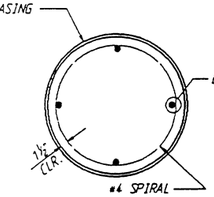

SECTION C

NOTE:
ACCEPTABLE ALTERNATES ARE
DEFORMED STEEL BAR #4 AASHTO M31 GR. 60
PLAIN STEEL BAR ½" ϕ AASHTO M31 GR. 60
DEFORMED WIRE D20 AASHTO M225
COLD DRAWN WIRE W20 AASHTO M32

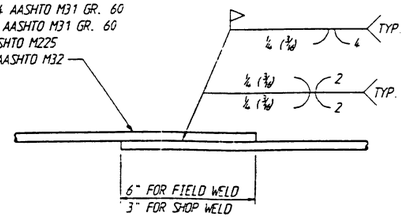

SPIRAL WELD DETAIL

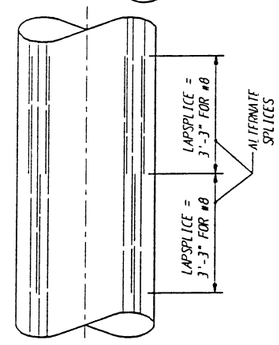

ALTERNATE LAPSPLICE DETAIL

NOTES:

1. SPLICE LOCATIONS:

   WITHIN 45 FEET OF ELEV. "A". LAP SPLICES FOR SPIRAL REINFORCEMENT WILL NOT BE ALLOWED IN THE TOP 15 FEET OR THE BOTTOM 25 FEET.

2. PILES SHALL BE DRIVEN TO A LOAD BEARING CAPACITY AS LISTED IN THE TABLE.

Bridge Design Engr.					DESIGN NO.	STATE	FED. AID PROJ. NO.	SHEET NO.	TOTAL SHEETS	BRIDGE AND STRUCTURES	DEADWATERROOT:\FGB\PILE_DETAILS.FGB; 1 09-JUN-92
Supervisor					10	WASH.					Washington State Department of Transportation
Designed By R.E. LIPTAK 4/92					JOB NUMBER						PILE DETAILS
Checked By J. KAPUR 4/92											
Detailed By B.H. CREWS 4/92											
Bridge Projects Engr.											
Prelim. Plan By											
Architect/Specialist	DATE	REVISION	BY	APP'D							BRIDGE SHEET NO. 4 SHEET OF SHEETS BRIDGE

ALLAN H. WALLEY STATE OF WASHINGTON 15547 REGISTERED PROFESSIONAL ENGINEER EXPIRES 12/13/93

Figure 1.3

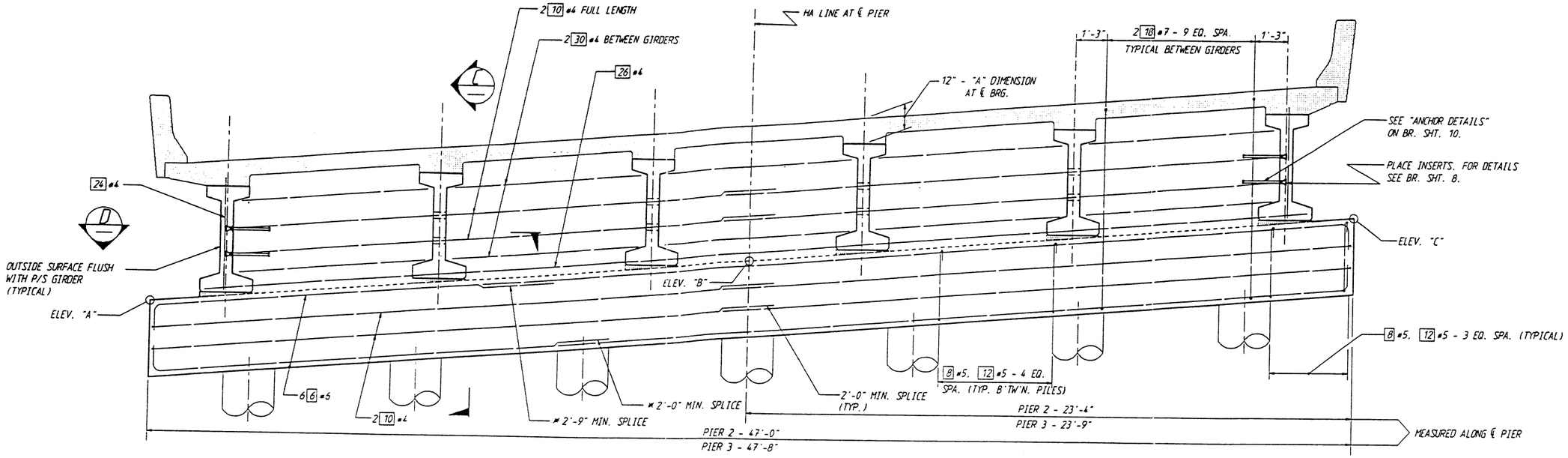

ELEVATION OF INTERMEDIATE PIER

PIER 2 SHOWN - PIER 3 SIMILAR AS NOTED
* ALTERNATE LOCATION OF SPLICE.

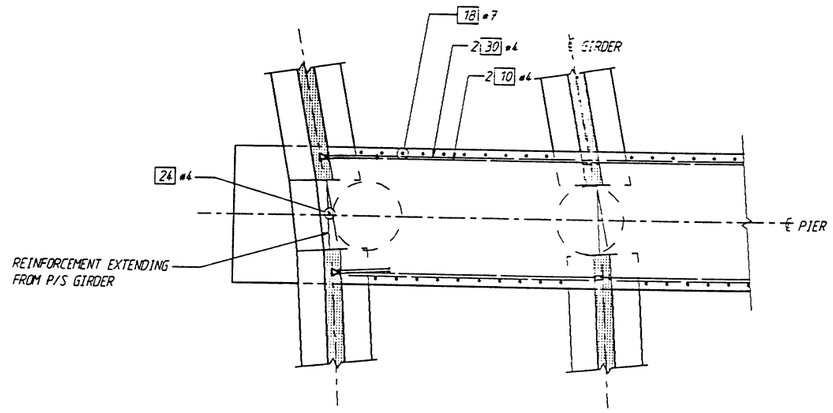

SECTION D

NOTE:

REINFORCEMENT BARS SHALL BE THREADED THROUGH HOLES IN GIRDERS PRIOR TO PLACING EXTERIOR GIRDERS.

ELEVATIONS ALONG ℄ PIER

PIER #	"A"	"B"	"C"
2	-3.11	-1.28	0.59
3	-2.67	-0.87	-0.95

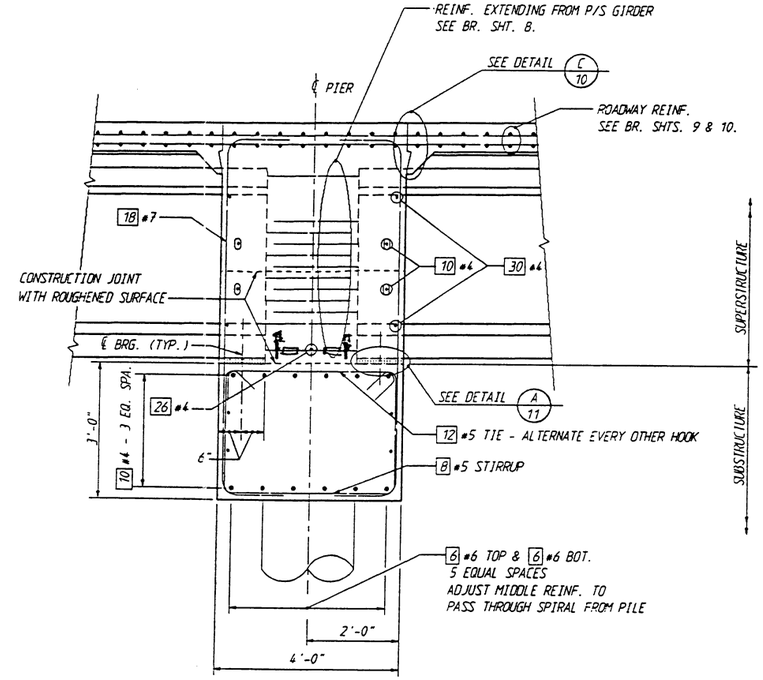

SECTION C
PIERS 2 & 3

NOTE : ALL DIMENSIONS NORMAL TO ℄ PIER.

dge Design Engr.					REGION NO.	STATE	FED. AID PROJ. NO	SHEET NO.	TOTAL SHEETS	BRIDGE AND STRUCTURES
pervisor					10	WASH.				
signed By R.E. LIPTAK 4/92					JOB NUMBER					
ecked By J. KAPUR 4/92										
talled By B.H. CREWS 4/92										
dge Projects Engr.										
elim. Plan By										
chitect/Specialist	DATE	REVISION	BY	APP'D						

DEADWATER ROOT: \FGB\PIER_2-3.FGB: 1 — 11-JUN-92

Washington State Department of Transportation

BRIDGE SHEET NO. 6

SHEET OF SHEETS

PIERS 2 & 3

Figure 1.4

Normalized 5% Damped Response Spectrum

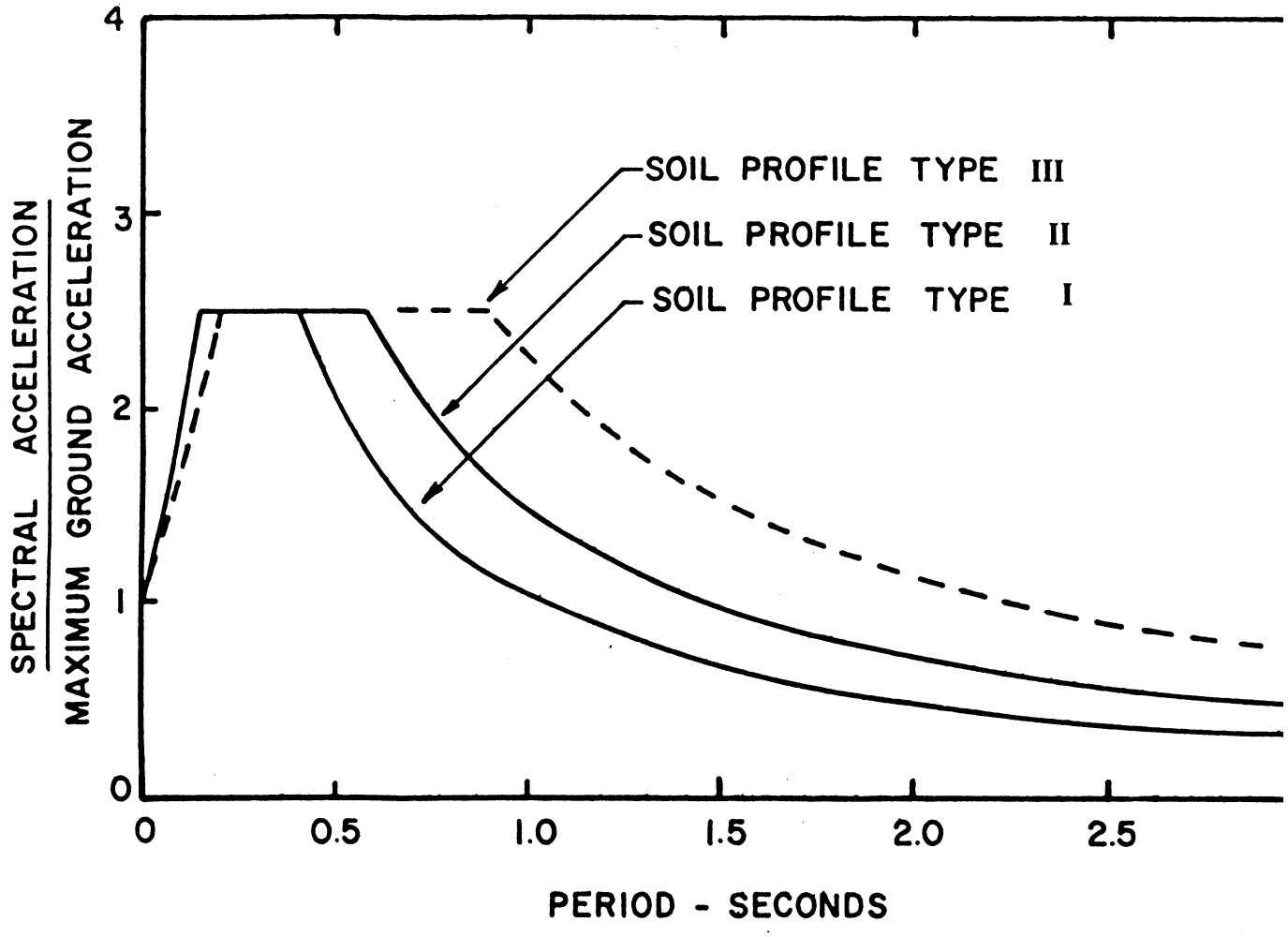

Reference: ATC-6 (1978)

Figure 2.1

3.0 SOIL PROPERTIES

The soil parameters provided by WSDOT for the soil layers are:

γ = total density in pcf
c = cohesion in psf
ϕ = friction angle in degrees
k = modulus of subgrade reaction in pci
G = low-strain shear modulus in psf or ksf
ν = Poisson's Ratio

Values of the modulus of subgrade reaction, k, where not determined by subsurface investigation, were obtained from Figure 4.6 of the Coldwater Creek example problem.

Because the behavior of soil is nonlinear during strong shaking, simple procedures were implemented to approximately account for the effect of this nonlinearity on the computation of the abutment and pier foundation stiffnesses. These procedures are described in Section 3.0 of the Coldwater Creek example problem and were implemented in the Deadwater Slough example problem herein because the ground acceleration coefficient, Z, was greater than 0.2.

4.0 PIER 1 STIFFNESS CALCULATION - FHWA METHOD

In this section the calculation of foundation stiffnesses using the FHWA (1986) method is presented for Pier 1 of the Deadwater Slough Bridge. (The use of the Novak method is illustrated in Section 5.0).

A side-elevation view of the abutment and the soil-property profile at Pier 1 (NW Abutment) is shown in Figure 4.1. As with the Coldwater Creek example, the basic

approach to compute the foundation stiffness matrix at this pier is to first compute the pile-group stiffness, pile-cap stiffness, and abutment-wall stiffness, and then combine these stiffnesses to obtain the abutment stiffness matrix at a specified point on the abutment foundation. This point (Point O in Figure 4.1) is located on top of the 3-foot thick footing at its geometric center.

4.1 PILE-STIFFNESS CALCULATION

Individual pile-head stiffnesses are first computed at the point where the piles enter the abutment footing. Several steps are involved in this calculation. First, the appropriate parameters of the steel-encased concrete piles are estimated (Section 4.1.1) and used in the calculation of the so-called t-z (vertical load - vertical deflection), Q-z (tip load - tip deflection), and p-y (lateral load - lateral deflection) curves, and in the calculation of the load-deflection curves of the pile heads.

The t-z and p-y curves specify the resistances provided by the soil bearing against the pile subjected to vertical and axial loads, and can be visualized as the force-deformation relationships of springs attached to small incremental pile segments comprising the pile. The Q-z curve is simply the force-deflection relationship of the pile tip and end-bearing soils. The calculation of the t-z and Q-z curves is illustrated in Sections 4.1.2 and 4.1.3, respectively; the p-y curve calculation is illustrated in Section 4.1.4. These curves are input to the computer program BMCOL-76 (Matlock et al, 1981) , which computes the load-deflection curves of the pile head under either the pinned-head or fixed-head condition for pile-head fixity. For this example problem, a fixed connection was assumed. The input to the BMCOL-76 program is described in Section 4.1.5 and the output is presented in Section 4.1.6. It should be noted that this program is similar to the COM624 program that has been used by WSDOT.

Because t-z, Q-z, and p-y curves are nonlinear, the pile-head load-deflection curves are also nonlinear. The procedure to compute the pile-head stiffnesses from the pile-head load-

deflection curves is described in Section 4.1.7. This procedure approximately considers the nonlinear soil behavior due to strong ground shaking.

The final step is to compute the pile-group stiffness matrix by using the GPILE program. Per the recommendation in the Task 1 report (Appendix A), group effects are neglected. The preparation of the input file and listing of the output from the GPILE program is presented in Section 4.1.8. The resulting pile-group stiffness matrix is listed in Section 4.1.9.

4.1.1 Estimation of Pile Parameters

The properties of the cylindrical concrete and steel-cased portions of the piles are provided in Table 4.1.

TABLE 4.1
PROPERTIES OF CYLINDRICAL CONCRETE, STEEL CASED PILES

Concrete Cylinder	Steel Casing
Diameter, D = 2 *ft*	*Inside Diam., D* = 2 *ft*
f_c' = 4,000 *psi*	*Thickness, t* = ⅜ *in*
$E_c = 57{,}000\sqrt{f_c'}$ = 3.60*E6 psi* = 5.18*E8 psf*	E_s = 29*E6 psi* = 4.18*E9 psf*
$I_c = \frac{\pi}{64} D^4$ = 0.785 ft^4	$I_s = \pi t R^3$, $2R=D$ = 0.098 ft^4
A_c = 3.14 ft^2	A_s = 0.197 ft^2

Thus, the axial (EA) and flexual (EI) rigidities of the composite section are:

$$EA = E_cA_c + E_sA_s = 2.45E09 \text{ lb}$$
$$EI = E_cI_c + E_sI_s = 8.19E08 \text{ lb-ft}^2$$

The above information was used in the calculation of the t-z, Q-z, and p-y curves, and the load-deflection curves of the pile-head.

4.1.2 Computation of t-z Curves

4.1.2.1 General Procedure. The general procedure for computing the t-z curve is explained in Section 4.1.2.1 of the Coldwater Creek example.

4.1.2.2 Application to Deadwater Slough Bridge Abutment Piles. The calculation of the t-z curves for input to the BMCOL-76 program is described below for piles supporting the Pier 1 abutment.

The values of the relevant soil parameters are shown in Figure 4.1. The input to BMCOL-76 only requires that the t-z curves be computed at the top and bottom of each soil layer (i.e. at Elevations A, C, D, E, F and G in Figure 4.1) and at the location of the water table, if it is along the pile (El. B). The calculation of the t-z curve is illustrated at Elevation C = -14 ft (at base of the Unit 2 - clay layer). The following equations from the Coldwater Creek example and information in Figure 4.1 of this example problem are used in the calculation:

Eqn. (4.5): f = c (cohesive soil)

Figure 4.1: c = 250 - 600 psf where 600 psf is applicable to bottom of cohesive layer (Unit 2) at El. -14 ft. Therefore, use c = 600 psf.

Pier 1
Abutmment Profile

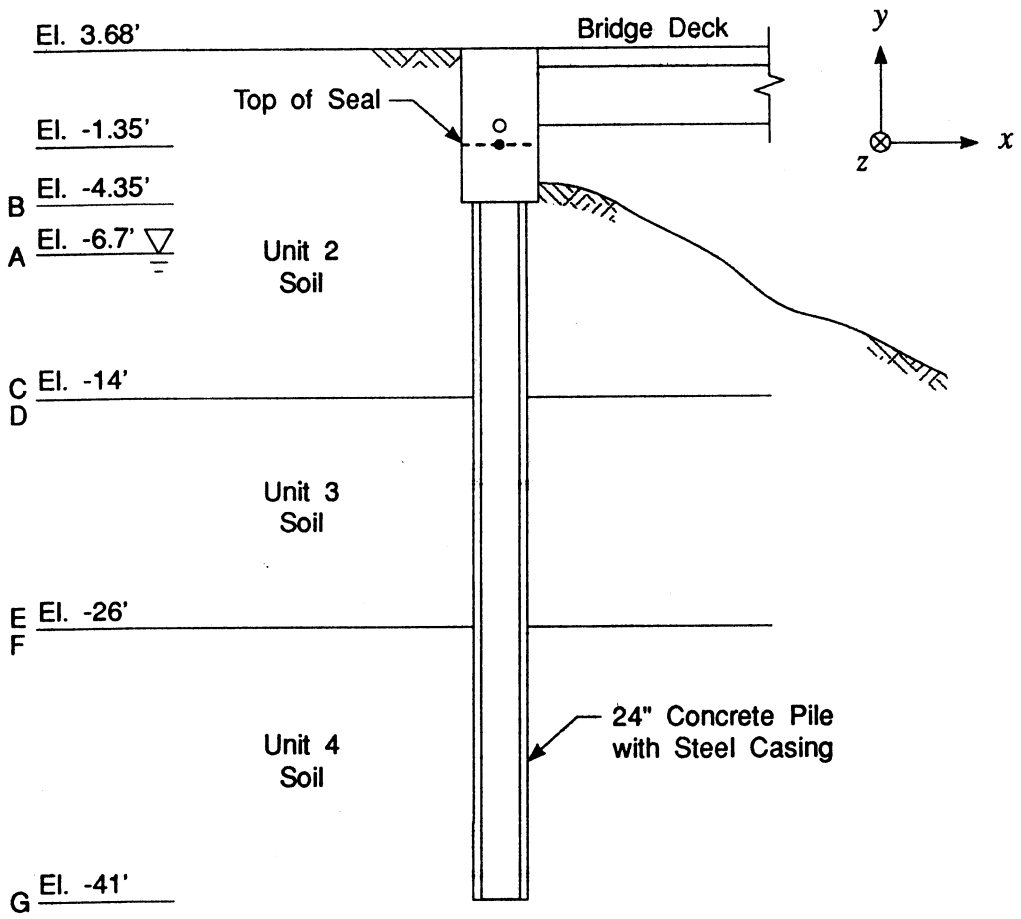

Unit 2:	γ = 93 pcf	ν = 0.45
	c = 250-600 psf	ϕ = 0
	G = 400 ksf	
Unit 3:	γ = 110 pcf	ν = 0.35
	c = 0	ϕ = 28°
	G = 800 ksf	
Unit 4:	γ = 130 pcf	ν = 0.30
	c = 0	ϕ = 40°
	G = 2800 ksf	

Figure 4.1

From Section 4.1.1, pile perimeter, $s = \pi d_o$, where d_o = outside pile diameter.

$d_o = 24\frac{3}{4}" = 2.0625$ ft

Therefore, $s = 6.48$ ft

Eqn. (4.2): $t_{max} = f \cdot s$

$= (0.60 \text{ ksf})\ (6.48 \text{ ft})$

$= 3.89$ kpf

Compute the length parameter, z_{ref} :

Eqn. (4.3): $z_{ref} = f / \bar{k}$

Eqn. (4.4): $\bar{k} = G\pi / 2s$

Figures 4.1: $G = 400\ ksf$

Therefore, $z_{ref} = \dfrac{(0.60\ ksf)(2)(6.48\ ft)}{(400\ ksf)(3.14)} = 0.00619\ ft = 0.0743\ in$

The above calculation pertains to ground acceleration coefficients, $Z < 0.2$. For this example, $Z = 0.25$. Therefore, reduce t_{max} by 50% per the general recommendation in Section 3.0 of the Coldwater Creek example, and construct the t-z curve. Thus,

Eqn. (4.1): $t = t_{max} \tanh(z / z_{ref}) = \left(\dfrac{3.89\ kpf}{2}\right) \tanh\left(\dfrac{z}{0.0743\ in}\right)$

A spread sheet containing the values of 10 points on the t-z curves at eight depths within the soil profile is provided in Table 4.2. The t-z curves for the last seven depths in this table were input to the BMCOL-76 program; these depths correspond to Points A through G in Figure 4.1.

4.1.3 Computation of Q-z Curve

4.1.3.1 General Procedure. The general procedure for computing the Q-z curve for each pile tip is explained in Section 4.1.3.1 of the Coldwater Creek example.

4.1.3.2 Application to Deadwater Slough Bridge Abutment Piles. The calculation of the Q-z curves for input to the BMCOL-76 program is described below for piles supporting the Pier 1 abutment. The pile tips bear on the Unit 4 cohesionless soil as shown in Figure 4.1. The following equations from the Coldwater Creek example and information in Figure 4.1 of this example problem are used in the calculation.

Eqn. (4.12): Unit end bearing, $q = p_o N_q$

where p_o = effective overburden pressure at pile tip
= (93 pcf) (3.68' + 6.7') + (93 - 62.4 pcf) (14' - 6.7')
+ (110 - 62.4 pcf) (12') + (130 - 62.4 pcf) (15')
= 2,770 psf

and N_q = dimensionless bearing capacity factor from
Table 4.3 of Coldwater Creek example
= 72 for $\phi = 40°$ (drilled pier)

Therefore, q = 200 ksf

Compute maximum resistance, Q_{max}

T-Z & Q-Z CURVES

Bridge: Deadwater Slough Overcrossing Pier 1 : high strain

Ground Surface Elevation:	3.68	ft		
Depth to water table:	10.38	ft	Elev: -6.7	ft
Average Pile Perimeter:	77.75	in		
Pile Tip Area:	481.11	in²		
Pile Type:	S	T=Timber,C=Concrete,S=Steel		
	D	O= Open Ended, D=Displacement		

SOIL	DEPTH	ELEV.	GAMMA	PHI	c	G	k	Po	Delta	f	f	Ks	Tmax	Zref
	ft	ft	γ	ϕ	ksf	psf	API RP2A	ksf	δ	ksf	psi	pci	lb/in	in
CLAY	0	3.68	93	-	0.25	4.00E+05	-	0.00	-	0.25	1.74	56	67	0.031
CLAY	8.03	-4.35	93	-	0.41	4.00E+05	-	0.75	-	0.41	2.84	56	110	0.051
CLAY	10.38	-6.7	93	-	0.46	4.00E+05	-	0.97	-	0.46	3.16	56	123	0.056
CLAY	17.68	-14	93	-	0.60	4.00E+05	-	1.19	-	0.60	4.17	56	162	0.074
SAND	17.68	-14	110	28	-	8.00E+05	1.0	1.19	20	0.43	3.00	112	117	0.027
SAND	29.68	-26	110	28	-	8.00E+05	1.0	1.76	20	0.64	4.45	112	173	0.040
SAND	29.68	-26	130	40	-	2.80E+06	1.0	1.76	20	0.64	4.45	393	173	0.011
SAND	44.68	-41	130	40	-	2.80E+06	1.0	2.77	20	1.01	7.01	393	273	0.018

SOIL	DEPTH	ELEV.	PHI	c	G	Po	q	q	Kt	Qmax	Zref
	ft	ft	ϕ	ksf	psf	ksf	ksf	psi	pci	k	in
SAND	44.68	-41	40	-	2.80E+06	2.77	200	1387	196	334	7.06

Table 4.2

Deadwater Slough Overcrossing Pier 1 : high strain T-Z & Q-Z CURVES

	DEPTH ft	ELEV. ft	Tmax lb/in	Zref in										
CLAY	0	3.68	67	0.031	T (lb/in)	0	17	31	43	51	57	61	64	67	67
					Z (in.)	0.000	0.008	0.015	0.023	0.031	0.039	0.046	0.054	0.077	2.000
CLAY	8.03	-4.35	110	0.051	T (lb/in)	0	27	51	70	84	94	100	104	109	110
					Z (in.)	0.000	0.013	0.025	0.038	0.051	0.063	0.076	0.089	0.127	2.000
CLAY	10.38	-6.7	123	0.056	T (lb/in)	0	30	57	78	94	104	111	116	121	123
					Z (in.)	0.000	0.014	0.028	0.042	0.056	0.070	0.085	0.099	0.141	2.000
CLAY	17.68	-14	162	0.074	T (lb/in)	0	40	75	103	123	137	147	152	160	162
					Z (in.)	0.000	0.019	0.037	0.056	0.074	0.093	0.111	0.130	0.186	2.000
SAND	17.68	-14	117	0.027	T (lb/in)	0	29	54	74	89	99	106	110	115	117
					Z (in.)	0.000	0.007	0.013	0.020	0.027	0.033	0.040	0.047	0.067	2.000
SAND	29.68	-26	173	0.040	T (lb/in)	0	42	80	110	132	147	157	163	171	173
					Z (in.)	0.000	0.010	0.020	0.030	0.040	0.050	0.059	0.069	0.099	2.000
SAND	29.68	-26	173	0.011	T (lb/in)	0	42	80	110	132	147	157	163	171	173
					Z (in.)	0.000	0.003	0.006	0.008	0.011	0.014	0.017	0.020	0.028	2.000
SAND	44.68	-41	273	0.018	T (lb/in)	0	67	126	173	208	231	247	257	269	273
					Z (in.)	0.000	0.004	0.009	0.013	0.018	0.022	0.027	0.031	0.045	2.000
					T (lb/in)										
					Z (in.)										
					T (lb/in)										
					Z (in.)										

Q-Z CURVE

	DEPTH ft	ELEV. ft	Qmax k	Zref in										
SAND	44.68	-41	334	7.062	Q (k)	0	82	154	212	254	283	302	314	329	334
					Z (in.)	0.000	1.765	3.531	5.296	7.062	8.827	10.592	12.358	17.654	35.308

Table 4.2 (cont.)

Eqn. (4.9): $Q_{max} = A \cdot q$

where A = cross-sectional area
$= \pi\ (24.75\ in/2)^2$
$= 481\ in^2 = 3.34\ ft^2$

Therefore, $Q_{max} = (3.34\ ft^2)\ (200\ ksf)$
$= 668\ k$

Compute length parameter, z_{ref}

Eqn (4.10): $z_{ref} = q/\overline{k}_t$

Eqn (4.11): $\overline{k}_t = G\pi/4s$

Figure 4.1: $G = 2800\ ksf$

Therefore, $z_{ref} = \dfrac{(200\ ksf)(4)(6.48\ ft)}{(2800\ ksf)(3.14)} = 0.590\ ft = 7.08\ in$

The above equations pertain to Z < 0.2. Since Z = 0.25, reduce Q_{max} by 50% and construct Q-z curve.

Eqn. (4.8):

$$Q = Q_{max} \tanh\ (z/z_{ref})$$
$$= \left(\frac{668\ k}{2}\right) \tanh\ (z/7.08\ in)$$

The values of 10 points on this curve are provided at the bottom of Table 4.2.

4.1.4 Computation of p-y Curves

4.1.4.1 General Procedure. The general procedure for computing the p-y curves is explained in Section 4.1.4.1 of the Coldwater Creek example.

4.1.4.2 Application to Deadwater Slough Bridge Abutment Piles. The calculation of the p-y curves for input to the BMCOL-76 program is described below for piles supporting the Pier 1 abutment.

The relevant soil parameters are provided in Figure 4.1. As with the t-z curves, the input to BMCOL-76 only requires that the p-y curves be computed at the top and bottom of each soil layer and at the location of the water table if it is along the pile. The calculation of the p-y curve is illustrated at Elevation C = -14 ft (at base of the Unit 2 clay layer in Figure 4.1). Equations and Table 4.4 from the Coldwater Creek example and Figure 4.1 in this example are used in the calculation.

Table 4.4: c = 600 psf; J = 0.50, ϵ_c = 0.010 (medium stiff clay)

Eqn. (4.8): $$p_u' = \min \left\{ \begin{array}{c} 3cD + p_o D + JcH \\ 9cD \end{array} \right\}$$

Eqn. (4.9): $y_c = 2.5\, \epsilon_c\, D$

For calculation of p_u', obtain the following parameter values:

Figure 4.1: H = 3.68 ft + 14 ft = 17.68 ft

p_o = (93 pcf)(3.68' + 6.7') + (93-62.4 pcf) (14' - 6.7')

= 1,190 psf

Section 4.1.1: D = 24.75 in = 2.06 ft

Therefore,

$$p_u' = \min \left\{ \begin{array}{l} (3)(0.60\ ksf)(2.06') + (1.19\ ksf)(2.06') + (0.5)(0.60\ ksf)(17.68') \\ (9)(0.60\ ksf)(2.06') \end{array} \right\}$$

$$= \min \left\{ \begin{array}{l} 11.5\ kpf \\ 11.1\ kpf \end{array} \right\}$$

$$= 11.1\ kpf$$

Also, y_c = 2.5 (0.01)(2.06') = 0.0515 ft = 0.618 in

The above calculation pertains to ground acceleration coefficients, Z < 0.2. For this example, Z = 0.25. Therefore, reduce p_u' by 50% per the recommendation in Section 3.0 and construct the p-y curve. Thus,

Eqn. (4.17):

$$p = \begin{Bmatrix} 1/2\, p_u' \,(y/y_c)^{1/3} & , y \le 8y_c \\ p_u' & , y > 8y_c \end{Bmatrix}$$

$$= \begin{Bmatrix} 1/2\,(\frac{11.1\ kpf}{2})\,(\frac{y}{0.618\ in})^{1/3} & , y \le 4.94\ in \\ (\frac{11.1\ kpf}{2}) & , y > 4.94\ in \end{Bmatrix}$$

Spreadsheets containing the values of 10 points on the p-y curves at eight depths within the abutment soil profile are provided in Table 4.3. The p-y curves for the last seven depths in this table were input to the BMCOL-76 program; these depths correspond to Points A through G in Figure 4.1.

4.1.5 Preparation of BMCOL-76 Input

The user guide titled, GUIDE FOR DATA INPUT FOR BMCOL-76, is provided in Appendix B. The text accompanying the guide is reproduced from the BMCOL-76 manual (Matlock et al, 1981), and is also provided in this Appendix. The preparation of the input was explained and illustrated for the Coldwater Creek example. The input file for the Deadwater Slough example will not be provided because it is similar to the Coldwater Creek input file.

4.1.6 BMCOL-76 Output

The output files for the axial load and lateral load cases were used to construct the load-deflection curves for the pile head. Refer to the Coldwater Creek example (Section 4.1.6) for explanation of the output file. Plots of the load-deflection curves for the pile head are

P-Y CURVES

Worksheet to link with d:\wash_dot\examples\deadwatr\axial\tz_one.xls
(including path and extension)

Bridge: Deadwater Slough Overcrossing Pier 1 : high strain
Ground Surface Elevation: 3.68
Depth to water table: 10.38 ft Elev: -6.7 ft
Average Pile Diameter: 24.75 in
Pile Type: S T=Timber,C=Concrete,S=Steel
D O= Open Ended, D=Displacement

SOIL	DEPTH ft	ELEV. ft	GAMMA γ	PHI (deg) ϕ	c ksf	PHI (rad) ϕ	Po ksf	C1	C2	C3	k lb / in^3	J	ε_c	Pu lb/in	Yc in
CLAY	0	3.68	93	-	0.25	-	0.00	-	-	-	-	0.50	0.010	129	0.619
CLAY	8.03	-4.35	93	-	0.41	-	0.75	-	-	-	-	0.50	0.010	476	0.619
CLAY	10.38	-6.7	93	-	0.46	-	0.97	-	-	-	-	0.50	0.010	598	0.619
CLAY	17.68	-14	93	-	0.60	-	1.19	-	-	-	-	0.50	0.010	928	0.619
SAND	17.68	-14	110	28	-	0.49	1.19	1.75	2.41	23	10	-	-	3551	1.506
SAND	29.68	-26	110	28	-	0.49	1.76	1.75	2.41	23	10	-	-	6812	1.721
SAND	29.68	-26	130	40	-	0.70	1.76	4.51	4.38	104	150	-	-	20971	0.353
SAND	44.68	-41	130	40	-	0.70	2.77	4.51	4.38	104	150	-	-	48703	0.545
0		0	0	0	0.00	0.00									
0		0	0	0	0.00	0.00									

SOIL	DEPTH ft	ELEV. ft	Pu lb/in	Yc in											
CLAY	0	3.68	129	0.619	P (lb/in)	0	32	41	46	51	55	59	62	64	64
					Y (in.)	0.000	0.619	1.238	1.856	2.475	3.094	3.713	4.331	4.950	6.188
CLAY	8.03	-4.35	476	0.619	P (lb/in)	0	119	150	172	189	204	216	228	238	238
					Y (in.)	0.000	0.619	1.238	1.856	2.475	3.094	3.713	4.331	4.950	6.188
CLAY	10.38	-6.7	598	0.619	P (lb/in)	0	149	188	216	237	256	272	286	299	299
					Y (in.)	0.000	0.619	1.238	1.856	2.475	3.094	3.713	4.331	4.950	6.188
CLAY	17.68	-14	928	0.619	P (lb/in)	0	232	292	335	368	397	422	444	464	464
					Y (in.)	0.000	0.619	1.238	1.856	2.475	3.094	3.713	4.331	4.950	6.188
SAND	17.68	-14	3551	1.506	P (lb/in)	0	391	738	1015	1217	1355	1446	1540	1576	1598
					Y (in.)	0.000	0.377	0.753	1.130	1.506	1.883	2.259	3.012	3.766	7.531
SAND	29.68	-26	6812	1.721	P (lb/in)	0	751	1417	1947	2335	2600	2775	2955	3024	3065
					Y (in.)	0.000	0.430	0.861	1.291	1.721	2.152	2.582	3.443	4.304	8.607
SAND	29.68	-26	20971	0.353	P (lb/in)	0	2311	4361	5994	7187	8005	8542	9098	9311	9436
					Y (in.)	0.000	0.088	0.177	0.265	0.353	0.442	0.530	0.707	0.883	1.766
SAND	44.68	-41	48703	0.545	P (lb/in)	0	5368	10128	13920	16692	18591	19838	21128	21623	21915
					Y (in.)	0.000	0.136	0.273	0.409	0.545	0.681	0.818	1.090	1.363	2.725
					P (lb/in)										
					Y (in.)										
					P (lb/in)										
					Y (in.)										

Table 4.3

presented in Figure 4.2 (axial direction) and Figure 4.3 (lateral direction). These curves were used to estimate the axial and lateral stiffnesses of the pile.

4.1.7 Calculation of Pile-Head Stiffnesses

The pile-head stiffnesses are computed from the load-deflection curves in Figures 4.2 and 4.3 as follows. For the axial load case, the axial pile-head stiffness is the slope of the load-deflection curve (Figure 4.2) at the origin (i.e. the initial tangent slope). For the lateral load case, the lateral pile-head stiffness is the slope of straight line from the origin to the point on the load-deflection curve corresponding to 0.50 in deflection. These rules for estimating pile-head stiffnesses were presented in Section 4.1.7 of the Coldwater Creek example.

According to WSDOT, the piles at Pier 1 are fixed to the abutment footing. Under this assumption, the pile-head stiffnesses resulting from the implementation of the above procedure (see Figures 4.2 and 4.3) are as follows:

$$K_z = 2.7 \times 10^6 \text{ lb/in (Axial)}$$
$$K_x = K_y = 9.2 \times 10^4 \text{ lb/in (Lateral)}$$

These stiffness values apply to each pile at Elevation -4.35 in Figure 4.1 (pile head location or bottom of pile cap).

4.1.8 Calculation of Pile-Group Stiffness Matrix

4.1.8.1 Assumptions. Two key assumptions are made in order to compute the 6 x 6 pile-group stiffness matrix: (1) pile-group effects (i.e. pile-soil-pile interaction) are neglected, and (2) because the piles are vertical and cylindrical, the individual pile-head stiffnesses computed in Section 4.1.7 apply to a local coordinate system that was established to be coincidental with the principal axes of the abutment, i.e. axial stiffness, K_z , is associated with the local z axis, which is parallel to the direction along the length of the pile; the transverse stiffness,

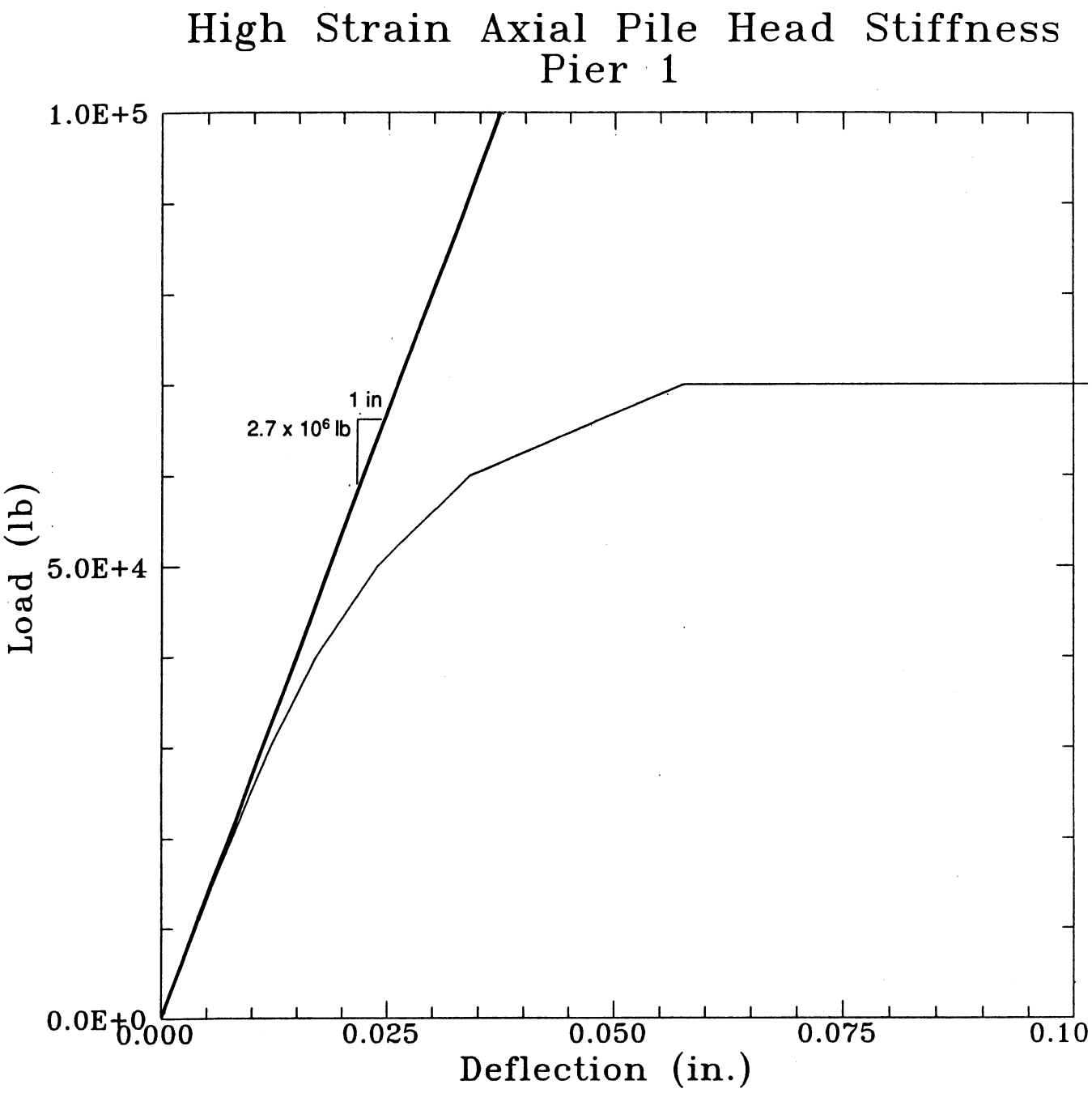
High Strain Axial Pile Head Stiffness
Pier 1
1.0E+5
5.0E+4
0.0E+0
Load (lb)
1 in
2.7 x 10^6 lb
0.000
0.025
0.050
0.075
0.10
Deflection (in.)

Figure 4.2

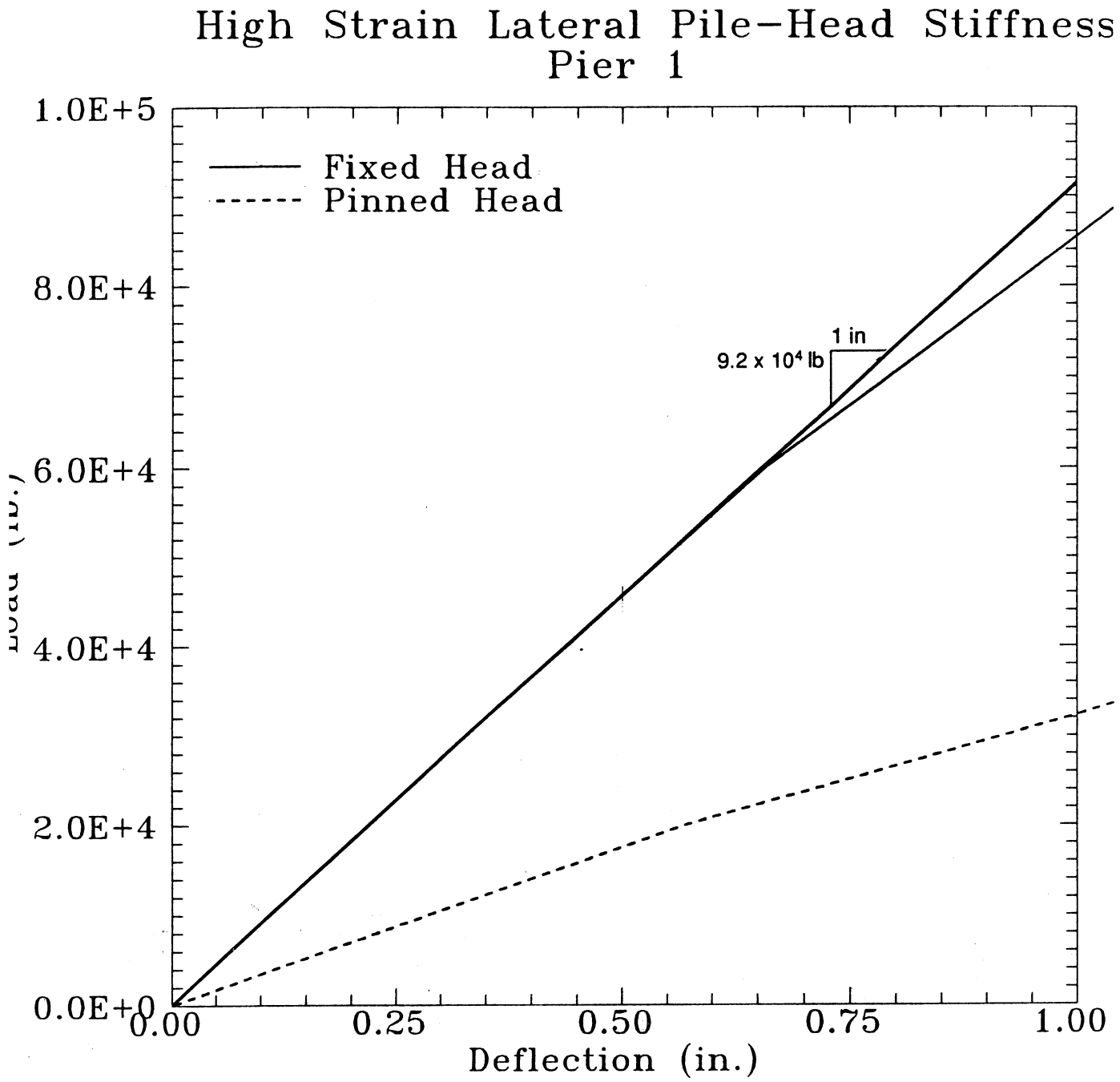
High Strain Lateral Pile-Head Stiffness
Pier 1
1.0E+5
8.0E+4
6.0E+4
4.0E+4
2.0E+4
0.0E+0
Load (lb.)
Fixed Head
Pinned Head
1 in
9.2 x 10⁴ lb
0.00
0.25
0.50
0.75
1.00
Deflection (in.)

Figure 4.3

transverse stiffness, K_y , is associated with the local y axis, which is coincident with the transverse direction of the abutment (i.e., parallel to the global z axis in Figure 4.1) and, the longitudinal stiffness, K_x , is associated with the local x axis, which is parallel to the global x axis in Figure 4.1 of the pile section.

4.1.8.2 Preparation of GPILE Input. The preparation of the input to the GPILE program, which computes the pile-group stiffness matrix, was discussed in Section 4.1.8.2 of the Coldwater Creek example. Refer to that section for details.

4.1.8.3 GPILE Output The GPILE output file for Pier 1 is shown in Table 4.4. The global group stiffness matrix, [K], and the local group stiffness matrix are listed. The global group stiffness matrix is used in the abutment stiffness calculation in Section 4.4. The local group stiffness matrix is not used because this matrix is for a different orientation of the global coordinate system. The global group stiffness matrix was computed at Point O in Figure 4.1 for the coordinate system shown in that figure. The origin of the coordinate system for the stiffness calculation is Point O.

4.2 ABUTMENT FOOTING STIFFNESSES

As recommended in the Task 1 report, the foundation stiffnesses of the pile caps are computed assuming the caps are footings fully embedded in the surrounding soil. These footing stiffnesses (along with the stiffness contributions from the abutment wall) are added to the pile-group stiffnesses to obtain the total abutment stiffness matrix.

4.2.1 Model and Assumptions

The theoretical model for estimating the stiffnesses of an embedded footing is presented in Section 4.2.1 of the Coldwater Creek example.

WASHINGTON STATE DEPARTMENT OF TRANSPORTATION 12/28/92 TIME 16:25:53 PAGE 4
*** GROUP PILE ANALYSIS *** REV 4/12/88

DEADWATER SLOUGH OVERCROSSING PILE STIFFNESS - PIER 1

GLOBAL GROUP STIFFNESS MATRIX:

	FX	FY	FZ	MX	MY	MZ
δX	0.773E+07	0.000E+00	0.000E+00	0.000E+00	0.000E+00	0.232E+0
δY	0.000E+00	0.227E+09	0.000E+00	0.000E+00	0.000E+00	0.000E+0
δZ	0.000E+00	0.000E+00	0.773E+07	-0.232E+08	0.000E+00	0.000E+0
ΘX	0.000E+00	0.000E+00	-0.232E+08	0.384E+11	0.000E+00	0.000E+0
ΘY	0.000E+00	0.000E+00	0.000E+00	0.000E+00	0.131E+10	0.000E+0
ΘZ	0.232E+08	0.000E+00	0.000E+00	0.000E+00	0.000E+00	0.696E+0

LOCAL GROUP STIFFNESS MATRIX:

	FX	FY	FZ	MX	MY	MZ
δX	0.227E+09	0.000E+00	0.000E+00	0.000E+00	0.000E+00	0.000E+0
δY	0.000E+00	0.773E+07	0.000E+00	0.000E+00	0.000E+00	-0.232E+0
δZ	0.000E+00	0.000E+00	0.773E+07	0.000E+00	0.232E+08	0.000E+0
ΘX	0.000E+00	0.000E+00	0.000E+00	0.131E+10	0.000E+00	0.000E+0
ΘY	0.000E+00	0.000E+00	0.232E+08	0.000E+00	0.384E+11	0.000E+0
ΘZ	0.000E+00	-0.232E+08	0.000E+00	0.000E+00	0.000E+00	0.696E+0

4.2.2 Calculation of Footing Stiffnesses

4.2.2.1 General Procedure. The general procedure to compute the foundation stiffnesses of an embedded footing (pile cap) is presented in Section 4.2.2.1 of the Coldwater Creek example.

4.2.2.2 Application to Deadwater Slough Abutment Footing. The calculation of the footing (pile cap) stiffness matrix for the Pier 1 abutment is described below. In Figure 1, the footing is defined as the portion of the abutment below Point O. The relevant equations given below are taken from the Coldwater Creek example (Section 4.2.2.1).

The footing dimensions from Figure 4.1:

Length: 2L = 45 ft - 9 in = 45.75 ft

Width: 2B = 4 ft

Thickness: D = 3 ft

Compute the effective soil depth:

Eqn. (4.29): $$h = \left(\frac{4BL}{\pi}\right)^{1/2} = \left(\frac{(45.75\ ft)(4\ ft)}{\pi}\right)^{1/2} = 7.63\ ft$$

Select the G and ν values at h = 7.63 ft beneath the bottom of footing:

Figure 4.1: G = 400 ksf, ν = 0.45

This modulus is the low-strain G. Because Z ≥ 0.2, reduce G by 50%. Thus, for subsequent calculations, use G = 200 ksf. Compute equivalent radii, R, R_x , R_y , and R_z , of the rectangular foundation using formula in Figure 4.11 of the Coldwater Creek example:

Translation: $R = h = 7.63\ ft$

Rotation: (about x axis) $R_x = \left[\frac{(2B)(2L)^3}{3\pi}\right]^{1/4} = \left[\frac{(4)(45.75)^3}{3\pi}\right]^{1/4} = 14.2\ ft$

Rotation: (about y axis) $R_y = \left[\frac{(2L)(2B)^3}{3\pi}\right]^{1/4} = \left[\frac{(45.75)(4)^3}{3\pi}\right]^{1/4} = 4.20\ ft$

Rotation: (about z axis) $R_z = \left[\frac{4BL(4B^2 + 4L^2)}{6\pi}\right]^{1/4} = \left[\frac{(4)(45.75)(4^2 + 45.75^2)}{6\pi}\right]^{1/4} = 12.0\ ft$

Compute the stiffnesses of equivalent circular footing, K_i^o:

Eqn. (4.24): $K_z^o = \frac{4GR}{1 - \nu} = \frac{4(200\ ksf)(7.63\ ft)}{1 - 0.45}\ x\left(\frac{1{,}000\ lb}{1k}\right) = 1.11\ x\ 10^7\ lb/ft$

Eqn. (4.25): $K_x^o = K_y^o = \frac{8GR}{2 - \nu} = \frac{8(200\ ksf)(7.63\ ft)}{2 - 0.45}\ x\left(\frac{1{,}000\ lb}{1k}\right) = 7.88\ x\ 10^6\ lb/ft$

Eqn. (4.26): $K_{\theta z}^o = \frac{16GR_z^3}{3} = \frac{16(200\ ksf)(12.0\ ft)^3}{3}\ x\left(\frac{1{,}000\ lb}{1k}\right) = 1.84\ x\ 10^9\ lb\text{-}ft$

Eqn. (4.27): $K_{\theta x}^o = \frac{8GR_x^3}{3(1 - \nu)} = \frac{8(200\ ksf)(14.2\ ft)^3}{3(1 - 0.45)}\ x\left(\frac{1{,}000\ lb}{1k}\right) = 2.78\ x\ 10^9\ lb\text{-}ft$

Eqn. (4.28): $K_{\theta y}^{o} = \frac{8GR_y^3}{3(1 - \nu)} = \frac{8(200\ ksf)(4.20\ ft)^3}{3(1 - 0.45)} \times \left(\frac{1{,}000\ lb}{1k}\right) = 7.18 \times 10^7\ lb\text{-}ft$

Compute values of α_i and β_i by first calculating L/B and D/R ratios:

L/B = 11.4

D/R = 3/7.63 = 0.393 (translation)

$D/R_x = 0.211$, $D/R_y = 0.714$, $D/R_z = 0.250$ (rotation)

The corresponding values of α_i and β_i were obtained from Figures 4.12 and 4.13 in the Coldwater Creek example, and are summarized in Table 4.5 below, along with the stiffnesses K_i^* and the final stiffnesses $K_i = \alpha_i \cdot \beta_1 \cdot K_i^*$ (Eqn. 4.22 in Coldwater Creek example).

TABLE 4.5
CALCULATION OF PIER 1 FOOTING STIFFNESSES

	K_i^o	α_i	β_i	K_i
K_x (lb/ft)	7.88×10^6	1.4	1.52	1.68×10^7
K_y (lb/ft)	7.88×10^6	1.4	1.52	1.68×10^7
K_z (lb/ft)	1.11×10^7	1.3	1.18	1.70×10^7
$K_{\phi x}$ (lb-ft)	2.78×10^9	1.3	1.26	4.55×10^9
$K_{\phi y}$ (lb-ft)	7.18×10^7	1.3	2.37	2.21×10^8
$K_{\phi z}$ (lb-ft)	1.84×10^9	1.3	1.75	4.19×10^9

Thus, the diagonal elements of the diagonal footing stiffness matrix, [K], are the values in the last column in Table 4.5. This stiffness matrix applies to the FHWA coordinate

system. Elements of this matrix will be rearranged in Section 4.4 to be compatible with the global coordinate system in Figure 4.1.

4.3 ABUTMENT WALL STIFFNESS

The stiffness due to the passive resistance of abutment backfill soil is also computed and added to the pile-group and footing stiffnesses.

4.3.1 Model and Assumptions

The model and assumptions for estimating the translational and rotational stiffnesses of the abutment wall-backfill system is provided in Section 4.3.1 of the Coldwater Creek example.

4.3.2 Calculation of Wall Stiffnesses

4.3.2.1 General Procedure. The formulas for the translational stiffness, K_x , and the rotational stiffness, $K_{\phi z}$, were provided in Section 4.3.2.1 of the Coldwater Creek example.

4.3.2.2 Application to Deadwater Slough Abutment Wall. The abutment-wall stiffness computation is illustrated for the Pier 1 abutment. The abutment wall height is assumed to be the distance from the top of the pile cap (i.e. Point O in Figure 4.1) to the top of the abutment. The stiffnesses are computed at Point O.

Obtain the appropriate length dimensions from Figures 1.2 and 4.1:

$B_w = 45.75$ ft

$H_w = 5.03$ ft

Thus, $h_1 = 0.37H_w = 1.86$ ft

Compute E_s using the high strain G, which is 50% less than the low-strain G of 400 ksf as explained in the abutment footing calculation:

Eqn. (4.35): $E_s = 2G(1 + \nu) = 2(200\ ksf)(1 + 0.45) = 580\ ksf$

Using the global coordinate system in Figure 4.1, the wall stiffnesses at Point O are:

Eqn. (4.32): $K_x = 0.425E_sB_w = 0.425(580\ ksf)(45.75\ ft)\ x \left(\frac{1{,}000\ lb}{1k}\right) = 1.13\ x\ 10^7\ lb/ft$

Eqn.(4.33): $K_{\theta z} = (0.425E_sB_w)h_1^2 + 0.072E_sB_wH_w^2$

$= (1.13\ x\ 10^7\ lb/ft)(1.86\ ft)^2 + 0.072(5.80\ x\ 10^5\ psf)(45.75\ ft)(5.03\ ft)^2$

$= 8.74\ x\ 10^7\ lb\text{-}ft$

Eqn. (4.34): $K_{x\theta z} = -(0.425E_sB_w)h_1 = -(1.13\ x\ 10^7\ lb/ft)(1.86\ ft) = -2.10\ x\ 10^7\ lb$

The minus sign in Eqn. (4.34) results from the fact that the sign convention for forces (moments) and displacements (rotations) in the FHWA (1986) report is slightly different from the convention adopted herein.

4.4 TOTAL ABUTMENT STIFFNESS MATRIX

4.4.1 General Procedure.

The total abutment stiffness matrix, $[K_t]$, at a given point is approximated as the sum of the stiffness matrices for the piles, $[K_p]$, footing or pile cap, $[K_f]$, and abutment wall, $[K_w]$, i.e.

$$[K_t] = [K_p] + [K_f] + [K_w]$$

Although this formula is simple, it is important to note that $[K_p]$, $[K_f]$, and $[K_w]$ must be computed at the same point in the same coordinate system used for the piles, footings, and wall.

4.4.2 Application to Deadwater Slough Abutment. The stiffness matrices $[K_p]$, $[K_f]$, and $[K_w]$ for the abutment system at Pier 1 were constructed from the stiffness calculations presented in Sections 4.1, 4.2, and 4.3, respectively. The xyz coordinate system is oriented as shown in Figure 4.1 with the origin at Point O.

The 6 x 6 stiffness matrices are:

From Table 4.4,

$$[K_p] = \begin{bmatrix} 7.73E6 & 0 & 0 & 0 & 0 & 2.32E7 \\ 0 & 2.27E8 & 0 & 0 & 0 & 0 \\ 0 & 0 & 7.73E6 & -2.32E7 & 0 & 0 \\ 0 & 0 & -2.32E7 & 3.84E10 & 0 & 0 \\ 0 & 0 & 0 & 0 & 1.31E9 & 0 \\ 2.32E7 & 0 & 0 & 0 & 0 & 6.96E7 \end{bmatrix}$$

From Table 4.5 (after converting from the FHWA to GPILE coordinate system),

$$\text{diag } [K_f] = \begin{bmatrix} 1.68E7 & & & & & \\ & 1.70E7 & & & & \\ & & 1.68E7 & & & \\ & & & 4.55E9 & & \\ & & & & 4.19E9 & \\ & & & & & 2.21E8 \end{bmatrix}$$

From Section (4.3.2.2),

$$[K_w] = \begin{bmatrix} 1.13E7 & 0 & 0 & 0 & 0 & -2.10E7 \\ 0 & 0 & 0 & 0 & 0 & 0 \\ 0 & 0 & 0 & 0 & 0 & 0 \\ 0 & 0 & 0 & 0 & 0 & 0 \\ 0 & 0 & 0 & 0 & 0 & 0 \\ -2.10E7 & 0 & 0 & 0 & 0 & 8.74E7 \end{bmatrix}$$

Therefore,

$$[K_t] = \begin{bmatrix} 3.58E7 & 0 & 0 & 0 & 0 & 2.20E6 \\ 0 & 2.44E8 & 0 & 0 & 0 & 0 \\ 0 & 0 & 2.45E7 & -2.32E7 & 0 & 0 \\ 0 & 0 & -2.32E7 & 4.30E10 & 0 & 0 \\ 0 & 0 & 0 & 0 & 5.50E9 & 0 \\ 2.20E6 & 0 & 0 & 0 & 0 & 3.78E8 \end{bmatrix}$$

The units are lb and ft.

5.0 PIER 1 STIFFNESS CALCULATION - NOVAK METHOD

The calculation of foundation stiffnesses using the Novak method is much simpler than the FHWA method primarily because a single computer program (DYNA3) is available to do all the required calculations. Furthermore, the theory upon which the program is based assumes linear elastic response of the soil-foundation system; consequently, fewer soil properties are required to characterize the soil medium, and nonlinear load-deflection relationships between the pile and soil (t-z, Q-z, p-y curves) are not required.

5.1 PILE AND FOOTING SIDE STIFFNESS

The Task 1 report recommended the use of the Pile & Footing Side option within the Novak computer program. With this option, the total pile-cap stiffness is the sum of the stiffnesses from the pile group and the passive resistance of the soil against the sides of the pile cap.

5.1.1 Soil Model

The soil model is shown in Figure 5.1, which was adapted from information in Figure 4.1. Note that shear-wave velocity, V_s, is given as an elastic property, rather than the shear modulus, G. In computing $V_s = \sqrt{G/\gamma_m}$ (where γ_m = mass density), the low-strain shear modulus values in Figure 4.1 were reduced by 50% to account for high soil strain.

Besides V_s, the other new soil parameter not shown in Figure 4.1 is the soil damping ratio for shear deformation, ζ. Values of $\zeta \leq 0.05$ are typically assumed and within this range, the effect of this parameter on the stiffness calculation is negligible. For this and all other example problems, $\zeta = 0.03$ was arbitrarily assumed.

5.1.2 Preparation of DYNA3 Input

The input file for Novak's DYNA3 computer program for Pier 1 is shown in Table 5.1. The preparation of this input file is very similar to the preparation of the input file for Pier 1

Soil Model for Novak Stiffness Calculation for Pile and Footing Side Case at Pier 1

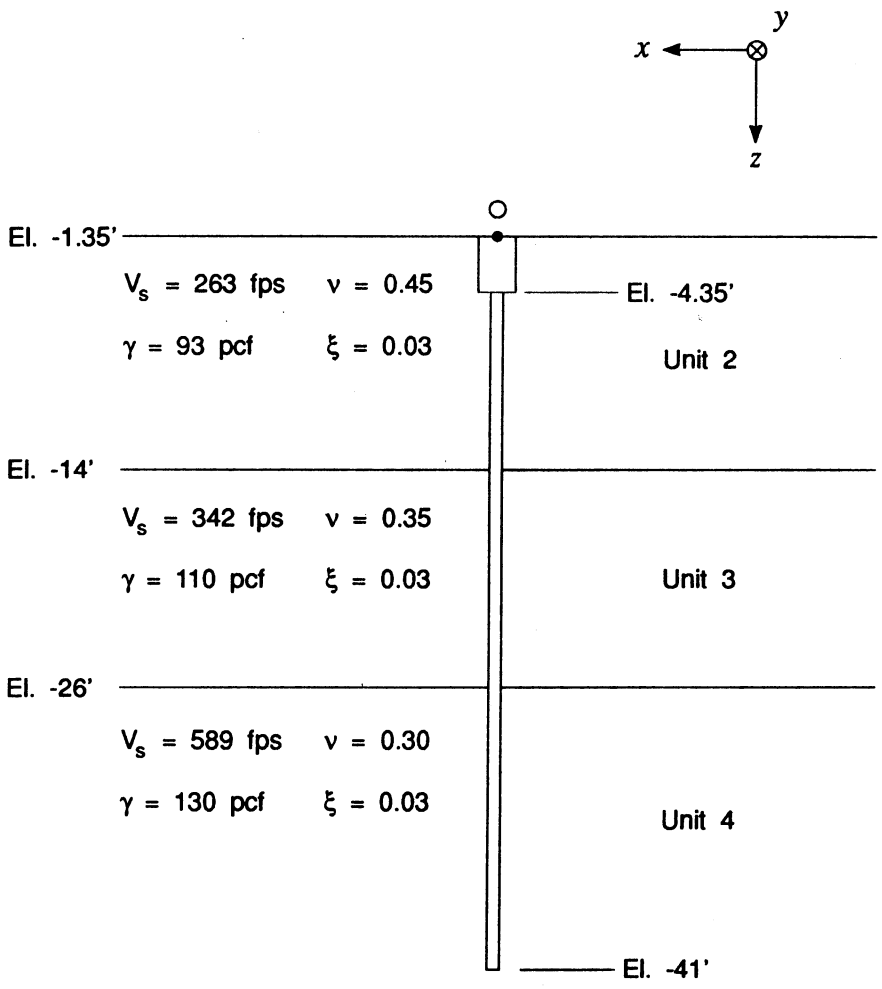

NOTES

V_s Shear-wave velocity $=\sqrt{G/\gamma_m}$ where G is the high-strain value of shear modulus = 50% of the low-strain G value in Figure 4.1. The parameter γ_m is mass density.

ξ Soil damping ratio (assumed).

xyz Coordinate system in this figure is oriented differently from the one in Figure 4.1. In Novak's model, the *z* coordinate axis is positive downward.

Figure 5.1

First, the pile head condition is assumed to be fixed for this example. Accordingly, the keyword "PINNED" has been changed to "FIXED." Also, the seven piles at Pier 1 of this example are vertical, removing the need to specify the batter pile data given in the Coldwater example.

Greater difficulty is encountered, however, in modelling the geometric properties of the composite pile sections utilized in the Deadwater Slough overcrossing. The input for the DYNA3 program can only accommodate properties for a uniform pile section. Therefore, the input pile properties, E', A', I_x', I_y', must be varied so that the products, $E'A'$, $E'I_x'$, $E'I_y'$, equal the values for the composite pile section. For this example, E' is arbitrarily set

$$E' = E_c = 5.18 \times 10^8 \ psf$$

The other properties are determined via the following relations:

$$A' = \frac{E_p A_p}{E'} = 4.73 \ ft^2$$

$$I_x' = I_y' = \frac{E_p I_p}{E'}$$

$$= 1.582 \ ft^4$$

Note that, as a consequence of the high value of E_s relative to E_c, the equivalent pile properties are considerably higher than for a plain section. The value of E' can conceivably vary from E_c to E_s. DYNA3 is insensitive to values of E' in this range, given that the products listed above remain constant.

5.1.3 DYNA3 Output

The output file from the DYNA3 program is listed in Table 5.2. The stiffnesses are in units of kips and ft. The values of CROSS-STIFFNESS (YZ PLANE) and CROSS-STIFFNESS (XZ PLANE) refer to $K_{y,\theta x}$ and $K_{x,\theta y}$, respectively.

5.2 ABUTMENT WALL STIFFNESS

The Task 1 report noted that the abutment-wall stiffness could be computed using Novak's method for a footing on an elastic half space whose properties are those of the backfill soil. However, the FHWA approach for retaining walls (Section 4.3) is slightly preferred over the Novak method. The stiffness matrix obtained using the FHWA method was presented in Section 4.4.

5.3 TOTAL PIER 1 STIFFNESS MATRIX

The total abutment stiffness matrix is $[K_t] = [K_{pfs}] + [K_w]$, where $[K_{pfs}]$ is the "pile + footing side" stiffness matrix, and K_w is the abutment wall stiffness matrix. From Table 5.2 of Section 5.1.3,

```
**************************************************
*                                                *
*        D Y N A 3   S I M U L A T I O N         *
*                                                *
*              RUN DATE -  1992/12/29            *
*              TIME     -  10:16:49              *
*              REVISION -  1991/07/30            *
*                                                *
**************************************************

DEADWATER SLOUGH PIER 1 [ PILES + EMBEDMENT ] [k ft

                                    RESULTS
                                    *******


FREQUENCY  -      .0010
*********


STIFFNESS CONSTANTS (K)
***********************

HORIZONTAL TRANSLATION  (X) ...   4.77869E+04
HORIZONTAL TRANSLATION  (Y) ...   4.77869E+04
VERTICAL TRANSLATION  (Z) .....   2.53185E+05
ROTATION ABOUT  (X) ...........   4.59864E+07
ROTATION ABOUT  (Y) ...........   3.01382E+06
TORSION ABOUT  (Z) ............   9.08932E+06
CROSS-STIFFNESS (YZ PLANE) ....   3.21732E+05
CROSS-STIFFNESS (XZ PLANE) .... -3.21732E+05

DAMPING CONSTANTS (C)
*********************
HORIZONTAL TRANSLATION  (X) ...   1.64217E+06
HORIZONTAL TRANSLATION  (Y) ...   1.64217E+06
VERTICAL TRANSLATION  (Z) .....   9.14033E+06
ROTATION ABOUT  (X) ...........   1.67440E+09
ROTATION ABOUT  (Y) ...........   1.24160E+08
TORSION ABOUT  (Z) ............   3.11989E+08
CROSS-DAMPING  (YZ PLANE) .....   1.20117E+07
CROSS-DAMPING  (XZ PLANE) ..... -1.20117E+07
```

$$[K_{pfs}] = \begin{bmatrix} 4.78E7 & 0 & 0 & 0 & -3.22E8 & 0 \\ 0 & 4.78E7 & 0 & 3.22E8 & 0 & 0 \\ 0 & 0 & 2.53E8 & 0 & 0 & 0 \\ 0 & 3.22E8 & 0 & 4.60E10 & 0 & 0 \\ -3.22E8 & 0 & 0 & 0 & 3.01E9 & 0 \\ 0 & 0 & 0 & 0 & 0 & 9.09E9 \end{bmatrix}$$

The units are lb and ft.

Because the coordinate system in Figure 4.1 is different from the Novak coordinate system (Figure 5.1), elements of $[K_w]$ from Section 4.4 were rearranged to be consistent with the coordinate system in Figure 5.1. Thus,

$$[K_w] = \begin{bmatrix} 1.13E7 & 0 & 0 & 0 & -2.10E7 & 0 \\ 0 & 0 & 0 & 0 & 0 & 0 \\ 0 & 0 & 0 & 0 & 0 & 0 \\ 0 & 0 & 0 & 0 & 0 & 0 \\ -2.10E7 & 0 & 0 & 0 & 8.74E7 & 0 \\ 0 & 0 & 0 & 0 & 0 & 0 \end{bmatrix}$$

Therefore,

$$[K_t] = \begin{bmatrix} 5.91E7 & 0 & 0 & 0 & -3.44E8 & 0 \\ 0 & 4.78E7 & 0 & 3.22E8 & 0 & 0 \\ 0 & 0 & 2.53E8 & 0 & 0 & 0 \\ 0 & 3.22E8 & 0 & 4.60E10 & 0 & 0 \\ -3.44E8 & 0 & 0 & 0 & 3.10E9 & 0 \\ 0 & 0 & 0 & 0 & 0 & 9.09E9 \end{bmatrix}$$

Note that $[K_t]$ is the stiffness matrix at Point O for the global coordinate system defined in Figure 5.1.

6.0 PIER 2 STIFFNESS CALCULATION - FHWA METHOD

Pier 2 of the Deadwater Slough bridge consists of a reinforced concrete ledger beam supported by seven vertical, 2′ diameter concrete columns (Figure 6.1). The columns extend into soils similar to those at Pier 1. The subsurface portions of the columns (piles) are encased in a 3/8" thick steel casing. The piles extend to a depth of approximately 33' below the mudline.

WSDOT has previously modelled this pier by considering the portions of the columns (piles) which extend from the mudline to the ledger beams as column elements for the finite element model. The portions of the columns (piles) below the mudline are modelled by 6 x 6 stiffness matrices placed on the neutral axis of each column element at the mudline (Figure 6.2).

Pier 2
Soil Profile

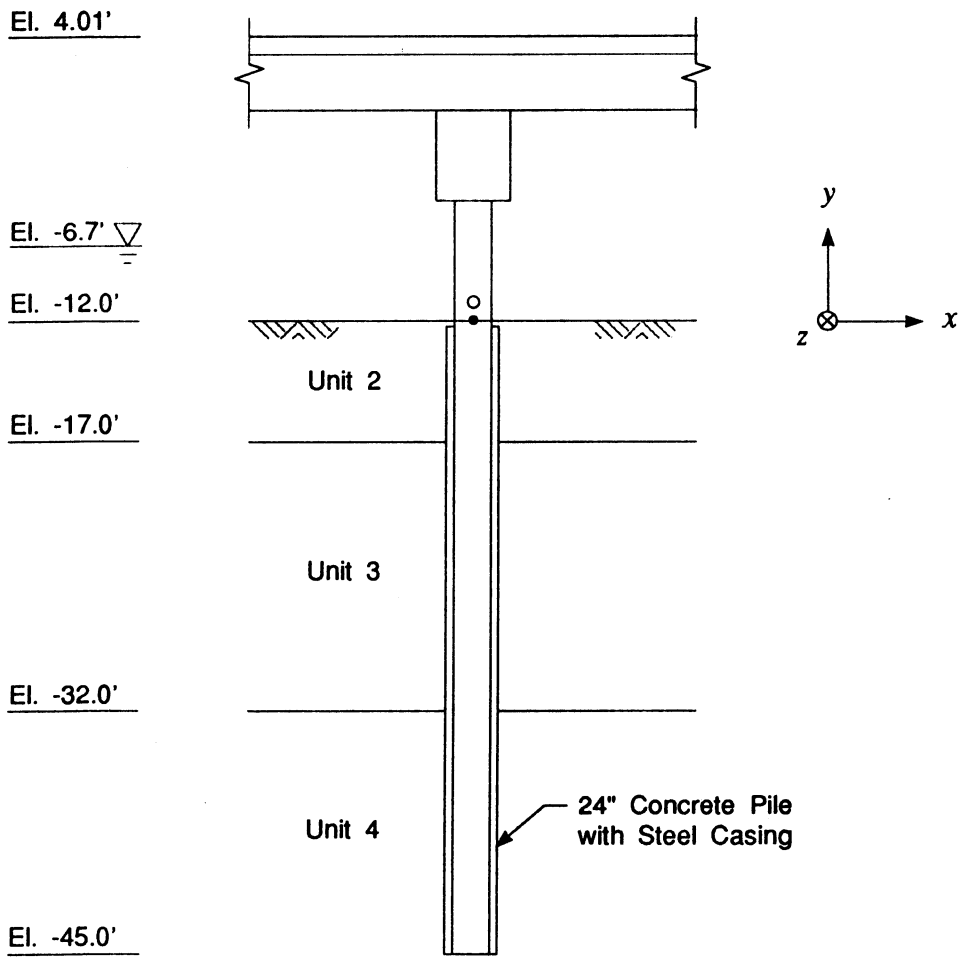

Soil properties are same as for Pier 1. See Figure 4.1.

Figure 6.1

Piers 2 and 3
Bent Structure

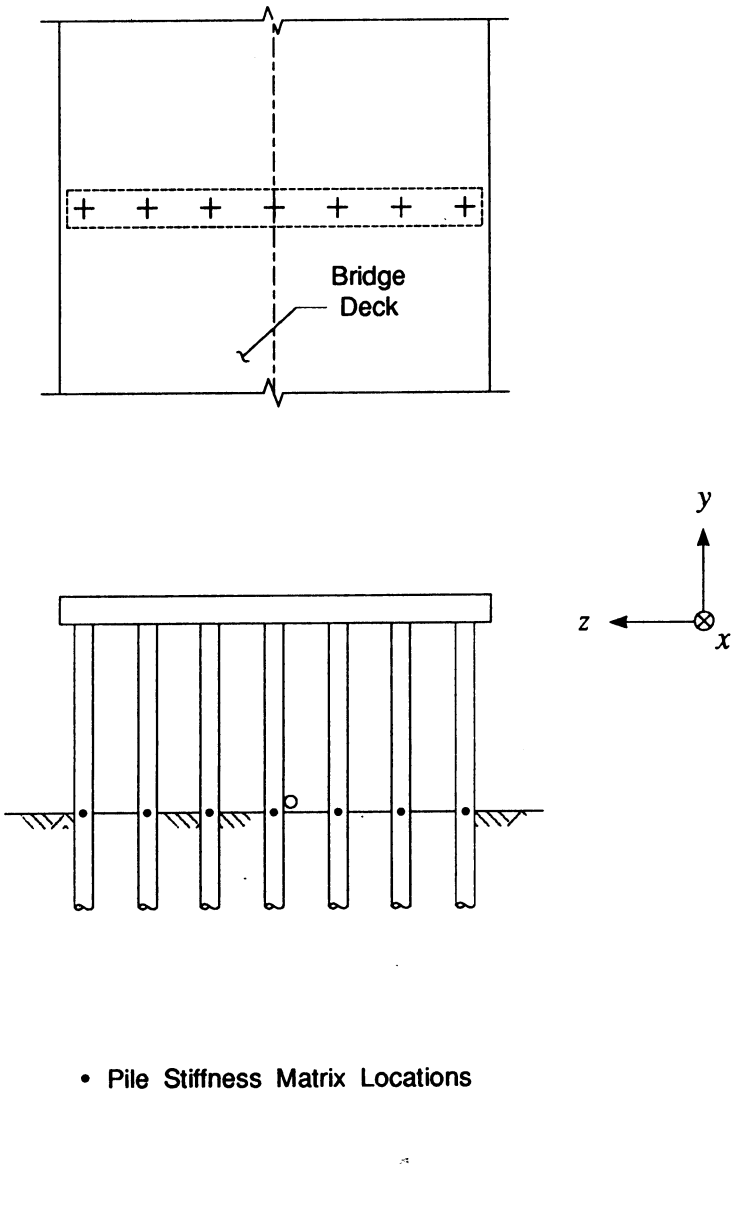

• Pile Stiffness Matrix Locations

Figure 6.2

6.1 PILE STIFFNESS CALCULATION

Pile stiffnesses are computed for a single pile extending from the mudline to the pile tip. Since these piles are continuous with the column sections extending to the ledger beams, a fixed-head condition is appropriate.

The pile-head stiffness matrix for the local pile-head coordinate system is of the form

$$[K_p] = \begin{bmatrix} K_x & 0 & 0 & 0 & 0 & K_{x,\theta y} \\ 0 & K_z & 0 & 0 & 0 & 0 \\ 0 & 0 & K_y & K_{y,\theta x} & 0 & 0 \\ 0 & 0 & K_{\theta x,y} & K_{\theta x} & 0 & 0 \\ 0 & 0 & 0 & 0 & 0 & 0 \\ K_{\theta y,x} & 0 & 0 & 0 & 0 & K_{\theta y} \end{bmatrix}$$

Because the pile cross-section is circular, the stiffness values in the two horizontal directions have the same absolute value, differing only by a sign change in the off-diagonal term. Thus, the stiffness matrix may be written as

$$[K_p] = \begin{bmatrix} K_x & 0 & 0 & 0 & 0 & K_{x,\theta y} \\ 0 & K_z & 0 & 0 & 0 & 0 \\ 0 & 0 & K_x & -K_{x,\theta y} & 0 & 0 \\ 0 & 0 & -K_{\theta y,x} & K_{\theta x} & 0 & 0 \\ 0 & 0 & 0 & 0 & 0 & 0 \\ K_{\theta y,x} & 0 & 0 & 0 & 0 & K_{\theta x} \end{bmatrix}$$

Of the five terms which must be evaluated, K_x and K_z are computed using the same methods as for Pier 1, taking into account the fixed head condition mentioned above.

Because each pile is treated as a separate foundation rather than as an element of a pile group, it is now necessary to compute the pile-head moment stiffness and force-moment coupling terms. In the calculation of the stiffness matrix for a pile group, these terms are typically neglected because (1) rotation of a pilecap results in translation of the piles which are positioned away from the center of rotation, and (2) the restoring moment arising from these translations is far greater than the restoring moment caused by rotation of the individual pile heads. For a single pile, however, this translational component is absent and, consequently, the rotation of the pile heads assumes a greater significance. Therefore, the moment-rotation terms cannot be neglected, nor can the off-diagonal force-rotation and moment-displacement terms.

The FHWA (1986) methodology neglects the torsional stiffnesses ($K_{\theta z}$) of individual piles. This stiffness should not influence the dynamic response of the bridge, and thus setting $K_{\theta z} = 0$ is an acceptable approximation.

The terms in the pile-head stiffness matrix are determined by first calculating the pile properties. These values are then used to evaluate the p-y, t-z, and Q-z curves which are reduced by 50% to account for the high-strain soil condition and used as input to the BMCOL-76 program. This exercise is very similar to the computations performed for Pier 1 which are presented in Sections 4.1.1-4.1.5.

6.1.1 Preparation of BMCOL-76 Input

Preparation of the BMCOL-76 input file for determination of K_x and K_z is similar to the input for the Coldwater Creek example, Pier 1. This explanation will not be repeated here.

The value of $K_{\theta y,x}$ can be evaluated from the "fixed-head" results from the lateral stiffness input file. In order to determine the values of $K_{\theta y}$ and $K_{x,\theta y}$, the input file must be modified so that (1) a moment, rather than a force, is applied to the pile head, and (2) the pile head is fixed against deflection, rather than rotation. This is achieved by altering Tables 7 and 8 of the input file (see Sec 4.1.6 of the Coldwater Example). No changes in the p-y curves are required. A similar option is available in the COM624 program used by WSDOT.

6.1.2 BMCOL-76 Output

The output files were used to generate lateral load-deflection curves and axial load-deflection curves similar to those for Pier 1 (Figures 6.3 and 6.4). Moment-displacement curves are generated by plotting the internal pile-head moments and corresponding displacements from the fixed-head lateral load condition (Figure 6.5).

Moment-rotation and force-rotation curves must be generated from the moment input file in order to evaluate the remaining stiffness terms. In the force-rotation curves, the shear within the pile section at the pile head is plotted against the corresponding pile-head rotation.

6.1.3 Calculation of Pile Head Stiffnesses

The pile-head stiffnesses are computed from the load-deflection curves in Figures 6.3 and 6.4 as follows. For the axial load case, the axial pile-head stiffness is the slope of the load-deflection curve (Figure 6.3) at the origin (i.e. the initial tangent slope). For the lateral load case (Figure 6.4), the lateral pile-head stiffness is the slope of straight line from the origin to the point on the load-deflection curve corresponding to 0.50 in deflection. These rules for estimating pile-head stiffnesses were presented in Section 4.1.7 of the Coldwater Creek example.

For the moment-rotation ($K_{\theta x}$), force-rotation ($K_{x,\theta y}$), and moment-deflection ($K_{\theta y,x}$) terms, the stiffnesses are equal to the initial tangent slope of the curve. Note that the values for $K_{x,\theta y}$ and $K_{\theta y,x}$ are numerically equal because the force-rotation and moment-deflection curves are linear for small deflections. If the non-linearity of the soil-pile system is considered (e.g. by taking a secant stiffness), the two values will not necessarily be equal.

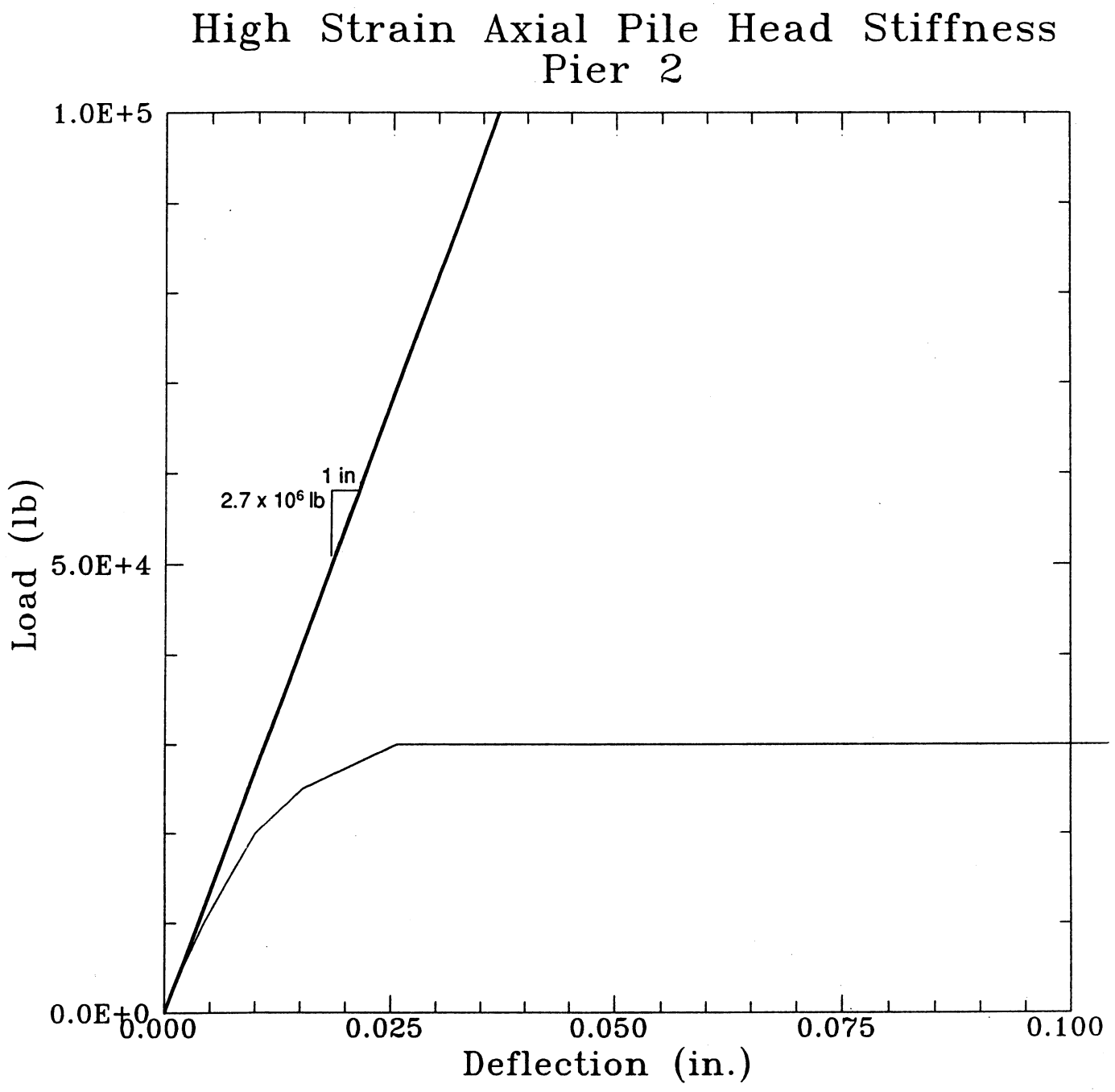
High Strain Axial Pile Head Stiffness
Pier 2
1.0E+5
5.0E+4
0.0E+0
Load (lb)
1 in
2.7 x 10^6 lb
0.000
0.025
0.050
0.075
0.100
Deflection (in.)

Figure 6.3

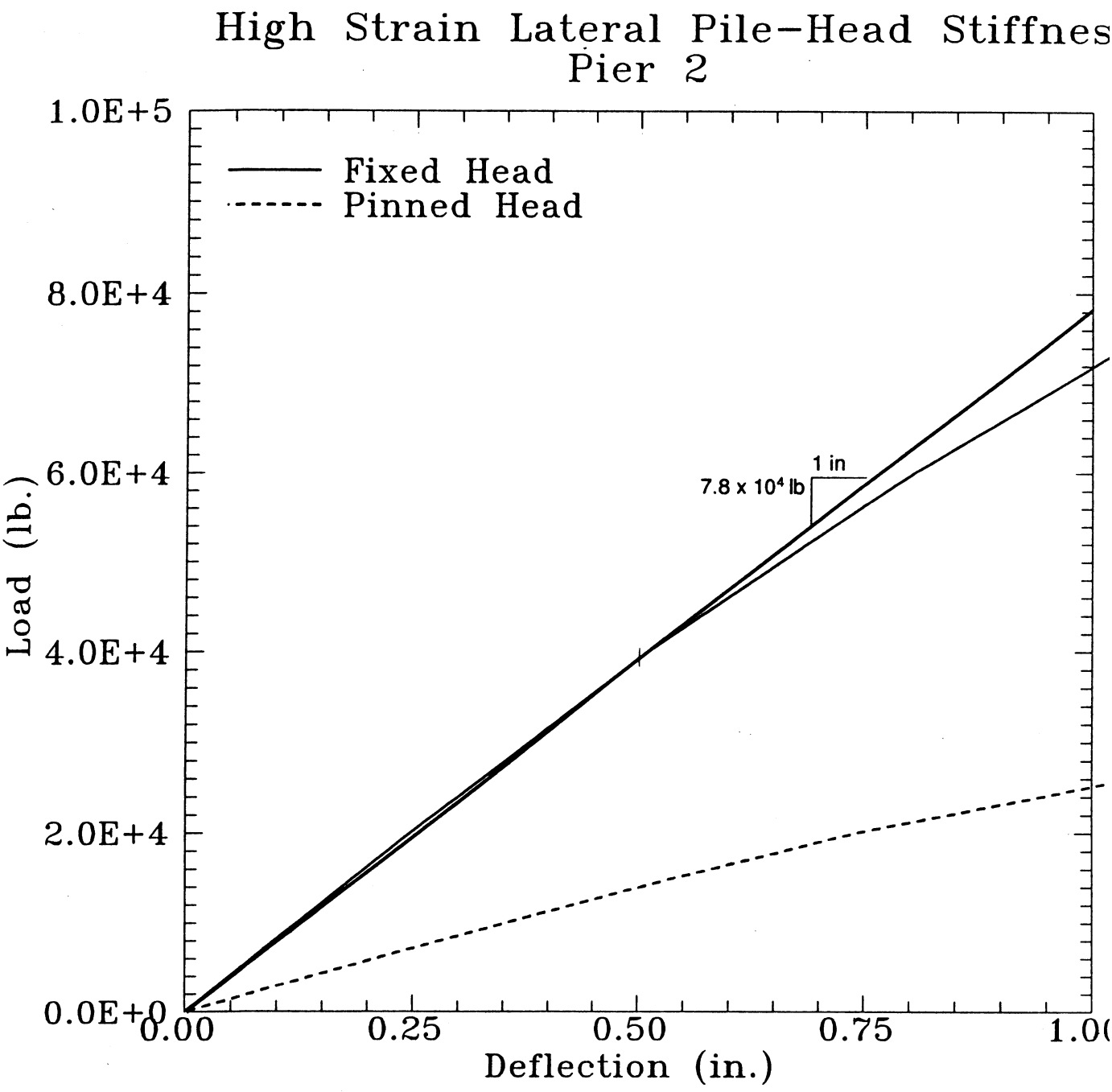
High Strain Lateral Pile-Head Stiffnes
Pier 2
Fixed Head
Pinned Head
1 in
7.8 x 10⁴ lb
Load (lb.)
1.0E+5
8.0E+4
6.0E+4
4.0E+4
2.0E+4
0.0E+0
0.00
0.25
0.50
0.75
1.0(
Deflection (in.)

Figure 6.4

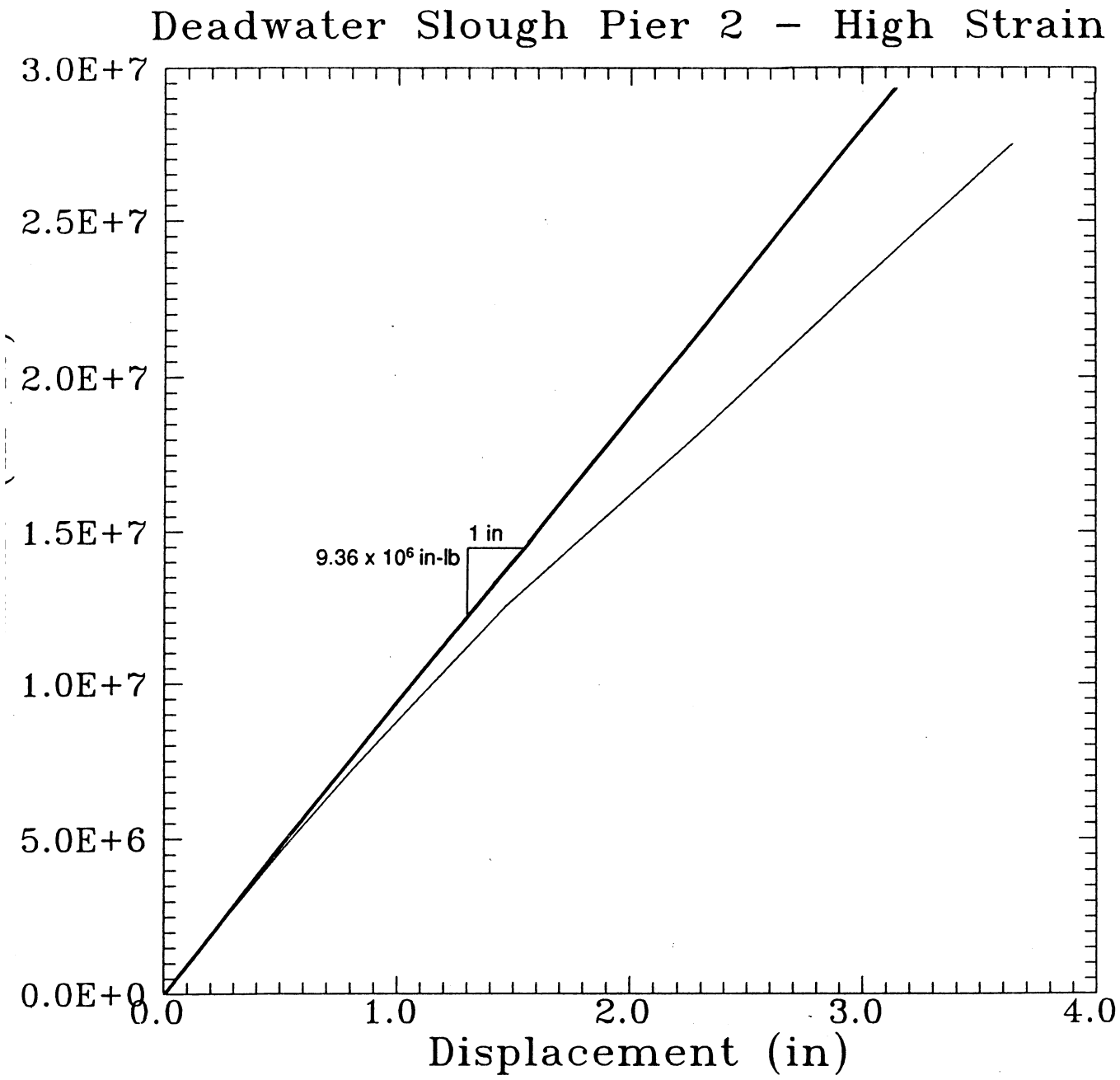
Deadwater Slough Pier 2 – High Strain
3.0E+7
2.5E+7
2.0E+7
1.5E+7
1.0E+7
5.0E+6
0.0E+0
0.0
1.0
2.0
3.0
4.0
Displacement (in)
1 in
9.36 x 10^6 in-lb

Figure 6.5

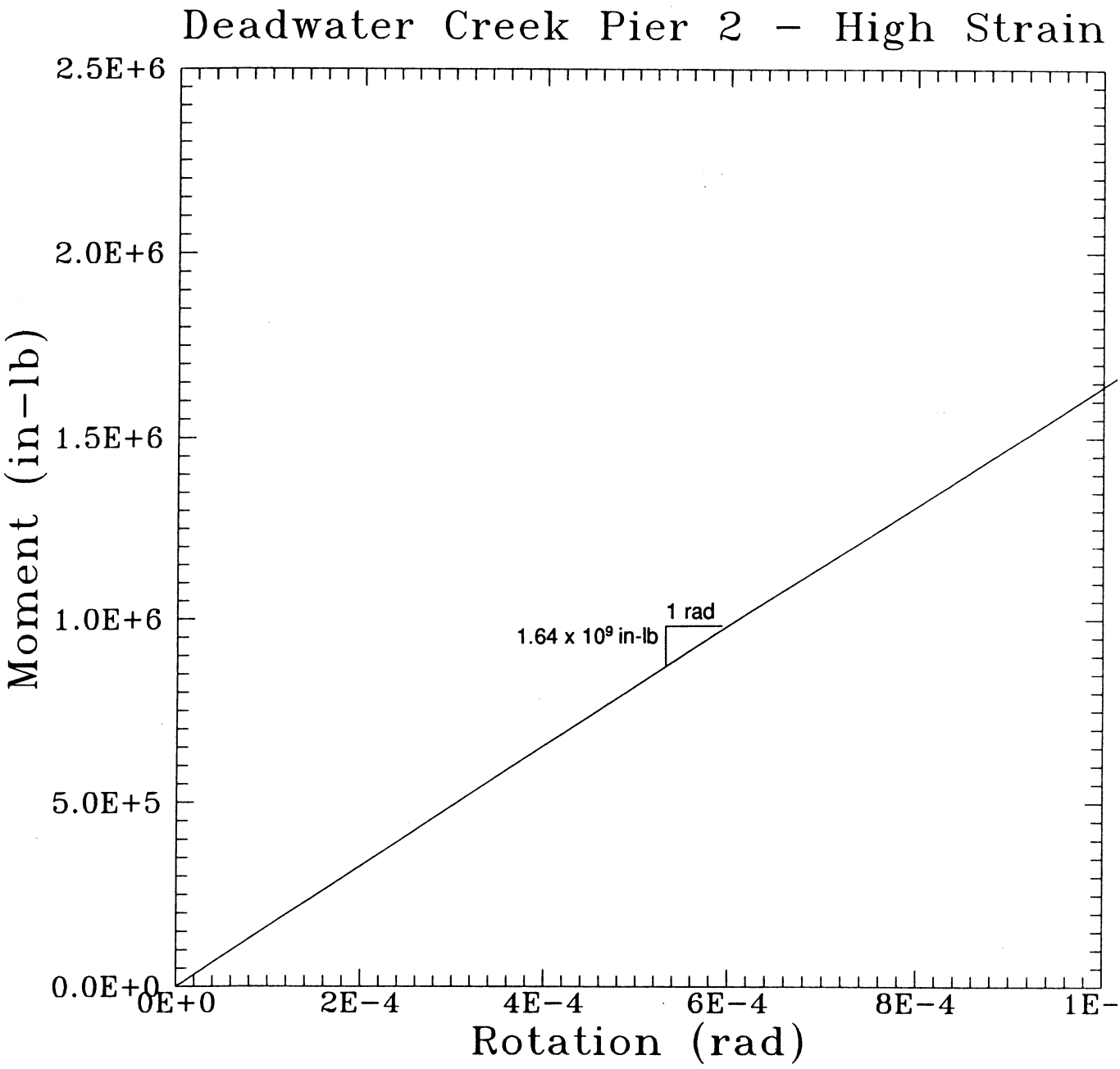
Deadwater Creek Pier 2 - High Strain
2.5E+6
2.0E+6
1.5E+6
1.0E+6
5.0E+5
0.0E+0
Moment (in-lb)
1 rad
1.64 x 10^9 in-lb
0E+0
2E-4
4E-4
6E-4
8E-4
1E-
Rotation (rad)

Figure 6.6

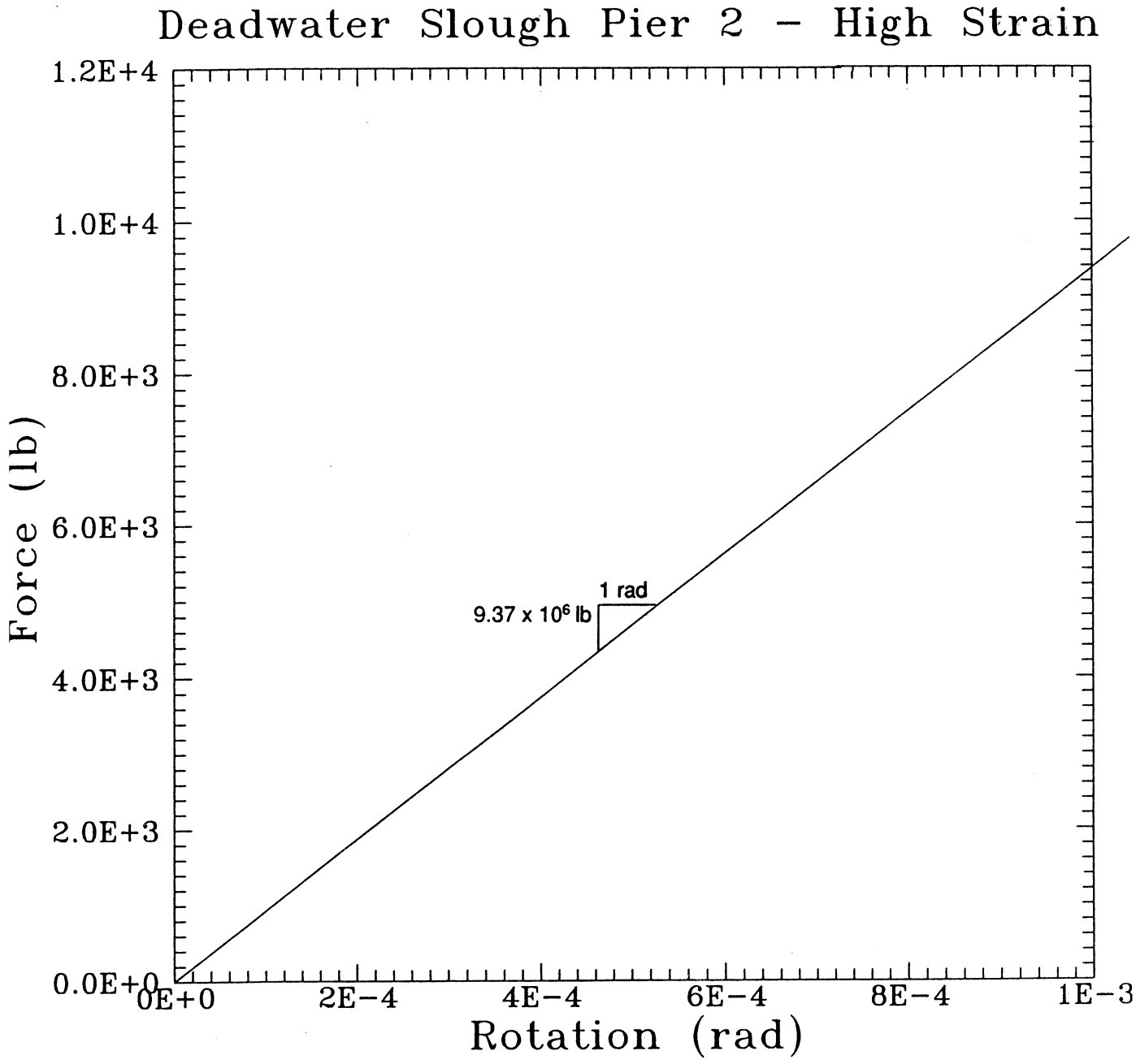
Deadwater Slough Pier 2 - High Strain
1.2E+4
1.0E+4
8.0E+3
6.0E+3
4.0E+3
2.0E+3
0.0E+0
Force (lb)
1 rad
9.37 x 10^6 lb
0E+0
2E-4
4E-4
6E-4
8E-4
1E-3
Rotation (rad)

Figure 6.7

As noted previously, the "piles" are continuous with the "columns" at Pier 2. A fixed condition is therefore used to compute pile head stiffnesses. The resulting values of stiffness (see Figures 6.3-6.7) are:

$$K_z = 2.7 \times 10^6 \text{ lb/in} = 3.24 \times 10^7 \text{ lb/ft}$$

$$K_x = K_y = 7.8 \times 10^4 \text{ lb/in} = 9.36 \times 10^5 \text{ lb/ft}$$

$$K_{\theta x} = K_{\theta y} = 1.6 \times 10^9 \text{ lb-in} = 1.33 \times 10^8 \text{ lb-ft}$$

$$K_{x,\theta y} = -K_{y,\theta x} = 9.4 \times 10^6 \text{ lb}$$

$$K_{\theta y,x} = -K_{\theta x,y} = 9.4 \times 10^6 \text{ lb}$$

The stiffness matrix for Pier 2 is:

$$[K_p] = \begin{bmatrix} 9.36E05 & 0 & 0 & 0 & 0 & 9.40E06 \\ 0 & 3.24E07 & 0 & 0 & 0 & 0 \\ 0 & 0 & 9.36E05 & -9.40E06 & 0 & 0 \\ 0 & 0 & -9.40E06 & 1.33E08 & 0 & 0 \\ 0 & 0 & 0 & 0 & 0 & 0 \\ 9.40E06 & 0 & 0 & 0 & 0 & 1.33E08 \end{bmatrix}$$

The units are lb and ft.

7.0 PIER 2 STIFFNESS CALCULATION - NOVAK METHOD

7.1 SOIL MODEL

The pier model used is described in Section 6.0 and shown in Figure 6.1. The soil model is shown in Figure 7.1. Values of shear-wave velocity, V_s, are computed using high-strain values of shear moduli. The damping ratio for the soil was assumed to be $\zeta = 0.03$.

7.2 PREPARATION OF DYNA3 INPUT

The DYNA3 input file for Pier 2 is listed in Table 7.1. The inputs are described in detail for Pier 1 of the Coldwater example. Note that there is only a single pile and that there is no footing. Therefore, the footing length and width are set equal to zero and the embedment option is omitted.

7.3 DYNA3 OUTPUT

The stiffness matrix for Pier 2 is given for a single pile only, and is given by $[K_p]$. From Table 7.2,

Soil Model for Novak Stiffness Calculation for Pile and Footing Side Case at Pier 2

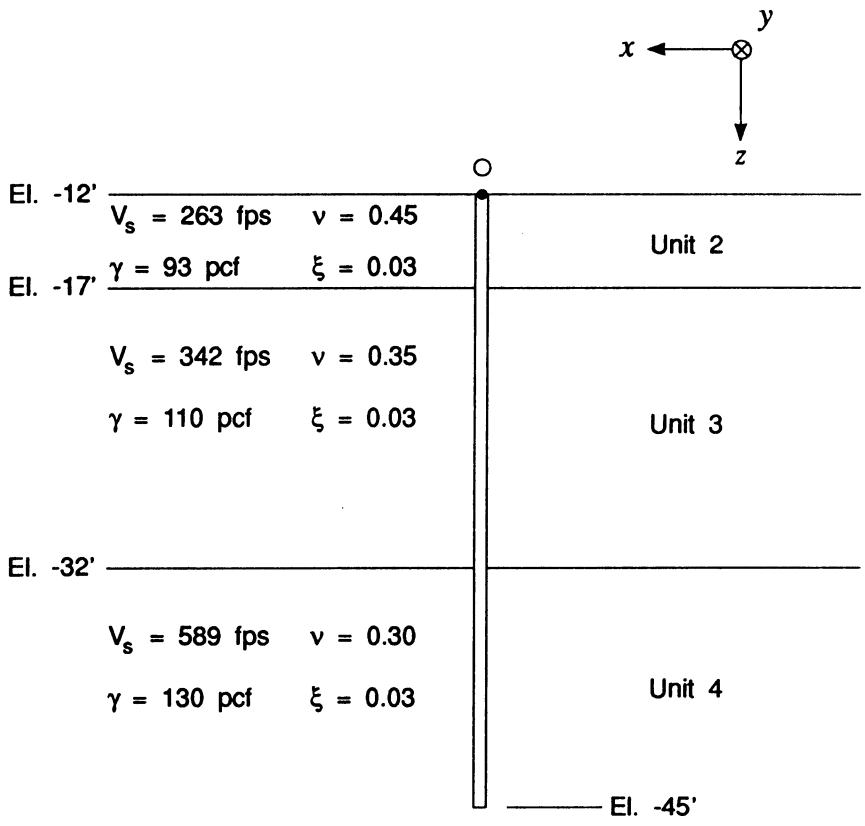

NOTES

V_s Shear-wave velocity $=\sqrt{G/\gamma_m}$, where G is the high-strain value of shear modulus = 50% of the low-strain G value in Figure 5.1. The parameter γ_m is mass density.

ξ Soil damping ratio (assumed).

xyz Coordinate system in this figure is oriented differently from the one in Figure 5.1.
In Novak's model, the *z* coordinate axis is positive downward.

Figure 7.1

```
TITLE=DEADWATER SLOUGH PIER 2 [ PILES + EMBEDMENT ] [k ft s]
MATRIX
GRAVITY=32.2
FOUNDATION=PILE
RECTANGULAR=0.,0.
MASS=100.,100.,100.,100.,100.,100.,100.
LAYERS=3
FIXED=1
 1  0.00    0.0
CONSTANTS=0.,0.,0.0,33.,.145,0.,0.17,0.05,1.11,5.18E05
ELEMENT
1   5.0  1.031  1.031  4.73  1.582 1.582 3.164
2  15.0  1.031  1.031  4.73  1.582 1.582 3.164
3  13.0  1.031  1.031  4.73  1.582 1.582 3.164
END-BEARING
NO-INTERACTION
SOIL
CONSTANTS
1   263.  .093  0.45 0.03
2   342.  .110  0.35 0.03
3   589.  .130  0.30 0.03
BELOW
589.  .130  .30  0.03
LOAD=HARMONIC
CONSTANTS
NONQUADRATIC
0.001  0.001  0.001  0.0  10.  0.0  0.  0.  0.
RUN
```

Table 7.1

```
*************************************************
*                                               *
*        D Y N A 3   S I M U L A T I O N        *
*                                               *
*              RUN DATE -  1992/12/29           *
*              TIME     -  10:16:57             *
*              REVISION -  1991/07/30           *
*                                               *
*************************************************

DEADWATER SLOUGH PIER 2 [ PILES + EMBEDMENT ] [k ft

                                    RESULTS
                                    *******


FREQUENCY  -     .0010
*********

STIFFNESS CONSTANTS (K)
***********************

HORIZONTAL TRANSLATION  (X) ...  7.30771E+03
HORIZONTAL TRANSLATION  (Y) ...  7.30771E+03
VERTICAL TRANSLATION  (Z) .....  3.53840E+04
ROTATION ABOUT  (X) ...........  2.24244E+05
ROTATION ABOUT  (Y) ...........  2.24244E+05
TORSION ABOUT  (Z) ............  5.32358E+04
CROSS-STIFFNESS (YZ PLANE) ....  2.92800E+04
CROSS-STIFFNESS (XZ PLANE) .... -2.92800E+04

DAMPING CONSTANTS (C)
*********************
HORIZONTAL TRANSLATION  (X) ...  2.55049E+05
HORIZONTAL TRANSLATION  (Y) ...  2.55049E+05
VERTICAL TRANSLATION  (Z) .....  1.24779E+06
ROTATION ABOUT  (X) ...........  9.93669E+06
ROTATION ABOUT  (Y) ...........  9.93669E+06
TORSION ABOUT  (Z) ............  2.22731E+06
CROSS-DAMPING  (YZ PLANE) .....  1.15456E+06
CROSS-DAMPING  (XZ PLANE) ..... -1.15456E+06
```

Table 7.2

$$[K_p] = \begin{bmatrix} 7.31E06 & 0 & 0 & 0 & -2.93E07 & 0 \\ 0 & 7.31E06 & 0 & 2.93E07 & 0 & 0 \\ 0 & 0 & 3.54E07 & 0 & 0 & 0 \\ 0 & 2.93E07 & 0 & 2.24E08 & 0 & 0 \\ -2.93E07 & 0 & 0 & 0 & 2.24E08 & 0 \\ 0 & 0 & 0 & 0 & 0 & 5.32E07 \end{bmatrix}$$

The units are lb and ft.

8.0 PIER 3 AND PIER 4 FOUNDATION STIFFNESSES

The FHWA and Novak methods were applied to Pier 3 and Pier 4. Because these pier foundations are similar to the Pier 1 and Pier 2 foundations, only the final results of the stiffness calculations are presented in Section 8.1 (Pier 3) and Section 8.2 (Pier 4). The stiffnesses are computed at the same point on the Pier 4 abutment (i.e., top of pile cap) and Pier 3 (i.e., top of "pile") as in the Piers 1 and 2 stiffness calculations.

8.1 PIER 3 FOUNDATION STIFFNESSES

8.1.1 FHWA Method

The Pier 3 soil profile is shown in Figure 8.1. The corresponding pile stiffness matrix is:

Pier 3
Soil Profile

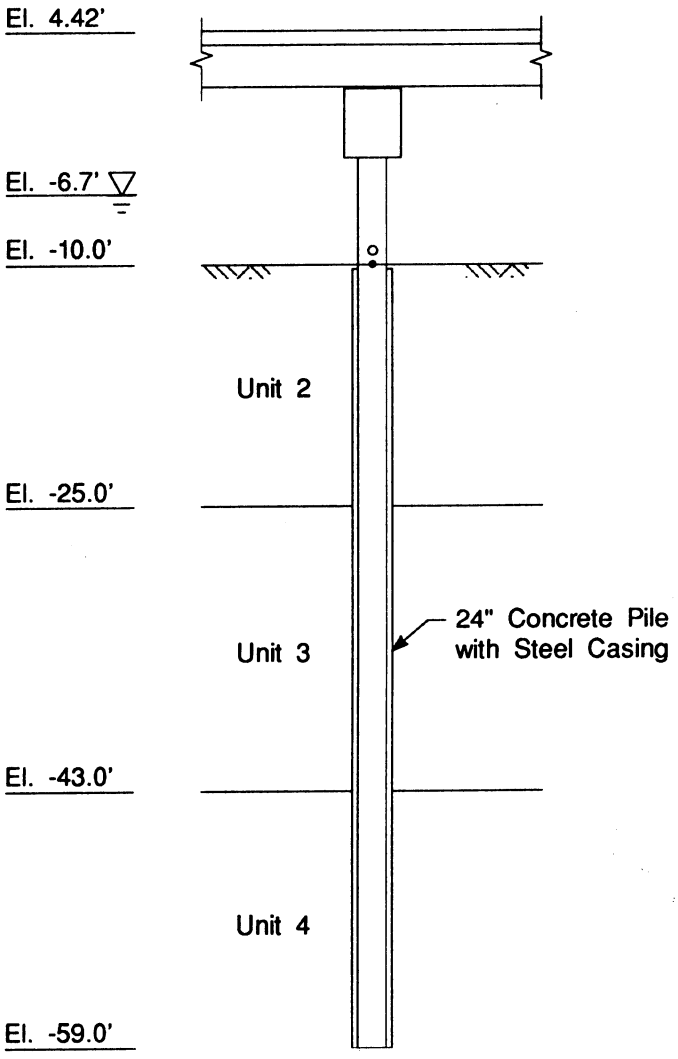

Soil properties are as for Pier 1. See Figure 1.

Coordinate Systems

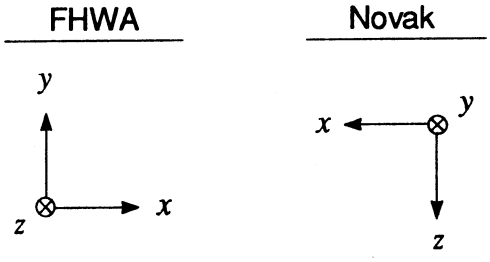

Figure 8.1

$$[K_p] = \begin{bmatrix} 6.48E05 & 0 & 0 & 0 & 0 & 6.84E06 \\ 0 & 3.24E07 & 0 & 0 & 0 & 0 \\ 0 & 0 & 6.48E05 & -6.84E06 & 0 & 0 \\ 0 & 0 & -6.84E06 & 1.15E08 & 0 & 0 \\ 0 & 0 & 0 & 0 & 0 & 0 \\ 6.84E06 & 0 & 0 & 0 & 0 & 1.15E08 \end{bmatrix}$$

The units are lb and ft. The coordinate system is defined as the local pile system shown in Figure 6.1.

8.1.2 Novak Method

The DYNA3 output file for Pier 3 is listed in Table 8.1. The coordinate system is defined as shown in Figure 7.1.

$$[K_p] = \begin{bmatrix} 6.33E6 & 0 & 0 & 0 & -2.50E7 & 0 \\ 0 & 6.33E6 & 0 & 2.50E7 & 0 & 0 \\ 0 & 0 & 3.58E7 & 0 & 0 & 0 \\ 0 & 2.50E7 & 0 & 2.04E8 & 0 & 0 \\ -2.50E7 & 0 & 0 & 0 & 2.04E8 & 0 \\ 0 & 0 & 0 & 0 & 0 & 4.58E7 \end{bmatrix}$$

```
************************************************
*                                              *
*        D Y N A 3   S I M U L A T I O N       *
*                                              *
*             RUN DATE -  1992/12/29           *
*             TIME     -  10:17: 5             *
*             REVISION -  1991/07/30           *
*                                              *
************************************************

DEADWATER SLOUGH PIER 3 [ PILES + EMBEDMENT ] [k ft

                                   RESULTS
                                   *******


FREQUENCY  -     .0010
*********

STIFFNESS CONSTANTS (K)
***********************

HORIZONTAL TRANSLATION  (X) ...  6.33039E+03
HORIZONTAL TRANSLATION  (Y) ...  6.33039E+03
VERTICAL TRANSLATION  (Z) .....  3.57623E+04
ROTATION ABOUT  (X) ...........  2.03883E+05
ROTATION ABOUT  (Y) ...........  2.03883E+05
TORSION ABOUT  (Z) ............  4.58072E+04
CROSS-STIFFNESS (YZ PLANE) ....  2.50342E+04
CROSS-STIFFNESS (XZ PLANE) .... -2.50342E+04

DAMPING CONSTANTS (C)
*********************
HORIZONTAL TRANSLATION  (X) ...  2.16561E+05
HORIZONTAL TRANSLATION  (Y) ...  2.16561E+05
VERTICAL TRANSLATION  (Z) .....  1.34892E+06
ROTATION ABOUT  (X) ...........  9.04653E+06
ROTATION ABOUT  (Y) ...........  9.04653E+06
TORSION ABOUT  (Z) ............  1.88671E+06
CROSS-DAMPING  (YZ PLANE) .....  9.79086E+05
CROSS-DAMPING  (XZ PLANE) ..... -9.79086E+05
```

Table 8.1

8.2 PIER 4 FOUNDATION STIFFNESSES

8.2.1 FHWA Method

The Pier 4 soil profile is shown in Figure 8.2. The final Pier 4 foundation stiffness matrix is:

$$[K_t] = \begin{bmatrix} 3.36E7 & 0 & 0 & 0 & 0 & -1.04E7 \\ 0 & 2.11E8 & 0 & 0 & 0 & 0 \\ 0 & 0 & 2.14E7 & -1.23E7 & 0 & 0 \\ 0 & 0 & -1.23E7 & 3.81E10 & 0 & 0 \\ 0 & 0 & 0 & 0 & 5.60E09 & 0 \\ -1.04E7 & 0 & 0 & 0 & 0 & 3.55E8 \end{bmatrix}$$

The units are lb and ft. The coordinate system is defined as shown in Figure 8.2 with the origin at Point O. Note that this global system is the same as the one for Pier 1 in Figure 4.1, although Pier 4 in Figure 8.2 is approximately a mirror image of Pier 1 in Figure 4.1[1].

[1]Piers 1 and 4 would be exact mirror images of each other in Figures 4.1 and 8.2 if the soil profiles were identical at both piers.

Pier 4
Abutment Profile

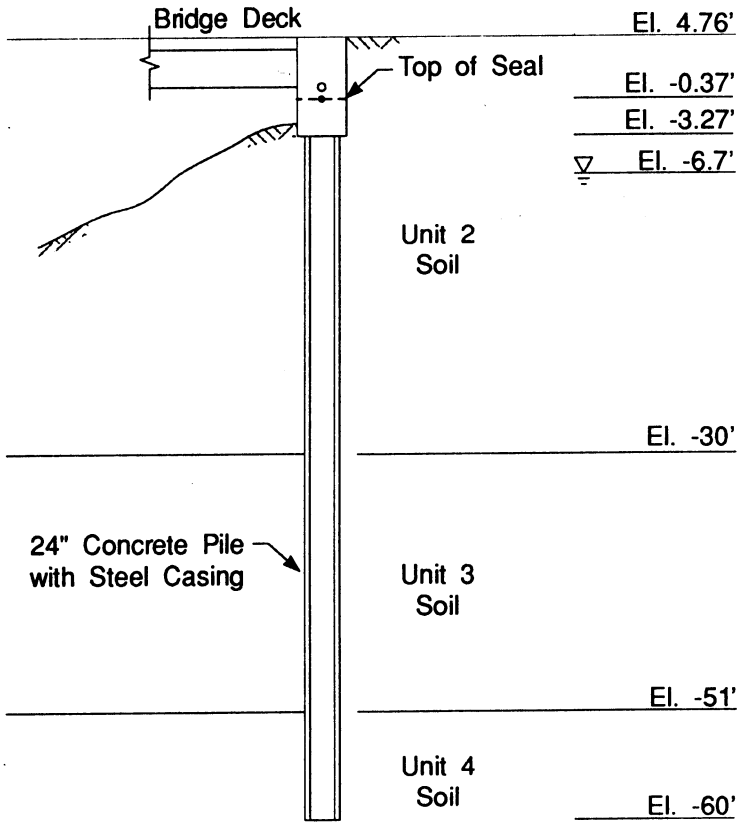

Soils are as for Pier 1. See figure 4.1.

Coordinate Systems

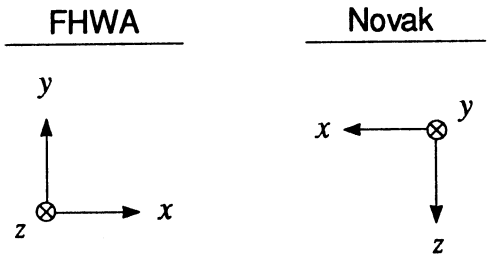

Figure 8.2

8.2.2 Novak Method

The final Pier 4 foundation stiffness matrix is:

$$[K_f] = \begin{bmatrix} 3.73E7 & 0 & 0 & 0 & -9.44E7 & 0 \\ 0 & 2.51E7 & 0 & 7.17E7 & 0 & 0 \\ 0 & 0 & 2.14E8 & 0 & 0 & 0 \\ 0 & 7.17E7 & 0 & 3.67E10 & 0 & 0 \\ -9.44E7 & 0 & 0 & 0 & 3.41E8 & 0 \\ 0 & 0 & 0 & 0 & 0 & 5.35E9 \end{bmatrix}$$

The units are lb and ft. The coordinate system is shown in Figure 8.1 with the origin at Point O. Relative to the entire bridge, this coordinate system is oriented the same as the coordinate system in Figure 5.1 for Pier 1.

9.0 APPLICATION TO SEISAB-I BRIDGE ANALYSIS

This example illustrates the use of SEISAB-I to conduct a response spectrum analysis of the Deadwater Slough Bridge, as described in Section 1.0.

The structure model is illustrated in Figure 9.1. In this example, Pier 1 abutment, Pier 2, Pier 3 and Pier 4 abutment are modeled in SEISAB-I analysis as Abutment 1, Bent 2, Bent 3 and Abutment 4, respectively. The bridge was analyzed twice to consider foundation stiffnesses determined by both the FHWA and Novak Methods.

9.1 ABUTMENT 1 MODEL

9.1.1 FHWA Method

Abutment 1 stiffness matrix $[K_t]$ given in Section 4.4.2 is for the GPILE coordinate system. The units are lb and ft. It is noted that for this example the GPILE coordinate system is the same as the SEISAB-I coordinate system, therefore, conversion to the SEISAB-I coordinate system is not required.

After converting from lb to kip units, we have:

$$[K_{SEISAB}] = \begin{bmatrix} 3.58E4 & 0 & 0 & 0 & 0 & 2.20E3 \\ & 2.44E5 & 0 & 0 & 0 & 0 \\ & & 2.45E4 & -2.32E4 & 0 & 0 \\ \text{Symmetrical} & & & 4.30E7 & 0 & 0 \\ & & & & 5.50E6 & 0 \\ & & & & & 3.78E5 \end{bmatrix}$$

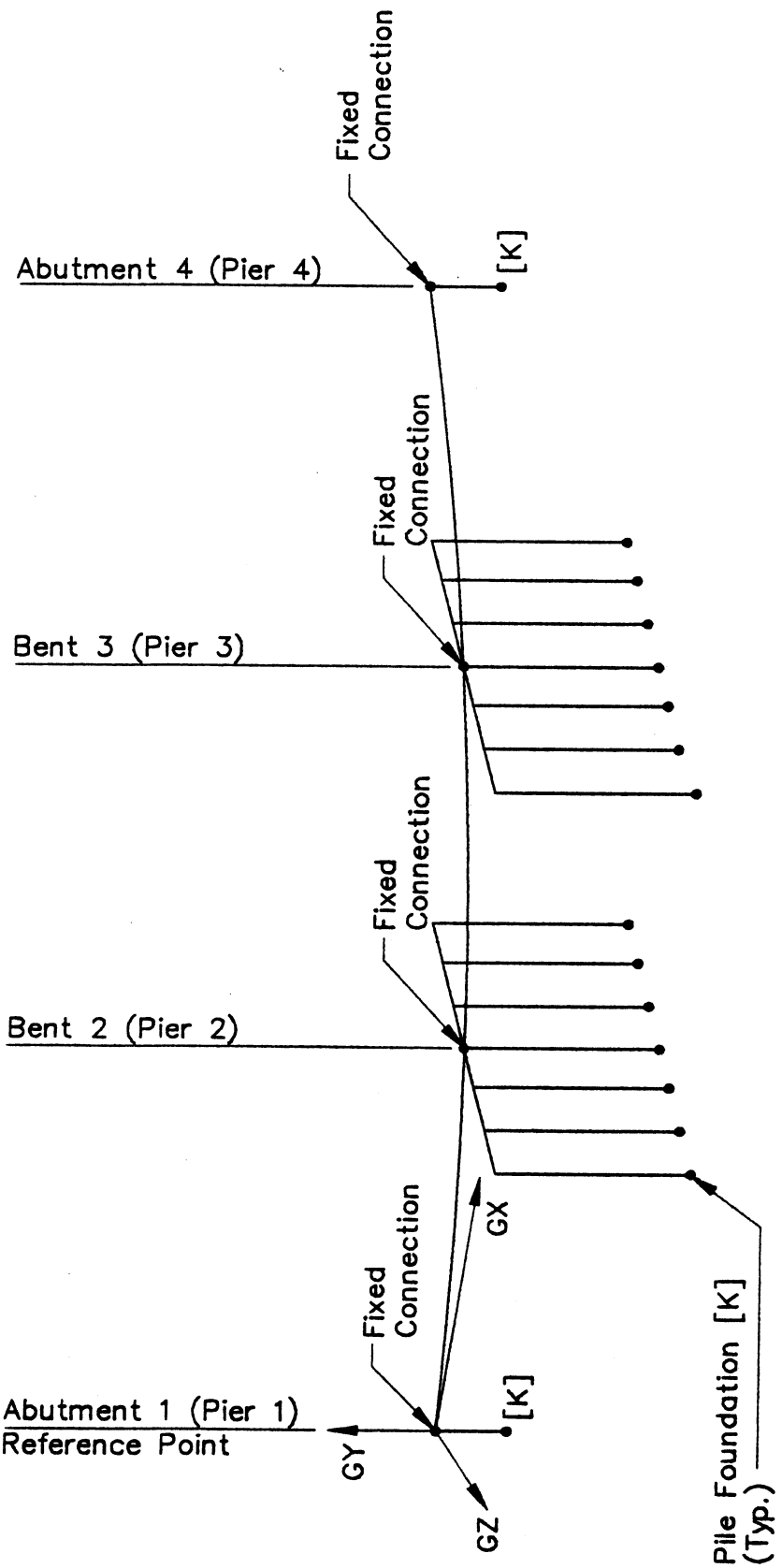

Deadwater Slough Structure Model

Figure 9.1

9.1.2 Novak Method

The Novak stiffness matrix given in Section 5.3 is for the Novak coordinate system. The units are lb and ft.

$$[K_{SEISAB}] = \begin{bmatrix} 5.91E7 & 0 & 0 & 0 & -3.44E8 & 0 \\ & 4.78E7 & 0 & 3.22E8 & 0 & 0 \\ & & 2.53E8 & 0 & 0 & 0 \\ \text{Symmetrical} & & & 4.60E10 & 0 & 0 \\ & & & & 3.10E9 & 0 \\ & & & & & 9.09E9 \end{bmatrix}$$

Converting to SEISAB-I coordinate system according to Appendix C-1 and from lb to kip units, we have:

$$[K_{SEISAB}] = \begin{bmatrix} 5.91E4 & 0 & 0 & 0 & 0 & -3.44E5 \\ & 2.53E5 & 0 & 0 & 0 & 0 \\ & & 4.78E4 & 3.22E5 & 0 & 0 \\ \text{Symmetrical} & & & 4.60E7 & 0 & 0 \\ & & & & 9.09E6 & 0 \\ & & & & & 3.10E6 \end{bmatrix}$$

9.2 BENT 2 MODEL

9.2.1 FHWA Method

The Bent 2 stiffness matrix $[K_p]$ given for each pile in Section 6.1.3 is for the coordinate system defined in Figure 6.1. This coordinate system is identical to the SEISAB-I coordinate system so conversion is not required. The units are lb and ft.

Converting from lb to kip units we have for each pile:

$$[K_{SEISAB}] = \begin{bmatrix} 9.36E2 & 0 & 0 & 0 & 0 & 9.40E3 \\ & 3.24E4 & 0 & 0 & 0 & 0 \\ & & 9.36E2 & -9.40E3 & 0 & 0 \\ \text{Symmetrical} & & & 1.33E5 & 0 & 0 \\ & & & & 0 & 0 \\ & & & & & 1.33E5 \end{bmatrix}$$

9.2.2 Novak Method

The Novak stiffness matrix is given for each pile in the Novak coordinate system in Section 7.3. The units are lb and ft.

$$[K_p] = \begin{bmatrix} 7.31E06 & 0 & 0 & 0 & -2.93E07 & 0 \\ & 7.31E06 & 0 & 2.93E07 & 0 & 0 \\ & & 3.54E07 & 0 & 0 & 0 \\ \text{Symmetrical} & & & 2.24E08 & 0 & 0 \\ & & & & 2.24E08 & 0 \\ & & & & & 5.32E07 \end{bmatrix}$$

Converting to SEISAB-I coordinate system according to Appendix C-1 and from lb to kip units we have:

$$[K_{SEISAB}] = \begin{bmatrix} 7.31E03 & 0 & 0 & 0 & 0 & -2.93E4 \\ & 3.54E4 & 0 & 0 & 0 & 0 \\ & & 7.31E3 & 2.93E4 & 0 & 0 \\ \text{Symmetrical} & & & 2.24ES & 0 & 0 \\ & & & & 5.32E4 & 0 \\ & & & & & 2.24E5 \end{bmatrix}$$

9.3 BENT 3 AND ABUTMENT MODELS

9.3.1 FHWA Method

The foundation stiffness matrices for these piers are given in Section 8.1.1 and 8.2.1, respectively. These stiffness matrices are used in the SEISAB-I analyses after converting from lb to kip units.

9.3.2 Novak Method

The foundation stiffness matrices are given in Section 8.1.2 and 8.2.2. Each was converted from Novak to SEISAB-I coordinate system and from lb to kip units. Conversion is the same as illustrated for Abutment 1 and Bent 2.

9.4 LOAD MODEL

The RESPONSE SPECTRUM must be input using the SEISAB ARBITRARY CURVE option in order to adjust the damping ratio as recommended in Task 1 Report, Section 6.2. In order to account for the 7-1/2 percent damping for those modes of vibration where soil-structure interaction is significant it is first necessary to identify those modes. This is done by first running the model using the seismic response spectrum (ACT6 CURVE) for 5 percent damping, SOIL TYPE II and ACCELERATION COEFFICIENT = 0.25, then recording R_a^t, R_d^t and R_d^v from the NORMALIZED SUPERSTRUCTURE MODE SHAPES output. The value theta is calculated and compared according to TASK 1 REPORT Section 5.2. Absolute displacement values are used for R_a^t, R_d^t and R_d^v. The response spectrum coefficient for each identified transverse mode is reduced by 15 percent to reflect the change to 7-

1/2 percent damping for that mode. It is convenient to construct the required SEISAB ARBITRARY CURVE using SEISAB-I output CS values for each mode period substituting reduced CS values described above where applicable. Run 2DEADFE2 is used to illustrate modification of the 5 percent damping ratio spectrum. Table 9.1 lists the spectrum modifications required.

TABLE 9.1
RUN 2DEADFE2 - RESPONSE SPECTRUM MODIFICATIONS FOR MODES WHERE SOIL-STRUCTURE INTERACTION IS SIGNIFICANT

MODE	R_a^t	R_d^t	R_d^v	θ	MODE PERIOD	MODIFIED SPECTRUM ORDINATE
1	0.513	1.000	0.012	0.507	0.302	0.536
4	0.996	0.892	0.886	0.560	0.151	0.536
7	0.991	0.666	0.031	1.422	0.078	0.536

1. Only transverse modes included.
2. $\theta = R_a^t/(R_d^t + R_d^v)$
3. For $\theta > 0.10$, Adjust Spectrum Ordinate
4. Modified spectrum ordinate is the spectrum ordinate for 5 percent damping reduced by 15% to convert to 7-1/2 percent damping. Note that spectrum ordinate for each period of vibration is output by SEISAB-I as CS.

EXAMPLE NO. 3

EBEY SLOUGH BRIDGE

TABLE OF CONTENTS

Section		Page
1.0	**DESCRIPTION OF BRIDGE AND FOUNDATION SOILS**	1
2.0	**SEISMIC DESIGN PARAMETERS**	1
3.0	**SOIL PROPERTIES**	2
4.0	**PIER 10 STIFFNESS CALCULATION - FHWA METHOD**	3
4.1	PILE STIFFNESS CALCULATION	3
4.1.1	Estimation of Pile Parameters	3
4.1.2	Computation of t-z Curves	3
4.1.2.1	General Procedure	3
4.1.2.2	Application to Ebey Slough Bridge Pier 10 Piles.	4
4.1.3	Computation of Q-z Curve	4
4.1.3.1	General Procedure.	4
4.1.3.2	Application to Ebey Slough Bridge Pier 10 Piles.	4
4.1.4	Computation of p-y Curves	4
4.1.4.1	General Procedure.	4
4.1.4.2	Application to Ebey Slough Bridge Pier 10 Piles.	4
4.1.5	Preparation of BMCOL-76 Input	4
4.1.6	BMCOL-76 Output	5
4.1.7	Calculation of Pile-Head Stiffnesses	5
4.1.8	Calculation of Pile-Group Stiffness Matrix	6
4.1.8.1	Assumptions.	6
4.1.8.2	Preparation of GPILE Input.	6
4.1.8.3	GPILE Output.	6
4.2	FOOTING STIFFNESSES	7
4.2.1	Model and Assumptions	7
4.2.2	Calculation of Footing Stiffnesses	7
4.2.2.1	General Procedure.	7
4.2.2.2	Application to Ebey Slough Pier 10 Pile Cap	7
4.3	WALL STIFFNESS	8
4.4	TOTAL PIER 10 STIFFNESS MATRIX	9
4.4.2	Application to Deadwater Slough Abutment.	9
5.0	**PIER 10 STIFFNESS CALCULATION - NOVAK METHOD**	10
5.1	PILE AND FOOTING SIDE STIFFNESS	11
5.1.1	Soil Model	11
5.1.2	Preparation of DYNA3 Input	11
5.1.3	DYNA3 Output	12
5.2	TOTAL PIER 10 STIFFNESS MATRIX	12

TABLE OF CONTENTS (Continued)

Section		Page
6.0 PIER 11 FOUNDATION STIFFNESSES		12
6.1	FHWA METHOD	13
6.2	NOVAK METHOD	13
7.0 PIER 12 FOUNDATION STIFFNESS		14
7.1	FHWA METHOD	14
7.1.1	Pile Stiffness	14
7.1.2	Footing Stiffness	15
7.1.3	Total Stiffness	15
7.2	NOVAK METHOD	16

8.0 APPLICATION TO SEISAB-I BRIDGE ANALYSIS 17
8.1 ABUTMENT MODELS 17
8.2 BENT MODELS 17
8.3 LOAD MODEL 19

1.0 DESCRIPTION OF BRIDGE AND FOUNDATION SOILS

The Ebey Slough Bridge is constructed of multiple bridge spans joined by bearing-hinges in the deck (Figure 1.1). For this example, only the section of the bridge which spans from the bearing-hinge west of Pier 10 to the bearing-hinge just east of Pier 12, a distance of approximately 466 feet, will considered. Hereafter, the word "bridge" will refer only to this section of the Ebey Slough Bridge.

The bridge section is a three-cell reinforced concrete box girder, approximately 7' 6" in depth and varying in width from 40 to 43 feet. The box girder is supported over its span by three piers constructed of a pile cap and a column section which extends from the top of the pile cap to the base of the box girder (Figures 1.2 and 1.3). The piers are designated as Pier 10, Pier 11, and Pier 12, numbering west to east. The piers are founded on pile groups of 20 (Piers 10 and 11) or 28 (Pier 12) 2' diameter reinforced concrete piles surrounded by a 3/8" steel sheathing (Figure 1.4). The piles are approximately 80 feet long, penetrating through a layer of soft clay and through alternating layers of dense and medium-dense sand. The piles extend upward through a 6' concrete seal and into a 6' thick reinforced concrete pile cap which supports the column section. The cap for Piers 10 and 11 is 28' long by 28' wide and 40' long by 34' wide for Pier 12. The seals are 2' larger in each dimension for each pier, resulting in total dimensions of 30' x 30' for Piers 10 and 11 and 42' x 36' for Pier 12.

2.0 SEISMIC DESIGN PARAMETERS

The ground acceleration coefficient for the seismic design of the Ebey Slough Bridge was 0.25. The appropriate soil category was Soil Type II, which is deep stiff soil over bedrock. The ATC-6, 5% damped response spectrum (Figure 2.1) for this soil type was normalized

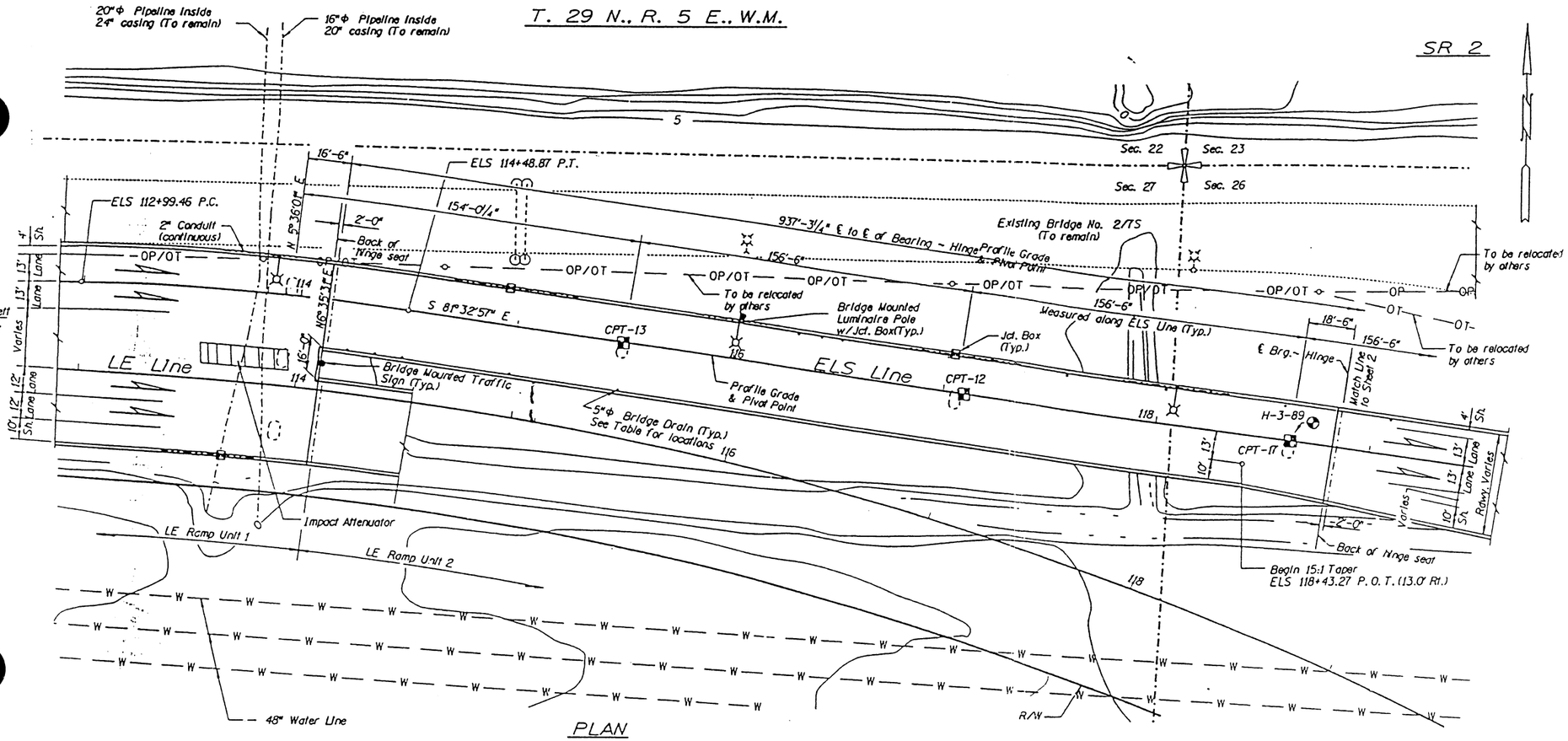

DATUM
...t I.Good.Vert.
...tum of 1929

POST TENSIONED
CONCRETE BOX GIRDER
LOADING: HS-20
OR
TWO 24 K AXLES & TRUCK

Figure 1.1

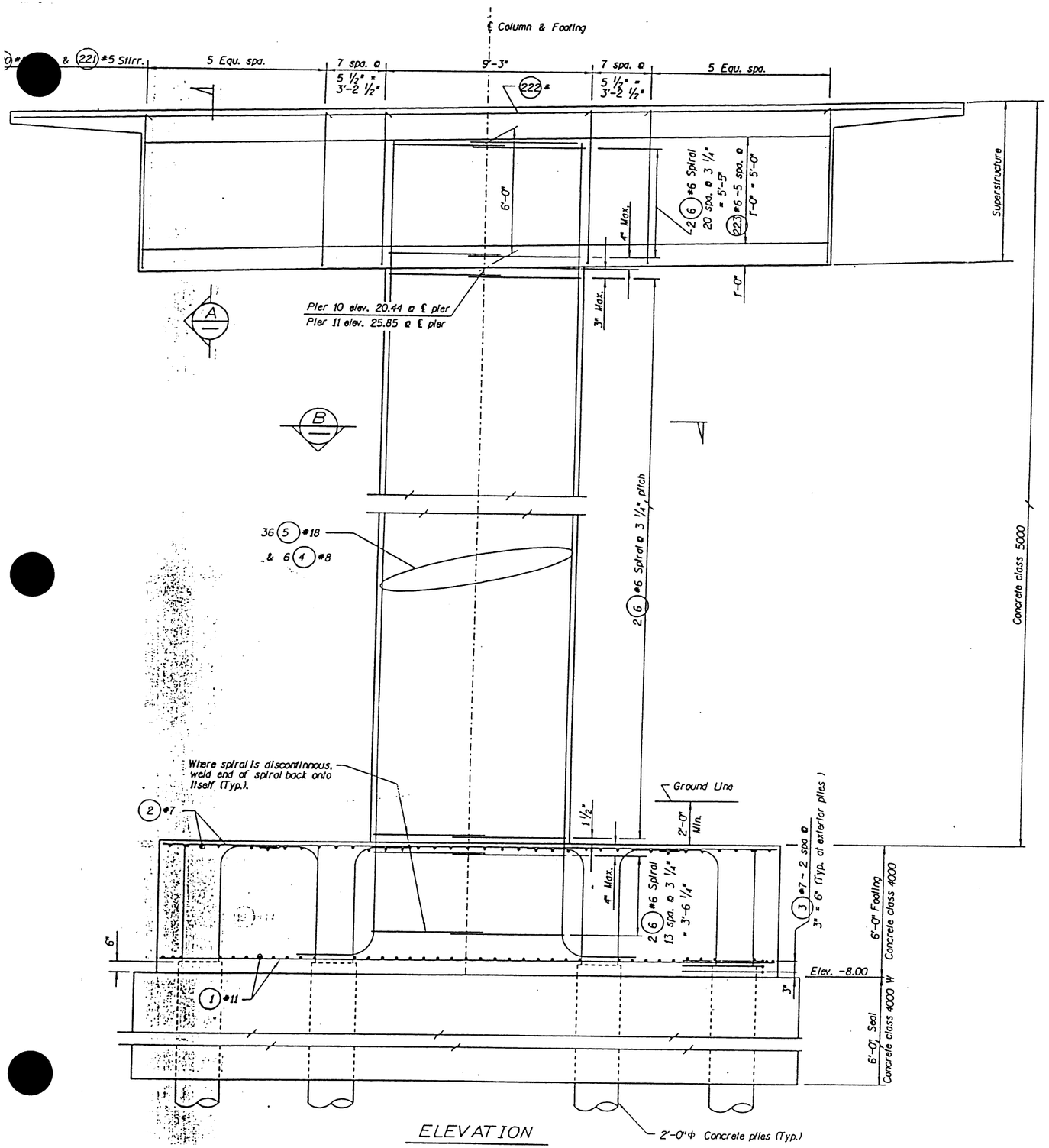

ELEVATION

PIER 10

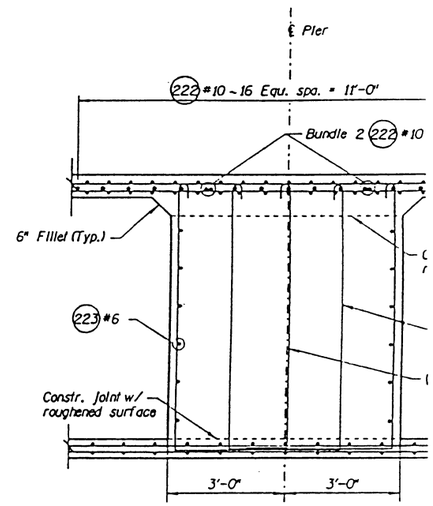

SECTION (A)

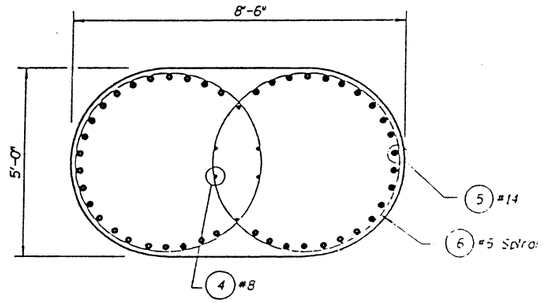

SECTION (B)

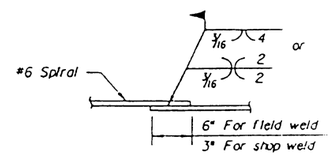

SPIRAL WELD DETAIL

Figure 1.2

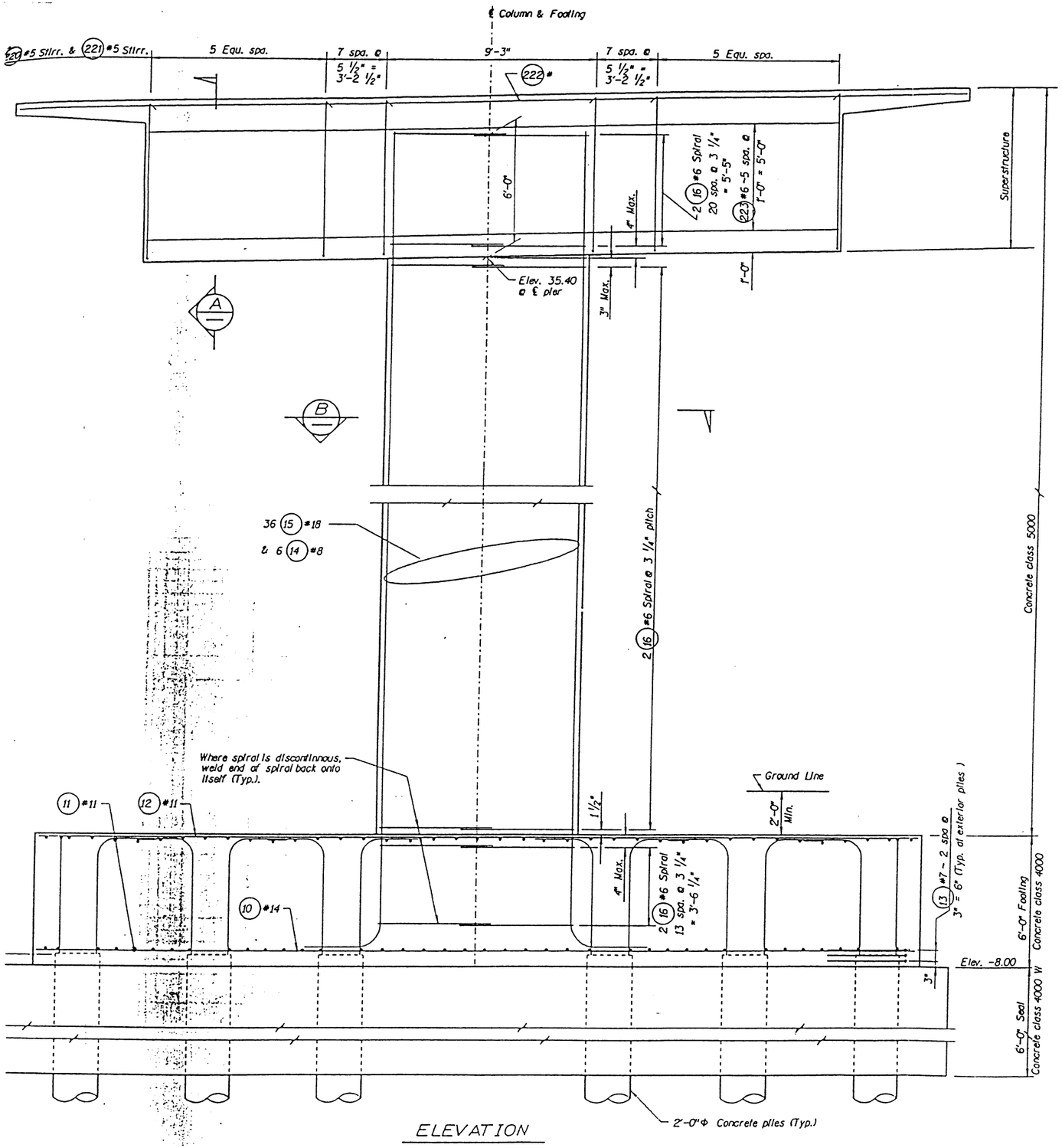

ELEVATION

PIER 12

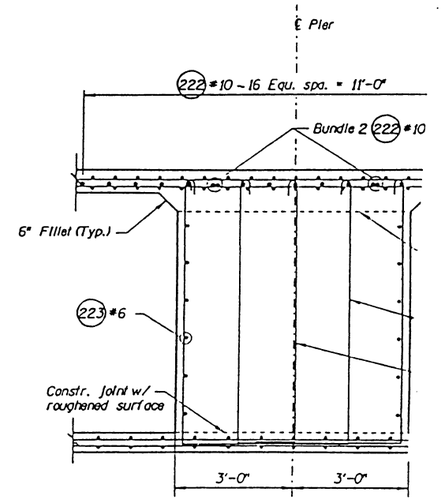

SECTION A

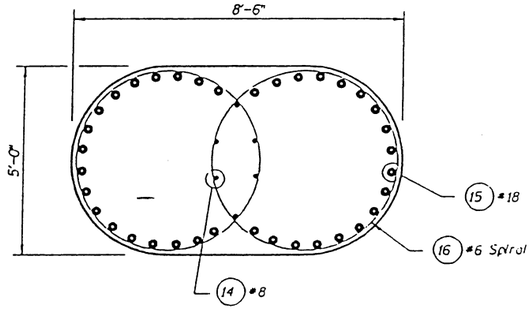

SECTION B

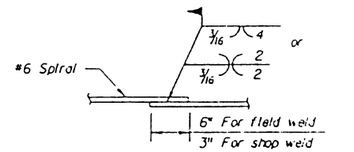

SPIRAL WELD DETAIL

Figure 1.3

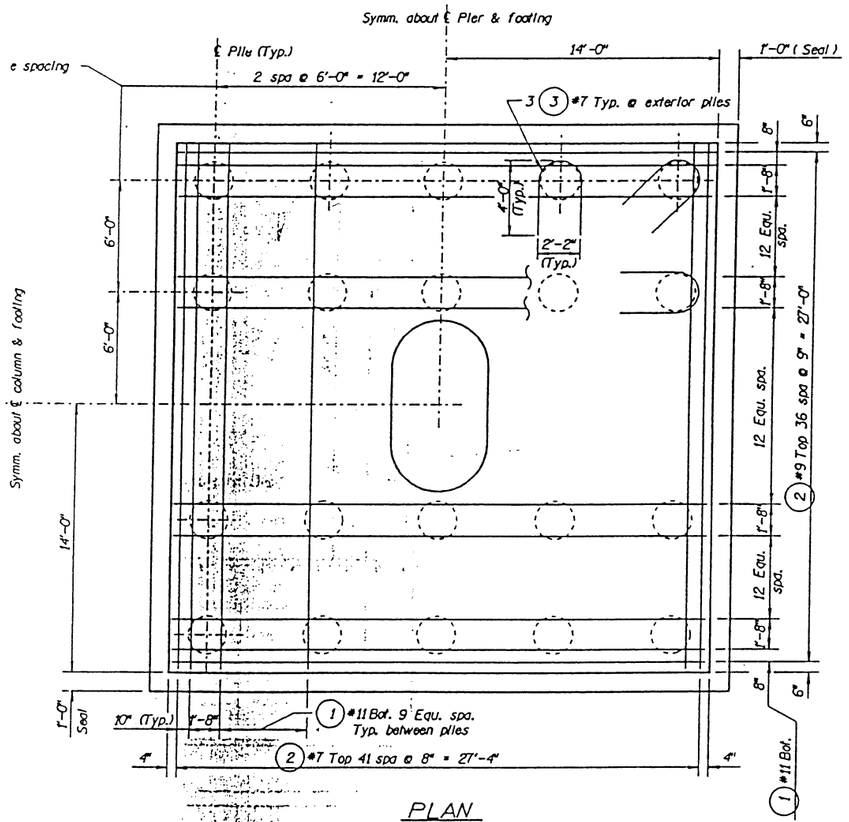

PLAN
PIERS 10 & 11 FOOTING

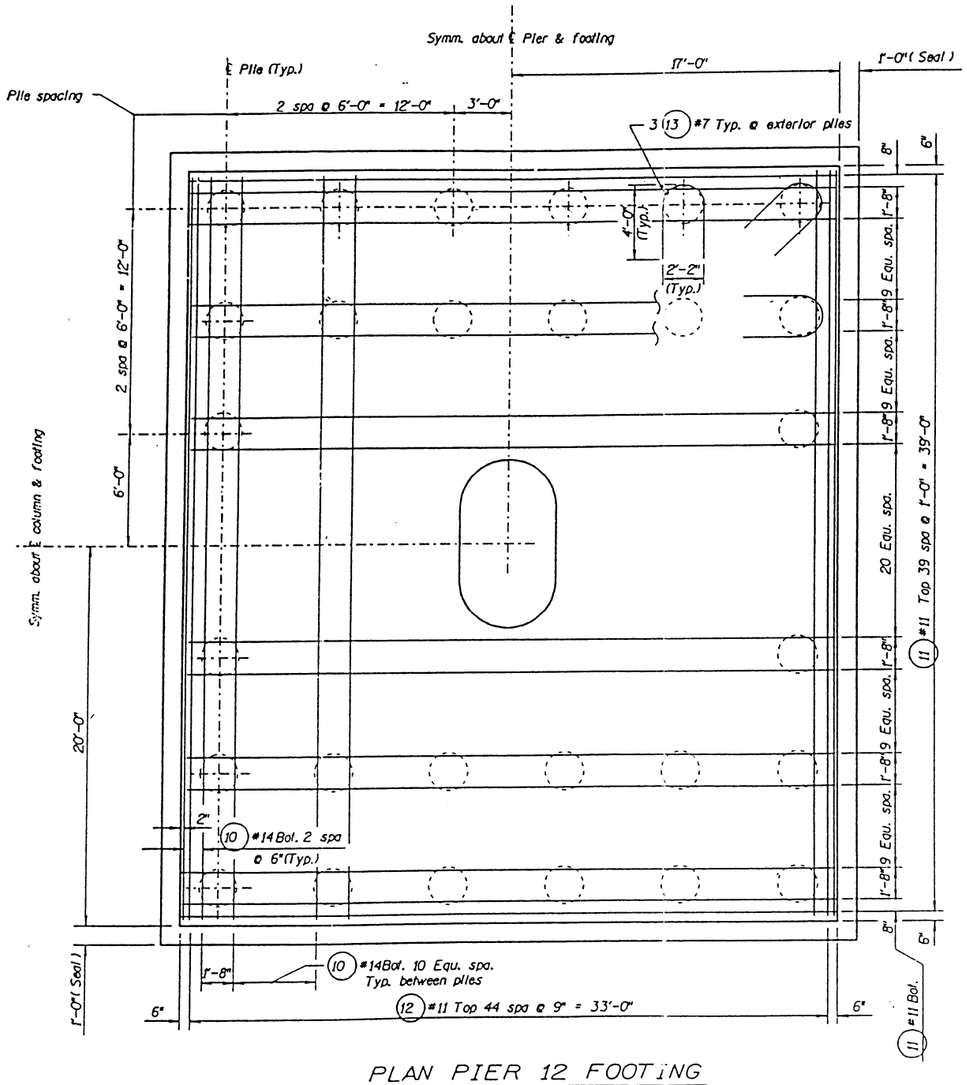

PLAN PIER 12 FOOTING

Figure 1.4

Normalized 5%
Damped Response Spectrum

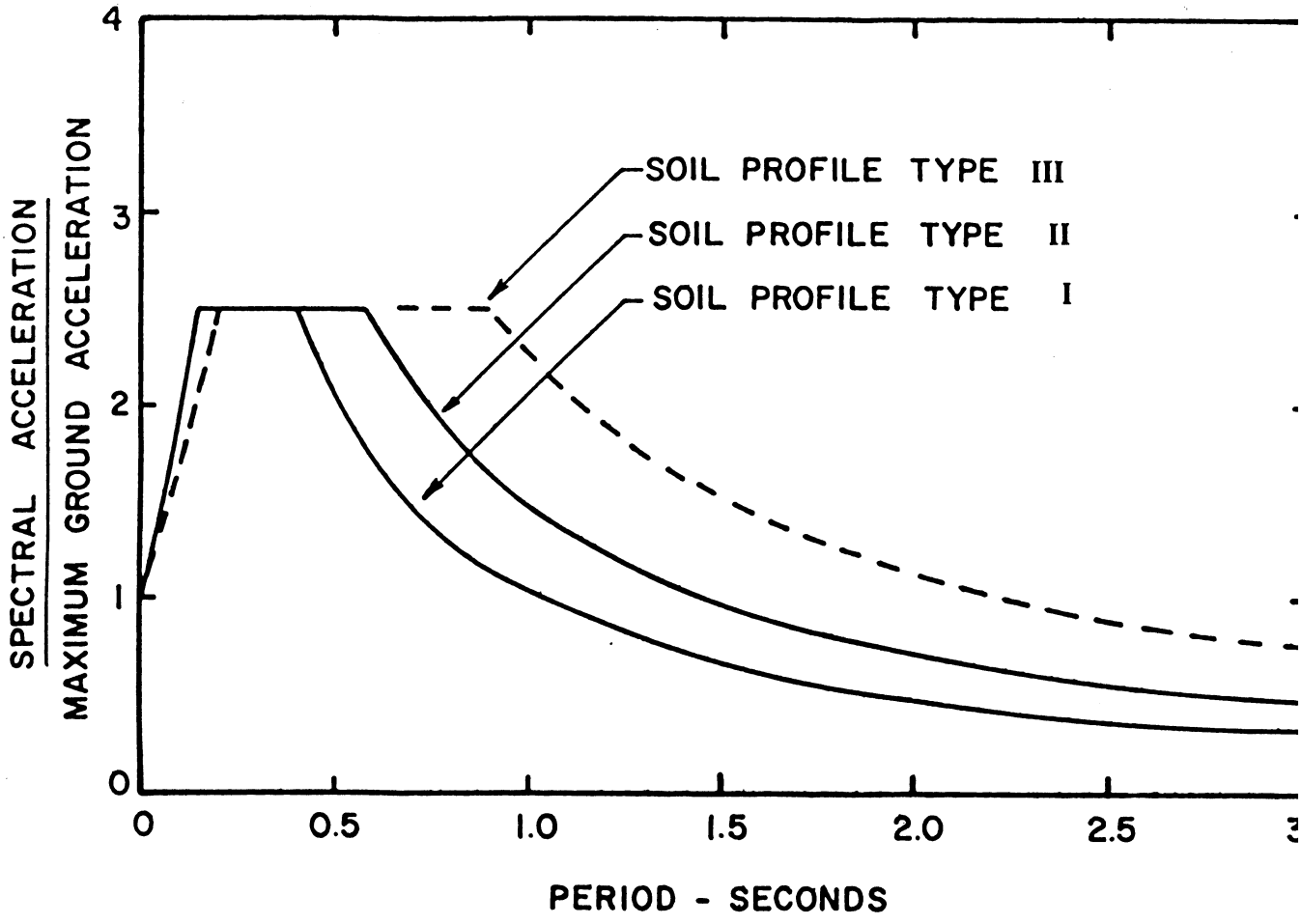

Reference: ATC-6 (1978)

Figure 2.1

to 0.25 g and was used in the dynamic response analysis of the bridge by WSDOT. This same spectrum will be used in the example problem presented herein for the bridge. The spectrum will be modified where appropriate to account for the 7½% damping recommended for those modes of vibration where soil-structure interaction is significant.

3.0 SOIL PROPERTIES

The soil parameters provided by WSDOT for the soil layers are:

- γ = total density in pcf
- c = cohesion in psf
- ϕ = friction angle in degrees
- k = modulus of subgrade reaction in pci
- G = low-strain shear modulus in psf or ksf
- ν = Poisson's Ratio

Values of the modulus of subgrade reaction, k, were obtained from Figure 4.6 of the Coldwater Creek example problem.

Because the behavior of soil is nonlinear during strong shaking, simple procedures were implemented to approximately account for the effect of this nonlinearity on the computation of the abutment and pier foundation stiffnesses. These procedures are described in Section 3.0 of the Coldwater Creek example problem and were implemented in the Ebey Slough example problem herein because the ground acceleration coefficient, Z, was greater than 0.2.

4.0 PIER 10 STIFFNESS CALCULATION - FHWA METHOD

In this section the calculation of foundation stiffnesses using the FHWA (1986) method is presented for Pier 10 of the Ebey Slough Bridge. Because the piers are similar, the method outlined in this section is also applied to Piers 11 and 12. The final results of the Pier 11 and 12 calculations are presented in Section 6.0 and 7.0, respectively.

A side-elevation view of Pier 10 is shown in Figure 4.1. Stiffness values for the pier are calculated for the top of the pile cap, at Point O. The method used is similar to that used for the Deadwater Slough Bridge Pier 1 abutment; however because Pier 10 is not an abutment, the foundation stiffness at this pier is calculated by first determining the stiffnesses of the pile group and pile cap (footing) and then combining these values to obtain a stiffness matrix for the pier.

4.1 PILE STIFFNESS CALCULATION

4.1.1 Estimation of Pile Parameters

The piles are identical to those used in the Deadwater Slough example problem. The pile properties are:

$$E_pA_p = 2.45E09 \text{ lb}$$
$$E_pI_p = 8.19E08 \text{ lb-ft}^2$$

4.1.2 Computation of t-z Curves

4.1.2.1 General Procedure. The general procedure for computing the t-z curves is explained in Section 4.1.2.1 of the Coldwater Creek example.

Pier 10 Soil Profile

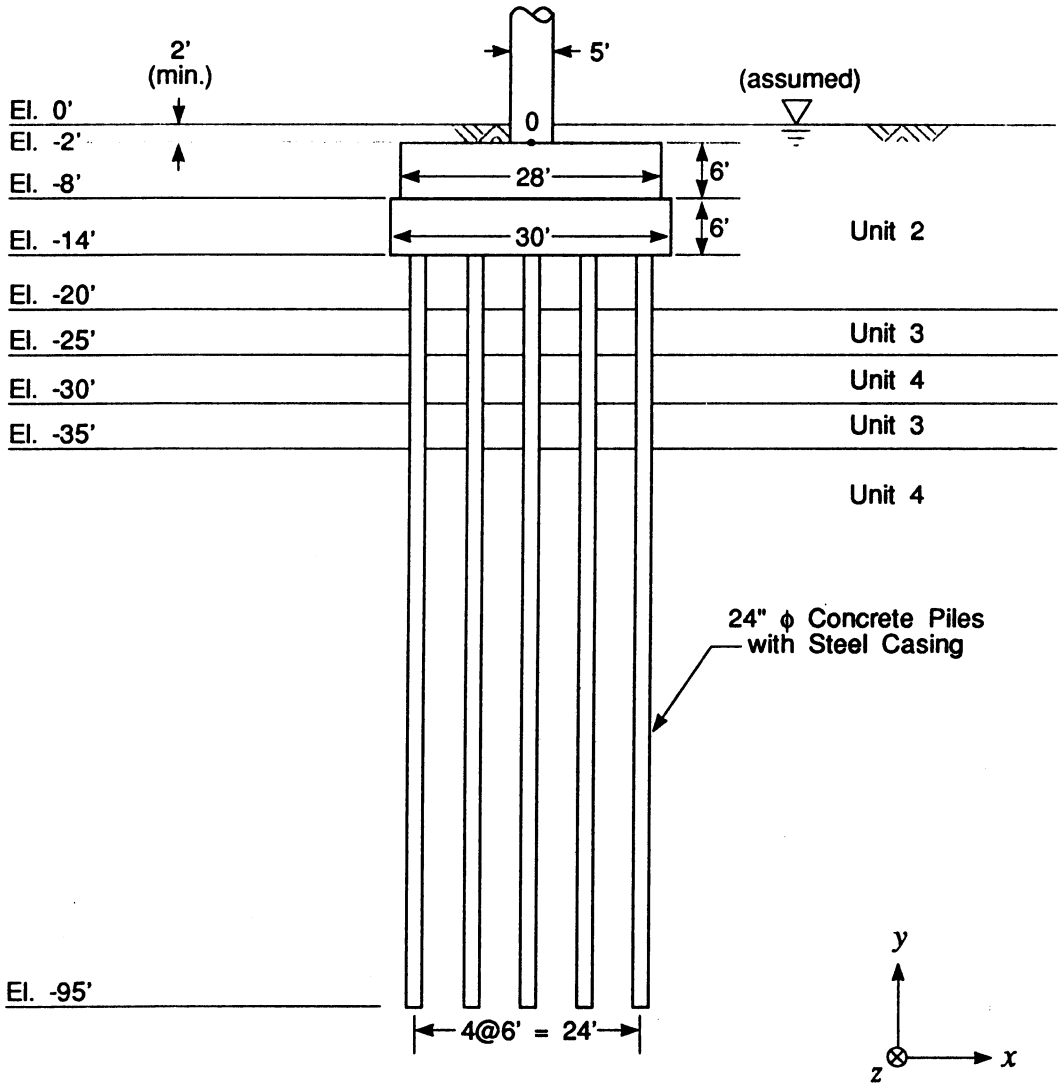

Soil Properties

Unit 2:	γ = 93 pcf	ϕ = 0°	c = 250-600 psf
		G = 400 ksf	ν = 0.45
Unit 3:	γ = 110 pcf	ϕ = 28°	c = 0
	K = 10 pci	G = 800 ksf	ν = 0.35
Unit 4:	γ = 130 pcf	ϕ = 40°	c = 0
	K = 150 pci	G = 2800 ksf	ν = 0.3

Figure 4.1

4.1.2.2 Application to Ebey Slough Bridge Pier 10 Piles. The methods for estimating values of the t-z curves are presented in Section 4.1.2.2 of the Coldwater Creek example for sand and in Section 4.1.2.2 of the Deadwater Slough example for clays.

The values of the relevant soil parameters are shown in Figure 4.1. The results of the t-z curve computation are shown in Table 4.1.

4.1.3 Computation of Q-z Curve

4.1.3.1 General Procedure. The general procedure for computing the Q-z curve for each pile tip is explained in Section 4.1.3.1 of the Coldwater Creek example.

4.1.3.2 Application to Ebey Slough Bridge Pier 10 Piles. The calculation of Q-z curves is very similar to the calculations shown in Section 4.1.3.2 of the Deadwater Slough example. The results for Pier 10 of the Ebey Slough bridge are shown in Table 4.1.

4.1.4 Computation of p-y Curves

4.1.4.1 General Procedure. The general procedure for computing the p-y curves is explained in Section 4.1.4.1 of the Coldwater Creek example.

4.1.4.2 Application to Ebey Slough Bridge Pier 10 Piles. The calculation of p-y curves is very similar to the calculations shown in Section 4.1.4.2 of the Deadwater Slough example. The p-y curves for Pier 10 of the Ebey Slough bridge are shown in Table 4.2.

4.1.5 Preparation of BMCOL-76 Input

The user guide titled, GUIDE FOR DATA INPUT FOR BMCOL-76, is provided in Appendix B. The text accompanying the guide is reproduced from the BMCOL-76 manual (Matlock et al, 1981), and is also provided in this Appendix. The preparation of the input

T-Z & Q-Z CURVES

Bridge: Ebey Slough Overcrossing Pier 10 : high strain

Ground Surface Elevation:	0	ft		
Depth to water table:	0	ft	Elev: 0	ft
Average Pile Perimeter:	77.75	in		
Pile Tip Area:	481.11	in²		
Pile Type:	S	T=Timber,C=Concrete,S=Steel		
	D	O= Open Ended, D=Displacement		

SOIL	DEPTH	ELEV.	GAMMA	PHI	c	G	k	Po	Delta	f	f	Ks	Tmax	Zref
	ft	ft	γ	ϕ	ksf	psf	API RP2A	ksf	δ	ksf	psi	pci	lb/in	in
CLAY	0	0	93	-	0.25	4.00E+05	-	0.00	-	0.25	1.74	56	67	0.031
CLAY	14	-14	93	-	0.50	4.00E+05	-	0.43	-	0.50	3.44	56	134	0.061
CLAY	20	-20	93	-	0.60	4.00E+05	-	0.61	-	0.60	4.17	56	162	0.074
SAND	20	-20	110	28	-	8.00E+05	1.0	0.61	20	0.22	1.55	112	60	0.014
SAND	25	-25	110	28	-	8.00E+05	1.0	0.85	20	0.31	2.15	112	84	0.019
SAND	25	-25	130	40	-	2.80E+06	1.0	0.85	20	0.31	2.15	393	84	0.005
SAND	30	-30	130	40	-	2.80E+06	1.0	1.19	20	0.43	3.00	393	117	0.008
SAND	30	-30	110	28	-	8.00E+05	1.0	1.19	20	0.43	3.00	112	117	0.027
SAND	35	-35	110	28	-	8.00E+05	1.0	1.43	20	0.52	3.60	112	140	0.032
SAND	35	-35	130	40	-	2.80E+06	1.0	1.43	20	0.52	3.60	393	140	0.009
SAND	95	-95	130	40	-	2.80E+06	1.0	5.48	20	2.00	13.86	393	539	0.035

SOIL	DEPTH	ELEV.	PHI	c	G	Po	q	q	Kp	Qmax	Zref
	ft	ft	ϕ	ksf	psf	ksf	ksf	psi	pci	k	in
SAND	95	-95	40	-	2.80E+06	5.48	395	2741	196	659	13.96

Table 4.1

Ebey Slough Overcrossing Pier 10 : high strain T-Z & Q-Z CURVES

	DEPTH ft	ELEV. ft	Tmax lb/in	Zref in										
CLAY	0	0	67	0.031	T (lb/in)	0	17	31	43	51	57	61	64	67	67
					Z (in.)	0.000	0.008	0.015	0.023	0.031	0.039	0.046	0.054	0.077	2.000
CLAY	14	-14	134	0.061	T (lb/in)	0	33	62	85	102	113	121	126	132	134
					Z (in.)	0.000	0.015	0.031	0.046	0.061	0.077	0.092	0.107	0.153	2.000
CLAY	20	-20	162	0.074	T (lb/in)	0	40	75	103	123	137	147	152	160	162
					Z (in.)	0.000	0.019	0.037	0.056	0.074	0.093	0.111	0.130	0.186	2.000
SAND	20	-20	60	0.014	T (lb/in)	0	15	28	38	46	51	54	57	59	60
					Z (in.)	0.000	0.003	0.007	0.010	0.014	0.017	0.021	0.024	0.034	2.000
SAND	25	-25	84	0.019	T (lb/in)	0	20	39	53	64	71	76	79	82	84
					Z (in.)	0.000	0.005	0.010	0.014	0.019	0.024	0.029	0.033	0.048	2.000
SAND	25	-25	84	0.005	T (lb/in)	0	20	39	53	64	71	76	79	82	84
					Z (in.)	0.000	0.001	0.003	0.004	0.005	0.007	0.008	0.010	0.014	2.000
SAND	30	-30	117	0.008	T (lb/in)	0	29	54	74	89	99	106	110	115	117
					Z (in.)	0.000	0.002	0.004	0.006	0.008	0.010	0.011	0.013	0.019	2.000
SAND	30	-30	117	0.027	T (lb/in)	0	29	54	74	89	99	106	110	115	117
					Z (in.)	0.000	0.007	0.013	0.020	0.027	0.033	0.040	0.047	0.067	2.000
SAND	35	-35	140	0.032	T (lb/in)	0	34	65	89	107	119	127	132	138	140
					Z (in.)	0.000	0.008	0.016	0.024	0.032	0.040	0.048	0.056	0.080	2.000
SAND	35	-35	140	0.009	T (lb/in)	0	34	65	89	107	119	127	132	138	140
					Z (in.)	0.000	0.002	0.005	0.007	0.009	0.011	0.014	0.016	0.023	2.000
SAND	95	-95	539	0.035	T (lb/in)	0	132	249	342	410	457	488	507	531	539
					Z (in.)	0.000	0.009	0.018	0.026	0.035	0.044	0.053	0.062	0.088	2.000

	DEPTH ft	ELEV. ft	Qmax k	Zref in

Table 4.1 (cont.)

P-Y CURVES

Worksheet to link with: d:\wash_dot\examples\ebey\axial\tz_10.xls
(including path and extension)

Bridge: Ebey Slough Overcrossing Pier 10 : high strain
Ground Surface Elevation: 0
Depth to water table: 0 ft Elev: 0 ft
Average Pile Diameter: 24.75 in
Pile Type: S T=Timber,C=Concrete,S=Steel
D O= Open Ended, D=Displacement

SOIL	DEPTH	ELEV.	GAMMA	PHI (deg)	c	PHI (rad)	Po	C1	C2	C3	k	J	ε_c	Pu	Yc
	ft	ft	γ	ϕ	ksf	ϕ	ksf				lb / in^3			lb/in	in
CLAY	0	0	93	-	0.25	-	0.00	-	-	-	-	0.50	0.01	129	0.62
CLAY	14	-14	93	-	0.50	-	0.43	-	-	-	-	0.50	0.01	618	0.62
CLAY	20	-20	93	-	0.60	-	0.61	-	-	-	-	0.50	0.01	915	0.62
SAND	20	-20	110	28	-	0.49	0.61	1.7	2.4	23	10	-	-	2035	0.76
SAND	25	-25	110	28	-	0.49	0.85	1.7	2.4	23	10	-	-	3290	0.99
SAND	25	-25	130	40	-	0.70	0.85	4.5	4.4	104	150	-	-	8632	0.17
SAND	30	-30	130	40	-	0.70	1.19	4.5	4.4	104	150	-	-	14299	0.24
SAND	30	-30	110	28	-	0.49	1.19	1.7	2.4	23	10	-	-	4598	1.15
SAND	35	-35	110	28	-	0.49	1.43	1.7	2.4	23	10	-	-	5520	1.18
SAND	35	-35	130	40	-	0.70	1.43	4.5	4.4	104	150	-	-	19845	0.28
SAND	95	-95	130	40	-	0.70	5.48	4.5	4.4	104	150	-	-	98130	0.52

SOIL	DEPTH	ELEV.	Pu	Yc											
	ft	ft	lb/in	in											
CLAY	0	0	129	0.619	P (lb/in)	0	32	41	46	51	55	59	62	64	64
					Y (in.)	0.000	0.619	1.238	1.856	2.475	3.094	3.713	4.331	4.950	6.188
CLAY	14	-14	618	0.619	P (lb/in)	0	154	195	223	245	264	281	295	309	309
					Y (in.)	0.000	0.619	1.238	1.856	2.475	3.094	3.713	4.331	4.950	6.188
CLAY	20	-20	915	0.619	P (lb/in)	0	229	288	330	363	391	415	437	457	457
					Y (in.)	0.000	0.619	1.238	1.856	2.475	3.094	3.713	4.331	4.950	6.188
SAND	20	-20	2035	0.763	P (lb/in)	0	224	423	582	697	777	829	883	903	916
					Y (in.)	0.000	0.191	0.381	0.572	0.763	0.954	1.144	1.526	1.907	3.815
SAND	25	-25	3290	0.987	P (lb/in)	0	363	684	940	1128	1256	1340	1427	1461	1480
					Y (in.)	0.000	0.247	0.494	0.740	0.987	1.234	1.481	1.974	2.468	4.935
SAND	25	-25	8632	0.173	P (lb/in)	0	951	1795	2467	2958	3295	3516	3745	3833	3884
					Y (in.)	0.000	0.043	0.086	0.129	0.173	0.216	0.259	0.345	0.432	0.863
SAND	30	-30	14299	0.238	P (lb/in)	0	1576	2974	4087	4901	5458	5824	6203	6349	6434
					Y (in.)	0.000	0.060	0.119	0.179	0.238	0.298	0.357	0.477	0.596	1.192
SAND	30	-30	4598	1.150	P (lb/in)	0	507	956	1314	1576	1755	1873	1995	2042	2069
					Y (in.)	0.000	0.287	0.575	0.862	1.150	1.437	1.724	2.299	2.874	5.748
SAND	35	-35	5520	1.183	P (lb/in)	0	608	1148	1578	1892	2107	2248	2394	2451	2484
					Y (in.)	0.000	0.296	0.591	0.887	1.183	1.478	1.774	2.366	2.957	5.914
SAND	35	-35	19845	0.284	P (lb/in)	0	2187	4127	5672	6801	7576	8083	8609	8811	8930
					Y (in.)	0.000	0.071	0.142	0.213	0.284	0.354	0.425	0.567	0.709	1.418
SAND	95	-95	98130	0.516	P (lb/in)	0	10815	20406	28047	33631	37459	39970	42570	43568	44155
					Y (in.)	0.000	0.129	0.258	0.387	0.516	0.646	0.775	1.033	1.291	2.582

Table 4.2

was explained and illustrated for the Coldwater Creek example. The input file for this example will not be provided because it is similar to the Coldwater Creek input file.

4.1.6 BMCOL-76 Output

The output files for the axial load and lateral load cases were used to construct the load-deflection curves for the pile head. Refer to the Coldwater Creek example (Section 4.1.6) for explanation of the output file. Plots of the load-deflection curves for the pile head are presented in Figure 4.2 (axial direction) and Figure 4.3 (lateral direction). These curves were used to estimate the axial and lateral stiffnesses of the pile.

4.1.7 Calculation of Pile-Head Stiffnesses

The pile-head stiffnesses are computed from the load-deflection curves in Figures 4.2 and 4.3 as follows. For the axial load case, the axial pile-head stiffness is the slope of the load-deflection curve (Figure 4.2) at the origin (i.e. the initial tangent slope). For the lateral load case, the lateral pile-head stiffness is the slope of straight line from the origin to the point on the load-deflection curve corresponding to 0.50 in deflection. These rules for estimating pile-head stiffnesses were presented in Section 4.1.7 of the Coldwater Creek example.

According to WSDOT, the piles at Pier 10 are fixed to the pile cap. Under this assumption, the pile-head stiffnesses resulting from the implementation of the above procedure (see Figures 4.2 and 4.3) are as follows:

$$K_z = 4.9 \times 10^6 \ lb/in = 5.88 \times 10^7 \ lb/ft \ (Axial)$$
$$K_x = K_y = 2.0 \times 10^5 \ lb/in = 2.40 \times 10^6 \ lb/ft \ (Lateral)$$

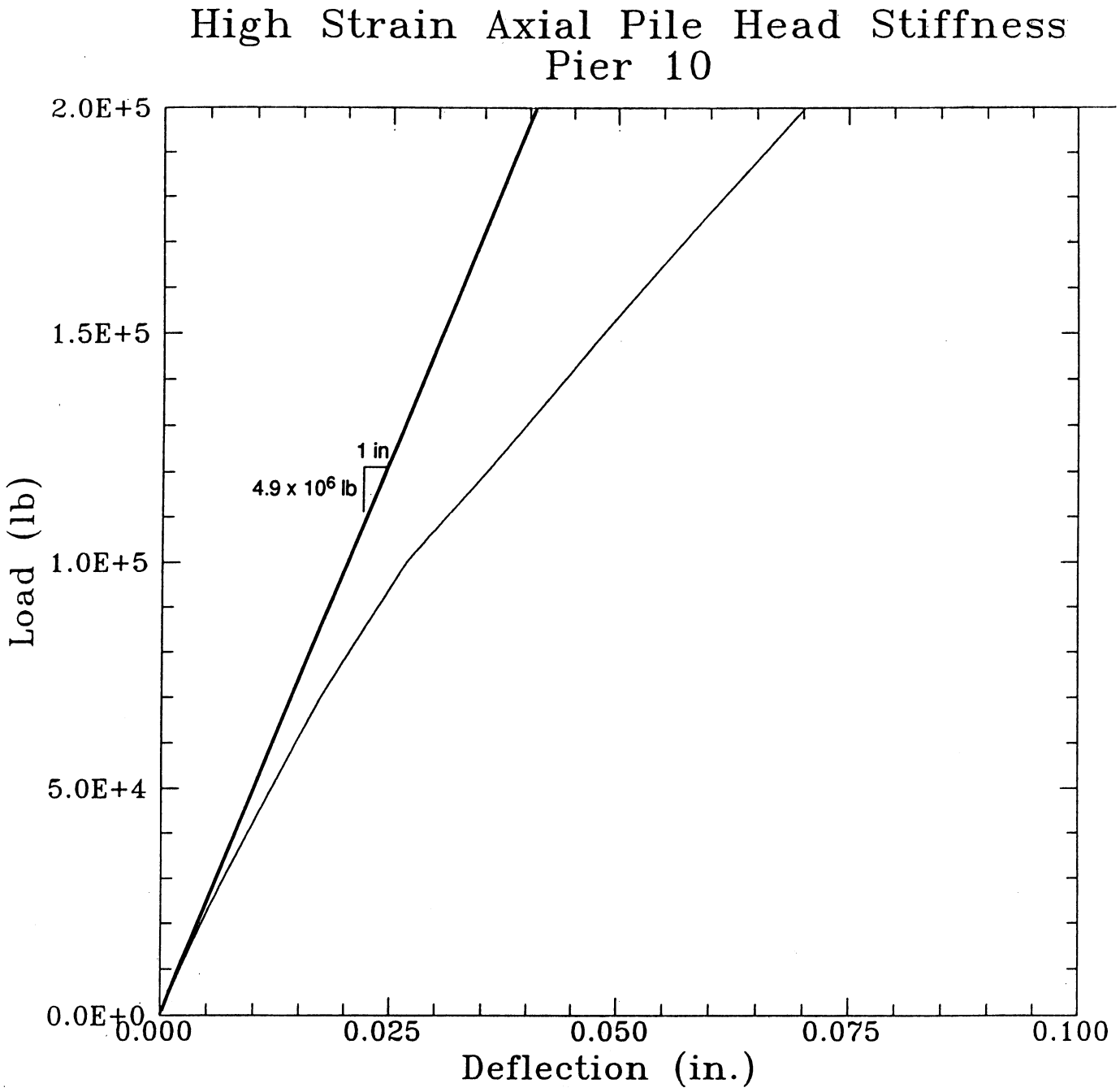
High Strain Axial Pile Head Stiffness
Pier 10
2.0E+5
1.5E+5
1.0E+5
5.0E+4
0.0E+0
Load (lb)
1 in
4.9 x 10^6 lb
0.000
0.025
0.050
0.075
0.100
Deflection (in.)

Figure 4.2

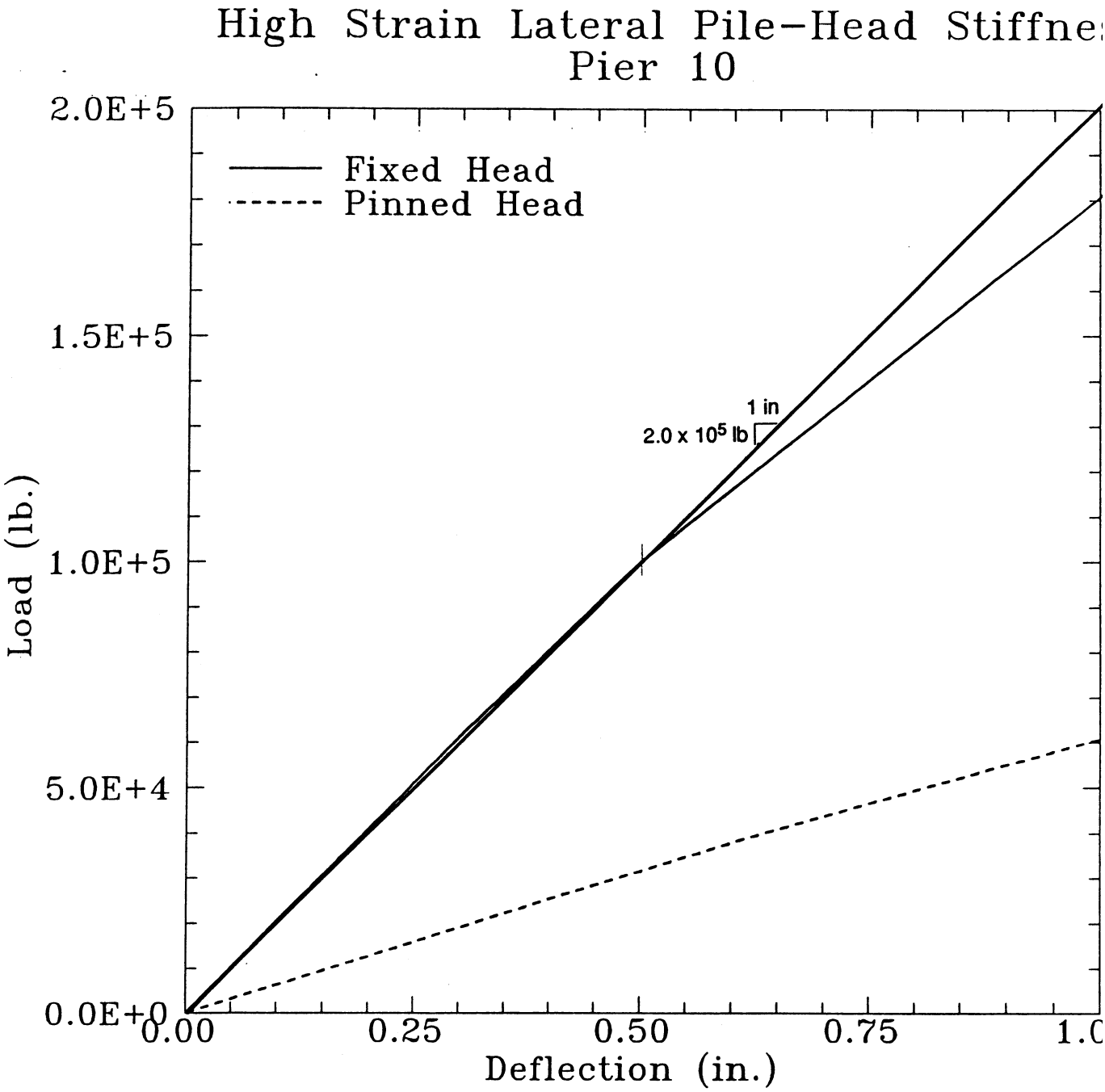
High Strain Lateral Pile-Head Stiffne
Pier 10
2.0E+5
1.5E+5
1.0E+5
5.0E+4
0.0E+0
Load (lb.)
Fixed Head
Pinned Head
1 in
2.0 x 10^5 lb
0.00
0.25
0.50
0.75
1.0
Deflection (in.)

Figure 4.3

These stiffness values apply to each pile at Elevation -14 in Figure 4.1 (pile head location or bottom of pile cap).

4.1.8 Calculation of Pile-Group Stiffness Matrix

4.1.8.1 Assumptions. Two key assumptions are made in order to compute the 6 x 6 pile-group stiffness matrix: (1) pile-group effects (i.e. pile-soil-pile interaction) are neglected, and (2) because the piles are vertical and cylindrical, the individual pile-head stiffnesses computed in Section 4.1.7 apply to a local coordinate system that was established to be coincidental with the principal axes of the pile cap, i.e. axial stiffness, K_z , is associated with the local z axis, which is parallel to the direction along the length of the pile; the transverse stiffness, K_y , is associated with the local y axis, which is coincident with the transverse direction of the pile cap (i.e., parallel to the global z axis in Figure 4.1) and, the longitudinal stiffness, K_x , is associated with the local x axis, which is parallel to the global x axis in Figure 4.4.

4.1.8.2 Preparation of GPILE Input. The input file for the GPILE program was prepared based on the pile-group dimensions shown in Figure 4.4. Preparation of this file was discussed in Section 4.1.8.2 of the Coldwater Creek example. Refer to that section for details.

4.1.8.3 GPILE Output. The GPILE output file for Pier 10 is shown in Table 4.4. The global group stiffness matrix, [K], and the local group stiffness matrix are listed. The global group stiffness matrix is used in the stiffness calculation in Section 4.4. The local group stiffness matrix is not used because this matrix is for a different orientation of the global coordinate system. The global group stiffness matrix was computed at Point O in Figure 4.1 for the coordinate system shown in that figure. The origin of the coordinate system for the stiffness calculation is Point O.

G Pile Input

Piers 10, 11

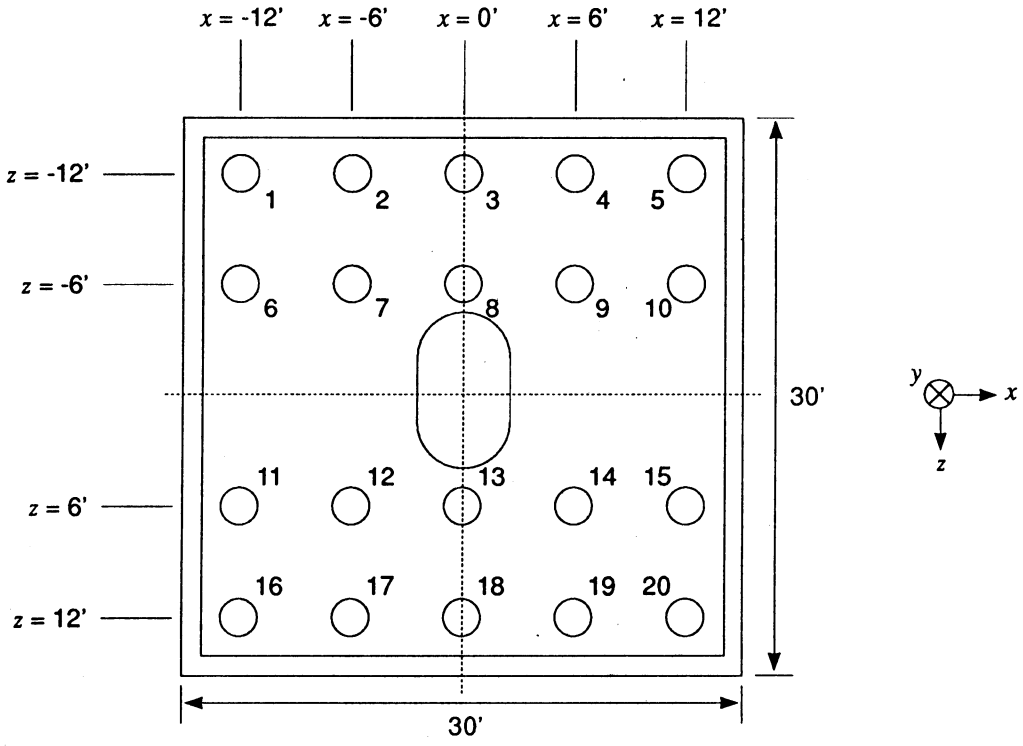

Pier 12

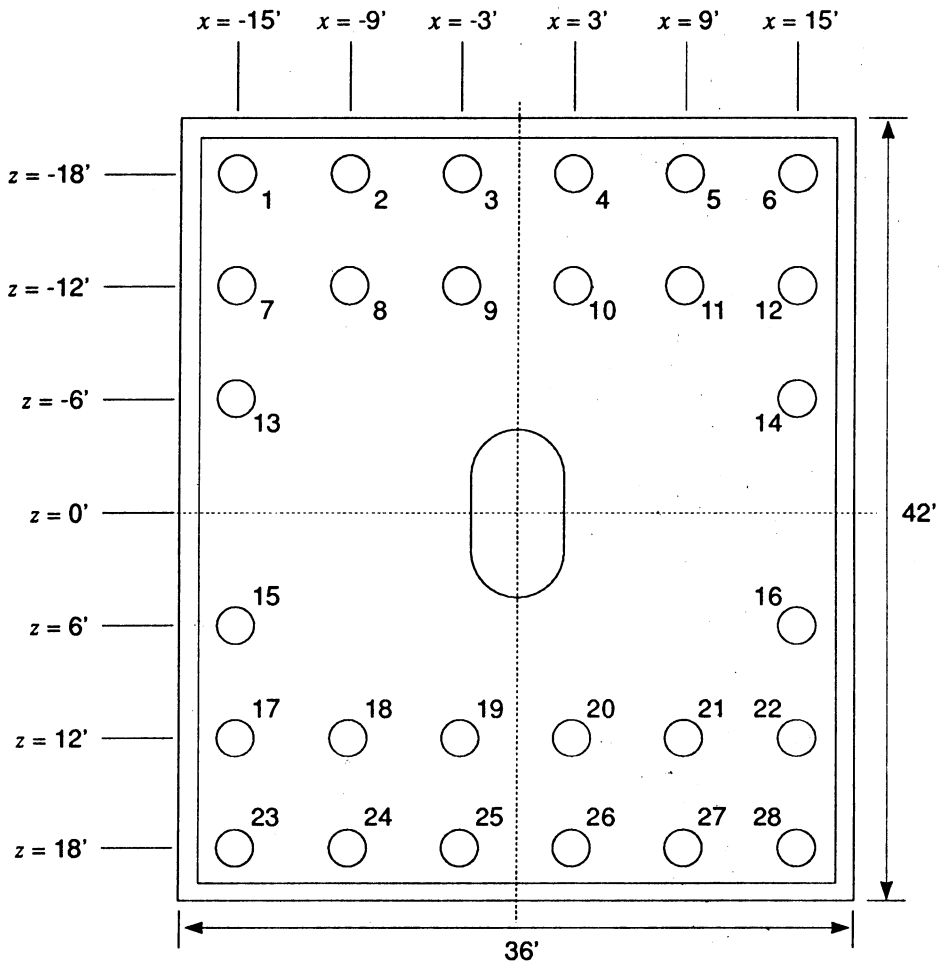

Figure 4.4

WASHINGTON STATE DEPARTMENT OF TRANSPORTATION 11/18/92 TIME 13:47:45 PAGE 6
*** GROUP PILE ANALYSIS *** REV 4/12/88

EBEY SLOUGH OVERCROSSING PILE STIFFNESS - PIER 10

GLOBAL GROUP STIFFNESS MATRIX:

	FX	FY	FZ	MX	MY	MZ
δX	0.480E+08	0.000E+00	0.000E+00	0.000E+00	0.000E+00	0.576E+09
δY	0.000E+00	0.118E+10	0.000E+00	-0.256E+03	0.000E+00	0.000E+00
δZ	0.000E+00	0.000E+00	0.480E+08	-0.576E+09	0.000E+00	0.000E+00
θX	0.000E+00	-0.256E+03	-0.576E+09	0.113E+12	0.000E+00	0.000E+00
θY	0.000E+00	0.000E+00	0.000E+00	0.000E+00	0.778E+10	0.000E+00
θZ	0.576E+09	0.000E+00	0.000E+00	0.000E+00	0.000E+00	0.916E+11

LOCAL GROUP STIFFNESS MATRIX:

	FX	FY	FZ	MX	MY	MZ
δX	0.118E+10	0.000E+00	0.000E+00	0.000E+00	0.256E+03	0.000E+00
δY	0.000E+00	0.480E+08	0.000E+00	0.000E+00	0.000E+00	-0.576E+09
δZ	0.000E+00	0.000E+00	0.480E+08	0.000E+00	0.576E+09	0.000E+00
θX	0.000E+00	0.000E+00	0.000E+00	0.778E+10	0.000E+00	0.000E+00
θY	0.256E+03	0.000E+00	0.576E+09	0.000E+00	0.113E+12	0.000E+00
θZ	0.000E+00	-0.576E+09	0.000E+00	0.000E+00	0.000E+00	0.916E+11

Table 4.4

4.2 FOOTING STIFFNESSES

As recommended in the Task 1 report, the foundation stiffnesses of the pile caps are computed assuming the caps are footings fully embedded in the surrounding soil. These footing stiffnesses are added to the pile-group stiffnesses to obtain the total stiffness matrix.

4.2.1 Model and Assumptions

The theoretical model for estimating the stiffnesses of an embedded footing is presented in Section 4.2.1 of the Coldwater Creek example.

4.2.2 Calculation of Footing Stiffnesses

4.2.2.1 General Procedure. The general procedure to compute the foundation stiffnesses of an embedded footing (pile cap) is presented in Section 4.2.2.1 of the Coldwater Creek example.

4.2.2.2 Application to Ebey Slough Pier 10 Pile Cap. The calculation of the footing (pile cap) stiffness matrix for the Pier 10 pile cap is described below. In Figure 4.1, the footing is defined as the portion of the pile cap below Point O. The relevant equations given below are taken from the Coldwater Creek example (Section 4.2.2.1). For simplicity, the footing is considered to be one rectangular block (instead of two as shown in Figure 4.1) with the following dimensions:

Length:	2L = 30 ft
Width:	2B = 30 ft
Thickness:	D = 12 ft

The corresponding values of α_i and $ß_i$ were obtained from Figures 4.12 and 4.13 in the Coldwater Creek example, and are summarized in Table 4.5 below, along with the stiffnesses K_i^o and the final stiffnesses $K_i = \alpha_i \cdot ß_1 \cdot K_i^o$ (Eqn. 4.22 in Coldwater Creek example).

The method used to compute footing stiffness are outlined in some detail in Section 4.2 of the Coldwater Creek example. The final pile cap stiffness values for Pier 10 are presented in Table 4.5 below.

TABLE 4.5
CALCULATION OF PIER 10 PILE CAP STIFFNESSES

	K_i^o	α_i	$ß_i$	K_i
K_x (lb/ft)	1.64×10^7	1.025	1.82	3.06×10^7
K_y (lb/ft)	1.64×10^7	1.025	1.82	3.06×10^7
K_z (lb/ft)	2.08×10^7	1.03	1.32	2.83×10^7
$K_{\theta x}$ (lb-ft)	4.10×10^9	1.05	2.26	9.74×10^9
$K_{\theta y}$ (lb-ft)	4.10×10^9	1.05	2.26	9.74×10^9
$K_{\theta z}$ (lb-ft)	5.36×10^9	1.05	2.79	1.57×10^{10}

Thus, the diagonal elements of the diagonal pile cap stiffness matrix, [K], are the values in the last column in Table 4.5. This stiffness matrix applies to the FHWA coordinate system. Elements of this matrix will be rearranged in Section 4.4 to be compatible with the global coordinate system in Figure 4.1.

4.3 WALL STIFFNESS

Not applicable--this pier does not have a wall.

4.4 TOTAL PIER 10 STIFFNESS MATRIX

4.4.1 General Procedure.

The total abutment stiffness matrix, $[K_t]$, at a given point is approximated as the sum of the stiffness matrices for the piles, $[K_p]$, and footing or pile cap, $[K_f]$, i.e.

$$[K_t] = [K_p] + [K_f]$$

Although this formula is simple, it is important to note that $[K_p]$ and $[K_f]$ must be computed at the same point in the same coordinate system used for the piles and footings.

4.4.2 Application to Deadwater Slough Abutment. The stiffness matrices $[K_p]$ and $[K_f]$ for the pile-cap system at Pier 10 were constructed from the stiffness calculations presented in Sections 4.1 and 4.2 respectively. The xyz coordinate system is oriented as shown in Figure 4.1 with the origin at Point O.

The 6 x 6 stiffness matrices are:

From Table 4.4,

$$[K_p] = \begin{bmatrix} 4.80E07 & 0 & 0 & 0 & 0 & 5.76E08 \\ 0 & 1.18E09 & 0 & 0 & 0 & 0 \\ 0 & 0 & 4.80E07 & -5.76E08 & 0 & 0 \\ 0 & 0 & -5.76E08 & 1.13E11 & 0 & 0 \\ 0 & 0 & 0 & 0 & 7.78E09 & 0 \\ 5.76E08 & 0 & 0 & 0 & 0 & 9.16E10 \end{bmatrix}$$

From Table 4.5 (after converting from the FHWA to GPILE coordinate system),

$$\text{diag. } [K_f] = \begin{bmatrix} 3.06E07 & & & & & \\ & 2.83E07 & & & & \\ & & 3.06E07 & & & \\ & & & 9.74E09 & & \\ & & & & 1.57E10 & \\ & & & & & 9.74E09 \end{bmatrix}$$

Therefore,

$$[K_t] = \begin{bmatrix} 7.86E07 & 0 & 0 & 0 & 0 & 5.76E08 \\ 0 & 1.21E09 & 0 & 0 & 0 & 0 \\ 0 & 0 & 7.86E07 & -5.76E08 & 0 & 0 \\ 0 & 0 & -5.67E08 & 1.23E11 & 0 & 0 \\ 0 & 0 & 0 & 0 & 2.35E10 & 0 \\ 5.67E08 & 0 & 0 & 0 & 0 & 1.01E11 \end{bmatrix}$$

The units are lb and ft.

5.0 PIER 10 STIFFNESS CALCULATION - NOVAK METHOD

The calculation of foundation stiffnesses using the Novak method is much simpler than the FHWA method primarily because a single computer program (DYNA3) is available to do all the required calculations. Furthermore, the theory upon which the program is based assumes linear elastic response of the soil-foundation system; consequently, fewer soil properties are required to characterize the soil medium, and nonlinear load-deflection relationships between the pile and soil (t-z, Q-z, p-y curves) are not required.

5.1 PILE AND FOOTING SIDE STIFFNESS

The Task 1 report recommended the use of the Pile & Footing Side option within the Novak computer program. With this option, the total pile-cap stiffness is the sum of the stiffnesses from the pile group and the passive resistance of the soil against the sides of the pile cap.

5.1.1 Soil Model

The soil model is shown in Figure 5.1, which was adapted from information in Figure 4.1. Note that shear-wave velocity, V_s, is given as an elastic property, rather than the shear modulus, G. In computing $V_s = \sqrt{G/\gamma_m}$ (where γ_m = mass density), the low-strain shear modulus values in Figure 4.1 were reduced by 50% to account for high soil strain.

Besides V_s, the other new soil parameter not shown in Figure 4.1 is the soil damping ratio for shear deformation, ζ. Values of $\zeta \leq 0.05$ are typically assumed and within this range, the effect of this parameter on the stiffness calculation is negligible. For this and all other example problems, $\zeta = 0.03$ was arbitrarily assumed.

5.1.2 Preparation of DYNA3 Input

The input file for Novak's DYNA3 computer program for Pier 10 is shown in Table 5.1. The preparation of this input file is very similar to the preparation of the input file for Pier 1 of the Coldwater example and therefore will not be discussed at length here.

Soil Model for Novak Stiffness Calculation for Pile and Footing Side Case at Pier 10

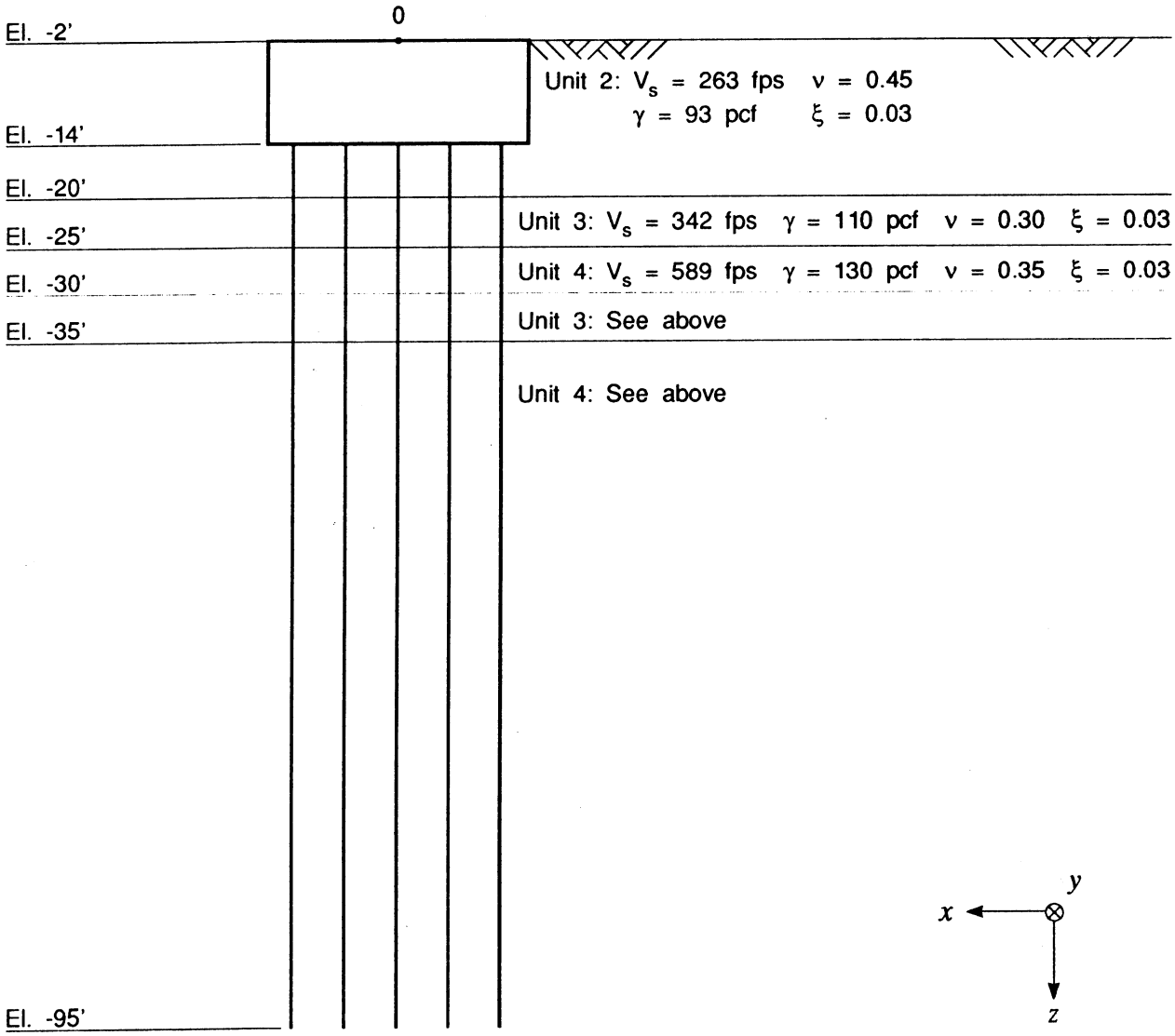

NOTES

V_s Shear-wave velocity = $\sqrt{G/\gamma_m}$, where G is the high-strain value of shear modulus = 50% of the low-strain G value in Figure 4.1. The parameter γ_m is mass density.

ξ Soil damping ratio (assumed).

xyz Coordinate system in this figure is oriented differently from the one in Figure 5.1.
In Novak's model, the *z* coordinate axis is positive downward.

Figure 5.1

```
TITLE=EBEY SLOUGH PIER 10 [ PILES + EMBEDMENT ] [k ft s]
MATRIX
GRAVITY=32.2
FOUNDATION=PILE
RECTANGULAR=30.0,30.0
MASS=100.,100.,100.,100.,100.,100.,100.
LAYERS=5
FIXED=20
  1 -12.0   12.0
  2  -6.0   12.0
  3   0.0   12.0
  4   6.0   12.0
  5  12.0   12.0
  6 -12.0    6.0
  7  -6.0    6.0
  8   0.0    6.0
  9   6.0    6.0
 10  12.0    6.0
 11 -12.0   -6.0
 12  -6.0   -6.0
 13   0.0   -6.0
 14   6.0   -6.0
 15  12.0   -6.0
 16 -12.0  -12.0
 17  -6.0  -12.0
 18   0.0  -12.0
 19   6.0  -12.0
 20  12.0  -12.0
CONSTANTS=0.,0.,12.,81.,.145,0.,0.17,0.05,1.11,5.18E05
ELEMENT
1   6.0  1.031  1.031  4.73  1.582 1.582 3.164
2   5.0  1.031  1.031  4.73  1.582 1.582 3.164
3   5.0  1.031  1.031  4.73  1.582 1.582 3.164
4   5.0  1.031  1.031  4.73  1.582 1.582 3.164
5  60.0  1.031  1.031  4.73  1.582 1.582 3.164
END-BEARING
NO-INTERACTION
SOIL
CONSTANTS
1   263.  .093  0.45 0.03
2   342.  .110  0.35 0.03
3   589.  .130  0.30 0.03
4   342.  .110  0.35 0.03
5   589.  .130  0.30 0.03
BELOW
589.  .130  .30  0.03
EMBEDDED=1
1  12.  263.  .093  0.45 0.03
LOAD=HARMONIC
CONSTANTS
NONQUADRATIC
0.001  0.001  0.001  0.0  10.  0.0  0.  0.  0.
RUN
```

Table 5.1

5.1.3 DYNA3 Output

The output file from the DYNA3 program is listed in Table 5.2. The stiffnesses are in units of kips and ft. The values of CROSS-STIFFNESS (YZ PLANE) and CROSS-STIFFNESS (XZ PLANE) refer to $K_{y\theta x}$ and $K_{x\theta y}$, respectively.

5.2 TOTAL PIER 10 STIFFNESS MATRIX

The total stiffness matrix is $[K_t] = [K_{pfs}]$, where $[K_{pfs}]$ is the "pile + footing side" stiffness matrix. From Table 5.2 of Section 5.1.3,

$$[K_{pfs}] = \begin{bmatrix} 1.54E8 & 0 & 0 & 0 & -2.39E9 & 0 \\ 0 & 1.54E8 & 0 & 2.39E9 & 0 & 0 \\ 0 & 0 & 1.11E9 & 0 & 0 & 0 \\ 0 & 2.39E9 & 0 & 1.42E11 & 0 & 0 \\ -2.39E9 & 0 & 0 & 0 & 1.22E11 & 0 \\ 0 & 0 & 0 & 0 & 0 & 3.34E10 \end{bmatrix}$$

The units are lb and ft.

$[K_{pfs}]$ defines the stiffness matrix at Point 0 for the global coordinate system defined in Figure 5.1.

6.0 PIER 11 FOUNDATION STIFFNESSES

The soil profile for Pier 11 is shown in Figure 6.1. The FHWA and Novak methods were applied to Pier 11 but, because of the extreme similarity of Piers 10 and 11, only the final results for Pier 11 will be presented here.

```
**********************************************
*
*        D Y N A 3   S I M U L A T I O N
*
*              RUN DATE -  1992/11/18
*              TIME     -  14: 9:42
*              REVISION -  1991/07/30
*
**********************************************

EBEY SLOUGH PIER 10 [ PILES + EMBEDMENT ] [k ft

                                    RESULTS
                                    *******


FREQUENCY  -     .0010
*********


STIFFNESS CONSTANTS (K)
***********************

HORIZONTAL TRANSLATION  (X) ...  1.54116E+05
HORIZONTAL TRANSLATION  (Y) ...  1.54116E+05
VERTICAL TRANSLATION  (Z) .....  1.11234E+06
ROTATION ABOUT  (X) ...........  1.42133E+08
ROTATION ABOUT  (Y) ...........  1.22180E+08
TORSION ABOUT  (Z) ............  3.33729E+07
CROSS-STIFFNESS (YZ PLANE) ....  2.38604E+06
CROSS-STIFFNESS (XZ PLANE) .... -2.38604E+06

DAMPING CONSTANTS (C)
*********************
HORIZONTAL TRANSLATION  (X) ...  5.42888E+06
HORIZONTAL TRANSLATION  (Y) ...  5.42888E+06
VERTICAL TRANSLATION  (Z) .....  4.57296E+07
ROTATION ABOUT  (X) ...........  5.71120E+09
ROTATION ABOUT  (Y) ...........  4.89014E+09
TORSION ABOUT  (Z) ............  1.14609E+09
CROSS-DAMPING  (YZ PLANE) .....  8.74711E+07
CROSS-DAMPING  (XZ PLANE) ..... -8.74711E+07
```

Table 5.2

Pier 11 Soil Profile

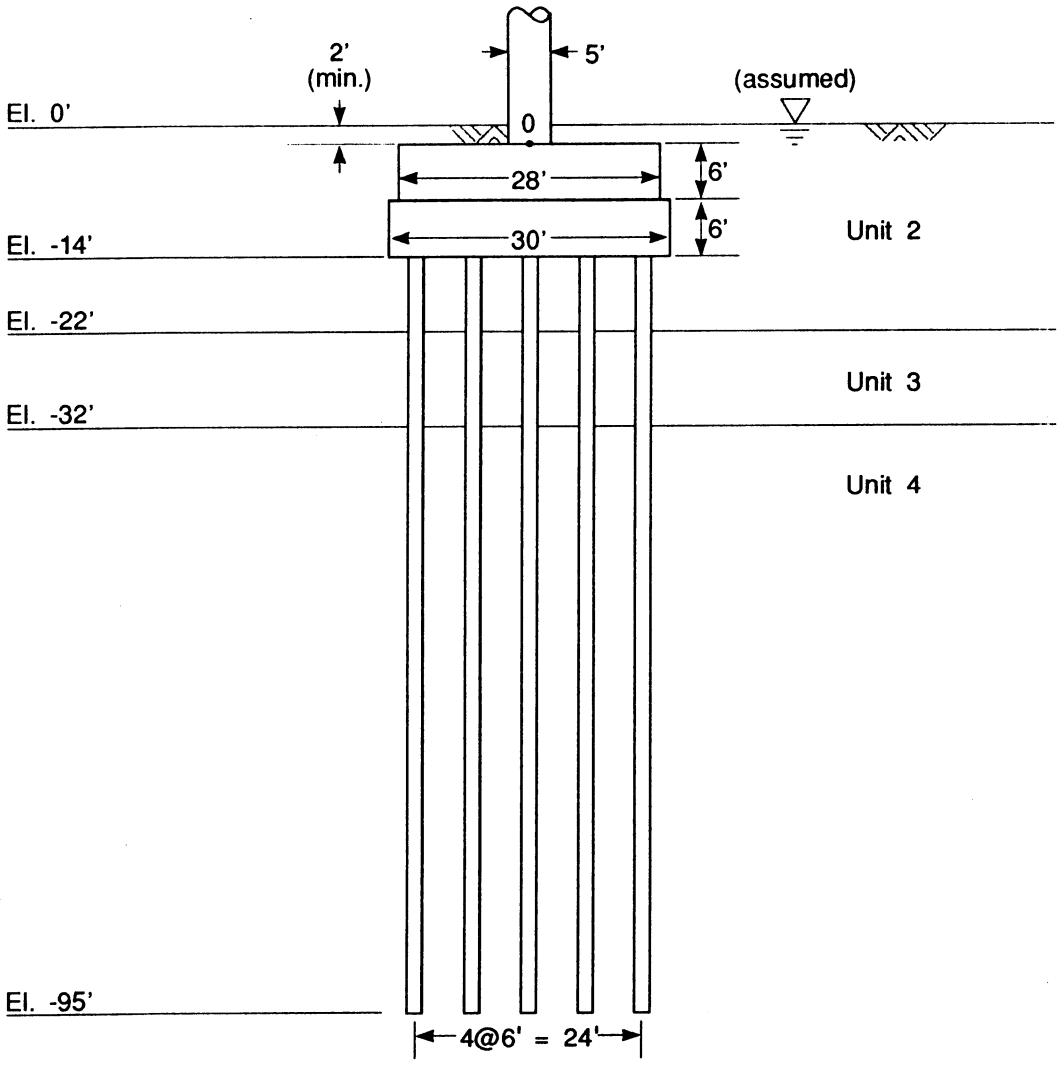

Soil properties are as for Pier 10. See Figure 4.1.

Coordinate Systems

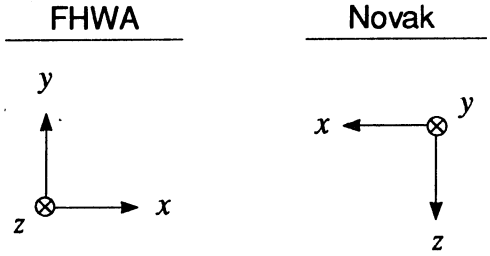

Figure 6.1

6.1 FHWA METHOD

The stiffness matrix is

$$[K_t] = \begin{bmatrix} 6.90E7 & 0 & 0 & 0 & 0 & 4.61E8 \\ 0 & 1.04E9 & 0 & 0 & 0 & 0 \\ 0 & 0 & 6.90E7 & -4.61E8 & 0 & 0 \\ 0 & 0 & -4.61E8 & 1.06E11 & 0 & 0 \\ 0 & 0 & 0 & 0 & 2.19E10 & 0 \\ 4.61E8 & 0 & 0 & 0 & 0 & 8.78E10 \end{bmatrix}$$

The units are lb and ft. The coordinate system is as shown in Figure 6.1.

6.2 NOVAK METHOD

The final stiffness matrix is

$$[K_t] = \begin{bmatrix} 1.43E8 & 0 & 0 & 0 & -2.20E9 & 0 \\ 0 & 1.43E8 & 0 & 2.20E9 & 0 & 0 \\ 0 & 0 & 1.06E9 & 0 & 0 & 0 \\ 0 & 2.20E9 & 0 & 1.34E11 & 0 & 0 \\ -2.20E9 & 0 & 0 & 0 & 1.15E11 & 0 \\ 0 & 0 & 0 & 0 & 0 & 3.15E10 \end{bmatrix}$$

The units are lb and ft. The coordinate system is as shown in Figure 6.1.

7.0 PIER 12 FOUNDATION STIFFNESS

The soil profile for Pier 12 is shown in Figure 7.1. This pier differs slightly in configuration from Piers 10 and 11. Note that Pier 12 is supported by a group of 28 piles, rather than 20 as for Piers 10 and 11, and that the Pier 12 pile cap is increased in size from 30' x 30' to 42' x 36'.

Only the results of the stiffness calculations for the FHWA and Novak methods are presented here.

7.1 FHWA METHOD

7.1.1 Pile Stiffness

The Pier 12 pile group stiffness contribution is

$$[K_p] = \begin{bmatrix} 5.71E7 & 0 & 0 & 0 & 0 & 6.85E9 \\ 0 & 1.51E9 & 0 & 0 & 0 & 0 \\ 0 & 0 & 5.71E7 & -6.85E9 & 0 & 0 \\ 0 & 0 & -6.85E9 & 3.19E11 & 0 & 0 \\ 0 & 0 & 0 & 0 & 1.87E10 & 0 \\ 6.85E9 & 0 & 0 & 0 & 0 & 1.93E11 \end{bmatrix}$$

The units are lb and ft.

Pier 12 Soil Profile

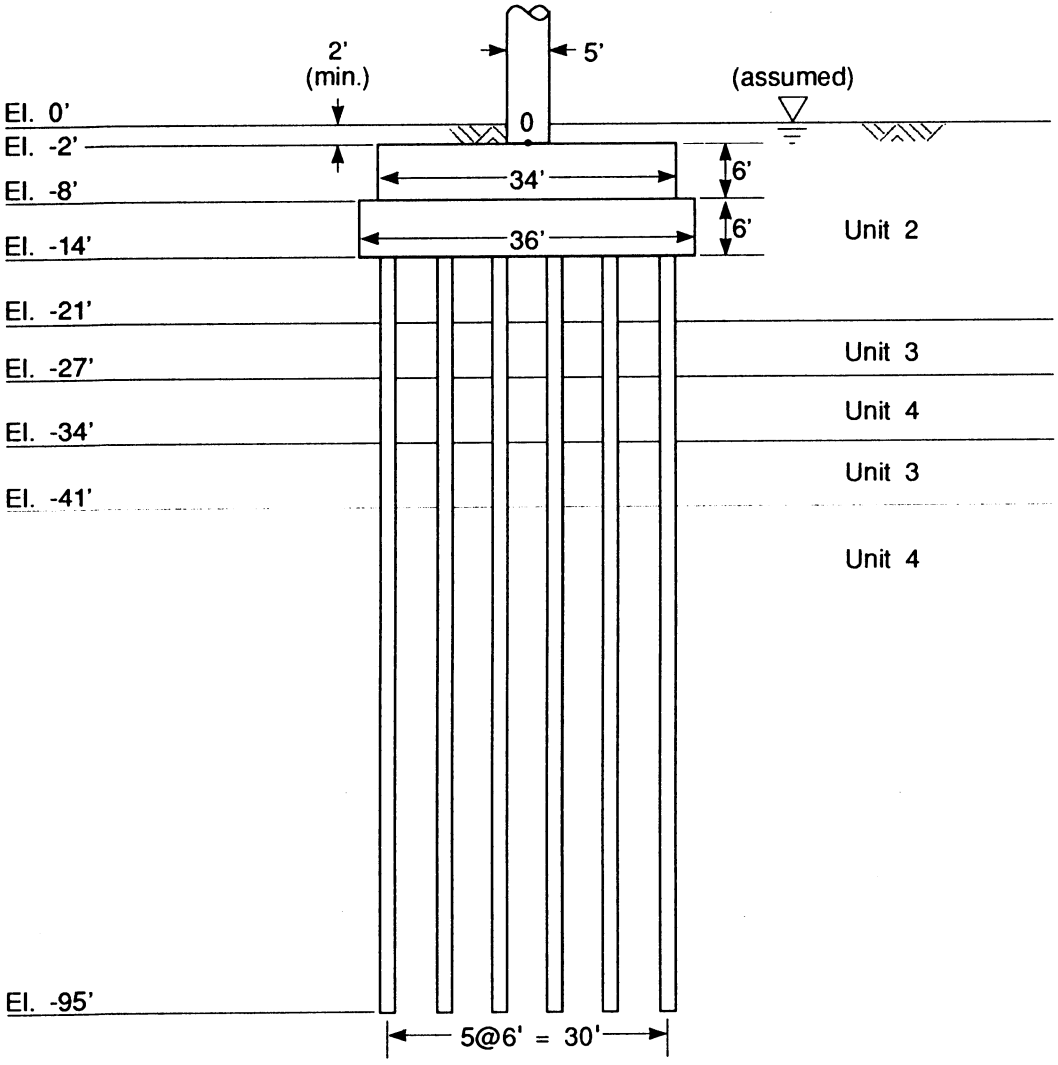

Soil properties are as for Pier 10. See Figure 4.1.

Coordinate Systems

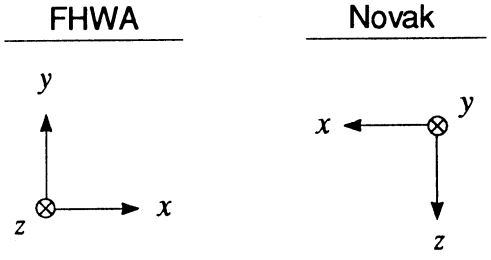

Figure 7.1

7.1.2 Footing Stiffness

TABLE 7.1
CALCULATION OF PIER 12 FOOTING STIFFNESSES

	α_i	β_i	K_i
K_x (lb/ft)	1.03	1.68	3.68×10^7
K_y (lb/ft)	1.017	1.68	3.63×10^7
K_z (lb/ft)	1.034	1.25	3.49×10^7
$K_{\theta x}$ (lb-ft)	1.052	1.84	1.94×10^{10}
$K_{\theta y}$ (lb-ft)	1.052	1.92	1.61×10^{10}
$K_{\theta z}$ (lb-ft)	1.052	2.47	3.06×10^{10}

Thus, the diagonal elements of the diagonal footing stiffness matrix, $[K_f]$, are the values in the last column in Table 7.1. This stiffness matrix applies to the FHWA coordinate system in Figure 7.1.

7.1.3 Total Stiffness

Adding the pile and footing stiffness contributions shown above, the total Pier 12 stiffness matrix is given by

$$[K_t] = \begin{bmatrix} 9.39E7 & 0 & 0 & 0 & 0 & 6.85E9 \\ 0 & 1.54E9 & 0 & 0 & 0 & 0 \\ 0 & 0 & 9.34E7 & -6.85E9 & 0 & 0 \\ 0 & 0 & -6.85E9 & 3.38E11 & 0 & 0 \\ 0 & 0 & 0 & 0 & 4.93E10 & 0 \\ 6.85E9 & 0 & 0 & 0 & 0 & 2.09E11 \end{bmatrix}$$

The units are lb and ft. The coordinate system is as shown in Figure 7.1.

7.2 NOVAK METHOD

$$[K_{pfs}] = \begin{bmatrix} 2.02E8 & 0 & 0 & 0 & -3.16E9 & 0 \\ 0 & 2.02E8 & 0 & 3.16E9 & 0 & 0 \\ 0 & 0 & 1.50E9 & 0 & 0 & 0 \\ 0 & 3.16E9 & 0 & 3.65E11 & 0 & 0 \\ -3.16E9 & 0 & 0 & 0 & 2.39E11 & 0 \\ 0 & 0 & 0 & 0 & 0 & 7.97E10 \end{bmatrix}$$

8.0 APPLICATION TO SEISAB-I BRIDGE ANALYSIS

This example illustrates the use of SEISAB-I to conduct a response spectrum analysis of the Ebey Slough Bridge, as described in Section 1.0.

The structure model is illustrated in Figure 8.1. In this example, Piers 10 through 18 are modeled in SEISAB-I analysis as Bents 2 through 10, respectively. The bridge was analyzed using foundation stiffnesses determined by the FHWA Method.

8.1 ABUTMENT MODELS

Since information was not furnished for abutting structures, Abutment 1 is assumed at the Station ELS. 114 + 14.73 Hinge Abutment 2 is assumed at the far end of the bridge. Both abutments are modeled as fixed transversely and free longitudinally.

8.2 BENT MODELS

Bent 2 stiffness matrix is given for each foundation in the coordinate system defined as the local pile system shown in Figure 4.1. This coordinate system is identical to the SEISAB-I coordinate system so conversion is not required. The units are lb and ft.

Converting from lb to kip units we have for each pile:

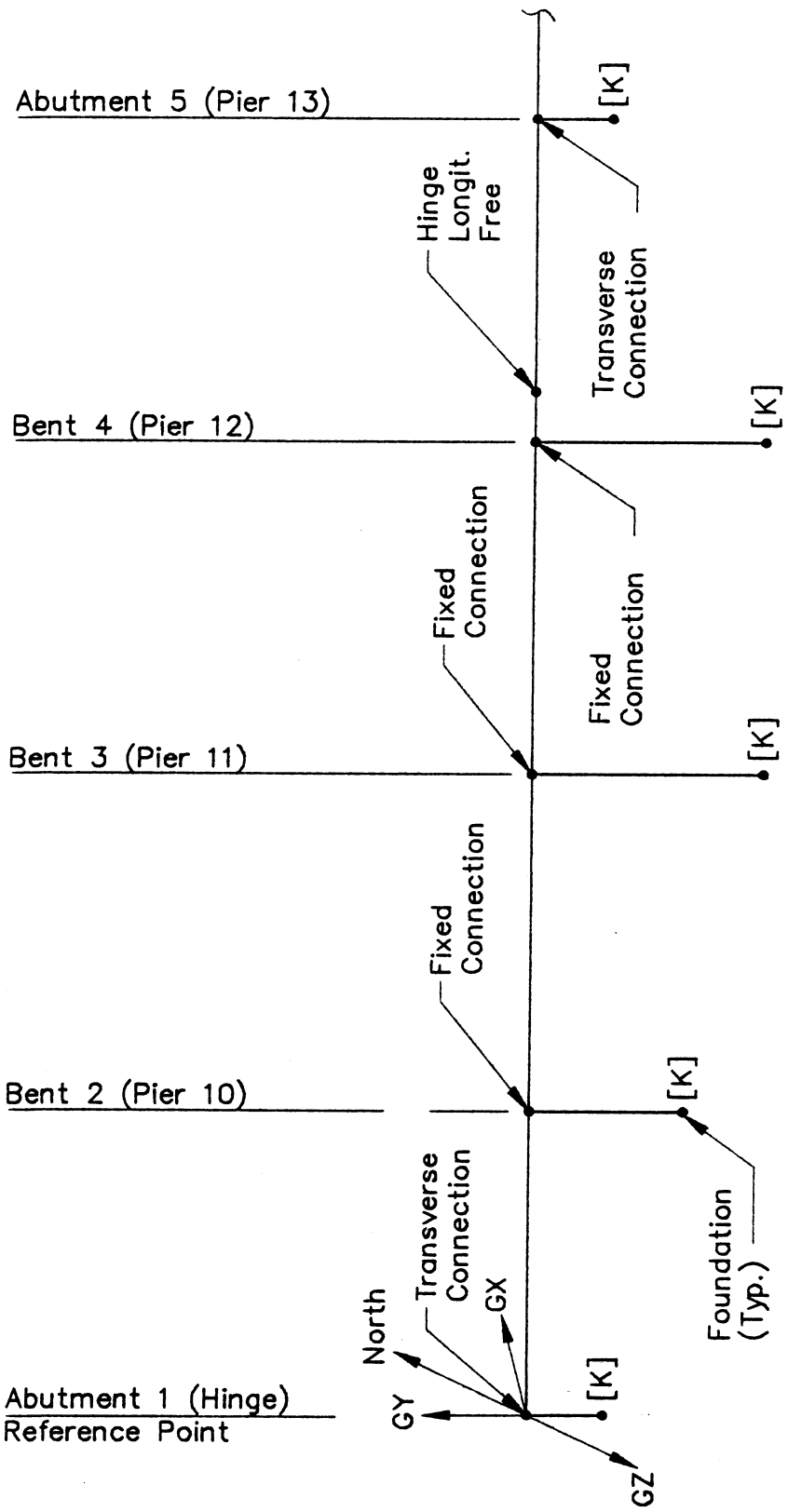

Ebey Slough Structure Model

Figure 8.1

$$[K_{SEISAB}] = \begin{bmatrix} 7.86E4 & 0 & 0 & 0 & 0 & 5.76E5 \\ & 1.21E6 & 0 & 0 & 0 & 0 \\ & & 7.86E4 & -5.76E5 & 0 & 0 \\ \text{Symmetrical} & & & 1.23E8 & 0 & 0 \\ & & & & 2.35E7 & 0 \\ & & & & & 1.01E11 \end{bmatrix}$$

Similarly, the Bent 3 stiffness matrix is:

$$[K_{SEISAB}] = \begin{bmatrix} 6.90E4 & 0 & 0 & 0 & 0 & 4.61E5 \\ & 1.04E6 & 0 & 0 & 0 & 0 \\ & & 6.90E4 & -4.61ES & 0 & 0 \\ \text{Symmetrical} & & & 1.06E8 & 0 & 0 \\ & & & & 2.19E7 & 0 \\ & & & & & 8.78E7 \end{bmatrix}$$

And the Bent 4 stiffness matrix is:

$$[K_{SEISAB}] = \begin{bmatrix} 5.71E4 & 0 & 0 & 0 & 0 & 6.85E6 \\ & 1.51E6 & 0 & 0 & 0 & 0 \\ & & 5.71E4 & -6.85E6 & 0 & 0 \\ \text{Symmetrical} & & & 3.19E8 & 0 & 0 \\ & & & & 1.87E7 & 0 \\ & & & & & 8.78E7 \end{bmatrix}$$

Bent 5 through Bent 7 foundation stiffness matrices are as provided by WSDOT.

Bent 8 through Bent 10 foundations are considered fixed as modeled by WSDOT.

8.3 LOAD MODEL

The response spectrum supplied by WSDOT was used without modification. Modification of modal damping ratios according to Task 1 Report Section 6.2 is not required since this example represents an interior section of a longer structure thus no real abutments are included in the model.

EXAMPLE NO. 4

NORTHRUP WAY OVERCROSSING

1.0 DESCRIPTION OF BRIDGE AND FOUNDATION SOILS 1

2.0 SEISMIC DESIGN PARAMETERS 1

3.0 SOIL PROPERTIES 2

4.0 PIER 1 STIFFNESS CALCULATION - FHWA METHOD 2
4.1 ABUTMENT FOOTING STIFFNESSES 3
4.1.1 Model and Assumptions 3
4.1.2 Calculation of Footing Stiffnesses 3
4.1.2.1 General Procedure 3
4.1.2.2 Application to Northrup Way Overcrossing Abutment Footing. 3
4.2 ABUTMENT WALL STIFFNESS 6
4.2.1 Model and Assumptions 6
4.2.2 Calculation of Wall Stiffnesses 7
4.2.2.1 General Procedure 7
4.2.2.2 Application to Northrup Way Overcrossing Abutment Wall. .. 7
4.3 TOTAL ABUTMENT STIFFNESS MATRIX 8
4.3.1 General Procedure 8
4.3.2 Application to Northrup Way Overcrossing Abutment. 8

5.0 PIER 1 STIFFNESS CALCULATION - NOVAK METHOD 10
5.1 FOOTING ON HALF-SPACE STIFFNESS 10
5.1.1 Soil Model 10
5.1.2 Preparation of DYNA3 Input 11
5.1.3 DYNA3 Output 11
5.2 ABUTMENT WALL STIFFNESS 12
5.3 TOTAL PIER 1 STIFFNESS MATRIX 12

6.0 PIER 2 AND PIER 3 FOUNDATION STIFFNESSES 13
6.1 FHWA METHOD 14
6.2 NOVAK METHOD 15

7.0 PIER 4 FOUNDATION STIFFNESS 15
7.1 FHWA METHOD 15
7.2 NOVAK METHOD 18

8.0 APPLICATION TO SEISAB-I BRIDGE ANALYSIS 19
8.1 BENT 2 MODEL 19
8.2 BENT 3 AND BENT 4 MODELS 20
8.3 BENT 5 MODEL 20
8.4 LOAD MODEL 21
8.5 DISCUSSION OF THE INPUT FILE 22
8.6 DISCUSSION OF THE OUTPUT FILE 23

1.0 DESCRIPTION OF BRIDGE AND FOUNDATION SOILS

The Northrup Way Overcrossing is a 3-span, prestressed concrete-girder bridge 162 feet long carrying a two-lane roadway approximately 25 feet wide (Figure 1.1). The "coed" abutments (Piers 1 and 4) at the ends of the bridge (Figures 1.2 and 1.3) consist of a monolithic reinforced concrete footing and wall system which provides a simple support for the bridge deck. Each of the two intermediate piers, Piers 2 and 3 (Figure 1.4), is comprised of a single reinforced concrete footing which supports two columns. These columns extend approximately 23 feet to a cross-beam which in turn supports the prestressed girders and the bridge deck.

2.0 SEISMIC DESIGN PARAMETERS

The ground acceleration coefficient for the seismic design of the Northrup Way Overcrossing was 0.25. The appropriate soil category was Soil Type II, which is deep stiff soil over bedrock. The ATC-6, 5% damped response spectrum (Figure 2.1) for this soil type was normalized to 0.25 g and was used in the dynamic response analysis of the bridge by WSDOT. This same spectrum will be used in the example problem presented herein for the bridge. The spectrum will be modified where appropriate to account for the 7½% damping recommended for those modes of vibration where soil-structure interaction is significant.

SEC. 20, T. 25 N., R. 5 E., W.M.
CITY OF BELLEVUE

SR 405

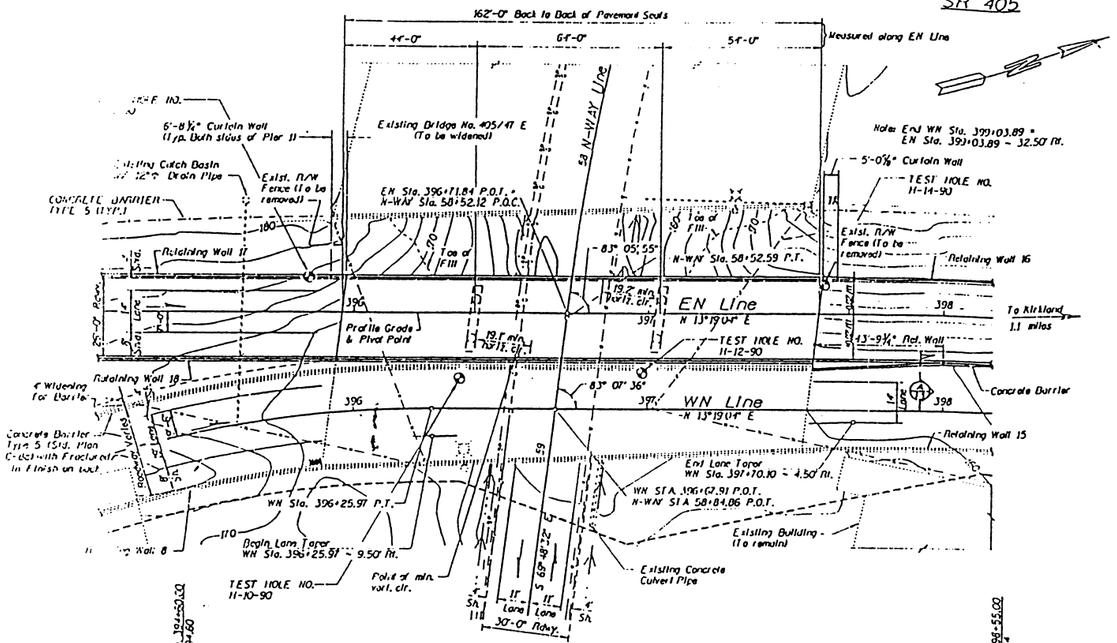

PLAN

Bearings of all plans = S 69°48'32" E

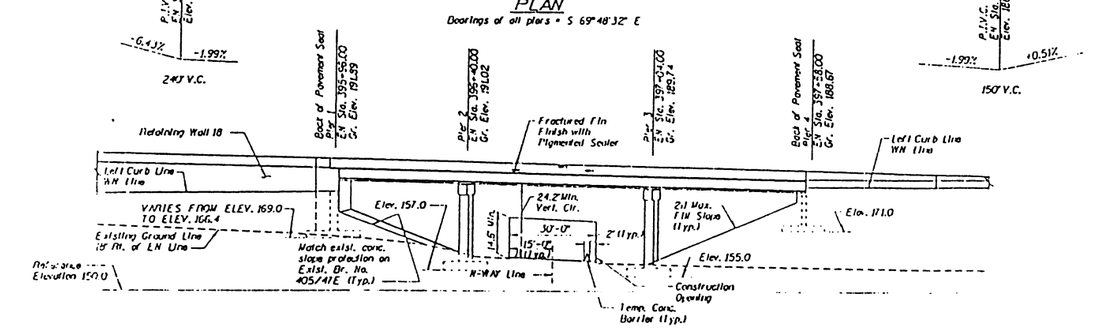

ELEVATION

Grade elevations shown are finish grades on EN Line at top of roadway slab and are equal to profile grade.

DATUM

City of Seattle

GENERAL NOTES

ALL MATERIAL AND WORKMANSHIP SHALL BE IN ACCORDANCE WITH THE REQUIREMENTS OF THE STATE OF WASHINGTON DEPARTMENT OF TRANSPORTATION STANDARD SPECIFICATIONS FOR ROAD, MUNICIPAL, AND BRIDGE CONSTRUCTION DATED 1991

THIS STRUCTURE HAS BEEN DESIGNED IN ACCORDANCE WITH THE REQUIREMENTS OF THE 1989 AASHTO STANDARD SPECIFICATIONS & INTERIM SPEC., THRU 1991. PRESTRESSED CONCRETE ELEMENTS HAVE BEEN DESIGNED BY ALLOWABLE STRESS DESIGN AND CHECKED FOR LOAD FACTOR DESIGN. ALL OTHER ELEMENTS HAVE BEEN DESIGNED BY LOAD FACTOR DESIGN.

SEISMIC DESIGN OF THIS STRUCTURE CONFORMS WITH THE PROVISIONS OF OF THE AASHTO GUIDE SPECIFICATIONS FOR SEISMIC DESIGN OF HIGHWAY BRIDGES, DATED 1983, AN ACCELERATION COEFFICIENT OF .25 HAS BEEN USED.

FOOTING ELEVATIONS AND SUBSTRUCTURE DETAILS ARE SUBJECT TO CHANGE DEPENDING UPON FOUNDATION MATERIAL ENCOUNTERED. REINFORCING STEEL FOR FOOTINGS AND WALLS SHALL NOT BE CUT UNTIL THE FINAL ELEVATIONS HAVE BEEN DETERMINED IN THE FIELD AND SUBSTRUCTURE DETAILS HAVE BEEN MODIFIED AS REQUIRED.

THE ALLOWABLE BEARING PRESSURE FOR PIER 1 & 4 ARE 2 AND HALF (2.5) TONS PER SQUARE FOOT AND FOR PIERS 2 & 3 SEVEN (7.0) TONS PER SQUARE FEET.

THE CONCRETE IN ALL CURTAIN WALLS, RETAINING WALLS AND PIERS 1 & 4 SHALL BE CLASS 4000 PSI. THE CONCRETE IN THE FOOTINGS OF PIER 2 & 3 SHALL BE 4000 PSI. ALL OTHER CAST IN PLACE CONCRETE SHALL BE 5000 PSI.

FALSEWORK SHALL BE CAREFULLY RELEASED TO PREVENT IMPACT OR UNDUE STRESS IN STRUCTURE. THE TRAFFIC BARRIER SHALL NOT BE POURED UNTIL THE FALSEWORK HAS BEEN RELEASED.

EXPOSED CONCRETE SURFACES SHALL RECEIVE PIGMENTED SEALER AS SHOWN ON THE PLANS.

UNLESS OTHERWISE SHOWN ON THE PLANS, CONCRETE COVER MEASURED FROM THE FACE OF THE CONCRETE TO THE FACE OF ANY REINFORCEMENT SHALL BE 2 1/2" AT THE TOP OF THE ROADWAY SLAB, 2" AT THE BOTTOM OF THE ROADWAY SLAB, 2" AT THE BOTTOM OF FOOTING AND 1 1/2" AT ALL OTHER LOCATIONS.

ALL EXPOSED CONCRETE SURFACES OF THE SUBSTRUCTURE TO ONE FOOT BELOW FINAL GROUND LINE SHALL RECEIVE PIGMENTED SEALER. SEE BRIDGE SHEET 9 FOR THE LIMIT OF PIGMENTED SEALER TO THE SUPERSTRUCTURE.

N-WAY LINE
EXISTING ELEVATIONS

ELEVATION	OFFSET LT.	STATION	OFFSET RT.	ELEVATION
159.1	11.5	58+20	11.0	160.4
159.5	11.5	58+30	11.0	160.6
159.9	11.5	58+40	11.0	160.9
160.3	11.5	58+50	11.0	161.2
160.7	11.4	58+60	11.3	161.5
161.1	11.3	58+70	11.5	161.7
161.4	11.2	58+80	11.8	162.0
161.8	11.1	58+90	12.0	162.2

CURVE DATA

P.I. STATION	Δ	RADIUS	TANGENT	S	LENGTH	BK. TANGENT
WN Sta. 394+32.30	101°57'05" Rt.	355.00'	438.02'	0.08'/Ft.	631.69'	N 69°38'05" E
N-WAY Sta 55+08.99	43°25'00" Lt.	955.37'	380.35'	Existing	723.95'	S 26°23'32" E

P.C. GIRDERS (W50G)
CONTINUOUS FOR LIVE LOA

LOADING: HS-20
OR
TWO 24^K AXLES @ 4' C.T.F.

DESIGN ENG.	DATE	REVISION	BY	APP'D
P.S. [illegible]	5/91			
[illegible]	6/91			
	5/91			

STATE 10 WASH. | FED. AID PROJ. NO. | SHEET NO. | TOTAL SHEETS | JOB NUMBER | CONTRACT NO.

BRIDGE AND STRUCTURES OFFICE

DATE

22-MAR-1991 I:\GS\405\SIP\NULDGN;2

Washington State Department of Transportation

LAYOUT

Figure 1.1

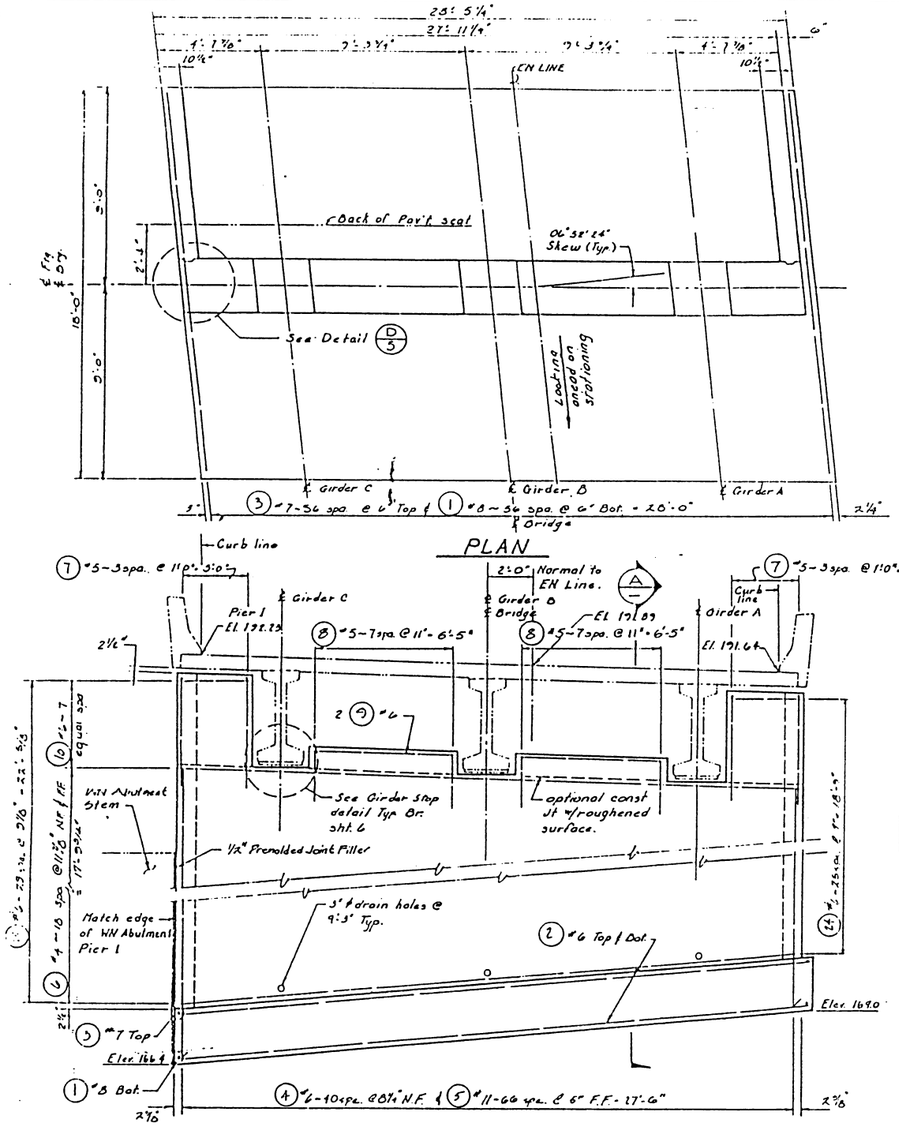

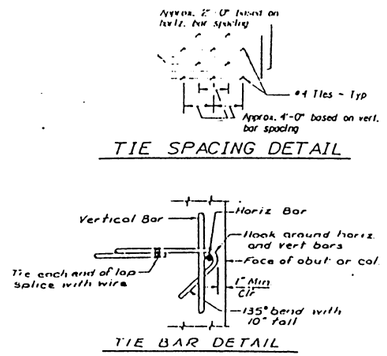

TOP OF GROUT ELEVATIONS	
GIRDER DESIGNATION	PIER 1
A	186.65
B	186.86
C	187.07

Note:
N.F. - Near Face
F.F. - Far Face

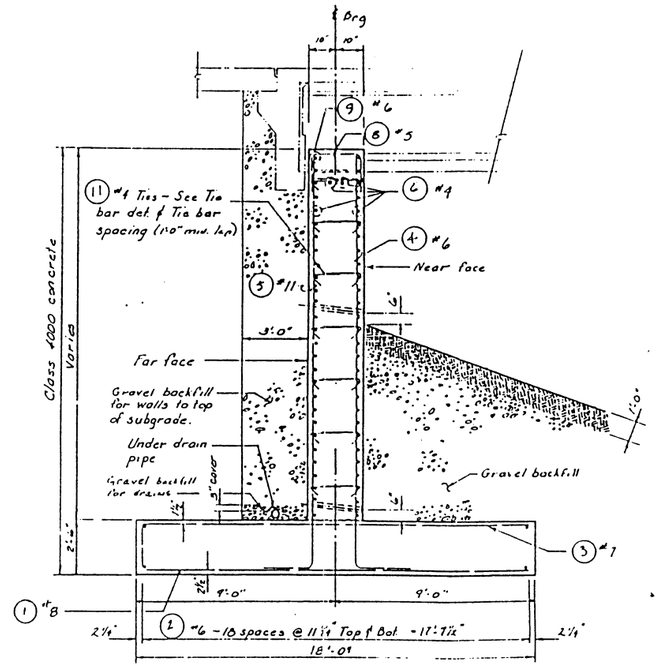

Bridge Design Engineer				REGION NO.	STATE	FED. AID PROJ. NO.	SHEET NO.	TOTAL SHEETS	BRIDGES AND STRUCTURES
Supervisor				10	WASH				
Reviewed By				JOB NUMBER					Washington State Department of Transportation
Designed By P.D. Kinderman 4/91									
Checked By Ilgh Sheikhizadeh 6/91				CONTRACT NO.					PIER 1
Detailed By L.H. Mower 7/91									
Architect									
Preliminary Plan By	DATE	REVISION	BY	APP'D					

APPROVED

BRIDGE SHEET NO 3 SHEET OF SHEETS

K-E ***** DOT FORM 221-013

Figure 1.2

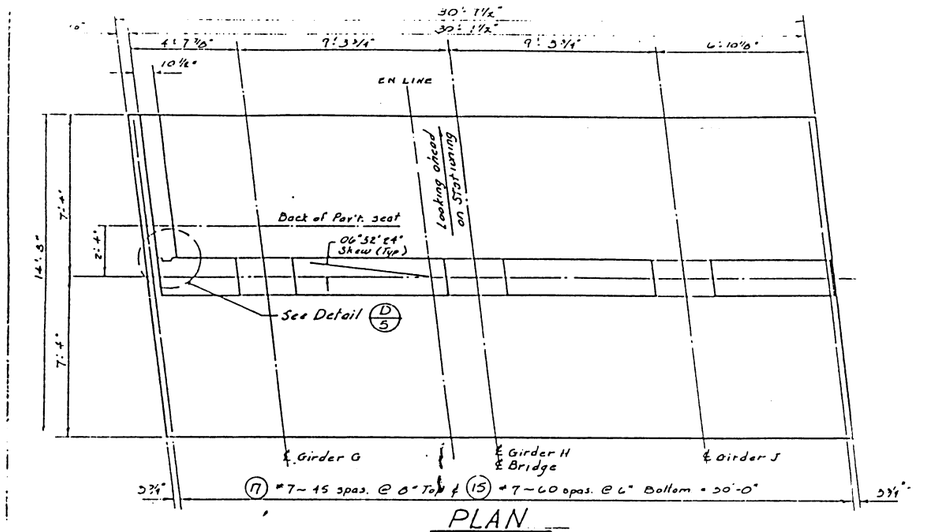

PLAN

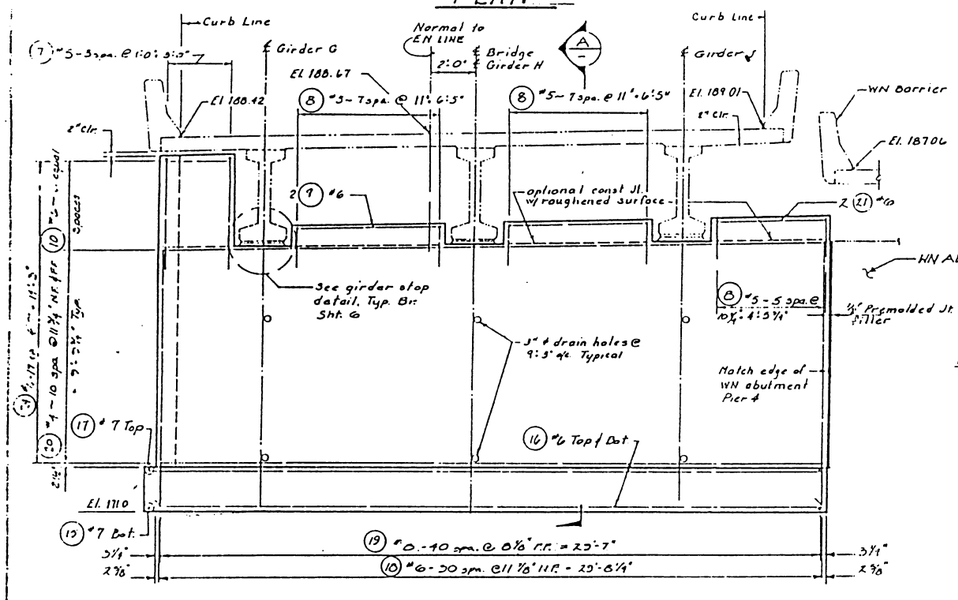

ELEVATION

Horiz. dimensions measured along ℄ Brg. except as noted
Elev. shown looking back on Stationing.

Note:
NF = Near Face
FF = For Face

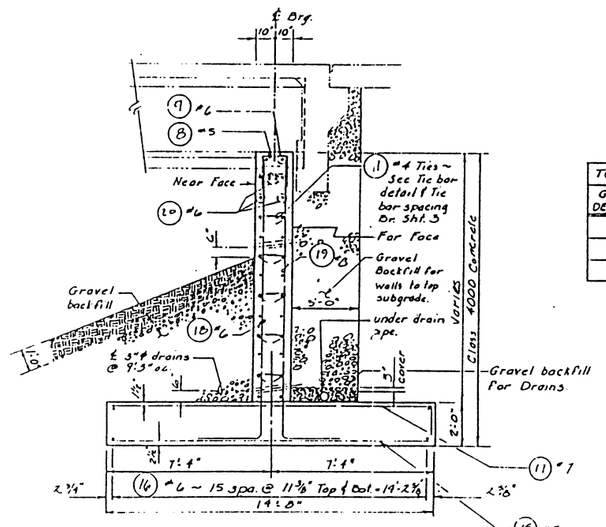

SECTION

TOP OF GROUT ELEVATIONS	
GIRDER DESIGNATIONS	PIER 4
G	183.53
H	183.74
J	183.95

Bridge Design Engineer					STATE	FED. AID PROJ. NO.	SHEET NO	TOTAL SHEETS	BRIDGES AND STRUCTURES
Superintendent									
Reviewed By									
Designed By P.D. Kinderman 4/91									
Checked By Hoh Sheikhzadeh 6/91									
Detailed By L.M. Mower 4/91									
Quantities									
Preliminary Plan By	DATE	REVISION	BY	APP'D					

ENGR. DIST. NO.	10
STATE	WASH
JOB NUMBER	
CONTRACT NO.	

APPROVED

Washington State Department of Transportation

PIER 4

BRIDGE SHEET NO 4

SHEET OF SHEETS

DOT FORM 221-013

Figure 1.3

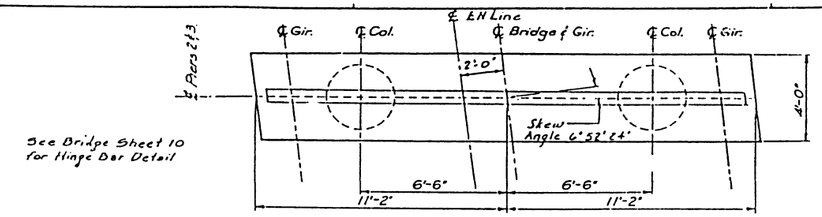

See Bridge Sheet 10 for Hinge Bar Detail

X-BEAM PLAN

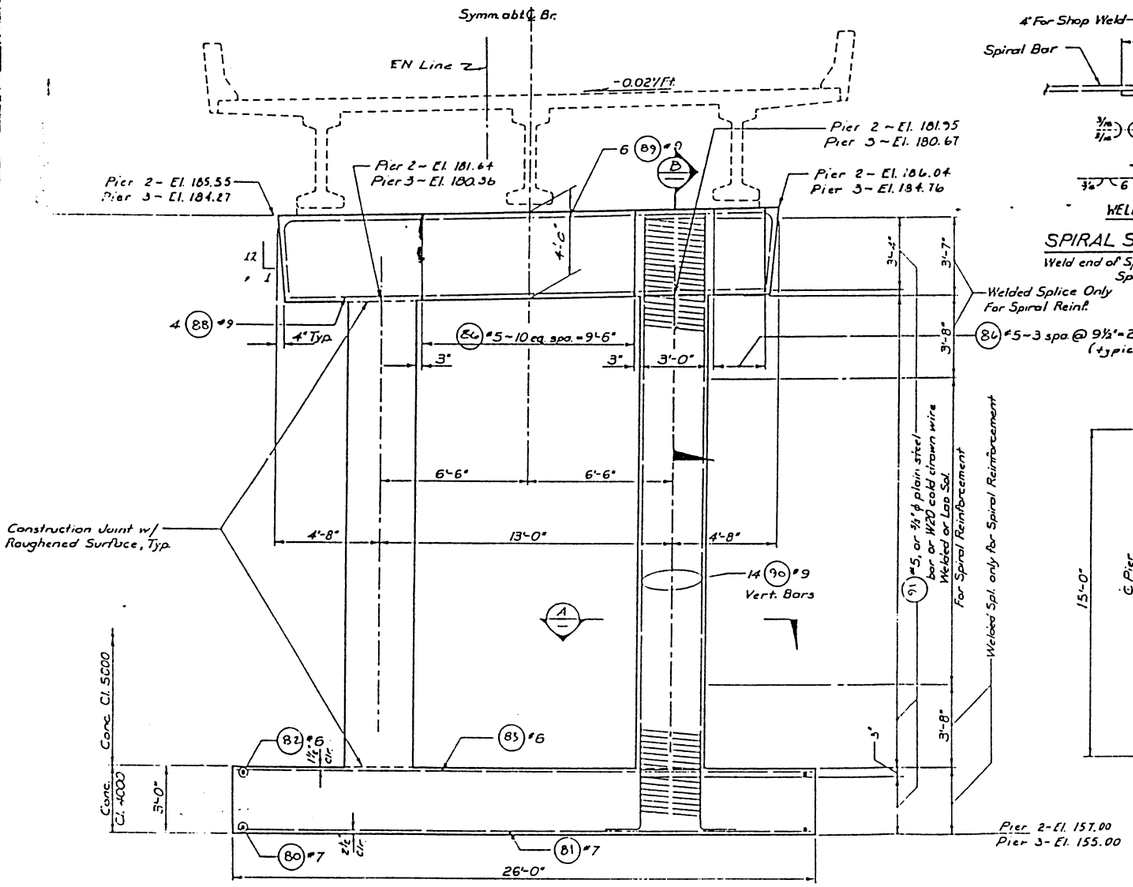

ELEVATION - PIERS 2 & 3

Elev. given @ ℄ of Pier
Shown normal to ℄ of Pier ahead on Stationing

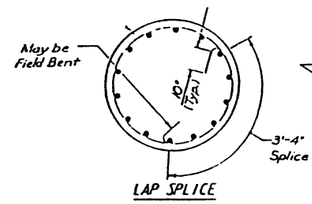

LAP SPLICE

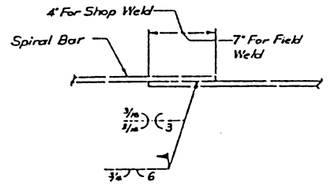

WELDED SPLICE

SPIRAL SPLICE DETAILS

Weld end of Spiral Back on Spiral @ Spiral Ends

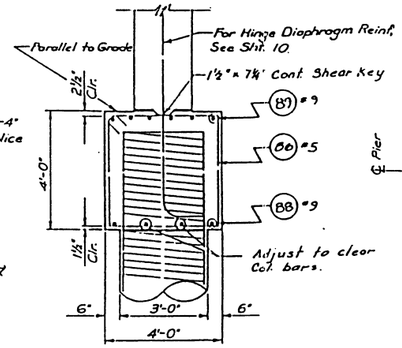

SECTION (B)

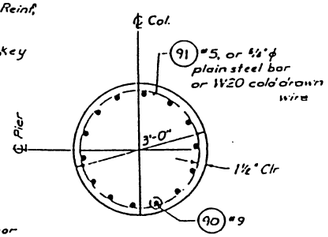

SECTION (A)

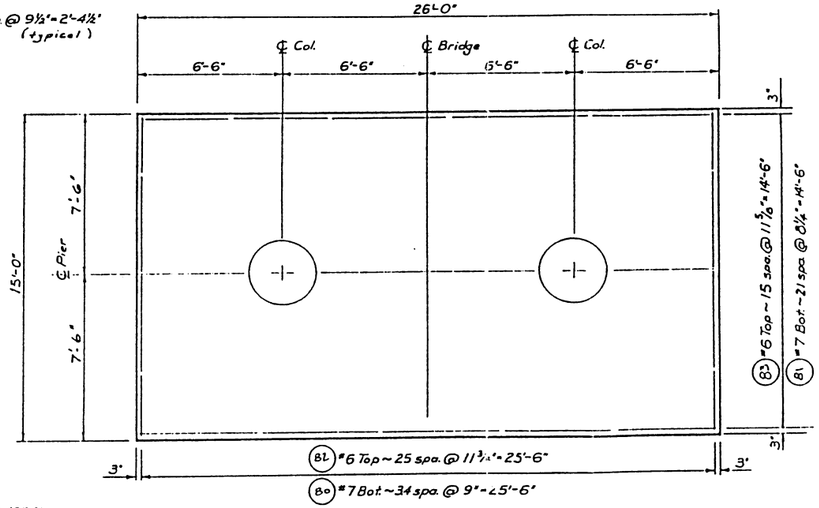

FOOTING PLAN

Design Engineer					REGION NO.	STATE	FED. AID PROJ. NO.	SHEET NO.	TOTAL SHEETS	BRIDGE SHEET NO. 7
Specified										
Reviewed By					10	WASH				
Checked By P.D. Kinderman 6/91					JOB NUMBER					SHEET OF SHEETS
Computed By S.H. Sheikhzadeh 6/91										
Detailed By B.H. Crews 10/90					CONTRACT NO.					
Architect										
Preliminary Plan By	DATE	REVISION	BY	APP'D						

DOT FORM 221-013 Revised 9/82

BRIDGES AND STRUCTURES

APPROVED

Washington State Department of Transportation

PIERS 2 & 3

Figure 1.4

Normalized 5% Damped Response Spectrum

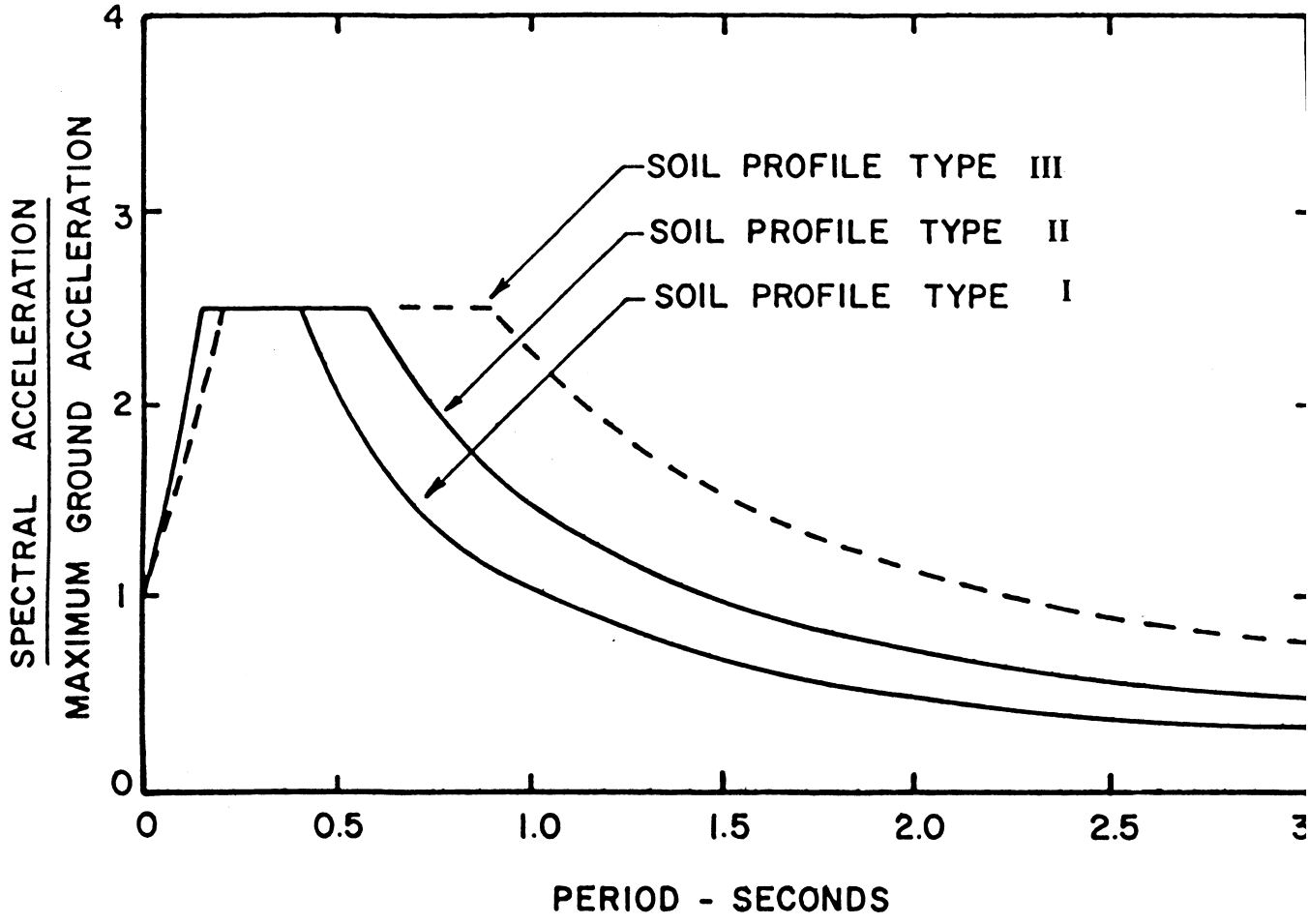

Reference: ATC-6 (1978)

Figure 2.1

3.0 SOIL PROPERTIES

The soil parameters provided by WSDOT for the soil layers are:

γ = total density in pcf
c = cohesion in psf
ϕ = friction angle in degrees
G = low-strain shear modulus in psf or ksf
ν = Poisson's Ratio

Because the behavior of soil is nonlinear during strong shaking, simple procedures were implemented to approximately account for the effect of this nonlinearity on the computation of the abutment and pier foundation stiffnesses. These procedures are described in Section 3.0 of the Coldwater Creek example problem and were implemented in the Northrup Way example problem herein because the ground acceleration coefficient, Z, was greater than 0.2.

4.0 PIER 1 STIFFNESS CALCULATION - FHWA METHOD

In this section the calculation of foundation stiffnesses using the FHWA (1986) method is presented for Pier 1 of the Northrup Way Overcrossing. (The use of the Novak method is illustrated in Section 5.0).

A side-elevation view of the abutment and the soil-property profile at Pier 1 is shown in Figure 4.1. As with the Coldwater Creek example, the basic approach to compute the foundation stiffness matrix at this pier is to first compute the footing stiffness and abutment-wall stiffness, and then combine these stiffnesses to obtain the abutment stiffness matrix at a specified point on the abutment foundation. This point (Point O in Figure 4.1) is located on top of the 2½-foot thick footing at its geometric center.

Pier 1
Soil Profile

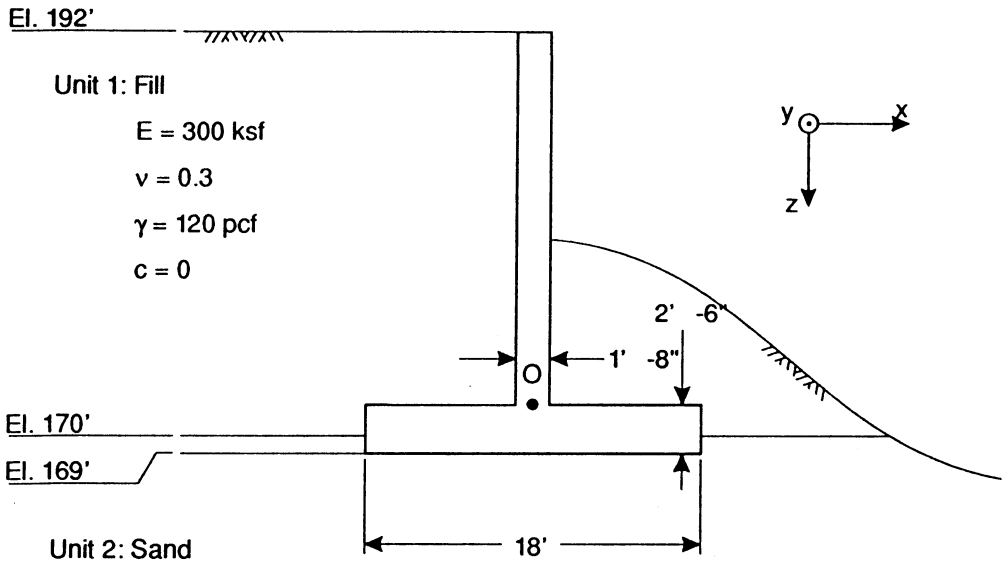

Unit 2: Sand

E = 2500 ksf

ν = 0.3

γ = 120 pcf

c = 0

El. 147'

Unit 3: Sand

E = 1500 ksf

ν = 0.4

γ = 110 pcf

c = 0

El. 134' ▽

Note: E = 2(1+ν)G

Figure 4.1

4.1 ABUTMENT FOOTING STIFFNESSES

As recommended in the Task 1 report, the foundation stiffnesses of the footings are computed by following the procedures specified in the FHWA (1986) report. These footing stiffnesses and the stiffness contributions from the abutment wall are added to obtain the total abutment stiffness matrix.

4.1.1 Model and Assumptions

The theoretical model for estimating the stiffnesses of an embedded footing is presented in Section 4.2.1 of the Coldwater Creek example.

4.1.2 Calculation of Footing Stiffnesses

4.1.2.1 General Procedure. The general procedure to compute the foundation stiffnesses of an embedded footing is presented in Section 4.2.2.1 of the Coldwater Creek example.

4.1.2.2 Application to Northrup Way Overcrossing Abutment Footing. The calculation of the footing stiffness matrix for the Pier 1 abutment is described below. In Figure 1, the footing is defined as the portion of the abutment below Point O. The relevant equations given below are taken from the Coldwater Creek example (Section 4.2.2.1).

The footing dimensions from Figure 4.1:

Length:	2L = 28 ft - 5¼ in = 28.44 ft
Width:	2B = 18 ft
Thickness:	D = 2.5 ft

Compute the effective soil depth:

Eqn. (4.29): $$h = \left(\frac{4BL}{\pi}\right)^{1/2} = \left(\frac{(28.44\ ft)(18\ ft)}{\pi}\right)^{1/2} = 12.8\ ft$$

Select the G and ν values at h = 12.8 ft beneath the bottom of footing:

Figure 4.1: G = E/2 (1 + υ) = 2500 ksf/2 (1.3) = 962 ksf, ν = 0.30

This modulus is the low-strain G. Because Z ≥ 0.2, reduce G by 50%. Thus, for subsequent calculations, use G = 481 ksf. Compute equivalent radii, R, R_x , R_y , and R_z , of the rectangular foundation using formula in Figure 4.11 of the Coldwater Creek example:

$$\textit{Translation:}\quad R = h = 12.8\ ft$$

$$\textit{Rotation: (about x axis)}\quad R_x = \left[\frac{(2B)(2L)^3}{3\pi}\right]^{1/4} = \left[\frac{(18)(28.44)^3}{3\pi}\right]^{1/4} = 14.5\ ft$$

$$\textit{Rotation: (about y axis)}\quad R_y = \left[\frac{(2L)(2B)^3}{3\pi}\right]^{1/4} = \left[\frac{(28.44)(18)^3}{3\pi}\right]^{1/4} = 11.5\ ft$$

$$\textit{Rotation: (about z axis)}\quad R_z = \left[\frac{4BL(4B^2 + 4L^2)}{6\pi}\right]^{1/4} = \left[\frac{(18)(28.44)(18^2 + 28.44^2)}{6\pi}\right]^{1/4} = 13.2\ ft$$

Compute the stiffnesses of equivalent circular footing, K_i^o:

Eqn. (4.24): $$K_z^o = \frac{4GR}{1 - \nu} = \frac{4(481\ ksf)(12.8\ ft)}{1 - 0.30}\ x\left(\frac{1{,}000\ lb}{1k}\right) = 3.51\ x\ 10^7\ lb/ft$$

Eqn. (4.25): $$K_x^o = K_y^o = \frac{8GR}{2 - \nu} = \frac{8(481\ ksf)(12.8\ ft)}{2 - 0.30}\ x\left(\frac{1{,}000\ lb}{1k}\right) = 2.89\ x\ 10^7\ lb/ft$$

Eqn. (4.26): $$K_{\theta z}^o = \frac{16GR_z^3}{3} = \frac{16(481\ ksf)(13.2\ ft)^3}{3}\ x\left(\frac{1{,}000\ lb}{1k}\right) = 5.96\ x\ 10^9\ lb\text{-}ft$$

Eqn. (4.27): $$K_{\theta x}^o = \frac{8GR_x^3}{3(1 - \nu)} = \frac{8(481\ ksf)(14.5\ ft)^3}{3(1 - 0.30)}\ x\left(\frac{1{,}000\ lb}{1k}\right) = 5.53\ x\ 10^9\ lb\text{-}ft$$

Eqn. (4.28): $$K_{\theta y}^o = \frac{8GR_y^3}{3(1 - \nu)} = \frac{8(481\ ksf)(11.5\ ft)^3}{3(1 - 0.30)}\ x\left(\frac{1{,}000\ lb}{1k}\right) = 2.79\ x\ 10^9\ lb\text{-}ft$$

Compute values of α_i and $ß_i$ by first calculating L/B and D/R ratios:

L/B = 1.6
D/R = 2.5/12.8 = 0.20 (translation)
$D/R_x = 0.17$, $D/R_y = 0.22$, $D/R_z = 0.19$ (rotation)

The corresponding values of α_i and $ß_i$ were obtained from Figures 4.12 and 4.13 in the Coldwater Creek example, and are summarized in Table 4.1 below, along with the stiffnesses K_i° and the final stiffnesses $K_i = \alpha_i \cdot ß_1 \cdot K_i^\circ$ (Eqn. 4.22 in Coldwater Creek example).

TABLE 4.1
CALCULATION OF PIER 1 FOOTING STIFFNESSES

	K_i^o	α_i	β_i	K_i
K_x (lb/ft)	2.90×10^7	1.050	1.29	3.91×10^7
K_y (lb/ft)	2.90×10^7	1.010	1.29	3.76×10^7
K_z (lb/ft)	3.52×10^7	1.040	1.11	4.05×10^7
$K_{\theta x}$ (lb-ft)	5.53×10^9	1.059	1.21	7.09×10^9
$K_{\theta y}$ (lb-ft)	2.79×10^9	1.059	1.31	3.87×10^9
$K_{\theta z}$ (lb-ft)	5.96×10^9	1.059	1.56	9.84×10^9

Thus, the diagonal elements of the diagonal footing stiffness matrix, [K], are the values in the last column in Table 4.1. This stiffness matrix applies to the global coordinate system in Figure 4.1.

4.2 ABUTMENT WALL STIFFNESS

The stiffness due to the passive resistance of abutment backfill soil is also computed and added to the footing stiffness.

4.2.1 Model and Assumptions

The model and assumptions for estimating the translational and rotational stiffnesses of the abutment wall-backfill system is provided in Section 4.3.1 of the Coldwater Creek example.

4.2.2 Calculation of Wall Stiffnesses

4.2.2.1 General Procedure. The formulas for the translational and rotational stiffnesses were provided in Section 4.3.2.1 of the Coldwater Creek example.

4.2.2.2 Application to Northrup Way Overcrossing Abutment Wall. The abutment-wall stiffness computation is illustrated for the Pier 1 abutment. The abutment wall height is assumed to be the distance from the top of the footing (i.e. Point O in Figure 4.1) to the top of the abutment. The stiffnesses are computed at Point O.

Obtain the appropriate length dimensions from Figures 1.2 and 4.1:

B_w = 27.69 ft
H_w = 20.5 ft

Thus, $h_1 = 0.37H_w$ = 7.59 ft

Compute E_s which is 50% less than the low-strain E of 300 ksf as explained in the abutment footing calculation:

Using the global coordinate system in Figure 4.1, the wall stiffnesses at Point O are:

Eqn. (4.32): $K_x = 0.425E_sB_w = 0.425(150\ ksf)(27.69\ ft)\ x\left(\frac{1{,}000\ lb}{1k}\right) = 1.77\ x\ 10^6\ lb/ft$

Eqn.(4.33): $K_{\theta y} = (0.425E_sB_w)h_1^2 + 0.072E_sB_wH_w^2$

$= (1.77\ x\ 10^6\ lb/ft)(7.59\ ft)^2 + 0.072(1.50\ x\ 10^5\ psf)(27.69\ ft)(20.5\ ft)^2$

$= 2.28\ x\ 10^8\ lb\text{-}ft$

Eqn. (4.34): $K_{x\theta y} = -(0.425E_sB_w)h_1 = -(1.77 \times 10^6\ lb/ft)(7.59\ ft) = -1.34 \times 10^7\ lb$

The minus sign in Eqn. (4.34) results from the fact that the sign convention for forces (moments) and displacements (rotations) in the FHWA (1986) report is slightly different from the convention adopted herein.

4.3 TOTAL ABUTMENT STIFFNESS MATRIX

4.3.1 General Procedure

The total abutment stiffness matrix, $[K_t]$, at a given point is approximated as the sum of the stiffness matrices for the footing $[K_f]$ and abutment wall, $[K_w]$, i.e.

$$[K_t] = [K_f] + [K_w]$$

Although this formula is simple, it is important to note that $[K_f]$ and $[K_w]$ must be computed at the same point in the same coordinate system used for the footings and wall.

4.3.2 Application to Northrup Way Overcrossing Abutment. The stiffness matrices $[K_f]$ and $[K_w]$ for the abutment system at Pier 1 were constructed from the stiffness calculations presented in Sections 4.1 and 4.2, respectively. The xyz coordinate system is oriented as shown in Figure 4.1 with the origin at Point O.

The 6 x 6 stiffness matrices are:

From Table 4.1,

$$\text{diag } [K_f] = \begin{bmatrix} 3.91E7 & & & & & \\ & 3.76E7 & & & & \\ & & 4.05E7 & & & \\ & & & 7.09E9 & & \\ & & & & 3.87E9 & \\ & & & & & 9.84E9 \end{bmatrix}$$

From Section (4.2.2.2),

$$[K_w] = \begin{bmatrix} 1.77E6 & 0 & 0 & 0 & -1.34E7 & 0 \\ 0 & 0 & 0 & 0 & 0 & 0 \\ 0 & 0 & 0 & 0 & 0 & 0 \\ 0 & 0 & 0 & 0 & 0 & 0 \\ -1.34E7 & 0 & 0 & 0 & 2.28E8 & 0 \\ 0 & 0 & 0 & 0 & 0 & 0 \end{bmatrix}$$

Therefore,

$$[K_t] = \begin{bmatrix} 4.09E7 & 0 & 0 & 0 & -1.34E7 & 0 \\ 0 & 3.76E7 & 0 & 0 & 0 & 0 \\ 0 & 0 & 4.05E7 & 0 & 0 & 0 \\ 0 & 0 & 0 & 7.09E9 & 0 & 0 \\ -1.34E7 & 0 & 0 & 0 & 4.10E9 & 0 \\ 0 & 0 & 0 & 0 & 0 & 9.84E9 \end{bmatrix}$$

The units are lb and ft.

5.0 PIER 1 STIFFNESS CALCULATION - NOVAK METHOD

The calculation of foundation stiffnesses using the Novak method is much simpler than the FHWA method primarily because a single computer program (DYNA3) is available to do all the required calculations. Furthermore, the theory upon which the program is based assumes linear elastic response of the soil-foundation system; consequently, fewer soil properties are required to characterize the soil medium.

5.1 FOOTING ON HALF-SPACE STIFFNESS

The Task 1 report recommended the use of the Pile & Footing Side option within the Novak computer program. The Northrup Way Overcrossing, however, is not supported by piles. In cases where the bridge is supported by footings only, the Footing on Half-Space option of the DYNA3 computer program is recommended. This option models the soil profile as a layered medium embedding the footing, while the soil below the footing is modelled by a linear elastic half-space.

5.1.1 Soil Model

The soil model is shown in Figure 5.1, which was adapted from information in Figure 4.1. Note that shear-wave velocity, V_s, is given as a low-strain elastic property, rather than the Young's modulus, E. In computing the proper $V_s = \sqrt{G/\gamma_m}$ (where γ_m = mass density) for input to DYNA3, the low-strain shear modulus values were reduced by 50% to account for high soil strain.

Besides V_s, the other new soil parameter in Figure 5.1 that was not shown in Figure 4.1 is the soil damping ratio for shear deformation, ζ. Values of $\zeta \leq 0.05$ are typically assumed and within this range, the effect of this parameter on the stiffness

Pier 1
Novak Soil Model

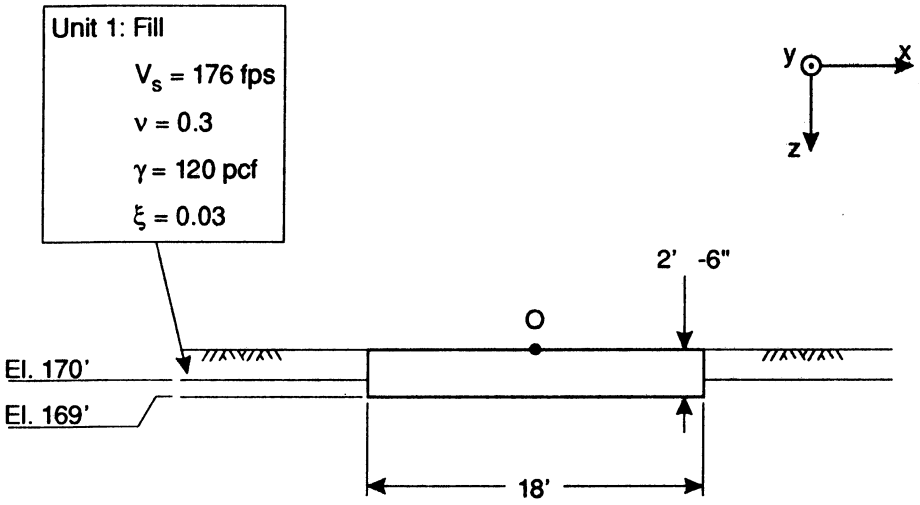

Unit 2: Sand

V_s = 508 fps

ν = 0.3

γ = 120 pcf

ξ = 0.03

Figure 5.1

calculation is negligible. For this and all other example problems, ζ = 0.03 was arbitrarily assumed.

5.1.2 Preparation of DYNA3 Input

The input file for Novak's DYNA3 computer program for Pier 1 is shown in Table 5.1. The lines in the input file are annotated with comments which appear on the right-hand side of the page. Most of the input items are self-explanatory, but a few will be elaborated upon here.

The lines beginning "RECTANGULAR=" and "MASS=" denote the plan dimensions and mass of the foundation system, respectively, just as for the PILE foundation type (see Section 5.1.2 of the Coldwater Creek problem). The line "CONSTANTS=0.,0.,2.5" indicates the location of Point O for DYNA3. As explained in the Coldwater Creek example, the value 2.5 indicates that Point O lies 2.5 ft above the bottom of the footing, and the sign is positive.

The soil properties are defined similarly to the pile example. First, the embedding soil layers are defined, numbering from the base of the footing to the top of the soil column. In order to remain consistent with the FHWA approach, the effect of that portion of the soil column overlying the top of the footing is neglected herein. The data for each layer consists of a layer number, the layer thickness, soil shear-wave velocity, soil unit weight, Poisson's ratio, and soil damping ratio for shear deformation. The half-space below the footing is defined by specifying the appropriate soil properties.

5.1.3 DYNA3 Output

The output file from the DYNA3 program is listed in Table 5.2. Please note that the form of the output file is very similar to the output for foundation systems containing

```
TITLE=Northup Way Overcrossing Pier 1 [k ft s]
MATRIX                                  | print stiffness and damping matrices
GRAVITY=32.2                            | gravitational constant
FOUNDATION=HALF-SPACE                   | footing overlying half-space
RECTANGULAR=18.0, 28.4                  | footing dimensions
MASS=0.,0.,0.,0.,0.,0.                  | mass properties of footing
CONSTANTS=0.,0.,2.5                     | location of Cg
SOIL
CONSTANTS=2                             | # of overlying soil layers
1   1.   508.  .120  0.3  0.03          | properties for first layer
                                        | layer number, thickness, Vs,
                                        | unit weight, Poisson's ratio, damping
2   1.5  176.  .120  0.3  0.03
BELOW                                   | half-space properties
508.  .120  .30  0.03                   | Vs, unit weight, Poisson's ration,
                                        | damping
LOAD=HARMONIC                           | minimal load specified
CONSTANTS
NONQUADRATIC
0.001  0.001  0.001  0.0  0.0  0.0  0.  0.  0.
RUN
```

Table 5.1

```
**********************************************
*
*        D Y N A 3   S I M U L A T I O N
*
*              RUN DATE -  1992/10/23
*              TIME     -  11:34:57
*              REVISION -  1991/07/30
*
**********************************************

Northrup Way Overcrossing Pier 1 [k ft s]

                                    RESULTS
                                    *******


FREQUENCY  -     .0010
*********


STIFFNESS CONSTANTS (K)
***********************

HORIZONTAL TRANSLATION  (X) ...  6.16354E+04
HORIZONTAL TRANSLATION  (Y) ...  6.16354E+04
VERTICAL TRANSLATION  (Z) .....  7.19199E+04
ROTATION ABOUT  (X) ...........  1.22031E+07
ROTATION ABOUT  (Y) ...........  6.43949E+06
TORSION ABOUT  (Z) ............  1.43819E+07
CROSS-STIFFNESS (YZ PLANE) ....  1.51392E+05
CROSS-STIFFNESS (XZ PLANE) .... -1.51392E+05

DAMPING CONSTANTS (C)
*********************
HORIZONTAL TRANSLATION  (X) ...  1.85043E+06
HORIZONTAL TRANSLATION  (Y) ...  1.85043E+06
VERTICAL TRANSLATION  (Z) .....  2.15936E+06
ROTATION ABOUT  (X) ...........  3.66100E+08
ROTATION ABOUT  (Y) ...........  1.93192E+08
TORSION ABOUT  (Z) ............  4.31458E+08
CROSS-DAMPING  (YZ PLANE) .....  4.54480E+06
CROSS-DAMPING  (XZ PLANE) ..... -4.54480E+06
```

Table 5.2

piles. The stiffnesses are in units of kips and ft. The values of CROSS-STIFFNESS (YZ PLANE) and CROSS-STIFFNESS (XZ PLANE) refer to $K_{y\theta x}$ and $K_{x\theta y}$, respectively.

5.2 ABUTMENT WALL STIFFNESS

The Task 1 report noted that the abutment-wall stiffness could be computed using Novak's method for a footing on an elastic half space whose properties are those of the backfill soil. However, the FHWA approach for retaining walls (Section 4.3) is slightly preferred over the Novak method. The stiffness matrix obtained using the FHWA method was presented in Section 4.3.

5.3 TOTAL PIER 1 STIFFNESS MATRIX

The total abutment stiffness matrix is $[K_t] = [K_f] + [K_w]$, where $[K_f]$ is the footing stiffness matrix, and $[K_w]$ is the abutment wall stiffness matrix. From Table 5.2 of Section 5.1.3,

$$[K_f] = \begin{bmatrix} 6.16E7 & 0 & 0 & 0 & -1.51E8 & 0 \\ 0 & 6.16E7 & 0 & 1.51E8 & 0 & 0 \\ 0 & 0 & 7.19E7 & 0 & 0 & 0 \\ 0 & 1.51E8 & 0 & 1.22E10 & 0 & 0 \\ -1.51E8 & 0 & 0 & 0 & 6.44E9 & 0 \\ 0 & 0 & 0 & 0 & 0 & 1.44E10 \end{bmatrix}$$

The units are lb and ft.

From Section 4.2,

$$[K_w] = \begin{bmatrix} 1.77E6 & 0 & 0 & 0 & -1.34E7 & 0 \\ 0 & 0 & 0 & 0 & 0 & 0 \\ 0 & 0 & 0 & 0 & 0 & 0 \\ 0 & 0 & 0 & 0 & 0 & 0 \\ -1.34E7 & 0 & 0 & 0 & 2.28E8 & 0 \\ 0 & 0 & 0 & 0 & 0 & 0 \end{bmatrix}$$

Therefore,

$$[K_t] = \begin{bmatrix} 6.34E7 & 0 & 0 & 0 & -1.64E8 & 0 \\ 0 & 6.16E7 & 0 & 1.51E8 & 0 & 0 \\ 0 & 0 & 7.19E7 & 0 & 0 & 0 \\ 0 & 1.51E8 & 0 & 1.22E10 & 0 & 0 \\ -1.64E8 & 0 & 0 & 0 & 6.67E9 & 0 \\ 0 & 0 & 0 & 0 & 0 & 1.44E10 \end{bmatrix}$$

Note that $[K_t]$ is the stiffness matrix at Point O for the global coordinate system defined in Figure 5.1.

6.0 PIER 2 AND PIER 3 FOUNDATION STIFFNESSES

The FHWA and Novak methods were applied to Pier 2 and Pier 3 (Figures 6.1 and 6.2). Because these pier foundations are similar to Pier 1, only the final stiffness results will be presented here. Furthermore, note that if the effect of the soil overlying Point O is neglected, as it is in this example, the footing calculations are identical. Accordingly, the Pier 3 results will not be presented, and may be taken to be numerically equal to the Pier 2 stiffness values.

Pier 2
Soil Profile

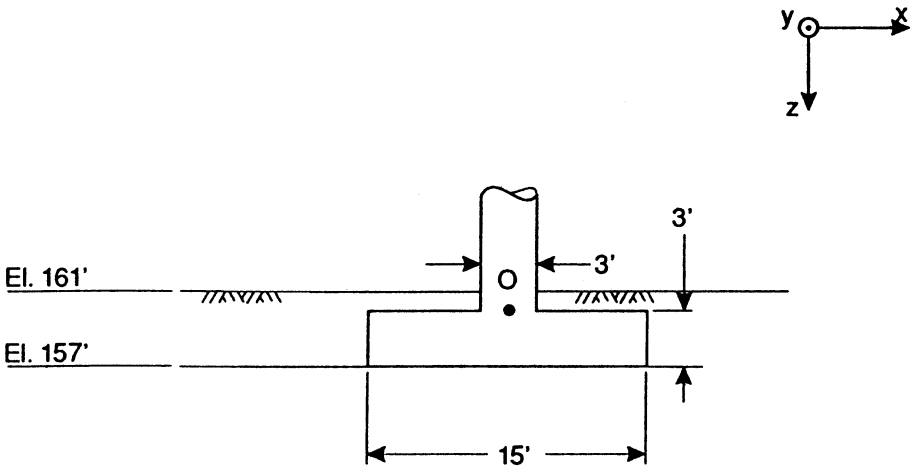

Unit 2: Sand

El. 138'

El. 134'

Unit 3: Clay

Soil properties as for Pier 1
See Figure 4.1

Figure 6.1

Pier 3
Soil Profile

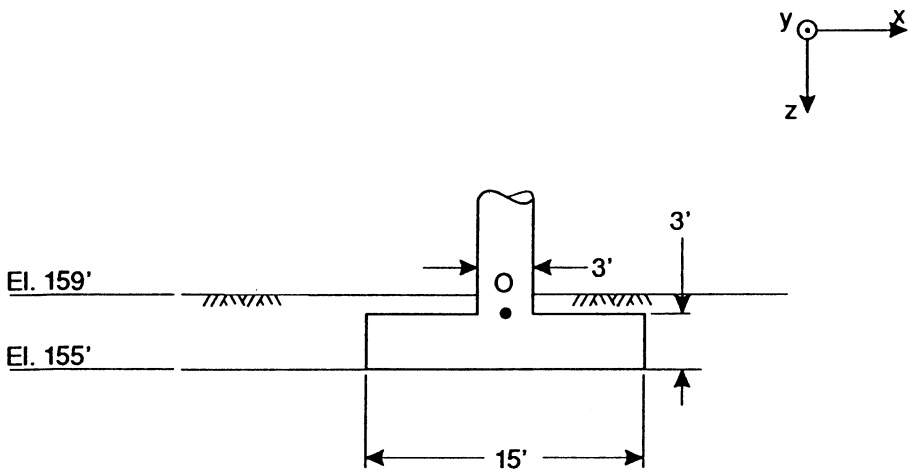

Unit 2: Sand

El. 138'

El. 134'

Unit 3: Clay

Soil properties as for Pier 1
See Figure 4.1

Figure 6.2

6.1 FHWA METHOD

The dimensions of the Pier 2 footing are as follows (Figures 1.4 and 6.1),

Length:	2L = 26 ft
Width:	2B = 15 ft
Thickness:	D = 3 ft

The soil properties at the effective soil depth, $H = \left(\frac{4BL}{\pi}\right)^{1/2} = 11.1$ ft, beneath the footing are

Figures 5.1 and 4.1: G = 962 ksf, ν = 0.30

This modulus is the low-strain G. Because $Z \geq 0.2$, reduce G by 50%. Thus, for subsequent calculations, use G = 481 ksf.

Note that, as no other elements contribute to the pier stiffness, $[K_t] = [K_f]$. The resulting 6 X 6 footing stiffness matrix, defined at Point O, is

$$[K_t] = \begin{bmatrix} 3.70E7 & 0 & 0 & 0 & 0 & 0 \\ 0 & 3.54E7 & 0 & 0 & 0 & 0 \\ 0 & 0 & 3.64E7 & 0 & 0 & 0 \\ 0 & 0 & 0 & 5.48E9 & 0 & 0 \\ 0 & 0 & 0 & 0 & 2.69E9 & 0 \\ 0 & 0 & 0 & 0 & 0 & 7.98E9 \end{bmatrix}$$

The units are lb and ft.

6.2 NOVAK METHOD

The input and output files for the DYNA3 program are shown in Tables 6.1 and 6.2, respectively. As noted previously, the pier stiffness is equal to the footing stiffness, defined at Point O as,

$$[K_t] = \begin{bmatrix} 6.04E7 & 0 & 0 & 0 & -1.66E8 & 0 \\ 0 & 6.04E7 & 0 & 1.66E8 & 0 & 0 \\ 0 & 0 & 6.59E7 & 0 & 0 & 0 \\ 0 & 1.66E8 & 0 & 9.92E9 & 0 & 0 \\ -1.66E8 & 0 & 0 & 0 & 4.83E9 & 0 \\ 0 & 0 & 0 & 0 & 0 & 1.31E10 \end{bmatrix}$$

The units are lb and ft.

7.0 PIER 4 FOUNDATION STIFFNESS

The soil profile for Pier 4 is shown in Figure 7.1. Because of the similarities between Piers 1 and 4, only an outline of the Pier 4 solution will be presented.

7.1 FHWA METHOD

The dimensions of the Pier 4 footing are as follows (Figures 1.3 and 7.1),

Length:	2L = 30 ft - 7½ in = 30.6 ft
Width:	2B = 14 ft - 8 in = 14.7 ft
Thickness:	D = 2 ft

Pier 4
Soil Profile

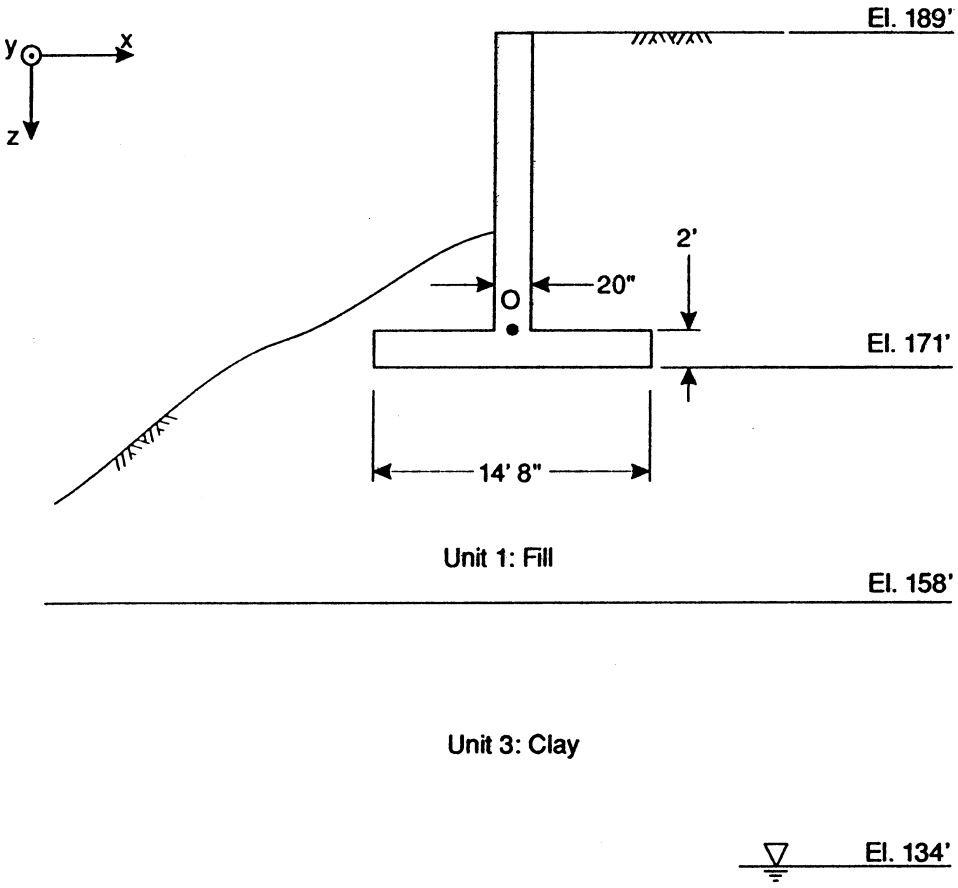

Soil properties as for Pier 1
See Figure 4.1

Figure 7.1

```
TITLE=Northrup Way Overcrossing Piers 2 and 3 [k ft
MATRIX
GRAVITY=32.2
FOUNDATION=HALF-SPACE
RECTANGULAR=15.0, 26.0
MASS=0.,0.,0.,0.,0.,0.,0.
CONSTANTS=0.,0.,3.0
SOIL
CONSTANTS=1
1   3.   508.  .120  0.3  0.03
BELOW
508.  .120  .30  0.03
LOAD=HARMONIC
CONSTANTS
NONQUADRATIC
0.001  0.001  0.001  0.0  0.0  0.0  0.  0.  0.
RUN
```

Table 6.1

```
**************************************************
*                                                *
*        D Y N A 3   S I M U L A T I O N         *
*                                                *
*              RUN DATE -  1992/10/23            *
*              TIME     -  11:35: 5              *
*              REVISION -  1991/07/30            *
*                                                *
**************************************************

Northrup Way Overcrossing Piers 2 and 3 [k ft s]

                                    RESULTS
                                    *******


FREQUENCY  -      .0010
*********


STIFFNESS CONSTANTS (K)
***********************

HORIZONTAL TRANSLATION  (X) ...   6.03500E+04
HORIZONTAL TRANSLATION  (Y) ...   6.03500E+04
VERTICAL TRANSLATION  (Z) .....   6.58508E+04
ROTATION ABOUT  (X) ...........   9.92421E+06
ROTATION ABOUT  (Y) ...........   4.83082E+06
TORSION ABOUT  (Z) ............   1.31334E+07
CROSS-STIFFNESS (YZ PLANE) ....   1.66163E+05
CROSS-STIFFNESS (XZ PLANE) .... -1.66163E+05

DAMPING CONSTANTS (C)
*********************
HORIZONTAL TRANSLATION  (X) ...   1.81196E+06
HORIZONTAL TRANSLATION  (Y) ...   1.81196E+06
VERTICAL TRANSLATION  (Z) .....   1.97729E+06
ROTATION ABOUT  (X) ...........   2.97735E+08
ROTATION ABOUT  (Y) ...........   1.44933E+08
TORSION ABOUT  (Z) ............   3.94001E+08
CROSS-DAMPING  (YZ PLANE) .....   4.98817E+06
CROSS-DAMPING  (XZ PLANE) ..... -4.98817E+06
```

Table 6.2

Compute the effective soil depth:

Eqn. (4.29): $h = \left(\frac{4BL}{\pi}\right)^{1/2} = \left(\frac{(30.6\ ft)(14.7\ ft)}{\pi}\right)^{1/2} = 12.0\ ft$

Select the G and ν values at h = 12.0 ft beneath the bottom of footing:

Figure 7.1: E = 300 ksf, ν = 0.30 $\therefore$ G = 115 ksf

The above shear modulus is the low-strain G. Because Z $\geq$ 0.2, reduce G by 50%. Thus, for subsequent calculations, use G = 58 ksf.

After performing the required computations, the resulting 6 X 6 footing stiffness matrix, defined at Point O, is

$$[K_f] = \begin{bmatrix} 4.35E6 & 0 & 0 & 0 & 0 & 0 \\ 0 & 4.08E6 & 0 & 0 & 0 & 0 \\ 0 & 0 & 4.49E6 & 0 & 0 & 0 \\ 0 & 0 & 0 & 8.43E8 & 0 & 0 \\ 0 & 0 & 0 & 0 & 2.96E8 & 0 \\ 0 & 0 & 0 & 0 & 0 & 1.06E9 \end{bmatrix}$$

The units are lb and ft.

The wall stiffnesses are computed for the following geometric and soil properties

Width:	B = 30 ft - 1½ in = 30.1 ft
Height:	H_w = 16 ft
Young's Modulus:	E_s = 300 ksf

This modulus is the low-strain E_s. Because $Z \geq 0.2$, reduce E_s by 50%. Thus, for subsequent calculations, use E_s = 150 ksf.

$$[K_w] = \begin{bmatrix} 1.92E6 & 0 & 0 & 0 & -1.17E7 & 0 \\ 0 & 0 & 0 & 0 & 0 & 0 \\ 0 & 0 & 0 & 0 & 0 & 0 \\ 0 & 0 & 0 & 0 & 0 & 0 \\ -1.17E7 & 0 & 0 & 0 & 1.54E8 & 0 \\ 0 & 0 & 0 & 0 & 0 & 0 \end{bmatrix}$$

Therefore,

$$[K_t] = \begin{bmatrix} 6.27E6 & 0 & 0 & 0 & -1.17E7 & 0 \\ 0 & 4.08E6 & 0 & 0 & 0 & 0 \\ 0 & 0 & 4.49E6 & 0 & 0 & 0 \\ 0 & 0 & 0 & 8.43E8 & 0 & 0 \\ -1.17E7 & 0 & 0 & 0 & 4.50E8 & 0 \\ 0 & 0 & 0 & 0 & 0 & 1.06E9 \end{bmatrix}$$

Note that $[K_t]$ is the stiffness matrix at Point O for the global coordinate system defined in Figure 7.1.

7.2 NOVAK METHOD

The input and output files for the DYNA3 program are shown in Tables 7.1 and 7.2, respectively. The footing stiffness is defined at Point O as,

$$[K_f] = \begin{bmatrix} 7.29E6 & 0 & 0 & 0 & -1.38E7 & 0 \\ 0 & 7.29E6 & 0 & 1.38E7 & 0 & 0 \\ 0 & 0 & 8.26E6 & 0 & 0 & 0 \\ 0 & 1.38E7 & 0 & 1.53E9 & 0 & 0 \\ -1.38E7 & 0 & 0 & 0 & 5.51E8 & 0 \\ 0 & 0 & 0 & 0 & 0 & 1.79E9 \end{bmatrix}$$

The units are lb and ft.

Adding these values to the wall stiffness values presented in Section 7.1, the resulting total stiffness matrix for Pier 4 is

$$[K_t] = \begin{bmatrix} 9.21E6 & 0 & 0 & 0 & -2.55E7 & 0 \\ 0 & 7.29E6 & 0 & 1.38E7 & 0 & 0 \\ 0 & 0 & 8.26E6 & 0 & 0 & 0 \\ 0 & 1.38E7 & 0 & 1.53E9 & 0 & 0 \\ -2.55E7 & 0 & 0 & 0 & 7.05E8 & 0 \\ 0 & 0 & 0 & 0 & 0 & 1.79E9 \end{bmatrix}$$

```
TITLE=Northrup Way Overcrossing Pier 4 [k ft s]
MATRIX
GRAVITY=32.2
FOUNDATION=HALF-SPACE
RECTANGULAR=14.7, 30.6
MASS=0.,0.,0.,0.,0.,0.,0.
CONSTANTS=0.,0.,2.
SOIL
CONSTANTS=1
1   2.   176.  .120  0.3  0.03
BELOW
176.  .120  .30  0.03
LOAD=HARMONIC
CONSTANTS
NONQUADRATIC
0.001  0.001  0.001  0.0  0.0  0.0  0.  0.  0.
RUN
```

Table 7.1

```
*************************************************
*
*        D Y N A 3   S I M U L A T I O N
*
*              RUN DATE -  1992/10/23
*              TIME     -  11:35:12
*              REVISION -  1991/07/30
*
*************************************************

Northrup Way Overcrossing Pier 4 [k ft s]

                                        RESULTS
                                        *******


FREQUENCY  -      .0010
*********


STIFFNESS CONSTANTS (K)
***********************

HORIZONTAL TRANSLATION  (X) ...  7.29451E+03
HORIZONTAL TRANSLATION  (Y) ...  7.29451E+03
VERTICAL TRANSLATION  (Z) .....  8.26294E+03
ROTATION ABOUT  (X) ...........  1.53209E+06
ROTATION ABOUT  (Y) ...........  5.50783E+05
TORSION ABOUT  (Z) ............  1.79597E+06
CROSS-STIFFNESS (YZ PLANE) ....  1.37948E+04
CROSS-STIFFNESS (XZ PLANE) .... -1.37948E+04

DAMPING CONSTANTS (C)
*********************
HORIZONTAL TRANSLATION  (X) ...  2.19306E+05
HORIZONTAL TRANSLATION  (Y) ...  2.19306E+05
VERTICAL TRANSLATION  (Z) .....  2.48479E+05
ROTATION ABOUT  (X) ...........  4.59641E+07
ROTATION ABOUT  (Y) ...........  1.65249E+07
TORSION ABOUT  (Z) ............  5.38790E+07
CROSS-DAMPING  (YZ PLANE) .....  4.14603E+05
CROSS-DAMPING  (XZ PLANE) ..... -4.14603E+05
```

Table 7.2

8.0 APPLICATION TO SEISAB-I BRIDGE ANALYSIS

This example illustrates the use of SEISAB-I to conduct a response spectrum analysis of the Northup Way Overcrossing, as described in Section 1.0.

The structure model is illustrated in Figure 8.1. Pier 1 abutment, Pier 2, Pier 3, and Pier 4 abutment are modeled in the SEISAB-I analysis as Bent 2, Bent 3, Bent 4, and Bent 5, respectively. SEISAB-I requires input of abutments so abutments of zero stiffness are used.

8.1 BENT 2 MODEL

Bent 2 is an abutment with backwall diaphragm connected to the superstructure. The diaphragm extends behind the abutment wall and provides a path for longitudinal loads directed toward mid-span. Load directed toward the approach cannot be transferred to the abutment wall due the presence of sliding bearings. Also, it is noted that, due to it's height and slope, the soil on the front side of the abutment wall will provide minimal resistance to lateral loads.

It is for these reasons that the wall stiffness [Kw] was removed from the BENT 2 foundation stiffness matrix. Stiffness of soil behind the backwall diaphragm is neglected. Therefore, only the diagonal footing stiffness matrix is considered. The units are lb and ft. The coordinate system is as shown in Figure 4.1.

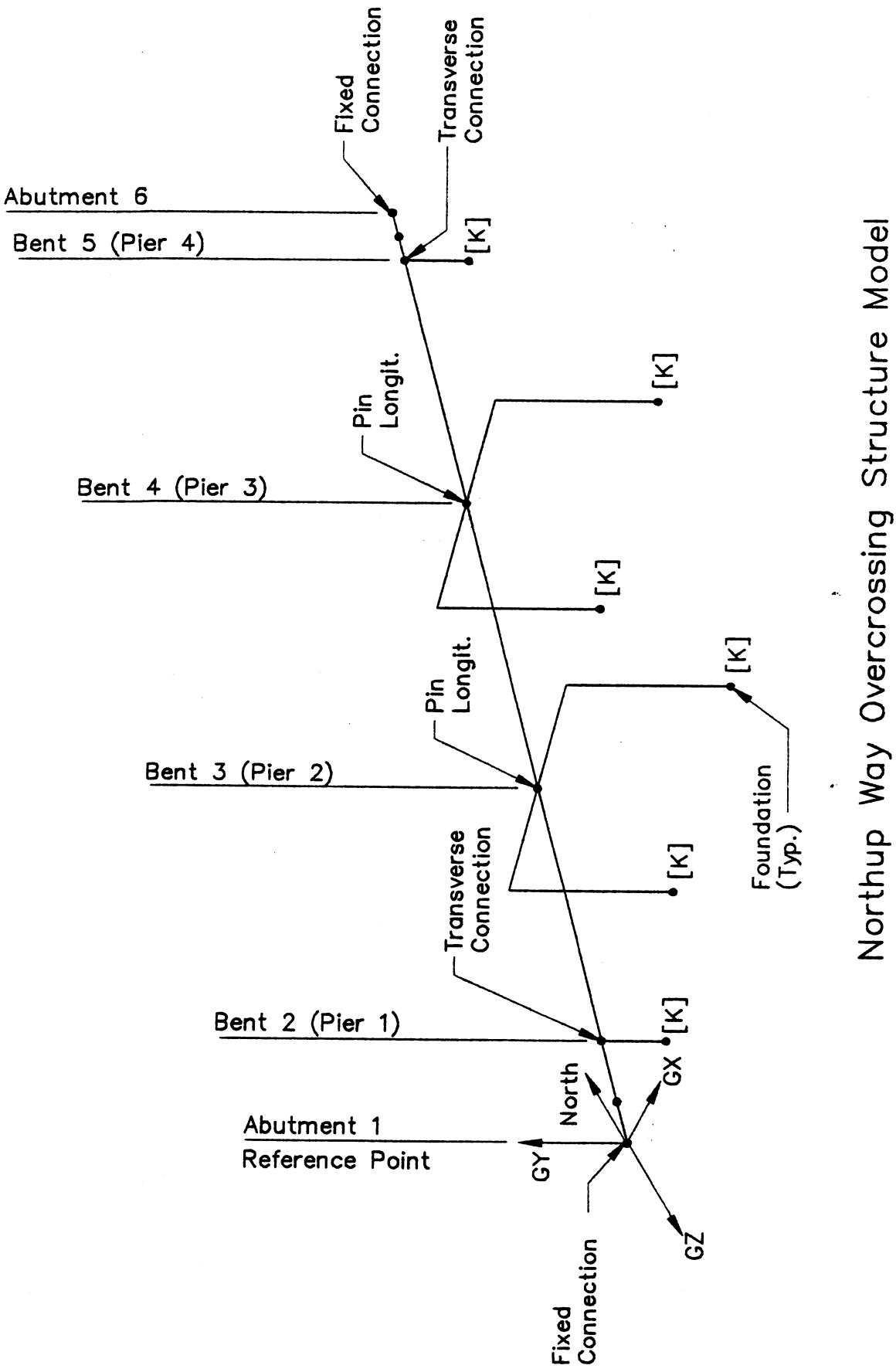
Northup Way Overcrossing Structure Model
Abutment 6
Bent 5 (Pier 4)
Bent 4 (Pier 3)
Bent 3 (Pier 2)
Bent 2 (Pier 1)
Abutment 1
Reference Point
Fixed Connection
Transverse Connection
Pin Longit.
Pin Longit.
Transverse Connection
Fixed Connection
[K]
[K]
[K]
[K]
[K]
[K]
Foundation (Typ.)
North
GX
GY
GZ

Figure 8.1

$$\text{Diag } [K_F] = \begin{bmatrix} 3.91E7 & 0 & 0 & 0 & 0 & 0 \\ 0 & 3.76E7 & 0 & 0 & 0 & 0 \\ 0 & 0 & 4.05E7 & 0 & 0 & 0 \\ 0 & 0 & 0 & 7.09E9 & 0 & 0 \\ 0 & 0 & 0 & 0 & 3.87E9 & 0 \\ 0 & 0 & 0 & 0 & 0 & 9.84E9 \end{bmatrix}$$

Transforming to SEISAB-I coordinate system according to Appendix C-2 and converting from lb to kip units we have:

$$\text{Diag } [K_{SEISAB}] = \begin{bmatrix} 3.91E4 & 0 & 0 & 0 & 0 & 0 \\ 0 & 4.05E4 & 0 & 0 & 0 & 0 \\ 0 & 0 & 3.76E4 & 0 & 0 & 0 \\ 0 & 0 & 0 & 7.09E6 & 0 & 0 \\ 0 & 0 & 0 & 0 & 9.84E6 & 0 \\ 0 & 0 & 0 & 0 & 0 & 3.87E6 \end{bmatrix}$$

8.2 BENT 3 AND BENT 4 MODELS

Bent 3 and Bent 4 have identical foundation matrices and calculated as for Bent 2. The resulting stiffness matrix in kip and ft units is:

$$\text{Diag } [K_{SEISAB}] = \begin{bmatrix} 3.70E4 & 0 & 0 & 0 & 0 & 0 \\ 0 & 3.64E4 & 0 & 0 & 0 & 0 \\ 0 & 0 & 3.54E4 & 0 & 0 & 0 \\ 0 & 0 & 0 & 5.48E6 & 0 & 0 \\ 0 & 0 & 0 & 0 & 7.98E6 & 0 \\ 0 & 0 & 0 & 0 & 0 & 2.69E6 \end{bmatrix}$$

8.3 BENT 5 MODEL

Bent 5 is an abutment with the same configuration as Bent 2. Following the methods used for Bent 2, we have for Bent 5:

$$\text{Diag } [K_{SEISAB}] = \begin{bmatrix} 4.35E3 & 0 & 0 & 0 & 0 & 0 \\ 0 & 4.49E3 & 0 & 0 & 0 & 0 \\ 0 & 0 & 4.08E3 & 0 & 0 & 0 \\ 0 & 0 & 0 & 8.43E5 & 0 & 0 \\ 0 & 0 & 0 & 0 & 1.06E6 & 0 \\ 0 & 0 & 0 & 0 & 0 & 2.96E5 \end{bmatrix}$$

8.4 LOAD MODEL

The RESPONSE SPECTRUM must be input using the SEISAB ARBITRARY CURVE option in order to adjust the damping ratio as recommended in Task 1, Report Section 6.2. In order to account for the 7 1/2 percent damping for those modes of vibration where soil-structure interaction is significant it is first necessary to identify those modes. This is done by running the model using the seismic response spectrum for 5 percent damping, recording R_a^t, R_d^t and R_d^v from the NORMALIZED SUPERSTRUCTURE MODE SHAPES output. The value theta is calculated and compared according to TASK 1 REPORT Section 5.2. Absolute displacement values are used for R_a^t, R_d^t and R_d^v. The response spectrum coefficient for each identified transverse mode is reduced by 15 percent to reflect the change to 7 1/2 percent damping for that mode. Run 4NORTFE2 is used to illustrate modification of the 5 percent damping ratio spectrum. Table 8.1 lists the spectrum modifications required.

TABLE 8.1
RUN 4NORTFE2 - RESPONSE SPECTRUM MODIFICATIONS FOR MODES WHERE SOIL-STRUCTURE INTERACTION IS SIGNIFICANT

MODE	R_a^t	R_d^t	R_d^v	θ	MODE PERIOD	MODIFIED SPECTRUM ORDINATE
2	0.506	0.998	0.001	0.507	0.423	.63→.536
4	0.715	1.000	0.009	0.709	0.189	.63→.536
5	0.828	1.000	0.003	0.826	0.183	.63→.536
6	0.461	1.000	0.035	0.445	0.142	.63→.536
8	0.865	0.997	0.012	0.857	0.127	.63→.536
10	0.924	0.993	0.021	0.911	0.095	.63→.536
11	0.992	0.992	0.007	0.993	0.092	.63→.536
15	0.614	0.985	0.822	0.340	0.048	.63→.536

1. Only transverse modes included.
2. $\theta = R_a^t/(R_d^t + R_d^v)$
3. For $\theta > 0.10$, Adjust Spectrum Ordinate
4. Modified Spectrum Ordinate is the spectrum ordinate for 5 percent damping reduced by 15 percent to convert from to 7-1/2 percent damping. Note that spectrum ordinate for each period of vibration is output by SEISAB-I as CS.

8.5 DISCUSSION OF THE INPUT FILE

The default units used in this example are kips, feet, seconds and radians.

The abutment-to-superstructure connections are specified as FIXED. To release the abutments and transfer all abutment forces to the dummy replacement bent, all abutment foundation spring values are set to zero in the FOUNDATION block.

The bent-to-superstructure connections are specified as FIXED by default.

Column tops at Piers 2 1nd 5 are specified as TRANSV in order to activate BEARING ELEMENTS at those locations while restricting tranv displacement within bearing elements.

COLUMN TOP JOINT SIZE is specified at Piers 3 and 4 to provide a rigid element from the top of each model column (superstructure centroid) to the top of each actual column so that true column stiffness is represented.

8.6 DISCUSSION OF THE OUTPUT FILE

Several iterative runs with varying BEARING KFIF1 stiffnesses were required to match the model displacement of bearing elements at Bent 2 and Bent 5 to the actual gap at the abutments. Results of each run were checked to:

1. Ascertain that the specified number of modes was found.
2. Confirm that output displacement for longitudinal load (LC 3) is equal to abutment gap of 0.125 ft.

EXAMPLE NO. 5

FHWA WORKSHOP BRIDGE

TABLE OF CONTENTS

Section		Page
1.0	**DESCRIPTION OF BRIDGE AND FOUNDATION SOILS**	1
2.0	**SEISMIC DESIGN PARAMETERS**	1
3.0	**SOIL PROPERTIES**	2
4.0	**PIER 1 STIFFNESS CALCULATION - FHWA METHOD**	2
4.1	PILE-STIFFNESS CALCULATION	3
4.1.1	Estimation of Pile Parameters	3
4.1.2	Computation of t-z Curves	3
4.1.2.1	General Procedure	3
4.1.2.2	Application to FHWA Workshop Bridge Abutment Piles.	3
4.1.3	Computation of p-y Curves	4
4.1.3.1	General Procedure.	4
4.1.3.2	Application to FHWA Workshop Bridge Abutment Piles.	4
4.1.4	Preparation of BMCOL-76 Input	4
4.1.5	BMCOL-76 Output	4
4.1.6	Calculation of Pile-Head Stiffnesses	5
4.1.7	Calculation of Pile-Group Stiffness Matrix	5
4.1.7.1	Assumptions.	5
4.1.7.2	Preparation of GPILE Input.	6
4.1.7.3	GPILE Output.	6
4.2	ABUTMENT FOOTING STIFFNESSES	6
4.2.1	Model and Assumptions	6
4.2.2	Calculation of Footing Stiffnesses	7
4.2.2.1	General Procedure.	7
4.2.2.2	Application to FHWA Workshop Abutment Footing.	7
4.3	ABUTMENT WALL STIFFNESS	8
4.3.1	Model and Assumptions	8
4.3.2	Calculation of Wall Stiffnesses	8
4.3.2.1	General Procedure.	8
4.3.2.2	Application to FHWA Workshop Abutment Wall.	8
4.4	TOTAL ABUTMENT STIFFNESS MATRIX	9
4.4.1	General Procedure.	9
4.4.2	Application to FHWA Workshop Abutment	9
5.0	**PIER 1 STIFFNESS CALCULATION - NOVAK METHOD**	11
5.1	PILE AND FOOTING SIDE STIFFNESS	11
5.1.1	Soil Model	12

TABLE OF CONTENTS (Continued)

Section	Page
5.1.2 Preparation of DYNA3 Input	12
5.1.3 DYNA3 Output	12
5.2 ABUTMENT WALL STIFFNESS	12
5.3 TOTAL PIER 1 STIFFNESS MATRIX	13
6.0 PIER 2 STIFFNESS RESULTS	14
6.1 FHWA METHOD	14
6.1.1 Pile Group Stiffness	14
6.1.2 Footing Stiffness	15
6.1.3 Total Stiffness	15
6.2 NOVAK METHOD	15
7.0 PIER 3 FOUNDATION STIFFNESSES	16
7.1 FHWA METHOD	16
7.2 NOVAK METHOD	17
8.0 PIER 4 STIFFNESS CALCULATION	17
8.1 FHWA METHOD	18
8.2 NOVAK METHOD	18

9.0 APPLICATION TO SEISAB-I BRIDGE ANALYSIS 20
9.1 ABUTMENT 1 AND 4 MODELS 20
9.1.1 FHWA Method 20
9.2 BENT 2 MODEL 21
9.2.1 FHWA Method 21
9.3 BENT 3 MODEL 21
9.3.1 FHWA Method 21
9.4 LOAD MODEL 22

1.0 DESCRIPTION OF BRIDGE AND FOUNDATION SOILS

The fifth example problem is excerpted from an FHWA workshop, "Seismic Design of Highway Bridges - Training Course." The bridge is a 3-span concrete box girder approximately 250 feet long (Figure 1.1). The monolithic abutments (Piers 1 and 4) at the ends of the bridge (Figure 1.2) are each supported by one row of seven vertical, 12" diameter x ¼" thick steel pipe piles backfilled with 4000 psi concrete. The piles penetrate through medium dense sand to a depth of approximately 70 ft (Figure 1.3). The piles are embedded in a concrete pile cap, 6' wide x 2' thick, which supports a small abutment approximately 15' high and 2' thick.

Each of the two intermediate bents (Piers 2 and 3) consists of a 4' diameter reinforced concrete column supporting the box girder. This column in turn is supported by a pile cap resting on nine vertical, 1' diameter steel pipe piles similar to those at Pier 1. At Pier 2, the piles and pile cap are fully embedded to the top of the pile cap. The piles at Pier 3, however, extend for a length of approximately 40' above the mudline. The pile cap is supported only by the piles and has no contact with the soil (see Figure 1.1). At both Piers 2 and 3 the piles extend to a depth of approximately 70 ft below the mudline.

2.0 SEISMIC DESIGN PARAMETERS

The ground acceleration coefficient for the seismic design of the FHWA Workshop Bridge was not specified. The appropriate soil category was Soil Type II, which is deep stiff soil over bedrock. The ATC-6, 5% damped response spectrum (Figure 2.1) for this soil type was normalized to 0.15 g and was used in the dynamic response analysis of the bridge presented herein. The spectrum will be modified where appropriate to account for the 7½% damping recommended for those modes of vibration where soil-structure interaction is significant.

FHWA Workshop Example

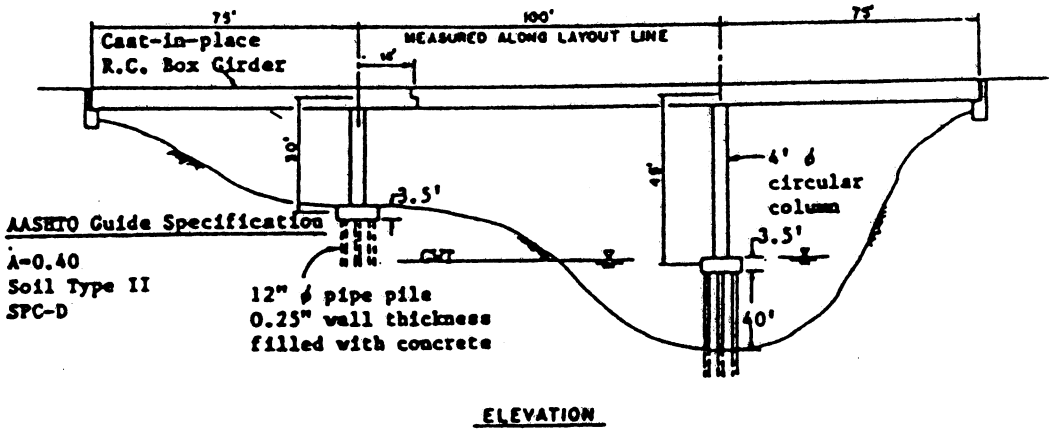

Bent 2 Bent 3

ELEVATION

SOURCE: FHWA Manual entitled: "Seismic Design of Highway Bridges - Training Course," page 5.1.2-31.

Figure 1.1

Normalized 5% Damped Response Spectrum

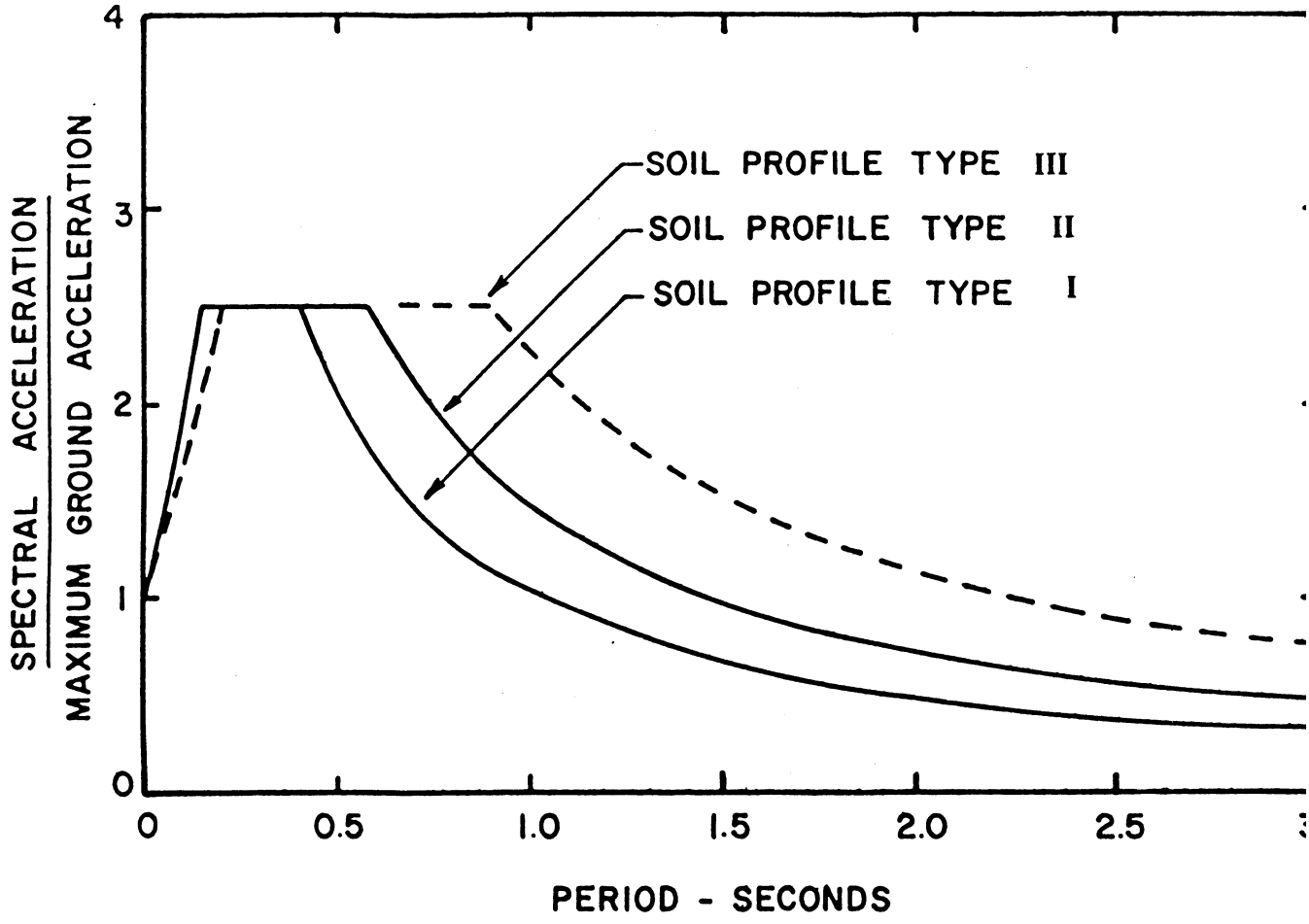

Reference: ATC-6 (1978)

Figure 2.1

3.0 SOIL PROPERTIES

The soil parameters provided by WSDOT for the soil layers are:

γ = total density in pcf
c = cohesion in psf
ϕ = friction angle in degrees
k = modulus of subgrade reaction in pci
G = low-strain shear modulus in psf or ksf
ν = Poisson's Ratio

Values of the modulus of subgrade reaction, k, were obtained from Figure 4.6 of the Coldwater Creek example problem.

Because the behavior of soil is nonlinear during strong shaking, simple procedures were implemented to approximately account for the effect of this nonlinearity on the computation of the abutment and pier foundation stiffnesses. These procedures are described in Section 3.0 of the Coldwater Creek example problem.

4.0 PIER 1 STIFFNESS CALCULATION - FHWA METHOD

In this section the calculation of foundation stiffnesses using the FHWA (1986) method is presented for Pier 1 of the FHWA Workshop Bridge. (The use of the Novak method is illustrated in Section 5.0).

A side-elevation view of the abutment and the soil-property profile at Pier 1 is shown in Figure 4.1. As with the Coldwater Creek example, the basic approach to compute the foundation stiffness matrix at this pier is to first compute the pile-group stiffness, pile-cap stiffness, and abutment-wall stiffness, and then combine these stiffnesses to obtain the

abutment stiffness matrix at a specified point on the abutment foundation. This point (Point O in Figure 4.1) is located on top of the 2-foot thick footing at its geometric center.

Note that no design value for peak ground acceleration has been specified. In order to demonstrate the computations which must be performed for low-strain conditions, a value of Z < 0.15g has been assumed. All calculations have therefore been carried out using low-strain soil properties, e.g. soil shear modulus, p-y curves, and t-z curves.

4.1 PILE-STIFFNESS CALCULATION

4.1.1 Estimation of Pile Parameters

The computation of the pile properties is similar to that performed for the Deadwater Slough Bridge in Section 4.1.1 of that example problem. The properties of the composite steel and concrete piles used in the FHWA Workshop bridge are

EA = 6.42E08 lb
EI = 5.35E07 lb-ft^2

The above information was used in the calculation of the t-z, Q-z, and p-y curves, and the load-deflection curves of the pile-head.

4.1.2 Computation of t-z Curves

4.1.2.1 General Procedure. The general procedure for computing the t-z curve is explained in Section 4.1.2.1 of the Coldwater Creek example.

4.1.2.2 Application to FHWA Workshop Bridge Abutment Piles. The calculation of Q-z curves is very similar to the calculations shown in Section 4.1.3.2 of the Deadwater Slough example. The results for Pier 1 of the FHWA Workshop bridge are shown in

Pier 1 Soil Profile

Soil Profile

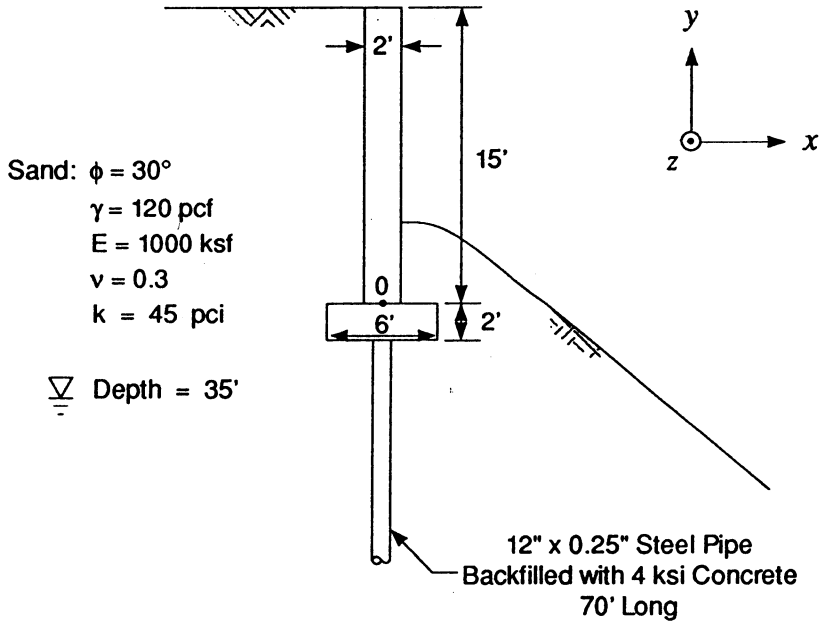

Plan

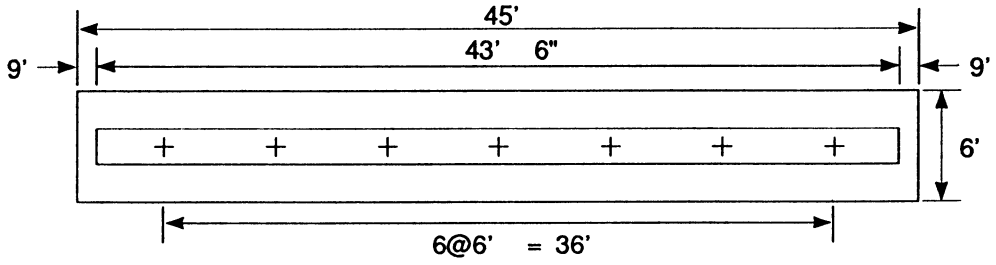

Figure

Table 4.1. Note that the calculations have been carried out using low-strain soil properties.

4.1.3 Computation of p-y Curves

4.1.3.1 General Procedure. The general procedure for computing the p-y curves is explained in Section 4.1.4.1 of the Coldwater Creek example.

4.1.3.2 Application to FHWA Workshop Bridge Abutment Piles. The calculation of p-y curves is very similar to the calculations shown in Section 4.1.4.2 of the Deadwater Slough example. The p-y curves for Pier 1 of the FHWA Workshop bridge are shown in Table 4.2. Note that the calculations have been carried out using low-strain soil properties.

4.1.4 Preparation of BMCOL-76 Input

The user guide titled, GUIDE FOR DATA INPUT FOR BMCOL-76, is provided in Appendix B. The text accompanying the guide is reproduced from the BMCOL-76 manual (Matlock et al, 1981), and is also provided in this Appendix. The preparation of the input was explained and illustrated for the Coldwater Creek example. The input file for the FHWA Workshop example will not be provided because it is similar to the Coldwater Creek input file.

4.1.5 BMCOL-76 Output

The output files for the axial load and lateral load cases were used to construct the load-deflection curves for the pile head. Refer to the Coldwater Creek example (Section 4.1.6) for explanation of the output file. Plots of the load-deflection curves for the pile head are presented in Figure 4.2 (axial direction) and Figure 4.3 (lateral direction). These curves were used to estimate the axial and lateral stiffnesses of the pile.

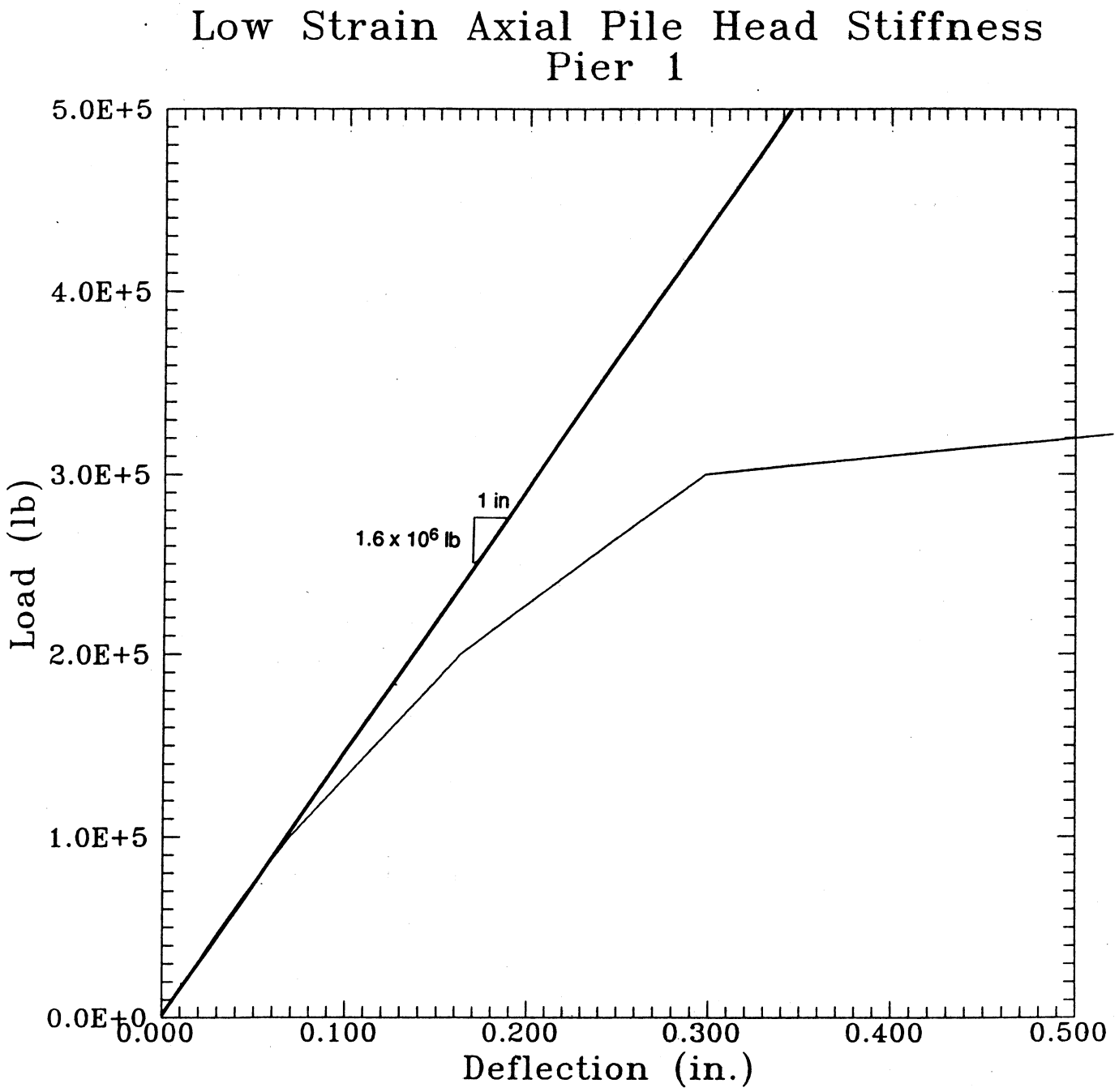
Low Strain Axial Pile Head Stiffness
Pier 1
5.0E+5
4.0E+5
3.0E+5
2.0E+5
1.0E+5
0.0E+0
Load (lb)
1 in
1.6 x 10^6 lb
0.000
0.100
0.200
0.300
0.400
0.500
Deflection (in.)

Figure 4.2

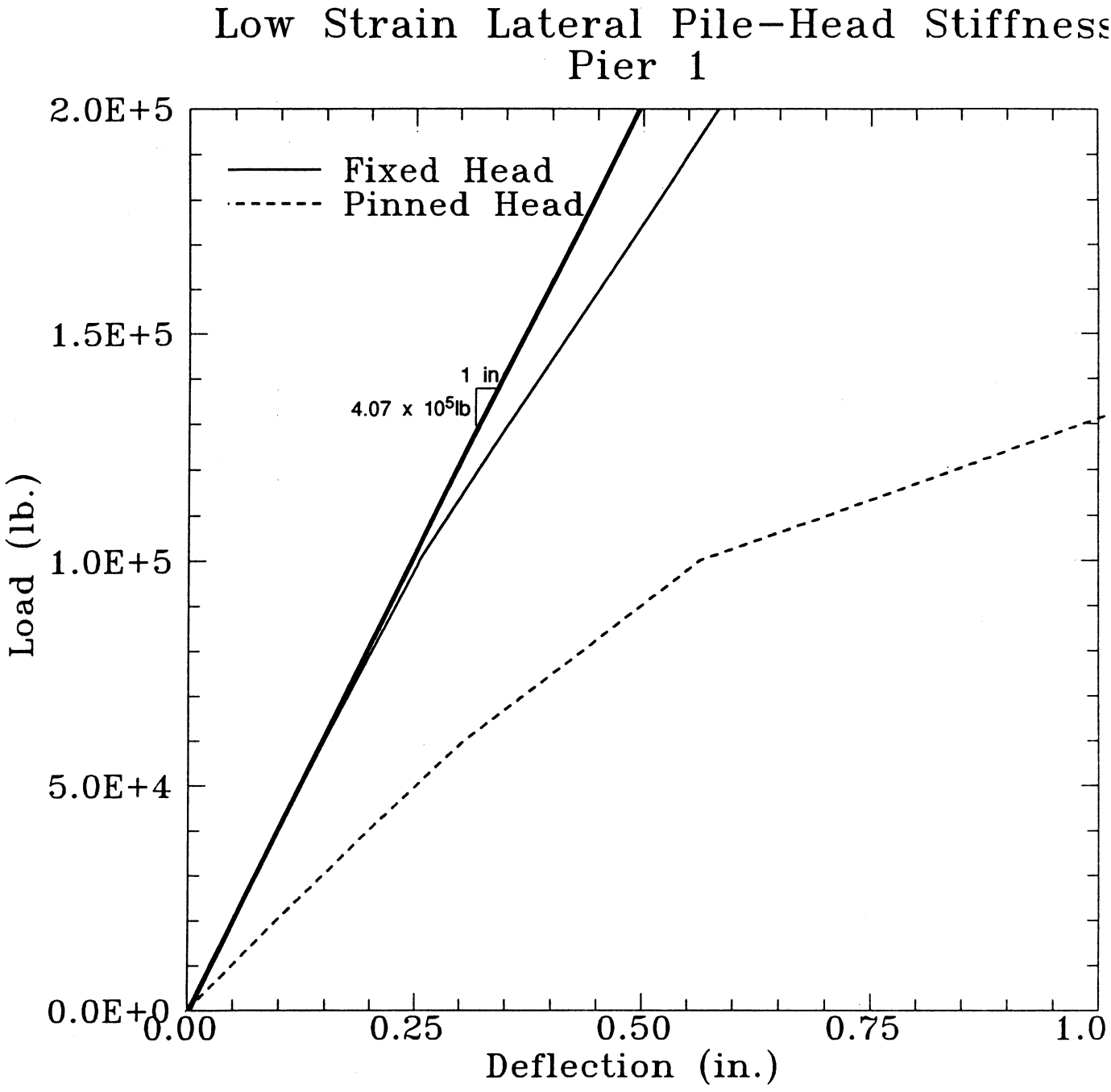
Low Strain Lateral Pile-Head Stiffness
Pier 1
2.0E+5
1.5E+5
1.0E+5
5.0E+4
0.0E+0
Load (lb.)
Fixed Head
Pinned Head
1 in
4.07 x 10^5 lb
0.00
0.25
0.50
0.75
1.0
Deflection (in.)

Figure 4.3

T-Z & Q-Z CURVES

Bridge: FHWA Example Piers 1 & 4 : low strain

Ground Surface Elevation:	0	ft		
Depth to water table:	35	ft	Elev: -35	ft
Average Pile Perimeter:	37.7	in		
Pile Tip Area:	113.1	in²		
Pile Type:	S	T=Timber,C=Concrete,S=Steel		
	D	O= Open Ended, D=Displacement		

SOIL	DEPTH	ELEV.	GAMMA	PHI	c	G	k	Po	Delta	f	f	Ks	Tmax	Zref
	ft	ft	γ	ϕ	ksf	psf	API RP2A	ksf	δ	ksf	psi	pci	lb/in	in
SAND	0	0	120	30	-	3.85E+05	1.0	0.00	20	0.00	0.00	111	0	0.000
SAND	17	-17	120	30	-	3.85E+05	1.0	2.04	20	0.74	5.16	111	194	0.046
SAND	35	-35	120	30	-	3.85E+05	1.0	4.20	20	1.53	10.62	111	400	0.095
SAND	35	-35	120	30	-	3.85E+05	1.0	4.20	20	1.53	10.62	111	400	0.095
SAND	87	-87	120	30	-	3.85E+05	1.0	7.20	20	2.62	18.19	111	686	0.163

SOIL	DEPTH	ELEV.	PHI	c	G	Po	Nq	q	q	Kp	Qmax	Zref
	ft	ft	ϕ	ksf	psf	ksf		ksf	psi	pci	k	in
SAND	87	-87	30	-	3.85E+05	7.20	21	151	1049	56	119	18.86

Table 4.1

FHWA Example Piers 1 & 4 : low strain T-Z & Q-Z CURVES

	DEPTH ft	ELEV. ft	Tmax lb/in	Zref in											
SAND	0	0	0	0.000	T (lb/in)	0	0	0	0	0	0	0	0	0	0
					Z (in.)	0.000	0.000	0.000	0.000	0.000	0.000	0.000	0.000	0.000	2.000
SAND	17	-17	194	0.046	T (lb/in)	0	48	90	123	148	165	176	183	192	194
					Z (in.)	0.000	0.012	0.023	0.035	0.046	0.058	0.069	0.081	0.116	2.000
SAND	35	-35	400	0.095	T (lb/in)	0	98	185	254	305	339	362	377	395	400
					Z (in.)	0.000	0.024	0.048	0.072	0.095	0.119	0.143	0.167	0.238	2.000
SAND	35	-35	400	0.095	T (lb/in)	0	98	185	254	305	339	362	377	395	400
					Z (in.)	0.000	0.024	0.048	0.072	0.095	0.119	0.143	0.167	0.238	2.000
SAND	87	-87	686	0.163	T (lb/in)	0	168	317	435	522	582	621	645	676	686
					Z (in.)	0.000	0.041	0.082	0.123	0.163	0.204	0.245	0.286	0.409	2.000
					T (lb/in)										
					Z (in.)										
					T (lb/in)										
					Z (in.)										
					T (lb/in)										
					Z (in.)										
					T (lb/in)										
					Z (in.)										
					T (lb/in)										
					Z (in.)										
					T (lb/in)										
					Z (in.)										

	DEPTH ft	ELEV. ft	Qmax k	Zref in

Table 4.1 (cont.)

P-Y CURVES

Worksheet to link with: d:\wash_dot\examples\fhwa\axial\tz_1.xls
(including path and extension)

Bridge: FHWA Example Piers 1 & 4 : low strain
Ground Surface Elevation: 0
Depth to water table: 35 ft Elev: -35 ft
Average Pile Diameter: 12 in
Pile Type: S T=Timber,C=Concrete,S=Steel
D O= Open Ended, D=Displacement

SOIL	DEPTH ft	ELEV. ft	GAMMA γ	PHI (deg) ϕ	c ksf	PHI (rad) ϕ	Po ksf	C1	C2	C3	k lb / in^3	J	ε c	Pu lb/in	Yc in
SAND	0	0	120	30	-	0.52	0.00	2.04	2.67	29	45	-	-	0	0.00
SAND	17	-17	120	30	-	0.52	2.04	2.04	2.67	29	45	-	-	4887	0.48
SAND	35	-35	120	30	-	0.52	4.20	2.04	2.67	29	45	-	-	10061	0.48
SAND	35	-35	120	30	-	0.52	4.20	2.04	2.67	29	30	-	-	10061	0.72
SAND	87	-87	120	30	-	0.52	7.20	2.04	2.67	29	30	-	-	17236	0.50
0		0	0	0	0.00	0.00									
0		0	0	0	0.00	0.00									
0		0	0	0	0.00	0.00									
0		0	0	0	0.00	0.00									
0		0	0	0	0.00	0.00									
0		0	0	0	0.00	0.00									

SOIL	DEPTH ft	ELEV. ft	Pu lb/in	Yc in											
SAND	0	0	0	0.000	P (lb/in)	0	0	0	0	0	0	0	0	0	0
					Y (in.)	0.000	0.000	0.000	0.000	0.000	0.000	0.000	0.000	0.000	0.000
SAND	17	-17	4887	0.479	P (lb/in)	0	1077	2032	2793	3349	3731	3981	4240	4339	4398
					Y (in.)	0.000	0.120	0.240	0.359	0.479	0.599	0.719	0.958	1.198	2.395
SAND	35	-35	10061	0.479	P (lb/in)	0	2218	4184	5751	6896	7681	8196	8729	8934	9054
					Y (in.)	0.000	0.120	0.240	0.359	0.479	0.599	0.719	0.958	1.198	2.395
SAND	35	-35	10061	0.719	P (lb/in)	0	2218	4184	5751	6896	7681	8196	8729	8934	9054
					Y (in.)	0.000	0.180	0.359	0.539	0.719	0.898	1.078	1.437	1.797	3.593
SAND	87	-87	17236	0.495	P (lb/in)	0	3799	7168	9852	11814	13159	14041	14954	15304	15511
					Y (in.)	0.000	0.124	0.248	0.371	0.495	0.619	0.743	0.991	1.238	2.476
					P (lb/in)										
					Y (in.)										
					P (lb/in)										
					Y (in.)										
					P (lb/in)										
					Y (in.)										
					P (lb/in)										
					Y (in.)										
					P (lb/in)										
					Y (in.)										
					P (lb/in)										
					Y (in.)										

Table 4.2

4.1.6 Calculation of Pile-Head Stiffnesses

The pile-head stiffnesses are computed from the load-deflection curves in Figures 4.2 and 4.3 as follows. For the axial load case, the axial pile-head stiffness is the slope of the load-deflection curve (Figure 4.2) at the origin (i.e. the initial tangent slope). For the lateral load case, the lateral pile-head stiffness is also the initial tangent slope. The rule for estimating axial pile-head stiffness was presented in Section 4.1.7 of the Coldwater Creek example, while the rule previously applied to lateral stiffness values has been modified to account for low-strain conditions.

According to WSDOT, the piles at Pier 1 are fixed to the abutment footing. Under this assumption, the pile-head stiffnesses resulting from the implementation of the above procedure (see Figures 4.2 and 4.3) are as follows:

$$K_z = 1.6 \times 10^6 \ lb/in = 1.92 \times 10^7 \ lb/ft \ (Axial)$$
$$K_x = K_y = 4.1 \times 10^5 \ lb/in = 4.92 \times 10^6 \ lb/ft \ (Lateral)$$

These stiffness values apply to each pile at the base of the pile cap shown in Figure 4.1.

4.1.7 Calculation of Pile-Group Stiffness Matrix

4.1.7.1 Assumptions. Two key assumptions are made in order to compute the 6 x 6 pile-group stiffness matrix: (1) pile-group effects (i.e. pile-soil-pile interaction) are neglected, and (2) because the piles are vertical and cylindrical, the individual pile-head stiffnesses computed in Section 4.1.7 apply to a local coordinate system that was established to be coincidental with the principal axes of the abutment, i.e. axial stiffness, K_z , is associated with the local z axis, which is parallel to the direction along the length of the pile; the transverse stiffness, K_y , is associated with the local y axis, which is coincident with the

transverse direction of the abutment (i.e., parallel to the global z axis in Figure 4.1) and, the longitudinal stiffness, K_x , is associated with the local x axis, which is parallel to the global x axis in Figure 4.1 of the pile section.

4.1.7.2 Preparation of GPILE Input. The preparation of the input to the GPILE program, which computes the pile-group stiffness matrix, was discussed in Section 4.1.8.2 of the Coldwater Creek example. Refer to that section for details.

4.1.7.3 GPILE Output. The GPILE output file for Pier 1 is shown in Table 4.4. The global group stiffness matrix, [K], and the local group stiffness matrix are listed. The global group stiffness matrix is used in the abutment stiffness calculation in Section 4.4. The local group stiffness matrix is not used because this matrix is for a different orientation of the global coordinate system. The global group stiffness matrix was computed at Point O in Figure 4.1 for the coordinate system shown in that figure. The origin of the coordinate system for the stiffness calculation is Point O.

4.2 ABUTMENT FOOTING STIFFNESSES

As recommended in the Task 1 report, the foundation stiffnesses of the pile caps are computed assuming the caps are footings fully embedded in the surrounding soil. These footing stiffnesses (along with the stiffness contributions from the abutment wall) are added to the pile-group stiffnesses to obtain the total abutment stiffness matrix.

4.2.1 Model and Assumptions

The theoretical model for estimating the stiffnesses of an embedded footing is presented in Section 4.2.1 of the Coldwater Creek example.

WASHINGTON STATE DEPARTMENT OF TRANSPORTATION 10/27/92 TIME 15:56:26 PAGE
*** GROUP PILE ANALYSIS *** REV 4/12/88

FHWA EXAMPLE PILE STIFFNESS - PIERS 1 AND 4

GLOBAL GROUP STIFFNESS MATRIX:

	FX	FY	FZ	MX	MY	M
δX	0.294E+08	0.000E+00	0.000E+00	0.000E+00	0.000E+00	0.588
δY	0.000E+00	0.134E+09	0.000E+00	0.000E+00	0.000E+00	0.000
δZ	0.000E+00	0.000E+00	0.294E+08	-0.588E+08	0.000E+00	0.000
θX	0.000E+00	0.000E+00	-0.588E+08	0.195E+11	0.000E+00	0.000
θY	0.000E+00	0.000E+00	0.000E+00	0.000E+00	0.423E+10	0.000
θZ	0.588E+08	0.000E+00	0.000E+00	0.000E+00	0.000E+00	0.118

LOCAL GROUP STIFFNESS MATRIX:

	FX	FY	FZ	MX	MY	M
δX	0.134E+09	0.000E+00	0.000E+00	0.000E+00	0.000E+00	0.000
δY	0.000E+00	0.294E+08	0.000E+00	0.000E+00	0.000E+00	-0.588
δZ	0.000E+00	0.000E+00	0.294E+08	0.000E+00	0.588E+08	0.000
θX	0.000E+00	0.000E+00	0.000E+00	0.423E+10	0.000E+00	0.000
θY	0.000E+00	0.000E+00	0.588E+08	0.000E+00	0.195E+11	0.000
θZ	0.000E+00	-0.588E+08	0.000E+00	0.000E+00	0.000E+00	0.118

Table 4.4

4.2.2 Calculation of Footing Stiffnesses

4.2.2.1 General Procedure. The general procedure to compute the foundation stiffnesses of an embedded footing (pile cap) is presented in Section 4.2.2.1 of the Coldwater Creek example.

4.2.2.2 Application to FHWA Workshop Abutment Footing. The footing (pile cap) stiffness matrix for the Pier 1 abutment is presented below. In Figure 4.1, the footing is defined as the portion of the abutment below Point O.

The footing dimensions from Figure 4.1:

Length:	2L = 45 ft
Width:	2B = 6 ft
Thickness:	D = 2 ft

The soil properties are:

Figure 4.1: E = 1000 ksf, ν = 0.30 $\therefore$ G = 385 ksf

The resulting diagonal stiffness matrix for the footing is

$$[K_f] = \begin{bmatrix} 3.08E07 & & & & & \\ & 2.94E07 & & & & \\ & & 3.08E07 & & & \\ & & & 8.79E09 & & \\ & & & & 8.59E09 & \\ & & & & & 5.32E08 \end{bmatrix}$$

The units are lb and ft.

4.3 ABUTMENT WALL STIFFNESS

The stiffness due to the passive resistance of abutment backfill soil is also computed and added to the pile-group and footing stiffnesses.

4.3.1 Model and Assumptions

The model and assumptions for estimating the translational and rotational stiffnesses of the abutment wall-backfill system is provided in Section 4.3.1 of the Coldwater Creek example.

4.3.2 Calculation of Wall Stiffnesses

4.3.2.1 General Procedure. The formulas for the translational stiffness, K_x , and the rotational stiffness, $K_{\theta z}$, were provided in Section 4.3.2.1 of the Coldwater Creek example.

4.3.2.2 Application to FHWA Workshop Abutment Wall. The abutment-wall stiffness computation is illustrated for the Pier 1 abutment. The abutment wall height is assumed to be the distance from the top of the pile cap (i.e. Point O in Figure 4.1) to the top of the abutment. The stiffnesses are computed at Point O.

Obtain the appropriate length dimensions from Figures 1.2 and 4.1:

B_w = 43 ft - 6 in = 43.5 ft
H_w = 15 ft

Compute wall stiffness values using the specified value of E_s = 1000 ksf. The resulting wall stiffness matrix is

$$[K_w] = \begin{bmatrix} 1.85E07 & 0 & 0 & 0 & 0 & -1.04E08 \\ 0 & 0 & 0 & 0 & 0 & 0 \\ 0 & 0 & 0 & 0 & 0 & 0 \\ 0 & 0 & 0 & 0 & 0 & 0 \\ 0 & 0 & 0 & 0 & 0 & 0 \\ -1.04E08 & 0 & 0 & 0 & 0 & 1.28E09 \end{bmatrix}$$

The units are lb and ft.

4.4 TOTAL ABUTMENT STIFFNESS MATRIX

4.4.1 General Procedure.

The total abutment stiffness matrix, $[K_t]$, at a given point is approximated as the sum of the stiffness matrices for the piles, $[K_p]$, footing or pile cap, $[K_f]$, and abutment wall, $[K_w]$, i.e.

$$[K_t] = [K_p] + [K_f] + [K_w]$$

Although this formula is simple, it is important to note that $[K_p]$, $[K_f]$, and $[K_w]$ must be computed at the same point in the same coordinate system used for the piles, footings, and wall.

4.4.2 Application to FHWA Workshop Abutment

The stiffness matrices $[K_p]$, $[K_f]$, and $[K_w]$ for the abutment system at Pier 1 were constructed from the stiffness calculations presented in Sections 4.1, 4.2, and 4.3, respectively. The xyz coordinate system is oriented as shown in Figure 4.1 with the origin at Point O.

The 6 x 6 stiffness matrices are:

From Table 4.4,

$$[K_p] = \begin{bmatrix} 3.42E7 & 0 & 0 & 0 & 0 & 6.83E7 \\ 0 & 1.34E8 & 0 & 0 & 0 & 0 \\ 0 & 0 & 3.42E7 & -6.83E7 & 0 & 0 \\ 0 & 0 & -6.83E7 & 1.95E10 & 0 & 0 \\ 0 & 0 & 0 & 0 & 4.92E9 & 0 \\ 6.83E7 & 0 & 0 & 0 & 0 & 1.37E8 \end{bmatrix}$$

From Section 4.2.2.2,

$$\text{diag } [K_f] = \begin{bmatrix} 3.08E7 & & & & & \\ & 2.94E7 & & & & \\ & & 3.08E7 & & & \\ & & & 8.79E9 & & \\ & & & & 8.59E9 & \\ & & & & & 5.32E8 \end{bmatrix}$$

From Section 4.3.2.2,

$$[K_w] = \begin{bmatrix} 1.85E7 & 0 & 0 & 0 & 0 & -1.04E8 \\ 0 & 0 & 0 & 0 & 0 & 0 \\ 0 & 0 & 0 & 0 & 0 & 0 \\ 0 & 0 & 0 & 0 & 0 & 0 \\ 0 & 0 & 0 & 0 & 0 & 0 \\ -1.04E8 & 0 & 0 & 0 & 0 & 1.28E9 \end{bmatrix}$$

Therefore,

$$[K_t] = \begin{bmatrix} 8.35E7 & 0 & 0 & 0 & 0 & -3.57E7 \\ 0 & 1.63E8 & 0 & 0 & 0 & 0 \\ 0 & 0 & 6.50E7 & -6.83E7 & 0 & 0 \\ 0 & 0 & -6.83E7 & 2.83E10 & 0 & 0 \\ 0 & 0 & 0 & 0 & 1.35E10 & 0 \\ -3.57E7 & 0 & 0 & 0 & 0 & 1.95E9 \end{bmatrix}$$

The units are lb and ft.

5.0 PIER 1 STIFFNESS CALCULATION - NOVAK METHOD

The calculation of foundation stiffnesses using the Novak method is much simpler than the FHWA method primarily because a single computer program (DYNA3) is available to do all the required calculations. Furthermore, the theory upon which the program is based assumes linear elastic response of the soil-foundation system; consequently, fewer soil properties are required to characterize the soil medium, and nonlinear load-deflection relationships between the pile and soil (t-z, Q-z, p-y curves) are not required.

5.1 PILE AND FOOTING SIDE STIFFNESS

The Task 1 report recommended the use of the Pile & Footing Side option within the Novak computer program. With this option, the total pile-cap stiffness is the sum of the stiffnesses from the pile group and the passive resistance of the soil against the sides of the pile cap.

5.1.1 Soil Model

The soil model is shown in Figure 5.1, which was adapted from information in Figure 4.1. Note that shear-wave velocity, V_s, is given as an elastic property, rather than the shear modulus, G. In computing $V_s = \sqrt{G/\gamma_m}$ (where γ_m = mass density), the low-strain shear modulus values in Figure 4.1 were used.

Besides V_s, the other new soil parameter not shown in Figure 4.1 is the soil damping ratio for shear deformation, ζ. Values of $\zeta \leq 0.05$ are typically assumed and within this range, the effect of this parameter on the stiffness calculation is negligible. For this and all other example problems, $\zeta = 0.03$ was arbitrarily assumed.

5.1.2 Preparation of DYNA3 Input

The input file for Novak's DYNA3 computer program for Pier 1 is shown in Table 5.1. The preparation of this input file is very similar to the preparation of the input file for Pier 1 of the Deadwater example and therefore will not be discussed here. The input file for Pier 1 is shown in Table 5.1.

5.1.3 DYNA3 Output

The output file from the DYNA3 program is listed in Table 5.2. The stiffnesses are in units of kips and ft. The values of CROSS-STIFFNESS (YZ PLANE) and CROSS-STIFFNESS (XZ PLANE) refer to $K_{y\theta x}$ and $K_{x\theta y}$, respectively.

5.2 ABUTMENT WALL STIFFNESS

The Task 1 report noted that the abutment-wall stiffness could be computed using Novak's method for a footing on an elastic half space whose properties are those of the

Pier 1 Novak Soil Model

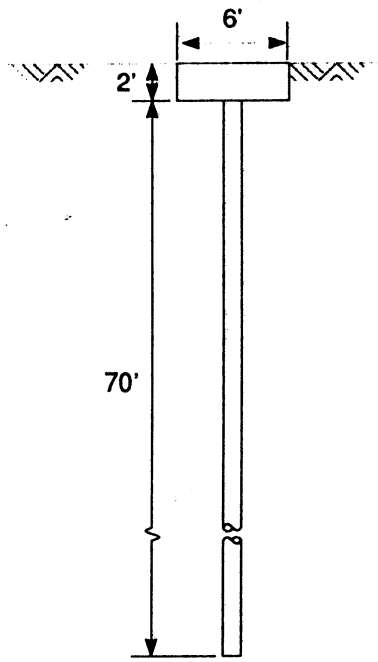

Sand: V_s = 321 fps
γ = 120 pcf
ν = 0.3
ξ = 0.03

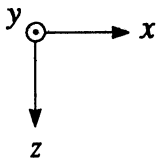

Figure 5.1

```
TITLE=FHWA Example PIERS 1 & 4 [ PILES + EMBEDMENT ] [k ft s]
MATRIX
GRAVITY=32.2
FOUNDATION=PILE
RECTANGULAR=6.0, 45.0
MASS=0.,0.,0.,0.,0.,0.,0.
LAYERS=1
FIXED=7
  1    0.0    18.0
  2    0.0    12.0
  3    0.0     6.0
  4    0.0     0.0
  5    0.0    -6.0
  6    0.0   -12.0
  7    0.0   -18.0
CONSTANTS=0.,0.,2.,70.,.145,0.,0.17,0.05,1.11,5.18E05
ELEMENT
1  70.0  0.5  0.5  1.24  0.103 0.103 0.206
FLOATING
NO-INTERACTION
SOIL
CONSTANTS
1   321.  .120  0.30 0.03
BELOW
321.  .120  .30  0.03
EMBEDDED=1
1  2.  321.  .120  0.30 0.03
LOAD=HARMONIC
CONSTANTS
NONQUADRATIC
0.001  0.001  0.001  0.0  10.  0.0  0.  0.  0.
RUN
```

Table 5.1

```
*************************************************
*                                               *
*        D Y N A 3   S I M U L A T I O N        *
*                                               *
*              RUN DATE -  1993/ 1/ 8           *
*              TIME     -  10:30:19             *
*              REVISION -  1991/07/30           *
*                                               *
*************************************************

FHWA Example PIERS 1 & 4 [ PILES + EMBEDMENT ] [k ft s

                                   RESULTS
                                   *******


FREQUENCY  -     .0010
*********


STIFFNESS CONSTANTS (K)
***********************

HORIZONTAL TRANSLATION  (X) ...  3.50694E+04
HORIZONTAL TRANSLATION  (Y) ...  3.50694E+04
VERTICAL TRANSLATION  (Z) .....  1.37113E+05
ROTATION ABOUT  (X) ...........  2.07150E+07
ROTATION ABOUT  (Y) ...........  6.44168E+05
TORSION ABOUT  (Z) ............  6.37973E+06
CROSS-STIFFNESS (YZ PLANE) ....  1.24304E+05
CROSS-STIFFNESS (XZ PLANE) .... -1.24304E+05

DAMPING CONSTANTS (C)
*********************
HORIZONTAL TRANSLATION  (X) ...  1.17944E+06
HORIZONTAL TRANSLATION  (Y) ...  1.17944E+06
VERTICAL TRANSLATION  (Z) .....  5.33050E+06
ROTATION ABOUT  (X) ...........  8.02027E+08
ROTATION ABOUT  (Y) ...........  2.46766E+07
TORSION ABOUT  (Z) ............  2.10214E+08
CROSS-DAMPING  (YZ PLANE) .....  4.47591E+06
CROSS-DAMPING  (XZ PLANE) ..... -4.47591E+06
```

Table 5.2

backfill soil. However, the FHWA approach for retaining walls (Section 4.3) is slightly preferred over the Novak method. The stiffness matrix obtained using the FHWA method was presented in Section 4.3.

5.3 TOTAL PIER 1 STIFFNESS MATRIX

The total abutment stiffness matrix is $[K_t] = [K_{pfs}] + [K_w]$, where $[K_{pfs}]$ is the "pile + footing side" stiffness matrix, and K_w is the abutment wall stiffness matrix. From Table 5.2 of Section 5.1.3,

$$[K_{pfs}] = \begin{bmatrix} 3.51E7 & 0 & 0 & 0 & -1.24E8 & 0 \\ 0 & 3.51E7 & 0 & 1.24E8 & 0 & 0 \\ 0 & 0 & 1.37E8 & 0 & 0 & 0 \\ 0 & 1.24E8 & 0 & 2.07E10 & 0 & 0 \\ -1.24E8 & 0 & 0 & 0 & 6.44E8 & 0 \\ 0 & 0 & 0 & 0 & 0 & 6.38E9 \end{bmatrix}$$

The units are lb and ft.

Because the coordinate system in Figure 4.1 is different from the Novak coordinate system (Figure 5.1), elements of $[K_w]$ from Section 4.3 were rearranged to be consistent with the coordinate system in Figure 5.1. Thus,

$$[K_w] = \begin{bmatrix} 1.85E7 & 0 & 0 & 0 & -1.04E8 & 0 \\ 0 & 0 & 0 & 0 & 0 & 0 \\ 0 & 0 & 0 & 0 & 0 & 0 \\ 0 & 0 & 0 & 0 & 0 & 0 \\ -1.04E8 & 0 & 0 & 0 & 1.28E9 & 0 \\ 0 & 0 & 0 & 0 & 0 & 0 \end{bmatrix}$$

Therefore,

$$[K_t] = \begin{bmatrix} 5.36E7 & 0 & 0 & 0 & -2.28E8 & 0 \\ 0 & 3.51E7 & 0 & 1.24E8 & 0 & 0 \\ 0 & 0 & 1.37E8 & 0 & 0 & 0 \\ 0 & 1.24E8 & 0 & 2.07E10 & 0 & 0 \\ -2.28E8 & 0 & 0 & 0 & 1.92E9 & 0 \\ 0 & 0 & 0 & 0 & 0 & 6.38E9 \end{bmatrix}$$

The units are lb and ft. Note that $[K_t]$ is the stiffness matrix at Point O for the global coordinate system defined in Figure 5.1.

6.0 PIER 2 STIFFNESS RESULTS

Pier 2 of the FHWA Workshop bridge consists of a reinforced concrete column supported by an embedded pile cap in turn supported by nine vertical, 1' diameter, steel pipe piles (Figure 6.1). The pipe piles have been backfilled with concrete of compressive strength f_c' = 4000 psi. The piles extend to a depth of approximately 70' below the mudline.

6.1 FHWA METHOD

6.1.1 Pile Group Stiffness

The pile stiffness calculations, p-y, t-z, and Q-z curve development and BMCOL76 operations, are similar to those performed for Pier 1. These operations will not be repeated here. The resulting pile group stiffness matrix is

Pier 2 Soil Profile

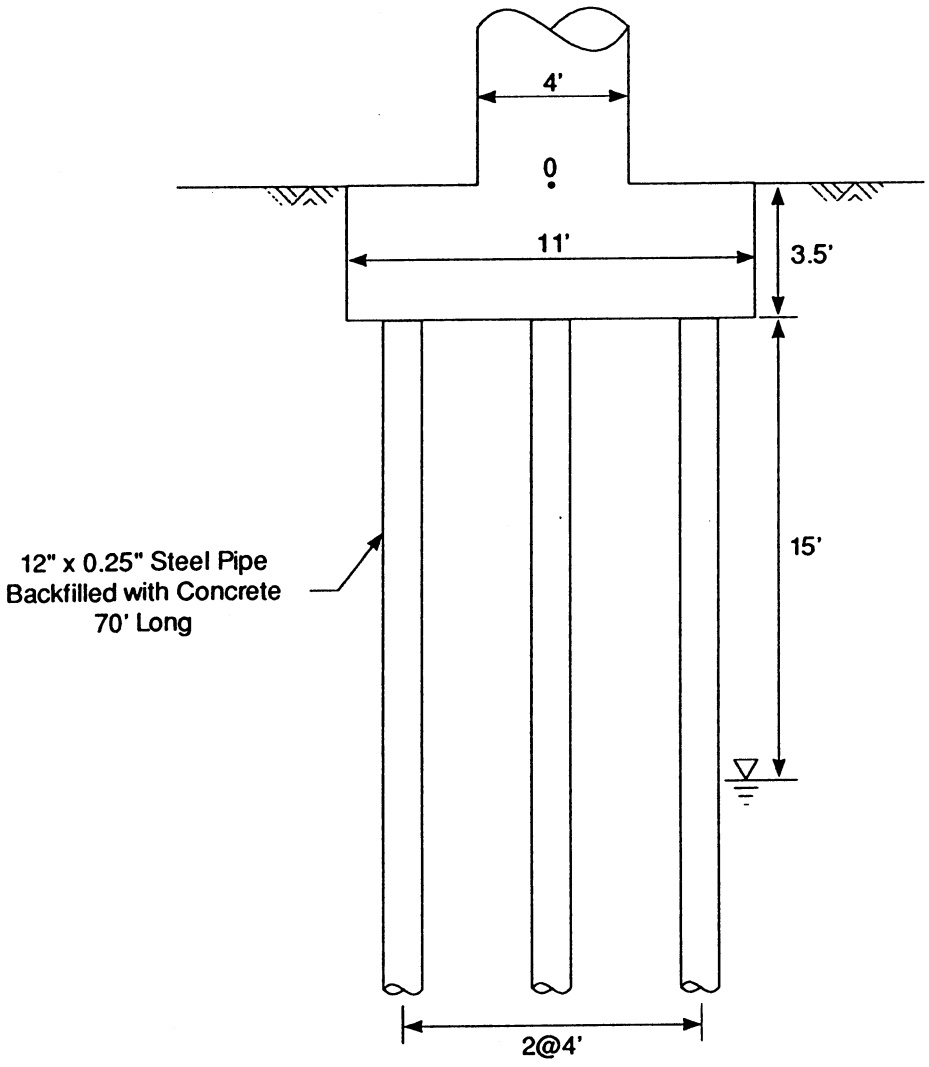

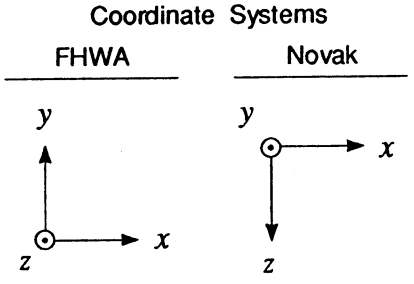

Soils as for Pier 1. See Figure 4.1.

Figure 6.1

$$[K_p] = \begin{bmatrix} 1.82E7 & 0 & 0 & 0 & 0 & 6.36E7 \\ 0 & 1.73E8 & 0 & 0 & 0 & 0 \\ 0 & 0 & 1.82E7 & -6.36E7 & 0 & 0 \\ 0 & 0 & -6.36E7 & 2.07E9 & 0 & 0 \\ 0 & 0 & 0 & 0 & 3.88E8 & 0 \\ 6.36E7 & 0 & 0 & 0 & 0 & 2.07E9 \end{bmatrix}$$

6.1.2 Footing Stiffness

$$\text{diag. } [K_f] = \begin{bmatrix} 1.96E7 & & & & & \\ & 1.77E7 & & & & \\ & & 1.96E7 & & & \\ & & & 7.32E8 & & \\ & & & & 1.34E9 & \\ & & & & & 7.32E8 \end{bmatrix}$$

6.1.3 Total Stiffness

$$[K_t] = \begin{bmatrix} 3.78E7 & 0 & 0 & 0 & 0 & 6.36E7 \\ 0 & 1.91E8 & 0 & 0 & 0 & 0 \\ 0 & 0 & 3.78E7 & -6.36E7 & 0 & 0 \\ 0 & 0 & -6.36E7 & 2.80E9 & 0 & 0 \\ 0 & 0 & 0 & 0 & 1.73E9 & 0 \\ 6.36E7 & 0 & 0 & 0 & 0 & 2.80E9 \end{bmatrix}$$

6.2 NOVAK METHOD

The input file used in the DYNA3 program is shown in Table 6.1. The resulting stiffness values, shown in Table 6.2, are

$$[K_{pfs}] = \begin{bmatrix} 4.63E7 & 0 & 0 & 0 & 2.27E8 & 0 \\ 0 & 4.63E7 & 0 & -2.27E8 & 0 & 0 \\ 0 & 0 & 1.77E8 & 0 & 0 & 0 \\ 0 & -2.27E8 & 0 & 3.34E9 & 0 & 0 \\ 2.27E8 & 0 & 0 & 0 & 3.34E9 & 0 \\ 0 & 0 & 0 & 0 & 0 & 1.62E9 \end{bmatrix}$$

The units are lb and ft. Note that this is the total Pier 2 stiffness matrix.

7.0 PIER 3 FOUNDATION STIFFNESSES

The FHWA and Novak methods were applied to Pier 3. This pier is very similar to Pier 2, differing in that the Pier 3 pile cap is not in contact with the supporting soil mass and the Pier 3 piles are unrestrained for the upper 40 ft of their length. This lack of restraint is easily modelled in both the FHWA and Novak methods by neglecting the shear resistance of the water column overlying the mudline. In the FHWA method, this is equivalent to specifying no p-y or t-z curves for the upper 40 ft of the pile section. An excerpt of the BMCOL input file for Pier 3 is shown in Table 7.1. In the Novak method, the water column is modelled by a fictitious "soil" layer with a shear wave velocity of zero. The DYNA3 input file is shown in Table 7.2

7.1 FHWA METHOD

As the pile cap does not contact the soil, and there is no wall element, the Pier 3 stiffness matrix is equal to the pile group stiffness given by:

Pier 3 Soil Profile

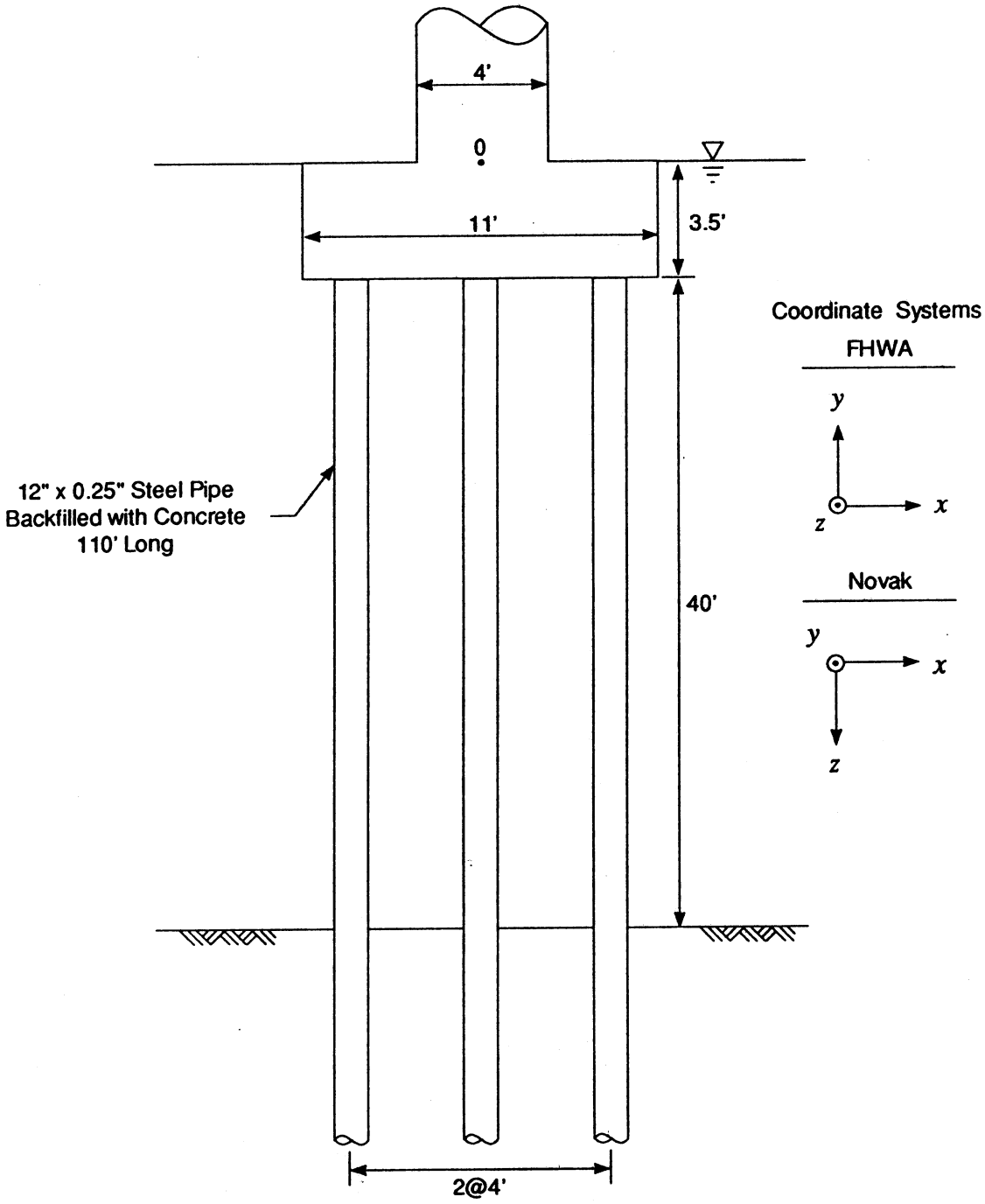

Soils as for Pier 1. See Figure 4.1.

Figure 7.1

```
PR3_FMT.IN                                                    04342-073
01-08-1993                  FHWA Example Pier 3 BMCOL input file (excerpt)
                                                              Page   1.

---FHWA Example PIER 3 -----                                  IDENTIFICATION OF RUN (2 LINES)
-------FIXED HEAD & FREE HEAD
1014     LATERAL LOAD ABUT 100 lb APPLIED LOAD FIXED HEAD     IDENTIFICATION OF PROBLEM
       2       0                        110    12.           TABLE 1: PROGRAM CONTROL DATA
      30       0   0   0   0       1   2   6       0   1     TABLE 6: LATERAL CONTROL DATA (2 CARDS)
             100. 1.00E-10       0   1   6  10  28                 ITERATION CONTROL DATA
       0       2          .00000001                          TABLE 7: SPECIFIED DEFLECTIONS AND SLOPES
       0 110      7.70E+09                                   TABLE 8: FIXED VALUES OF LATERAL STIFFNESS AND
       0   0                  100.
      40       1 -1.2E+01  1.0E-03   2   1                  TABLE 9: LATERAL SUPPORT CURVES
                           0   0                                    NOTE : NO SUPPORT FOR UPPER 40 FT OF F
                           0 2000
         110   0 -1.2E+01  1.0E-03  10   1
                           0 2129 4017 5521 6620 7374 7868 8380 8576 8692
                           0   86  172  259  345  431  517  690  862 1725
1017     LATERAL LOAD ABUT 200 LB APPLIED LOAD FIXED HEAD     NEXT PROBLEM
```

Table 7.1

$$[K_p] = \begin{bmatrix} 5.40E4 & 0 & 0 & 0 & 0 & 1.89E5 \\ 0 & 2.16E7 & 0 & 0 & 0 & 0 \\ 0 & 0 & 5.40E4 & -1.89E5 & 0 & 0 \\ 0 & 0 & -1.89E5 & 2.31E8 & 0 & 0 \\ 0 & 0 & 0 & 0 & 1.15E6 & 0 \\ 1.89E5 & 0 & 0 & 0 & 0 & 2.31E8 \end{bmatrix}$$

The units are lb and ft. Coordinate system is defined as shown in Figure 7.1.

7.2 NOVAK METHOD

The DYNA3 output file for Pier 3 is listed in Table 7.3. The coordinate system is defined as shown in Figure 7.1.

$$[K_p] = \begin{bmatrix} 5.02E4 & 0 & 0 & 0 & -1.24E6 & 0 \\ 0 & 5.02E4 & 0 & 1.24E6 & 0 & 0 \\ 0 & 0 & 7.91E7 & 0 & 0 & 0 \\ 0 & 1.24E6 & 0 & 8.82E8 & 0 & 0 \\ -1.24E6 & 0 & 0 & 0 & 8.82E8 & 0 \\ 0 & 0 & 0 & 0 & 0 & 9.96E6 \end{bmatrix}$$

The units are lb and ft.

8.0 PIER 4 STIFFNESS CALCULATION

A side-elevation view of the abutment and the soil-property profile at Pier 4 is shown in Figure 8.1. It should be noted that Piers 1 and 4 are mirror-images of one another

```
TITLE=FHWA Example PIER 3 [ PILES + EMBEDMENT ] [k ft s]
MATRIX
GRAVITY=32.2
FOUNDATION=PILE
RECTANGULAR=11.0, 11.0
MASS=0.,0.,0.,0.,0.,0.
LAYERS=2
FIXED=9
  1  -4.0    4.0
  2  -4.0    0.0
  3  -4.0   -4.0
  4   0.0    4.0
  5   0.0    0.0
  6   0.0   -4.0
  7   4.0    4.0
  8   4.0    0.0
  9   4.0   -4.0
CONSTANTS=0.,0.,3.5,110.,.145,0.,0.17,0.05,1.11,5.18E05
ELEMENT
1  40.0  0.5  0.5  1.24  0.103 0.103 0.206
2  70.0  0.5  0.5  1.24  0.103 0.103 0.206
FLOATING
NO-INTERACTION
SOIL
CONSTANTS
1     0.  .120  0.30 0.03
2   321.  .120  0.30 0.03
BELOW
321.  .120  .30  0.03
LOAD=HARMONIC
CONSTANTS
NONQUADRATIC
0.001  0.001  0.001  0.0  10,  0.0  0.  0.  0.
RUN
```

Table 7.2

```
**************************************************
*                                                *
*        D Y N A 3   S I M U L A T I O N         *
*                                                *
*             RUN DATE -  1993/ 1/ 8             *
*             TIME     -  10:30:31               *
*             REVISION -  1991/07/30             *
*                                                *
**************************************************

FHWA Example PIER 3 [ PILES + EMBEDMENT ] [k ft s

                                   RESULTS
                                   *******


FREQUENCY  -     .0010
*********


STIFFNESS CONSTANTS (K)
***********************

HORIZONTAL TRANSLATION  (X) ...  5.01763E+01
HORIZONTAL TRANSLATION  (Y) ...  5.01763E+01
VERTICAL TRANSLATION  (Z) .....  7.90960E+04
ROTATION ABOUT  (X) ...........  8.81888E+05
ROTATION ABOUT  (Y) ...........  8.81889E+05
TORSION ABOUT  (Z) ............  9.96401E+03
CROSS-STIFFNESS (YZ PLANE) ....  1.23945E+03
CROSS-STIFFNESS (XZ PLANE) .... -1.23945E+03

DAMPING CONSTANTS (C)
*********************
HORIZONTAL TRANSLATION  (X) ...  1.75101E+03
HORIZONTAL TRANSLATION  (Y) ...  1.75101E+03
VERTICAL TRANSLATION  (Z) .....  3.55909E+06
ROTATION ABOUT  (X) ...........  3.92601E+07
ROTATION ABOUT  (Y) ...........  3.92601E+07
TORSION ABOUT  (Z) ............  4.70172E+05
CROSS-DAMPING  (YZ PLANE) .....  4.26494E+04
CROSS-DAMPING  (XZ PLANE) ..... -4.26494E+04
```

Pier 4
Soil Profile

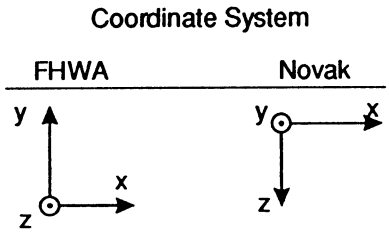

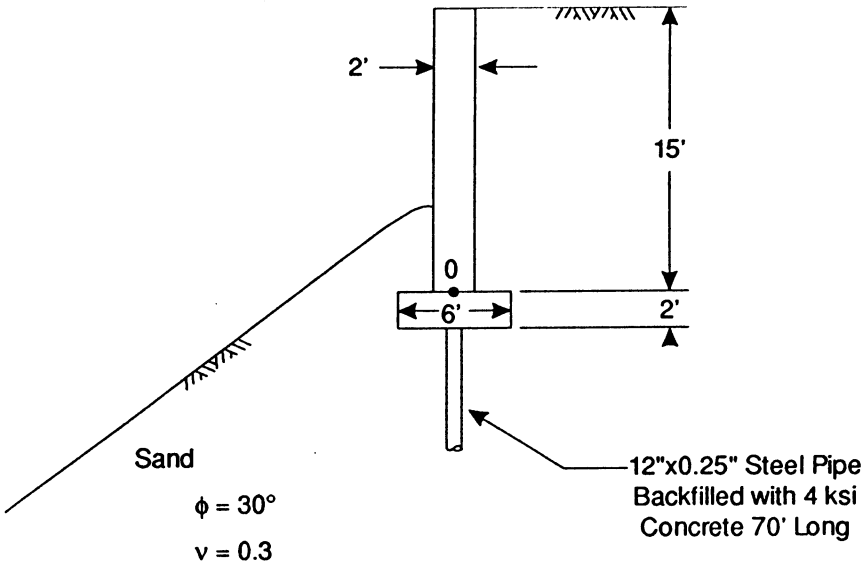

$\phi = 30°$

$\nu = 0.3$

$\gamma = 120$ pcf

$k = 45$ pci

$E = 1000$ ksf

∇ Depth = 35'

Figure 8.1

and that the piles are vertical and symmetrically placed about the transverse axis of the pile cap. Therefore, the stiffness values are numerically equal for Piers 1 and 4.

8.1 FHWA METHOD

After the Pier 1 results presented in Section 4.4, the final Pier 4 stiffness matrix is given by:

$$[K_t] = \begin{bmatrix} 8.35E7 & 0 & 0 & 0 & 0 & -3.57E7 \\ 0 & 1.63E8 & 0 & 0 & 0 & 0 \\ 0 & 0 & 6.50E7 & -6.83E7 & 0 & 0 \\ 0 & 0 & -6.83E7 & 2.83E10 & 0 & 0 \\ 0 & 0 & 0 & 0 & 1.35E10 & 0 \\ -3.57E7 & 0 & 0 & 0 & 0 & 1.95E9 \end{bmatrix}$$

The units are lb and ft. The coordinate system is defined as shown in Figure 8.1 with the origin at Point O.

8.2 NOVAK METHOD

The final Pier 4 foundation stiffness matrix is:

$$[K_t] = \begin{bmatrix} 5.36E7 & 0 & 0 & 0 & -2.28E8 & 0 \\ 0 & 3.51E7 & 0 & 1.24E8 & 0 & 0 \\ 0 & 0 & 1.37E8 & 0 & 0 & 0 \\ 0 & 1.24E8 & 0 & 2.07E10 & 0 & 0 \\ -2.28E8 & 0 & 0 & 0 & 1.92E9 & 0 \\ 0 & 0 & 0 & 0 & 0 & 6.38E9 \end{bmatrix}$$

The units are lb and ft. The coordinate system is shown in Figure 8.1 with the origin at Point O.

9.0 APPLICATION TO SEISAB-I BRIDGE ANALYSIS

This example illustrates the use of SEISAB-I to conduct a response spectrum analysis of the FHWA Workshop Bridge, as described in Section 1.0.

The structure model is illustrated in Figure 9.1. In this example, Pier 1 through Pier 4 are modeled in SEISAB-I as Abutment 1, Bent 2, Bent 3 and Abutment 4, respectively. The bridge was analyzed to consider foundation stiffnesses determined by the FHWA Method.

9.1 ABUTMENT 1 AND 4 MODELS

9.1.1 FHWA Method

Abutment 1 and 4 stiffness matrix given in Section 4.4.2 and 8.1, respectively, for the GPILE coordinate system. The units are lb and ft. It is noted that for this example the GPILE coordinate system is the same as the SEISAB-I coordinate system, therefore, conversion to the SEISAB-I coordinate system is not required.

After converting from lb to kip units, we have:

$$[K_{SEISAB}] = \begin{bmatrix} 8.35E4 & 0 & 0 & 0 & 0 & -3.57E4 \\ & 1.63E5 & 0 & 0 & 0 & 0 \\ & & 6.50E4 & -6.83E4 & 0 & 0 \\ \text{Symmetrical} & & & 2.83E7 & 0 & 0 \\ & & & & 1.35E7 & 0 \\ & & & & & 1.95E6 \end{bmatrix}$$

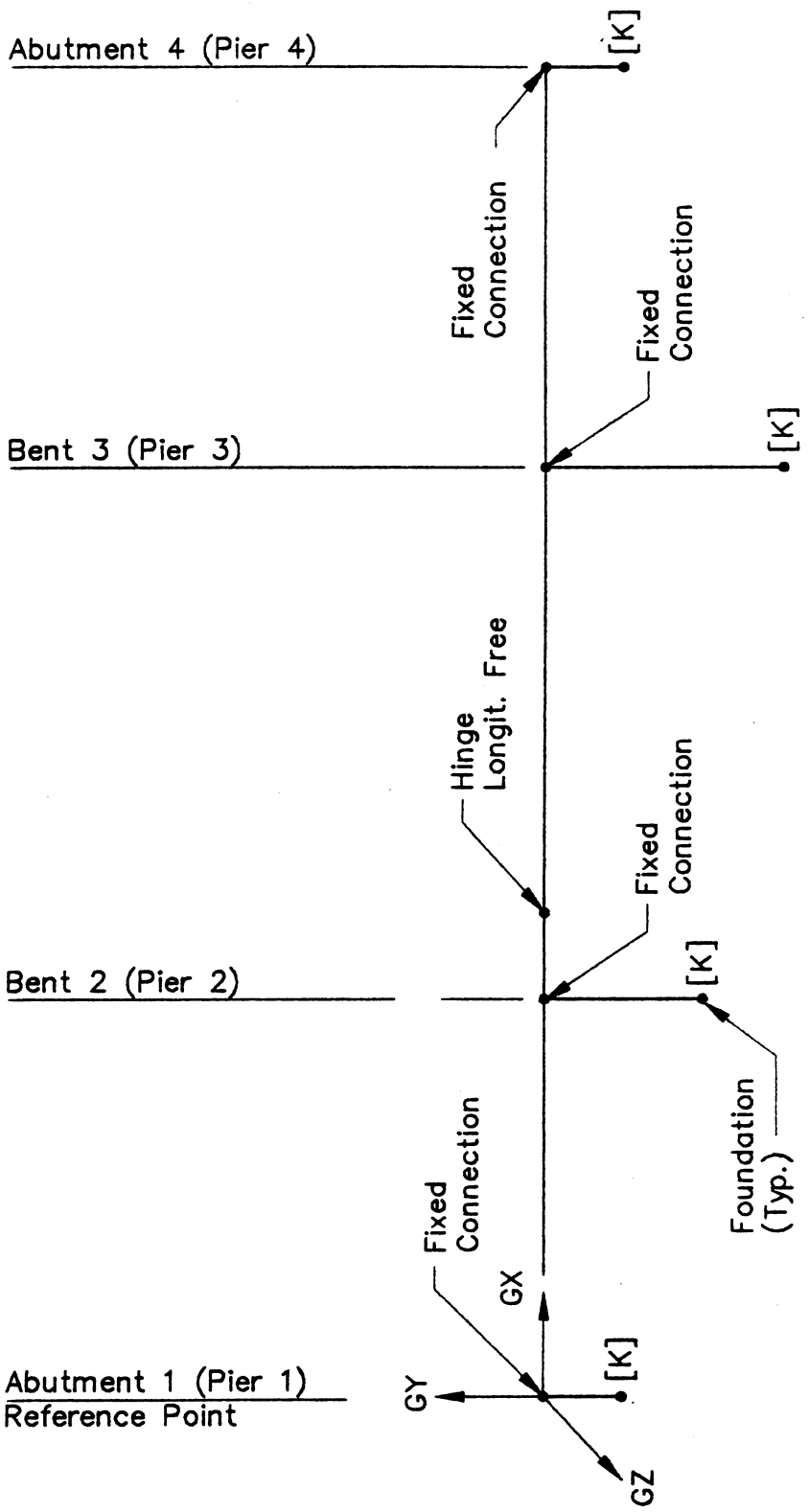

FHWA Workshop Structure Model

Figure 9.1

9.2 BENT 2 MODEL

9.2.1 FHWA Method

Pier 2 (Bent 2) stiffness matrix given for each pile in the coordinate system defined as the local pile system shown in Figure 6.1.3. This coordinate system is identical to the SEISAB-I coordinate system so conversion is not required. The units are lb and ft.

Converting from lb to kip units we have for each pile:

$$[K_{SEISAB}] = \begin{bmatrix} 3.78E4 & 0 & 0 & 0 & 0 & 6.36E4 \\ & 1.91E5 & 0 & 0 & 0 & 0 \\ & & 3.78E4 & -6.36E4 & 0 & 0 \\ \text{Symmetrical} & & & 2.80E6 & 0 & 0 \\ & & & & 1.73E6 & 0 \\ & & & & & 2.80E6 \end{bmatrix}$$

9.3 BENT 3 MODEL

9.3.1 FHWA Method

Pier 3 (Bent 3) stiffness matrix is given for each pile in the coordinate system defined as the local pile system shown in Figure 7.1. This coordinate system is identical to the SEISAB-I coordinate system so conversion is not required. The units are lb and ft.

Converting from lb to kip units, we have for each pile:

$$[K_{SEISAB}] = \begin{bmatrix} 4.63E4 & 0 & 0 & 0 & 2.27E5 & 0 \\ & 4.63E4 & 0 & -2.27E5 & 0 & 0 \\ & & 1.77E5 & 0 & 0 & 0 \\ \text{Symmetrical} & & & 3.34E6 & 0 & 0 \\ & & & & 3.34E6 & 0 \\ & & & & & 1.62E6 \end{bmatrix}$$

9.4 LOAD MODEL

The RESPONSE SPECTRUM must be input using the SEISAB ARBITRARY CURVE option in order to adjust the damping ratio as recommended in Task 1 Report, Section 6.2. In order to account for the 7-1/2 percent damping for those modes of vibration where soil-structure interaction is significant it is first necessary to identify those modes. This is done by running the model using the seismic response spectrum for 5 percent damping, recording R_a^t, R_d^t and R_d^v from the NORMALIZED SUPERSTRUCTURE MODE SHAPES output. The value theta is calculated and compared according to TASK 1 REPORT Section 5.2. Absolute displacement values are used for R_a^t, R_d^t and R_d^v. The response spectrum coefficient for each identified transverse mode is reduced by 15 percent to reflect the change to 7-1/2 percent damping for that mode. Run 5FHWAFE2 is used to illustrate modification of the 5 percent damping ratio spectrum. Table 9.1 lists the spectrum modifications required.

TABLE 9.1
RUN 5FHWAFE2 - RESPONSE SPECTRUM MODIFICATIONS FOR MODES WHERE SOIL-STRUCTURE INTERACTION IS SIGNIFICANT

MODE	R_a^t	R_d^t	R_d^v	θ	MODE PERIOD	MODIFIED SPECTRUM ORDINATE
1	0.047	0	1	0.047	1.317	0.50→0.43
5	0.430	0	1	0.430	4.054	0.63→0.536
8	0.595	0	0.958	0.621	5.759	0.63→0.536

1. Only transverse modes included.
2. $\theta = R_a^t/(R_d^t + R_d^v)$
3. For $\theta > 0.10$, Adjust Spectrum Ordinate
4. Spectrum ordinate for 5 percent damping is reduced by 15 percent to convert to 7-1/2 percent damping. Note that spectrum ordinate for each period of vibration is output by SEISAB-I as CS.

Appendix A

TASK 1 REPORT
EVALUATION OF METHODS TO ESTIMATE STIFFNESS AND DAMPING OF BRIDGE FOUNDATIONS

Submitted To:

WASHINGTON STATE DEPARTMENT OF TRANSPORATION
JOB NO. 4342-073-004
April 1992

CBC

DAMES & MOORE

TASK 1 REPORT

EVALUATION OF METHODS TO ESTIMATE STIFFNESS AND DAMPING OF BRIDGE FOUNDATIONS

Submitted to:

Washington State Department of Transportation
Transportation Building, KF-01
Olympia, Washington 98504-5201

Prepared by:

Dames & Moore
500 Market Place Tower
2025 First Avenue
Seattle, Washington 98121

WSDOT Agreement No. Y-4711
Dames & Moore Job No. 4342-073-04

April 1992

DAMES & MOORE
500 MARKET PLACE TOWER, 2025 FIRST AVENUE, SEATTLE, WASHINGTON 98121
(206) 728-0744 FAX: (206) 448-7994

April 30, 1992

Washington State Department of Transportation
Planning, Research Public Transportation
Transportation Building, KF-01
Olympia, WA 98504-5201

Attention: Pat LaViollette

Task 1 Reprot
WSDOT Project "Effects of Foundation-Soil Interaction"
Dames & Moore Project No. 4342-073-004

Dear Pat:

Dames & Moore is pleased to submit 5 bound copies and 1 unbound copy of the subject report. If you have any questions, please contact us. We look forward to beginning Task 2 after you have finished reviewing the Task 1 report.

Yours very truly,

DAMES & MOORE, INC.

C.B. Crouse, Ph.D., P.E.
Principal Engineer/Associate

Attachments

TABLE OF CONTENTS

Section		Page
1.0	INTRODUCTION	1
2.0	METHODS FOR PILE FOUNDATIONS	2
2.1	METHODS SELECTED FOR COMPARATIVE STUDY	3
2.2	TEST DATA	5
2.3	COMPARATIVE ANALYSES	7
2.4	CONCLUSIONS	10
3.0	METHODS FOR FOOTINGS	11
3.1	METHODS SELECTED FOR COMPARATIVE STUDY	12
3.2	TEST DATA	13
3.3	COMPARATIVE ANALYSES	15
3.4	CONCLUSIONS	16
4.0	METHODS FOR ABUTMENT SYSTEMS	16
4.1	METHODS SELECTED FOR COMPARATIVE STUDY	17
4.2	TEST DATA	18
4.3	COMPARATIVE ANALYSES	19
4.4	CONCLUSIONS	19
5.0	METHODS FOR MODAL DAMPING	20
5.1	METHODS TO ESTIMATE MODAL DAMPING	20
5.2	TEST DATA AND ANALYSIS	22
5.3	CONCLUSIONS	23
6.0	RECOMMENDATIONS	23
6.1	FOUNDATION STIFFNESS	23
6.2	MODAL DAMPING	24
6.3	GEOTECHNICAL PARAMETERS	25
7.0	REFERENCES	26

1.0 INTRODUCTION

This report presents the results of Task 1, Literature Search, of the Dames & Moore research study for the Washington State Department of Transportation (WSDOT) titled, "Effects of Foundation-Soil Interaction." The overall objective of the research program is to develop methods for incorporating the effects of foundation-soil interaction into procedures for the seismic design of WSDOT bridges. The objective of Task 1 was to evaluate the state-of-the-art methods to estimate stiffness and damping of bridge foundations for use in dynamic soil-structure interaction analysis of bridges. The foundation types included piles and footings supporting piers and abutment systems.

The state-of-the-art assessment consisted of an evaluation of the various methods available to estimate stiffness and damping of bridge foundations. This evaluation focussed on (1) the accuracy of these methods when tested against experimental data from bridges and other structures, and (2) the practicality of the methods and ease of their use in the WSDOT bridge design office.

Many publications dealing with the topic of computing foundation stiffnesses and damping were compiled and reviewed. The methods appearing in these publications ranged from relatively simple practical methods to ones that were mathematically complex requiring extensive computational effort. The complex methods were eliminated from further evaluation. The practical methods were then reviewed in more detail. The ones developed during the 1960s and 1970s have been superseded by ones developed between 1980 and the present. These newer methods either are more general, are incorporated into commercially available computer programs, or have been calibrated against a larger experimental database than the earlier methods. Therefore, these newer methods were selected as candidates for possible use by WSDOT. The essential features of these methods have been summarized in tables provided in Appendix A of this report. The candidate methods were also tested against the experimental database, where appropriate. This database resulted from (1) forced vibration testing of four bridges and two other structures with foundations similar to bridge-piers foundations, and (2) earthquake-generated motions recorded on one of the bridges.

Our evaluations of methods to estimate the stiffness and damping of pile foundations, footings, and abutment systems are presented in Sections 2.0, 3.0, and 4.0, respectively. Methods to estimate the modal damping ratios of bridge-foundation systems are summarized in Section 5.0. Based on the results of these evaluations, methods recommended for use by the WSDOT bridge design office are provided in Section 6.0.

2.0 METHODS FOR PILE FOUNDATIONS

Several practical and widely-used methods to estimate the stiffness of pile foundations were published by Poulos (Poulos, 1968, 1971a, 1971b) in the late 1960s and early 1970s. His solutions were subsequently published and condensed in Poulos and Davis (1980). These solutions were for static loading of elastic piles embedded in an elastic homogeneous half space. Other practical methods for static loading were developed by Matlock and Reese, and others, in which the soil medium was modeled as a Winkler spring, and the theory of subgrade reaction was used (Matlock and Reese, 1960; Broms, 1964a, b; Hetenyi, 1946).

Practical methods to estimate the dynamic stiffness and damping of piles were first introduced by Novak in the early 1970s (Novak, 1974). The solutions were for elastic piles in an elastic, homogeneous half space.

High-speed digital computers and the evolution of the finite element and boundary element methods (FEM and BEM) made it possible to solve more complex problems in soil-pile interaction. Although FEM and BEM methods enable the user to model the pile geometry and soil stratigraphy more precisely, these methods are tedious and impractical for use by designers because of the time involved in building the models and the computer time required to obtain solutions. These methods were not selected for further evaluation.

Many of the aforementioned practical methods have further evolved during the last ten years, and were selected for the Task 1 evaluation. Five methods were identified for single piles (Novak, Matlock,

Reese, Gazetas, and Lam); and five methods were identified for pile groups (Novak, FHWA, Reese, Lam, and Gazetas).

The Matlock method for single piles was largely incorporated into the FHWA method for pile groups. Similarly, the Reese, Novak, and Gazetas methods for single piles were incorporated into their respective methods for pile groups. The Lam method for single piles was extended by Dames & Moore for the comparative study to provide solutions for pile groups under the assumption that pile-group effects were negligible. This assumption is common to the FHWA approach also. The other approaches for pile groups have various approximate methods to account for pile-group effects.

The essential features, strengths, and limitations of each method for single piles and pile groups are summarized on pages 1-4 of the foldout tables in Appendix A at the end of this report. All of these methods are user friendly in the sense that solutions can be readily obtained from charts, figures, simple formulas, or commercially available computer programs.

The Matlock and Reese methods for single piles, as well as the FHWA and Reese methods for pile groups, are essentially equivalent. Consequently, in the comparative studies with the experimental database, the Matlock/FHWA method was selected over the Reese method for these comparisons because the computer programs to implement the Matlock/FHWA method were available in the Dames & Moore computer library.

Because most pile foundations consist of pile groups (rather than single piles), the remainder of the discussion in this section will focus on (1) the four methods selected for pile groups, and (2) the comparisons of the stiffnesses predicted from these methods with stiffnesses estimated from forced vibration response data obtained from two bridges and two transformer foundations.

2.1 METHODS SELECTED FOR COMPARATIVE STUDY

As noted above methods to compute pile-head stiffnesses were selected for the comparative study: (1) FHWA (Lam and Martin, 1986), (2) Novak (Novak et al, 1991), (3) Lam (Lam et al, 1991), and (4) Gazetas (Gazetas, 1991). The FHWA method, which was specifically developed for bridge foundations,

is based on methods first developed by Matlock, Reese, and coworkers. In this approach, the pile is modeled as discrete, linearly elastic beam elements, and the interaction between these elements and the surrounding soil is modeled by nonlinear force-deflection relationships (e.g., Matlock and Reese, 1961; Matlock, 1970; Matlock et al, 1981; Reese and Cox, 1975; O'Neill and Murchison, 1983). The cornerstone of this approach is the development of these force-deflection relationships (or so-called p-y, t-z, and q-z curves), which can be a relatively time-consuming process. The pile-head stiffness is equal to the tangent or secant modulus of the force (moment) vs. deflection (rotation) curve computed for the pile-head.

To circumvent the computation of the force-deflection curves, Lam et al (1991) conducted sensitivity studies and discovered a simpler procedure for floating piles in soils characterized by a constant coefficient of variation of soil reaction, f. Based on the results of their studies, Lam et al developed simple charts to obtain the lateral and rotational pile-head stiffnesses, which are only functions of f and the flexural rigidity, EI, of the pile. The authors have not developed charts for obtaining vertical pile-head stiffness, which is critical for estimating the rotational stiffness of pile groups. Nonetheless, the Lam et al method was selected for evaluation because of its simplicity.

Both the Lam et al and the FHWA methods are based on nonlinear force-deflection relationships between the soil and pile. As a result, the methods are limited to the estimation of static stiffness. On the other hand, the Novak and Gazetas methods are completely linear methods and can be used to estimate static and dynamic stiffnesses. Like the Lam et al method, the Gazetas method is only applicable to floating piles modeled as linear elastic beams, but it provides the user with the option to select from several different types of viscoelastic isotropic soil profiles, in which the elastic soil modulus (E_s) is either: (1) constant with depth (z), (2) proportional to z, or (3) proportional to $\sqrt{z}$. Gazetas made approximations to the elastic theory of dynamic soil-pile interaction to obtain relatively simple formulas to compute pile-head stiffnesses.

Novak's method is more general than the Gazetas approach and involves fewer approximations. The computer programs (PILAY 2 and DYNA 3) are required to obtain the solutions. In this approach, the soil is modeled as linear, viscoelastic, isotropic layers over a half space, and the pile is modeled as a linear elastic beam of constant or variable cross section. The PILAY 2 program computes a 6 X 6 pile-

head stiffness matrix for each pile and the DYNA 3 program combines them to obtain the 6 X 6 pile-group stiffness matrix. The DYNA 3 program has the option to include or neglect the pile-soil-pile interaction (i.e., pile-group effects) in the pile-group stiffness computation. The program also provides the user the option of considering the contribution of the soil surrounding an embedded pile cap to the foundation stiffness. Because of these features, the DYNA 3 program was used to investigate the differences between the static and dynamic stiffnesses, pile-group effects, and the stiffness of an embedded pile cap relative to the stiffness of the piles supporting the cap.

2.2 TEST DATA

Four sets of data were selected for the comparative study. Three of these data sets were low-amplitude forced vibration data from the MRO bridge (Douglas et al, 1990; Werner et al, 1990), the Rose Creek bridge (Douglas and Reid, 1982), and the transformer foundations at the Duwamish substation (Crouse and Cheang, 1987). The fourth set was the accelerogram data recorded on the MRO during the 1979 Imperial Valley earthquake (Werner et al, 1987).

MRO Bridge

The MRO bridge near El Centro, California, is a monolithic, two-span, reinforced concrete box girder bridge (Figure 1). The central pier is supported by a 5 X 5 square grid of wooden piles assumed to be pin-connected to a two-tiered concrete pile cap. The lower tier is 15 ft X 15 ft X 3.5 ft thick; the upper tier is 10 ft X 10 ft X 2 ft thick. The piles are about 40 ft long, 3 ft apart, and 1 ft in diameter at the top and taper slightly toward their tips. The piles are embedded in alternating layers of clayey sand, silty sand, silty clay, and silty sand (Norris, 1986b) (Figure 1).

The abutments are supported by a single row of 7 wooden piles driven into an embankment fill consisting of stiff clay overlying the native material mentioned in the preceding paragraph (Figure 1). These piles are similar to the pier foundation piles in terms of diameter and taper but are 5'4" apart and about 20 ft longer. The pile cap, which is integral with the abutment wall, is 3 ft wide, 35 ft long, and 1.75 ft thick.

Forced vibration tests using a hydraulic ram device were conducted on the MRO bridge in May, 1988 to determine its dynamic soil-structure interaction characteristics. Results of these tests are reported in Douglas et al (1990) and Werner et al (1990). The fundamental transverse frequency of 3.2 Hz measured during these tests was significantly greater than the 2.5 Hz frequency deduced from the accelerogram data recorded on the bridge during the 1979 Imperial Valley earthquake, which induced much larger strains in the bridge and soil than during the vibration tests (Werner et al, 1987; Douglas et al, 1984).

Abutment and pier foundation stiffnesses were estimated from the forced vibration test data (Douglas et al, 1991; Crouse, unpublished calculations). Some stiffnesses have been estimated from the earthquake response data also (Norris, 1986b; Wilson and Tan, 1990).

Rose Creek Bridge

The Rose Creek bridge in Nevada is a five-span concrete box girder bridge with piers supported by tubular steel piles filled with concrete (Figure 2). The steel piles are about 25 ft long, and 12 ¾" in diameter, ⅜" thick, and embedded in mostly medium stiff to stiff clay (Norris, 1986a: Norris and Sackman, 1986) (Figure 2). The spacing between the piles is 3 ft. The piles comprising the Piers 1 and 4 foundations were arranged in a 3 X 5 rectangular grid, whereas the piles comprising the Piers 2 and 3 foundations were arranged in a 4 X 5 rectangular grid.

Douglas and Reid (1982) conducted forced vibration tests on a bridge similar to those at the MRO bridge. Norris (1986a) and Norris and Sackman (1986) estimated transverse and rotational stiffnesses of the four pile caps from the test data.

Duwamish Substation

Two large transformer banks (Banks 77 and 79) at the Duwamish substation in Seattle, Washington are supported on tubular steel piles filled with concrete (Figure 3). The pile geometry, size, and spacing are different at each bank. Bank 77 consists of 16 piles, either battered or vertical, whereas Bank 79 consists of six slightly smaller vertical piles. The piles at both banks are embedded in approximately

40 ft of mainly loose to medium dense sand to silty sand over hard glacial till which provide end bearing for the piles.

Forced vibration tests using a quick-release apparatus were conducted on both banks to determine the fundamental frequencies of the soil-structure system in both principal lateral directions (Crouse and Cheang, 1987). Because the transformers were essentially rigid, the fundamental frequencies were functions of the inertial properties of the pile cap and transformer and the flexibility of the soil-pile system.

2.3 COMPARATIVE ANALYSES

The four methods discussed in the METHODS section and the information presented in the TEST DATA section were used to estimate the foundation stiffnesses and/or natural frequencies for each test case. These predictions are compared to the observed experimental values in Table 1 (MRO vibration test), Table 2 (MRO earthquake), Table 3 (Rose Creek), and Table 4 (Duwamish).

The types of information presented in each table are similar, but require explanation before making the comparisons. The left-hand column in each table labeled "Observed Experimental Values" are the foundation stiffnesses and/or natural frequencies of the soil-structure system derived from the vibration-test or earthquake-response data. The first value listed for each stiffness is the best-estimate value. The values in parentheses define the range of values obtained by different methods or authors. The next three major column headings, "Piles Only," "Piles and Footing," and "Piles and Footing Side," represent the assumptions regarding the stiffness contributions from the piles and embedded pile cap. The "Piles Only" column means that the stiffness provided by the soil around the cap was neglected in the theoretical calculations. The "Piles and Footing" column means that the stiffnesses computed for an embedded cap, assumed to be a footing without piles, was added to the pile stiffnesses. The "Piles and Footing Side" column means that the passive resistance from the soils along the sides of the cap were added to the pile stiffnesses. The stiffness solutions for this case were only available with the Novak et al (1991) DYNA 3 program. Under the "Piles Only," "Piles and Footing," and "Piles and Footing Side" columns, foundation stiffnesses and/or natural frequencies are listed for the four methods. The following subscript convention was adopted for the foundation stiffnesses, K_x, K_y, K_z, $K_{\theta x}$, $K_{\theta y}$, $K_{\theta z}$. The

subscripts x, y, and z refer to, respectively, the: (1) longitudinal direction parallel to the plane of the elevation views in Figures 1, 2, and 3, (2) transverse direction normal to the plane of the elevation views, and (3) vertical direction. The subscripts θx, θy, and θz refer to rotations about the x, y, and z directions, respectively. The cross-coupling stiffnesses were not measured and therefore were not included in the comparisons.

The foundation stiffnesses listed in Tables 1 to 4 for each method are static stiffnesses without pile-group effects, i.e., pile-soil-pile interaction neglected. The differences between static and dynamic stiffnesses at the natural frequencies listed in the tables were insignificant based on calculations using Novak's method. The potential pile-group effects are considered at the end of this section.

The stiffnesses estimated for the MRO vibration-test and earthquake-response cases (Tables 1 and 2) differ because the low-strain soil shear moduli (Figure 1), assumed in the calculation of the vibration-test stiffnesses, were reduced by 50% for the earthquake stiffness calculations. This reduction was based on studies by Crouse and Hushmand (1990) at the nearby Differential Array accelerograph station, which also recorded the ground motions generated by the 1979 earthquake. The low-strain shear modulus was used to estimate the stiffnesses for the other two vibration-test cases (Tables 3 and 4).

The piles were assumed to be pin-connected to the caps. This assumption was thought to be more appropriate than the alternative fixed-head assumption based on the available drawings and knowledge of the general design practice for the pile-to-cap connection at the times when the foundations were designed.

After reviewing the results in the four tables, several observations and conclusions were made. The Lam et al method ("Lam-Charts" in tables) generally underestimated the observed stiffnesses for the MRO (Table 1) and Rose Creek (Table 3) vibration tests, the only two cases for which the method could be tested. The method provided estimates of the transverse stiffness, K_y, that were reasonably consistent with the observed MRO values if the stiffness contribution of the cap ("Piles and Footing") was included in the stiffness calculation. However, the method consistently underestimated the observed transverse stiffnesses for Rose Creek regardless of whether or not the cap contribution was included.

The Gazetas method tended to underestimate the transverse stiffnesses for the MRO vibration test case (Table 1) without the cap resistance included and tended to overestimate them when the cap was included. The vertical stiffnesses were overestimated in both cases. When the foundation stiffnesses estimated for the "Piles Only" and "Piles and Footing" cases were substituted into a SAP90 model of the MRO bridge-foundation system, the resulting fundamental frequencies, which corresponded to the fundamental transverse mode involving substantial foundation interaction, bracketed the frequencies measured during the vibration test and 1979 earthquake (Tables 1 and 2). The Gazetas method, like the Lam et al method, underestimated the Rose Creek foundation stiffnesses (Table 3).

The more interesting comparisons are between the results from the FHWA and Novak methods, not only because these methods could be applied to all four test cases, but also because the methods involve different approaches to estimate pile stiffness. The FHWA and Novak results for the MRO vibration-test case (Table 1) are similar for the pier foundation. The results are also similar for the abutment foundation for the "Piles and Footing" case, but differ significantly for the "Piles Only" case where the Novak stiffnesses are much greater than the FHWA stiffnesses. The fundamental transverse frequencies (f_1) computed from the Novak stiffnesses for "Piles Only," "Piles and Footing," and "Piles and Footing Side" cases are all slightly greater (~ 10 % or less) than the observed frequency (3.2 Hz). The FHWA stiffnesses for the "Piles Only" and "Piles and Footing" cases yielded frequencies, f_1, that bracketed the observed frequency.

For the MRO earthquake case (Table 2), the f_1 values estimated from Novak's results are roughly 50 % larger than the observed value of 2.5 Hz, whereas the FHWA approach yielded f_1 values that bracketed the observed frequency. The f_1 values computed using the FHWA method were based on pile-head stiffnesses which were taken as the secant moduli of the force-deflection curves for the pile head. The deflections used to calculate the secant moduli were arbitrarily taken to be 1" (horizontal) and 1/2" vertical (I.P. Lam, personal written communication, 1991). Subsequent calculations, using an iterative procedure to estimate pile-head deflections and associated secant stiffness, indicated that the assumed 1" deflection was larger than the actual deflection by about a factor of five. The pile-cap stiffness, K_y, estimated from this iterative approach was similar to the K_y value obtained from Novak's method.

For the Rose Creek test case (Table 3), the Novak results are generally similar to the observed stiffnesses for the "Piles and Footing" or the "Piles and Footing Sides" cases. The FHWA method generally underestimates the stiffnesses for the "Piles Only" and "Piles and Footing" cases, although the underestimation is not that great for the latter case.

Because only natural frequencies were measured during the Duwamish vibration tests (Table 4), the FHWA and Novak methods were compared based on these data only. The Novak method overestimates the fundamental frequencies at Bank 77 by about 10 to 40 %; for Bank 79 Novak's estimates are generally similar to the observed frequencies. The agreement is particularly good for the "Pile and Footing Side" case for both banks. The FHWA method for the "Piles Only" case produces natural frequencies similar to the observed frequencies at Bank 77 but underestimates the observed frequencies at Bank 79. For the "Piles and Footing" case, the FHWA method generally overestimates the frequencies for both banks.

One of the key issues is whether or not to include pile-group effects in the calculation of pile stiffnesses. This issue was addressed using Novak's method which has the option to include pile-group effects in the stiffness calculation. Novak's method was repeated using this option for the Rose Creek and Duwamish test cases. The results, presented in Tables 5 and 6, show that the group-effects option reduces the stiffnesses (or natural frequencies) to levels that are generally well below the observed values.

2.4 CONCLUSIONS

The FHWA and Novak methods of estimating foundation stiffnesses can be applied to bridge foundations with some level of confidence based on the results of this study. Overall, the Novak method produced results somewhat more consistent with the observations than did the FHWA method.

The use of static, rather than dynamic, foundation stiffnesses would appear to be an acceptable practice for modeling the dynamic interaction of bridge foundation systems in the frequency range where this interaction is likely to be significant. The results also suggest that the interaction between the pile cap and surrounding soil should also be included in the stiffness calculation. Of the two options

studied in this paper, the one including only the passive resistance of the soil against the sides of the pile cap tended to yield results more consistent with the data than the one in which the cap was treated as an embedded footing.

The inclusion of group-interaction effects into stiffness-estimation models for piles cannot be recommended based on the results of this study. The stiffnesses (or natural frequencies) computed using Novak's interaction factors for group effects were much lower than the observed experimental values.

On the other hand, the data from the MRO vibration-test and MRO earthquake-response cases, as well as other information, clearly demonstrated the importance of nonlinear soil behavior, and particularly, the reduction of soil stiffness during strong earthquake excitation. The reduction in shear modulus at the MRO during the 1979 earthquake was apparently greater than the reduction estimated from accelerogram data recorded at a nearby site. Norris (1986a) postulates that liquefaction of the soil in various layers around the pier foundation significantly reduced the foundation stiffness. The possible occurrence of the liquefaction at this site and its impact on the dynamic response of the MRO are currently being investigated by Dames & Moore for another project.

3.0 METHODS FOR FOOTINGS

Methods to estimate the stiffness and damping of footing foundations have evolved over the last 50 years, with most of the development occurring between the mid-1960s and mid-1980s. An excellent summary of the historical development of these methods can be found in Gazetas (1983). The earlier methods pertained to a rigid disk on an elastic, homogeneous, isotropic half space. Lysmer (1965), Richart and Whitman (1967), Richart et al (1970), and Whitman (1967), developed simple approximate expressions for the stiffness and damping ratio for vertical, horizontal, rocking, and torsional vibrations for this type of footing foundation. These expressions have been widely used by engineers for soil dynamics' problems.

As with piles, high-speed digital computers enabled researchers to obtain numerical solutions to more complex problems, such as footings of different shapes resting on, or embedded in, a layered viscoelastic half space. These solutions were obtained by FEM or BEM methods, or sophisticated numerical solution techniques applied to the mixed boundary-value elastodynamic problem. The FEM, BEM, or numerical solution techniques can be used to obtain the stiffness and damping of a footing on a case-by-case basis, but this approach is not practical because it is labor intensive. The methods were not selected for further evaluation.

3.1 METHODS SELECTED FOR COMPARATIVE STUDY

Practical methods are available, in which solutions can be obtained from charts, figures, or a commercially available computer program. These methods (Novak, Gazetas, Wong, Dominguez, FHWA) are summarized on pages 5 and 6 of the foldout tables in Appendix A and apply to more realistic situations than a disk over a half space. All of the methods are linear, and all of them except the FHWA method provide dynamic stiffness and damping for all 6 degrees of freedom of the footing. The FHWA method only provides static stiffnesses.

The Novak method (Novak et al, 1991) is part of the same computer software that contains subroutines for piles (see Section 2.0 and foldout tables). Because the method has been integrated into a software package, it is more versatile than the other four methods, which are applicable to a narrower range of soil or foundation models. For example, Gazetas obtained approximate solutions (Gazetas, 1991) applicable only to half-space or soil-layer-over-rock models; however, his formulas can be applied to embedded or surface foundations of arbitrary shape. Wong's method involved the numerical solution of integral equations (Wong and Luco, 1978, 1985). Solutions in the form of tables were obtained for either (1) a square surface foundation on a soil layer over a half space, or (2) a rectangular foundation over a half space. The Dominguez's BEM solutions (Dominguez, 1978) are in graphical format and pertain to a square or rectangular foundation resting on the surface of, or embedded in, an elastic half space. The FHWA report (Lam and Martin, 1986) provides simple equations and figures to account for circular or rectangular footings on the surface of, or embedded in, an elastic half space. The equations and figures were obtained from Richart et al (1970) and Gazetas (1983).

Because the Dominguez solutions were more restrictive and yielded results similar to the FHWA, Gazetas, or Novak methods, the Dominguez method was not considered in the comparative study.

3.2 TEST DATA

Three sets of data were selected for the comparative study. One set comprised the low-amplitude forced harmonic vibration data from the Horsethief bridge (Crouse et al, 1987). Another data set was obtained during similar tests conducted at the Differential Array accelerograph station (Crouse and Hushmand, 1989). The third data set consisted of the accelerograms recorded at this station during the 1979 Imperial Valley Earthquake (Crouse and Hushmand, 1990).

Horsethief Bridge

The Horsethief bridge (Figure 4) near Corona, California, is a single-span, monolithic, prestressed concrete, box-girder bridge. Vertical support is provided by a rectangular concrete footing beneath each abutment. The footing is not structurally tied to the abutment wall; rather, a thin neoprene strip separates the bottom of the abutment from the top of the footing.

The footings rest on sandy soil with some coarse gravel content. The average shear-wave velocity, V_s, of the upper 3 m (10 ft) of soil beneath the footings is about 260 mps (850 fps). The backfill soil consists of similar material except the average V_s is about 210 mps (700 fps). Both estimates were obtained by spectral analysis of surface waves, excited by a vertical impulse load applied near each abutment.

Forced harmonic vibration tests were performed on the bridge in 1984. During the testing, the response of the bridge was measured with 30 accelerometers placed at various locations on the bridge deck, abutment walls, and the top of the footings near the inside edges of the abutment walls. The accelerometers were positioned so that the rigid body and flexural motions of the footing, abutment and deck could be determined.

Natural frequencies, mode shapes, and footing foundation stiffnesses were computed from the response data (Crouse et al, 1987; Crouse and Hushmand, 1987).

Differential Array Station

The Differential Array Station (Figure 5) in El Centro, California, is a 2.44-m (8 ft) tall reinforced masonry-block structure with a plywood roof. The foundation consists of a 2.44-m (8 ft) square by 0.10-m (4 in) thick concrete slab supported by a 0.30-m (2 ft) thick by 0.61-m (2 ft) deep rectangular concrete wall around its perimeter. The total mass of this station is 13,860 kg (30,490 lb) (Crouse and Hushmand, 1989).

The Differential Array site is underlain by a deep alluvial deposit. The upper 30 m (98 ft) of soil consist mostly of medium stiff silty clay with occasional layers of fine sand or coarse sand. The surficial soil consists of interbedded dense to medium dense very fine sand and soft to medium stiff silty clay to a depth of 5 m (16 ft).

Shear-wave velocity profiles of the surficial soil (Figure 5) were estimated from results of two geophysical tests: the Spectral Analysis of Surface Waves (SASW) and the downhole methods. These methods yielded consistent values of the average shear-wave velocity over the first 10 m (33 ft) of soil of approximately 170 m/sec (560 fps). The higher-resolution SASW method indicated the presence of a softer 0.7-m (2.3 ft) thick layer at about 1 m (3.3 ft) depth with a shear-wave velocity of about 80 m/sec (260 fps).

This station and a free-field site 8 m (26 ft) away recorded strong motions generated during the 1979 Imperial Valley earthquake. (Recall the MRO bridge recorded motions during this event also). In 1986, low-amplitude forced harmonic vibration tests were conducted at the station. The response data generated during this test and the earthquake were used to estimate the fundamental frequencies of the soil-structure system for low and high dynamic soil strains (Crouse and Hushmand, 1989, 1990).

3.3 COMPARATIVE ANALYSES

The four models discussed in the METHODS section and the information presented in the TEST DATA section were used to estimate the foundation stiffnesses and/or natural frequencies for each test case. These predictions are compared to the observed experimental values in Table 7 (Horsethief), Table 8 (Differential Array earthquake), and Table 9 (Differential Array vibration test).

For the Horsethief test case (Table 7), the stiffnesses and natural frequencies estimated from Gazetas' method agree most closely with the observed experimental values. Generally, the other three methods underpredict the stiffnesses and natural frequencies. However, for the two key stiffnesses that contribute significantly to the soil-structure interaction (K_y and $K_{\theta x}$), the differences between the predictions from all four methods and the observations are not that great. For example, the natural frequencies predicted for the third mode, where the interaction is substantial, are within 5-17% of the experimental value of 8.2 Hz.

The comparisons presented in Tables 8 and 9 for the Differential Array test cases are revealing. The reduction in fundamental frequency from a low-strain value of 12 Hz (Table 9) to a high-strain value of 8.7 Hz (Table 8) measured during the earthquake clearly indicate that the soil shear modulus was reduced by 50% during the earthquake. However, when this modulus value was used, the four methods predicted much higher fundamental frequencies, based on a 2.44-m (8 ft) square foundation assumption, than the observed frequency of 8.7 Hz. This result suggested that the thin slab foundation was not experiencing significant shear forces from the soil beneath it, and that most of the load transfer between the soil and foundation was occurring at the perimeter wall. When only the perimeter-wall foundation was considered, the foundation stiffnesses predicted by the four methods were reduced such that the resulting computed fundamental frequencies were within about 10-20% of the measured value. The fundamental frequency predicted from the FHWA stiffnesses was closest to the observed frequency.

Under the assumption that the perimeter wall provides the load transfer between the soil and foundation, stiffnesses and fundamental frequencies were computed for the Differential Array vibration test case, and the results are listed in Table 9. Two sets of results are provided: one set for static foundation stiffnesses, and the other for dynamic foundation stiffnesses computed at a frequency of

12 Hz. The FHWA method was not included in the latter results because it can only be used to compute static stiffnesses. The results indicate that the differences between the static and dynamic foundation stiffnesses are negligible. The static foundation stiffnesses and fundamental frequencies predicted by the four methods are similar to each other and are also close to the observed frequency of 12 Hz.

3.4 CONCLUSIONS

The above comparisons for footings suggest that all four methods may be used with confidence. Overall, the Gazetas method yielded slightly better predictions than did the other methods.

Similar to the conclusion reached in Section 2.0, the use of static foundation stiffnesses would appear to be an acceptable practice for modeling the interaction between the soil and footing.

4.0 METHODS FOR ABUTMENT SYSTEMS

Each component of a foundation system in contact with the soil has some contribution to the overall soil-foundation stiffness of the system. The elements of an abutment system that contribute to the stiffness include the footing, abutment wall, wingwall, and any piles that may be supporting the footing or wingwall. Wilson (1988) published a simple method for combining the individual stiffness contributions from each element into a foundation stiffness matrix for the abutment system (see p. 9 of foldout tables in Appendix A). The overall concept has merit, but some of the details are not internally consistent. For example, for a pile-supported footing, the stiffness contribution from the footing is included in the longitudinal and transverse stiffness estimate, but ignored in the vertical stiffness estimate. Another concern with the approach is that from the standpoint of the element stiffness calculations, each element is assumed to be independent of the other elements. Furthermore, Wilson suggests computing the stiffnesses of the wall elements by assuming they are rigid footings on an elastic half space. Whereas this assumption may be reasonable for abutment walls, treating the wingwall as a rigid footing may not be appropriate because it is more apt to act as a flexible cantilever.

Despite the above shortcomings, certain aspects of Wilson's method need to be retained or revised to estimate the stiffness of an abutment system. The difficulty in selecting a revised methodology is the lack of experimental data that can be used to isolate the contribution of each element. From the standpoint of earthquake loading, the transverse direction is perhaps the most important one based on the AASHTO guidelines and the response data recorded to date. The comparative studies presented in Sections 2.0 and 3.0 for the MRO and Horsethief bridges suggest that contributions from the abutment wall and wingwall to the estimation of the transverse stiffness, K_y, and rotational stiffness, $K_{\theta x}$, of the abutment system can be neglected. However, the abundance of experimental load-test data for retaining walls suggests that the backfill soils offer a significant amount of passive resistance to the abutment wall. Thus, the contribution of the abutment wall to the longitudinal stiffness, K_x, and the rotational stiffness, $K_{\theta y}$, of the abutment system should be included. Methods to estimate these stiffnesses are presented below.

4.1 METHODS SELECTED FOR COMPARATIVE STUDY

A number of relatively simple methods are available to estimate the stiffness, K_x, and $K_{\theta y}$, for an abutment wall. The usual approximation is to assume a 2-D plane strain model of a rigid retaining wall translating or rotating into an elastic, homogenous, isotropic quarter or half space. Another approximation is to assume that the wall is a footing on an elastic half space.

Five candidate methods were identified (Wood, Finn, FHWA, Lam, Wilson) and are presented in pages 7 and 8 of the foldout tables in Appendix A. Each method incorporates one of the two aforementioned approximations.

The methods of Wood (Wood and Elms, 1990; Wood, 1985), Finn (Finn, 1963; Poulos and Davis, 1980), and FHWA (Lam and Martin, 1986) employ the 2-D approximation. The main limitation of the 2-D approximation is that the longitudinal stiffness, K_x, is independent of the height of the abutment wall, which is physically implausible, but which appears to provide reasonable stiffness estimates for typical abutment wall dimensions (I. Lam, personal communication, 1991).

Wood presents pressure distribution diagrams which must be integrated by hand to obtain the stiffnesses. Several diagrams are presented for different cases such as rigid or flexible walls, and linear or nonlinear backfill soils.

Finn provides formulas for the pressure distribution which must be integrated numerically to obtain the stiffnesses. Before integrating, however, the stress at the base of the wall must be modified to remove the singularity or infinite stress concentration.

The FHWA document provides simple formulas for the wall stiffnesses, K_x and $K_{\theta y}$; the authors simplified one of Wood's pressure distribution diagrams and performed the required integrations. The formulas are applicable to all abutment walls and backfill soils.

The Lam (Lam et al, 1991) and Wilson (1988) methods treat the retaining wall as a footing on an elastic half space. Lam provides a simple equation and convenient chart for obtaining the stiffness, K_x, but does not provide any information to compute $K_{\theta y}$. Wilson simply refers the user to other references, such as Poulos and Davis (1980), to obtain the stiffnesses.

Of the five methods presented above, the one by Finn was eliminated from further consideration because of the singularity problem at the base of the wall.

4.2 TEST DATA

The bridge test data relevant to the estimation of the transnational and rotational stiffnesses for abutment walls are limited to the MRO and Horsethief bridges. For these data, the uncertainty in the experimental stiffnesses associated with the longitudinal direction is greater than the uncertainty in stiffnesses associated with the transverse direction. The primary reason is that the fundamental longitudinal soil-structure interaction mode was not excited during the test program at the MRO bridge, and only partially excited at the Horsethief bridge.

4.3 COMPARATIVE ANALYSES

Table 10 presents the comparisons for the MRO vibration test case. The observed experimental values are for the entire abutment system and reflect the contribution for the abutment wall, footings, and piles. The actual contribution from each element could not be isolated from the test data. The Novak solutions from Table 1 for the "Piles Only" and the "Pile + Footing Side" cases are shown in Table 10, together with the solutions from the four retaining wall methods. The purpose of presenting these results is to indicate the possible relative contributions of the different elements comprising the abutment system. The calculations show that the abutment wall has a significant contribution to the stiffness. As expected, the 2-D methods (FHWA, Wood) for retaining walls predict somewhat lower stiffnesses than the footing-on-half-space methods (Lam, Wilson).

Table 11 presents the results for the Horsethief bridge. The observed experimental stiffness, K_x, represents the contribution of the abutment wall only, although as previously noted, the uncertainty in this value is thought to be much greater than that associated with K_y. This value of K_x was estimated from a partially-excited higher mode of vibration of the bridge-abutment system which involved a significant amount of longitudinal movement of the wall. The uncertainty in the experimental value is due to the fact that a complete definition of the modal quantities could not be obtained because the forced vibration test had to be terminated prematurely before the peak response was reached.

The values of K_x predicted by the FHWA, Wilson, and Wood methods are similar to the observed value, while the Lam value is 50% greater. All four predicted values are considered to lie within the range of uncertainty associated with the experimental value. Again, the 2-D model predictions are somewhat smaller than the predictions from the footing-on-half-space model.

4.4 CONCLUSIONS

The four methods evaluated for estimating abutment wall stiffnesses appear to provide reasonably consistent results. The FHWA method is the easiest to apply, but not that much easier than the others. The use of the solutions for a footing-on-half-space model has some appeal because it limits the

aforementioned problem associated with the 2-D approach, and because solutions for footings are readily obtained from the methods cited in this section or in Section 3.0.

5.0 METHODS FOR MODAL DAMPING

Most dynamic response analyses are performed using modal superposition with a design response spectrum (or spectra) used as the definition of the input motion to the model. Thus, for each mode of vibration of the soil-structure model, a modal damping value must be estimated or assumed, and the corresponding response spectral acceleration must be obtained from the design spectrum. Usually for bridges, a damping value of 5% of critical damping is considered for all modes of vibration. However, research conducted by the project team has demonstrated that the modal damping values for a particular bridge vary, and values larger than 5% have been observed. The factor that appears to affect the modal damping depends on (1) the superstructure and foundation damping, and (2) the relative deformations of the bridge and its foundation elements. These factors indicate that the modal damping depends on the bridge-foundation system considered.

5.1 METHODS TO ESTIMATE MODAL DAMPING

Two relatively straightforward methods to estimate the modal damping of a soil-structure system were found in the literature. One method is based on strain energy (Hansen, 1970; Roesset et al, 1973) in which the modal damping ratio for a particular mode of the soil-structure system is the weighted average of the structural and foundation damping values. The weights are proportional to the strain energies stored in the superstructure and foundation elements for that mode.

Another method to estimate modal damping for a soil-structure system was developed by Luco (1981). Luco derived a formula to compute the modal damping ratio as a function of the fixed-base modal properties of the system (e.g. natural frequencies, damping ratios, mode shapes), certain properties of the soil-structure system (i.e. natural frequencies, mode shapes), and the foundation damping. In applying this method, the natural frequencies and mode shapes would be computed by

a dynamic analysis computer program (i.e. SEISAB, STRUDL, etc.) and the foundation damping would be estimated by methods such as those evaluated in this report. The fixed-base structural damping would be assigned (e.g. 5% or less depending on the structure and anticipated level of shaking).

Unfortunately, both methods outlined above were derived for structures supported by one foundation. The theory for multiple foundations has not been developed. An attempt by the project team to adapt and apply the energy-based method to the Horsethief bridge, the simplest of the bridge foundation systems, was unsuccessful; the resulting damping ratios were much larger than the observed values.

Modal damping ratios could be estimated for the lower modes of vibration, where the important transverse modes of vibration are likely to be, by constructing a dynamic model of the soil-structure system involving the mass, damping, and stiffness matrices. The damping matrix for the superstructure could be assigned and the damping matrix for the foundation could be estimated using the methods presented in this report. The mass and stiffness matrices would be generated in the usual manner; the portion of the stiffness matrix associated with the soil-foundation interaction would also be estimated using the methods in this report. This model could then be excited by harmonic motions covering a wide frequency band. The peaks of the amplitude response curve at a particular location on the bridge model could be used to estimate the modal damping by employing the simple half-power method or more formal systems identification techniques. However, this cumbersome method to estimate modal damping is of questionable practical value because once the mass, damping, and stiffness matrices are specified, then the seismic response can be computed directly, using a time-history, rather than a modal superposition method. However, many users are uncomfortable with such a direct approach to estimate seismic response because of their lack of experience or knowledge in specifying the damping matrix and the time histories, and the larger computer output generated by the time-history approach. As more users become familiar with it, this approach may replace, or at least be used in conjunction with, the modal superposition method.

Despite the absence of a practical and reliable physically-based method to estimate modal damping for structures with multiple foundations, the vibration test data for bridges suggest that a simple empirical approach may be used instead.

5.2 TEST DATA AND ANALYSIS

The relevant test data for modal damping consist of vibration response data from the MRO, Horsethief, and Moses Lake bridges. The mode shapes, natural frequencies, and modal damping values were compiled from these data and examined. The MRO and Horsethief bridges were described earlier; the Moses Lake bridge in Washington is currently being studied by Professor M. Eberhard at the University of Washington, who employed Dames & Moore to conduct forced harmonic vibration tests on the bridge. The bridge is a three-span concrete I girder bridge whose pier and abutment foundations are supported on footings. The Moses Lake bridge vibration data were not used in the methodology evaluation for footings (Section 3.0) because geotechnical properties of the embankment soils supporting the abutments have not been measured to date. Nonetheless, the response data were useful for examining modal damping.

Table 12 is a compilation of the modal data from each bridge vibration data set that was considered relevant. Only the data from the transverse modes, where the soil-structure interaction was thought to be significant, are included in the table. Listed in the table are the natural frequencies, modal deflections, and modal damping ratios. The modal deflections listed are the average transverse translation of the abutments ($\bar{R}_a^t$), the maximum transverse deflection of the deck (R_d^t), and the maximum vertical deflection of the deck (R_d^v), which for these data sets was primarily due to torsion of the deck about the longitudinal axis. The transverse modal deflections at the pier foundations of the MRO and Moses Lake bridges were not included in Table 12 because they were roughly an order of magnitude smaller than the abutment deflections, ($\bar{R}_a^t$).

If significant soil-structure interaction is defined as values of $\theta = \bar{R}_a^t/(R_d^t + R_d^v) \geq 0.1$, then all modes satisfying this criterion in Table 12 have modal damping ratios $\zeta > 6\%$. The range of ζ is between 6% and 15%. For $0.05 \leq \theta < 0.1$, modal damping ratios, $\zeta > 6\%$, were also observed for higher order transverse modes of the MRO. For $\theta < 0.05$, $\zeta < 0.05$ for the data in Table 12. The ζ = 7.2% for the MRO-1979 earthquake data was derived by Werner et al (1987). Dodd (1986) estimated values of ζ as large as 18% for the same data.

5.3 CONCLUSIONS

The empirical data strongly suggest that damping ratios $\zeta > 0.05$ are justified in cases where the soil-structure interaction is significant. However, because no physically-based model for estimating modal damping is available, the use of damping ratios higher than the traditional 5% value should be conservatively established and confined to bridges with a small number of spans, i.e. 1 to 3, where higher damping values have been measured.

6.0 RECOMMENDATIONS

6.1 FOUNDATION STIFFNESS

Based on the methods to estimate the stiffnesses of pile foundations, footings, and abutment systems that were evaluated in this report, we recommend that WSDOT use either the ones developed by Novak or FHWA. The Novak method is preferred slightly over the FHWA method because it is easier to implement; however, WSDOT is more familiar with the FHWA approach for piles because it presently uses an approach by Reese which is essentially equivalent to the FHWA Matlock-based approach.

The Novak method is particularly attractive from a user standpoint because it is contained within one computer program and can be used for piles, footings, and abutment walls. The Novak program can also compute foundation damping; this capability will become useful when a physically-based procedure for computing modal damping is developed in the future.

The FHWA method for piles is nonlinear, whereas Novak's method is linear. However, both approaches yielded similar results for the MRO earthquake case, assuming a soil shear modulus reduction of 50%. For severe cases of soil degradation, e.g. liquefaction, both approaches can be used by either specifying a residual strength or a very low shear modulus for the liquefied soil.

One attractive feature of the FHWA (and WSDOT) approach for piles is that the same computer program to estimate individual pile-head stiffnesses (i.e. BMCOL76) can be used to estimate the bending moments and deflections within the pile. Novak's program to estimate a pile-cap stiffness matrix could be used in conjunction with the BMCOL76 program (or its equivalent) to compute pile moments and deflections. However, if Novak's program is used to estimate the pile-cap stiffness matrix, then the compatibility check of pile-cap displacements, resulting from the dynamic analysis using SEISAB (or any other structural analysis program) and from the BMCOL76 (or its equivalent) program used for the pile-response analysis, would be of questionable value. Even if BMCOL76 is used to estimate the stiffness matrix, such a check is probably not warranted anyway, unless the relative displacement between the pile and soil is large enough to cause yielding in the soil adjacent to the pile.

In computing pile-head stiffnesses, we recommend that static (rather than dynamic) stiffnesses be calculated and pile-group effects be ignored. The passive resistance of an embedded pile cap should be included in the calculation of pile cap stiffness.

Static stiffnesses are also recommended for footings and the embedment of the footings should be considered in the stiffness estimate.

The methods recommended above are suggested for pile-supported or footing-supported abutments also. In calculating the overall abutment-system stiffness matrix, we recommend that the wingwalls be ignored. Shearing resistance of the abutment wall can also be ignored in the estimation of K_y, K_z, $K_{\theta x}$ for the abutment system. The passive resistance of the wall should be included in the calculation of K_x and $K_{\theta y}$, and can be included in the calculation of $K_{\theta z}$ at the user's discretion.

6.2 MODAL DAMPING

We recommend that modal damping ratios (ζ) greater than 5% only be used for bridges having 1 to 3 spans, where the total length of the bridge from one abutment to the other is less than about 250 ft. Although the data suggested some correlation between the modal deflection ratio θ and ζ (see Table 12), we recommend that ζ = 7½% be presently used for all transverse modes for which $\theta \geq 0.1$.

6.3 GEOTECHNICAL PARAMETERS

To characterize the soil, Novak's method only requires two linear (or equivalent linear) elastic properties (i.e. shear modulus and Poisson's ratio) and the soil density for each layer. Ideally, the shear modulus should be obtained from in-situ seismic velocity surveys or from published correlations between shear-wave velocity (or shear modulus) and Standard Penetration Test (SPT) values (Dobry et al, 1991). Reductions in shear modulus (G) for large shearing strains (γ) induced during strong ground motion should also be made before estimating the foundation stiffnesses. Curves relating G/G_{max} to γ can be found in the Dobry et al (1991) reference.

For most situations encountered in practice, the total soil density will vary between 90 and 130 pcf. In lieu of density measurements, a unit weight from the literature (e.g. Peck et al, 1974; Bowles, 1988), or a nominal value of 110 pcf is recommended unless the soil is loose saturated peat, for example, where densities as low as 70 pcf have been measured. In these extreme cases, the user should select a density based on judgment if soil samples are not available for direct measurement.

If the FHWA approach for piles is used, then soil-strength parameters (e.g. friction angle for sands, ϕ, and undrained shear strength for clays, c) and the friction coefficient between the pile and soil (δ) are required for each layer. If these properties are not measured, then they can be obtained from correlations in the literature. For example, values of ϕ for sand can be read from Figure 22, page 59, of the Volume II FHWA report (Lam and Martin, 1986). Values of c can be estimated by dividing by 2 the unconfined compressive strength values listed in Table 1.5, p. 20, of Peck et al (1974). Values of δ can be found in API RP2A (1991) or NAVFAC DM 7.02 (NAVFAC, 1986). Once these parameter values have been estimated or measured, then we suggest that procedures in API RP2A (1991) be used to develop the p-y, t-z, and Q-z curves.

7.0 REFERENCES

API RP 2A, 1991, "API Recommended Practice for Planning, Designing and Constructing Fixed Offshore Platforms," 19th edition, American Petroleum Institute, Washington, D.C.

Bowles, J.E., 1988, Foundation Analysis and Design, 4th edition, McGraw-Hill, 1004 p.

Broms, B.B., 1964a, "Lateral Resistance of Piles in Cohesionless Soils," Journal of the Soil Mechanics and Foundations Division, ASCE, Vol. 90, No. SM3, Paper 3909, May, pp. 123-156.

Broms, B.B., 1964b, "Lateral Resistance of Piles in Cohesive Soils," Journal of the Soil Mechanics and Foundations Division, ASCE, Vol. 90, No. SM2, Proc. Paper 382S, March, pp. 27-63.

Crouse, C.B., B. Hushmand, and G.R. Martin, 1987, "Dynamic Soil-Structure Interaction of a Single-Span Bridge," Journal of Earthquake Engineering and Structural Dynamics, Vol. 15, pp. 711-729.

Crouse, C.B., and L. Cheang, 1987, "Dynamic Testing of Pile-Group Foundations," Dynamic Response of Pile Foundations," Experiment, Analysis, and Observation, ASCE Geotechnical Special Publication No. 11, pp. 79-98.

Crouse, C.B., and B. Hushmand, 1987, "Estimation of Bridge Foundation Stiffnesses from Forced Vibration Data," Proceedings, 3rd International Conference on Soil Dynamics, and Earthquake Engineering, Princeton University, Princeton, N.J., June.

Crouse, C.B., and B. Hushmand, 1989, "Soil-Structure Interaction at CDMG and USGS Accelerograph Stations," Bull. Seism. Soc. Am., Vol. 79, pp. 1-14.

Crouse, C.B., and B. Hushmand, 1990, "Soil-Structure Interaction, and Nonlinear Site Response at the Differential Array Accelerograph Station," Proceedings, Fourth U.S. National Conference on Earthquake Engineering, Vol. 3, pp. 815-823.

Dobry, R., et al., 1991, "Low-, and High-Strain Cyclic Material Properties," Proceedings, NSF/EPRI Workshop on Dynamic Soil Properties, and Site Characterization, Vol. 1, Chap. 3, pp. 1-100.

Dodd, L.L., 1986, "The Use of Simple Models to Analyze the Meloland Road Overcrossing Subjected to the 1979 Imperial Valley Earthquake," M.S. Thesis, Civil Engineering Dept., Univ. Nevada at Reno, 177 p.

Dominquez, J., 1978, "Dynamic Stiffness of Rectangular Foundations," Department of Civil Engineering, Report No. R78-20, Massachusetts Institute of Technology, Cambridge, Massachusetts.

Douglas, B.M., C.B. Crouse, S.D. Werner, and E.A. Maragakis, 1992, "Quick-Release Dynamic Tests of the Meloland Road Overcrossing," University of Nevada at Reno, Center for Earthquake Engineering, Research Report, under preparation.

Douglas, B.M., E.A. Maragakis, and S. Vrontinos, 1991, "Parameter Identification Studies of the Meloland Road Overcrossing," Proceedings, Pacific Conference on Earthquake Engineering, Vol. 1, pp. 105-116.

Douglas, B.M., E.A. Maragakis, S. Vrontinos, and B.J. Douglas, 1990, "Analytical Studies of the Static and Dynamic Response of the Meloland Road Overcrossing," Proceedings, Fourth U.S. National Conference on Earthquake Engineering, Vol. 1, pp. 987-992.

Douglas, B.M., G.M. Norris, L. Dodd, and J. Richardson, 1984, "Behavior of Meloland Road Overcrossing During the 1979 Imperial Valley Earthquake," Proceedings, Seismic Research for Highway Bridges (U.S.-Japan Program), Department of Civil Engineering, University of Pittsburgh, Pittsburgh, Pennsylvania, 686 pp.

Douglas, B.M., and W.H. Reid, 1982, "Dynamic Tests and System Identification of Bridges," Journal of the Structural Division, ASCE, Vol. 108, pp. 2295-2312.

Finn, W.D.L., 1963, "Boundary Value Problems of Soil Mechanics," ASCE Journal of Soil Mechanics and Foundations Division, Vol. 89, Part 1, pp. 39-72.

Gazetas, G., 1983, "Analysis of Machine Foundation Vibration: State of the Art," Journal of Soil Dynamics and Earthquake Engineering, Vol. 2, No. 1, pp. 2-42.

Gazetas, G., 1991, "Foundation Vibrations," Foundation Engineering Handbook, 2nd Edition, H.Y. Fang, ed, Van Nostrand Reinhold, pp. 553-593.

Hansen, R.J., ed., 1970, Seismic Design for Nuclear Power Plants, The MIT Press, Cambridge, Mass.

Hetenyi, M., 1946, "Beams on Elastic Foundations," University of Michigan Press.

Lam, I.P., and G.R. Martin, 1986, "Seismic Design of Highway Bridge Foundations," FHWA Report Nos. FHWA/RD-861, FHWA/RD-86/102, and RHWA/RD-86/103.

Lam, I.P., G.R. Martin, and R. Imbsen, 1991, "Modeling Bridge Foundations for Seismic Design, and Retrofitting," Transportation Research Record 1290, Vol. 2, pp. 113-126.

Luco, J.E., 1981, "Linear Soil-Structure Interaction," Report UCRL-15272, PSA #7249809, Lawrence Livermore Laboratory, Livermore, California.

Lysmer, J., 1965, "Vertical Motions of Rigid Footings," Ph.D. thesis, University of Michigan, Ann Arbor.

Martin, G.R., and I.P. Lam, 1985, "Seismic Design Procedures for Bridge Foundations," Proceedings, Second Joint U.S.-New Zealand Workshop on Seismic Resistance of Highway Bridges, Applied Technology Council, ATC-12-1, pp. 129-146.

Werner, S.D., J.L. Beck, and M.B. Levine, 1987, "Seismic Response Evaluation of Meloland Road Overpass Using 1979 Imperial Valley Earthquake Records." Journal of Earthquake Engineering and Structural Dynamics, Vol. 15, pp. 249-274.

Werner, S.D., J.L. Beck, and A. Nisar, 1990, "Dynamic Tests, and Seismic Excitation of a Bridge Structure," Proceedings, Fourth U.S. National Conference on Earthquake Engineering, Vol. 1, pp. 1037-1046.

Whitman, R.V., 1976, "Soil-Platform Interaction," Proceedings, Conference on Behavior of Offshore Structures, NGI, Oslo, Vol. 1, p. 817.

Wilson, J.C., 1988, "Stiffness of Non-skew Monolithic Bridge Abutments for Seismic Analysis," Journal of Earthquake Engineering and Structural Dynamics, Vol. 16, pp. 867-883.

Wilson, J.C., and B.S. Tan, 1990, "Bridge Abutments: Formulation of a Simple Model for Earthquake Response Analysis," Journal of Engineering Mechanics, ASCE, Vol. 116, pp. 1828-1837.

Wong, H.L., and J.E. Luco, 1978, "Tables of Impedance Functions and Input Motions for Rectangular Foundations," Department of Civil Engineering, Report No. CE78-15, University of Southern California, Los Angeles, CA, 92 p.

Wong, H.L., and J.E. Luco, 1985, "Tables of Impedance Functions for Square Foundations on Layered Media," Journal of Soil Dynamics and Earthquake Engineering, Vol. 4, pp. 64-81.

Wood, J.H., 1985, "Earthquake Pressures on Monolithic Bridge Abutment Walls," Report No. M1.85/3, Central Laboratories, Lower Hutt, New Zealand.

Wood, J.H., and D.G. Elms, 1990, "Bridge Design, and Research Seminar; Volume 2: Seismic Design of Bridge Abutments, and Retaining Walls," RRU Bulletin 84, Road Research Unit, Transit, New Zealand, 90 p.

Table 1. Meloland Road Overpass Foundation Stiffness and Natural Frequency Values - Vibration Test

			Observed Experimental Values	Piles Only				Piles + Footing				Piles + Footing Side Soil
				FWA	Norwk	Lam. + Chords	Combs	FWA	Norwk	Lam. + Chords	Combs	Norwk
Pier	K_y	lb/ft	7.0E+07 (4.2-9.3E7)	7.8E+07	9.1E+07	6.8E+06	9.8E+06	1.6E+08	1.8E+08	9.1E+07	1.3E+08	1.3E+08
	K_z	lb/ft	2.0E+08 (1.3-2.0E8)	3.0E+08	3.8E+08	—	9.7E+08	3.9E+08	4.9E+08	—	9.7E+08	3.9E+08
	K_{tx}	lb-ft/rad	3.0E+10 (0.3-6.8E10)	7.3E+09	7.2E+09	—	1.6E+10	1.3E+10	1.3E+10	—	2.3E+10	1.0E+10
Abutment	K_y	lb/ft	3.0E+07 (2.5-3.8E7)	3.4E+06	3.4E+07	1.3E+06	3.2E+06	7.2E+07	8.5E+07	7.0E+07	1.0E+08	4.8E+07
	K_z	lb/ft	6.0E+07 (5.5-7.2E7)	4.5E+07	1.9E+08	—	5.7E+08	1.1E+08	2.3E+08	—	6.6E+08	1.9E+08
	K_{tx}	lb-ft/rad	2.0E+10 (1.0-2.6E10)	5.2E+09	2.1E+10	—	6.5E+10	1.8E+10	2.9E+10	—	7.7E+10	2.3E+10
	K_{ty}	lb-ft/rad	2.0E+09 (2.0 E9)	0.0E+00	0.0E+00	—	0.0E+00	3.9E+08	3.3E+08	—	6.6E+08	1.7E+08
	K_{tz}	lb-ft/rad	4.0E+10 (0.8-4.0E10)	3.8E+08	4.0E+09	—	3.8E+08	1.1E+10	1.4E+10	—	3.5E+10	8.3E+09
Modal Frequency	f_1	Hz	3.2	2.6	3.5	—	2.2	3.5	3.8	—	3.9	3.7
	f_2	Hz	3.4	2.8	3.4	—	3.1	3.5	3.6	—	3.5	3.5
	f_3	Hz	4.7	4.2	4.5	—	4.4	4.5	4.6	—	4.6	4.6
	f_4	Hz	6.6	5.1	7.0	—	5.2	7.5	7.7	—	7.6	7.5

Table 2. Meloland Road Overpass Foundation Stiffness and Natural Frequency Values - 1979 Earthquake

			Observed Experimental Values	Piles Only				Piles + Footing				Piles + Footing Side Soil
				FWA	Norwk	Lam. + Chords	Combs	FWA	Norwk	Lam. + Chords	Combs	Norwk
Pier	K_y	lb/ft	—	3.6E+07	5.3E+07	3.5E+06	6.3E+06	7.8E+07	9.6E+07	4.6E+07	6.5E+07	7.2E+07
	K_z	lb/ft	—	3.9E+07	2.7E+08	—	4.4E+08	8.6E+07	3.0E+08	—	4.9E+08	2.7E+08
	K_{tx}	lb-ft/rad	2.8E+08	1.6E+09	5.1E+09	—	8.0E+09	4.6E+09	8.1E+09	—	1.2E+10	6.6E+09
Abutment	K_y	lb/ft	1.1E+07	1.3E+06	2.0E+07	1.0E+06	2.0E+06	3.6E+07	4.6E+07	3.5E+07	5.0E+07	2.7E+07
	K_z	lb/ft	2.9E+07	9.2E+06	1.3E+08	—	2.9E+08	4.2E+07	1.5E+08	—	3.3E+08	1.3E+08
	K_{tx}	lb-ft/rad	—	1.0E+09	1.5E+10	—	3.2E+10	5.7E+09	1.8E+10	—	3.8E+10	1.5E+10
	K_{ty}	lb-ft/rad	—	0.0E+00	0.0E+00	—	0.0E+00	1.9E+08	1.7E+08	—	3.4E+08	8.7E+07
	K_{tz}	lb-ft/rad	—	1.5E+08	2.3E+09	—	2.3E+08	5.7E+09	7.4E+09	—	1.7E+10	4.5E+09
Modal Frequency	f_1	Hz	2.5	1.6	3.2	—	1.8	2.9	3.5	—	3.7	3.6
	f_3	Hz	4.6	3.4	4.4	—	4.3	4.2	4.5	—	4.6	4.6

*Modal frequencies correspond to the following mode shapes.

1 : Fundamental Transverse
2 : First Antisymmetric Vertical
3 : First Symmetric Vertical
4 : Fundamental Torsional

Matlock, H., 1970, "Correlations for Design of Laterally Loaded Piles in Soft Clay," Proceedings, 2nd Annual Offshore Technology Conference, Houston, Texas, OTC 1204.

Matlock, H., D. Bogard, and I.P. Lam, 1981, "BMCOL 76: A Computer Program for the Analysis of Beam-Columns Under Static Axial, and Lateral Loading," In-House Documentation Report, Ertec, Inc., June.

Matlock, H., and L.C. Reese, 1961, "Generalized Solutions for Laterally Loaded Piles," Journal of Soil Mechanics Division, ASCE, Vol. 86, pp. 673-694; also in Transactions, ASCE, Paper No. 3370, Vol. 127, Part I, 1962, pp.1120-1269.

NAVFAC, 1986, "Foundations and Earth Structures," NAVFAC DM 7.02, Dept. of Navy.

Norris, G.M., 1986a, "Evaluation of the Nonlinear Stabilized Rotational Stiffness of Pile Groups," Proceedings, 37th Highway Geology Symposium, Helena, Montana.

Norris, G.M., 1986b, "Nonstable Rotational Stiffness of a Pile Group," Proceedings, Third U.S. National Conference on Earthquake Engineering, pp. 635-646.

Norris, G.M., and R.L. Sackman, 1986, "Evaluation of the Lateral Stiffness of Pile Groups for Seismic Analysis of Highway Bridges: Parts A, and B," Proceedings, 22nd Symposium on Engineering Geology, and Soils Engineering, pp. 323-363.

Novak, M., 1974, "Dynamic Stiffness and Damping of Piles," Canadian Geotech. Journal, Vol 11, pp. 574-598.

Novak, M., M. Sheta, L. El-Hifnawy, H.El-Marsafawi, and O. Ramadan, 1991, "DYNA 3, A Computer Program for Calculation of Foundation Response to Dynamic Loads, User Manual," University of Western Ontario Geotechnical Research Centre, Report No. GEOP 90-02, Vol. 1, Rev. 2.

O'Neill, M.W., and J.M. Murchison, 1983, "An Evaluation of P-Y Relationships in Sands," Report to American Petroleum Institute, (PRAC 82-41-1).

Peck, R.B., W.E. Hanson, and T.H. Thornburn, 1974, Foundation Engineering, 2nd edition, John Wiley and Sons, Inc., 514 p.

Poulos, H.G., 1968, "Analysis of the Settlement of Pile Groups," Geotechnique, Vol. 18, London, England, pp. 449-471.

Poulos, H.G., 1971, "Behavior of Laterally-Loaded Piles II: Pile Groups," Journal of the Soil Mechanics and Foudnations Division, ASCE 97, SM5, pp. 773-751.

Poulos, H.G., 1971, "The Displacement of Laterally Loaded Piles: I-Single Piles," Journal of the Soil Mechanics and Foundations Division, ASCE, Vol. 97, No. SM5, Proc. Paper 8092, May, pp. 711-731.

Poulos, H.G., and E.H. Davis, 1980, Pile Foundation Analysis and Design. New York: John Wiley and Sons, Inc., 411 p.

Reese, L.C., and W.R. Cox, 1975, "Field Testing, and Analysis of Laterally Loaded Piles in Stiff Clay," Proceedings, Offshore Technology Conference, OTC 2312.

Roesset, J.M., R.V. Whitman, and R. Dobry, 1973, "Modal Analysis for Structures with Foundation Interaction," ASCE Journal of Structural Division, Vol. 99, pp. 399-416.

Richart, F.E., and Whitman, R.V., 1967, "Comparison of Footing Vibration Tests with Theory," Journal of Soil Mechanics and Foudnations Division, Vol. 93, pp. 143-168.

Richart, F.E. Jr., J.E. Hall Jr., and R.D. Woods, 1970, "Vibrations of Soils and Foundations," Prentice-Hall International, Inc., New Jersey.

Table 3. Rose Creek Foundation Stiffness Values - Vibration Test

		Observed Experimental Values	Piles Only				Piles + Footing				Piles + Footing Side
			FHWA	Nowak	Lam - Charts	Gazetas	FHWA	Nowak	Lam - Charts	Gazetas	Nowak
Pier 1:	K_y (k/in)	1825 (1700-2100)	917	1975	210	630	1480	2660	780	1630	2175
	K_{ox} (k in/rad)	6.3E+07 (5.4 - 7.0E7)	4.6E+07	5.4E+07	—	1.9E+07	4.9E+07	6.1E+07	—	3.6E+07	5.6E+07
Pier 2:	K_y (k/in)	7567 (3900-9800)	10000	2160	280	830	10600	4190	881	2160	2500
	K_{ox} (k in/rad)	7.3E+07 (6.0 - 9.8E7)	6.2E+07	4.9E+07	—	2.6E+07	6.6E+07	6.9E+07	—	3.7E+07	5.6E+07
Pier 3:	K_y (k/in)	5450 (4000-6000)	2830	5240	530	1400	3430	6100	1131	2320	5575
	K_{ox} (k in/rad)	9.1E+07 (6.5 - 13.5E7)	6.5E+07	7.7E+07	—	5.2E+07	6.9E+07	8.6E+07	—	6.4E+07	8.1E+07
Pier 4:	K_y (k/in)	1560 (1200-2100)	750	1970	210	630	1314	2920	780	1630	2200
	K_{ox} (k in/rad)	6.6E+07 (5.4 - 7.8E7)	3.2E+07	5.4E+07	—	1.7E+07	3.7E+07	6.1E+07	—	2.6E+07	4.2E+07

Table 4. Duwamish Power Station Static Stiffness and Fundamental Frequency Values - Vibration Test

			Observed Experimental Values	Piles Only		Piles + Footing		Piles + Footing Side
				FHWA	Nowak	FHWA	Nowak	Nowak
Bank 77	K_x	lb/ft	—	3.0E+07	6.3E+07	6.6E+07	9.3E+07	7.0E+07
	K_y	lb/ft	—	3.0E+07	6.3E+07	6.8E+07	9.3E+07	7.0E+07
	K_z	lb/ft	—	3.7E+08	4.3E+08	4.1E+08	4.6E+08	4.3E+08
	K_{ox}	lb-ft/rad	—	4.2E+09	4.8E+09	5.8E+09	6.1E+09	5.2E+09
	K_{oy}	lb-ft/rad	—	8.7E+09	9.9E+09	1.2E+10	1.3E+10	1.0E+10
	K_{oz}	lb-ft/rad	—	1.1E+09	2.4E+09	5.9E+09	6.2E+09	4.1E+09
	f_x	Hz	6.30	6.49	7.39	8.39	8.74	7.71
	f_y	Hz	5.80	4.35	6.15	6.11	7.04	6.34
Bank 79	K_x	lb/ft	—	7.1E+06	2.0E+07	3.1E+07	4.1E+07	2.4E+07
	K_y	lb/ft	—	7.1E+06	2.0E+07	3.2E+07	4.1E+07	2.4E+07
	K_z	lb/ft	—	1.2E+08	1.5E+08	1.4E+08	1.7E+08	1.5E+08
	K_{ox}	lb-ft/rad	—	7.2E+08	9.1E+08	1.2E+09	1.4E+09	1.0E+09
	K_{oy}	lb-ft/rad	—	1.7E+09	2.1E+09	2.7E+09	3.0E+09	2.3E+09
	K_{oz}	lb-ft/rad	—	1.5E+08	4.5E+08	1.1E+09	1.8E+09	1.0E+09
	f_x	Hz	4.60	3.18	4.32	5.08	5.47	4.59
	f_y	Hz	3.80	2.58	3.24	3.78	4.10	3.42

Table 5. Rose Creek Static Stiffness Values - Vibration Test (Novak results)

		Observed Experimental Value	No Group Interaction			Group Interaction		
			Pile Only	Pile + Footing	Pile + Footing, SVA	Pile Only	Pile + Footing	Pile + Footing, SVA
Pier 1:	K_y (k/in)	1825 (1700-2100)	1975	2660	2175	601	1286	803
	$K_{\theta x}$ (k-in/rad)	6.3E+07 (5.4 - 7.0E7)	5.4E+07	6.1E+07	5.6E+07	3.7E+07	4.4E+07	3.9E+07
Pier 2:	K_y (k/in)	7567 (3900-9800)	2160	4190	2500	509	2539	850
	$K_{\theta x}$ (k-in/rad)	7.3E+07 (6.0 - 9.8E7)	4.9E+07	6.9E+07	5.6E+07	3.0E+07	5.0E+07	3.4E+07
Pier 3:	K_y (k/in)	5450 (4000-6000)	5240	6100	5575	1200	2060	1540
	$K_{\theta x}$ (k-in/rad)	9.1E+07 (6.5 - 13.5E7)	7.7E+07	8.6E+07	8.1E+07	4.6E+07	5.5E+07	4.9E+07
Pier 4:	K_y (k/in)	1560 (1200-2100)	1970	2920	2200	516	1466	750
	$K_{\theta x}$ (k-in/rad)	6.6E+07 (5.4 - 7.8E7)	5.4E+07	6.1E+07	4.2E+07	2.6E+07	3.3E+07	2.8E+07

Table 6. Duwamish Power Station Static Stiffness and Fundamental Frequency Values - Vibration Test (Novak results)

			Observed Experimental Value	No Group Interaction			Group Interaction		
				Pile Only	Pile + Footing	Pile + Footing, SVA	Pile Only	Pile + Footing	Pile + Footing, SVA
Bank 77:	K_x	lb/ft	—	6.3E+07	9.3E+07	7.0E+07	2.1E+07	5.1E+07	2.7E+07
	K_y	lb/ft	—	6.3E+07	9.3E+07	7.0E+07	2.1E+07	5.1E+07	2.7E+07
	K_z	lb/ft	—	4.3E+08	4.6E+08	4.3E+08	9.2E+07	1.3E+08	9.5E+07
	$K_{\theta x}$	lb-ft/rad	—	4.8E+09	6.1E+09	5.2E+09	3.8E+09	5.1E+09	4.2E+09
	$K_{\theta y}$	lb-ft/rad	—	9.9E+09	1.3E+10	1.0E+10	6.4E+09	9.0E+09	7.0E+09
	$K_{\theta z}$	lb-ft/rad	—	2.4E+09	6.2E+09	4.1E+09	1.3E+09	5.1E+09	3.0E+09
	f_x	Hz	6.30	7.39	8.74	7.71	4.86	6.90	5.45
	f_y	Hz	5.80	6.15	7.04	6.34	4.49	5.99	4.87
Bank 79:	K_x	lb/ft	—	2.0E+07	4.1E+07	2.4E+07	1.1E+07	3.2E+07	1.5E+07
	K_y	lb/ft	—	2.0E+07	4.1E+07	2.4E+07	1.1E+07	3.2E+07	1.6E+07
	K_z	lb/ft	—	1.5E+08	1.7E+08	1.5E+08	6.1E+07	8.4E+07	6.3E+07
	$K_{\theta x}$	lb-ft/rad	—	9.1E+08	1.4E+09	1.0E+09	1.2E+09	1.6E+09	1.3E+09
	$K_{\theta y}$	lb-ft/rad	—	2.1E+09	3.0E+09	2.3E+09	2.4E+09	3.3E+09	2.6E+09
	$K_{\theta z}$	lb-ft/rad	—	4.5E+08	9.1E+08	1.0E+09	3.8E+08	8.4E+08	9.4E+08
	f_x	Hz	4.60	4.32	5.47	4.59	3.89	5.41	4.32
	f_y	Hz	3.80	3.24	4.10	3.42	3.27	4.26	3.54

Table 7. Horsethief Canyon Underpass Static Stiffness and Natural Frequency Values - Vibration Test

		Observed Experimental Values	CANA	Novak	Quazaks	Wong & Luco
Footing	K_x lb/ft	2.7E+08	1.8E+08	1.4E+08	2.8E+08	1.3E+08
	K_y lb/ft	1.7E+08	1.8E+08	1.4E+08	2.4E+08	1.2E+08
	K_z lb/ft	3.6E+08	1.9E+08	1.5E+08	2.5E+08	1.6E+08
	$K_{\theta x}$ lb ft/rad	1.4E+11	1.0E+11	9.0E+10	1.3E+11	4.2E+10
Modal Frequency	f_1 Hz	4.7	4.52	4.28	4.51	4.29
	f_2 Hz	6.4	6.27	5.80	6.34	5.71
	f_3 Hz	8.2	9.21	8.58	10.62	8.17
	f_4 Hz	10.6	11.01	11.13	11.02	11.02
	f_5 Hz	14	12.85	11.66	13.28	11.77

- Modal frequencies correspond to the following mode shapes.
  1 : Fundamental Vertical
  2 : Torsional with small transverse footing displacements
  3 : Torsional with large transverse footing displacements
  4 : Symmetric Slab Mode
  5 : Second Vertical

Table 8. Differential Array Static Stiffness and Fundamental Frequency Values -Earthquake (Modulus Reduction = 0.5)

		Observed Experimental Values	Full Footing Footprint				Perimeter Foundation Only			
			FEM	Novak	Barkan	Wong & Luco	FEM	Novak	Barkan	Wong & Luco
K_x	lb/ft	—	1.7E+07	1.4E+07	1.8E+07	1.2E+07	2.9E+06	2.9E+06	3.1E+06	2.9E+06
K_z	lb/ft	—	1.7E+07	1.6E+07	1.7E+07	1.5E+07	3.8E+06	3.6E+06	3.8E+06	3.7E+06
K_{xy}	lb ft/rad	—	4.7E+08	2.8E+08	3.3E+08	2.1E+08	3.1E+08	1.7E+08	1.7E+08	1.2E+08
K_{yz}	lb ft/rad	—	5.5E+08	4.8E+08	6.0E+08	2.8E+08	2.9E+08	2.5E+08	3.0E+08	1.6E+08
K_{xz}	lb	—	0.0E+00	2.0E+07	8.8E+06	4.3E+06	0.0E+00	1.7E+07	1.6E+06	1.9E+06
f	Hz	8.70	15.39	14.23	14.41	11.53	8.08	7.25	7.94	7.40

Table 9. Differential Array Static and Dynamic Stiffness and Fundamental Frequency Values - Vibration Test (Perimeter Foundation Only)

		Observed Experimental Values	Static Values				Values at f=12Hz		
			FEM	Novak	Barkan	Wong & Luco	Novak	Barkan	Wong & Luco
K_x	lb/ft	---	5.8E+06	5.8E+06	6.2E+06	5.8E+06	5.7E+06	6.5E+06	5.8E+06
K_z	lb/ft	---	7.5E+06	7.2E+06	7.5E+06	7.4E+06	7.3E+06	7.3E+06	7.2E+06
K_{xy}	lb ft/rad	---	6.2E+08	3.3E+08	3.4E+08	2.4E+08	2.8E+08	3.0E+08	2.3E+08
K_{yz}	lb ft/rad	---	5.8E+08	5.0E+08	6.0E+08	3.2E+08	5.0E+08	5.7E+08	3.1E+08
K_{xz}	lb	---	0.0E+00	3.5E+07	3.2E+06	3.7E+06	0.0E+00	3.2E+06	4.5E+06
f	Hz	12.00	11.43	10.25	11.23	10.47	10.21	11.13	10.46

Table 10. Meloland Road Overpass Static Stiffness Values - Vibration Test (no pile group interaction)

		Observed Experimental Values	Piles Only	Piles + Footing Side	Retaining Wall			
			Novak	Novak	FHWA	Lam – Charts	Wilson	Wood
Abutment	K_x lb/ft	---	3.4E+07	4.8E+07	2.0E+08	4.2E+08	3.6E+08	2.2E+08
	$K_{\theta y}$ lb-ft/rad	2.0E+09 (2.0 E9)	0.0E+00	1.7E+08	7.1E+09	---	2.6E+10	1.2E+10
	$K_{\theta z}$ lb-ft/rad	4.0E+10 (0.8-4.0E10)	4.0E+09	8.3E+09	1.9E+10	4.0E+10	7.7E+10	2.1E+10

Table 11. Horsethief Canyon Underpass Static Stiffness Values - Vibration Test

		Observed Experimental Values	Retaining Wall			
			FHWA	Lam – Charts	Wilson	Wood
Abutment Wall	K_x lb/ft	1.9E+08	1.6E+08	2.8E+08	2.2E+08	1.7E+08
	$K_{\theta y}$ lb ft/rad	---	8.6E+09	---	1.5E+10	1.3E+10
	$K_{\theta z}$ lb ft/rad	---	6.4E+10	1.1E+11	1.7E+11	6.8E+10

TABLE 12
MODAL DAMPING RATIOS FOR TRANSVERSE MODES OF VIBRATION OF BRIDGES

Bridge Test Case	Transverse Mode No.	Natural Frequency	Modal Deflections			Modal Damping	θ
			$\bar{R}_a^t$	R_d^t	R_d^v		
1. MRO-vib. (21 kip load)	1	3.3 Hz	0.11	0.31	0.18	6.2%	0.22
	2	12.7	0.029	0.096	0.30	8.8	0.073
	3	22.1	~0	0.19	0.38	3.2	~ 0
2. MRO-vib. (141 kip load)	1	3.2 Hz	0.094	0.33	0.14	6.5%	0.2
	2	13.2	0.02	0.10	0.32	11.6	0.05
	3	22.4	~0	0.96	0.34	3.4	~ 0
3. MRO-1979 EQ	1	2.5 Hz	0.66	1.0	0.37	7.2%	0.48
4. Horsethief	1	6.4 Hz	< 0.01	0.03	0.27	3.5%	~ 0
	2	8.2	0.8	1.25	0.39	15.0	0.49
5. Moses Lake (Test 1)	1	6.6 Hz	0.31	1.0	0.22	9.1%	0.25
	2	7.4	0.26	1.0	0.45	6.8	0.18
6. Moses Lake (Test 2)	1	6.5 Hz	0.24	1.0	0.26	6.2%	0.19
	2	7.1	0.40	1.0	0.42	8.5	0.28

$\bar{R}_a^t$ = average transverse deflection of abutments

R_d^t = maximum transverse deflection of deck

R_d^v = maximum vertical deflection of deck

$\theta = \bar{R}_a^t/(R_d^t + R_d^v)$

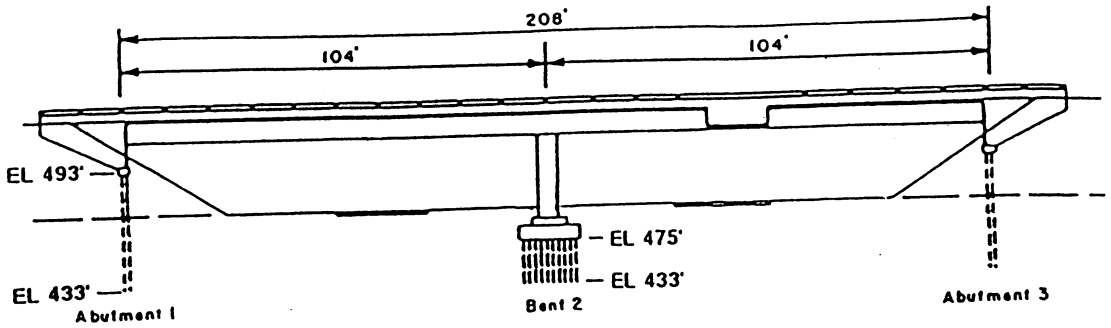

ELEVATION
No Scale

Abutment Soil Profile

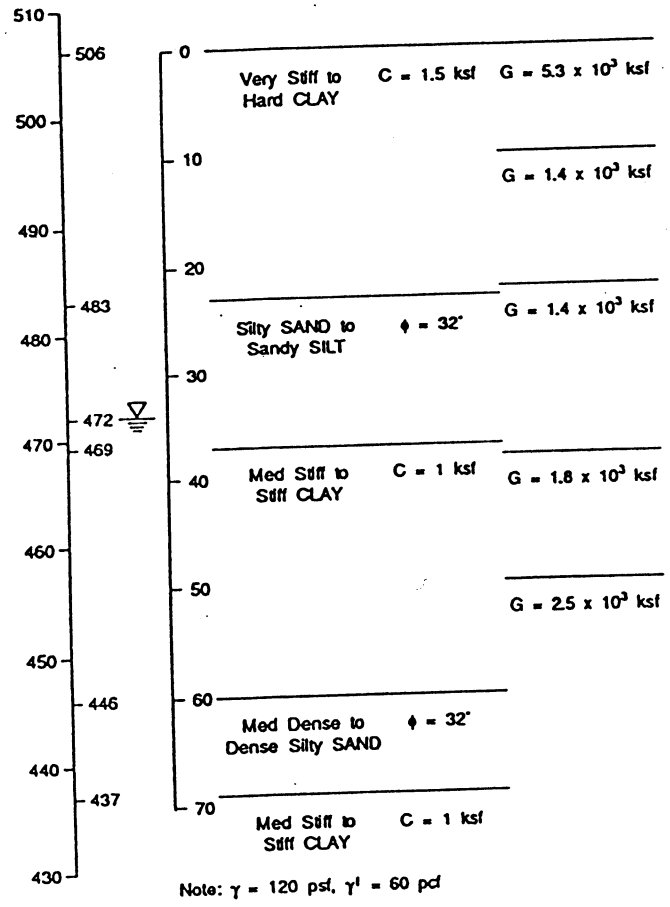

Pier Soil Profile

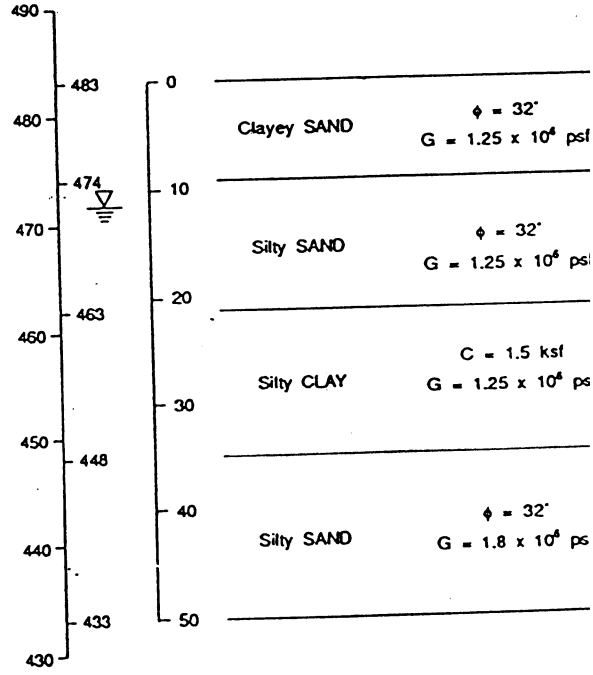

Reference: Douglas et al (1992), Martin and Lam (1985)

Symbols: γ = total unit weight, γ' = submerged unit we
ϕ = internal friction angle, c = cohesion,
G = low-strain shear modulus

Figure 1
Meloland Road Overcrossing Bridge and Soil Profiles

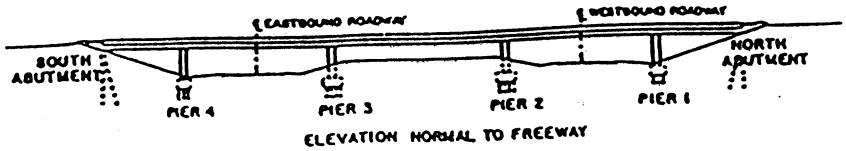

ELEVATION NORMAL TO FREEWAY

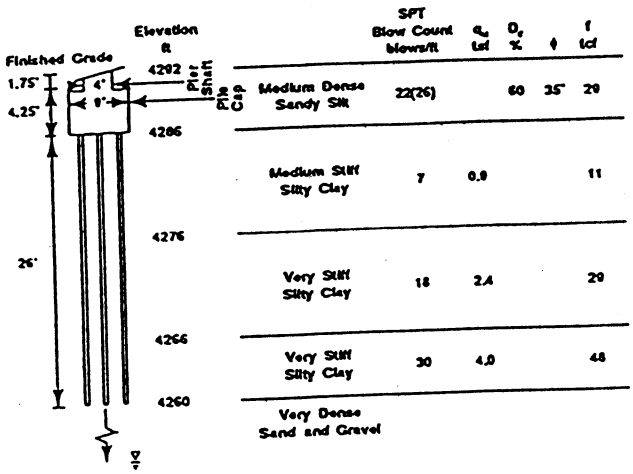

SOIL PROFILE FOR PILE GROUP 1

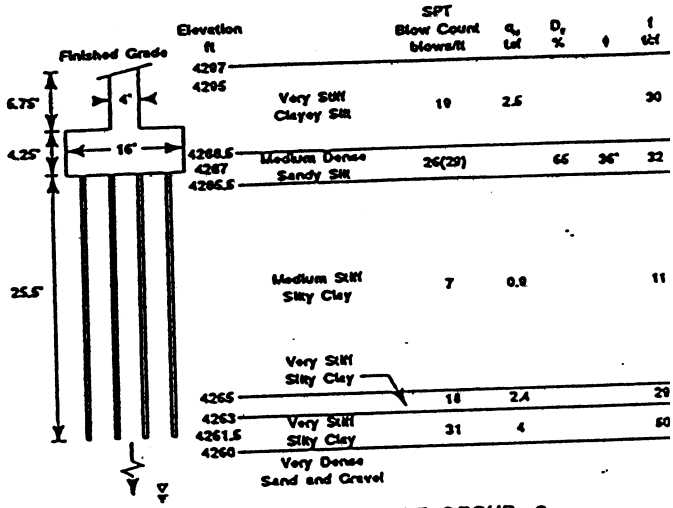

SOIL PROFILE FOR PILE GROUP 2

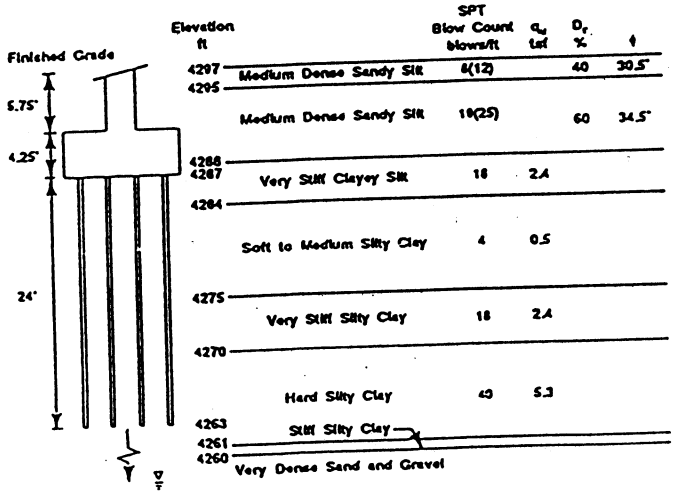

SOIL PROFILE FOR PILE GROUP 3

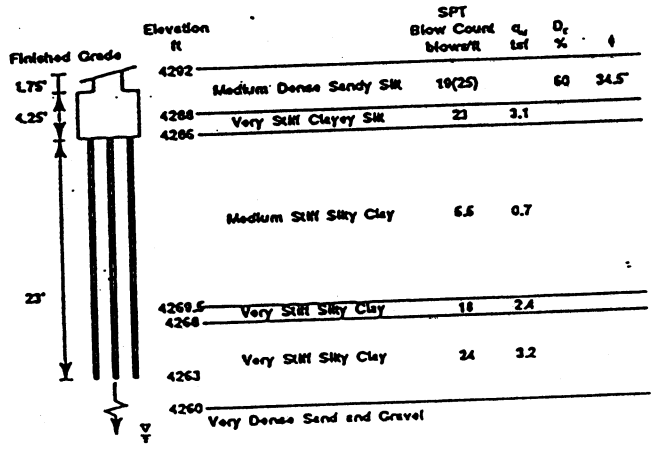

SOIL PROFILE FOR PILE GROUP 4

Symbols: q_u = Unconfined compressive strength, D_r = relative density,
ϕ = internal friction angle, f = constant of subgrade moulus variation

References: Douglas and Reid (1982), Norris and Sackman (1986), Norris (1986a).

Figure 2
Rose Creek Bridge Foundations and Soil Profiles

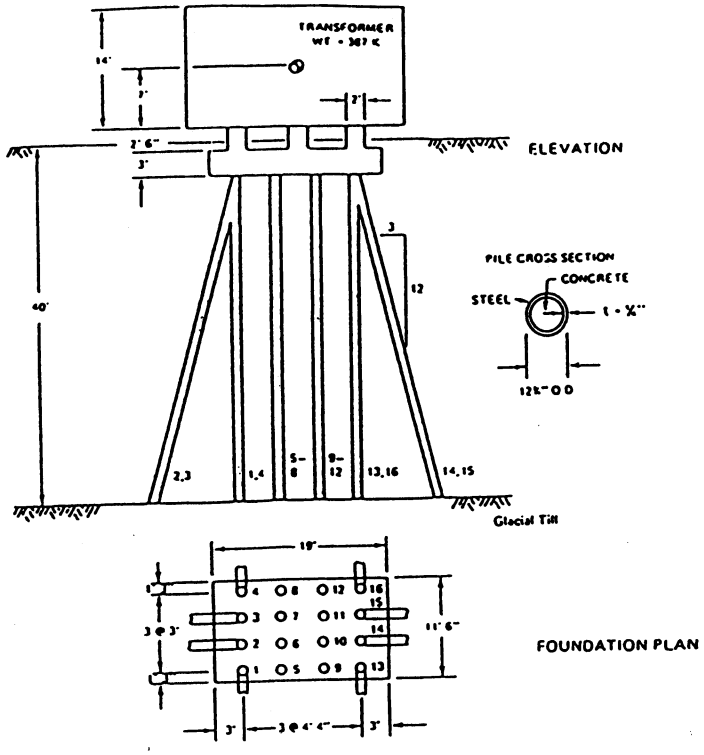

TRANSFORMER BANK 77.

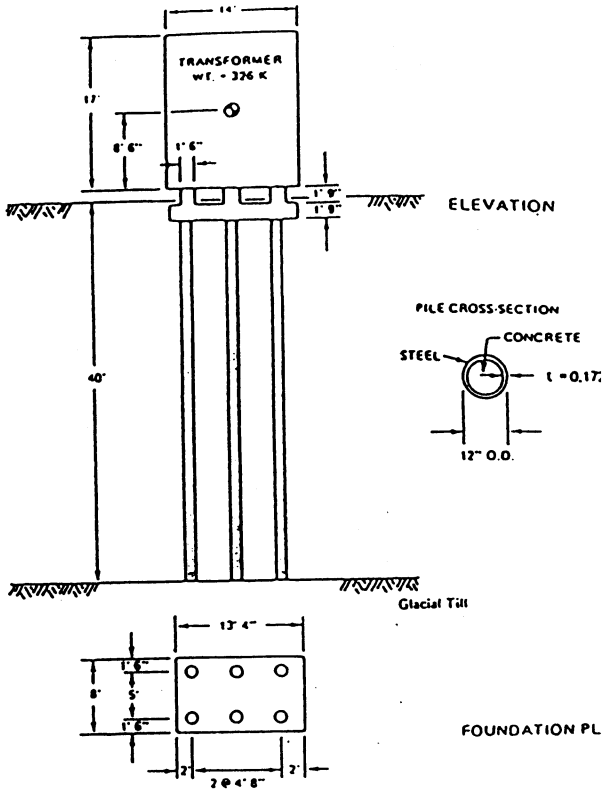

TRANSFORMER BANK 79.

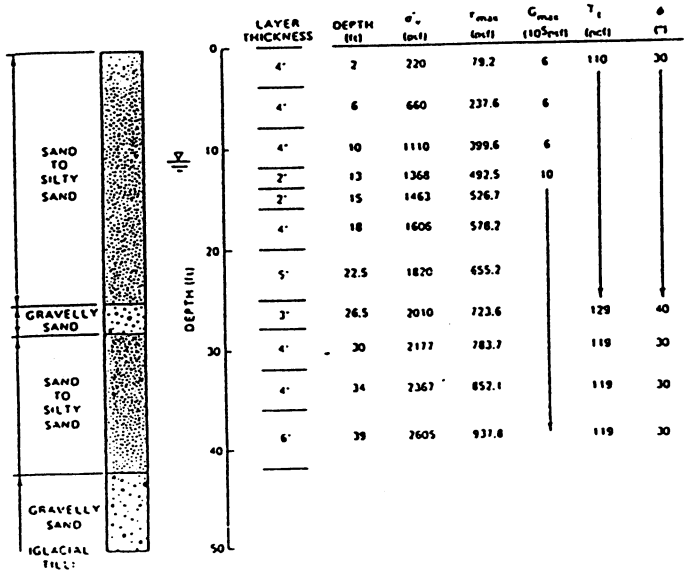

SYMBOLS

σ'_v = VERTICAL CONFINING STRESS

τ_{max} = SHEAR STRENGTH

G_{max} = LOW STRAIN SHEAR MODULUS

γ_t = TOTAL DENSITY

ϕ = INTERNAL FRICTION ANGLE

IDEALIZED SOIL PROFILE

Reference: Crouse and Cheang (1987)

Figure 3
Duwamish Transformer Foundations and Soil Profile

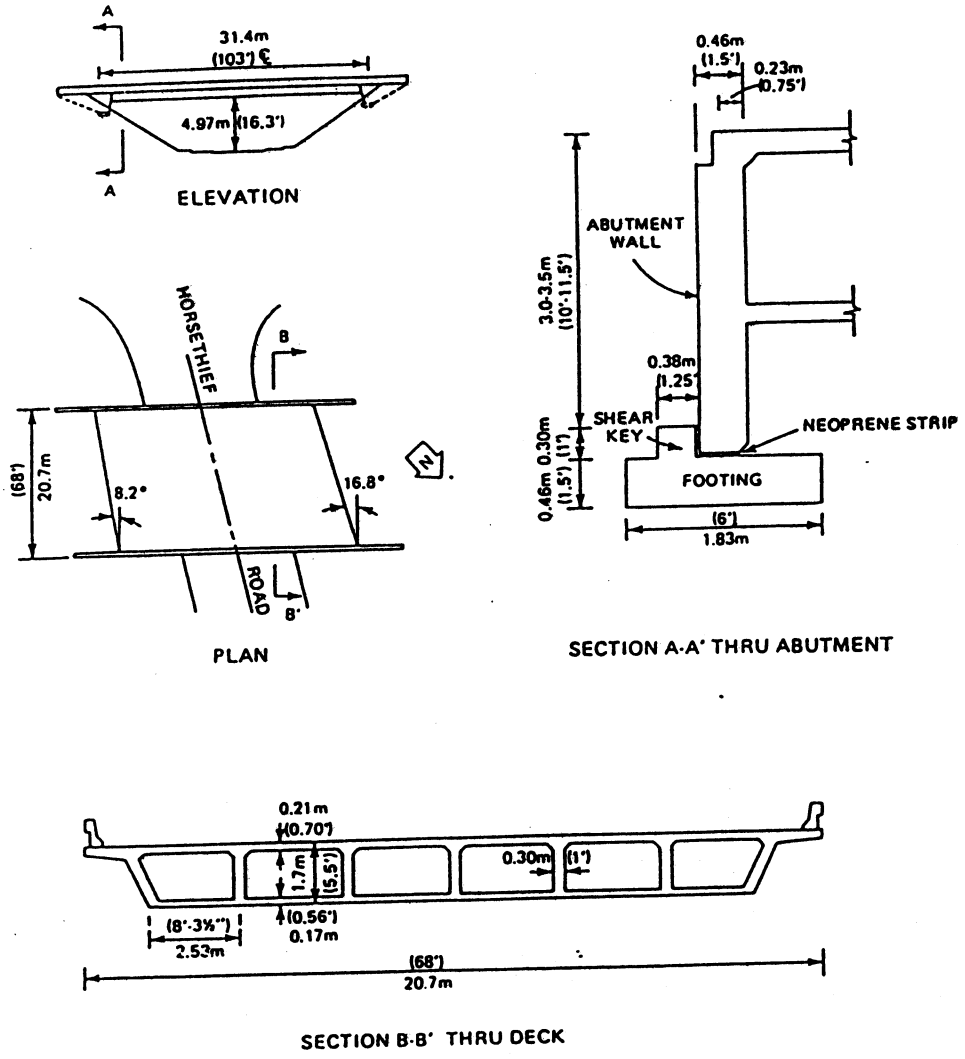

Reference: Crouse et al (1987)

Figure 4

Horsethief Road Undercrossing Bridge

DAMES & MOORE

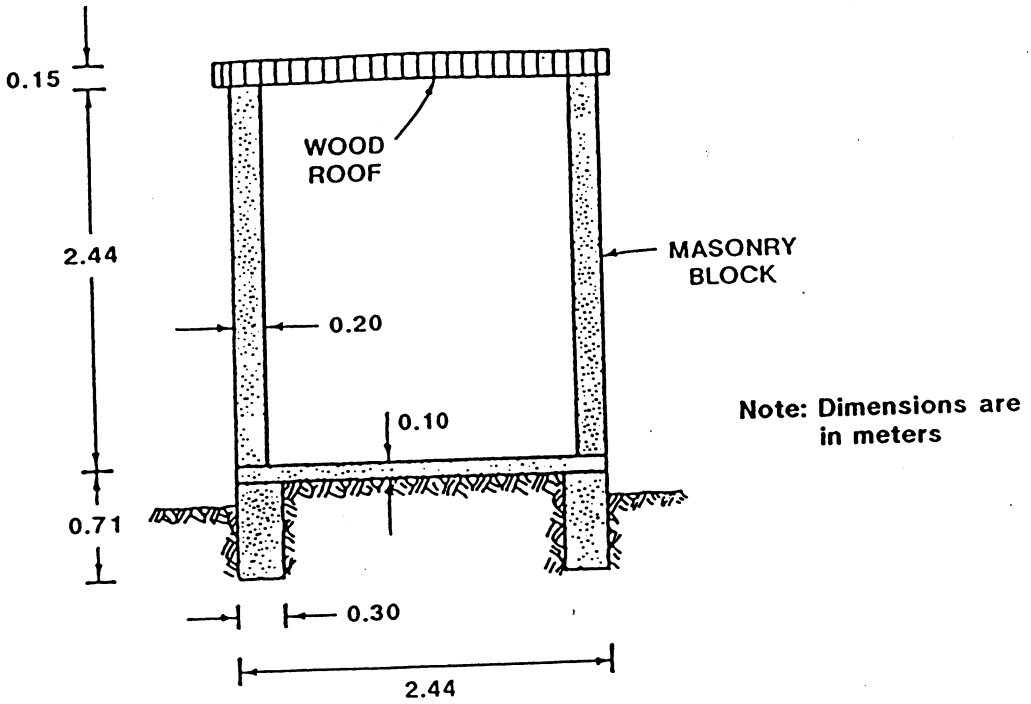

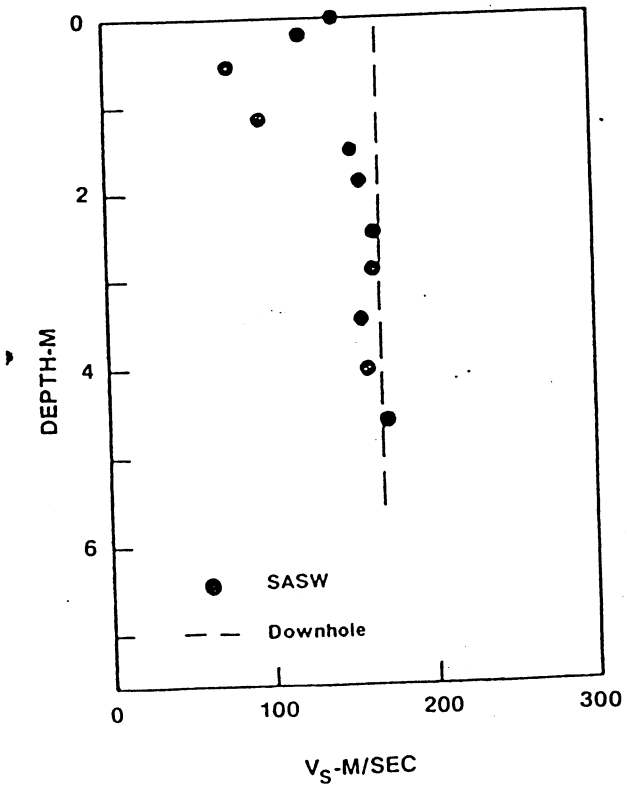

Reference: Crouse and Hushmand (1989)

Figure 5

Differential Array Accelerograph Station

APPENDIX A

METHODS TO COMPUTE FOUNDATION STIFFNESS AND DAMPING

METHODS TO COMPUTE FOUNDATION STIFFNESS AND DAMPING

Foundation Type	Method Author	Method Type: Linear/ Nonlinear	Method Type: Static/ Dynamic	Soil Model	Foundation Model	Boundary Conditions	Solution Obtained by	Input Parameters	Output Parameters	Advantages (A)/Limitations (L)	References
I. Single Vertical Pile	1. Novak	Linear	Dynamic	Linear, viscoelastic, isotropic, horizontal layers over ½ space	Linear, elastic beam model of pile with constant or variable cross-section.	• Welded contact between soil and pile • Fixed or pinned connection between pile and cap.	Computer program PILAY 2. PC version available	• pile: E, I, d, L for ea. pile segment • soil: G, ρ, υ, β, h for each soil layer • fixity condition of pile head and tip where: E= Young's modulus I = moment of inertia d= diameter L= length G= shear modulus ρ= density υ= Poisson's ratio β= damping ratio h= layer thickness.	6x6 pile head stiffness and damping matrix which is frequency dependent. Because of axial symmetry, lateral stiffnesses are equal ($K_x = K_y$) and rocking stiffnesses are equal ($K_x = K_y$). Associated off-diagonal terms are equal.	A: Only commercially available computer program to compute dynamic stiffness and dynamic damping matrices for pile head. A/L: Effect of gaping and nonlinear soil behavior can be approximately modeled, but only by adjusting linear stiffness and damping properties of soil. L: Constant values of stiffness must be selected from frequency dependent solutions by user for input to SEISAB.	User Manual by Novak et al (1990). Revised August 1991. This manual is for the more general program DYNA3, which incorporates the PILAY2 program. Other background references listed in manual.
	2. Matlock	Linear or nonlinear options available	Static	Load-deflection relationships or soil-resistance curves that model the interaction between the pile and soil for each increment of pile length. Relationships are linearly or nonlinearly elastic.	Linear, elastic beam model of pile with constant or variable cross section.	Fixed or pinned or arbitrary rotational restraint at head, tip, or along any segment of pile. Nonlinear springs representing soil resistance are attached to each pile segment.	Computer program BMCOL 76. PC version available.	• pile: E, I, A, L A = cross section area • soil resistance: p-y, t-z, Q-z curves • fixed, free or arbitrary rotational restraint at head or tip or along any segment of pile	Linear or nonlinear curves of lateral force vs. lateral deflection, axial force vs. axial deflection, and moment about horizontal axis vs. rotation.	A: Program can model nonlinear soil resistance. Procedures to specify soil resistance (p-y, t-z, Q-z) curves have been checked against pile-load test data. L: Method restricted to static loads (and thus, damping not computed). p=y, t-z, Q-z curves must be generated by user. Torsion not considered. Pile-head stiffnesses must be estimated by user.	User Manual by Matlock et al (1981)

METHODS TO COMPUTE FOUNDATION STIFFNESS AND DAMPING

Foundation Type	Method Author	Method Type: Linear/ Nonlinear	Method Type: Static/ Dynamic	Soil Model	Foundation Model	Boundary Conditions	Solution Obtained by	Input Parameters	Output Parameters	Advantages (A)/Limitations (L)	References
I. Single Vertical Pile	3. Reese	Nonlinear but user can input linear soil resistance curves	Static	Load-deflection relationships or soil-resistance curves that model the interaction between the pile and soil for each increment of pile length. Relationships are linearly or nonlinearly elastic.	Linear, elastic beam model of pile with constant or variable cross section.	• Fixed or pinned or arbitrary rotational restraint at pile head • Free condition at pile tip	Computer programs: • LPILE 3 (lateral loads & bending moments about horizontal axis). • APILE 2 (axial load) PC versions available	LPILE 3 • pile: E, I, d, L • soil resistance p-y curves • boundary conditions as described in column (7). Distributed lateral load can be applied along pile APILE 2 • pile: E, A, d, L • soil resistance t-z, Q-z curves	LPILE 3 • Linear or nonlinear curves of lateral force vs. lateral deflection, and moment about horizontal axis vs. rotation APILE • Linear or nonlinear curve of axial load vs. axial deflection	A: Programs can model nonlinear soil resistance. Procedures to specify soil resistance (p-y, t-z, Q-z) curves have been checked against pile-load test data. Programs can generate p-y, t-z, Q-z curves internally for select procedures. L: Methods restricted to static loads (and thus, damping not computed). Torsion not considered. Pile-head stiffnesses must be estimated by user from output.	LPILE 3 Public domain user manual for similar COM624P program published by FHWA, Rept. No. FHWA-SA-91-002. APILE 2 User manual published by ENSOFT
	4. Gazetas	Linear	Dynamic	Linear, viscoelastic isotropic, homogeneous or simple vertically heterogeneous layer over rock. Elastic modulus profiles are: (1) E_s = constant (2) $E_s = c\,z$ (3) $E_s = c\,\sqrt{z}$ where z = depth c = constant	Linear elastic beam model of cylindrical pile with constant cross section	• Welded contact between soil and pile • Free head condition • Floating pile (end bearing piles not considered)	Simple closed-form algebraic equations	• pile: E, d, L • soil: - $\bar{E}_s$ = elastic modulus at z = d - h, v,	5x5 pile head stiffness and damping matrix which is frequency dependent. Because of axial symmetry, $K_x = K_y$ and $K_x = K_y$. Associated off-diagonal terms are equal. Torsional stiffness not provided.	A: Method is quick and simple to use. Equations for stiffness and damping can be easily solved by hand calculator or by a simple computer program. Lateral and rocking stiffness solutions are frequency independent. Axial stiffness solution is approximately frequency independent. A/L: Three modulus profiles cover most practical situations, but method may be difficult to apply to unusual profiles. L/A: Nonlinear soil behavior cannot be modeled exactly, but equivalent linear properties can be selected. L: Solutions not available for end-bearing piles. Methods are approximate. Torsion not considered.	Gazetas (1991)
	5. Lam	Linear	Linear	Linear elastic soil with $E_s = c\,z$.	Linear elastic beam model of cylindrical pile with constant cross section.	• Welded contact between soil and pile • free head condition	Simple charts	• pile: E, I • soil: E_s or f where f is coefficient of variation of soil reaction	4x4 pile head stiffness matrix. Axial and torsional stiffnesses not provided.	A: Method is very quick and simple to use. Charts provided to easily obtain f for clays and sands. L: Method limited to soil profile with constant f. Axial & torsional stiffnesses not provided. Static solution only, and damping not computed.	Lam et al (1991)

METHODS TO COMPUTE FOUNDATION STIFFNESS AND DAMPING

Foundation Type	Method Author	Method Type: Linear/ Nonlinear	Method Type: Static/ Dynamic	Soil Model	Foundation Model	Boundary Conditions	Solution Obtained by	Input Parameters	Output Parameters	Advantages (A)/Limitations (L)	References
II. Group Pile	1. Novak	Linear	Static or Dynamic	Linear, viscoelastic, isotropic horizontal layers over ½ space	Linear, elastic, beam model of pile with constant or variable cross section. Piles attached to rigid cap or footing.	• Welded contact between soil and pile • Fixed or pinned connection between piles and cap.	Computer program DYNA 3 which incorporates PILAY 2 and subroutine to account for pile-group effects. PC version available.	Same as for PILAY 2 (see p. 1) plus pile group geometry.	6x6 pile group stiffness and damping matrix.	Same as for PILAY 2 (see p.1) plus the following: A: Three user options available to account for (or neglect) group effects through interaction factors: 1. No interaction 2. Static interaction 3. Dynamic interaction L: Interaction factors are approximate A: Vertical and battered piles can be considered within pile group.	User Manual by Novak et al (1990). Revised August, 1991.
	2. Lam	Linear or Nonlinear	Static	see I.2 (p.1) Matlock	Linear, elastic beam model of pile with constant or variable cross section. Piles attached to rigid cap.	• see I.2 (p.1) Matlock • Fixed or pinned condition between piles and cap or arbitrary rotational restraint	1. Substitution of individual pile-head stiffnesses into formulas for pile-group stiffness. Pile-head stiffnesses obtained from BMCOL 76. or 2. Computer program PILECAP	Individual pile-head stiffnesses and pile-group geometry.	6x6 pile group stiffness matrix.	Same as for BMCOL 76 (see I.2 Matlock p.1) plus the following: A/L: Formulas for obtaining pile-group stiffness matrix are simple, but not explicitly provided L: Group effects are neglected. A; Vertical and battered piles can be considered within group when using PILECAP program	Lam & Martin (1986) FHWA Rept. No. FHWA/RD-86/102, vol. II, outlines procedure for obtaining 6x6 pile-group stiffness matrix from individual pile-head stiffnesses. Vol. III of that FHWA report provides the user guide and source code for the program PILECAP.

METHODS TO COMPUTE FOUNDATION STIFFNESS AND DAMPING

Foundation Type	Method Author	Method Type: Linear/ Nonlinear	Method Type: Static/ Dynamic	Soil Model	Foundation Model	Boundary Conditions	Solution Obtained by	Input Parameters	Output Parameters	Advantages (A)/Limitations (L)	References
II. Group Pile	3. Reese.	Linear or Nonlinear	Static	See I.3 (p.2) Reese	Linear elastic beam model of pile with constant or variable cross section. Piles attached to rigid cap.	• See I.3 (p.2) Reese • Fixed, pinned or elastic restraint between piles and cap	Computer program GROUP	Similar to LPILE 3 and APILE 2 or output from these programs can be input to GROUP. Pile-group geometry.	Load vs. displacement and moment vs. rotation of pile cap, which can be used to estimate 5x5 pile cap stiffness matrix.	Same as for LPILE 3 & APILE 2 plus the following: A/L: Group-effects can be considered, but only by user reducing single-pile results, which is a very approximate procedure. A: Vertical and battered piles can be considered within pile group. L: Torsion neglected.	User Manual published by ENSOFT.
	4. Gazetas	Linear	Dynamic	See I.4 (p.2) Gazetas	Linear elastic beam model of cylindrical pile with constant cross section. Piles attached to rigid cap.	• See I.4 (p.2) Gazetas • Fixed or pinned condition between piles and cap.	Hand calcs following procedures in Gazetas publications.	See I.4 (p.2) Gazetas. Pile group geometry.	5x5 pile cap stiffness and damping matrix. Torsional stiffness not provided.	Same as for I.4 (p.2) plus the following: A/L: Group effects considered through approximate dynamic interaction factors which are frequency dependent in most cases. L: No formulas are provided for lateral interaction factors for linear and parabolic E_s profiles A/L: Computer program is not available, but formulas are not very complicated L: Battered piles not considered. Torsion not considered.	Procedures and formulas found in Dobry & Gazetas (1988) and Gazetas (1991).

METHODS TO COMPUTE FOUNDATION STIFFNESS AND DAMPING

Foundation Type	Method Author	Method Type: Linear/ Nonlinear	Method Type: Static/ Dynamic	Soil Model	Foundation Model	Boundary Conditions	Solution Obtained by	Input Parameters	Output Parameters	Advantages (A)/Limitations (L)	References
III. Single Footing	1. Novak	Linear	Static & Dynamic	Several Options: • Half Space • Layer over ½ space • Layer over Rock • Layered Medium Each soil layer is homogeneous, isotropic and viscoelastic. For layer-over-½ space model, a linearly varying shear-wave velocity can be considered within the layer.	Footing is rigid and is: • Surface or embedded • Cylindrical or rectangular	Bonded contact between footing and soil.	Subroutines within computer program DYNA 3. These options are HALF-SPACE, STRATUM, RIGID-BODY, COMPOSITE-MEDIUM	Foundation dimensions: • length (radius) • width • depth Embedment Soil properties: • Shear Modulus • Density • Poisson's Ratio • Material Damping for each layer	6x6 footing stiffness and damping matrix which is frequency dependent. Subroutine MATRIX is used.	A: Wide range of foundation and soil conditions can be considered. L: Constant values of stiffness must be selected from frequency-dependent solutions for input to SEISAB.	User Manual by Novak et al (1990). Revised August 1991. This manual is for the more general program DYNA3, which incorporates the subroutines listed in Col. (8).
	2. Gazetas	Linear	Static & Dynamic	Several Options: • Half Space (Homogeneous or Inhomogeneous) • Layer over Rock. Soil is isotropic and viscoelastic	Footing is rigid and is: • Surface or embedded • Rectangular or arbitrary plan shape	Bonded contact between footing and soil.	Simple closed-form algebraic equations. Graphs also available for combinations of soil and foundation parameters.	Foundation dimensions of circumscribed rectangle. Area of footing in plan. Embedment.	6x6 footing stiffness and damping matrix, which is frequency dependent.	A: Method is relatively simple to use. Equations for stiffness and damping can be easily solved by a hand calculator or simple computer program. A/L: Many practical situations can be modeled by the soil models and foundation models listed, but many others are not covered. L: Method is approximate. L: Constant values of stiffness must be selected from frequency-dependent solutions for input to SEISAB	Gazetas (1991)

METHODS TO COMPUTE FOUNDATION STIFFNESS AND DAMPING

Foundation Type	Method Author	Method Type: Linear/ Nonlinear	Method Type: Static/ Dynamic	Soil Model	Foundation Model	Boundary Conditions	Solution Obtained by	Input Parameters	Output Parameters	Advantages (A)/Limitations (L)	References
III. Single Footing	3. Wong	Linear	Static & Dynamic	Several Options: • Half Space • Homogeneous or Inhomogeneous layer over half-space. Inhomogeneous layer assumed to have linearly varying shear-wave velocity with depth	Rigid rectangular foundation for half-space soil model. Square foundation for layer-over-half-space model. Both foundations rest on surface (i.e. no embedment)	Bonded contact between foundation and soil	Tables	Foundation length and length/width ratio. Shear-wave velocity, density, Poisson's Ratio, and material damping ratio of soil media	6x6 footing stiffness and damping matrix which is frequency dependent.	A: Tables containing solutions are easy to use. A: Solutions are obtained by rigorous analytical and numerical methods. L: Foundation and soil models are limited. L: Constant values of stiffness must be selected from frequency-dependent solutions for input to SEISAB.	Wong & Luco (1978, 1985)
	4. Dominguez	Linear	Static & Dynamic	Half Space	Rigid rectangular surface or embedded foundation	Bonded contact between foundation and soil	Figures	Foundation length and width. Embedment. Shear-modulus.	6x6 footing stiffness and damping matrix, which is frequency dependent.	A: Figures containing solutions are fairly easy to use. L: Foundation and soil models are too limited. L: Constant values of stiffness must be selected from frequency-dependent solutions for input to SEISAB	Dominguez (1978)
	5. FHWA	Linear	Static	Linearly elastic isotropic half-space	Rigid circular or rectangular footing on surface or embedded in half-space	Bonded contact between footing and soil.	Simple equations and figures	Radius or length and width of foundation. Embedment. Shear modulus and Poisson's ratio of soil	6x6 diagonal static stiffness matrix.	A: Method is very simple and quick to use. L: Method not provided for off-diagonal terms of stiffness matrix (rocking-translation coupling) which may be important for embedded footings L: Dynamic stiffness and damping not provided	Lam & Martin (1986) FHWA Rept. No. FHWA/RD-86/102, vol. II, pp. 40-51.

METHODS TO COMPUTE FOUNDATION STIFFNESS AND DAMPING

Foundation Type	Method Author	Method Type: Linear/ Nonlinear	Method Type: Static/ Dynamic	Soil Model	Foundation Model	Boundary Conditions	Solution Obtained by	Input Parameters	Output Parameters	Advantages (A)/Limitations (L)	References
IV. Retaining or Abutment Wall	1. Wood	Linear	Static	Linear, elastic, homogeneous, isotropic, plane strain, finite element model. (Some solutions available for flexible wall)	Rigid wall translating or rotating into soil. (some solutions available for flexible wall)	Smooth or bonded contact between wall and soil.	Graphs (Hand-calc. integration of curves required to obtain stiffnesses)	Young's Modulus, E_s, of soil (Poisson's ratio, $\nu = 0.3$ assumed). Dimensions of wall area (H x B) in contact with backfill (Strictly speaking, wall depth dimension, H, is not needed to obtain trans. stiffness — H cancels out during integration. H is needed for rotational stiffness)	Translational and rotational stiffness. (Translational stiffness in direction normal to face of wall. Rotational stiffness is about axis parallel to face of wall.)	A/L: Graphs are simple but integration of curves is required L: Solutions only available for limited cases. L: Translational & rotational stiffnesses associated with shearing resistance between soil & wall not provided. Torsional stiffness about vertical axis not provided. L: Dynamic stiffness and damping not computed. L: Stiffness independent of wall height (a result of 2-D plane strain approximation)	Wood & Elms (1990), Wood (1985)
	2. Finn	Linear	Static	Linear, elastic, homogeneous, isotropic, plane strain quarter space	Rigid wall translating or rotating into soil	Smooth or bonded contact between wall and soil	Formulas (Formulas are simple but must be integrated to obtain stiffnesses)	E_s , ν, H, B (same comment about H as in IV.1 above)	Translational and rotational stiffness similar to IV.1 above.	A/L: Formulas are simple, but require numerical integration L: Translational and rotational stiffness associated with shearing resistance between soil and wall not provided. Torsional stiffness about vertical axis also not provided. L: Solution not available for dynamic stiffness and damping. L: Stiffness independent of wall height.	Finn (1963) or Poulos & Davis (1974)
	3. FHWA	Linear	Static	Linear, elastic homogeneous, isotropic, plane strain, finite element model	Rigid wall translating or rotating into soil.	Bonded contact.	Simple equation	E_s, H, B	Translational and rotational stiffness similar to IV.1 above.	A: Equations for stiffnesses are very simple and easy to use L: Same limitation as IV.1 above	Lam & Martin (1986) FHWA Rept. No. FHWA/RD-86/ 102, vol. II, p. 135.

METHODS TO COMPUTE FOUNDATION STIFFNESS AND DAMPING

Foundation Type	Method Author	Method Type: Linear/ Nonlinear	Method Type: Static/ Dynamic	Soil Model	Foundation Model	Boundary Conditions	Solution Obtained by	Input Parameters	Output Parameters	Advantages (A)/Limitations (L)	References
IV. Retaining or Abutment Wall	4. Lam	Linear	Static	Linear, elastic, homogeneous, isotropic half space	Rigid foundation (wall) translating into half space	Bonded contact	Simple equation	E_s, ν, B, I (I is influence coefficient that depends on H/B)	Translational stiffness similar to IV.1 above	A: Equation is very simple and easy to use. A/L: Wall height is more accurately considered using ½-space rather than 2-D, ¼-space theory, but stiffness will be somewhat overestimated L: Other stiffnesses not provided. L: Solution not available for dynamic stiffness & damping	Lam et al (1991)
	5. Wilson	Linear	Static	Linear, elastic homogeneous, isotropic half space	Rigid foundation (wall) translating into half space	Bonded contact	Equations	E_s, ν, B, I (I is influence coefficient that depends on H/B).	Translational stiffness similar to IV.1 above, torsional stiffness about vertical axis, rotational stiffness about transverse axis. Stiffnesses associated with shearing resistance between wall & soil not provided.	A: Equations are fairly simple A/L: Wall height is more accurately considered using ½-space rather than 2-D, ¼-space theory, but stiffnesses will be somewhat overestimated. A/L: User has choice of references to obtain influence coefficients, which are not provided in Wilson paper. L: Stiffnesses associated with shearing resistance between soil & wall not provided.	Wilson (1988) (paper suggests Poulos & Davis (1974) for influence coefficients)

METHODS TO COMPUTE FOUNDATION STIFFNESS AND DAMPING

Foundation Type	Method Author	Method Type: Linear/ Nonlinear	Method Type: Static/ Dynamic	Soil Model	Foundation Model	Boundary Conditions	Solution Obtained by	Input Parameters	Output Parameters	Advantages (A)/Limitations (L)	References
V. Abutment System (including abutment wall, abutment footing with or without piles, and wingwalls)	1. Wilson	Linear	Static	Linear, elastic homogeneous, isotropic half space. Model permits solutions for other types of media.	Rigid elements for abutment wall, footing and wingwall. Elastic piles.	Depends on solutions selected for individual elements comprising abutment system.	Equations which superimpose solutions for individual elements comprising abutment system	Dimensions of: abutment wall and footing, wingwall and wingwall footing. Soil modulus (E_s) and Poisson's ratio (v). Influence coefficients, I, for wall and footings. Pile-head stiffnesses (translational).	6x6 Abutment stiffness matrix at a point on abutment wall representing the centroid of the bridge-deck cross section.	A: Equations are fairly simple A/L: User can implement methods of his choice to compute the stiffnesses of elements comprising abutment system. Thus, other references must be used. L: Contribution of footing stiffness included in longitudinal and transverse stiffness of system but ignored in the vertical system stiffness, which is inconsistent. L: Rotational stiffnesses of wall and footing elements based on uniform distribution of translational stiffnesses, may be inappropriate for certain length/width ratios. L: Wingwall stiffness contribution may be overestimated for abutments on embankments L: Solutions not available for dynamic stiffness and damping.	Wilson (1988)
VI. Abutment-Embankment System	1. Wilson	Linear	Static	Linear, elastic, isotropic, homogeneous, 2-D, plane strain model of trapezoidal cross section of embankment.	Abutment geometry ignored, except for length of wingwall	Embankment rests on rigid base	Simple equations	Height (H), Width (W), Slope (S), and shear modulus (G) of embankment. Length of wingwalls	Transverse & vertical stiffnesses of abutment.	A: Equations are very simple A: Abutment configuration can be ignored L: Total stiffness is obtained by multiplying the stiffness of 2-D unit depth model by depth wingwall extends into backfill, which is arbitrary. L: Other stiffnesses not provided L: Solution not available for dynamic stiffness and damping	Wilson & Tan (1990)

Appendix B

GUIDE FOR DATA INPUT FOR BMCOL 76

With Supplementary Notes

Extract from

A COMPUTER PROGRAM FOR

THE ANALYSIS OF BEAM-COLUMNS UNDER

STATIC AXIAL AND LATERAL LOADING

by

Hudson Matlock
Dewaine Bogard
Ignatius Lam

Ertec, Inc.
Long Beach, California

15 October 1980

IDENTIFICATION OF RUN (2 alphanumeric cards per run)

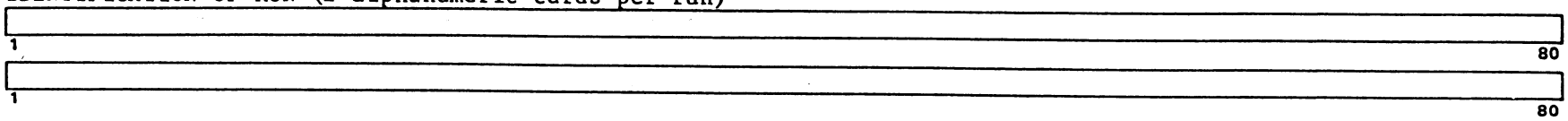

IDENTIFICATION OF PROBLEM (1 alphanumeric card each problem)

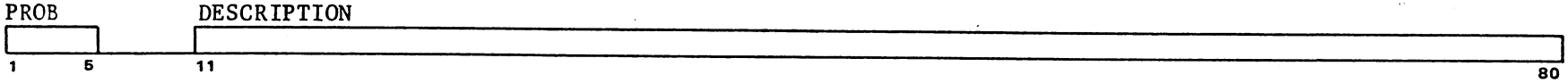

TABLE 1. PROGRAM CONTROL DATA

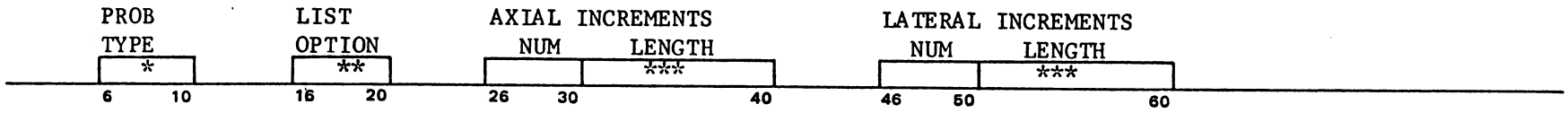

* 1=axial
2=lateral
3=combination

** 1=suppress listing of data cards

*** axial increment length must be an integral multiple of lateral

TABLE 2. AXIAL CONTROL DATA (1 card for linear problems, 2 cards for iterating solution)

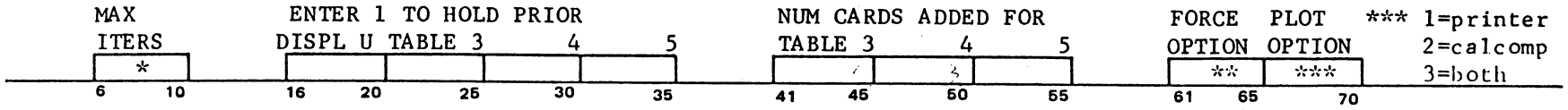

* 0 = linear solution

** 1 = optional output of force components (Table 13)

ITERATION CONTROL CARD (1 card for iterating solution, none for linear problem)

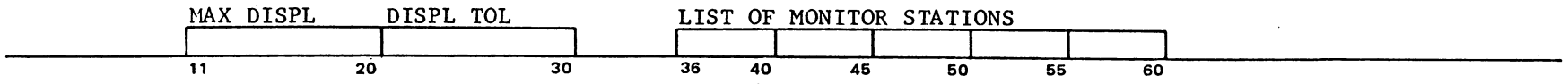

TABLE 3. SPECIFIED AXIAL DISPLACEMENTS (number of cards according to Table 2; none if prior Table 3 held)

STATION DISPLACEMENT

TABLE 4. FIXED VALUES OF AXIAL STIFFNESS AND LOAD (number of cards according to Table 2) See page 9 for procedures. Data algebraically added to storage as lumped quantities per increment length, linearly interpolated between values input at indicated end stations. Half values of loads Q and springs S are applied at end stations but, since axial stiffness AE is a property of the bars, a full value is stored at each bar. Concentrated loads Q and springs S are established as full values at single stations by setting TO STA = FROM STA.

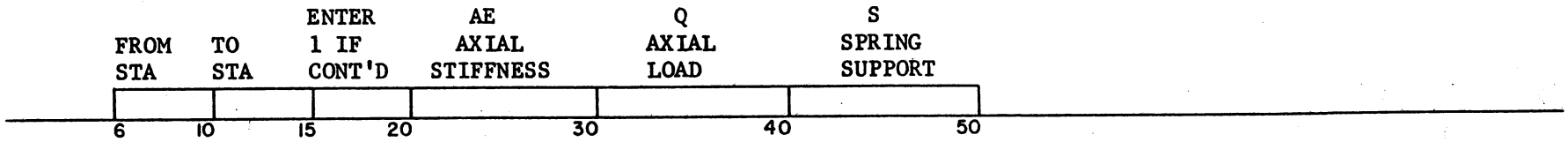

TABLE 5. AXIAL LOAD AND SUPPORT CURVES (3 cards per curve according to Table 2) Procedure for distributing values to stations between input curves corresponds to that for Table 4, except that values of force Q and spring stiffness S (determined by linear interpolation along curves according to previously computed displacements) are added to storage in each iteration. Distance to origin of curve at each station is linearly interpolated between end stations of adjacent curves. Also see page 9.

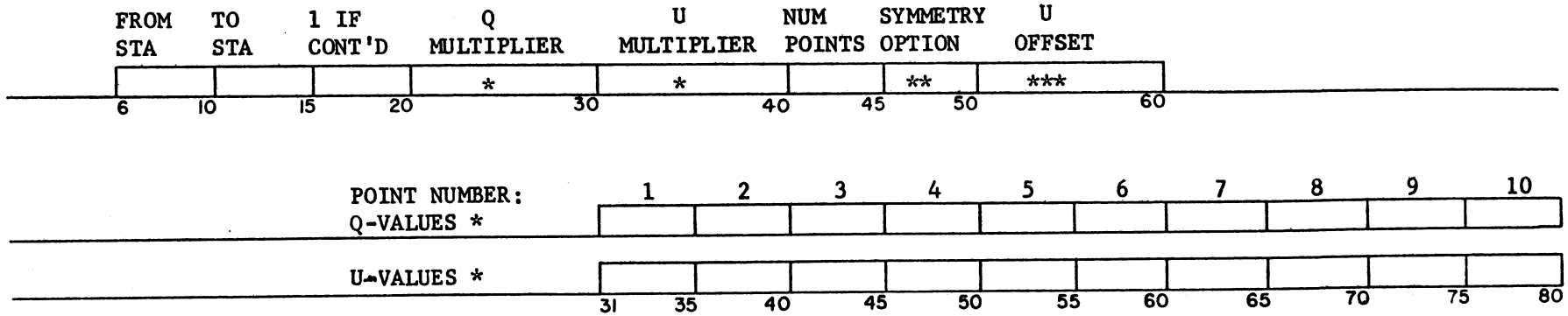

* Final Q or U in storage will be the product of MULTIPLIER and VALUE.

** Enter 1 if curve symmetric about origin; final U's entered must be positive.

*** Distance from BMCOL origin (U = 0) to curve origin (U-VALUE = 0)

TABLE 6. LATERAL CONTROL DATA (1 card for linear problem; 2 cards for iterating solution)

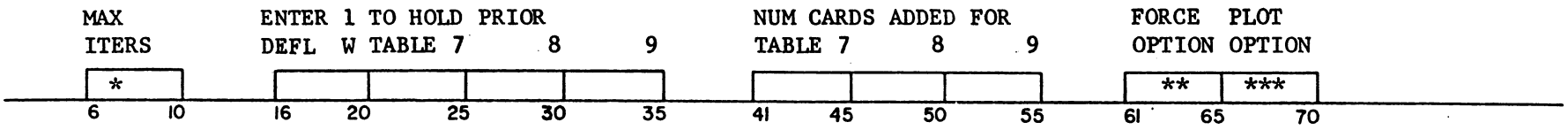

* 0 = linear solution
** 1 = optional output of force components (Table 16)
*** 1 = printer, 2 = calcomp, 3 = both

ITERATION CONTROL CARD (1 card for iterating solution; none for linear problem)

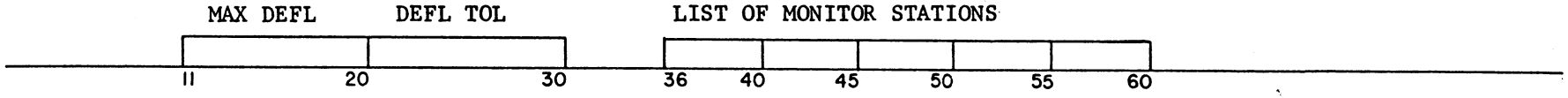

TABLE 7. SPECIFIED DEFLECTIONS AND SLOPES

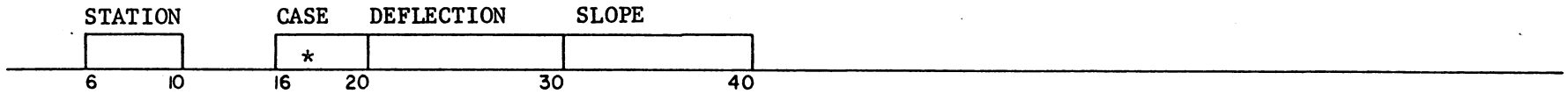

* CASE = 1 for defl, 2 for slope, 3 for both

TABLE 8. FIXED VALUES OF LATERAL STIFFNESS AND LOAD (number of cards according to Table 6) See page 9 for procedures. Data algebraically added to storage as lumped quantities per increment length, linearly interpolated between values input at indicated end stations, with half-values at each end station. Concentrated values are established as full values at single stations by setting TO STA = FROM STA.

FROM STA	TO STA	ENTER 1 IF CONT'D	F BENDING STIFFNESS	Q LATERAL LOAD	S SPRING SUPPORT	C APPLIED COUPLE	R ROTATIONAL RESTRAINT

TABLE 9. LATERAL LOAD AND SUPPORT CURVES (3 cards per curve according to Table 6) Procedure for distributing values for stations between input curves corresponds to that for Table 8, except that the values of force Q and spring stiffness S (determined by linear interpolation along curves according to previously computed deflections) are added to storage in each iteration. Distance to origin of a curve at a station is linearly interpolated between end stations of adjacent curves. Also see page 9.

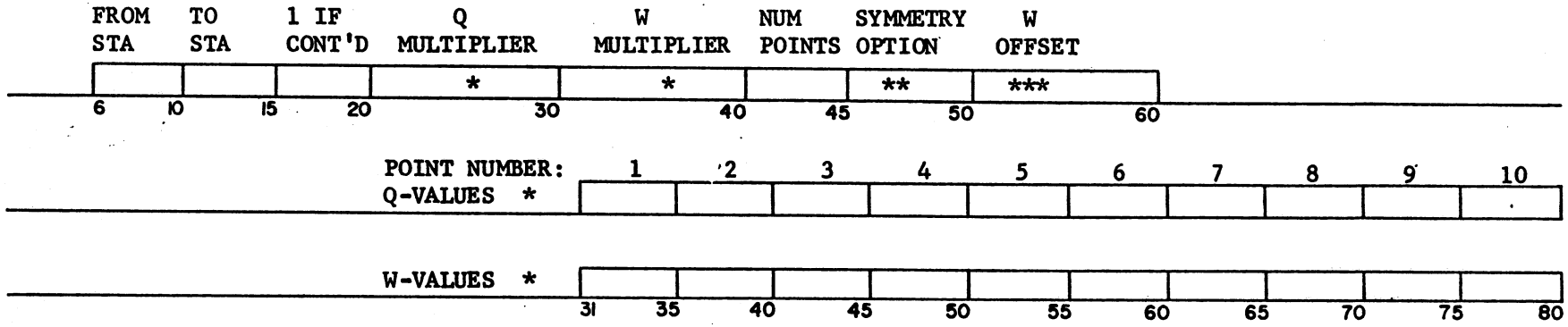

* Final Q or W in storage will be the product of VALUE and MULTIPLIER.
** Enter 1 if curve symmetric about its origin; final W's entered must be positive.
*** Distance from BMCOL origin (W = 0) to curve origin (W-VALUE = 0).

STOP CARD. Enter STOP to terminate run.

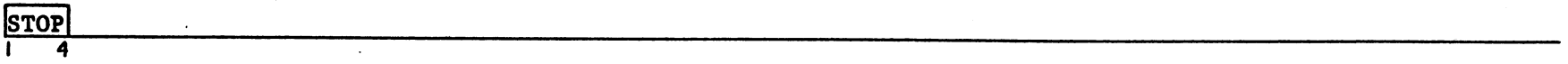

BMCOL 76 GUIDE FOR DATA INPUT - Supplementary Notes

GENERAL PROGRAM NOTES

The data cards must be stacked in the proper order for the program to run.

A consistent set of units must be used for all input data, for example: inches and pounds.

All 5-space words are understood to be integers or whole decimal numbers . . . . . | -1 2 3 4 |

All 10-space words are floating-point decimal numbers . . . . . | - 1 . 2 3 4 E + 0 3 |

The user is cautioned that nonlinear axial and lateral solutions do not necessarily converge to a unique solution even though closure is achieved at each station. The validity of a solution may be tested by approaching the solution from two different beginning sets of deflection or displacement by means of the HOLD options provided in Tables 2 and 6.

TABLE 1. PROGRAM CONTROL DATA

The LIST OPTION being set equal to one will suppress the listing of data cards as they are read. The use of the listed input data is encouraged, for errors in the input data may be easily found. The list is printed on a separate page which may be discarded.

The maximum number of increments into which the beam-column may be divided is 200.

TABLES 2 AND 6. AXIAL AND LATERAL CONTROL DATA

Each of these tables is read as specified by the problem type in Table 1.

Iterating solutions will start with all values of displacement or deflection equal to zero unless options are exercised to hold them from the preceding problem.

For Tables 3 and 7, a choice must be made between holding all data from a previous problem or entering entirely new data. If the hold-option is set equal to one, the number of cards in these tables must be zero.

For each of Tables 4 and 8, the input data are stored in card-image form and are redistributed for each problem. The maximum number of card images accumulated for any problem, including those held, is 50.

The same is true for Tables 5 and 9 but the maximum accumulation is 20 curves or 60 cards.

The card count for each table should be carefully checked after the coding of each problem is completed.

The maximum number of iterations should be set to avoid excessive machine computation. Most structural problems should close within 10 iterations, an allowed maximum of 20 is usually adequate.

The primary purpose of the maximum allowable displacement or deflection is to stop the program if an unreasonably large value is reached at any station. It should therefore be set to a value large enough to not interfere with the normal trial-and-correction process of the iterative solution.

The closure tolerance has the same units as the displacement or deflection. If it is unreasonably small, closure may be difficult to achieve. For most structural problems, a value in the range of 0.001 to 0.0001 inch is satisfactory.

The monitor data are printed on separate sheets which may be discarded. However, to encourage the understanding of the engineering or structural aspects of the solution process, the program requires that 5 monitor stations be designated for all problems that require an iterative solution.

TABLES 3 AND 7. SPECIFIED CONDITIONS

The maximum number of stations in either table at which conditions may be specified is 20.

Cards must be arranged in increasing order of station numbers.

A slope may not be specified closer than 3 increments from another specified slope.

A deflection may not be specified closer than two increments from a specified slope, except that both slope and deflection may be specified at the same station.

TABLES 4 AND 8. AXIAL AND LATERAL STIFFNESS AND LOAD DATA

Typical units, values per station	AE	Q	S	F	C	R
	lb	lb	lb/in	lb x in^2	in x lb	in x lb/radian

Data may be input at any station number regardless of the length of the real beam-column; values which occur beyond the end are ignored.

For the interpolation and distribution process, there are four variations in the station numbering and in referencing for continuation to succeeding cards. These variations are explained and illustrated on page 8.

There are no restrictions on the order of cards in these tables, except that stations within each distribution sequence must be in increasing order.

TABLES 5 AND 9. NONLINEAR SUPPORT CURVES

Typical units, values per station:	Q lb	U and W inches

The Q-U and Q-W curves in Tables 5 and 9 are intended primarily to express the effects of reactions which do not vary in linear proportion to the response of the beam-column. Values of Q and S are obtained by linear interpolation, with respect to displacement or deflection, between points along a curve (See Fig 1), and also by linear interpolation, with respect to distance along the beam-column, between adjacent curves.

For the usual types of nonlinear supports, positive beam or column responses are resisted by negative forces; therefore, negative Q-values should usually accompany positive U-values and W-values, and vice-versa. Where a support has similar resistance characteristics for both positive and negative values of displacement or deflection, the curve symmetry option may be set equal to one and input data points must then be limited to the region of positive values of displacement U or deflection W (See Fig 2). Since the curve is symmetric about the origin, the curve point at the origin (0,0) may be omitte

The maximum number of points which may be input on any given curve is 10, although additional points up to a total of 20 may be created internally if the curve symmetry option is exercised.

The process of distributing Q and S values to each station by linear interpolation between curves is directly parallel to the arrangements for Tables 4 and 8 input except that interpolations and distributions are made repeatedly during iterative solutions. The variations in input-data station numbering and sequence-continuations are therefore the same as for Tables 4 and 8.

Curves may be input at any station number, regardless of the length of the real beam-column. No Q and S values from Q-U or Q-W curves are computed for stations beyond the end of the real beam-column; furthermore, when the right end of the beam-column falls between two Q-U or Q-W curves of an interpolation-distribution sequence, the Q and S values at the end station are automatically set to half values.

There are no restrictions on the order of Q-U or Q-W curves except that within a distribution sequence the stations must be in increasing order. More than one curve may be placed at a station.

For any particular curve, the signs and the order of the data must provide that the final values of U or W in storage (U-value X U-multiplier and W-value X W-multiplier) be arranged in algebraically increasing order. The curve interpolation procedure does not permit discontinuous jumps in Q at any value of U or W, that is, with two successive values of U or W that are equal. There must be only one possible point on any curve for any given value of displacement or deflection.

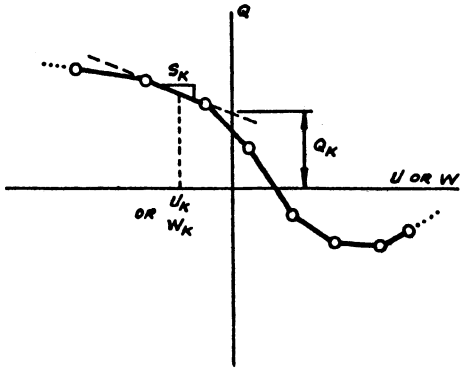

Fig 1. Interpolation for tangent modulus from a single nonlinear support curve.

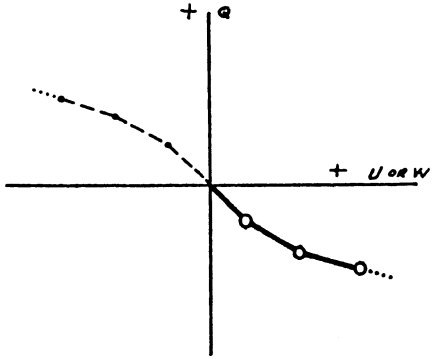

Fig. 2. Left side of curve is internally completed by using symmetry option.

Individual Card Input

Data concentrated at one station .....

Axial stiffness in one bar .....

Data uniformly distributed .....

Multiple-Card Sequence

First of sequence .....

Interior of sequence .....

End of sequence .....

FROM STA	TO STA	CONT'D TO NEXT CARD?	F,Q,S, C,R	AE	
2	2	0=No	2.0		●
1	2	0=No		2.0	◔
5	15	0=No	2.0	1.0	○
11	15	0=No	1.0	2.0	◒
20		1=Yes	2.0	2.0	■
	25	1=Yes	2.0	2.0	■
	30	0=No	0.0	2.0	■
31		1=Yes	2.0	0.0	□
	35	0=No	2.0	4.0	□

Resulting Distribution of Data in Computer Storage

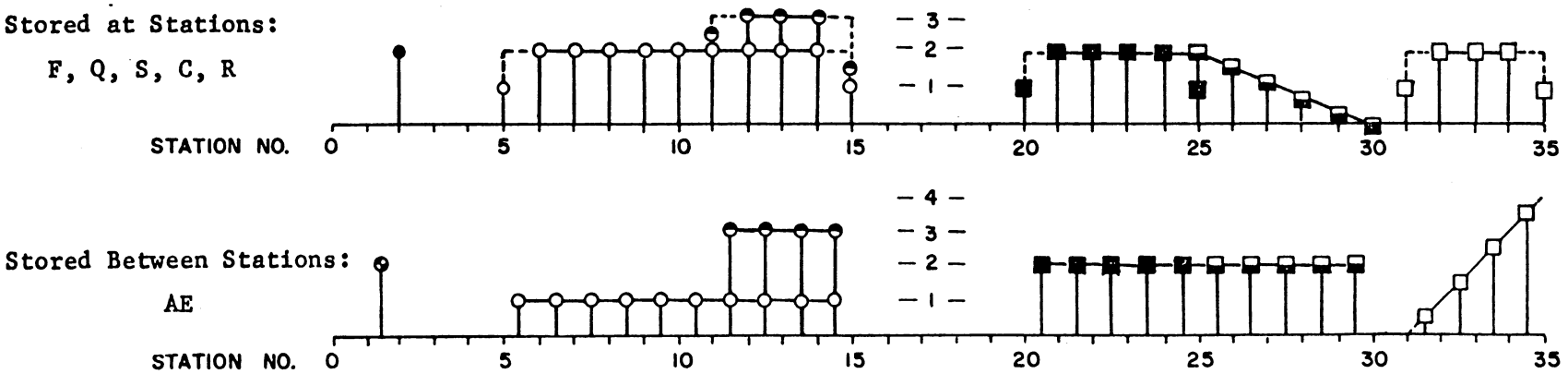

Appendix C

APPENDIX C

FHWA/NOVAK TO SEISAB COORDINATE SYSTEM TRANSFORMATION C-1
FHWA TO SEISAB COORDINATE SYSTEM TRANSFORMATION C-2
STIFFNESS MATRIX TRANSLATION OF VERTICAL POSITION C-3

FHWA/NOVAK TO SEISAB COORDINATE SYSTEM TRANSFORMATION

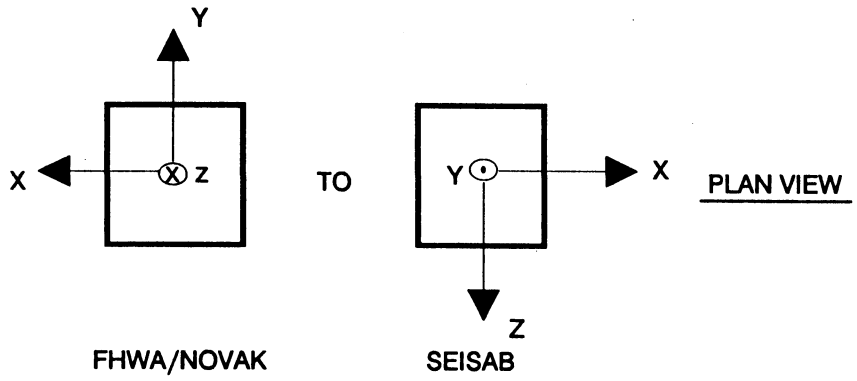

$$[K_{FHWA}] = \begin{bmatrix} a_{11} & a_{12} & a_{13} & \cdot & \cdot & \cdot \\ a_{21} & a_{22} & \cdot & \cdot & \cdot & \cdot \\ a_{31} & \cdot & \cdot & \cdot & \cdot & \cdot \\ \cdot & \cdot & \cdot & \cdot & \cdot & \cdot \\ \cdot & \cdot & \cdot & \cdot & \cdot & \cdot \\ \cdot & \cdot & \cdot & \cdot & \cdot & \cdot \end{bmatrix}$$

Where a_{mn} = FHWA or NOVAK stiffness value

Note that:

SEISAB-I	x	=	FHWA -x	=	NOVAK -x
SEISAB-I	y	=	FHWA -z	=	NOVAK -z
SEISAB-I	z	=	FHWA -y	=	NOVAK -y

First, multiply each x column by -1 and exchange y and z columns after multiplying y and z columns by -1.

$$\begin{bmatrix} -a_{11} & -a_{13} & -a_{12} & -a_{14} & -a_{16} & -a_{15} \\ -a_{21} & -a_{23} & -a_{22} & -a_{24} & -a_{26} & -a_{25} \\ -a_{31} & -a_{33} & -a_{32} & -a_{34} & -a_{36} & -a_{35} \\ -a_{41} & -a_{43} & -a_{42} & -a_{44} & -a_{46} & -a_{45} \\ -a_{51} & -a_{53} & -a_{52} & -a_{54} & -a_{56} & -a_{55} \\ -a_{61} & -a_{63} & -a_{62} & -a_{64} & -a_{66} & -a_{65} \end{bmatrix}$$

Next, multiply each x row by -1 and exchange y and z rows after multiplying y and z rows by -1.

$$[K_{SEISAB}] = \begin{bmatrix} a_{11} & a_{13} & a_{12} & a_{14} & a_{16} & a_{15} \\ a_{31} & a_{33} & a_{32} & a_{34} & a_{36} & a_{35} \\ a_{21} & a_{23} & a_{22} & a_{24} & a_{26} & a_{25} \\ a_{41} & a_{43} & a_{42} & a_{44} & a_{46} & a_{45} \\ a_{61} & a_{63} & a_{62} & a_{64} & a_{66} & a_{65} \\ a_{51} & a_{53} & a_{52} & a_{54} & a_{56} & a_{55} \end{bmatrix}$$

FHWA TO SEISAB COORDINATE SYSTEM TRANSFORMATION

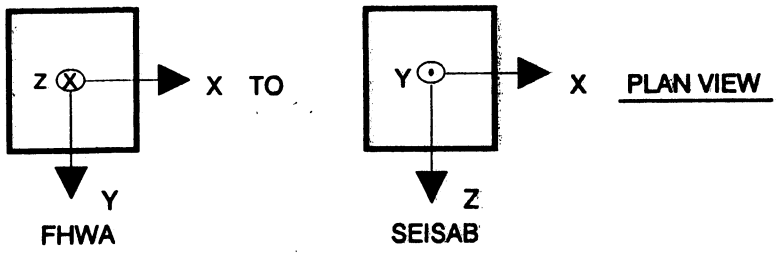

$$[K_{FHWA}] = \begin{bmatrix} a_{11} & a_{12} & \cdot & \cdot & \cdot & \cdot \\ a_{21} & a_{22} & \cdot & \cdot & \cdot & \cdot \\ a_{31} & \cdot & \cdot & \cdot & \cdot & \cdot \\ \cdot & \cdot & \cdot & \cdot & \cdot & \cdot \\ \cdot & \cdot & \cdot & \cdot & \cdot & \cdot \\ \cdot & \cdot & \cdot & \cdot & \cdot & \cdot \end{bmatrix}$$

Where a_{mn} = FHWA Stiffness value

Note that: SEISAB-I x = FHWA x
SEISAB-I y = FHWA -z
SEISAB-I z = FHWA y

First exchange x and z columns after multiplying each FHWA z column by -1.

$$\begin{bmatrix} a_{11} & -a_{13} & a_{12} & a_{14} & -a_{16} & a_{15} \\ a_{21} & -a_{23} & a_{22} & a_{24} & -a_{26} & a_{25} \\ a_{31} & -a_{33} & a_{32} & a_{34} & -a_{36} & a_{35} \\ a_{41} & -a_{43} & a_{42} & a_{44} & -a_{46} & a_{45} \\ a_{51} & -a_{53} & a_{52} & a_{54} & -a_{56} & a_{55} \\ a_{61} & -a_{63} & a_{62} & a_{64} & -a_{66} & a_{65} \end{bmatrix}$$

Next, exchange y and z rows after multiplying each z row by -1.

$$[K_{SEISAB}] = \begin{bmatrix} a_{11} & -a_{13} & a_{12} & a_{14} & -a_{16} & a_{15} \\ a_{31} & a_{33} & -a_{32} & -a_{34} & a_{36} & -a_{35} \\ a_{21} & -a_{23} & a_{22} & a_{24} & -a_{26} & a_{25} \\ a_{41} & -a_{43} & a_{42} & a_{44} & -a_{46} & a_{45} \\ -a_{61} & a_{63} & -a_{62} & -a_{64} & a_{66} & -a_{65} \\ a_{51} & -a_{53} & a_{52} & a_{54} & -a_{56} & a_{55} \end{bmatrix}$$

Transform general six by six spring stiffness matrix for vertical position as shown in Figure C-1.

Let a = stiffness at position a
b = stiffness at position b
d = vertical distance from position a to position b

At point "a" $[Ka] = \begin{bmatrix} a_{11} & a_{12} & \cdot & \cdot & \cdot & \cdot \\ \cdot & & & & & \\ \cdot & & & 6 & x & 6 \\ \cdot & & & & & \\ \cdot & & & & & \\ \cdot & & & & & \end{bmatrix}$

Such that: $[Ka]\begin{Bmatrix} \delta_x^a \\ \delta_y^a \\ \delta_z^a \\ \theta_x^a \\ \theta_y^a \\ \theta_z^a \end{Bmatrix} = \begin{Bmatrix} F_x^a \\ F_y^a \\ F_z^a \\ M_x^a \\ M_y^a \\ M_z^a \end{Bmatrix}$

Transform spring stiffness $[Ka]$ at point "a" to $[Kb]$ at point "b". Assume rigid body translation.

1. Transform displacements using rigid body kinetics.

$$\delta_x^b = \delta_x^a + d\theta_y^a \qquad \theta_x^b = \theta_x^b$$
$$\delta_y^b = \delta_y^a \qquad d \qquad \theta_x^a \qquad \theta_y^b = \theta_y^b$$
$$\delta_z^b = \delta_z^a \qquad \theta_z^b = \theta_z^b$$

$$\{\delta^b\} = \begin{bmatrix} 1 & 0 & 0 & 0 & d & 0 \\ 0 & 1 & 0 & -d & 0 & 0 \\ 0 & 0 & 1 & 0 & 0 & 0 \\ 0 & 0 & 0 & 1 & 0 & 0 \\ 0 & 0 & 0 & 0 & 1 & 0 \\ 0 & 0 & 0 & 0 & 0 & 1 \end{bmatrix} \{\delta^a\}$$

$$\{\delta^b\} = [T_\delta]\{\delta^a\}$$

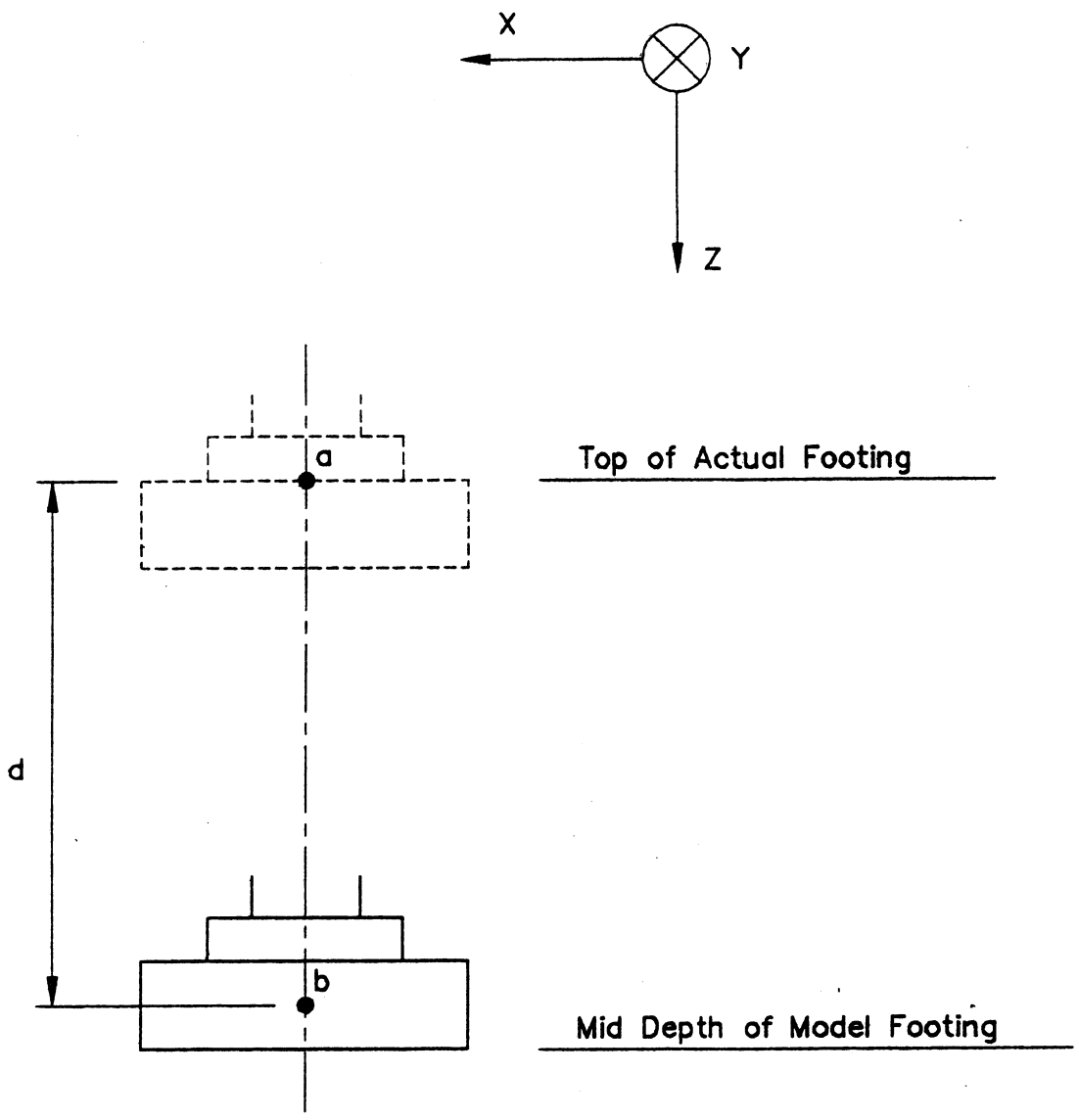

Transformation Model

Figure C.1

2. Transform forces while maintaining equilibrium.

$$\sum F_i^a = \sum F_i^b$$

and

$$\sum M_i^a = \sum M_i^b \qquad \text{(about "b")}$$

$$M_x^b = M_x^a + dF_y^a \qquad F_x^b = F_x^a$$

$$M_y^b = M_y^a - dF_x^a \qquad F_y^b = F_y^a$$

$$M_z^b = M_z^a \qquad F_z^b = F_z^a$$

$$\{F^b\} = \begin{bmatrix} 1 & 0 & 0 & 0 & 0 & 0 \\ 0 & 1 & 0 & 0 & 0 & 0 \\ 0 & 0 & 1 & 0 & 0 & 0 \\ 0 & +d & 0 & 1 & 0 & 0 \\ -d & 0 & 0 & 0 & 1 & 0 \\ 0 & 0 & 0 & 0 & 0 & 1 \end{bmatrix} \{F^a\}$$

$$\{F^b\} = [T_F]\{F^a\}$$

3. Solve for $[K_b]$.

$$[K_b]\{\delta^b\} = \{F^b\}$$
$$[K_b][T_\delta]\{\delta^a\} = [T_F]\{F^a\}$$
$$\{F^a\} = [K_a]\{\delta^a\}$$
$$[K_b][T_\delta]\{\delta^a\} = [T_F][K_a]\{\delta^a\}$$
$$[K_b][T_\delta] = [T_F][K_a]$$
$$[K_b][T_\delta][T_\delta]^{-1} = [T_F][K_a][T_\delta]^{-1}$$
$$[K_b] = [T_F][K_a][T_\delta]^{-1}$$

Determine $[T\delta]^{-1}$

$$[T\delta] = \begin{bmatrix} 1 & 0 & 0 & 0 & d & 0 \\ 0 & 1 & 0 & -d & 0 & 0 \\ 0 & 0 & 1 & 0 & 0 & 0 \\ 0 & 0 & 0 & 1 & 0 & 0 \\ 0 & 0 & 0 & 0 & 1 & 0 \\ 0 & 0 & 0 & 0 & 0 & 1 \end{bmatrix} \qquad \begin{bmatrix} 1 & 0 & 0 & 0 & 0 & 0 \\ 0 & 1 & 0 & 0 & 0 & 0 \\ 0 & 0 & 1 & 0 & 0 & 0 \\ 0 & 0 & 0 & 1 & 0 & 0 \\ 0 & 0 & 0 & 0 & 1 & 0 \\ 0 & 0 & 0 & 0 & 0 & 1 \end{bmatrix}$$

$$\begin{bmatrix} 1 & 0 & 0 & 0 & 0 & 0 \\ 0 & 1 & 0 & 0 & 0 & 0 \\ 0 & 0 & 1 & 0 & 0 & 0 \\ 0 & 0 & 0 & 1 & 0 & 0 \\ 0 & 0 & 0 & 0 & 1 & 0 \\ 0 & 0 & 0 & 0 & 0 & 1 \end{bmatrix} \qquad [T\delta]^{-1} = \begin{bmatrix} 1 & 0 & 0 & 0 & -d & 0 \\ 0 & 1 & 0 & d & 0 & 0 \\ 0 & 0 & 1 & 0 & 0 & 0 \\ 0 & 0 & 0 & 1 & 0 & 0 \\ 0 & 0 & 0 & 0 & 1 & 0 \\ 0 & 0 & 0 & 0 & 0 & 1 \end{bmatrix}$$

$$[TF][Ka] = \begin{bmatrix} 1 & 0 & 0 & 0 & 0 & 0 \\ 0 & 1 & 0 & 0 & 0 & 0 \\ 0 & 0 & 1 & 0 & 0 & 0 \\ 0 & +d & 0 & 1 & 0 & 0 \\ -d & 0 & 0 & 0 & 1 & 0 \\ 0 & 0 & 0 & 0 & 0 & 1 \end{bmatrix} \begin{bmatrix} a_{11} & a_{12} & a_{13} & a_{14} & a_{15} & a_{16} \\ a_{21} & a_{22} & a_{23} & a_{24} & a_{25} & a_{26} \\ a_{31} & a_{32} & a_{33} & a_{34} & a_{35} & a_{36} \\ a_{41} & a_{42} & a_{43} & a_{44} & a_{45} & a_{46} \\ a_{51} & a_{52} & a_{53} & a_{54} & a_{55} & a_{56} \\ a_{61} & a_{62} & a_{63} & a_{64} & a_{65} & a_{66} \end{bmatrix}$$

$$= \begin{bmatrix} a_{11} & a_{12} & a_{13} & a_{14} & a_{15} & a_{16} \\ a_{21} & a_{22} & a_{23} & a_{24} & a_{25} & a_{26} \\ a_{31} & a_{32} & a_{33} & a_{34} & a_{35} & a_{36} \\ a_{41}+da_{21} & a_{42}+da_{22} & a_{43}+da_{23} & a_{44}+da_{24} & a_{45}+da_{25} & a_{46}+da_{26} \\ a_{51}-da_{11} & a_{52}-da_{12} & a_{53}-da_{13} & a_{54}-da_{14} & a_{55}-da_{15} & a_{56}-da_{16} \\ a_{61} & a_{62} & a_{63} & a_{64} & a_{65} & a_{66} \end{bmatrix}$$

$$[K_b] = [T_F][Ka][Ts]^{-1}$$

$$[K_b] = \begin{bmatrix} a_{11} & a_{12} & a_{13} & da_{12} + a_{14} & a_{15} - da_{11} & a_{16} \\ a_{21} & a_{22} & a_{23} & da_{22} + a_{24} & a_{25} - da_{21} & a_{26} \\ a_{31} & a_{32} & a_{33} & da_{32} + a_{34} & a_{35} - da_{31} & a_{36} \\ a_{41} + da_{21} & a_{42} + da_{22} & a_{43} + da_{23} & da_{42} + d^2a_{22} + a_{44} + da_{24} & -da_{41} - d^2a_{21} + a_{45} + da_{25} & a_{46} + da_{26} \\ a_{51} - da_{11} & a_{52} - da_{12} & a_{53} - da_{13} & da_{52} - d^2a_{12} + a_{54} - da_{14} & -da_{51} + d^2a_{11} + a_{55} - da_{15} & a_{56} - da_{16} \\ a_{61} & a_{62} & a_{63} & a_{64} & a_{65} & a_{66} \end{bmatrix}$$